ELSEVIER

World Journal of Gastroenterology®

Supported by NSFC 2005-2006

Volume 11 Number 14
April 14, 2005

National Journal Award 2005

Contents

World Journal of Gastroenterology®
Volume 11 **Number** 14 **April** 14, 2005

Contents

World Journal of Gastroenterology®
Volume 11 **Number** 14 **April** 14, 2005

Contents

Editorial Coordinator for this issue: Anitha Kumaran

World Journal of Gastroenterology (*World J Gastroenterol , WJG*), a leading international journal in gastroenterology and hepatology, has an established reputation for publishing first class research on esophageal cancer, gastric cancer, liver cancer, viral hepatitis, colorectal cancer, and *Helicobacter pylori* infection, providing a forum for both clinicians and scientists, and has been indexed and abstracted in Index Medicus, MEDLINE, PubMed, Chemical Abstracts, EMBASE, Abstracts Journals, Nature Clinical Practice Gastroenterology and Hepatology, CAB Abstracts and Global Health. Impact factor of ISI JCR during 2000-2003 is 0.993, 1.445, 2.532 and 3.318 respectively. *WJG* is a weekly journal published jointly by The *WJG* Press and Elsevier Inc. The publication date is on 7th, 14th, 21st, and 28th every month. The *WJG* is supported by The National Natural Science Foundation of China, No. 30224801 and No.30424812, which was founded with a name of *China National Journal of New Gastroenterology* on October 1,1995, and renamed as *WJG* on January 25, 1998.

PUBLISHED JOINTLY BY
The WJG Press and Elsevier Inc

PRINTING GROUP
Printed in Beijing on acid-free paper by Beijing Kexin Printing House

 Print ISSN 1007-9327 CN 14-1219/R.

SPECIAL STATEMENT
All articles published in this journal represent the viewpoints of the authors except where indicated otherwise.

EDITORIAL OFFICE
Editor: *World Journal of Gastroenterology*,
The WJG Press, Apartment 1066 Yishou Garden, 58 North Langxinzhuang Road, PO Box 2345, Beijing 100023, China
Telephone: +86-(0)10-85381901-1023
Fax:+86-10-85381893
E-mail: wjg@wjgnet.com
http://www.wjgnet.com

Public Relationship Manager
Shi-Yu Guo
The WJG Press, Apartment 1066 Yishou Garden, 58 North Langxinzhuang Road, PO Box 2345, Beijing 100023, China
Telephone: +86-(0)10-85381901-1023
Fax: +86-10-8538 1893
E-mail: s.y.guo@wjgnet.com
http://www.wjgnet.com

SUBSCRIPTION INFORMATION
Foreign
Elsevier (Singapore) Pte Ltd, 3 Killiney Road #08-01, Winsland House I, Singapore 239519
Telephone: +65-6349 0200
Fax: +65-6733 1817
E-mail: r.garcia@elsevier.com
http://asia.elsevierhealth.com
Institutional Rates Print-2005 rates: USD1 500.00
Personal Rates Print-2005 rates: USD700.00

Domestic
Local Post Offices Code No. BM 82-261

Author Reprints and Commercial Reprints
The WJG Press, Apartment 1066 Yishou Garden, 58 North Langxinzhuang Road, PO Box 2345, Beijing 100023, China
Telephone: +86-(0)10-85381901-1023
Fax:+86-10-85381893
E-mail: wjg@wjgnet.com
http://www.wjgnet.com

ADVERTISING
Rosalia Da Carcia
Elsevier Science
Journals Marketing & Society Relations Health Science Asia
3 Killiney Road #08-01, Winsland House 1 Singapore 239519
Telephone: +65-6349 0200
Fax +65- 6733 1817
E-mail: r.garcia@elsevier.com
http://asia.elsevierhealth.com

INSTRUCTIONS TO AUTHORS
Full instructions are available online at http://www.wjgnet.com/wjg/help/instructions.jsp If you do not have web access please contact the editorial office.

World Journal of Gastroenterology®

Editorial Board

2004-2006

Published by The WJG Press and Elsevier Inc., PO Box 2345, Beijing 100023, China
Fax: +86-(0)10-85381893 E-mail: wjg@wjgnet.com http://www.wjgnet.com

Bulgaria
Zahariy Alexandrov Krastev, *Sofia*

Canada
Wang-Xue Chen, *Ottawa*
Richard N Fedorak, *Edmonton*
Hugh James Freeman, *Vancouver*
Samuel S Lee, *Calgary*
Philip Martin Sherman, *Toronto*
Alan BR Thomson, *Edmonton*
Eric M Yoshida, *Vancouver*

China
Francis KL Chan, *Hong Kong*
Xiao-Ping Chen, *Wuhan*
Jun Cheng, *Beijing*
Chi-Hin Cho, *Hong Kong*
Zong-Jie Cui, *Beijing*
Da-Jun Deng, *Beijing*
Er-Dan Dong, *Beijing*
Sheung-Tat Fan, *Hong Kong*
Xue-Gong Fan, *Changsha*
Jin Gu, *Beijing*
De-Wu Han, *Taiyuan*
Shao-Heng He, *Shantou*
Fu-Lian Hu, *Beijing*
Wayne HC Hu, *Hong Kong*
Ching Lung Lai, *Hong Kong*
Kam Chuen Lai, *Hong Kong*
Wai-Keung Leung, *Hong Kong*
Zhi-Hua Liu, *Beijing*
Ai- Ping Lu, *Beijing*
Jing-Yun Ma, *Beijing*
Lun-Xiu Qin, *Shanghai*
Yu-Gang Song, *Guangzhou*
Peng Shang, *Xi'an*
Qin Su, *Beijing*
Yuan Wang, *Shanghai*
Benjamin Wong, *Hong Kong*
Wai-Man Wong, *Hong Kong*
Hong Xiao, *Shanghai*
Dong-Liang Yang, *Wuhan*
Xue-Biao Yao, *Hefei*
Yuan Yuan, *Shenyang*
Man-Fung Yuen, *Hong Kong*
Jian-Zhong Zhang, *Beijing*
Zhi-Rong Zhang, *Chengdu*
Xiao-Hang Zhao, *Beijing*
Shu Zheng, *Hangzhou*

Costa Rica
Edgar M Izquierdo, *San José*

Croatia
Marko Duvnjak, *Zagreb*

Denmark
Flemming Burcharth, *Herlev*
Peter Bytzer, *Copenhagen*
Hans Gregersen, *Aalborg*
Jens H Henriksen, *Hvidovre*
Fin Stolze Larsen, *Copenhagen*
Søren Møller, *Hvidovre*

Egypt
Abdel-Rahman El-Zayadi, *Giza*

Finland
Pentti Sipponen, *Espoo*

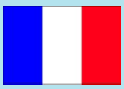

France
Charles Paul Balabaud, *Bordeaux*
Jacques Belghiti, *Clichy*
Pierre Brissot, *Rennes*
Franck Carbonnel, *Besancon*
Bruno Clément, *Rennes*
Jacques Cosnes, *Paris*
Francoise Degos, *Clichy*
Francoise Lunel Fabian, *Angers*
Gérard Feldmann, *Paris*
Jean Fioramonti, *Toulouse*
Rene Lambert, *Lyon*
Didier Lebrec, *Clichy*
Francis Mégraud, *Bordeaux*
Richard Moreau, *Clichy*
Jose Sahel, *Marseille*
Jean-Yves Scoazec, *Lyon*
Jean-Pierre Henri Zarski, *Grenoble*

Germany
HD Allescher, *Garmisch-Partenkirchen*
Rudolf Arnold, *Marburg*
Hubert Blum, *Freiburg*
Peter Born, *Muchen*
Heinz J Buhr, *Berlin*
Haussinger Dieter, *Düsseldorf*
Dietrich CF, *Bad Mergentheim*
Wolfram W Domschke, *Muenster*
Ulrich Robert Fölsch, *Kiel*
Peter R Galle, *Mainz*
Burkhard Göke, *Munich*
Axel M Gressner, *Aachen*
Eckhart Georg Hahn, *Erlangen*
Werner Hohenberger, *Erlangen*
RG Jakobs, *Ludwigshafen*
Joachim Labenz, *Siegen*
Ansgar W Lohse, *Hamburg*
Peter Malfertheiner, *Magdeburg*
Andrea Dinah May, *Wiesbaden*
Stephan Miehlke, *Dresden*
Gustav Paumgartner, *Munich*
Ulrich Ks Peitz, *Magdeburg*
Giuliano Ramadori, *Göttingen*
Tilman Sauerbruch, *Bonn*
Hans Seifert, *Oldenburg*
J Ruediger Siewert, *Munich*
Manfred V Singer, *Mannheim*
Jurgen M Stein, *Frankfurt*
Manfred Stolte, *Bayreuth*
Wolfgang R Stremmel, *Heidelberg*
Hans Ludger Tillmann, *Leipzig*
Siegfried Wagner, *Deggendorf*
Bertram Wiedenmann, *Berlin*

Greece
Arvanitakis C, *Thessaloniki*
Elias A Kouroumalis, *Heraklion*

Hungary
Simon A László, *Szekszárd*
János Papp, *Budapest*

Iceland
Hallgrimur Gudjonsson, *Reykjavik*

India
Sujit Kumar Bhattacharya, *Kolkata*
Chawla YK, *Chandigarh*
Radha Dhiman K, *Chandigarh*
Sri Prakash Misra, *Allahabad*
Kartar Singh, *Lucknow*

Iran
Reza Malekzadeh, *Tehran*

Israel
Abraham Rami Eliakim, *Haifa*
Yaron Niv, *Pardesia*

Italy
Giovanni Addolorato, *Roma*
Alfredo Alberti, *Padova*
Annese V, *San Giovanni Rotondo*
Giovanni Barbara, *Bologna*
Gabrio Bassotti, *Perugia*
Franco Bazzoli, *Bologna*
Adolfo Francesco Attili, *Roma*
Antomio Benedetti, *Ancona*
Giovanni Cammarota, *Roma*
Antonino Cavallari, *Bologna*
Dario Conte, *Milano*
Gino Roberto Corazza, *Pavia*
Guido Costamagua, *Roma*
Antonio Craxi, *Palermo*
Fabio Farinati, *Padua*
Giovanni Gasbarrini, *Roma*
Paolo Gentilini, *Florence*
Edoardo G Giannini, *Genoa*

Paolo Gionchetti, *Bologna*
Roberto De Giorgio, Bologna
Mario Guslandi, *Milano*
Giovanni Maconi, *Milan*
Giulio Marchesini, *Bologna*
Giuseppe Montalto, *Palermo*
Luisi Pagliaro, *Palermo*
Fabrizio R Parente, *Milan*
Perri F, *San Giovanni Rotondo*
Raffaele Pezzilli, *Bologna*
Pilotto A, *San Giovanni Rotondo*
Massimo Pinzani, *Firenze*
Gabriele Bianchi Porro, *Milano*
Piero Portincasa, *Bari*
Giacomo Laffi, *Firenze*
Enrico Roda, *Bologna*
Massimo Rugge, *Padova*
Vincenzo Savarino, *Genova*
Vincenzo Stanghellini, *Bologna*
Calogero Surrenti, *Florence*
Roberto Testa, *Genoa*
Dino Vaira, *Bologna*

Japan

Kyoichi Adachi, *Izumo*
Takashi Aikou, *Kagoshima*
Taiji Akamatsu, *Matsumoto*
Takafumi Ando, *Nagoya*
Akira Andoh, *Otsu*
Taku Aoki, *Tokyo*
Masahiro Arai, *Tokyo*
Tetsuo Arakawa, *Osaka*
Yasuji Arase, *Tokyo*
Masahiro Asaka, *Sapporo*
Hitoshi Asakura, *Tokyo*
Yutaka Atomi, *Tokyo*
Takeshi Azuma, *Fukui*
Nobuyuki Enomoto, *Yamanashi*
Kazuma Fujimoto, *Saga*
Toshio Fujioka, *Oita*
Yoshihide Fujiyama, *Otsu*
Hiroyuki Hanai, *Hamamatsu*
Kazuhiro Hanazaki, *Nagano*
Naohiko Harada, *Fukuoka*
Makoto Hashizume, *Fukuoka,*
Tetsuo Hayakawa, *Nagoya*
Kazuhide Higuchi, *Osaka*
Ichiro Hirata, *Osaka*
Keiji Hirata, *Kitakyushu*
Takafumi Ichida, *Shizuoka*
Kenji Ikeda, *Tokyo*
Kohzoh Imai, *Sapporo*
Fumio Imazeki, *Chiba*
Masayasu Inoue, *Osaka*
Hiromi Ishibashi, *Nagasaki*
Shunji Ishihara, *Izumo*
Toru Ishikawa, *Niigata*
Kei Ito, *Sendai*
Masayoshi Ito, *Tokyo*
Hiroaki Itoh, *Akita*
Hiroshi Kaneko, *Aichi-Gun*
Shuichi Kaneko, *Kanazawa*
Takashi Kanematsu, *Nagasaki*
Junji Kato, *Sapporo*
Mototsugu Kato, *Sapporo*
Shinzo Kato, *Tokyo*
Sunao Kawano, *Osaka*
Yoshikazu Kinoshita, *Izumo*
Masaki Kitajima, *Tokyo*
Tsuneo Kitamura, *Chiba*
Seigo Kitano, *Oita*
Hironori Koga, *Kurume*
Satoshi Kondo, *Sapporo*
Shoji Kubo, *Osaka*
Shigeki Kuriyama, *Kagawa*
Masato Kusunoki, *Mie*
Takashi Maeda, *Fukuoka*
Shin Maeda, *Tokyo*
Osamu Matsui, *Kanazawa*
Yasushi Matsuzaki, *Tsukuba*
Hiroto Miwa, *Hyogo*
Masashi Mizokami, *Nagoya*
Motowo Mizuno, *Hiroshima*
Morito Monden, *Suita*
Hisataka S Moriwaki, *Gifu*
Yoshiharu Motoo, *Kanazawa*
Akihiro Munakata, *Hirosaki*
Kazunari Murakami, *Oita*
Kunihiko Murase, *Tusima*
Masato Nagino, *Nagoya*
Yujl Naito, *Kyoto*
Hisato Nakajima, *Tokyo*
Hiroki Nakamura, *Yamaguchi*
Shotaro Nakamura, *Fukuoka*
Akimasa Nakao, *Nagoya*
Mikio Nishioka, *Niihama*
Susumu Ohmada, *Maebashi*
Masayuki Ohta, *Oita*
Tetsuo Ohta, *Kanazawa*
Susumu Okabe, *Kyoto*
Katsuhisa Omagari, *Nagasaki*
Saburo Onishi, *Nankoku*
Morikazu Onji, *Ehime*
Hiromitsu Saisho, *Chiba*
Hidetsugu Saito, *Tokyo*
Takafumi Saito, *Yamagata*
Isao Sakaida, *Yamaguchi*
Michiie Sakamoto, *Tokyo*
Iwao Sasaki, *Sendai*
Motoko Sasaki, *Kanazawa*
Chifumi Sato, *Tokyo*
Shuichi Seki, *Osaka*
Hiroshi Shimada, *Yokohama*
Mitsuo Shimada, *Tokushima*
Hiroaki Shimizu, *Chiba*
Tooru Shimosegawa, *Sendai*
Tadashi Shimoyama, *Hirosaki*
Ken Shirabe, *Iizuka City*
Yoshio Shirai, *Niigata*
Katsuya Shiraki, *Mie*
Yasushi Shiratori, *Okayama*
Yasuhiko Sugawara, *Tokyo*
Toshiro Sugiyama, *Toyama*
Kazuyuki Suzuki, *Morioka*
Hidekazu Suzuki, *Tokyo*
Tadatoshi Takayama, *Tokyo*
Tadashi Takeda, *Osaka*
Koji Takeuchi, *Kyoto*
Kiichi Tamada, *Tochigi*
Akira Tanaka, *Kyoto*
Eiji Tanaka, *Matsumoto*
Noriaki Tanaka, *Okayama*
Shinji Tanaka, *Hiroshima*
Kyuichi Tanikawa, *Kurume*
Tadashi Terada, *Shizuoka*
Akira Terano, *Shimotsugagun*
Kazunari Tominaga, *Osaka*
Hidenori Toyoda, *Ogaki*
Akihito Tsubota, *Chiba*
Shingo Tsuji, *Osaka*
Takato Ueno, *Kurume*
Shinichi Wada, *Tochigi*
Hiroyuki Watanabe, *Kanazawa*
Sumio Watanabe, *Akita*
Toshio Watanabe, *Osaka*
Yuji Watanabe, *Ehime*
Chun-Yang Wen, *Nagasaki*
Koji Yamaguchi, *Fukuoka*
Takayuki Yamamoto, *Yokkaichi*
Takashi Yao, *Fukuoka*
Hiroshi Yoshida, *Tokyo*
Masashi Yoshida, *Tokyo*
Norimasa Yoshida, *Kyoto*
Kentaro Yoshika, *Toyoake*
Masahide Yoshikawa, *Kashihara*

Lithuania

Sasa Markovic, *Japljeva*

Macedonia

Vladimir Cirko Serafimoski, *Skopje*

Malaysia

Andrew Seng Boon Chua, *Ipoh*
Jayaram Menon, *Sabah*
Khean-Lee Goh, *Kuala Lumpur*

Monaco

Patrick Rampal, *Monaco*

Netherlands

Louis MA Akkermans, *Utrecht*
Karel Van Erpecum, *Utrecht*
Albert K Groen, *Amsterdam*
Dirk Joan Gouma, *Amsterdam*
Jan BMJ Jansen, *Nijmegen*
Evan Anthony Jones, *Abcoude*
Ernst Johan Kuipers, *Rotterdam*
Chris JJ Mulder, *Amsterdam*
Michael Müller, *Wageningen*

Pena AS, *Amsterdam*
Andreas Smout, *Utrecht*
RW Stockbrugger, *Maastricht*
GP Vanberge-Henegouwen, *Utrecht*

New Zealand
Ian David Wallace, *Auckland*

Norway
Trond Berg, *Oslo*
Helge Lyder Waldum, *Trondheim*

Pakistan
Muhammad S Khokhar, *Lahore*

Philippines
Eulenia Rasco Nolasco, *Manila*

Poland
Tomasz Brzozowski, *Cracow*
Andrzej Nowak, *Katowice*

Portugal
Miguel Carneiro De Moura, *Lisbon*

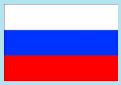

Russia
Vladimir T Ivashkin, *Moscow*
Leonid Lazebnik, *Moscow*
Vasiliy I Reshetnyak, *Moscow*

Singapore
Bow Ho, *Kent Ridge*
Francis Seow-Choen, *Singapore*

Slovakia
Anton Vavrecka, *Bratislava*

South Africa
Michael C Kew, *Parktown*

South Korea
Jin-Hong Kim, *Suwon*
Myung-Hwan Kim, *Seoul*
Yun-Soo Kim, *Seoul*
Yung-Il Min, *Seoul*
Jae-Gahb Park, *Seoul*
Dong Wan Seo, *Seoul*

Spain
Abraldes JG, *Barcelona*
Fernando Azpiroz, *Barcelona*
Ramon Bataller, *Barcelona*
Josep M Bordas, *Barcelona*
Maria Buti, *Barcelon*
Xavier Calvet, *Sabadell*
Antoni Castells, *Barcelona*
Manuel Daz-Rubio, *Madrid*
Juan C Garcia-Pagán, *Barcelona*
Genover JB, *Barcelona*
Javier P Gisbert, *Madrid*
Jaime Guardia, *Barcelona*
Angel Lanas, *Zaragoza*
Ricardo Moreno-Otero, *Madrid*
Julian Panes, *Barcelona*
Miguel Perez-Mateo, *Alicante*
Josep M Pique, *Barcelona*
Jesus Prieto, *Pamplona*
Luis Rodrigo, *Oviedo*

Sri Lanka
Janaka De Silva, *Ragama*

Swaziland
Gerd Kullak-Ublick, *Zurich*

Sweden
Lars Christer Olbe, *Molndal*
Curt Einarsson, *Huddinge*
Lars R Lundell, *Stockholm*
Xiao-Feng Sun, *Linkoping*

Switzerland
Christoph Beglinger, *Basel*
Michael W Fried, *Zurich*
Bruno Stieger, *Zurich*
Arthur Zimmermann, *Berne*

Turkey
Yusuf Bayraktar, *Ankara*
Figen Gurakan, *Ankara*
Cihan Yurdaydin, *Ankara*

United Kingdom
Axon ATR, *Leeds*
Paul Jonathan Ciclitira, *London*
Amar Paul Dhillon, *London*
Stuarts Forbes
Subrata Ghosh, *London*
Brian T Johnston, *Belfast*
David EJ Jones, *Newcastle*
Michael A Kamm, *Harrow*
Hong-Xiang Liu, Cambridge
Giorgina Mieli-Vergani, *London*
Nikolai V Naoumov, *London*
John P Neoptolemos, *Liverpool*
James Neuberger, *Birmingham*
Colm Antoine O'Morain, *Dublin*
Simon D Taylor-Robinson, *London*
Frank Ivor Tovey, *Basingstoke*
Min Zhao, *Foresterhill*

United States
Firas H Ac-Kawas, *Washington*
Gianfranco D Alpini, *Temple*
Paul Angulo, *Rochester*
Jamie S Barkin, *Miami Beach*
Todd Baron, *Rochester*
Kim Elaine Barrett, *San Diego*
Jennifer D Black, *Buffalo*
Xu Cao, *Birmingham*
David L Carr-Locke, *Boston*
Marc F Catalano, *Milwaukee*
Xian-Ming Chen, *Rochester*
James M Church, *Cleveland*
Vincent Coghlan, *Beaverton*
James R Connor, *Hershey*
Pelayo Correa, *New Orleans*
John Cuppoletti, *Cincinnati*
Peter V Danenberg, *Los Angeles*
Kiron Moy Das, *New Brunswick*
Hala El-Zimaity, *Houston*
Ronnie Fass, *Tucson*
Emma E Furth, *Pennsylvania*
John Geibel, *New Haven*
Graham DY, *Houston*
Joel S Greenberger, *Pittsburgh*
Anna S Gukovskaya, *Los Angeles*
Gavin Harewood, *Rochester*
Atif Iqbal, *Omaha*
Hajime Isomoto, *Rochester*
Dennis M Jensen, *Los Angeles*
Leonard R Johnson, *Memphis*
Peter James Kahrilas, *Chicago*
Anthony Nicholas Kalloo, *Baltimore*
Neil Kaplowitz, *Los Angeles*
Emmet B Keeffe, *Palo Alto*
Joseph B Kirsner, *Chicago*
Burton I Korelitz, *New York*
Robert J Korst, *New York*
Richard A Kozarek, *Seattle*
Shiu-Ming Kuo, *Buffalo*
Frederick H Leibach, *Augusta*
Andreas Leodolter, *La Jolla*
Ming Li, *New Orleans*
Lenard M Lichtenberger, *Houston*
Gary R Lichtenstein, *Philadelphia*
Josep M Llovet, *New York*
Martin Lipkin, *New York*

Manuscript reviewers of *World Journal of Gastroenterology*

PO Box 2345, Beijing 100023, China
www.wjgnet.com
wjg@wjgnet.com

ELSEVIER

World J Gastroenterol 2005;11(14):2051-2054
World Journal of Gastroenterology ISSN 1007-9327

• *REVIEW* •

Portal vein embolization before major hepatectomy

Hai Liu, Yong Fu

Hai Liu, Yong Fu, Department of Surgical Oncology, Hainan Provincial People's Hospital, Haikou 570311, Hainan Province, China
Correspondence to: Dr. Hai Liu, MD, Department of Surgical Oncology, Hainan Provincial People's Hospital, Haikou 570311, Hainan Province, China. dr_liuhai@hotmail.com
Telephone: +86-898-68642223 Fax: +86-898-68653685
Received: 2004-03-23 Accepted: 2004-05-23

Abstract

To discuss the rationale, techniques and the unsolved issues regarding preoperative portal vein embolization (PVE) before major hepatectomy. After a systematic search of Pubmed, we reviewed and retrieved literature related to PVE. Preoperative PVE is an approach that is gaining increasing acceptance in the preoperative treatment of selected patients prior to major hepatic resection. Induction of selective hypertrophy of the nondiseased portion of the liver with PVE in patients with either primary or secondary hepatobiliary, malignancy with small estimated future liver remnants (FLR) may result in fewer complications and shorter hospital stays following resection. Additionally, PVE performed in patients initially considered unsuitable for resection due to lack of sufficient remaining normal parenchyma may add to the pool of candidates for surgical treatment. The results suggest that PVE is recomm-endable in treating the cirrhotic patients before major liver resection.

Key words: Portal vein embolization; Hepatectomy

Liu H, Fu Y. Portal vein embolization before major hepatectomy. *World J Gastroenterol* 2005; 11(14): 2051-2054
http://www.wjgnet.com/1007-9327/11/2051.asp

INTRODUCTION

Complete resection of hepatic tumors remains the first choice for curative treatment of primary and secondary liver malignancies, giving the patient the only chance of long-term survival. In up to 45% of primary and secondary liver tumors, extended liver resection is necessary to achieve clear resection margins[1]. The reason for unresectability is that often the remnant liver is of insufficient volume to support postoperative liver function, which itself is still the principal cause of postoperative death after major hepatectomy. The mortality rate after major liver resection ranges from 3.2% to 7% in patients with noninjured liver parenchyma and increases up to 32% in patients with cirrhosis[1-3]. It has been demonstrated that liver failure is directly related to the size of remnant functional liver volume, and various procedures have been developed to induce liver regeneration. Preoperative occlusion of the portal vein branches feeding the hepatic segments to be resected reduced the risk of postoperative liver failure after major liver resection and increased the number of resectable patients[2-4].

Pathophysiological characteristics of liver after PVE

Portal vein ligation (PVL) not only led to atrophy of the ipsilateral lobe and hypertrophy of contralateral lobe in rats[5], but also led to ipsilateral lobe atrophy and contralateral lobe hypertrophy in humans[1,6,7]. These basic observations provide the foundation for the study of portal vein embolization (PVE) for clinical purpose. The mechanisms underlying the atrophy-hypertrophy complex are poorly understood. The liver cells have the remarkable ability to dedifferentiate and expand clonally. Stimuli leading to hypertrophy include a combination of hepatic and extrahepatic factors. The physiological trigger for hypertrophy is unknown. Some cytokine, such as hepatocyte growth factor (HGF), transforming growth factor, and interleukin-6 may be involved[8]. Insulin and glucagon are both two natural nutrient factors for liver cells and the increase of insulin and glucagon may contribute to the hypertrophy of future liver remnant (FLR) after PVE. Immediately after embolization, portal vein blood flow to the unembolized liver measured by transcutaneous Doppler ultrasonography increased significantly, and the resulting hypertrophy rate correlated with blood flow rate[9-11]. Regeneration rate of non-cirrhotic liver was 12-21 cm^3 per d 2 wk after embolization, about 11 cm^3 per d at 4 wk and 6 cm^3 per d at 32 d. For comparison, the rate was slower at 2 wk in cirrhotic liver, only 9 cm^3 per d[2,12,13]. So, liver resection is always performed 4 wk following PVE. Several reasons could explain the failure of hypertrophy after technically successful PVE, among them are the activity of the underlying chronic liver disease, the presence of diabetes[14], the possible vascular recannulization of the embolized portal vein branches and the presence of major portal hypertension with portosystemic shunts[15,16].

Indications and contraindications for PVE

Indications At present, four factors are important to decide whether and when to perform PVE. First, the ratio of FLR to total estimated liver volume (TELV) should be calculated. Second, cases need to be categorized into those with and those without underlying liver diseases because these factors will determine how much FLR is needed to reduce postoperative morbidity and mortality. The minimum absolute liver volume necessary to support post-resection

hepatic function has not been clearly defined. However, an FLR/TELV ratio of at least 25% is recommended in patients with normal livers, with a ratio of at least 40% in patients in whom the liver is considered stable (e.g., from chronic liver disease or high-dose chemotherapy)[17]. When FLR/TELV ratios are below these levels, PVE may be performed in an attempt to increase FLR volume. Third, the presence of systemic disease such as diabetes mellitus may limit hepatic hypertrophy[14]. Insulin is a comitogenic factor with HGF that often leads to fast rates of regeneration. Fourth, planning for the type and extent of the anticipated surgical procedure (e.g., right hepatectomy and pancreaticoduodenectomy) is important because more functional hepatic reserve may be required to reduce postoperative morbidity. Recent clinical studies show that PVE with two-stage hepatectomy is practicable for patients with multiple metastases in both right and left liver[4]. From above, it comes that the PVE should be considered in the following circumstances: (1) major hepatectomy for patients with chronic liver diseases; (2) extended hemihepatectomy for patients with normal liver; (3) two-stage strategy for patients with multiple bilobar metastases. The FLR ratio is calculated with data obtained by three-dimensional volum-etric computed tomography after PVE with the following formula: FLR/TELV = FLR/(total liver volume-tumor volume)×100%.

Contraindications

Patients with metastatic diseases such as distant metastases or periportal lymphadenopathy cannot undergo resection and therefore are not candidates for PVE. Patients with bilobar multiple metastases were not considered as the candidates for PVE before[18], but recent studies confirm that some of these patients can benefit from PVE in combination with two-stage hepatectomy[4]. Other relative contraindications for PVE include an uncorrectable coagulopathy, tumor invasion of the portal vein, tumor precluding safe transhepatic access, biliary dilatation (in cases of biliary tree obstruction, drainage is recommended), portal hypertension, and renal failure that requires dialysis. PVE in cases of tumor invasion of the portal vein may not be warranted because there may be no significant benefit from the procedure.

Issues regarding clinical practice

Preparation for PVE Prior to PVE, a complete patient history is taken and a thorough physical examination performed. Laboratory studies including complete blood cell count, prothrombin time, liver function tests, and blood urea nitrogen/creatinine levels are essential prior to PVE. If patient has an elevated total bilirubin (>3.0 mg/dL), percutaneous or endoscopic biliary drainage is beneficial. CT scanning is a fundamental radiological investigation prior to PVE, for it documents the extent of disease (i.e., extrahepatic disease or involvement of the planned FLR), FLR size, and portal venous anatomy.

PVE techniques

Percutaneous transhepatic preoperative PVE is the most used routine for PVE nowadays[2-4]. On the day of the procedure, prophylactic broad-spectrum antibiotics (e.g., cefazolin, ceftriaxone sodium) are administered intrave-nously for prevention of biliary sepsis. Although general anesthetic may be requested, the procedure is most often performed with local anesthetic (1% lidocaine hydrochloride) and intravenously administered sedatives that allow the patient to remain conscious. Ultrasonography of the liver is performed to determine the best access route into the portal venous system. Under sterile conditions, access into the portal venous system is gained under ultrasonic or fluoro-scopic guidance or both. The ipsilateral approach (access through the portion of the liver to be resected) is recom-mended so as not to injure the FLR. A portal venous access through tumor should be avoided, for it may exacerbate tumor spread or cause subcapsular hematoma. If the tumor burden is high, the contralateral approach (i.e., access through the FLR) may be used. However, this option must be wei-ghed against the possibility of causing injury to the FLR or the portal veins that supply it. In addition, transileocolical venous approach is an alternative performed by a surgeon at open laparotomy with direct cannulation of ileocolic vein[1]. It is particularly practicable for the patients of colorectal cancer with liver metastasis, for the PVE can be done at the surgery of primary tumor.

Choice of embolic agents

Various substances used have yielded different rates or degrees of hypertrophy of unembolized segments. Gelfoam, coil, cyanoacrylate, polyvinyl alcohol, polydocanal, absolute alcohol, fibrin, and lipiodol are used[3,19-22]. Both gelfoam and coil are always used along with other substances for the embolization of large branches of portal vein[19,20]. Gelatin sponge is a generally used embolic material, but frequent recanalization is found, especially 2 wk after embolization if used alone. Fibrin glue has also been used as an embolic agent, but PVE with fibrin glue is incomplete and it allows recanalization in short time if used alone, whereas fibrin mixed with lipiodol can achieve very good embolic effect[23]. But it is very expensive compared to other embolic agents. Cyanoacrylate has a strong embolic effect and has been used for obliteration of gastric coronary vein and esophageal varices. It ensures PVE, which lasts for 4 wk, but massive peribiliary fibrosis and casting of portal vein may increase operative difficulty technically[21]. Polyvinyl alcohol is safe, it causes little periportal reaction, and generates durable portal vein occlusion while used in combination with coils[19]. PVE with absolute alcohol may be particularly useful for hepatocellular carcinoma, although obvious alteration was found in measured liver function following the embolization. Lipiodol is a common embolic agent used for hepatic artery embolization, and it results in very effective embolization when used in combination with cyanoacrylate[3,20]. Polidocanol induces thrombosis and necrotizing inflammation, so it is used in sclerotherapy for esophageal varices. Comparison of embolic effect between different agents shows that the combination of polidocanol with gelatin sponge achieves the best effects, followed by cyanocrylate, gelatin sponge, and fibrin[20]. The effectiveness and safety of a new embolic agent, Embol-78, have been reported, the mean volume of the FLR increased to 38% in the hepatocellular carcinoma group, and by 46% in the nonhepatocellular carcinoma group[22]. Compared with other embolic agents, the authors think that Embol-78 has several advantages. The partially hydrolyzed

polymer Embol-78 was soluble in a less concentrated ethanol solution and miscible in larger quantities of water-soluble contrast media. The improved radiopacity (190 mg of iodine/mL) was thus adequate to permit monitoring of the embolization process with conventional fluoroscopy instead of digital subtraction angiography. Concern about the systemic toxicity of ethanol was also reduced because of the hydrolysis reaction[22].

Efficiency of PVE

Surgical resection has been recognized as the most effective treatment for patients with colorectal liver metastases. Indeed, the mortality rate after hepatectomy has been reduced to less than 5%, and satisfactory 5-year survival rates after hepatectomy have also been reported up to 30%[21]. However, hepatectomy can be applied only for approximately 10-20% of patients with colorectal liver metastases. Among the factors that are contraindications for hepatectomy, insufficient functional volume of remnant liver after hepatic resection can cause postoperative hepatic failure and it is still an obstacle to a major hepatic resection. As one of the solutions to this dilemma and in order to increase the indications for a major hepatectomy, preoperative PVE has been proposed to induce compensatory hypertrophy of the contralateral FLR in patients with metastatic diseases. Two to eight weeks after PVE, FLR may increase by 20-46% with various embolic agents for patients with or without liver parenchyma disease, and 70-100% patients can undergo hemihepatectomy or extended hemihepatectomy after PVE[3,4,20,22]. PVE not only increases the pool of candidates for hepatectomy, but also decreases significantly the incidence of postoperative complications as well as the intensive care unit stay and total hospital stay after right hepatectomy[2,3]. Therefore, Farges adopted routine performance of PVE before major hepatectomy in patients with chronic liver disease[3]. It was only the patients with tumors confined to hemiliver that were considered as candidates for PVE before. However, the recent clinical studies show that PVE with two-stage hepatectomy is practicable for patients with multiple bilobar metastases[4]. In two-stage strategy, the tumors in the FLR are removed at first operation, then followed by PVE and second hemihepatectomy or extended hemihepatectomy. But this strategy should be limited to patients with no more than three nodules in FLR, which are less than 2.5 cm in diameter each. With two-stage strategy, 70% patients can undergo second hemihepatectomy or extended hemihepatectomy after PVE, and the 3-year survival rate was 53%, which was comparable to that of one-stage group or non-PVE group[4]. Broering *et al*[1], found that PVE and PVL were both feasible and safe methods of increasing the remnant functional liver volume and achieving resectability of extended liver tumors without increasing mortality and morbidity. Ligation or PVE with direct cannulation of ileocolic vein of the tumor bearing portal vein branch is reasonable for the patients with liver metastasis from colorectal cancer, and it can be done at the same surgery of the resection of primary tumor. However, Jaeck *et al*[4], argued against this attitude, holding that (1) development of portal cavernoma with collateral circulation to the ligated lobe reduces the efficiency of portal branch ligation; and (2) development of severe adhesions owing to the hilar diss-ection needed for the ligation of the right portal branch consequently makes it more difficult to perform second hepatectomy.

Complications of PVE

PVE is considerably less toxic than arterial embolization, so side effects are minimal. Signs and symptoms of post-embolization syndrome, such as nausea and vomiting, are rare. Fever and pain are infrequent. Changes in liver function following PVE are usually minor and transient (50% of patients have no appreciable change). When transaminase levels rise, they usually peak at a level less than three times baseline 1-3 d after embolization and return to baseline in 7-10 d, regardless of the embolic materials used. Slight changes in total bilirubin value and white blood cell count may be seen. Synthetic function (e.g., prothrombin time) was almost never affected. But mesenterioportal venous thrombosis occurred in one patient[4]. This patient developed acute gastrointestinal bleeding and encephalopathy, which were conservatively treated, and a later ischemic duodenojejunal stenosis with subsequent mechanical occlusion occurred. It is essential to avoid the reflux of embolizing material into the portal venous branches of the remnant liver. The balloon catheter is designed for this purpose[3,20].

Important unsolved issues regarding PVE

The purpose of PVE is to increase the hepatic functional reserve of FLR as well as its volume[24]. However, there are three major problems facing PVE: (1) PVE stimulates the growth of hepatic tumor[2,25,26]; (2) PVE may fail to increase the volume of FLR in some patients, especially those with fibrotic or cirrhotic liver[3]; (3) Is PVE safe in patients with high-grade varices? The mechanisms of fast tumor growth after PVE are still poorly understood. Kokudo *et al*[26], assessed the proliferative activity of intrahepatic metastases in the embolized liver after PVE in 18 patients with colorectal metastases and found a significantly increased tumor Ki-67 labeling index in the metastases group with PVE compared to hepatic metastases without PVE. It was postulated that the tumor growth after PVE might be controlled by three factors: Malignant potential of the tumors; changes in cytokines or growth factors induced by PVE; and changes in blood supply after PVE. Animal models of portal vein branch ligation demonstrated that HGF-mRNA markedly increased in the non-ligated growing lobe, but was only slightly elevated in the ligated shrinking lobe. Increased tissue levels of HGF might increase the level in plasma, thus stimulating the growth of hepatic tumors. Barbaro *et al*[25], recently noted a significant increase in hepatic tumor volume from colorectal carcinoma after PVE, while hepatic tumor volume from carcinoid tumor was unchanged. Another factor potentially stimulating tumor growth after PVE is increased hepatic arterial blood flow in embolized liver after PVE, for supply of intrahepatic metastases depends solely on arterial blood supply[23]. But these cannot explain why PVE increased hepatic tumor volume from colorectal carcinoma, while did not stimulate the growth of carcinoid tumor. Butyrate is known to stimulate proliferation of normal crypt cells, whereas it induces apoptosis and has antiangiogenic effects on colon cancer cells[27]. Therefore,

the lack of butyrate from portal vein blood may contribute to the increase in hepatic metastasis volume of colorectal carcinoma and, meanwhile, the enrichment of butyrate in FLR may help prevent tumor recurrence in patients treated with two-stage strategy. Hepatic arterial blood flow in embolized liver is increased after PVE and the supply of intrahepatic metastases depends solely on arterial blood supply, so PVE combined with transcatheter arterial embolization (TAE) may help prevent tumor growth and at the same time accelerate the hypertrophy of FLR. Pioneering reports from Inaba *et al*, and Sugawara *et al*, have confirmed that PVE in combination with TAE is safe, effective, and hence recommendable. Portal vein pressure rises about 4 cm H_2O after PVE[22], however, there is no report of PVE-related acute variceal hemorrhage. Liver transplantation is an excellent alternative to liver resection in treating the cirrhotic patient with small oligonodular HCC, but for large HCCs, partial liver resection remains the best therapeutic option for cure because neither liver transplantation nor percutaneous treatments are indicated. So PVE has become an important tool to induce hypertrophy of the FLR before major liver resection in cirrhotic patients.

REFERENCES

1 **Broering DC,** Hillert C, Krupski G, Fischer L, Mueller L, Achilles EG, Schulte am Esch J, Rogiers X. Portal vein embolization *vs* portal vein ligation for induction of hypertrophy of the future liver remnant. *J Gastrointest Surg* 2002; **6**: 905-913; discussion 913

2 **Hemming AW,** Reed AI, Howard RJ, Fujita S, Hochwald SN, Caridi JG, Hawkins IF, Vauthey JN. Preoperative portal vein embolization for extended hepatectomy. *Ann Surg* 2003; **237**: 686-691; discussion 691-693

3 **Farges O,** Belghiti J, Kianmanesh R, Regimbeau JM, Santoro R, Vilgrain V, Denys A, Sauvanet A. Portal vein embolization before right hepatectomy: prospective clinical trial. *Ann Surg* 2003; **237**: 208-217

4 **Jaeck D,** Bachellier P, Nakano H, Oussoultzoglou E, Weber JC, Wolf P, Greget M. One or two-stage hepatectomy combined with portal vein embolization for initially nonresectable colorectal liver metastases. *Am J Surg* 2003; **185**: 221-229

5 **Schweizer W,** Duda P, Tanner S, Balsiger D, Hoflin F, Blumgart LH, Zimmermann A. Experimental atrophy/hypertrophy complex (AHC) of the liver: portal vein, but not bile duct obstruction, is the main driving force for the development of AHC in the rat. *J Hepatol* 1995; **23**: 71-78

6 **Takayasu K,** Muramatsu Y, Shima Y, Moriyama N, Yamada T, Makuuchi M. Hepatic lobar atrophy following obstruction of the ipsilateral portal vein from hilar cholangiocarcinoma. *Radiology* 1986; **160**: 389-393

7 **Lee KC,** Kinoshita H, Hirohashi K, Kubo S, Iwasa R. Extension of surgical indications for hepatocellular carcinoma by portal vein embolization. *World J Surg* 1993; **17**: 109- 115

8 **Michalopoulos GK,** DeFrances MC. Liver regeneration. *Science* 1997; **276**: 60-66

9 **Goto Y,** Nagino M, Nimura Y. Doppler estimation of portal blood flow after percutaneous transhepatic portal vein embolization. *Ann Surg* 1998; **228**: 209-213

10 **Gerunda GE,** Bolognesi M, Neri D, Merenda R, Miotto D, Barbazza F, Zangrandi F, Bisello M, Valmasoni M, Gangemi A, Gagliesi A, Faccioli AM. Preoperative selective portal vein embolization (PSPVE) before major hepatic resection. Effectiveness of Doppler estimation of hepatic blood flow to predict the hypertrophy rate of non-embolized liver segments. *Hepatogastroenterology* 2002; **49**: 1405-1411

11 **Shimada R,** Imamura H, Nakayama A, Miyagawa S, Kawasaki S. Changes in blood flow and function of the liver after right portal vein embolization. *Arch Surg* 2002; **137**: 1384-1388

12 **Shimamura T,** Nakajima Y, Une Y, Namieno T, Ogasawara K, Yamashita K, Haneda T, Nakanishi K, Kimura J, Matsushita M, Sato N, Uchino J. Efficacy and safety of preoperative percutaneous transhepatic portal embolization with absolute ethanol: a clinical study. *Surgery* 1997; **121**: 135-141

13 **de Baere T,** Roche A, Vavasseur D, Therasse E, Indushekar S, Elias D, Bognel C. Portal vein embolization: utility for inducing left hepatic lobe hypertrophy before surgery. *Radiology* 1993; **188**: 73-77

14 **Shirabe K,** Shimada M, Gion T, Hasegawa H, Takenaka K, Utsunomiya T, Sugimachi K. Postoperative liver failure after major hepatic resection for hepatocellular carcinoma in the modern era with special reference to remnant liver volume. *J Am Coll Surg* 1999; **188**: 304-309

15 **Imamura H,** Shimada R, Kubota M, Matsuyama Y, Nakayama A, Miyagawa S, Makuuchi M, Kawasaki S. Preoperative portal vein embolization: an audit of 84 patients. *Hepatology* 1999; **29**: 1099-1105

16 **Tanaka H,** Hirohashi K, Kubo S, Ikebe T, Tsukamoto T, Hamba H, Shuto T, Wakasa K, Kinoshita H. Influence of histological inflammatory activity on regenerative capacity of liver after percutaneous transhepatic portal vein embolization. *J Gastroenterol* 1999; **34**: 100-104

17 **Shoup M,** Gonen M, D'Angelica M, Jarnagin WR, DeMatteo RP, Schwartz LH, Tuorto S, Blumgart LH, Fong Y. Volumetric analysis predicts hepatic dysfunction in patients undergoing major liver resection. *J Gastrointest Surg* 2003; **7**: 325–330

18 **Madoff DC,** Hicks ME, Vauthey JN, Charnsangavej C, Morello FA Jr, Ahrar K, Wallace MJ, Gupta S. Transhepatic portal vein embolization: anatomy, indications, and technical considerations. *Radiographics* 2002; **22**: 1063-1076

19 **Madoff DC,** Hicks ME, Abdalla EK, Morris JS, Vauthey JN. Portal vein embolization with polyvinyl alcohol particles and coils in preparation for major liver resection for hepatobiliary malignancy: safety and effectiveness-study in 26 patients. *Radiology* 2003; **227**: 251-260

20 **Kaneko T,** Nakao A, Takagi H. Clinical studies of new material for portal vein embolization: comparison of embolic effect with different agents. *Hepatogastroenterology* 2002; **49**: 472-477

21 **Elias D,** Ouellet JF, De Baere T, Lasser P, Roche A. Preoperative selective portal vein embolization before hepatectomy for liver metastases: long-term results and impact on survival. *Surgery* 2002; **131**: 294-299

22 **Ko GY,** Sung KB, Yoon HK, Kim JH, Weon YC, Song HY. Preoperative portal vein embolization with a new liquid embolic agent. *Radiology* 2003; **227**: 407-413

23 **Kito Y,** Nagino M, Nimura Y. Doppler sonography of hepatic arterial blood flow velocity after percutaneous transhepatic portal vein embolization. *AJR Am J Roentgenol* 2001; **176**: 909-912

24 **Kubo S,** Shiomi S, Tanaka H, Shuto T, Takemura S, Mikami S, Uenishi T, Nishino Y, Hirohashi K, Kawamura E, Kinoshita H. Evaluation of the effect of portal vein embolization on liver function by $^{(99m)}$tc-galactosyl human serum albumin scintigraphy. *J Surg Res* 2002; **107**: 113-118

25 **Barbaro B,** Di Stasi C, Nuzzo G, Vellone M, Giuliante F, Marano P. Preoperative right portal vein embolization in patients with metastatic liver disease. Metastatic liver volumes after RPVE. *Acta Radiol* 2003; **44**: 98-102

26 **Kokudo N,** Tada K, Seki M, Ohta H, Azekura K, Ueno M, Ohta K, Yamaguchi T, Matsubara T, Takahashi T, Nakajima T, Muto T, Ikari T, Yanagisawa A, Kato Y. Proliferative activity of intrahepatic colorectal metastases after preoperative hemihepatic portal vein embolization. *Hepatology* 2001; **34**: 267-272

27 **Zgouras D,** Wachtershauser A, Frings D, Stein J. Butyrate impairs intestinal tumor cell-induced angiogenesis by inhibiting HIF-1alpha nuclear translocation. *Biochem Biophys Res Commun* 2003; **300**: 832-838

Science Editor Zhu LH **Language Editor** Elsevier HK

PO Box 2345, Beijing 100023, China
www.wjgnet.com
wjg@wjgnet.com

ELSEVIER

World J Gastroenterol 2005;11(14):2055-2060
World Journal of Gastroenterology ISSN 1007-9327

• *ESOPHAGEAL CANCER* •

Loss of heterozygosity in multistage carcinogenesis of esophageal carcinoma at high-incidence area in Henan Province, China

Ji-Ye An, Zong-Min Fan, Shan-Shan Gao, Ze-Hao Zhuang, Yan-Ru Qin, Ji-Lin Li, Xin He, George Sai-Wah Tsao, Li-Dong Wang

Ji-Ye An, Laboratory for Cancer Research and the Third Teaching Hospital, College of Medicine, Zhengzhou University, Zhengzhou 450052, Henan Province, China
Zong-Min Fan, Ze-Hao Zhuang, Yan-Ru Qin, Shan-Shan Gao, Xin He, Li-Dong Wang, Henan Key Laboratory for Esophageal Cancer, Laboratory for Cancer Research, College of Medicine, Zhengzhou University, Zhengzhou 450052, Henan Province, China
Ji-Lin Li, Department of Pathology, Yaocun Esophageal Cancer Hospital, Linzhou 456592, Henan Province, China
George Sai-Wah Tsao, Laboratory for Cell Biology, Hong Kong University, Hong Kong, China
Supported by National Outstanding Young Scientist Foundation of China, No. 30025016; State Basic Research Development Program of China, No. G1998051206; Foundation of Henan Education Committee, No. 1999125 and the US NIH Grant, No. CA65871
Correspondence to: Professor Li-Dong Wang, Henan Key Laboratory for Esophageal Cancer, Laboratory for Cancer Research, College of Medicine, Zhengzhou University, Zhengzhou 450052, Henan Province, China. ldwang@zzu.edu.cn
Telephone: +86-11-371-66658335 Fax: +86-11-371-66658335
Received: 2004-04-07 Accepted: 2004-05-24

Abstract

AIM: Microsatellites are the repeated DNA sequences scattered widely within the genomes and closely linked with many important genes. This study was designed to characterize the changes of microsatellite DNA loss of heterozygosity (LOH) in esophageal carcinogenesis.

METHODS: Allelic deletions in 32 cases of matched precancerous, cancerous and normal tissues were examined by syringe microdissection under an anatomic microscope and microsatellite polymorphism analysis using 15 polymorphic markers on chromosomes 3p, 5q, 6p, 9p, 13q, 17p, 17q and 18q.

RESULTS: Microsatellite DNA LOH was observed in precancerous and cancerous tissues, except D9S1752. The rate of LOH increased remarkably with the lesions progressed from basal cell hyperplasia (BCH) to squamous cell carcinoma (SCC) (P<0.05). Three markers, D9S171, D13S260 and TP53, showed the highest incidence of LOH (>60%). LOH loci were different in precancerous and cancerous tissues. LOH in D3S1234 and TP53 was the common event in different lesions from the same patients.

CONCLUSION: Microsatellite DNA LOH occurs in early stage of human esophageal carcinogenesis, even in BCH. With the lesion progressed, gene instability increases, the accumulation of this change may be one of the important mechanisms driving precancerous lesions to cancer.

Key words: Esophageal cancer; Precancerous lesion; LOH

An JY, Fan ZM, Gao SS, Zhuang ZH, Qin YR, Li JL, He X, Tsao GSW, Wang LD. Loss of heterozygosity in multistage carcinogenesis of esophageal carcinoma at high-incidence area in Henan Province, China. *World J Gastroenterol* 2005; 11(14): 2055-2060

http://www.wjgnet.com/1007-9327/11/2055.asp

INTRODUCTION

Esophageal carcinoma (EC) is one of the six most common malignant diseases in the world with a remarkable geographical distribution. The prognosis of EC is very poor, its 5-year survival rate is only about 10% for the patients at late or advanced stage. Linzhou city (formerly Linxian) and nearby counties in Henan Province, China, have been well recognized as the high incidence area in the world. In the past years, scientists from China and other countries have made much research work in this area and found that esophageal carcinogenesis was a multistep progressive process characterized by multiple genetic changes (accumulation and overlap). The early characteristic of the subjects predisposed to EC is the abnormal proliferation of epithelial cells, morphologically manifested as basal cell hyperplasia (BCH), dysplasia (DYS) and carcinoma *in situ* (CIS), which could be considered as precancerous lesions of EC. The precancerous lesions are instable, i.e., they can develop to cancer, or stay for a couple of years without any changes, or even return to normal. What is the most important factor to decide the precancerous lesions to develop in different directions, especially in those with a similar morphology? What is the key point to induce mild precancerous lesions to develop cancer? Our assumption is that there exist different molecular changes in precancerous lesions with a similar morphology. To characterize the molecular changes in carcinogenesis of EC, the mechanism of EC could be elucidated and the biomarkers for early diagnosis and mass survey of high-risk populations could be established[1].

Microsatellites are the repeated DNA sequences scattered widely within the genomes and closely linked with many important genes[2]. In recent years many researches have indicated that the alteration of microsatellite DNA is one of the important markers, which could induce normal cells to undergo immortal and neoplastic transformations. It was reported that an extensive loss of microsatellite DNA was discovered in many tumors such as colon cancer. Some

microsatellite loci often exist in the hot spots of LOH at a high frequency in some specific malignancies. Tumor suppressor genes, which are associated with the development and progression of tumors, may harbor in the vicinity of these hot spots.

To characterize the changes of microsatellite DNA in esophageal carcinogenesis, loss of heterozygosity (LOH) in specific loci was analyzed in 32 surgically resected EC specimens using microsatellite polymorphic markers. Allelic deletions were examined using 15 polymorphic markers on chromosomes 3p, 5q, 6p, 9p, 13q, 17p, 17q and 18q.

MATERIALS AND METHODS

Precancerous and cancerous tissues

Thirty-two surgically resected squamous cell carcinoma (SCC) specimens were collected from Linxian Country, a high-incidence area of EC in Henan Province, China. Of the EC patients, 18 were males and 14 were females with an average age of 59 years (range 44-73 years). All the SCC patients were not treated by either chemotherapy or radiotherapy before operation. Surgically resected specimens were divided into two parts: One was fixed with 85% ethanol and paraffin embedded for histopathological diagnosis, and the other was stored in liquid nitrogen and then transferred in a -80 ℃ freezer for further use. Ten of thirty-two cases were taken from cancer and adjacent tissues. Various tissues from cancer and adjacent parts were frozen and cut into 5-μm thick sections and 30-60 slides were used for DNA extraction and LOH analysis. Five slides were stained with hematoxylin-eosin (HE) for histopathological diagnosis. According to cell morphologic changes, the esophageal epithelia were divided into BCH, DYS, CIS and SCC[3].

Syringe microdissection under anatomic microscope and DNA extraction

According to the distribution of cells in HE-stained sections, we dropped glycerol in matched spots, separated precancerous, cancerous and normal cells by a 5-mL syringe under an anatomy microscope, put them into 180 μL lysis buffer, added 20 μL proteinase K (50 μg/μL), and kept overnight at 56 ℃. By this method, 90% purified cells could be collected[4]. DNA was extracted according to the protocols of the QIAGEN DNA Mini Kit.

LOH analysis

According to the results based on our previous work in esophageal carcinogenesis at high-incidence area for EC in Henan Province, China[5], we chose 15 microsatellite DNA loci for LOH analysis using a circulating p53-Rb system. These loci represented D3S966 (RASSF1A), D3S1234 and D3S1300 (FHIT), D5S82 (DP1), D5S346 (APC), D6S497 (HLA, Waf1), D9S1752 (INK4a), D9S171 (INK4b), D13S260 (BRCA2), D13S321 and D13S233 (Rb1), TP53 and D17S786 (p53), D17S855 (BRCA1) and D18S858 (DCC).

Microsatellite polymorphism analysis

Each locus was amplified from 40 to 50 ng of template DNA by PCR using paired primers, of which the forward primer was 5' end-labeled with [γ-^{32}P] ATP. Eight percent of nondenaturing polyacrylamide gel electrophoresis was performed at 1 650 V for 2-3 h. After electrophoresis, the gel was transferred to a 3 MM chromatography paper and dried in a vacuum gel dryer at 80 ℃ for 1 h. The dried gel was placed into an X-ray film cassette with an intensifying screen and exposed to a Kodak film at -70 ℃ or at room temperature for 2-48 h.

Result determination

Three individuals examined the relative intensities of polymorphic alleles in different lesions. LOH status was established if the intensity of one allele in the tumor was significantly reduced as compared with its corresponding allele in constitutive DNA. When the decision was not unanimous, the density of alleles was determined by quantitative densitometry. Reduction of 30% intensity of one allele in tumor DNA compared to its matching allele in the constitutive DNA was chosen as the criteria for LOH status. Individual results were classified into three categories: LOH (loss of one allele), heterozygosity retained (no allelic loss), and uninformative (homozygous alleles)[6].

Statistical analysis

The data were analyzed by SPSS10.0 statistical software. LOH frequency was performed by χ^2 test. $P<0.05$ was considered statistically significant.

RESULTS

Relationship between LOH frequency and lesions (Figures 1 and 2, Table 1)

Microsatellite DNA LOH was observed in precancerous and cancerous tissues, except D9S1752. The rate of LOH increased remarkably with the lesion developed from BCH to SCC ($P<0.05$). At least on LOH locus was 41% (7/17) in BCH, 82% (14/17) in DYS, 100% (17/17) in CIS and 97% (31/32) in SCC. Three samples from SCC and one sample from CIS were found to have deletions in 18 loci.

Distribution of microsatellite DNA LOH in different lesions (Figure 3)

LOH loci were different in precancerous and cancerous tissues. In BCH, DYS and SCC, the highest LOH loci were TP53 (20%), D13S260 (33.3%) and TP53 (68.2%) respectively. In CIS, the highest LOH markers had three loci, D13S260, D9S171 and D3S966 (50%). Three markers, D9S171, D13S260 and TP53, showed the highest incidence of LOH (>60%). LOH in D3S1234 and TP53 was the common event in different lesions of the same patients.

DISCUSSION

Inactivation of tumor suppressor genes appears to be one of the genetic mechanisms involved in the development of esophageal cancer. This process includes mutation of one allele, followed by a deletion of the remaining one (LOH) or homozygous deletion of both alleles. Allelic deletions detected as LOH have been proved useful for mapping regions of DNA that contain tumor suppressor genes[7]. LOH at specific chromosomal regions strongly suggested

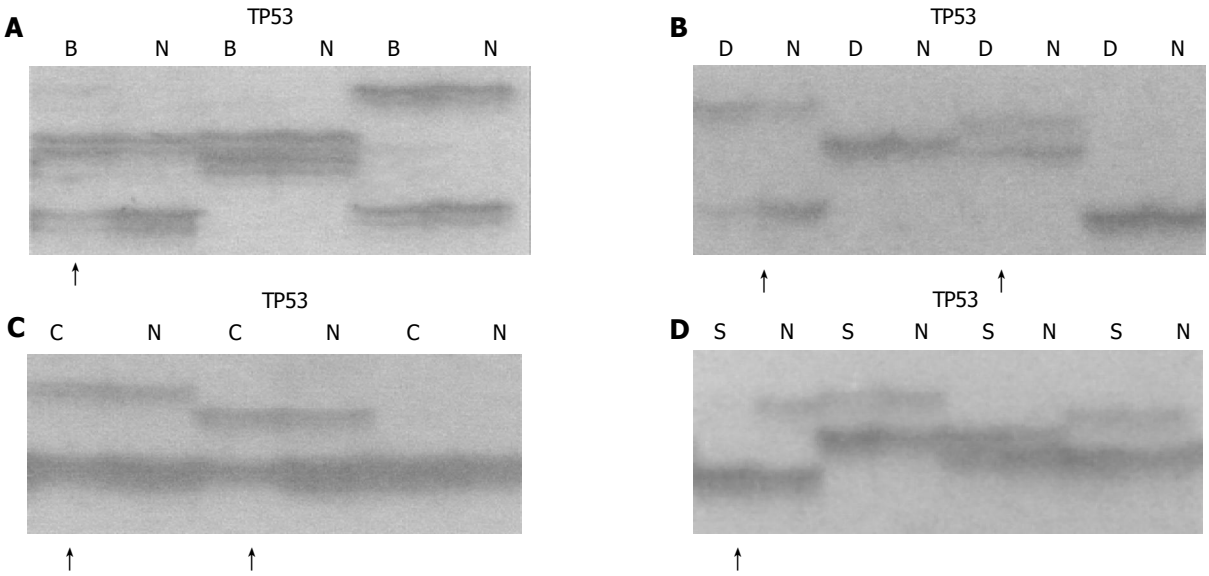

Figure 1 Allelic deletion patterns in TP53 microsatellite loci. Arrows indicate LOH in different lesions. B: basal cell hyperplasia (BCH), D: dysplasia (DYS), C: carcinoma *in situ* (CIS), S: squamous cell carcinoma(SCC), N: normal tissue, A: LOH in BCH; B: LOH in DYS; C: LOH in CIS; D: LOH in SCC.

the existence of tumor suppressor genes at the relevant segments[8]. We performed deletion mapping analyses in 32 cases of matched precancerous, cancerous and normal tissues using 15 microsatellite markers on chromosomes 3p, 5q, 6p, 9p, 13q, 17p, 17q and 18q and found that microsatellite DNA LOH occurred in early precancerous stage and in BCH. With the development of the disease, the rate of LOH increased, indicating that the genetic changes occurred in the early stage of EC. With the lesion progressed, gene instability increased, the accumulation of this change may be one of the important mechanisms transforming precancerous lesions to cancer. LOH loci were different even at the same stages (such as DYS), indicating that there existed different molecular changes in precancerous lesions with a similar morphology. These changes might be the key factors to decide precancerous lesions developing in different directions, especially in those with a similar morphology. Esophageal carcinogenesis is a multistep progressive process characterized by multiple genetic changes (accumulation and overlap). The changes of $p15^{INK4b}$, BRAC2 and p53 genes are common molecular events in esophageal carcinogenesis. LOH in D3S1234 and TP53 is the common event in different lesions of patients, indicating that the alternations of fragile histidine triad (FHIT) and p53 might be the key points to induce mild precancerous lesions to cancer. RASSF1A - one of the candidate TSGs - might be

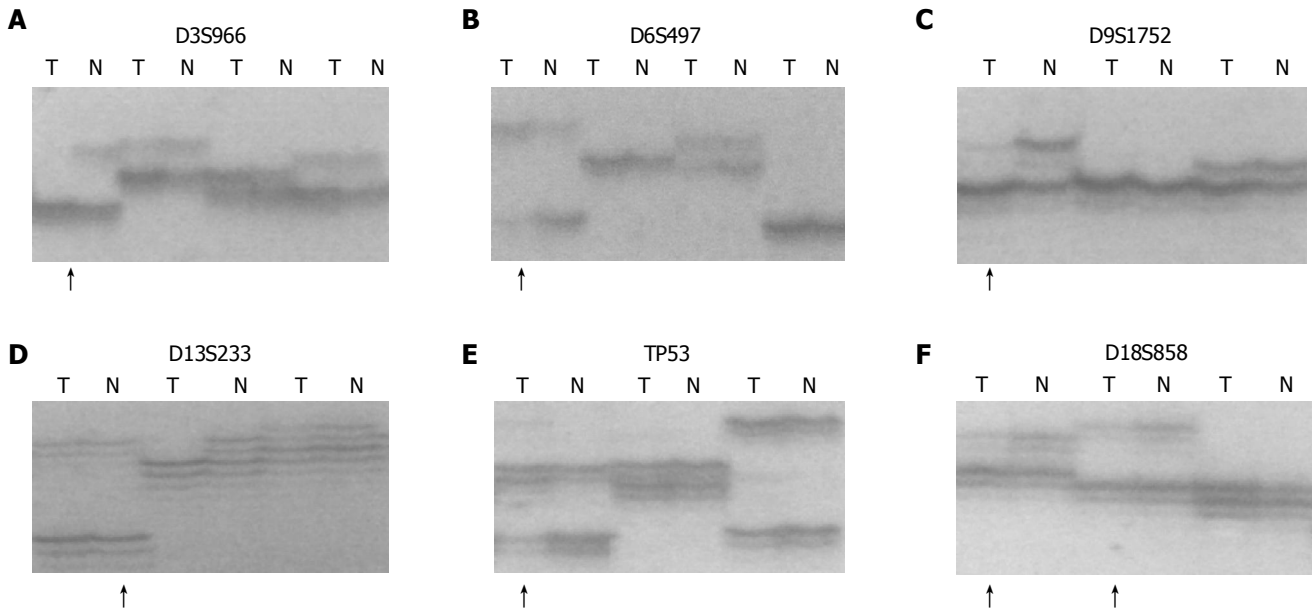

Figure 2 Allelic deletion patterns of various microsatellite markers in ESCC. Paired tumor DNA (T) and non-neoplastic DNA (N) were examined for each case. Arrows indicate LOH in tumor samples. A: D3S966 LOH; B: D6S497 LOH; C: D9S1752 LOH; D: D13S233 LOH; E: TP53 LOH; F: D18S858 LOH.

Table 1 Comparison between frequency of microsatellite LOH in different lesions of esophagus

MSM	LOH frequency *n* (%)				*P*
	BCH	DYS	CIS	SCC	
D3S1234	1/14 (7.1)	3/12 (25)	5/15 (33.30)	9/23 (39.1)	0.042
D3S1300	0/11 (0)	2/10 (20)	4/10 (40)	10/26 (38.5)	0.024
D3S966	0/13 (0)	3/13 (23.1)	8/16 (50)	11/20 (55.0)	0.001
D5S82	0/12 (0)	2/12 (16.7)	6/15 (40)	8/20 (40.0)	0.010
D5S346	2/12 (16.7)	3/12 (25)	4/10 (40)	14/25 (56.0)	0.011
D6S497	0/10 (0)	0/13 (0)	0/12 (0)	9/26 (34.6)	0.001
D9S1752	1/15 (6.7)	2/12 (16.7)	3/15 (20)	5/25 (20.0)	0.315
D9S171	0/13 (0)	5/16 (31.3)	7/14 (50)	14/23 (60.8)	0.000
D13S233	0/11 (0)	3/13 (23.1)	6/16 (37.5)	10/21 (47.6)	0.006
D13S321	0/14 (0)	3/12 (25)	6/14 (42.9)	11/25 (44.0)	0.006
D13S260	0/16 (0)	4/12 (33.3)	7/14 (50)	16/26 (61.5)	0.000
D17S855	2/13 (15.4)	4/14 (28.6)	6/15 (40)	14/26 (53.8)	0.014
TP53	3/15 (20)	4/13 (30.8)	7/16 (43.8)	15/22 (68.2)	0.002
D17S786	0/14 (0)	3/12 (25)	6/15 (40)	12/22 (54.5)	0.001
D18S858	0/13 (0)	3/16 (18.8)	4/12 (33.3)	10/18 (55.6)	0.000

MSM: microsatellite marker; LOH: loss of heterozygosity; BCH: basal cell hyperplasia DYS: dysplasia; CIS: carcinoma *in situ*; SCC: squamous cell carcinoma -: not done.

involved in the esophageal carcinogenesis in Henan Province, China.

The $p15^{INK4b}$ gene is an inhibitor of cyclin-dependent kinase 4, which has been identified in 95% genome sequence homogeneity with $p16^{INK4a}$. They encode two important cyclin-dependent kinase inhibitors, which could negatively regulate G_1-S transition of the proliferating cells by contributing to the maintenance of pRb in an active state[9]. Xing *et al*[10], reported that both $p15^{INK4b}$ and $p16^{INK4a}$ genes were frequently inactivated in EC, but the inactivation of $p15^{INK4b}$ and $p16^{INK4a}$ involved different mechanisms, with $p16^{INK4a}$ predominantly affected by aberrant methylation and $p15^{INK4b}$ by deletion. We analyzed the allelic loss of $p15^{INK4b}$ and $p16^{INK4a}$ using D9S1752 and D9S171 microsatellite markers, and found that the LOH frequency of $p15^{INK4b}$ was much higher than that of $p16^{INK4a}$ in precancerous and cancerous lesions. Our results support the speculation of Xing *et al*[10], and suggest that the deletion of $p15^{INK4b}$ gene might be involved in the multistage development of EC at the high-incidence area in Henan Province, China. LOH of $p16^{INK4a}$ might not be an important event in the esophageal carcinogenesis in the area.

BRCA1 and BRCA2 are tumor suppressor genes in familial breast-ovarian carcinoma syndrome and are located in different chromosomes. The BRCA2 gene is located on chromosome 13q12[11]. Extensive genetic and biochemical characterization has shown that BRCA2 is involved in the maintenance of chromosomal stability. It could serve as a critical mediator of DNA repair through direct interactions with Rad51 and might play an important role in recombination-mediated double-strand DNA break repair[12]. Harada *et al*[13], performed a fine deletion mapping on 13q by analyzing 60 EC patients with 18 polymorphic markers and found the frequent loss at D13S260 (43.7%). Up to now, to our knowledge, there are no other reports on the changes of BRCA2 in precancerous tissues. In our experiment, BRCA2 gene alternations were detected as 0% in BCH, 33% in DYS, 50% in CIS, and 61.5% in SCC, indicating that the deletion of BRCA2 might be involved in the development of EC and is one of the common molecular events in the esophageal carcinogenesis.

The p53 tumor suppressor gene is located on chromosome

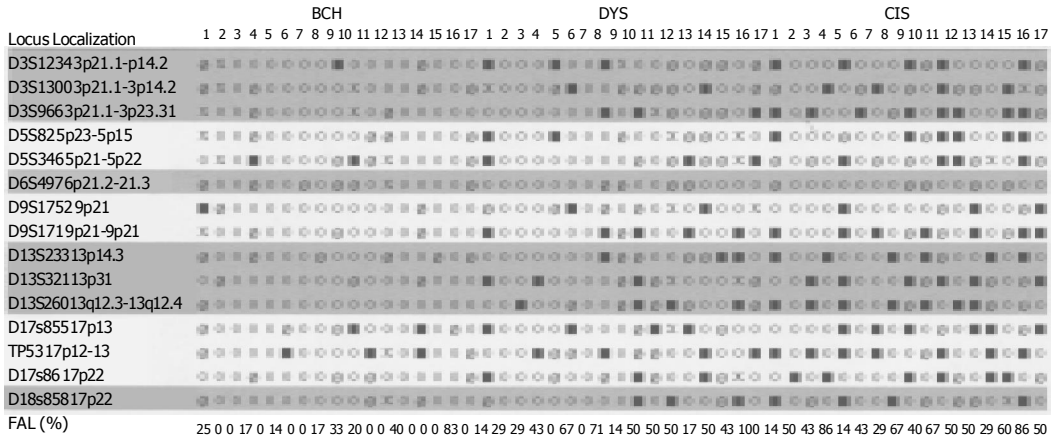

Figure 3 Distributions of microsatellite DNA-LOH in different precancerous lesions of esophagus FAL: fractional allelic loss for each tumor ○ retention of heterozygosity ■ loss of heterozygosity Ø uninformative, X not done.

17p13.1 and encodes a 53 ku nuclear phosphoprotein that binds to DNA and blocks the progression of the cell cycle in response to DNA damage and mediates apoptosis[14]. Allelic loss of p53 gene on chromosome 17p13.1 has been demonstrated to be one "hit" of inactivation of p53 gene. It was reported that the frequencies of LOH ranged from 65% to 83.8%, and often co-existed with mutations ("two hits") in EC[15]. In our experiments, the deletion of p53 occurred in the early stage of BCH (20%), indicating that the alternations of p53 might be the key points to induce mild precancerous lesions to cancer.

Frequent allele loss has been observed on chromosome 3p in EC and its premalignant lesions, indicating that inactivation of putative tumor suppressor genes on 3p may be involved in early stages of esophageal carcinogenesis. It has been reported that FHIT gene is a novel tumor suppressor gene located on chromosome 3p14.2[16]. Highly frequent abnormal transcripts of FHIT gene have been found in a variety of human cancers, including cancers of the digestive tract, lung, breast, and head and neck[17,18]. Point mutations of the FHIT gene were also seen in gastric and breast carcinomas, but very rarely. A review of the literature showed that different results were obtained by different researches[19-21]. Zou *et al*[19], reported that the deletions of FHIT were involved in 11 of 50 (22%) EC samples. On the other hand, Mori *et al*[22], observed that the LOH frequency of the FHIT gene was 76%. In our experiment, loss of FHIT was detectable in 7% BCH, 20% DYS, 33% CIS and 39% SCC. Although the LOH frequency of FHIT gene was low in our results, the change occurred in each stage of esophageal carcinogenesis. Exposure to different environmental carcinogens might be one of the reasons why there existed differences in different areas.

RASSF1A is a novel tumor suppressor gene that was isolated recently from the lung tumor suppressor locus *3p21.3*[23]. The presence of a Ras associated domain in RASSF1A suggested that this protein might function as an effector of Ras signaling in normal cells. Its protein structure also suggested that RASSF1A might participate in the DNA damage response or in DNA damage-induced regulation of other cell signaling events[24]. Chan *et al*[25], demonstrated the methylation status of RASSF1A and the frequency of LOH in *3p21.3* region in bladder cancer and found that the frequency of LOH and methylation of RASSF1A were 57.9% and 47.5% respectively, showing that RASSF1A might be inactivated in accordance with the two-hit inactivation model, involving deletion of one allele and hypermethylation of the other[26]. Up to now, much research work has been done in promoter hypermethylation of RASSF1A. In the present study, we observed that the LOH frequency of D3S966 was 23.1% in DYS, 50% in CIS and 55% in SCC, indicating that RASSF1A might be involved in the esophageal carcinogenesis at the high-incidence area in Henan Province, China. To our knowledge, this report is the first to identify allelic loss of RASSF1A during esophageal carcinogenesis in Henan Province, China.

REFERENCES

1 **Wang LD,** Zheng S. The mechanism of esophageal and gastric cardia carcinogenesis from the subjects at high-incidence area for esophageal cancer in Henan. *Zhengzhou Daxue Xuebao* 2002; **37**: 717-729

2 **Cullis CA.** The use of DNA polymorphisms in genetic mapping. *Genet Eng (N Y)* 2002; **24**: 179-189

3 **Wang LD,** Shi ST, Zhou Q, Goldstein S, Hong JY, Shao P, Qiu SL, Yang CS. Changes in p53 and cyclin D1 protein levels and cell proliferation in different stages of human esophageal and gastric-cardia carcinogenesis. *Int J Cancer* 1994; **59**: 514-519

4 **Wang LD,** Zhou Q, Hong JY, Qiu SL, Yang CS. p53 protein accumulation and gene mutations in multifocal esophageal precancerous lesions from symptom free subjects in a high incidence area for esophageal carcinoma in Henan, China. *Cancer* 1996; **77**: 1244-1249

5 **Wang LD,** Hong JY, Qiu SL, Gao H, Yang CS. Accumulation of p53 protein in human esophageal precancerous lesions: a possible early biomarker for carcinogenesis. *Cancer Res* 1993; **53**: 1783-1787

6 **Reed AL,** Califano J, Cairns P, Westra WH, Jones RM, Koch W, Ahrendt S, Eby Y, Sewell D, Nawroz H, Bartek J, Sidransky D. High frequency of p16 (CDKN2/MTS-1/INK4A) inactivation in head and neck squamous cell carcinoma. *Cancer Res* 1996; **56**: 3630-3633

7 **Thiagalingam S,** Foy RL, Cheng KH, Lee HJ, Thiagalingam A, Ponte JF. Loss of heterozygosity as a predictor to map tumor suppressor genes in cancer: molecular basis of its occurrence. *Curr Opin Oncol* 2002; **14**: 65-72

8 **Kinzler KW,** Nilbert MC, Vogelstein B, Bryan TM, Levy DB, Smith KJ, Preisinger AC, Hamilton SR, Hedge P, Markham A. Identification of a gene located at chromosome 5q21 that is mutated in colorectal cancers. *Science* 1991; **251**: 1366-1370

9 **Xing EP,** Nie Y, Song Y, Yang GY, Cai YC, Wang LD, Yang CS. Mechanisms of inactivation of p14ARF, p15INK4b, and p16INK4a genes in human esophageal squamous cell carcinoma. *Clin Cancer Res* 1999; **5**: 2704-2713

10 **Xing EP,** Nie Y, Wang LD, Yang GY, Yang CS. Aberrant methylation of p16INK4a and deletion of p15INK4b are frequent events in human esophageal cancer in Linxian, China. *Carcinogenesis* 1999; **20**: 77-84

11 **Wooster R,** Neuhausen SL, Mangion J, Quirk Y, Ford D, Collins N, Nguyen K, Seal S, Tran T, Averill D. Localization of a breast cancer susceptibility gene, *BRCA2*, to chromosome 13q12-13. *Science* 1994; **265**: 2088-2090

12 **Shamoo Y.** Structural insights into BRCA2 function. *Curr Opin Struct Biol* 2003; **13**: 206-211

13 **Harada H,** Tanaka H, Shimada Y, Shinoda M, Imamura M, Ishizaki K. Lymph node metastasis is associated with allelic loss on chromosome 13q12-13 in esophageal squamous cell carcinoma. *Cancer Res* 1999; **59**: 3724-3729

14 **Hu N,** Huang J, Emmert-Buck MR, Tang ZZ, Roth MJ, Wang C, Dawsey SM, Li G, Li WJ, Wang QH, Han XY, Ding T, Giffen C, Goldstein AM, Taylor PR. Frequent inactivation of the TP53 gene in esophageal squamous cell carcinoma from a high-risk population in China. *Clin Cancer Res* 2001; **7**: 883-891

15 **Baker SJ,** Kinzler KW, Vogelstein B. Knudson's hypothesis and the TP53 revolution. *Genes Chromosomes Cancer* 2003; **38**: 329

16 **Pekarsky Y,** Palamarchuk A, Huebner K, Croce CM. FHIT as tumor suppressor: mechanisms and therapeutic opportunities. *Cancer Biol Ther* 2002; **1**: 232-236

17 **Scully C,** Field JK, Tanzawa H. Genetic aberrations in oral or head and neck squamous cell carcinoma 2: chromosomal aberrations. *Oral Oncol* 2000; **36**: 311-327

18 **Yang Q,** Yoshimura G, Sakurai T, Kakudo K. The Fragile Histidine Triad gene and breast cancer. *Med Sci Monit* 2002; **8**: RA140-RA144

19 **Zou TT,** Lei J, Shi YQ, Yin J, Wang S, Souza RF, Kong D, Shimada Y, Smolinski KN, Greenwald BD, Abraham JM, Harpaz N, Meltzer SJ. FHIT gene alterations in esophageal cancer and ulcerative colitis (UC). *Oncogene* 1997; **15**: 101-105

20 **Mimori K,** Inoue H, Shiraishi T, Matsuyama A, Mafune K, Tanaka Y, Mori M. Microsatellite instability is often observed in esophageal carcinoma patients with allelic loss in the FHIT/

FRA3B locus. *Oncology* 2003; **64**: 275-279
21 **Roth MJ,** Hu N, Emmert-Buck MR, Wang QH, Dawsey SM, Li G, Guo WJ, Zhang YZ, Taylor PR. Genetic progression and heterogeneity associated with the development of esophageal squamous cell carcinoma. *Cancer Res* 2001; **61**: 4098-4104
22 **Mori M,** Mimori K, Shiraishi T, Alder H, Inoue H, Tanaka Y, Sugimachi K, Huebner K, Croce CM. Altered expression of Fhit in carcinoma and precarcinomatous lesions of the esophagus. *Cancer Res* 2000; **60**: 1177-1182
23 **Chow LS,** Lo KW, Kwong J, To KF, Tsang KS, Lam CW, Dammann R, Huang DP. RASSF1A is a target tumor suppressor from 3p21.3 in nasopharyngeal carcinoma. *Int J Cancer* 2004; **109**: 839-847
24 **Dammann R,** Li C, Yoon JH, Chin PL, Bates S, Pfeifer GP. Epigenetic inactivation of a RAS association domain family protein from the lung tumour suppressor locus 3p21.3. *Nat Genet* 2000; **25**: 315-319
25 **Chan MW,** Chan LW, Tang NL, Lo KW, Tong JH, Chan AW, Cheung HY, Wong WS, Chan PS, Lai FM, To KF. Frequent hypermethylation of promoter region of RASSF1A in tumor tissues and voided urine of urinary bladder cancer patients. *Int J Cancer* 2003; **104**: 611-616
26 **Kuroki T,** Trapasso F, Yendamuri S, Matsuyama A, Alder H, Mori M, Croce CM. Allele loss and promoter hypermethylation of VHL, RAR-beta, RASSF1A, and FHIT tumor suppressor genes on chromosome 3p in esophageal squamous cell carcinoma. *Cancer Res* 2003; **63**: 3724-3728

Science Editor Zhang JZ, Wang XL and Li WZ **Language Editor** Elsevier HK

PO Box 2345, Beijing 100023, China
www.wjgnet.com
wjg@wjgnet.com

ELSEVIER

World J Gastroenterol 2005;11(14):2061-2066
World Journal of Gastroenterology ISSN 1007-9327

Clinical analysis of the risk factors for recurrence of HCC and its relationship with HBV

Di-Peng Ou, Lian-Yue Yang, Geng-Wen Huang, Yi-Ming Tao, Xiang Ding, Zhi-Gang Chang

Di-Peng Ou, Lian-Yue Yang, Geng-Wen Huang, Yi-Ming Tao, Xiang Ding, Zhi-Gang Chang, Liver Cancer Laboratory, Department of Surgery, Xiangya Hospital, Central South University, Changsha 410008, Hunan Province, China
Supported by the National Key Technologies R and D Program, No. 2001BA703B04 and Hunan Province Developing Planning Committee, No. 2001907
Correspondence to: Professor. Lian-Yue Yang, Liver Cancer Laboratory, Department of Surgery, Xiangya Hospital, Central South University, Changsha 410008, Hunan Province, China. lianyueyang@hotmail.com
Telephone: +86-731-4327326 Fax: +86-731-4327332
Received: 2004-10-19 Accepted: 2004-11-08

Abstract

AIM: To comprehend the risk factors of recurrence of hepatocellular carcinoma (HCC) and its relationship with the infection patterns of hepatitis B virus (HBV).

METHODS: All materials of 270 cases of postoperative HCC were statistically analyzed by SPSS software. Recurrence and metastasis were classified into early (≤2 years) and late phase (>2 years). Risk factors for recurrence and metastasis after surgery in each group were analyzed.

RESULTS: Out of 270 cases of HCC, 162 cases were followed up in which recurrence and metastasis occurred in 136 cases. There were a lot of risk factors related to recurrence and metastasis of HCC; risk factors contributing to early phase recurrence were serum AFP level, vascular invasion, incisal margin and operative transfusion, gross tumor classification and number of intrahepatic node to late phase recurrence. The HBV infective rate of recurrent HCC was 94.1%, in which "HBsAg, HBeAb, HBcAb" positive pattern reached 45.6%. The proportion of HBV infection in solitary large hepatocellular carcinoma (SLHCC) evidently decreased compared to nodular hepatocellular carcinoma (NHCC) (P<0.05).

CONCLUSION: The early and late recurrence and metastasis after hepatectomy of HCC were associated with different risk factors. The early recurrence may be mediated by vascular invasion and remnant lesion, the late recurrence by tumor's clinical pathology propert, as multicentric carcinogenesis or intrahepatic carcinoma de novo. HBV replication takes a great role in this process. From this study, we found that SLHCC has more satisfactory neoplasm biological behavior than NHCC.

Key words: Hepatocellular carcinoma; Recurrence and metastasis; Risk factor; Hepatitis B virus

Ou DP, Yang LY, Huang GW, Tao YM, Ding X, Chang ZG. Clinical analysis of the risk factors for recurrence of HCC and its relationship with HBV. *World J Gastroenterol* 2005; 11 (14): 2061-2066
http://www.wjgnet.com/1007-9327/11/2061.asp

INTRODUCTION

Because of the advances in surgical techniques and perioperative management, hepatectomy of hepatocellular carcinoma (HCC) has become a safe operation with low operative mortality. However, the long-term prognosis remains poor due to a high incidence of recurrence and metastasis of HCC, ranging from 50% to 80%[1-3]. The effect of HCC's therapy is also unpleasant; the high rate of recurrence and metastasis after HCC resection has always disturbed clinical surgeon nowadays. There are lots of reports based on the fact that intrahepatic recurrence or multicentric carcinogenesis de novo were found after resection of HCC[4,5]. Because different risk factors for recurrence and metastasis have been identified in previous articles[6], it is a controversy regarding the way of recurrence and metastasis, which need us continue to disclose its mechanism.

Hepatitis B virus (HBV) is a hepadnavirus, discussed worldwide as resulting in viral hepatitis in humans. HBV gets distributed at various ages, the infectious rate of HBV has reached 10% in China. Once it infects the human body, the HBV gets replicated and proliferated into hepatocytes, induces hepatocyte lesion and develops into chronic hepatitis. It has been reported that HBV is the prime cause for the development of HCC. In order to discuss the relationship between HBV and the recurrence and metastasis of HCC, we studied the clinical data of postoperative HCC and its follow-up.

MATERIALS AND METHODS

Population

The base population consisted of 270 consecutive patients who had undergone initial and curative hepatic resection for HCCs at Central South University Xiangya Hospital from 1992 to 2002. The indication of surgical resection and operative procedure was determined according to the decision criteria based on the liver function test including ascites, serum bilirubin level, and image data. Systematic resection of Couinaud's segment was a preferred operative

Table 1 Baseline characteristics in 270 patients (mean±SD)

Variable factors	All patients (n = 270)	Recurrent patients (n = 136)	Recurrent patients (n = 136)	
			Early phase (n = 107)	Late phase (n = 29)
Age (yr)	46.9±13.0	4.0±11.5	44.2±11.1	47.7±12.9
Sex (male/female)	247/23	126/10	99/8	27/2
Gross tumor classification (small/solitary/nodular)	66/168/36	35/77/24	23/63/21	12/14/3
Edmondson classification (I–II/III–IV)	128/142	65/71	46/61	19/10
Tumor capsule (present/absent)	55/215	23/113	13/94	10/19
Vascular invasion (present/absent)	145/125	79/57	62/45	7/12
Alpha-fetoprotein (positive/negative)	141/129	85/51	75/32	10/19
Hepatocirrhosis (positive/negative)	200/70	105/31	82/25	23/6
Type of liver resection (non-anatomical/anatomical)	149/121	78/58	59/48	19/10
Incisal margin (≤1 cm/>1 cm)	22/258	15/131	14/93	1/28
HBV infection (positive/negative)	239/31	128/8	102/5	26/3
Blood transfusion (yes/no)	199/71	100/36	75/32	25/4
Survival time (d)	–	575.9±499.6	384.7±313.1	1 248.5±450.9
Recurrent time (d)	–	435.6±417.9	23.1±199.6	1 072.2±396.9

Note: Small HCC (SHCC), solitary large HCC (SLHCC), nodular HCC (NHCC).

procedure if the patient's liver functional reserve permitted. Curative resection was defined as removal of all recognizable tumors with a clear margin. As regards the tumor margin, resection with 1 cm was defined as curative so long as no tumor invasion was observed at the surgical cut surface[7]. By retrospectively investigating these data of 270 patients, 162 gained follow-up and finally entered into the analyses. One hundred and eight patients were excluded for the following reasons: data lacked follow-up for 96 and incomplete pathological analysis in 12. Out of 162 patients only 132 presented recurrence. We divided time of recurrence into early phase (amongst 2 years) and later phase (excluding 2 years); there were 107 cases of recurrence and metastasis in early phase and 29 cases in later phase. The baseline characteristics of these 162 patients classified according to viral infection pattern are presented in Table 1. Gross HCC classification was divided into small HCC (SHCC), solitary large HCC (SLHCC) and nodular HCC (NHCC) according to our previous study on HCC's basic and clinical characteristics[8]. Various surgical procedures were classified as anatomical or non-anatomical resections. Anatomical resection involves resecting the tumor together with the tumor-containing portal vein and corresponding hepatic territory and includes hemihepatectomy (right or left), sectorectomy (right lateral, right paramedian, left medial, and the left lateral sector), and segmentectomy (resection of Couinaud's segments). All other types of resection such as limited resection and tumor enucleation are classified as non-anatomical resection.

Follow-up and end point

After discharge, monthly follow-up by tumor marker (alpha-fetoprotein, AFP) and ultrasound (US) as well as helical computed tomographic (CT) scan for every 4 mo were conducted for 1 year. Then, we screened patients by tumor marker measurement and US for every 2 mo and helical CT for every 6 mo thereafter, and hepatic angiography when recurrence was suspected. Recurrence was diagnosed based on the combined findings of these clinical examinations. The end point of this study was time-to-recurrence, which was defined as the period between surgery and the diagnosis of recurrence and metastasis. Patients who died for reasons not related to HCC were censored at the time of death. All follow-up data were summarized by the end of April 2004.

Variables analyzed

Discrete variables were computed directly, whereas continuous variables were classified into binary or polytomous categorical data. Cut-off points for AFP were 20 μg/L, and maximal tumor diameter were determined according to operative records, which gave the best discrimination between time-to-recurrence curves among several stratifications[5].

The studied variables could be classified as host-, cancer-, or surgery-related (Table 1). The host-related factors were age, sex, viral markers (HBsAg-, HBeAg-, HBsAb-, HBeAb-, HBcAb-). HBV infection pattern was graded according to the difference of viral markers positive expression. Fibrosis was assessed using non-cancerous parts of the resected specimens. The stage of liver fibrosis was classified into four categories (no, mild, moderate, and cirrhosis) to represent the severity of liver disease. Cancer-related factors were gross classification of the tumor[6,9], tumor multiplicity, maximum diameter of tumor, microscopically assessed vascular invasion, intrahepatic metastasis, microscopically assessed presence and/or invasion of a tumor capsule, tumor cell

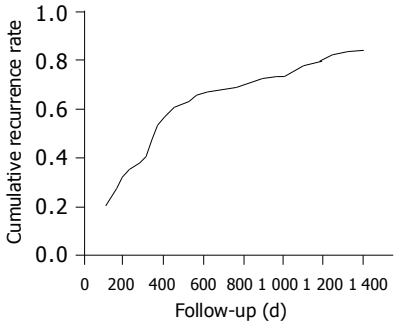

Figure 1 Curve of overall cumulative recurrence and metastasis rate metastasis rate present in 136 HCC patients.

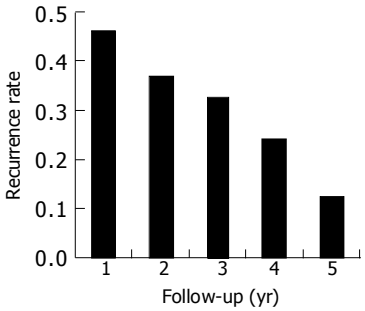

Figure 2 Bar graph of recurrence and metastasis rate present in 136 patients at each year.

differentiation, serum AFP level. Multiple tumor nodules and intrahepatic metastasis were differentiated based on macro- and microscopical findings. In brief, multiple tumors were classified into intrahepatic metastases if they were (a) tumors apparently growing from portal venous tumor thrombi, or (b) multiple satellite nodules surrounding a main tumor with similar or poorer degree of cell differentiation. Surgery-related factors included type of resection (anatomical *vs* non-anatomical) and surgical free margin (>1 cm *vs* <1 cm).

Statistical analysis

The overall hazard function for recurrence and metastasis was also estimated to visually depict chronological change in the recurrence rate after hepatectomy. We investigated factors contributing to early and late phase recurrence, separately, setting 2 years as the cut-off between the early and late phases[7]. For this purpose, we first conducted a multiple regression analysis by setting the different baseline hazard functions for respective institutions and by censoring patients without recurrence at 2 years after surgery at this time point. Then, we performed a landmark analysis on recurrence-free status at 2 years after surgery. Finally, the relationship between the viral infection patterns was investigated using the Mantel-Haenszel trend test on data from patients showing only one of two hepatitis markers. As additional sets of analyses, we performed the same analyses exclusively in patients with solitary tumor. Likewise, we also performed analyses dividing patients with and without liver cirrhosis. All statistical analyses in the present study were performed using the Statistical Package for Social Sciences (SPSS11.0 software).

RESULTS

Analysis of the recurrence and metastasis of HCC

Among the 162 cases of follow-up, the median follow-up time was 1 742 d (range 7-4 200 d). Recurrence and metastasis were observed in 136 patients. There was a patient who survived more than 11 years. Overall cumulative recurrence and metastasis rate curves for all patients are shown in Figure 1, and Figure 2 depicts the overall recurrence and metastasis at each year after operation, which peaked at the first year postoperatively, then gradually decreased year by year. The overall cumulative recurrence and metastasis rate were 32.7% (200 d), 59.2% (400 d), 64.5% (600 d), 69.8% (800 d), 73.5% (1 000 d), 80.3% (1 200 d), 84.1% (1 400 d); there were 46.3% (1st year), 36.8% (2nd year), 32.7% (3rd year), 24.3% (4th year) and 12.4% (5th year) respectively from 1st to 5th year.

Factors contributing to early (≤2 years) phase recurrence and metastasis

Recurrence and metastasis before 2 years was observed in 107 patients. Multiple regression analysis identified four variables as contributing to early phase recurrence and metastasis: Serum AFP (alpha-fetoprotein) level, vascular invasion, incisal margin and operative transfusion (Table 2). As a result, the causes of recurrence and metastasis for early phase were the factors correlated to surgery.

Factors contributing to late (>2 years) phase recurrence and metastasis

In the same way, recurrence and metastasis was observed in 29 patients. Factors related to late phase recurrence and metastasis were gross tumor classification and number of intrahepatic node (Table 2). NHCC had higher recurrence and metastasis rate than SLHCC ($P = 0.026$). It was coincident to the results of our prophase study on the SLHCC characterization at basic and clinical[10].

Relationship on the HBV infection with recurrence and metastasis of HCC

It has been confirmed by lots of epidemiological survey that HCC genesis is closely related to the HBV infection. Our further study disclosed that the HBV infection has related to the recurrence and metastasis of HCC. In this paper, the infective rate was 88.5% on 270 cases of HCC, but 94.1% on 136 cases of recurrence and metastasis of HCC. Among the 162 cases of follow-up, there were 128 recurrences with HBV infection (147 cases) and only 8 recurrences without HBV infection (15 cases). Statistic comparison had high significant difference ($\chi^2 = 11.501$, $P = 0.001$); it prompted that the HBV infection was an important cause of recurrence and metastasis of HCC.

The HBV infective pattern was different in various clinical classifications of HCC. Contrast analysis of the HBV infective pattern among 270 HCC patients that accepted operation with 136 HCC patients showed that recurrence and metastasis occurred; we found that HBV infection not only related to

Table 2 Multiple regression analysis of recurrence and metastasis of 136 HCC patients

Variable	Results on early phase			Results on late phase		
	Regression coefficient	*t*	*P*	Regression coefficient	*t*	*P*
AFP level	-0.328	-3.693	0.000	-0.280	-1.306	0.208
Hepatocirrhosis	0.024	0.274	0.785	-0.377	-1.530	0.143
Type of liver resection	0.023	0.260	0.795	0.245	1.235	0.233
Incisal margin	0.217	2.485	0.015	0.106	0.420	0.679
Blood transfusion	-0.223	2.553	0.012	0.268	1.266	0.222
Gross tumor classification	-0.051	-0.583	0.561	-0.518	-2.433	0.026
Vascular invasion	0.266	3.013	0.003	-0.361	-1.562	0.136
Tumor capsule	0.023	0.259	0.797	-0.281	-1.111	0.281
Edmondson classification	0.126	1.444	0.152	0.065	0.292	0.774

Note: Dependent variable was the time of recurrence and metastasis (d).

Table 3 Statistics of the HBV infective pattern

Serum markers	All patients (n = 270)		Recurrent patients (n = 136)	
	Positive number	Ratio (%)	Positive number	Ratio (%)
HBsAg+HBeAg+HBcAb+	20	7.4	14	10.3
HBsAg+HBeAb+HBcAb+	118	43.7	62	45.6
HBsAg+HBcAb+	57	21.1	32	23.5
HBsAb+	9	3.3	6	4.4
HBcAb+	2	0.7	2	1.5
HBeAb+HBcAb+	7	2.6	1	0.7
HBsAg+	16	5.9	9	6.6
HBsAb+HBeAb+HBcAb+	2	0.7	0	0.0
HBsAg+HBeAb+	6	2.2	1	0.7
HBsAb+HBeAb+	2	0.7	1	0.7
HBV negative	31	11.5	8	5.9

the HCC genesis and recurrence, but also that their infective pattern varied (t = 2.407, P = 0.037, Table 3). Further comparison of the infective pattern of recurrent SLHCC and recurrent NHCC, results showed the HBV infection pattern of recurrent NHCC, which was obviously different compared with SLHCC, and the proportion of recurrent NHCC with HBV infection was obviously step-up than recurrent SLHCC (P<0.05, Table 4).

DISCUSSION

Recurrence and metastasis of HCC could divide into intrahepatic recurrence and extrahepatic metastasis, but 90% of recurrence were intrahepatic, which could be expressed in mono-, poly- and omni-hepatic dissemination. Extrahepatic metastasis means primary lesion of HCC spreading to distant location, it can also accompany with intrahepatic recurrence. Multi-center carcinogenesis of HCC was closely related to postoperative recurrence. It has reported that recurrent rate reach to peak amongst 2 year, about 62-82%. This time after hepatectomy was the most risky period for recurrence and metastasis[11]. Therefore, we divided the recurrent time into early and late phase according to the point of 2 years postoperatively. In this study, recurrent risk factors at early phase were serum AFP level, vascular invasion, incisal margin and operative transfusion. Serum AFP was synthesized on embryo hepatocyte, it was not expressed on normal hepatocytes, but was expressed specifically on hepatic cancer cells. Now serum AFP level usually assayed as utility data contributing to judgment of operative effect on whether it descents to normal level (<20 μg/L). It has reported that serum AFP level would be descended to negative in 18% postoperative patients, and obvious descended in 40%[12]. Nowadays image examination such as B-US, CT scan, magnetic resonance imaging and digital subtraction angiography are limited, even the LR-CT with ultra-iodized oil image through hepatic artery can only find tumor >0.5 cm, and it is difficult to find the micro carcinoma <0.3 cm. So it is important for the surveillance of the recurrence and metastasis of postoperative HCC. Serum AFP level will be changed pre- and post-operation at HCC patients. Our material shows 85 cases occurred positive expression.

Surgery-related vascular invasion, incisal margin and operative transfusion were immediate causes for postoperative recurrence and metastasis at early phase, it means the HCC incision was not radical, and remnant carcinoma continues to grow after operation. As the way of enlarged incisal margin peremptory to prevent postoperative recurrence and metastasis is undesirable, it could not reduce the recurrence and metastasis but lead the patient to liver function failure or death[13-15]. Our experiences are to adopt limited hepatectomy, incisal margin is kept in 1-2 cm especially for the tumor with capsule or pseudocapsule. Owing to abundant liver blood supply, operative transfusion is usually inevitable even though there are lots of hemostasia measures to manipulate hepatic hemorrhage on operation. Investigation has made clear that operative hetero-transfusion could bring out many troubles[16,17]. Our study detected the recurrent rate obviously

Table 4 Compare the HBV infective pattern between SLHCC and NHCC

Serum markers	All patients (n = 270)		Recurrent patients (n = 136)		χ^2	P
	SLHCC ratio (%)	NHCC ratio (%)	SLHCC ratio (%)	NHCC ratio (%)		
HBsAg+HBeAg+HBcAb+	40.0	13.3	33.3	25.0	4.244	0.039
HBsAg+HBeAb+HBcAb+	56.3	12.5	53.1	12.2	0.003	0.955
HBsAg+HBcAb+	70.2	12.8	73.1	11.5	0.079	0.778
HBsAb+	71.4	14.3	60.0	20.0	1.833	0.176
HBeAb+HBcAb+	75.0	12.5	0.0	100.0	4.876	0.000
HBsAg+	63.2	5.3	50.0	12.5	4.867	0.027
HBV negative	69.6	4.3	87.5	0.0	4.877	0.027

increased in whom accepted transfusion compared to non-transfusion (P = 0.012), indicated operative transfusion is auxo-action for recurrence and metastasis at the early phase of postoperation. The mechanism maybe: Thrombosis is the advantage of cancer cell implantation, growth factors are released to reinforce cancer cell growth directly or indirectly, to inhibit the NK cell's activity and result in the function of NK immunocytes decreased, to accelerate the growth of remnant cancer cells. Therefore surgeon should weigh the merits and demerits while performing HCC hepatectomy, adopt acrobatic hepatectomy technique, reduced operative hepatic bleeding and blood transfusion as far as possible, to adopt self-transfusion when necessary. Preoperative vascular invasion or carcinoma thrombosis are fundamental cause for postoperative recurrence and metastasis, leading to decrease of postoperative survival rate. Above all, the micro vascular invasion under microscopy could not be judged, which directly lead to recurrence and metastasis at early phase after hepatectomy[18].

The clinical classification of HCC was the independence related risk factor during the late phase of postoperation. On the basement of previous abundant basic and clinical research, we divided HCC into small HCC (SHCC), solitary large HCC (SLHCC) and nodular HCC (NHCC) according to its clinical pathology propert. Analyzed 29 cases of recurrent data at late phase in contrast with 107 cases at early phase, we found the proportion of SLHCC decreased obviously than NHCC (58.9% *vs* 48.3%), there was a significant difference (χ^2 = 3.929, P = 0.047). It indicated SLHCC has more satisfactory neoplasm biological behavior than NHCC, which coincided with the results of our prophase research[10].

Chronic HBV infection is the main cause of HCC genesis in China. We statistically analyzed the materials of in-patients accepted hepatectomy at our hospital, the HBV infective rate reached 90%. The closed relation between HBV infection and HCC could manifest in the concordance on their epidemiologic character, such as local distribution, sex, age and family history[19]. The main HBV infective pattern of 270 patients was positive "HBsAg, HBeAb, HBcAb" viral markers. Positive HBsAg shows those patients existing with HBV infection, positive HBeAb and HBcAb shows HBV replicated in hepatocytes at lower level. If HBeAb presented long-term positive, the HBV-DNA has been integrated with host hepatocyte chromosome DNA, kept latentiation ever since[20,21]. Our data on 136 cases of recurrence and metastasis shows that the pattern of positive HBcAb was distinctly enhanced. We could explain that the HCC patients with HBV infection have lower immunological function, with decreased resistant ability, HBV promoted recurrence and metastasis by various kinds of pathway as activating HBx function, integrating host cell DNA, destructing apoptosis of normal hepatocyte, inactivating P53 gene, facilitating extracellular matrix degradation[22-24].

Among the recurrent HCC, the HBV infective pattern of NHCC was evidently different from that of SLHCC, furthermore, the proportion of NHCC with HBV infection was evidently increased (P<0.05). It is interpreted that NHCC more easily combines with HBV reproduction than SLHCC in the course of recurrence and metastasis. So the prognosis that NHCC is worse than SLHCC could be elucidated from another point of view.

In conclusion, this study provides an epidemiological evidence that intrahepatic recurrence and metastasis of HCC after hepatic resection has two obvious etiologies. The early recurrence may be mediated by vascular invasion and remnant lesion, the late recurrence by tumor's clinical pathology propert, as multicentric carcinogenesis or intrahepatic carcinoma de novo. So we could prevent recurrence and metastasis of HCC in the following way: to adopt limited hepatectomy and acrobatic hepatectomy technique, to reduce operative hepatic bleeding and blood transfusion as far as possible, to control HBV infection in HCC patients. In this way, we can increase postoperative survival rate of HCC on whole.

REFERENCES

1 **Chen XP**, Qiu FZ, Wu ZD, Zhang BX. Chinese experience with hepatectomy for huge hepatocellular carcinoma. *Br J Surg* 2004; **91**: 322-326

2 **Chen WT**, Chau GY, Lui WY, Tsay SH, King KL, Loong CC, Wu CW. Recurrent hepatocellular carcinoma after hepatic resection: prognostic factors and long-term outcome. *Eur J Surg Oncol* 2004; **30**: 414-420

3 **Shimozawa N**, Hanazaki K. Longterm prognosis after hepatic resection for small hepatocellular carcinoma. *J Am Coll Surg* 2004; **198**: 356-365

4 **Huo TI**, Lui WY, Wu JC, Huang YH, King KL, Loong CC, Lee PC, Chang FY, Lee SD. Deterioration of hepatic functional reserve in patients with hepatocellular carcinoma after resection: incidence, risk factors, and association with intrahepatic tumor recurrence. *World J Surg* 2004; **28**: 258-262

5 **Imamura H,** Matsuyama Y, Tanaka E, Ohkubo T, Hasegawa K, Miyagawa S, Sugawara Y, Minagawa M, Takayama T, Kawasaki S, Makuuchi M. Risk factors contributing to early and late phase intrahepatic recurrence of hepatocellular carcinoma after hepatectomy. *J Hepatol* 2003; **38**: 200-207

6 **Tung-Ping Poon R**, Fan ST, Wong J. Risk factors, prevention, and management of postoperative recurrence after resection

of hepatocellular carcinoma. *Ann Surg* 2000; **232**: 10-24
7 **Cha C**, Fong Y, Jarnagin WR, Blumgart LH, DeMatteo RP. Predictors and patterns of recurrence after resection of hepatocellular carcinoma. *J Am Coll Surg* 2003; **197**: 753-758
8 **Yang LY**, Wang W, Peng JX, Yang JQ, Huang GW. Differentially expressed genes between solitary large hepatocellular carcinoma and nodular hepatocellular carcinoma. *World J Gastroenterol* 2004; **10**: 3569-3573
9 **Hui AM,** Takayama T, Sano K, Kubota K, Akahane M, Ohtomo K, Makuuchi M. Predictive value of gross classification of hepatocellular carcinoma on recurrence and survival after hepatectomy. *J Hepatol* 2000; **33**: 975-979
10 **Wang W**, Yang LY, Huang GW, Lu WQ, Yang ZL, Yang JQ, Liu HL. Genomic analysis reveals RhoC as a potential marker in hepatocellular carcinoma with poor prognosis. *Br J Cancer* 2004; **90**:2349-2355
11 **Hanazaki K**, Kajikawa S, Shimozawa N, Mihara M, Shimada K, Hiraguri M, Koide N, Adachi W, Amano J. Survival and recurrence after hepatic resection of 386 consecutive patients with hepatocellular carcinoma. *J Am Coll Surg* 200; **191**: 381-388
12 **Huo TI**, Huang YH, Lui WY, Wu JC, Lee PC, Chang FY, Lee SD. Selective prognostic impact of serum alpha-fetoprotein level in patients with hepatocellular carcinoma: analysis of 543 patients in a single center. *Oncol Rep* 2004; **11**: 543-550
13 **Jaeck D**, Bachellier P, Oussoultzoglou E, Weber JC, Wolf P. Surgical resection of hepatocellular carcinoma. Post-operative outcome and long-term results in Europe: an overview. *Liver Transpl* 2004; **10**: S58-S63
14 **Cho A**, Okazumi S, Miyazawa Y, Makino H, Miura F, Ohira G, Yoshinaga Y, Tohma T, Kudo H, Matsubara K, Ryu M, Ochiai T. Limited resection based on reclassification of segment 8 of the liver. *Hepatogastroenterology* 2004; **51**: 575-576
15 **Vauthey JN**, Pawlik TM, Abdalla EK, Arens JF, Nemr RA, Wei SH, Kennamer DL, Ellis LM, Curley SA. Is extended hepatectomy for hepatobiliary malignancy justified? *Ann Surg* 2004; **239**: 722-730; discussion 730-732
16 **Kooby DA**, Jarnagin WR. Surgical management of hepatic malignancy. *Cancer Invest* 2004; **22**: 283-303
17 **Rui JA**, Zhou L, Liu FD, Chu QF, Wang SB, Chen SG, Qu Q, Wei X, Han K, Zhang N, Zhao HT. Major hepatectomy without blood transfusion: report of 51 cases. *Chin Med J* 2004; **117**: 673-676
18 **Poon RT**, Fan ST, Ng IO, Lo CM, Liu CL, Wong J. Different risk factors and prognosis for early and late intrahepatic recurrence after resection of hepatocellular carcinoma. *Cancer* 2000; **89**: 500-507
19 **Chen CH**, Chen YY, Chen GH, Yang SS, Tang HS, Lin HH, Lin DY, Lo SK, Du JM, Chang TT, Chen SC, Liao LY, Kuo CH, Lin KC, Tai DI, Changchien CS, Chang WY, Sheu JC, Chen DS, Liaw YF, Sung JL. Hepatitis B virus transmission and hepatocarcinogenesis: a 9 year retrospective cohort of 13676 relatives with hepatocellular carcinoma. *J Hepatol* 2004; **40**: 653-659
20 **Ohata K**, Hamasaki K, Toriyama K, Ishikawa H, Nakao K, Eguchi K. High viral load is a risk factor for hepatocellular carcinoma in patients with chronic hepatitis B virus infection. *J Gastroenterol Hepatol* 2004; **19**: 670-675
21 **Chen JD**, Liu CJ, Lee PH, Chen PJ, Lai MY, Kao JH, Chen DS. Hepatitis B genotypes correlate with tumor recurrence after curative resection of hepatocellular carcinoma. *Clin Gastroenterol Hepatol* 2004; **2**: 64-71
22 **Pal J**, Somogyi C, Szmolenszky A A, Szekeres G, Sipos J, Hegedus G, Martzinovits I, Molnar J, Nemeth P. Immunohistochemical assessment and prognostic value of hepatitis B virus X protein in chronic hepatitis and primary hepatocellular carcinomas using anti-HBxAg monoclonal antibody. *Pathol Oncol Res* 2001; **7**: 178-184
23 **Feitelson MA**, Zhu M, Duan LX, London WT. Hepatitis B x antigen and p53 are associated in vitro and in liver tissues from patients with primary hepatocellular carcinoma. *Oncogene* 1993; **8**: 1109-1117
24 **Theret N**, Musso O, Turlin B, Lotrian D, Bioulac-Sage P, Campion JP, Boudjema K, Clement B. Increased extracellular matrix remodeling is associated with tumor progression in human hepatocellular carcinomas. *Hepatology* 2001**; 34**: 82-88

Science Editor Li WZ **Language Editor** Elsevier HK

PO Box 2345, Beijing 100023, China
www.wjgnet.com
wjg@wjgnet.com

ELSEVIER

World J Gastroenterol 2005;11(14):2067-2071
World Journal of Gastroenterology ISSN 1007-9327

Hepatic resection for hepatocellular carcinoma in end-stage renal disease patients: Two decades of experience at Chang Gung Memorial Hospital

Chun-Nan Yeh, Wei-Chen Lee, Miin-Fu Chen

Chun-Nan Yeh, Wei-Chen Lee, Miin-Fu Chen, Department of General Surgery, Chang Gung Memorial Hospital, Chang Gung University, Taoyuan, Taiwan, China
Correspondence to: Dr. Chun-Nan Yeh, Department of General Surgery, Chang Gung Memorial Hospital, 5 Fu-Hsing Street, Kwei-Shan, Taoyuan, Taiwan, China. ycn@adm.cgmh.org.tw
Telephone: +886-3-3281200-3219 Fax: +886-3-3285818
Received: 2004-10-13 Accepted: 2004-12-23

Key words: HCC; ESRD

Yeh CN, Lee WC, Chen MF. Hepatic resection for hepatocellular carcinoma in end-stage renal disease patients: Two decades of experience at Chang Gung Memorial Hospital. *World J Gastroenterol* 2005; 11(14): 2067-2071
http://www.wjgnet.com/1007-9327/11/2067.asp

Abstract

AIM: Hepatocellular carcinoma (HCC) is a common disease in Taiwan. The prevalence of viral hepatitis infection and the subsequent development of HCC are well known to be higher in patients with end-stage renal disease (ESRD) requiring hemodialysis (HD) or peritoneal dialysis (PD) than among the general population. However, information on hepatic resection for ESRD-HCC patients is limited.

METHODS: The clinical features of 26 ESRD-HCC patients who underwent hepatic resection from 1982 to 2001 were retrospectively reviewed. Meanwhile, the clinicopathological features and the outcome of 1 198 HCC patients without ESRD undergoing hepatic resection were used for comparison.

RESULTS: Of 1 224 surgically resected HCC patients, 26 (4.2%) were ESRD-HCC. Univariate analysis revealed more associated disease, more physical signs of anemia and postoperative complications, lower hemoglobin, platelet, α-fetoprotein, elevated blood urea nitrogen (BUN) and creatinine levels, smaller tumors, lower HBsAg positivity, higher HCV positivity, and longer hospital stays in the ESRD-HCC group compared with the HCC group. Furthermore, multivariate stepwise logistic regression analysis revealed that elevated BUN and creatinine levels were the only two independently significant factors in the patients in the ESRD-HCC group. Overall and disease-free survival rates were similar between the ESRD-HCC and HCC groups.

CONCLUSION: Elevated BUN and creatinine were the only two main independent factors differentiating ESRD-HCC from HCC patients. ESRD should not be a contraindication of hepatic resection in HCC patients; however, careful operative techniques and perioperative care are crucial to achieving lower morbidity and mortality. Comparable overall survival and disease-free survival can be achieved in selected ESRD-HCC patients undergoing hepatic resection when compared with conventional HCC patients.

INTRODUCTION

Hepatocellular carcinoma (HCC) is a common disease in Taiwan, with an annual age-adjusted prevalence of 28.7/100 000 population. HCC is the leading cause of cancer-related death among men, and second among women in Taiwan[1].

Although liver transplantation provides an alternative option for the surgical management of HCC, partial hepatic resection remains the mainstay of treatment. With improvements in surgical techniques and perioperative care, surgical mortality rates in HCC patients receiving hepatectomy have recently reduced significantly[2]. The prevalence of viral hepatitis infection and the subsequent development of HCC are well known to be higher in patients with end-stage renal disease (ESRD) requiring hemodialysis (HD) or peritoneal dialysis (PD) than among the general population[3,4]. Such patients are usually immunocompromised and have various degrees of associated coagulopathy[4-6]. Because hemorrhage, infection, and liver failure are the main causes of death after liver resection, HCC resection should be particularly risky for patients with ESRD[7]. However, few reports exist on liver resection for HCC in such patients[3,6,7]. This study attempted to determine the outcome of liver resection for HCC in ESRD patients.

MATERIALS AND METHODS

From 1982 to 2001, 1 224 consecutive HCC patients underwent surgery at the Department of Surgery, Chang Gung Memorial Hospital, Taipei, Taiwan. Among them, 26 HCC patients (4.2%) suffering ESRD treated with HD, and/or continuous ambulatory peritoneal dialysis (CAPD) undergoing curative surgery were classified as ESRD-HCC group, while the remaining 1 198 patients were classified as HCC group. Sixty-seven patients were excluded from the survival analysis due to incomplete follow-up records. Totally

Table 1 Demographic data of 1 224 HCC patients undergoing hepatectomy with and without ESRD

	ESRD–HCC (%) (n = 26)	HCC (%) (n = 1 198)	P
Age (yr)	53.4±13.2	54.3±13.7	0.748
Gender (M:F)	22:4	937:261	0.433
Associated disease	19 (73.1)	406 (33.9)	0.0001
Symptoms (+)	17 (65.4)	799 (66.7)	0.889
Physical findings (+)	13 (50.0)	289 (24.1)	0.002
HBsAg (+)	11 (42.3)	782/1 101 (71.0)	0.002
Anti-HCV Ab (+)	15 (62.5)	314/854 (36.8)	0.01
Dual infection (+)	2/23 (8.7)	99/816 (36.8)	1.0
Associated cirrhosis (+)	14 (53.8)	647/1 187 (54.5)	0.947
child-pugh grade			
A	19 (76.0)	1 014 (89.5)	
B+C	6 (24)	119 (10.5)	0.055

M: male; F: female; HBsAg: hepatitis B surface antigen; HCV: hepatitis C virus; Ab: antibody.

1 157 patients were enrolled in this study for survival analysis. In this study, 66 HCC patients (including three ESRD-HCC patients) died within one month after surgery (surgical mortality rate 5.4%; 66/1 224). Laboratory tests were performed on the day before surgery. Differences in demographics, symptomatology, physical examination, laboratory data, presence of cirrhosis, operative findings, and pathological features between the two groups were compared. Clinicopathological features were conditioned as presence or absence; resection margin less than 1 cm *vs* a margin of more than 1 cm; and low histological grading *vs* high grade. Resections included segmentectomy, lobectomy, extended lobectomy, subsegmentectomy, and wedge resection. Segmentectomy is a resection of one of the four segments (lateral, medial, anterior, or posterior) of the liver as classified by Healey and Schroy. Subsegmentectomy is a resection of a Couinaud segment. Histopathological findings of HCC were divided into four grades according to Edmondson and Stainer's system. Grades I and II were conditioned as low-grade, and grades III and IV as high-grade HCC (described as previously)[8].

Table 2 Laboratory data of 1 224 HCC patients undergoing hepatectomy with and without ESRD

	ESRD–HCC (%) (n = 26)	HCC (%) (n = 1 198)	P
AFP (ng/mL)	2 143.7±1 0365.5	6 520.9±9 9070.2	0.825
AFP>400 ng/mL	2/25 (8.0)	392/1 098 (35.7)	0.003
Hemoglobin (g/dL)	10.6±2.5	13.0±2.1	0.0001
WBC (/μL)	6 284.6±3 031.0	7 467.6±7 956.4	0.449
Platelet (10^3/μL)	134.7±77.0	179.4±99.2	0.023
PT/PT (normal control)	0.85±1.6	0.96±1.9	0.778
INR (%)	1.10±0.16	1.10±0.18	0.953
Albumin (g/dL)	3.70±0.67	3.90±0.62	0.115
Bilirubin (direct) (mg/dL)	0.30±0.14	0.51±1.16	0.588
Bilirubin (total) (mg/dL)	0.80±0.36	1.12±1.27	0.207
BUN (mg/dL)	54.9±26.9	15.5±7.1	0.0001
Creatinine (mg/dL)	6.64±4.01	1.21±1.69	0.0001
AST (IU/L)	63.5±55.5	72.6±96.0	0.631
ALT (IU/L)	46.6±51.1	63.9±71.0	0.236
ALP (IU/L)	101.5±45.2	114.7±295.6	0.827
ICG 15 (%)	19.4±15.6	14.5±13.9	0.143

AFP: α-fetoprotein; PT: prothrombin time; INR: international normalized ratio; BUN: blood urea nitrogen; AST: aspartate aminotransferase; ALT: alanine aminotransferase; ALP: alkaline phosphatase; ICG 15: indocyanine green retention rate at 15 min.

Before admission for liver resection, one patient received CAPD and the remaining 25 patients underwent regular HD thrice weekly. Etiologies diagnosed in the 26 patients were as follows: idiopathic nephropathy (12), diabetic nephropathy (5), gouty nephropathy (2), nephrolithiasis (1), nephrotic syndrome (1), gouty nephropathy (1), malignancy (transitional cell carcinoma) associated nephropathy (1), hypertensive nephropathy (2), and polycystic kidney disease (1). The duration of dialysis ranged from 2 to 152 mo (median/mean: 37/46.3 mo). The patient who underwent CAPD shifted to HD about 1 wk before surgery. HD was conducted on the day before surgery, and then continued post-surgery was being conducted on alternate days, starting from the first day of post-surgery. CAPD was resumed for one patient after discharge.

Statistical analysis

All data are presented as percentage of patients or mean with standard deviation. Numerical data were compared by independent student two-sample t tests. Nominal data were compared by Pearson χ^2 test, Fisher exact test, or multiple forward stepwise logistic regression when appropriate. Survival was calculated and plots constructed according to the Kaplan-Meier method and compared with a log-rank test between groups. All statistical analyses were performed using the SPSS computer software package (Version 10.0, Chicago, IL). A value of $P<0.05$ was considered significant.

RESULTS

The ESRD-HCC group contained 22 men and 4 women, with a mean age of 53.4±13.2 years (range, 30-83 years). The ESRD-HCC and HCC groups displayed similar age distributions and gender ratios (Table 1). However, associated disease and anemia (hemoglobin <10 gm/dL) were more common in the ESRD-HCC group than the HCC group (Tables 1 and 4). Hypertension was the most commonly associated disease (10/19; 52.6%), followed by diabetes mellitus (DM; 8/19; 42.1%) (Table 4). Notably, ESRD-HCC patients displayed a lower percentage of positive

Table 3 Operative, macroscopic, and microscopic findings of HCC patients with and without ESRD

	ESRD–HCC (%) (n = 26)	HCC (%) (n = 1 198)	P
Major hepatectomy	17/26 (65.4)	603/1 198 (50.3)	0.129
Blood loss (cc)	955.8±771.2	1 358.6±1 593.3	0.199
Blood transfusion (cc)	462.0±580.1	1 037.9±2 261.9	0.204
Tumor size (cm)	4.1±2.0	6.2±4.5	0.0001
Tumor size >5 cm	6/26 (23.1)	545/1 171 (46.5)	0.018
Grading (Edmondson and Stainer)			
Low-grade (I+II)	10/25 (40.0)	504/948 (53.2)	
High-grade (III+IV)	15/25 (60.0)	444/948 (46.8)	0.193
Capsule formation (+)	16/21 (76.2)	676/1 012 (66.8)	0.365
Capsule invasion (+)	8/15 (53.3)	359/625 (57.4)	0.751
Macroscopic vascular invasion (+)	8/24 (33.3)	431/1 150 (37.5)	0.678
Satellite lesions (+)	5/25 (20.0)	336/1 155 (29.1)	0.321
Resection margin >1 cm	12/23 (52.2)	373/1 051 (35.5)	0.099
Rupture (+)	3/26 (11.5)	140/1 167 (12.0)	0.943
Complication	11/26 (42.3)	240/1 198 (20.0)	0.005
Hospital stay (d)	26.8±11.7	21.7± 12.7	0.046
Mortality	3/26 (11.5)	63/1 198 (5.3)	0.161

Table 4 Associated disease, morbidity, and postoperative mortality of 26 ESRD–HCC and 1 198 HCC patients treated with hepatectomy

	ESRD–HCC (n = 26)		HCC (n = 1 198)
Associated disease	19 (73.1%)	Associated disease	406 (33.9%)
ESRD only	7	Peptic ulcer	121
Hypertension	10	DM	111
DM	8	Hypertension	88
Heart disease	3	DM+hypertension	42
TCC	1	DM+peptic ulcer	20
Peptic ulcer	6	Heart disease	31
		CVA	11
		Biliary tract disease (GB stone or CBD stone or IHD stone)	27
		Lung disease	27
		Others	71
Morbidity	11 (42.3%)	Cause of mortality	66 (5.3%)
Pleural effusion	4	Hepatic failure	12
Ascites	2	Infection-induced hepatic failure	10
Jaundice	1	Intra-abdominal bleeding	23
Pneumonia	1	Cholangitis	1
Intra-abdominal abscess	1	Bile leakage	1
Wound infection	1	ARDS	2
Fever	1	EV bleeding	2
Cause of mortality	3 (11.5%)	Peptic ulcer bleeding	3
Sepsis	2	Combine EV and peptic ulcer bleeding	1
Pulmonary embolism	1	Renal failure	4
		Pneumonia/ pulmonary embolism	1/1
		VT/heart failure	1/1
		Ischemic bowel /hollow organ perforation	1/1
		DIC	1

TCC: transitional cell carcinoma; DM: diabetes mellitus; CVA: cerebrovascular disease; GB: gallbladder; CBD: common bile duct; IHD: intrahepatic duct; ARDS: adult respiratory distress syndrome; EV: esophageal variceal; VT: ventricular tachycardia; DIC: disseminated intravascular coagulopathy.

Table 5 Univariate and multiple forward stepwise logistic regression analysis of clinicopathological features in 1 224 HCC patients after hepatectomy between ESRD and non-ESRD groups

	Univariate analysis P	Multivariate logistic regression analysis P
Associate disease	0.001	NS
Presence of physical findings	0.002	NS
Positive HBsAg	0.002	NS
Positive anti-HCV Ab	0.002	NS
Platelet<150 000/mL	0.011	NS
Hb<10 g/dL	0.0001	NS
BUN>30 mg/dL	0.0001	0.0001
Cr>1.5 mg/dL	0.0001	0.002
AFP>400 ng/L	0.003	NS
Tumor size<5 cm	0.018	NS
Hospital stay>21 d	0.035	NS
Complication	0.005	NS

HBsAg: hepatitis B surface antigen; HCV: hepatitis C virus; Ab: antibody; Hb: hemoglobin; BUN: blood urea nitrogen; Cr: creatinine; AFP: α-fetoprotein.

hepatitis B and higher percentage of hepatitis C compared to the HCC group. Although rates of underlying liver cirrhosis did not differ significantly between the two groups, ESRD-HCC patients tended to have lower percentage of Child-Pugh grade A (P = 0.055) (Table 1).

Table 2 displays the results of all preoperative laboratory tests. Levels of AFP, hemoglobin, platelet, blood urea nitrogen (BUN), and creatinine differ between the two groups.

Table 3 lists the operative, macroscopic, and microscopic findings. Patients in the ESRD-HCC group displayed similar extent of hepatectomy, blood loss, and blood transfusion to those in the HCC group. Notably, tumor size was smaller in the ESRD-HCC group than the HCC group (P = 0.0001). However, the percentages of low-grade and high-grade HCC were similar in both groups. Generally, the tumors in the ESRD-HCC group had similar capsule formation, capsular invasion, vascular invasion, satellite lesions, rupture rate, and clearance margins to those in the HCC group (Table 3). Table 4 displays the causes of operative mortality of ESRD-HCC and HCC patients. Overall mortality rate was 5.4% (66/1 224). The mortality rates of the ESRD-HCC (11.5%) patients undergoing hepatic resection are higher than the HCC groups (5.3%), although it is not statistically significant (P = 0.161). Meanwhile, more complications and longer stay at hospital were noted in the ESRD-HCC patients than the HCC patients (P = 0.005 and 0.046).

Univariate analysis showed that associated disease, physical signs of anemia, lower hepatitis B positivity, higher hepatitis C positivity, lower hemoglobin and platelet count, elevated BUN, creatinine and AFP levels, smaller tumor size, more complications, and longer stay at hospital were associated with ESRD-HCC. However, multivariate logistic regression analysis showed that elevated BUN and creatinine were the only two independent factors differentiating ESRD-HCC from HCC (Table 5).

All the 1 157 patients who underwent hepatic resection were followed regularly until death. The duration of follow-up for 26 ESRD-HCC and 1 131 HCC patients ranged from 0.01 to 97.6 mo (median = 15.0 mo) and 0.01 to 213.5 mo (median = 14.6 mo), respectively. Table 6, Figures 1A and B display overall and disease-free survival for the ESRD-HCC and HCC groups. The 1-, 3-, and 5-year overall survival rates were 82.0%, 38.1%, 38.1% in the ESRD-HCC group and 70.6, 48.6, 34.8% in the HCC group, respectively. Moreover, the 1-, 3-, and 5-year disease-free survival rates were 63.1%, 49.1%, and 16.4% in the ESRD-HCC group, and 55.2%, 35.4%, 26.9% in the HCC group, respectively. Notably, the patients in the ESRD-HCC group had similar overall and disease-free survival to those in the HCC group.

DISCUSSION

Contrary to Cheng's report, ESRD-HCC patients displayed comparable clinicopathological features to HCC patients with exception of displaying lower hemoglobin and higher serum creatinine levels[7]. This study demonstrated that ESRD-HCC patients undergoing hepatectomy differed from HCC patients in several respects. ESRD-HCC patients undergoing hepatectomy had higher rate of underlying associated disease, as well as physical findings of anemia,

Table 6 Prognosis of HCC patients undergoing hepatectomy with and without ESRD

	ESRD-HCC (%) (n = 26)	HCC (%) (n = 1 131)	P
Overall survival (mo)			
mean	47.9	63.3	
Median	23.6	32.8	
95%CI of mean	27.3; 68.4	55.7; 71.0	
Log-rank			0.7034
DFS (mo)			
mean	35.9	52.0	
Median	14.8	15.5	
95%CI of mean	17.0; 54.7	43.7; 60.3	
Log-rank			0.6123

CI: confidence interval; DFS: disease-free survival.

lower positivity of hepatitis B infection, and higher positivity of hepatitis C infection. Hypertension is the disease most commonly associated with ESRD, followed by DM. Hepatitis B and C are two common pathogens causing chronic hepatitis in patients with ESRD. The acceptance of hepatitis B surface antigen screening has led the infected patients being identified and isolated over the past 20 years. Consequently, hepatitis B is now encountered less frequently in dialysis units. However, while hepatitis B has become less problematic, hepatitis C has been recognized as a significant problem since 1979. The prevalence of anti-HCV in HD patients is quite variable, ranging from 5 to over 50%[9]. In Taiwan, the rate of anti-HCV in HD patients is 30.5% [10], and is significantly lower in patients with CAPD[11]. Anti-HCV positivity is associated with previous blood transfusion, mode of therapy, and duration of HD.

ESRD-HCC patients undergoing hepatectomy exhibited lower hemoglobin level than HCC patients, explaining the higher positivity for physical findings of anemia in ESRD-HCC patients. Anemia can be a complication of the HD procedure itself, with its associated blood loss. ESRD-HCC patients also had lower platelet count than HCC patients. Reduced platelet counts were more common in patients on dialysis, particularly in HCV-positive HD patients, and the failure of megakaryocyte production by the bone marrow is a fundamental cause of this platelet reduction in both HD and CAPD patients[12].

ESRD-HCC patients exhibited lower AFP level and significantly lower percentage of AFP >400 ng/mL compared with HCC patients without ESRD. That ESRD-HCC patients have lower percentage of HBsAg positivity and smaller tumor size may explain the lower AFP values[8,13]. From the world literature on factors affecting the prognosis of surgically treated patients, previous European and Japanese reports emphasize the importance of preoperative AFP value[14,15]. The Italian group proposed the CLIP scoring system for the staging for HCC based partly on AFP value[14]. The specific reason for raised AFP level worsening the prognosis is uncertain. AFP may be a unique biological variable expressing grade of malignancy, and has suppressive effects on the immunologic reaction directed against tumor cells[16]. Regarding tumor markers, several investigations have demonstrated that AFP level is not influenced by uremic status and maintains its specificity for tumor monitoring in uremic status[17]. ESRD-HCC patients had smaller tumors and lower percentage of tumor size >5 cm compared with HCC patients without ESRD. HCC screening for chronic hepatitis B and hepatitis C carriers in endemic areas using AFP and/or abdominal ultrasound could identify tumors, especially smaller ones, explaining the observation. Our previous study demonstrated that HCV patients had smaller tumors[18]. We also demonstrated that HCC patients with larger tumor size had higher percentages of positive hepatitis B infection and lower percentage of hepatitis C infection. Meanwhile, overall survival and disease-free survival for HCC patients undergoing hepatic resection with tumor larger than 10 cm is worse than for those with tumor less than 10 cm, which is significantly influenced by the high value of AFP[8]. Smaller tumor size, lower AFP level, and significantly lower percentage of AFP >400 ng/mL in ESRD-HCC patients may partly explain no significant survival difference to HCC patients.

This study observed a higher prevalence of postoperative complications among ESRD-HCC patients after hepatectomy, explaining the longer hospital stays and higher mortality rate of ESRD-HCC patients. Notably, a higher percentage of HCV infection, Child-Pugh grade, and more associated disease may partially contribute to the more eventful postoperative courses of ESRD-HCC patients compared to HCC patients. Our previous study demonstrated that HCV-related HCC patients were older, and tended to have severe, and progressive liver disease[18]. Generally, septic problems occur most frequently with advanced cirrhosis and contribute heavily to the increased mortality. The increased infection rate may be partially explained by the

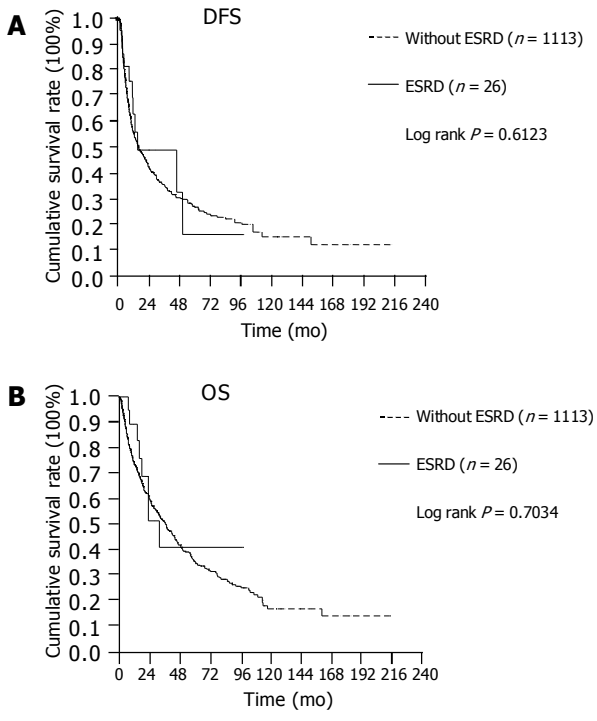

Figure 1 A: Disease-free survival of 26 HCC patients with ESRD undergoing hepatectomy *vs* 1 131 HCC patients without ESRD undergoing hepatectomy; B: Overall survival of 26 HCC patients with ESRD undergoing hepatectomy *vs* 1 131 HCC patients without ESRD undergoing hepatectomy.

impairment of Kupffer cell function, which reduces intravascular clearance of the enteric organism[19]. Additionally, ascitic fluid may provide an ideal growth medium for bacterial contaminants released during cholecystectomy[19]. Overall, the relative risk of septic complications depends on the severity of cirrhosis. Numerous investigations have correlated the prevalence of sepsis with the patient's Child-Pugh classification[19]. This study finds that pleural effusion and ascites are the two most common complications after hepatic resection. For hepatic surgeons, careful operative techniques and perioperative care are crucial to achieving an uneventful postoperative course and preventing postoperative wound infection and intra-abdominal abscess, even mortality.

As for prognosis, comparable overall survival and disease-free survival can be achieved in selected ESRD-HCC patients undergoing hepatic resection when compared to conventional HCC patients in this study. Since the first combined liver-kidney transplant was proposed in 1983[20], this procedure has gained increasing popularity for liver failure and irreversible renal insufficiency[20]. To the best of our knowledge, no report regarding combined liver-kidney transplant for ESRD-HCC patients is noted in the literature.

In summary, elevated BUN and creatinine values were the only two independent factors differentiating ESRD-HCC from HCC patients. ESRD should not be a contraindication of hepatic resection in HCC patients; however, careful operative techniques and perioperative care are crucial to achieving lower morbidity and mortality. Comparable overall survival and disease-free survival to conventional HCC patients can be achieved in selected ESRD-HCC patients undergoing hepatic resection.

REFERENCES

1 Department of Health, Executive Yuan, Republic of China. Annual report of cancer registration, 2001
2 **Fan ST**, Lo CM, Liu CL, Lam CM, Yuen WK, Yeung C, Wong J. Hepatectomy for hepatocellular carcinoma: toward zero hospital deaths. *Ann Surg* 1999; **229**: 322-330
3 **Hayashi H**, Ohtake Y, Kashima T, Irie Y, Murata M, Hayashi H, Kobayashi S, Okuda K. Hepatocellular carcinoma among hemodialysis patients infected with hepatitis C virus-early evolution and rapid progression. *Clin Nephrol* 1999; **51**: 321-323
4 **Mailloux LU**, Bellucci AG, Wilkes BM, Napolitano B, Mossey RT, Lesser M, Bluestone PA. Mortality in dialysis patients: analysis of the causes of death. *Am J Kidney Dis* 1991; **18**: 326-335
5 **Remuzzi G.** Bleeding in renal failure. *Lancet* 1988; **1**: 1205-1208
6 **Yamagata M**, Kanematsu T, Matsumata T, Nishizaki T, Utsunomiya T, Sugimachi K, Okuda S. Possibility of hepatic resection in patients on maintenance hemodialysis. *Hepatogastroenterology* 1993; **40**: 249-252
7 **Cheng SB**, Wu CC, Shu KH, Ho WL, Chen JT, Yeh DC, Liu TJ, P'eng FK. Liver resection for hepatocellular carcinoma in patients with end-stage renal failure. *J Surg Oncol* 2001; **78**: 241-246; discussion 246-247
8 **Yeh CN,** Lee WC, Chen MF. Hepatic resection and prognosis for patients with hepatocellular carcinoma larger than 10 cm: two decades of experience at Chang Gung memorial hospital. *Ann Surg Oncol* 2003; **10**: 1070-1076
9 **Huang CC.** Hepatitis in patients with end-stage renal disease. *J Gastroenterol Hepatol* 1997; **12**: S236-S241
10 **Hung CC.** Dialysis therapy in Taiwan: 1995 National Surveillance Report. *J Nephrol ROC* 1995; **9**: 71-83
11 **Huang CC,** Wu MS, Lin DY, Liaw YF. The prevalence of hepatitis C virus antibodies in patients treated with continuous ambulatory peritoneal dialysis. *Perit Dial Int* 1992; **12**: 31-33
12 **Paganini EP.** Overview of anemia associated with chronic renal disease: primary and secondary mechanisms. *Semin Nephrol* 1989; **9**: 3-8
13 **Nomura F,** Ohnishi K, Tanabe Y. Clinical features and prognosis of hepatocellular carcinoma with reference to serum alpha-fetoprotein levels. Analysis of 606 patients. *Cancer* 1989; **64**: 1700-1707
14 **Primary liver cancer in Japan.** Clinicopathologic features and results of surgical treatment. *Ann Surg* 1990; **211**: 277-287
15 **A new prognostic system for hepatocellular carcinoma: a retrospective study of 435 patients: the Cancer of the Liver Italian Program (CLIP) investigators**. *Hepatology* 1998; **28**: 751-755
16 **Yachnin S,** Soltani K, Lester EP. Further studies on the mechanism of suppression of human lymphocyte transformation by human alpha-fetoprotein. *J Allergy Clin Immunol* 1980; **65**: 127–135
17 **Odagiri E**, Jibiki K, Takeda M, Sugimura H, Iwachika C, Abe Y, Kihara K, Kihara Y, Itou M, Nomura T. Effect of hemodialysis on the concentration of the seven tumor markers carcinoembryonic antigen, alpha-fetoprotein, squamous cell carcinoma-related antigen, neuron-specific enolase, CA 125, CA 19-9 and CA 15-3 in uremic patients. *Am J Nephrol* 1991; **11**: 363-368
18 **Chen MF,** Jeng LB, Lee WC. Surgical results in patients with hepatitis virus-related hepatocellular carcinoma in Taiwan. *World J Surg* 2002; **26**: 742-747
19 **Mansour A,** Watson W, Shayani V, Pickleman J. Abdominal operations in patients with cirrhosis: still a major surgical challenge. *Surgery* 1997; **122**: 730-735; discussion 735-736
20 **Margreiter R**, Kramar R, Huber C, Steiner E, Niederwieser D, Judmaier G, Vogel W. Combined liver and kidney transplantation. *Lancet* 1984; **1**: 1077-1078
21 **Jeyarajah DR**, McBride M, Klintmalm GB, Gonwa TA. Combined liver-kidney transplantation: what are the indications? *Transplantation* 1997; **64**: 1091-1096

Science Editor Guo SY **Language Editor** Elsevier HK

PO Box 2345, Beijing 100023, China
www.wjgnet.com
wjg@wjgnet.com

ELSEVIER

World J Gastroenterol 2005;11(14):2072-2079
World Journal of Gastroenterology ISSN 1007-9327

• *LIVER CANCER* •

Expression of heat shock proteins (HSP27, HSP60, HSP70, HSP90, GRP78, GRP94) in hepatitis B virus-related hepatocellular carcinomas and dysplastic nodules

Seung Oe Lim, Sung Gyoo Park, Jun-Hi Yoo, Young Min Park, Hie-Joon Kim, Kee-Taek Jang, Jae Won Cho, Byung Chul Yoo, Gu-Hung Jung, Cheol Keun Park

Seung Oe Lim, Sung Gyoo Park, Jun-Hi Yoo, Guhung Jung, School of Biological Sciences, Seoul National University, Seoul, Korea
Young Min Park, Hepatology Center and Laboratory of Hepatocarcinogenesis, Bundang Jesaeng General Hospital, Kyungkido, Korea
Hie-Joon Kim, School of Chemistry, Seoul National University, Seoul, Korea
Kee-Taek Jang, Cheol Keun Park, Department of Pathology, Samsung Medical Center, Sungkyunkwan University School of Medicine, Seoul, Korea
Jae Won Cho, General Surgery, Samsung Medical Center, Sungkyunkwan University School of Medicine, Seoul, Korea
Byung Chul Yoo, Internal Medicine, Samsung Medical Center, Sungkyunkwan University School of Medicine, Seoul, Korea
Supported by the fund from the Korea Science and Engineering Foundation (Grant No. R01-2001-00098). Seung Oe Lim was supported by BK21 Research Fellowship from the Ministry of Education and Human Resources Development
Co-correspondents: Cheol Keun Park and Guhung Jung
Correspondence to: Cheol Keun Park, MD, PhD, Department of Pathology, Samsung Medical Center, Sungkyunkwan University School of Medicine, Seoul 135-710, Korea. ckpark@smc.samsung.co.kr
Telephone: +82-2-3410-2766 Fax: +82-2-3410-0025
Received: 2004-10-05 Accepted: 2004-12-08

Abstract

AIM: Expression of heat shock proteins (HSPs) is frequently up-regulated in hepatocellular carcinoma (HCC), which evolves from dysplastic nodule (DN) and early HCC to advanced HCC. However, little is known about the differential expression of HSPs in multistep hepatocarcinogenesis. It was the purpose of this study to monitor the expression of HSPs in multistep hepatocarcinogenesis and to evaluate their prognostic significance in hepatitis B virus (HBV)-related HCC.

METHODS: Thirty-eight HCC and 19 DN samples were obtained from 52 hepatitis B surface antigen-positive Korean patients. Immunohistochemical and dot immunoblot analyses of HSP27, HSP60, HSP70, HSP90, glucose regulated protein (GRP)78, and GRP94 were performed and their expression at different stages of HCC development was statistically analyzed.

RESULTS: Expression of HSP27, HSP70, HSP90, GRP78, and GRP94 increased along with the stepwise progression of hepatocarcinogenesis. Strong correlation was found only in GRP78 (Spearman's $r = 0.802$). There was a positive correlation between the expressions of GRP78, GRP94, HSP90, or HSP70 and prognostic factors of HCC. Specifically, the expression of GRP78, GRP94, or HSP90 was associated significantly with vascular invasion and intrahepatic metastasis.

CONCLUSION: The expressions of HSPs are commonly up-regulated in HBV-related HCCs and GRP78 might play an important role in the stepwise progression of HBV-related hepatocarcinogenesis. GRP78, GRP94, and HSP90 may be important prognostic markers of HBV-related HCC, strongly suggesting vascular invasion and intrahepatic metastasis.

Key words: Heat shock protein; Hepatocellular carcinoma; Dysplastic nodule; Hepatocarcinogenesis; Immunohistochemistry; Dot immunoblot analysis

Lim SO, Park SG, Yoo JH, Park YM, Kim HJ, Jang KT, Cho JW, Yoo BC, Jung GH, Park CK. Expression of heat shock proteins (HSP27, HSP60, HSP70, HSP90, GRP78, GRP94) in hepatitis B virus-related hepatocellular carcinomas and dysplastic nodules. *World J Gastroenterol* 2005; 11(14): 2072-2079
http://www.wjgnet.com/1007-9327/11/2072.asp

INTRODUCTION

Worldwide hepatocellular carcinoma (HCC) is a common malignant tumor that takes the lives of about one million people annually. Even after resection, the overall survival rate of patients with HCC is still unsatisfactory due to frequent recurrences[1]. Hepatitis B virus (HBV) is one of the known risk factors for HCC, but it is not yet clear how this factor leads to HCC[1]. HCC is characterized by multistage process of tumor progression. Recently, dysplastic nodule (DN) has been described as a precancerous lesion in the multistep hepatocarcinogenesis and is divided into low grade and high grade DN depending on the degree of cytologic atypia on histological examination[2]. Early HCC does not destroy the underlying liver structure and is uniformly composed of well differentiated cancer cells with little cellular atypia. At the tumor-nontumor boundary, well-differentiated cancer cells proliferate as though they are replacing normal hepatocytes ('replacing growth')[3,4]. The appearance of a regenerative nodule in the liver might be the first step of

hepatocarcinogenesis, subsequently developing into advanced HCC through low-grade dysplastic nodule (LGDN), high-grade dysplastic nodule (HGDN), and early HCC (in a multistep fashion)[5]. However, the molecular mechanisms implicated in the progression to HBV-related HCC remain largely unknown.

Mammalian cells express a family of highly conserved proteins in response to heat as well as many other stressful stimuli[6]. This family of stress proteins include heat shock proteins (HSPs) and glucose regulated proteins (GRPs)[7,8]. These proteins are multifunctional molecular chaperones. In neoplasms, expression of HSP has been implicated in the regulation of apoptosis, in immune response against tumors, and in multidrug resistance[9,10]. Increased HSP levels make cells to be more resistant to apoptosis. HSP, being one of the most immunogenic molecules known, can also act by increasing cellular immunity[11]. Understanding the roles of HSPs in carcinogenesis has important implications regarding tumor behavior and potential prognostics[12].

Up-regulated expression of HSPs has been reported in several cancers (e.g., breast cancer, renal cancer, various leukemias, bladder cancer, *etc.*)[13-16]. The overexpression of HSPs in tumorous tissues has been implicated to have prognostic value in patients with breast, renal, and bladder cancer[13,17]. Recently, we have observed up-regulation of HSP60, HSP70, HSP90, GRP78, and GRP94 in HCCs by proteome analysis[18,19]. Correlation between HSP27 expression and histological grade and survival of patients with HCC has been reported[20]. Tanaka *et al*[21], reported that the expression of GRP94 mRNA increased along with the histological grade of the HCC. However, the prognostic significance of the expression of HSPs in HCC is largely unknown at this time and so further studies are needed. Also, it is not known whether the expression of HSPs play a role in the initiation or progression of HBV-related multistep hepatocarcinogenesis. In the present study, in order to determine whether the expression of the HSPs is involved in HBV-related hepatocarcinogenesis, and if so, to which stage it is linked, we performed immunohistochemical (IHC) and dot immunoblot analyses of HSP27, HSP60, HSP70, HSP90, GRP78, and GRP94 on a series of hepatocellular tumors which includes premalignant lesions.

MATERIALS AND METHODS

Tissue specimen and histopathology

Immediately after hepatectomy for primary HCC, freshly removed liver tissues were serially sliced from top to bottom edge at 4-5 mm intervals and then examined by a pathologist (C.K.P.) for the presence of nodular lesions. Any nodules greater than 10 mm in diameter and any bulging nodules different in color macroscopically, from the surrounding liver, regardless of size, were snap-frozen in liquid nitrogen and stored at -80 ℃. Subsequent sections from the same nodule were fixed in 10% neutral formalin for confirming morphological diagnosis. Early HCC was matched to the diagnostic criteria of Liver Cancer Study Group of Japan[22]. Advanced HCCs were graded histologically according to the Edmondson and Steiner's criteria[23], and DNs were subdivided into LGDN and HGDN by two pathologists (C.K.P. and K.J.), according to the guidelines of the International Working Party[2]. From this, 38 HCCs (early HCC, 5; Edmondson grade I HCC, 12; grade II, 11; grade III, 10 cases) and 19 DNs (LGDN, 11; HGDN, 8) were obtained from 52 Korean patients at Samsung Medical Center between 2000 and 2003. Informed consent was obtained from each patient included in the study. Non-tumorous tissues were taken far from the tumor as possible and were snap-frozen in liquid nitrogen and stored at -80 ℃. Non-tumorous liver revealed cirrhosis in 48 patients and chronic hepatitis in four. None of the patients had any preoperative chemotherapy. All patients were seropositive for hepatitis B surface antigen but had no serum antibody against hepatitis C virus. Among the 38 patients with HCC, 28 were men and 10 were women with a mean age of 50 years (range 25-65 years). Thirteen of the 14 patients with DNs were men and 1 was a woman with a mean age of 52 years (range 33-62 years). The histopathologic features of HCCs examined were histological differentiation, tumor size, tumor capsule formation, microvascular invasion, major portal vein invasion, intrahepatic metastasis, and tumor stage. Microvascular invasion was considered as present when at least one or more endothelial cells or the tunica media of the vessel were recognized to surround a neoplastic cell group. Intrahepatic metastasis and tumor capsule formation were matched to the criteria of the Liver Cancer Study Group of Japan[22]. The tumor stage was determined according to the AJCC cancer staging criteria[24]. Blocks of normal liver were prepared as controls from five patients with metastatic colonic carcinoma of the liver.

Immunohistochemistry

Formalin-fixed, paraffin-embedded tissue including both HCC or DN and adjacent non-tumorous liver were sectioned with 4 μm thickness. IHC study was performed using the streptavidin-biotin complex method and TechMate™ 1 000 automated staining system (DakoChemmate, Glostrup, Denmark). Primary antibodies used and working dilutions employed are as follows: HSP27 mouse monoclonal antibody (mAb) (SPA-800, StressGen, Victoria, Canada) (1∶200), HSP60 mouse mAb (SPA-806, StressGen) (1∶1 500), HSP70 mouse mAb (sc-24, Santa Cruz, San Francisco, USA) (1∶200), HSP90 mouse mAb (sc-13 119, Santa Cruz) (1∶800), GRP78 goat polyclonal antibody (pAb) (sc-1050, Santa Cruz) (1∶30), and GRP94 rat mAb (SPA-850, StressGen) (1∶1 600). Deparaffinized sections were treated with 3% hydrogen peroxide in methanol for 10 min to inhibit endogenous peroxidase. Sections were immersed in 0.05 mol/L citrate buffer (pH 6.0) and heated in a microwave oven for 10 min. Sections were then incubated with the primary antibody for 60 min at room temperature. Each section was treated sequentially with biotinylated secondary antibody (anti-mouse or anti-goat immunoglobulin) and streptavidin–peroxidase complex (DakoChemmate). 3,3'-diaminobenzidine tetrahydrochloride was used as a chromogen, and then Mayer's hematoxylin counterstain was applied. Negative controls (isotype-matched irrelevant antibody or preimmune goat serum as primary antibody) were made to run simultaneously. The results of staining were evaluated by two independent pathologists (C.K.P. and K.J.) and the difference in interpretation was resolved by consensual agreement. At least equally intensive nuclear or cytoplasmic staining

compared with bile ducts was considered positive[25]. Positive cells were counted by monitoring at least 1 000 cells in HCC or DN and non-tumorous liver from more than five high power fields where positive cells were present at a relatively uniform density. For each tissue section, staining was assessed as negative (0-5% positive cells), + (6-25% positive cells), ++ (26-50% positive cells), +++ (51-75% positive cells), or ++++ (>75% positive cells).

Immunoblot analysis

Sample preparation and immunoblot analysis were performed as previously described[19]. All samples were diluted at 2 μg/μL. Protein samples (10-20 μg) were subjected to SDS-PAGE and transferred to polyvinylidene difluoride membrane. Primary antibodies, β-actin mAb (Sigma, St. Louis, USA) (1∶5 000), HSP27 mAb (StressGen) (1∶1 000), HSP60 mAb (StressGen) (1∶10 000), HSP70 mAb (Santa Cruz) (1∶1 000), HSP90 mAb (Santa Cruz) (1∶1 000), GRP78 mAb (Santa Cruz) (1∶500), and GRP94 mAb (StressGen) (1∶1 000) were diluted in PBS/5% skim milk/0.1% Tween 20.

Dot immunoblot analysis

Before performing dot immunoblot analysis, each antibody was validated for specificity by performing immunoblot analysis as described above, using the same tissue protein sample. The linear range of loading volume in the dot immunoblot analysis was tested using serially diluted protein samples. Using Bio Dot™ (Bio-Rad, Hercules, USA), protein samples (0.8-1.6 μg) were loaded onto each well of dot blot apparatus and transferred to polyvinylidene difluoride membrane overnight at 4 ℃. Every protein sample was loaded as a triplicate. Same primary antibodies were used in immunoblot analysis above. The rest of the experimental procedure was the same except that the membrane was washed for 2 h with PBS/0.13% Tween 20. Using the ImageMaster 2D Elite software 4.01 (Amersham, Upsala, UK), the intensity of the dot was determined by integrating the optical density over the spot area (dot volume). The changes in the expression of HSPs were evaluated by dividing the dot volume of tumor by that of non-tumorous tissue.

Statistical analysis

The relationship between the expression of HSPs and hepatocellular tumors including DNs was analyzed by calculating Spearman's correlation coefficient (r). The relationship between the enhancement of expression of HSPs and hepatocellular tumors in dot immunoblot analysis was analyzed by Jonckheere-Terpstra test. Correlation between the expression of HSPs and prognostic factors of HCCs was analyzed by Jonckheere-Terpstra test, Mann-Whitney test, or Kruskal-Wallis test. P values of less than 0.05 were considered statistically significant.

RESULTS

Immunohistochemical analysis

In our earlier proteome analysis, we observed that the expression of many HSPs increased in HCC[18,19]. However, the determination of how the level of expression changes during the stepwise progression of hepatocarcinogenesis was not identified. So, we performed IHC analysis on a series of hepatocellular tumors including DNs. Immunoreactivity for HSP27, HSP60, or HSP90 was observed only in the cytoplasm of hepatocytes of tumor tissues. Immunoreactivity for HSP70 was observed in both the nucleus and cytoplasm, and, in most cases, the intensity of staining of the cytoplasm corresponded to that of the nucleus. Immunoreactivity for GRP78 or GRP94 was observed mostly in the cytoplasm, but was also observed in the nucleus although rarely. The bile duct epithelium always showed cytoplasmic immunoreactivity and thus served as an internal standard of positive staining (Figure 1D). There was a higher expression of HSP27, HSP90, GRP78, or GRP94 in HCC than in the adjacent non-tumorous liver. The expression of HSP60 in HCC was similar to that in the non-tumorous liver. There was either no immunoreactivity or focal staining for HSP70 in the non-tumorous liver (Table 1). Immunoreactivity for HSPs in normal livers was similar to that in the non-tumorous liver. Positive immunoreactivity (>5% positive hepatocytes) for HSP27 was demonstrated in 10.5% of DNs and 76.3% of HCCs. The proportion of positive immunoreactivity was 100% in DNs and 97.4% in HCCs for HSP60, 0% in DNs and 68.4% in HCCs for HSP70, 5.3% in DNs and 55.3% in HCCs for HSP90, 63.2% in DNs and 94.7% in HCCs for GRP78, and 68.4% in DNs and 86.8% in HCCs for GRP94 (Table 1 and Figure 1).

Expression of HSP27, HSP70, HSP90, GRP78, and GRP94 increased along with the stepwise progression of hepatocarcinogenesis (from LGDN to HCC grade III) (Spearman's r = 0.6-0.802). Strong correlation was found only in GRP78 (Spearman's r = 0.802) (Figures 1F-H). Expression of HSP60 decreased along with the stepwise progression of hepatocarcinogenesis (P = 0.012), but with weak correlation (Spearman's r = -0.329) (Table 1).

Dot immunoblot analysis

It was deemed necessary to confirm the IHC results by immunoblot analysis. However, conventional immunoblot analysis involves separation of the tissue proteins by SDS-PAGE and takes much time. Therefore, faster dot immunoblot analysis was used. In dot immunoblot analysis, the expression level of a certain protein can be determined simultaneously from 96 tissue samples using 96 wells on a plate. Smaller amount of protein is needed than by immunoblot analysis (dot immunoblot, 0.8-1.6 μg; immunoblot, 20-30 μg).

Before investigating the expression of six HSPs (HSP27, HSP60, HSP70, HSP90, GRP78, GRP94) in hepatocellular tumors by dot immunoblot analysis, validity of the dot immunoblot method was established by analyzing the expression levels of HSP27, HSP60, and HSP90 in the same tissue protein samples by both the dot immunoblot analysis and the immunoblot analysis. Figure 2 shows that consistent results are obtained by the two methods for all three proteins (P = 0.000, P = 0.034, P = 0.003 for HSP27, HSP60, HSP90, respectively). Figure 2 also shows the reproducibility by the three replicate dot immunoblot analyses of the same sample.

Dot immunoblot analysis showed up-regulation (≥1.5-fold increase) in 15.8% of DNs and 68.4% of HCCs for HSP27, 15.8% of DNs and 52.6% of HCCs for HSP60,

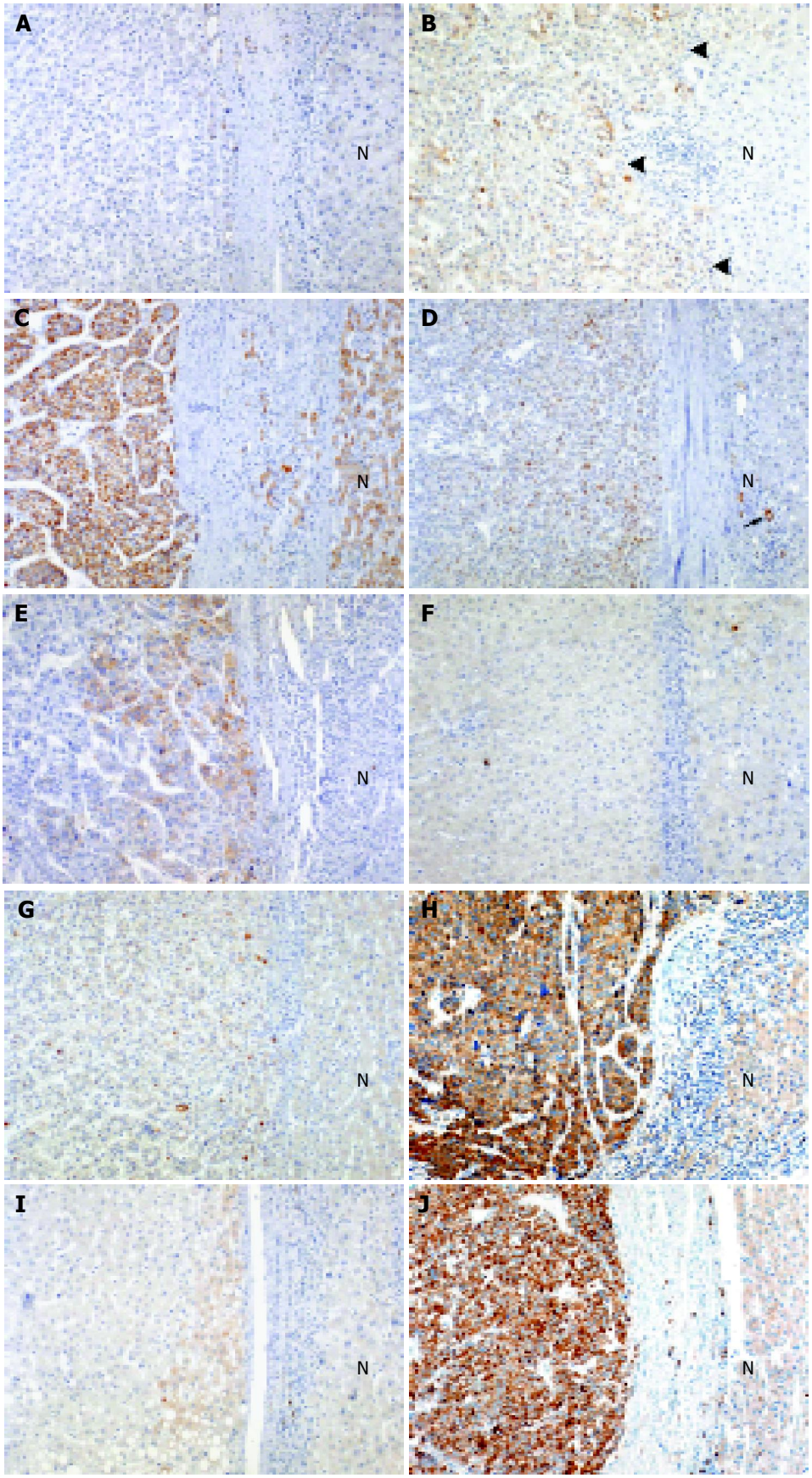

Figure 1 IHC staining of HSP in DN and HCC (original magnification, ×100). A: Rare immunoreactivity for HSP27 in high-grade DN; B: 25% immunoreactivity for HSP27 in early HCC. The borders between early HCC and non-tumorous liver are indicated by arrowheads; C: 96% immunoreactivity for HSP60 in HCC Grade II; D: 30% immunoreactivity for HSP70 in HCC Grade I. Bile duct epithelium shows cytoplasmic immunoreactivity (arrow); E: 35% immunoreactivity for HSP90 in HCC Grade II; F: Rare immunoreactivity for GRP78 in low-grade DN; G: 10% immunoreactivity for GRP78 in HCC Grade I; H: 93% immunoreactivity for GRP78 in HCC Grade III; I: 15% immunoreactivity for GRP94 in high-grade DN; J: 95% immunoreactivity for GRP94 in HCC Grade III. N, non-tumorous liver.

Table 1 Expression of HSPs in hepatocarcinogenesis obtained by IHC analysis

HSP	Percentage of positive cells (%)	NL	DN		HCC				*P* (*r*)
		(*n* = 57)	LGDN (*n* = 11)	HGDN (*n* = 8)	E-HCC (*n* = 5)	GI (*n* = 12)	GII (*n* = 11)	GIII (*n* = 10)	
HSP27	0-5	42	11	6		5	2	2	
	6-25	12		2	4	5	3	3	0.000[1]
	26-50	3					2	1	(0.600)
	51-75				1	1	2		
	>75					1	2	4	
HSP60	0-5							1	
	6-25								0.012[1]
	26-50	3					3		(–0.329)
	51-75	2						1	
	>75	52	11	8	5	12	8	8	
HSP70	0-5	57	11	8	3	4	3	2	
	6-25				1	3	2		0.000[1]
	26-50				1	3	2	1	(0.669)
	51-75					1	2	4	
	>75					1	2	3	
HSP90	0-5	56	10	8	5	8	4		
	6-25	1	1			2	4	3	0.000[1]
	26-50					2	2	3	(0.707)
	51-75						1	2	
	>75							2	
GRP78	0-5	5	6	1	1	1			
	6-25	22	5	7	4	5	2		0.000[1]
	26-50	17				1	2	1	(0.802)
	51-75	9				3	2	1	
	>75	4				2	5	8	
GRP94	0-5	16	3	3	2	1	2		
	6-25	26	7	4	2	2			0.000[1]
	26-50	9	1	1	1	7	3	2	(0.708)
	51-75	3				1	3		
	>75	3				1	3	8	

NL: non-tumorous liver; DN: dysplastic nodule; LGDN: low-grade DN; HGDN: high-grade DN; HCC: hepatocellular carcinoma; E: early; G: Edmondson-Steiner's grade; *n*: number of cases; *P*: Spearman correlation (from LGDN to HCC GIII); (*r*): Correlation coefficient; [1]Value was statistically significant.

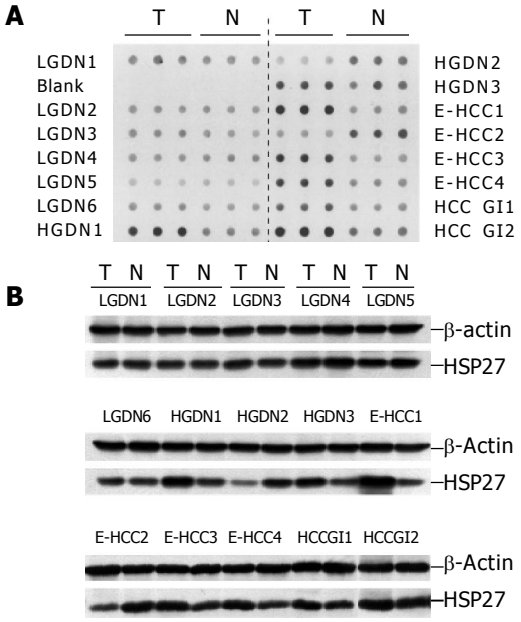

Figure 2 Examples of dot immunoblot and immunoblot analysis of HSP27 in the same tissue samples. A: Dot immunoblot analysis of HSP27 in tumor (T) and non-tumorous tissue (N) of 15 patients (LGDN, six; HGDN, three; E-HCC, four; HCC GI, two cases); B: Immunoblot analysis of HSP27 in tumor and non-tumorous tissue of 15 patients. Dot immunoblotting and immunoblotting with HSP27 monoclonal antibody were performed as described in Materials and Methods. β-actin was used as a reference. The results of dot immunoblot analysis revealed the same expression patterns as the immunoblot analysis. LGDN: low-grade dysplastic nodule, HGDN: high-grade dysplastic nodule, E: early, HCC: hepatocellular carcinoma, G: Edmondson-Steiner's grade.

31.6% of DNs and 65.8% of HCCs for HSP70, 42.1% of DNs and 73.7% of HCCs for HSP90, 52.6% of DNs and 71.1% of HCCs for GRP78, and 57.9% of DNs and 65.8% of HCCs for GRP94 (Table 2).

Expression of HSP27 increased along with the stepwise progression of hepatocarcinogenesis (Spearman's $r = 0.407$). Expression of HSP60, HSP90, and GRP78 increased likewise ($P<0.05$), but the correlation was weak (Spearman's $r<0.4$) (Table 2). There was a significant correlation between the expression levels of HSP27, HSP60, HSP90, and GRP78 and hepatocellular tumors including DNs ($P = 0.018$, $P = 0.004$, $P = 0.021$, $P = 0.005$, respectively) (Table 3).

Correlation between the expression of HSPs and prognostic factors of HCC

IHC analysis showed a positive correlation between the expression of GRP78 or GRP94 and poorer histological grade of differentiation, tumor size of >2 cm, lack of tumor capsule, microvascular invasion, major portal vein invasion, intrahepatic metastasis, and higher tumor stage. Expression of HSP90 was significantly associated with six prognostic factors except for tumor size. Expression of HSP70 was significantly correlated with poorer histological grade of differentiation, lack of tumor capsule, and microvascular invasion. Specifically, there was a significant correlation between the expression of GRP78, GRP94, or HSP90 and microvascular invasion, major portal vein invasion, and intrahepatic metastasis (Table 4).

Table 2 Expression of HSPs in hepatocarcinogenesis obtained by dot immunoblot analysis

HSP	Tumor/ non-tumor	DN		HCC				*P* (*r*)
		LGDN (*n* = 11)	HGDN (*n* = 8)	E-HCC (*n* = 5)	GI (*n* = 12)	GII (*n* = 11)	GIII (*n* = 10)	
HSP27	< 0.5		1	1				
	0.5–1.5	9	6		3	4	4	0.002[1]
	1.5–2.5	2	1	2	6	2	2	(0.407)
	> 2.5			2	3	5	4	
HSP60	< 0.5				1			
	0.5–1.5	10	6	4	4	5	4	0.004[1]
	1.5–2.5	1	2	1	4	6	4	(0.372)
	> 2.5				3		2	
HSP70	< 0.5							
	0.5–1.5	6	7	3	3	2	5	0.100
	1.5–2.5	5		2	4	8	4	(0.220)
	> 2.5		1		5	1	1	
HSP90	< 0.5			1				
	0.5–1.5	5	6	3	2	2	2	0.007[1]
	1.5–2.5	6	2	1	4	7	6	(0.353)
	> 2.5				6	2	2	
GRP78	< 0.5		1				1	
	0.5–1.5	5	3	3	2	3	2	0.007[1]
	1.5–2.5	5	4	1	4	3		(0.355)
	> 2.5	1		1	6	5	7	
GRP94	< 0.5						1	
	0.5–1.5	7	1	2	1	5	4	0.571
	1.5–2.5	2	6	3	5	4	1	(0.077)
	> 2.5	2	1		6	2	4	

DN: dysplastic nodule; LGDN: low-grade DN; HGDN: high-grade DN; HCC: hepatocellular carcinoma; E: early; G: Edmondson-Steiner's grade; *n*: number of cases; *P*: Spearman Correlation; (*r*): Correlation coefficient; [1]Value was statistically significant.

DISCUSSION

The present study confirms the results from earlier proteomic analysis and shows that HSPs are frequently up-regulated in HCCs. Up-regulation of HSPs in various cancers suggest that they might be involved in tumorigenesis[8]. Enhancement of tumorigenesis by overexpression of HSP27 and HSP70 has been implicated in a rodent model[26-29]. HSPs are known to be essential for the survival of cancer cells in different cancers[16,28,29]. HSPs as molecular chaperones might sustain cancer cells by modulating the activity of different proteins involved in cell cycle and apoptosis. In fact many HSPs are known to regulate apoptosis and even prevent apoptosis induced by anticancer drugs[8]. For example, there has been an implication that HSP27 prevents depolymerization of F-actin by cytochalasin D and subsequent cytochrome C release[30]. HSP70 helps to maintain the genomic stability of telomerase[31]. HSP90 plays a role in breast and prostate cancer by maintaining the functional quality of proteins involved in the progression of cancer[31,32]. Schamhart *et al*[33], reported that HCC cell lines respond to heat stress with a transient increase in the synthesis of HSPs (molecular weights of 107, 89, 70, 68, and 27 ku). Up-regulation of HSP27 and HSP70 in HCCs in microarray studies has been reported[34,35]. Takashima *et al*[36], reported that HSP70,

Table 3 Enhancement of HSP expression relative to non-tumorous tissue in hepatocarcinogenesis obtained by dot immunoblot analysis

Group	*n*	Enhancement of expression (mean±SD)					
		HSP27	HSP60	HSP70	HSP90	GRP78	GRP94
LGDN	11	1.25±0.31	1.07±0.43	1.37±0.45	1.55±0.45	1.65±0.85	1.61±1.02
HGDN	8	1.22±0.72	1.15±0.44	1.32±0.58	1.20±0.32	1.42±0.71	2.45±1.87
E-HCC	5	2.52±1.57	0.93±0.41	1.18±0.49	1.04±0.64	1.72±1.16	1.63±0.54
HCCGI	12	2.17±1.06	1.96±1.20	2.69±1.72	2.76±1.70	7.41±8.65	13.70±25.68
HCCGII	11	3.26±3.19	1.58±0.41	1.80±0.55	1.95±0.56	2.65±1.30	1.87±0.90
HCCGIII	10	2.68±2.34	2.14±1.58	1.66±0.84	2.22±1.33	4.54±4.79	3.02±2.70
P		0.018[1]	0.004[1]	0.123	0.021[1]	0.005[1]	0.373

LGDN: low-grade dysplastic nodule; HGDN: high-grade dysplastic nodule; E: early; HCC: hepatocellular carcinoma; G: Edmondson-Steiner's grade; *n*: number of cases; SD: standard deviation; *P*: Jonckheere-Terpstra test; [1]Value was statistically significant.

Table 4 Correlation between HSP immunostaining and prognostic factors in 38 HCCs

	P					
	HSP27	HSP60	HSP70	HSP90	GRP78	GRP94
Histological grade						
E–HCC (5)						
HCC GI (12)	0.150	0.085	0.009[1]	0.000[1]	0.000[1]	0.000[1]
HCC GII (11)						
HCC GIII (10)						
Tumor size						
≤2 cm (10)	0.097	0.158	0.077	0.079	0.000[1]	0.019[1]
>2 cm (28)						
Encapsulation						
E-HCC (5)						
Positive (27)	0.434	0.634	0.049[1]	0.001[1]	0.011[1]	0.005[1]
Negative (6)						
Microvascular invasion						
Positive (16)	0.413	0.339	0.042[1]	0.000[1]	0.002[1]	0.000[1]
Negative (22)						
Major portal vein invasion						
Positive (3)	0.271	0.489	0.739	0.012[1]	0.050[1]	0.028[1]
Negative (35)						
Intrahepatic metastasis						
Positive (7)	0.798	0.189	0.158	0.000[1]	0.010[1]	0.050[1]
Negative (31)						
Tumor stage						
I (25)						
II (10)	0.800	0.816	0.128	0.000[1]	0.002[1]	0.000[1]
III (3)						

E: early; G: Edmondson-Steiner's grade; ( ): number of cases; *P*: Jonckheere-Terpstra test, Mann–Whitney test, or Kruskal–Wallis test; [1]Value was statistically significant.

HSP70.1, GRP75, and GRP78 were simultaneously up-regulated in hepatitis C virus-related HCCs in proteomic and immunoblot analysis. However, it has not yet been known whether the expression of HSPs is involved in HBV-related multistep hepatocarcinogenesis. We performed IHC and dot immunoblot analyses of HSP27, HSP60, HSP70, HSP90, GRP78, and GRP94 on a series of hepatocellular tumors including premalignant lesions. IHC analysis is used often in clinical studies to investigate the expression of specific proteins. However, immunohistochemistry is inadequate for a quantitative comparison of protein expression in both non-tumorous and tumorous tissues. Thus we performed dot immunoblot analysis which is suitable for quantification of protein expression in multiple samples, in order to supplement the IHC results. Both immunohistochemistry and dot immunoblot analysis showed an overall increase in HSP27, HSP90, and GRP78 correlating with the stepwise progression of hepatocarcinogenesis ($P<0.05$). Dot immunoblot analysis enabled us to quantitatively compare the level of protein expression at various stages of hepatocellular tumor (Table 3).

In IHC analysis, we showed that HSP27, HSP70, HSP90, GRP78, and GRP94 were expressed increasingly correlating with the stepwise progression of HBV-related hepatocarcinogenesis. Strong correlation was found only in GRP78 (Spearman's $r = 0.802$). Moderate correlation (Spearman's $r = 0.4$-0.75) was found in HSP27, HSP70, HSP90, and GRP94. It is possible that HSP expression increases as a result of tumorigenesis, due to stimulation of HSPs by a stressful environment. However, the role of HSPs involved in hepatocarcinogenesis is unknown, at this time. Correlation between HSP27 expression and histological grade in HCC has been reported[20]. Chuma *et al*[25], reported that HSP70 expression gradually increased according to the stepwise progression of hepatocarcinogenesis, which is consistent with the result of this study. Shuda *et al*[37], reported that mRNA and protein expression of GRP78 was up-regulated as the histological grade of HCC increased and that its expression could be regulated by endoplasmic reticulum stress response elements. Tanaka *et al*[21], reported that the expression of GRP94 mRNA increased as the histological grade of HCC increased. To our knowledge, this is the first report of the correlations between the expression of HSP27, HSP90, GRP78, and GRP94 and hepatocellular tumors including premalignant lesions. In this study, GRP78 and GRP94 were commonly up-regulated in DN, although their expression levels were not that high. We think that GRP78 and GRP94 might play a role in the early stage of HBV-related hepatocarcinogenesis.

Progression of HCCs often leads to vascular invasion and intrahepatic metastasis. A tumor capsule may act as a barricade preventing the spread of cancer cells and may have a positive role in the prognosis of HCC[38]. There was a positive correlation between the expression of GRP78, GRP94, HSP90, or HSP70 and prognostic factors of HBV-related HCC, which implies that the expression of these HSPs is closely correlated with tumor progression and aggressive behavior of HCC. In this study, there was no relation between the HSP27 expression and prognostic factors of HBV-related HCC. This is at variance with a previous report by King *et al*[20], who found correlation between HSP27 expression and histological grade of HCC in cases with high rate of HBV infection. The relation between histological grade and HSP27 expression in HBV-related HCC needs further analysis. To our knowledge, this is the first report of the correlation between the expression of GRP78, GRP94, HSP90, and HSP70 and prognostic factors of HCC. Although the implication of the overexpression of GRP78, GRP94, and HSP90 in HCCs is not clear at present, results of this study suggest that the above HSPs could be important prognostic markers of HBV-related HCC, which strongly suggests the presence of vascular invasion and intrahepatic metastasis.

In conclusion, the expressions of HSPs are commonly up-regulated in HCCs and their expression patterns tend to be closely associated with stepwise progression of HBV-related hepatocarcinogenesis. GRP78 might play an important role in the stepwise progression of HBV-related hepatocarcinogenesis. Expression of GRP78, GRP94, HSP90, or HSP70 is closely correlated with tumor progression and aggressive behavior of HBV-related HCC. Specifically, GRP78, GRP94, and HSP90 may be important prognostic markers which strongly suggest the presence of vascular invasion and intrahepatic metastasis.

REFERENCES

1 **Anthony PP.** Hepatocellular carcinoma: an overview. *Histopathology* 2001; **39**: 109-118

2 **Terminology of nodular hepatocellular lesions**. *Hepatology* 1995; **22**: 983-993
3 **Hirohashi S,** Ishak KG, Kojiro M, Wanless IR, Theise ND, Tsukama H, Blum HE, Deugnier Y, Laurent Puig P, Fischer HP, Sakamoto M. Tumors of the liver and intrahepatic bile ducts. Hepatocellular carcinoma In: Hamilton SR, Aaltonen LA, eds. WHO classification. Tumours of the digestive system. 2nd ed. Lyon: *IARC* 2000: 167
4 **Kojiro M.** Pathological evolution of early hepatocellular carcinoma. *Oncology* 2002; **62** Suppl 1: 43-47
5 **Sakamoto M,** Hirohashi S, Shimosato Y. Early stages of multistep hepatocarcinogenesis: adenomatous hyperplasia and early hepatocellular carcinoma. *Hum Pathol* 1991; **22**: 172-178
6 **Lindquist S,** Craig EA. The heat-shock proteins. *Annu Rev Genet* 1988; **22**: 631-677
7 **Little E,** Ramakrishnan M, Roy B, Gazit G, Lee AS. The glucose-regulated proteins (GRP78 and GRP94): functions, gene regulation, and applications. *Crit Rev Eukaryot Gene Expr* 1994; **4**: 1-18
8 **Garrido C,** Gurbuxani S, Ravagnan L, Kroemer G. Heat shock proteins: endogenous modulators of apoptotic cell death. *Biochem Biophys Res Commun* 2001; **286**: 433-442
9 **Ciocca DR,** Clark GM, Tandon AK, Fuqua SA, Welch WJ, McGuire WL. Heat shock protein hsp70 in patients with axillary lymph node-negative breast cancer: prognostic implications. *J Natl Cancer Inst* 1993; **85**: 570-574
10 **Levine AJ,** Momand J, Finlay CA. The p53 tumour suppressor gene. *Nature* 1991; **351**: 453-456
11 **Kaufmann SH.** Heat shock proteins and the immune response. *Immunol Today* 1990; **11**: 129-136
12 **Lebret T,** Watson RW, Fitzpatrick JM. Heat shock proteins: their role in urological tumors. *J Urol* 2003; **169**: 338-346
13 **Lebret T,** Watson RW, Molinie V, O'Neill A, Gabriel C, Fitzpatrick JM, Botto H. Heat shock proteins HSP27, HSP60, HSP70, and HSP90: expression in bladder carcinoma. *Cancer* 2003; **98**: 970-977
14 **Helmbrecht K,** Zeise E, Rensing L. Chaperones in cell cycle regulation and mitogenic signal transduction: a review. *Cell Prolif* 2000; **33**: 341-365
15 **Jaattela M.** Escaping cell death: survival proteins in cancer. *Exp Cell Res* 1999; **248**: 30-43
16 **Jolly C,** Morimoto RI. Role of the heat shock response and molecular chaperones in oncogenesis and cell death. *J Natl Cancer Inst* 2000; **92**: 1564-1572
17 **Mosser DD,** Morimoto RI. Molecular chaperones and the stress of oncogenesis. *Oncogene* 2004; **23**: 2907-2918
18 **Kim W,** Oe Lim S, Kim JS, Ryu YH, Byeon JY, Kim HJ, Kim YI, Heo JS, Park YM, Jung G. Comparison of proteome between hepatitis B virus- and hepatitis C virus-associated hepatocellular carcinoma. *Clin Cancer Res* 2003; **9**: 5493-5500
19 **Lim SO,** Park SJ, Kim W, Park SG, Kim HJ, Kim YI, Sohn TS, Noh JH, Jung G. Proteome analysis of hepatocellular carcinoma. *Biochem Biophys Res Commun* 2002; **291**: 1031-1037
20 **King KL,** Li AF, Chau GY, Chi CW, Wu CW, Huang CL, Lui WY. Prognostic significance of heat shock protein-27 expression in hepatocellular carcinoma and its relation to histologic grading and survival. *Cancer* 2000; **88**: 2464-2470
21 **Tanaka K,** Kondoh N, Shuda M, Matsubara O, Imazeki N, Ryo A, Wakatsuki T, Hada A, Goseki N, Igari T, Hatsuse K, Aihara T, Horiuchi S, Yamamoto N, Yamamoto M. Enhanced expression of mRNAs of antisecretory factor-1, gp96, DAD1 and CDC34 in human hepatocellular carcinomas. *Biochim Biophys Acta* 2001; **1536**: 1-12
22 Liver Cancer Study Group of Japan. The general rules for the clinical and pathological study of primary liver cancer. 4th ed. Tokyo: *Kanehara* 2000: 32-33
23 **Edmondson HA,** Steiner PE. Primary carcinoma of the liver: a study of 100 cases among 48 900 necropsies. *Cancer* 1954; **7**: 462-503
24 **Greene FL,** Page DL, Fleming ID. AJCC cancer staging manual. 6th ed. New York: *Springer* 2002: 132-138
25 **Chuma M,** Sakamoto M, Yamazaki K, Ohta T, Ohki M, Asaka M, Hirohashi S. Expression profiling in multistage hepatocarcinogenesis: identification of HSP70 as a molecular marker of early hepatocellular carcinoma. *Hepatology* 2003; **37**: 198-207
26 **Garrido C,** Fromentin A, Bonnotte B, Favre N, Moutet M, Arrigo AP, Mehlen P, Solary E. Heat shock protein 27 enhances the tumorigenicity of immunogenic rat colon carcinoma cell clones. *Cancer Res* 1998; **58**: 5495-5499
27 **Jaattela M.** Over-expression of hsp70 confers tumorigenicity to mouse fibrosarcoma cells. *Int J Cancer* 1995; **60**: 689-693
28 **Conroy SE,** Latchman DS. Do heat shock proteins have a role in breast cancer? *Br J Cancer* 1996; **74**: 717-721
29 **Gibbons NB,** Watson RW, Coffey RN, Brady HP, Fitzpatrick JM. Heat-shock proteins inhibit induction of prostate cancer cell apoptosis. *Prostate* 2000; **45**: 58-65
30 **Paul C,** Manero F, Gonin S, Kretz-Remy C, Virot S, Arrigo AP. Hsp27 as a negative regulator of cytochrome C release. *Mol Cell Biol* 2002; **22**: 816-834
31 **Jaattela M,** Wissing D, Kokholm K, Kallunki T, Egeblad M. Hsp70 exerts its anti-apoptotic function downstream of caspase-3-like proteases. *EMBO J* 1998; **17**: 6124-6134
32 **Isaacs JS,** Xu W, Neckers L. Heat shock protein 90 as a molecular target for cancer therapeutics. *Cancer Cell* 2003; **3**: 213-217
33 **Schamhart DH,** van Walraven HS, Wiegant FA, Linnemans WA, van Rijn J, van den Berg J, van Wijk R. Thermotolerance in cultured hepatoma cells: cell viability, cell morphology, protein synthesis, and heat-shock proteins. *Radiat Res* 1984; **98**: 82-95
34 **Iizuka N,** Oka M, Yamada-Okabe H, Mori N, Tamesa T, Okada T, Takemoto N, Tangoku A, Hamada K, Nakayama H, Miyamoto T, Uchimura S, Hamamoto Y. Comparison of gene expression profiles between hepatitis B virus- and hepatitis C virus-infected hepatocellular carcinoma by oligonucleotide microarray data on the basis of a supervised learning method. *Cancer Res* 2002; **62**: 3939-3944
35 **Okabe H,** Satoh S, Kato T, Kitahara O, Yanagawa R, Yamaoka Y, Tsunoda T, Furukawa Y, Nakamura Y. Genome-wide analysis of gene expression in human hepatocellular carcinomas using cDNA microarray: identification of genes involved in viral carcinogenesis and tumor progression. *Cancer Res* 2001; **61**: 2129-2137
36 **Takashima M,** Kuramitsu Y, Yokoyama Y, Iizuka N, Toda T, Sakaida I, Okita K, Oka M, Nakamura K. Proteomic profiling of heat shock protein 70 family members as biomarkers for hepatitis C virus-related hepatocellular carcinoma. *Proteomics* 2003; **3**: 2487-2493
37 **Shuda M,** Kondoh N, Imazeki N, Tanaka K, Okada T, Mori K, Hada A, Arai M, Wakatsuki T, Matsubara O, Yamamoto N, Yamamoto M. Activation of the ATF6, XBP1 and grp78 genes in human hepatocellular carcinoma: a possible involvement of the ER stress pathway in hepatocarcinogenesis. *J Hepatol* 2003; **38**: 605-614
38 **Kemeny F,** Vadrot J, Wu A, Smadja C, Meakins JL, Franco D. Morphological and histological features of resected hepatocellular carcinoma in cirrhotic patients in the West. *Hepatology* 1989; **9**: 253-257

Science Editor Guo SY **Language Editor** Elsevier HK

PO Box 2345, Beijing 100023, China
www.wjgnet.com
wjg@wjgnet.com

ELSEVIER

World J Gastroenterol 2005;11(14):2080-2087
World Journal of Gastroenterology ISSN 1007-9327

• *BASIC RESEARCH* •

Controlled and reversible induction of differentiation and activation of adult human hepatocytes by a biphasic culture technique

Marcus K.H. Auth, Kim A. Boost, Kerstin Leckel, Wolf-Dietrich Beecken, Tobias Engl, Dietger Jonas, Elsie Oppermann, Philip Hilgard, Bernd H. Markus, Wolf-Otto Bechstein, Roman A. Blaheta

Marcus K.H. Auth, Universitäts-Kinderklinik Essen, Abteilung für Allgemeine Pädiatrie, Germany
Kim A. Boost, Zentrum der Anästhesiologie und Wiederbelebung, Johann Wolfgang Goethe-Universität, Frankfurt am Main, Germany
Kerstin Leckel, Elsie Oppermann, Wolf-Otto Bechstein, Klinik für Allgemein- und Gefäßchirurgie, Germany
Wolf-Dietrich Beecken, Tobias Engl, Dietger Jonas, Roman A. Blaheta, Klinik für Urologie und Kinderurologie, Zentrum der Chirurgie, Johann Wolfgang Goethe-Universität, Frankfurt am Main, Germany
Philip Hilgard, Universitätsklinikum Essen, Abteilung für Gastroenterologie und Hepatologie, Germany
Bernd H. Markus, Klinik für Allgemein- und Viszeralchirurgie, Städt. Klinikum Kemperhof, Koblenz, Germany
Supported by the "Matthias Lackas-Stiftung", "Paul und Ursula Klein-Stiftung", "Heinrich und Erna Schaufler-Stiftung", "Gisela Stadelmann-Stiftung", and study grants from the Johann Wolfgang Goethe-Universitätsklinikum, Universitätsklinikum Essen (IFORES), and Deutsche Forschungsgemeinschaft (AU 117/4-1)
Correspondence to: Dr. Marcus K.H. Auth, Department of General Pediatrics, Children's Hospital, University of Essen, Hufelandstr. 55, D-45122 Essen, Germany. marcus.auth@uni-essen.de
Telephone: +49-201-723-3632 Fax: +49-201-723-3360
Received: 2004-11-09 Accepted: 2004-11-23

Abstract

AIM: Clinical application of human hepatocytes (HC) is hampered by the progressive loss of growth and differentiation *in vitro*. The object of the study was to evaluate the effect of a biphasic culture technique on expression and activation of growth factor receptors and differentiation of human adult HC.

METHODS: Isolated HC were sequentially cultured in a hormone enriched differentiation medium (DM) containing nicotinamide, insulin, transferrin, selenium, and dexamethasone or activation medium (AM) containing hepatocyte growth factor (HGF), epidermal growth factor (EGF), and granulocyte-macrophage colony-stimulating factor (GM-CSF). Expression, distribution and activation of the HC receptors (MET and EGFR) and the pattern of characteristic cytokeratin (CK) filaments were measured by fluorometry, confocal microscopy and Western blotting.

RESULTS: In the biphasic culture system, HC underwent repeated cycles of activation (characterized by expression and activation of growth factor receptors) and re-differentiation (illustrated by distribution of typical filaments CK-18 but low or absent expression of CK-19). In AM increased expression of MET and EGFR was associated with receptor translocation into the cytoplasm and induction of atypical CK-19. In DM low expression of MET and EGFR was localized on the cell membrane and CK-19 was reduced. Receptor phosphorylation required embedding of HC in collagen type I gel.

CONCLUSION: Control and reversible modulation of growth factor receptor activation of mature human HC can be accomplished *in vitro*, when defined signals from the extracellular matrix and sequential growth stimuli are provided. The biphasic technique helps overcome de-differentiation, which occurs during continuous stimulation by means of growth factors.

Key words: Human hepatocytes; Differentiation; Hepatocyte growth factor; Epidermal growth factor; HGF receptor; EGF receptor; Cytokeratin; Collagen gel

Auth MKH, Boost KA, Leckel K, Beecken WD, Engl T, Jonas D, Oppermann E, Hilgard P, Markus BH, Bechstein WO, Blaheta RA. Controlled and reversible induction of differentiation and activation of adult human hepatocytes by a biphasic culture technique. *World J Gastroenterol* 2005; 11(14): 2080-2087
http://www.wjgnet.com/1007-9327/11/2080.asp

INTRODUCTION

Liver regeneration requires the remaining hepatocytes (HC) not only to retain their ability to proliferate but also to perform all essential functions needed for homeostasis *in vivo*[1]. In recent years, some obstacles encountered during the culturing of human liver cells have been overcome, emphasizing the role of soluble growth factors[2], extracellular matrix (ECM)[3,4], cellular cross-talk[5-7] and the existence of a compartment of progenitor cells[6]. However, little attention has been attributed to the dynamics of this process, which requires adaptation of parenchymal cells to systemic signals and changes in their microenvironment. Sequential coordination of this complex process finally determines if successful regeneration (growth and repair) or irreversible liver failure occurs.

Current *in vitro* models have suggested that *in vitro* growth of HC involves de-differentiation, characterized by induction

of alpha-fetoprotein (AFP) or cytokeratin 19 (CK-19)[2,3,8,9]. In human liver, CK-19 is expressed in fetal hepatic progenitor cells and in mature bile duct epithelial cells, but not in mature HC[10]. Models of HC transplantation suggest that HC proliferation in the adult liver is not associated with de-differentiation[9]. In cell culture models with rat HC, proliferation triggered by hepatocyte growth factor (HGF) and epidermal growth factor (EGF) has been associated with the loss of liver-specific proteins [albumin, cytochrome P450 (CY P450)] and induction of AFP and CK-19[2,3,5,11,12]. Re-differentiation to the HC phenotype has been attributed to the presence of either EHS gel, a basement membrane analogue from the Engelbreth-Holm-Swarm mouse sarcoma, which contains several ECM components and growth factors[2], or collagen type I gel[8]. Growth arrest has been associated with re-differentiation, possibly as a result of decreased expression of growth receptors for EGF (EGFR) and HGF (MET)[2,4].

However, in these systems, the continuous exposure to hepatic mitogens is not physiologic and does not reflect the situation *in vivo*, where paracrine secretion of growth factors and matrix deposition occur in a sequential manner[13]. With regard to organ development, it is well established that tyrosine kinase receptors are critical components in the pertinent response to mesenchymal signals, requiring receptor expression at the appropriate times[14]. In current culture models, continuous exposure of cultured HC to high levels of HGF and EGF has enabled substantial proliferation of rodent HC *in vitro*[2], but subsequent transmission of this model to human HC *in vitro* has not yielded comparable results[4]. Decrease in tyrosine phosphorylation and down-regulation of receptor proteins have been suggested to account for the decline, but as yet this dilemma has not been resolved.

Expansion of mature human HC *in vitro* and controlling their differentiation is essential to employing human liver cells in bioartificial liver support, would help improve the outcome of gene therapy and HC transplantation and would open new perspectives for stem cell engineering. In this paper we describe a novel, defined culture model based upon a biphasic culture technique of human HC. We have analyzed the effects of culture medium providing either factors of metabolic support (differentiation medium (DM), containing dexamethasone, insulin, transferrin, selenium, and high amounts of nicotinamide) or mitogenic stimulation (activation medium (AM), containing moderate amounts of EGF, HGF, granulocyte-macrophage colony-stimulating factor (GM-CSF)) onto expression and bioactivity of MET and EGFR in human HC. We have examined receptor expression, distribution (membrane or cytoplasmic) and functional activity (phosphorylation) of these receptors and the corresponding phenotype of these cells (pattern of CK-18 and CK-19).

We provide compelling evidence that control of differentiation and activation of human HC is feasible in a reversible manner by sequential modulation of soluble nutrients. In contrast to other models, we demonstrate that biological response of human HC to soluble growth factors is not inhibited, but supported by a surrounding 3D ECM, if chemically defined collagen type I gel is applied.

MATERIALS AND METHODS

Human hepatocytes

For isolation of primary human HC, normal human liver tissue was obtained from hemihepatectomy specimen (due to secondary liver metastases) or from unused liver transplant tissue (reduced sized grafts). For cell isolation purposes, the normal hepatic tissue was carefully resected at a safe distance to the tumor tissue and the resection edge. The patients' sex was equally distributed, their age ranged from 20 to 60 years, and tissue was only isolated if primary liver disease was excluded. Informed consent was obtained, and the study was approved by the local ethical committee in accordance with the Declaration of Helsinki. Human HC were isolated by the two-step collagenase perfusion technique and seeded on a 2D collagen I matrix or within a 3D collagen sandwich as described elsewhere[8].

Culture media and incubation protocol

HC were cultured continuously either in a chemically defined DM or AM. Both media consisted of DMEM (Invitrogen, Karlsruhe, Germany), supplemented with 50 mL/L pooled human serum, 20 mmol/L Hepes, and 50 μg/mL gentamycin. DM was enriched with nicotinamide, insulin, transferrin, selenium, and dexamethasone. AM was deprived of hormones but instead enriched with the mitogens EGF, HGF, and GM-CSF. The full description of both media is shown in Table 1.

In subsequent studies, both media were used alternately in 5-d intervals. Freshly isolated HC were incubated with DM (incubation code A) or AM (incubation code B) for 5 d, followed by a switch to AM (incubation code A) or DM (incubation code B) for the next 5 d. Then a further medium change was carried out to recover the initial culture conditions. Figure 1 shows the experimental design.

Table 1 Cell culture media

	DM	AM
	DMEM	DMEM/Ham's F12
	20 mmol/L Hepes	20 mmol/L Hepes
	50 μg/mL gentamycin	50 μg/mL gentamycin
	50 mL/L human serum	50 mL/L human serum
		10 ng/mL EGF
		1 ng/mL HGF
		1 ng/mL GM-CSF
D-glucose	2 g/L	3.15 g/L
Galactose	2 g/L	
Ornithine	0.1 g/L	
L-proline	0.03 g/L	0.02 g/L
Nicotinamide	305 mg/L	2.02 mg/L
$ZnCl_2$	0.544 mg/L	
$ZnSO_4$ $7H_2O$	0.75 mg/L	0.432 mg/L
$CuSO_4$ $5H_2O$	0.2 mg/L	0.0013 mg/L
$MnSO_4$	0.025 mg/L	
L-glutamine	580 mg/L	365 mg/L
ITS[1]	0.5 g/L	
Dexamethasone	1.0 g/L	

[1]ITS = rh-insulin 5.0 mg/L, human transferrin 5.0 mg/L, selenium 5.0 μg/L.

MET and EGFR surface expression

Receptor surface expression was detected using a FACscan

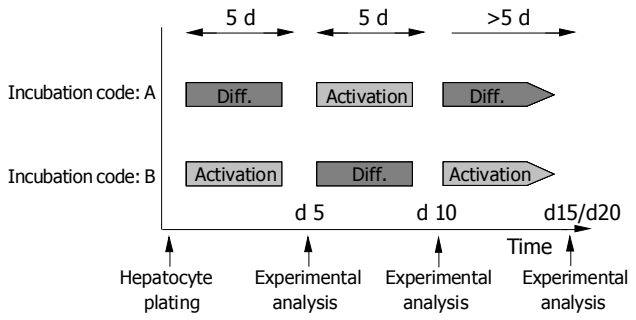

Figure 1 Experimental design. HC were alternately cultured in AM or DM. Environmental switch was carried out on d 5 and 10 after plating. Incubation code A confers to initial incubation in DM, code B to initial incubation in AM. Experimental analysis of HC was carried out on d 5, 10, 15, and 20, if not otherwise indicated.

(Becton Dickinson, Heidelberg, Germany)[8]. The following antibodies were used: anti-MET (rabbit, polyclonal; Santa Cruz Biotechnology, Heidelberg, Germany), anti-EGFR (mouse, clone LA22; Santa Cruz Biotechnology), anti-cytokeratin 18 (mouse, clone Ks18.04; Progen, Heidelberg, Germany), anti-cytokeratin 19 (mouse, clone Ks19.1; Progen). FITC-conjugated goat-anti-rabbit IgG or goat anti-mouse IgG served as the secondary antibody.

Confocal microscopy

HC were plated on round cover slips (pretreated with collagen I) and incubated for 60 min with unconjugated anti-MET or anti-EGFR antibody. Indocarbocyanine (Cy 3™; Dianova; working dilution: 1:50) conjugated goat-anti-mouse IgG or goat anti-rabbit IgG was added as the secondary antibody. Specimens were viewed after embedding in an antifade reagent/mounting medium mixture (ProLong™ Antifade Kit, MoBiTec, Göttingen, Germany) using a confocal laser scanning microscope (LSM 10; Zeiss, Jena, Germany)[6].

Western blot

HC lysates were applied to a 7% polyacrylamide gel and electrophoresed for 90 min at 60 V. The protein was then transferred to nitrocellulose membranes. After blocking, the membranes were incubated overnight with the anti-MET (dilution 1:10 000) or anti-EGFR (dilution 1:100) antibody. HRP-conjugated goat-anti-mouse IgG (Upstate Biotechnology, Lake Placid, NY; dilution 1:5 000) served as the secondary antibody. The membrane was briefly incubated with ECL detection reagent (ECL™, Amersham) to visualize the proteins and exposed to an X-ray film (Hyperfilm™ ECL™, Amersham). The cell line A431 served as the positive control.

Receptor phosphorylation

At several time points after plating, cell culture medium was removed and replaced by a serum- and growth-factor-free medium. After 20-h incubation, HC were stimulated for 3 min with either 10 ng/mL EGF or 1 ng/mL HGF. Subsequently, HC were rinsed with ice-cold PBS, lysed for 5 min in lysis buffer and the Western blot assay was carried out as described above. The monoclonal antibody p-Tyr (Santa Cruz Biotechnology; clone PY99, 1:250 dilution) was used to detect ligand-induced tyrosine phosphorylation.

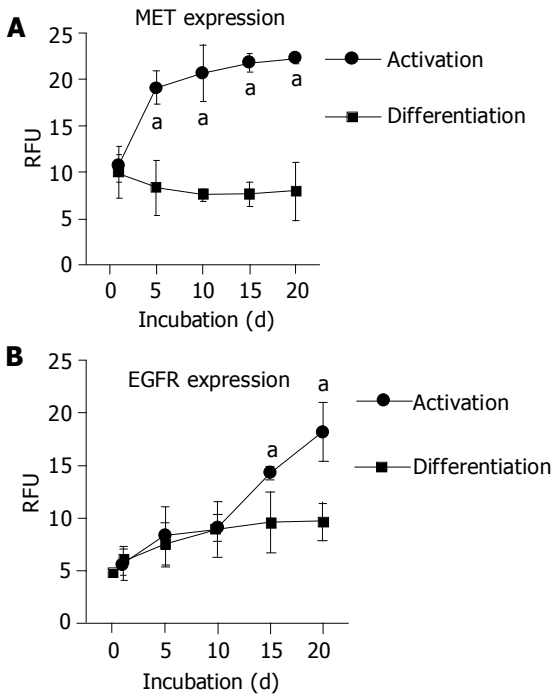

Figure 2 Expression kinetics of growth factor receptors. A: MET expression; B: EGFR expression. HC were permanently cultured either in a AM or in a DM. The receptor level was detected by flow cytometry and expressed as relative fluorescence units (RFU). mean±SD (n = 6), $^aP<0.05$ between groups.

Statistical analysis

All experiments with flow cytometry were performed six times. Data presented in the graphics are expressed as mean±SD. Statistical analysis was conducted by the Wilcoxon-Mann-Whitney-U test. Differences were considered statistically significant at $P<0.05$.

RESULTS

Expression of MET and EGFR

When HC were permanently incubated in AM, membranous MET expression rapidly increased and reached a plateau phase within 10 d. In contrast, MET expression remained low in the continuous presence of growth-factor-free DM (Figure 2A). Confocal examination of receptor distribution, 8 h after HC isolation, demonstrated weak receptor expression mainly along the plasma membrane. Prolonged cultivation in DM typically resulted in distinct surface assembly of MET. This pattern remained stable for 3 wk. A different feature was observed in the presence of AM, as MET strongly accumulated in the cytoplasm, already 5 d after plating out the HC (Figure 3A).

Contrary to the dynamic alterations of MET, membranous EGFR expression was not enhanced by growth factors during the early period of cell cultivation. Rather, EGFR was not up-regulated until after a 10-d lag phase (Figure 2B). Simultaneous confocal analysis showed initial cytoplasmic EGFR location, followed by a strong intracellular accumulation when cultivated in AM, or by a distinct enrichment at the hepatocellular membrane when cultivated in DM (Figure 3B).

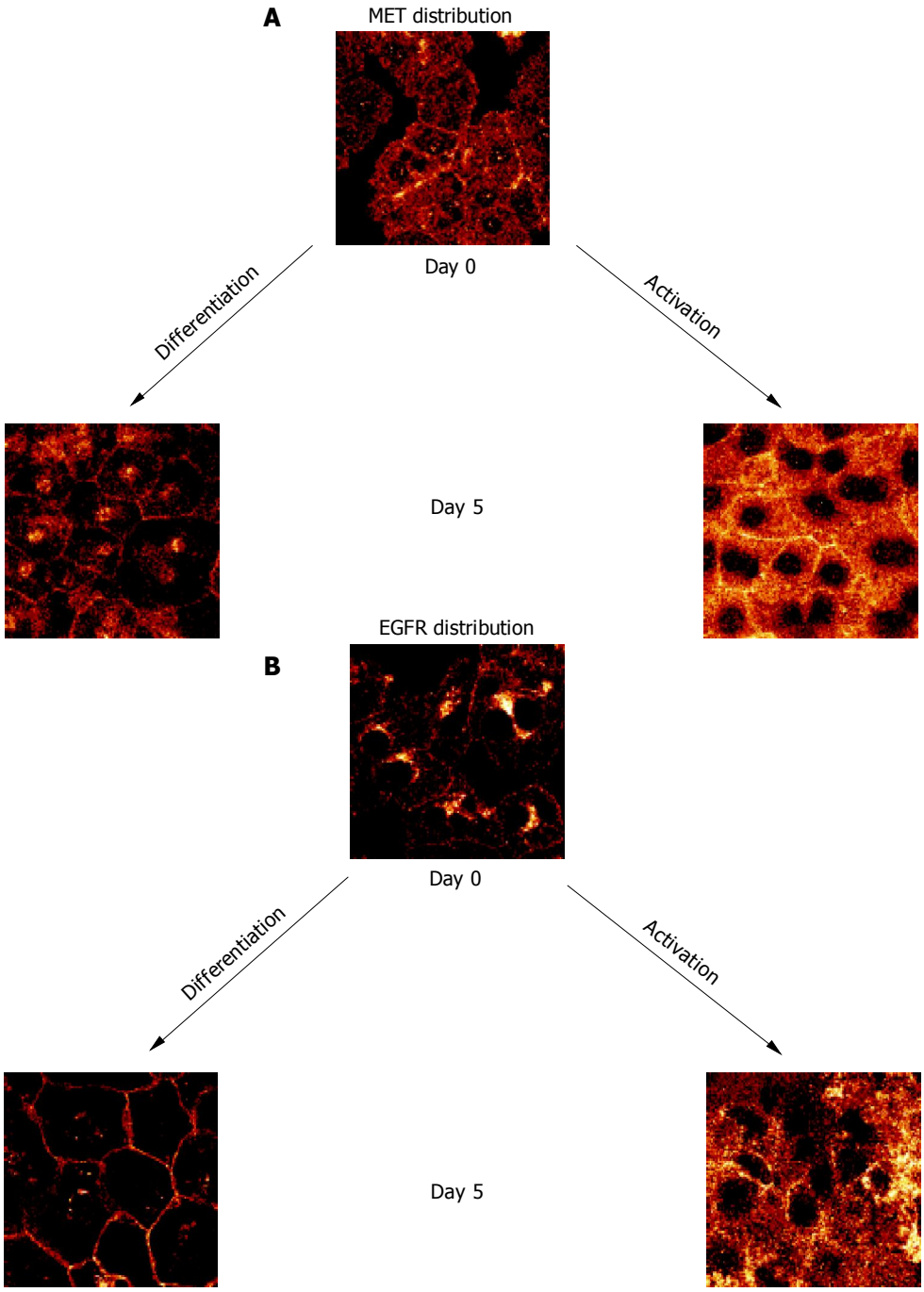

Figure 3 Confocal analysis of distribution pattern of growth factor receptors on d 0 and 5 after culture onset. A: MET distribution; B: EGFR distribution. HC were cultured either in DM or in AM. Indocarbocyanine staining, ×100/1.3 oil immersion objective. Each figure is representative for three separate experiments.

Reversible induction of differentiation and activation of human HC in a biphasic culture system

When using DM and AM alternately, MET and EGFR expression kinetics strictly followed the extracellular conditions. When HC were initially treated with DM for 5 d, MET remained constant during this time (Figure 4A, code A). However, the subsequent switch to AM evoked a nearly two-fold increase in MET by d 10. This process was reversible, as the MET level nearly returned to basal values when the initial culture conditions were established again (d 20). Reversal of the differentiation status was also possible when HC were cultured in the order AM-DM-AM (Figure 4A, code B).

In good accordance with the fluorometric analyses, Western blot data showed reversible changes of total MET protein content, which were strongly dependent on the cell culture conditions (Figure 5).

Similar changes were observed with respect to the EGFR. However, due to the lag phase of the EGFR expression kinetics, which has been demonstrated in Figure 2B, reversible receptor changes in response to the cell culture medium did not occur immediately (as seen with respect to MET expression), but with 5-10 d delay (Figure 4B).

As CK are well-established differentiation markers, all

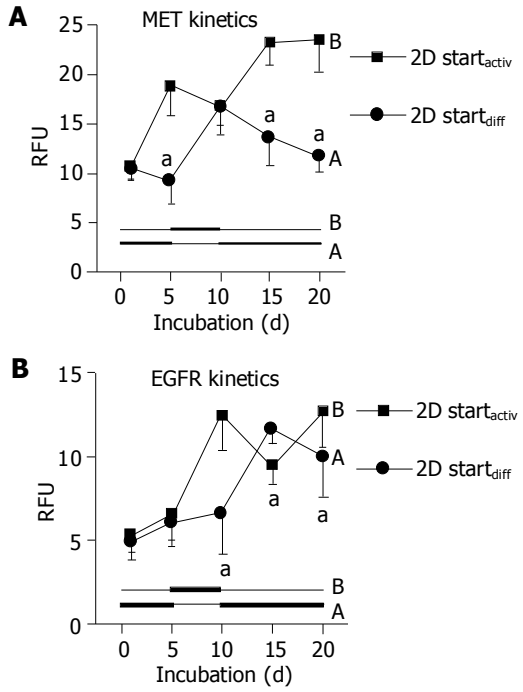

Figure 4 Dynamics of growth factor receptor expression. A: MET kinetics; B: EGFR kinetics. HC were plated on a 2D collagen matrix and incubated alternately in AM or DM. Code A (2D start$_{diff}$) is related to initial 5-d incubation in DM, followed by 5-d incubation in AM and subsequent incubation in DM. Code B (2D start$_{activ}$) concerns the incubation order AM-DM-AM. The receptor level was detected by flow cytometry and expressed as RFU. mean±SD (n = 6), ^aP<0.05 between groups.

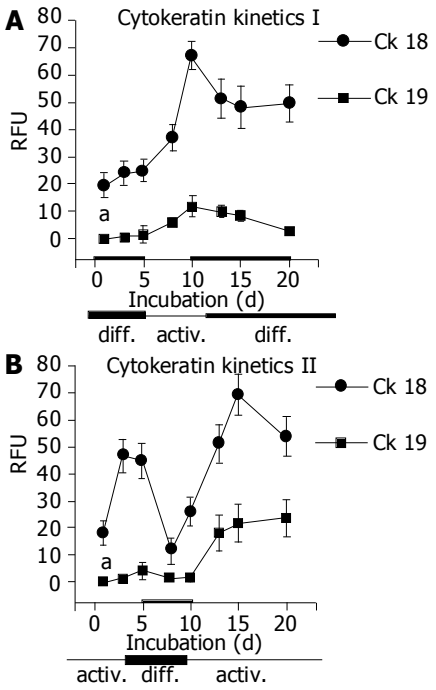

Figure 6 CK 18 and 19 expression, several time points after cell plating. A: Kinetic part I is related to initial 5-d incubation in DM, followed by 5-d incubation in AM and subsequent incubation in DM; B: Kinetic part II is related to the incubation order AM-DM-AM. HC were seeded on a 2D collagen matrix and incubated alternately in AM or DM. CK level was detected by flow cytometry and expressed as RFU. mean±SD (n = 6); ^aP<0.05 between groups.

experiments were repeated with respect to CK-18 and CK-19 expression. AM triggered up-regulation of CK-18 and de novo expression of CK-19. In contrast, DM evoked stable CK-18 expression level and prevented CK-19 synthesis. The processes were reversible, a switch from AM to DM was paralleled by a strong down-regulation of both CK-18 and CK-19. The subsequent switch to AM increased the filament expression level again. CK-18 and CK-19 were also regulated in a reversible manner when HC were cultured in the order DM-AM-DM (Figures 6 and 7).

Dynamics of growth receptor distribution in the biphasic culture system

Figure 8 shows that EGFR localization followed the time-dependent medium changes in a reversible manner. When freshly isolated HC were initially incubated in AM up to d 5, and then exposed to DM (d 5 until d 10), intracellular EGFR became re-distributed along the plasma membrane (Figure 8A). In contrast, cultivation in the order DM up to d 5, AM from d 5 until d 10, was accompanied by a loss of EGFR surface expression, and a rapid internalization of this receptor (Figure 8B). A further switch back to DM was paralleled by a distinct re-accumulation of EGFR onto the surface of the plasma membrane (Figure 8C), which corresponds to the initial culture state.

Receptor phosphorylation depends on three-dimensional cell shape

When HC were seeded on a 2D collagen matrix, only a weak MET phosphorylation signal was detected in the early

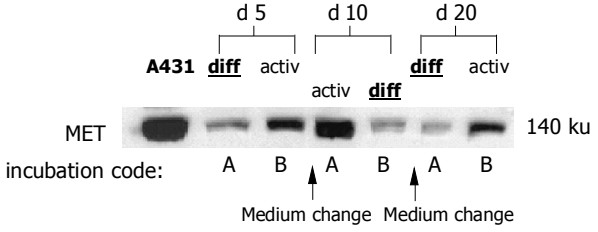

Figure 5 Western blot analysis of MET protein content. HC were incubated alternately in AM or DM. Medium was changed on days 5 and 10. Incubation code A indicates initial 5-d incubation in DM, followed by 5-d incubation in AM and subsequent incubation in DM. Incubation code B is related to initial incubation in AM, followed by incubation in DM and, subsequently, in AM. A431 cells served as positive controls. The blots are representative for three separate experiments.

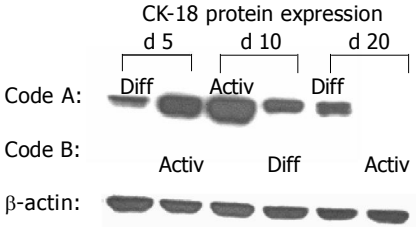

Figure 7 Western blot analysis of CK 18 protein content. HC were incubated alternately in AM or DM. Medium was changed on d 5 and 10. Code A indicates initial 5-d incubation in DM, followed by 5-d incubation in AM and subsequent incubation in DM. Code B is related to initial incubation in AM, followed by incubation in DM and, subsequently, in AM. β-actin served as the internal control. The blot is representative for three separate experiments.

cultivation period, independent of the cell culture medium used (Figure 9, right lanes, d 5). However, when HC retained their 3D structure by embedding them in a 3D collagen sandwich, a distinct activation of MET was evoked in response to a short-course stimulus by soluble HGF. The response was strongly dependent on the extracellular milieu. Figure 9, left lanes, demonstrates that MET phosphorylation was most prominent in a growth factor free, but hormone enriched environment DM. Receptor responsiveness could be induced in a controlled and reversible manner, as MET activity was high in presence of DM, was down-regulated in the presence of AM, but became reactivated when the starting conditions DM were re-introduced.

DISCUSSION

Over more than a decade there has been the hope of growing and expanding human HC *in vitro*[2,4,15,16]. While a medium with high amounts of HGF, EGF and nicotinamide has enabled proliferation of rodent HC[2], comparable results have not been achieved with human cells[4]. To prevent receptor down-regulation, which is associated with constant culture conditions, we developed a novel, biphasic culture technique. Hereby, we were able to demonstrate a controlled switch from hepatocellular differentiation to activation in a reversible manner.

The mixture of hormones and growth factors may exert counteracting effects in the downstream cascade, e.g., HGF and EGF activate the protein kinases ERK1/2, and the transcription factors NF-kappa B and AP-1, whereas dexamethasone inhibits them[17-19]. Therefore, we devised two distinct media (DM and AM) for alternate incubation.

Our composition of AM contained biologically active[20,21], but lower amounts of HGF, EGF, and nicotinamide than other models[2,4]. In order to synergize with HGF's mode of action, we substituted with GM-CSF, which promotes activation of ERK1/2, NF-kappa B and AP-1[22-24]. In AM, we detected high receptor expression, but translocation into the cytoplasm, accompanied by increase of atypical intermediate filaments CK-19 ("ductular phenotype"), suggesting de-differentiation as described before[2,8].

Our composition of DM included dexamethasone, high levels of nicotinamide, insulin in a beneficial mixture with transferrin and selenium, metabolic substrates which have been shown to induce albumin expression, cytochrome P450 activity, and amino acid uptake[4,25-27]. We omitted HGF, which down-regulates CYP450-expression and synthesis of acute-phase proteins[11,12]. In DM, tyrosine kinase receptor expression was reduced, but accompanied by proper distribution along the plasma membrane. This correlated with reduction of atypical CK-19 expression, indicating more physiological differentiation (CK-18 positive, CK-19 negative) of parenchymal HC.

These observations suggest that continuous exposure to soluble mitogens does not go along with an adequate biological response. Conversely, presence of a growth-factor-free, but hormonally enriched environment DM supports not only cytoskeletal differentiation, but also enables appropriate receptor distribution.

To reflect variable metabolic demand and growth responsiveness, our dynamic model was based upon alternating stimulation by SM or DM in 5-d intervals. Hereby, we considered the dependency of liver-specific metabolic genes on hormonal changes[28], the capability of proliferation without shutting down liver-specific functions[1], the sequential course of organ development and regeneration *in vivo*[14], and the balanced interplay of positive and negative signals in this process[1].

It is possible that complete down-regulation of tyrosine kinase receptors was prevented in our system by lack of continuous exposure to mitogens and omission of nuclear hormones in AM[2,4]. Our activation interval was adjusted to the kinetics of liver cell proliferation *in vivo*[29] and *in vitro*[16,20,21]. In other models, continuously high mitogenic stimulation was associated with an increase of AFP and CK-19 over time[2,4], possibly reflecting a situation such as encountered in fulminant hepatitis, where very high levels of serum HGF induce ductular structures, eventually inhibiting liver regeneration and causing irreversible hepatic failure. Remarkably, in our model, re-differentiation could repeatedly be accomplished by a medium switch to DM. Therefore, our experiments indicate that an unphysiologic

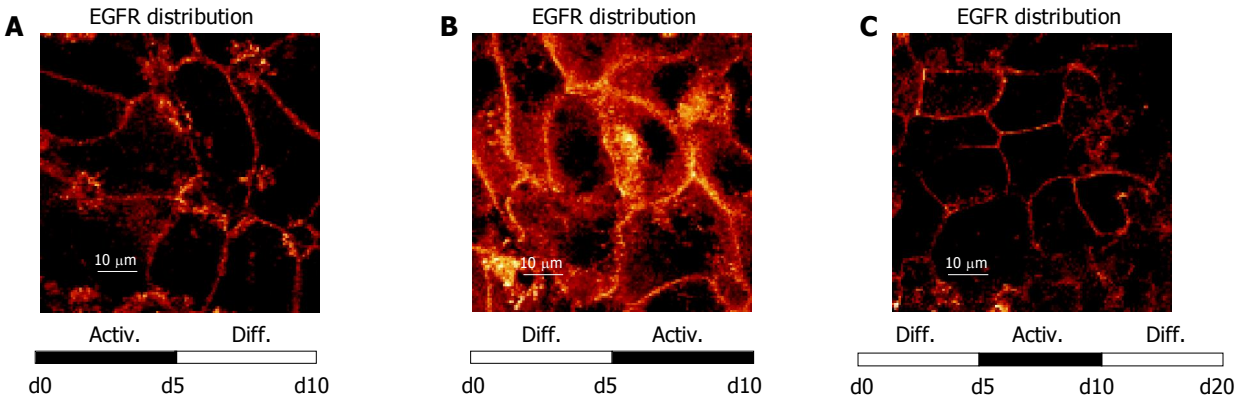

Figure 8 Dynamics of EGFR distribution depending on modulation of the culture environment. A: Receptor localization along the plasma membrane after switching the extracellular milieu from de-differentiation (activation) to differentiation inducing conditions (d 10); B: The reverse order (DM-AM) evoked a distinct receptor translocation into the cytoplasm (d 10); C: Receptor re-localization onto the cell surface was induced again after a further 10-d incubation in DM (d 20). Confocal microscopy, ×100/1.3 oil immersion objective. Each figure is representative for three separate experiments.

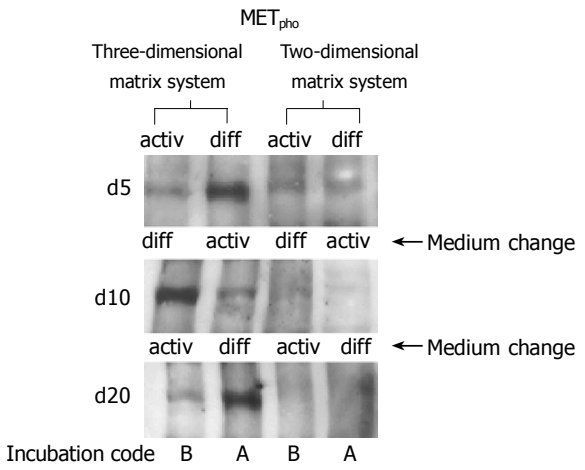

Figure 9 Western blot analysis of milieu dependent shift of MET phosphorylation (MET_{pho}). Environmental switch has been carried out on d 5 and 10. Left lanes indicate HC cultivation within a 3D collagen matrix (sandwich), right lanes confer to a 2D culture system (collagen matrix). Incubation code A indicates initial 5-d incubation in DM, followed by 5-d incubation in AM and subsequent incubation in DM. Incubation code B is related to initial incubation in AM, followed by incubation in DM and subsequent incubation in AM. The blots are representative of three separate experiments.

ductular phenotype may be induced by the continuous presence of growth factors. This process could be counteracted by a predominance of hormonal and metabolic substrates, suggesting that the maintenance of hepatic growth and metabolism may be feasible *in vitro*[9,28].

In our model, tyrosine kinase phosphorylation, physiologic expression of CK-18, and significant reduction of CK-19 levels depended on embedding in 3D collagen type I gel. It is well established that cell shape determines whether an individual cell will grow, differentiate, or die in response to growth factors[30]. Our findings are supported by previous reports, illustrating that collagen type I sandwich gel increased HC transcriptional activity and maintained liver-specific genes[31]. Furthermore, it has been tested as the only substrate enabling both maintenance of liver-specific genes and proliferation[1]. For the first time, we have been able to demonstrate the synergism of cell-matrix effects and soluble signals on differentiation and growth factor responsiveness of human HC.

The capacity for liver cell proliferation correlates with expression of MET, but not serum levels of HGF[32,33]. MET and EGFR are members of the transmembrane growth factor receptor tyrosine kinase family. Ligand-induced activation is characterized by receptor dimerization, autophosphorylation in the cytoplasmic domain, attracting cytosolic protein complexes, followed by phosphorylation of mitogen-activated protein kinase and kinases[14,28,34]. In our sequential model, a strong receptor expression associated with translocation into the cytoplasm was induced by the presence of exogenous growth factors. On the contrary, receptor expression was low, but distributed along the plasma membrane, when growth factors were omitted and a hormone-rich milieu was supplied. The appropriate localization and subsequent activation of growth receptors on human HC illustrate that essential biological requirements for liver repair and regeneration are provided by our culture model.

This biphasic technique represents progress in controlling growth and differentiation of human HC *in vitro*. Sequential stimulation of liver cells may help uncover the links between metabolism and the complex cascade of gene activation required for DNA replication[22]. Eventually, these studies might promote the application of human liver cells in HC transplantation, gene therapy, adult stem cell transfer, and bioartificial liver support[35,36].

ACKNOWLEDGMENTS

We would like to thank Karen Nelson for critically reading the manuscript.

REFERENCES

1 **Bucher NL,** Robinson GS, Farmer SR. Effects of extracellular matrix on hepatocyte growth and gene expression: implications for hepatic regeneration and the repair of liver injury. *Semin Liver Dis* 1990; **10**: 11-19

2 **Block GD,** Locker J, Bowen WC, Petersen BE, Katyal S, Strom SC, Riley T, Howard TA, Michalopoulos GK. Population expansion, clonal growth, and specific differentiation patterns in primary cultures of hepatocytes induced by HGF/SF, EGF and TGF alpha in a chemically defined (HGM) medium. *J Cell Biol* 1996; **132**: 1133-1149

3 **Nishikawa Y,** Tokusashi Y, Kadohama T, Nishimori H, Ogawa K. Hepatocytic cells form bile duct-like structures within a three-dimensional collagen gel matrix. *Exp Cell Res* 1996; **223**: 357-371

4 **Runge DM,** Runge D, Dorko K, Pisarov LA, Leckel K, Kostrubsky VE, Thomas D, Strom SC, Michalopoulos GK. Epidermal growth factor- and hepatocyte growth factor-receptor activity in serum-free cultures of human hepatocytes. *J Hepatol* 1999; **30**: 265-274

5 **Michalopoulos GK,** Bowen WC, Zajac VF, Beer-Stolz D, Watkins S, Kostrubsky V, Strom SC. Morphogenetic events in mixed cultures of rat hepatocytes and nonparenchymal cells maintained in biological matrices in the presence of hepatocyte growth factor and epidermal growth factor. *Hepatology* 1999; **29**: 90-100

6 **Mitaka T,** Sato F, Mizuguchi T, Yokono T, Mochizuki Y. Reconstruction of hepatic organoid by rat small hepatocytes and hepatic nonparenchymal cells. *Hepatology* 1999; **29**: 111-125

7 **Michalopoulos GK,** Bowen WC, Mule K, Lopez-Talavera JC, Mars W. Hepatocytes undergo phenotypic transformation to biliary epithelium in organoid cultures. *Hepatology* 2002; **36**: 278-283

8 **Blaheta RA,** Kronenberger B, Woitaschek D, Auth MK, Scholz M, Weber S, Schuldes H, Encke A, Markus BH. Dedifferentiation of human hepatocytes by extracellular matrix proteins *in vitro*: quantitative and qualitative investigation of cytokeratin 7, 8, 18, 19 and vimentin filaments. *J Hepatol* 1998; **28**: 677-690

9 **Dabeva MD,** Laconi E, Oren R, Petkov PM, Hurston E, Shafritz DA. Liver regeneration and alpha-fetoprotein messenger RNA expression in the retrorsine model for hepatocyte transplantation. *Cancer Res* 1998; **58**: 5825-5834

10 **Van Eyken P,** Sciot R, Callea F, Van der Steen K, Moerman P, Desmet VJ. The development of the intrahepatic bile ducts in man: a keratin-immunohistochemical study. *Hepatology* 1988; **8**: 1586-1595

11 **Guillen MI,** Gomez-Lechon MJ, Nakamura T, Castell JV. The hepatocyte growth factor regulates the synthesis of acute-phase proteins in human hepatocytes: divergent effect on interleukin-6-stimulated genes. *Hepatology* 1996; **23**: 1345-1352

12 **Donato MT,** Gomez-Lechon MJ, Jover R, Nakamura T, Castell JV. Human hepatocyte growth factor down-regulates the expression of cytochrome P450 isozymes in human hepatocytes in primary culture. *J Pharmacol Exp Ther* 1998; **284**: 760-767
13 **Yang Y,** Spitzer E, Meyer D, Sachs M, Niemann C, Hartmann G, Weidner KM, Birchmeier C, Birchmeier W. Sequential requirement of hepatocyte growth factor and neuregulin in the morphogenesis and differentiation of the mammary gland. *J Cell Biol* 1995; **131**: 215-226
14 **Diehl AM,** Rai RM. Liver regeneration 3: Regulation of signal transduction during liver regeneration. *FASEB J* 1996; **10**: 215-227
15 **Stolz DB,** Michalopoulos GK. Comparative effects of hepatocyte growth factor and epidermal growth factor on motility, morphology, mitogenesis, and signal transduction of primary rat hepatocytes. *J Cell Biochem* 1994; **55**: 445-464
16 **Gomez-Lechon MJ,** Guillen I, Ponsoda X, Fabra R, Trullenque R, Nakamura T, Castell JV. Cell cycle progression proteins (cyclins), oncogene expression, and signal transduction during the proliferative response of human hepatocytes to hepatocyte growth factor. *Hepatology* 1996; **23**: 1012-1019
17 **Liu F,** Su Y, Li B, Ni B. Regulation of amyloid precursor protein expression and secretion via activation of ERK1/2 by hepatocyte growth factor in HEK293 cells transfected with APP751. *Exp Cell Res* 2003; **287**: 387-396
18 **Thoresen GH,** Guren TK, Christoffersen T. Role of ERK, p38 and PI3-kinase in EGF receptor-mediated mitogenic signalling in cultured rat hepatocytes: requirement for sustained ERK activation. *Cell Physiol Biochem* 2003; **13**: 229-238
19 **Kassel O,** Sancono A, Kratzschmar J, Kreft B, Stassen M, Cato AC. Glucocorticoids inhibit MAP kinase via increased expression and decreased degradation of MKP-1. *EMBO J* 2001; **20**: 7108-7116
20 **Ismail T,** Howl J, Wheatley M, McMaster P, Neuberger JM, Strain AJ. Growth of normal human hepatocytes in primary culture: effect of hormones and growth factors on DNA synthesis. *Hepatology* 1991; **14**: 1076-1082
21 **Strain AJ,** Ismail T, Tsubouchi H, Arakaki N, Hishida T, Kitamura N, Daikuhara Y, McMaster P. Native and recombinant human hepatocyte growth factors are highly potent promoters of DNA synthesis in both human and rat hepatocytes. *J Clin Invest* 1991; **87**: 1853-1857
22 **Fausto N.** Liver regeneration. *J Hepatol* 2000; **32**: 19-31
23 **Bozinovski S,** Jones JE, Vlahos R, Hamilton JA, Anderson GP. Granulocyte/macrophage-colony-stimulating factor (GM-CSF) regulates lung innate immunity to lipopolysaccharide through Akt/Erk activation of NFkappa B and AP-1 *in vivo*. *J Biol Chem* 2002; **277**: 42808-42814
24 **Jubinsky PT,** Short MK, Mutema G, Witte DP. Developmental expression of Magmas in murine tissues and its co-expression with the GM-CSF receptor. *J Histochem Cytochem* 2003; **51**: 585-596
25 **Inui T,** Shinomiya N, Fukasawa M, Kobayashi M, Kuranaga N, Ohkura S, Seki S. Growth-related signaling regulates activation of telomerase in regenerating hepatocytes. *Exp Cell Res* 2002; **273**: 147-156
26 **Runge D,** Runge DM, Jager D, Lubecki KA, Beer-Stolz D, Karathanasis S, Kietzmann T, Strom SC, Jungermann K, Fleig WE, Michalopoulos GK. Serum-free, long-term cultures of human hepatocytes: maintenance of cell morphology, transcription factors, and liver-specific functions. *Biochem Biophys Res Commun* 2000; **269**: 46-53
27 **Pachernik J,** Esner M, Bryja V, Dvorak P, Hampl A. Neural differentiation of mouse embryonic stem cells grown in monolayer. *Reprod Nutr Dev* 2002; **42**: 317-326
28 **Taub R.** Liver regeneration 4: transcriptional control of liver regeneration. *FASEB J* 1996; **10**: 413-427
29 **Michalopoulos GK,** DeFrances MC. Liver regeneration. *Science* 1997; **276**: 60-66
30 **Mooney D,** Hansen L, Vacanti J, Langer R, Farmer S, Ingber D. Switching from differentiation to growth in hepatocytes: control by extracellular matrix. *J Cell Physiol* 1992; **151**: 497-505
31 **Dunn JC,** Tompkins RG, Yarmush ML. Hepatocytes in collagen sandwich: evidence for transcriptional and translational regulation. *J Cell Biol* 1992; **116**: 1043-1053
32 **Tsubouchi H,** Niitani Y, Hirono S, Nakayama H, Gohda E, Arakaki N, Sakiyama O, Takahashi K, Kimoto M, Kawakami S. Levels of the human hepatocyte growth factor in serum of patients with various liver diseases determined by an enzyme-linked immunosorbent assay. *Hepatology* 1991; **13**: 1-5
33 **D'Errico A,** Fiorentino M, Ponzetto A, Daikuhara Y, Tsubouchi H, Brechot C, Scoazec JY, Grigioni WF. Liver hepatocyte growth factor does not always correlate with hepatocellular proliferation in human liver lesions: its specific receptor c-met does. *Hepatology* 1996; **24**: 60-64
34 **Runge DM,** Runge D, Foth H, Strom SC, Michalopoulos GK. STAT 1alpha/1beta, STAT 3 and STAT 5: expression and association with c-MET and EGF-receptor in long-term cultures of human hepatocytes. *Biochem Biophys Res Commun* 1999; **265**: 376-381
35 **Strain AJ,** Neuberger JM. A bioartificial liver-state of the art. *Science* 2002; **295**: 1005-1009
36 **Mahler S,** Desille M, Fremond B, Chesne C, Guillouzo A, Campion JP, Clement B. Hypothermic storage and cryopreservation of hepatocytes: the protective effect of alginate gel against cell damages. *Cell Transplant* 2003; **12**: 579-592

Science Editor Li WZ **Language Editor** Elsevier HK

PO Box 2345, Beijing 100023, China
www.wjgnet.com
wjg@wjgnet.com

ELSEVIER

World J Gastroenterol 2005;11(14):2088-2094
World Journal of Gastroenterology ISSN 1007-9327

• *BASIC RESEARCH* •

Identification of the immunogenic domains in HBsAg preS1 region using overlapping preS1 fragment fusion proteins

Wei-Guo Hu, Jun Wei, Heng-Chuan Xia, Xin-Xiu Yang, Feng Li, Guang-Di Li, Yuan Wang, Zu-Chuan Zhang

Wei-Guo Hu, Jun Wei, Heng-Chuan Xia, Xin-Xiu Yang, Feng Li, Guang-Di Li, Yuan Wang, Zu-Chuan Zhang, Key Laboratory of Proteomics, Institute of Biochemistry and Cell Biology, Shanghai Institutes for Biological Sciences, Chinese Academy of Sciences, 320 Yue-yang Road, Shanghai 200031, PR China
Jun Wei, Department of Pathology, Baylor College of Medicine, One Baylor Plaza, Houston, TX 77030, USA
Correspondence to: Zu-Chuan Zhang, Key Laboratory of Proteomics, Institute of Biochemistry and Cell Biology, Shanghai Institutes for Biological Sciences, Chinese Academy of Sciences, 320 Yue-yang Road, Shanghai 200031, China. zhangzc@sunm.shcnc.ac.cn
Telephone: +86-21-54921281 Fax: +86-21-54921011
Received: 2004-04-28 Accepted: 2004-06-24

Abstract

AIM: The incorporation of hepatitis B virus (HBV) preS1 region into epitope-based vaccines against HBV has been accepted widely, but the incorporate site and size of preS1 sequence is controversial. Therefore our purpose was to further investigate its immunogenic domains for the epitope-based hepatitis B vaccine design.

METHODS: Eight GST fusion proteins containing overlapping preS1 fragments in preS1 (21-119) region were expressed in *E.coli*. Using these purified fusion proteins, the immunogenic domains in preS1 region were identified in detail in mice and humans by Western blot analysis and ELISA.

RESULTS: The results in mice showed that the immunogenic domains mainly existed in preS1 (21-59) and preS1 (95-109). Similarly, these fragments had strong immunogenicity in humans; whereas the other parts except for preS1 (60-70) also had some immunogenicity. More importantly, a major immunogenic domain, preS1 (34-59), which has much stronger immunogenicity, was identified. Additionally, the antibodies against some preS1 fragments, especially preS1 (34-59), were speculated to be virus-neutralizing.

CONCLUSION: Eight GST fusion proteins containing overlapping preS1 fragments were prepared successfully. They were used for the study on the immunogenic domains in preS1 (21-119) region. The preS1 (34-59) fragments were the major immunogenic domains in the preS1 region, and the antibodies against these fragments were speculated to be virus-neutralizing. Therefore, the incorporation of preS1 (34-59) fragments into epitope-based HBV vaccines may be efficient for enhancement of immune response. Additionally, the results also imply that there are more complex immune responses to preS1 region and more abundant immunogenic domains in humans.

Key words: HBV; preS1; GST fusion protein; Immunogenic domain; Overlapping

Hu WG, Wei J, Xia HC, Yang XX, Li F, Li GD, Wang Y, Zhang ZC. Identification of the immunogenic domains in HBsAg preS1 region using overlapping preS1 fragment fusion proteins. *World J Gastroenterol* 2005; 11(14): 2088-2094
http://www.wjgnet.com/1007-9327/11/2088.asp

INTRODUCTION

Hepatitis B virus (HBV) is a small enveloped DNA virus, whose envelope contains three related surface glycoproteins called the large (L), middle (M) and small (S) proteins. All these proteins are the products of a single open reading frame, which is divided into preS1, preS2 and S regions[1]. They arise from three separate translation initiation AUG codons and share a common C-terminal. The S protein (226 amino acid residues) is encoded by the S gene. The M protein contains preS2 (55 amino acid residues) and S regions, while L protein contains preS1 (108 or 119 amino acid residues, depending on the subtype), preS2 and S regions.

HBV is the major etiologic agent for hepatitis B in humans[2]. It may cause acute and chronic hepatitis with serious sequelae such as cirrhosis and hepatocellular carcinoma (HCC)[3]. There are about 400 million HBV carriers worldwide[4] with about one million deaths per year due to HBV-associated liver cancer[5]. Whereas a previous study claimed that mass vaccination was effective in preventing HBV infection and in declining the incidence of HCC[6]. These enormous successes were achieved with plasma-derived vaccines, and later with yeast-derived recombinant vaccines[7,8]. However, both vaccines have a none-response rate of up to 10% in healthy vaccines after immunization with the licensed vaccines containing only the S-protein component of HBV surface antigen (HBsAg) particles[9]. Therefore, it is necessary to develop more effective and highly immunogenic vaccines.

For the development of vaccines against HBV, the preS1 sequence of HBsAg has been shown to be a particularly efficient immunogen at T-and B-cell levels[10,11]. In general, epitopes of proteins should be incorporated into recombinant vaccines for the production of poly-and monoclonal antibodies[12]. Great deals of studies have shown that there are many immunogenic B-cell epitopes in the preS1 domain. Five distinct antibody-binding sites within the preS1 region of HBsAg/P43 of the *adw* subtype: preS1 (16-27), preS1 (32-53), preS1 (41-53), preS1 (94-105) and preS1 (106-117) have been determined in mice[13]. A putative B-cell epitope biased to the C-terminal region, preS1 (57-119), was

identified in a commercially available immunoglobulin prepared from chronically HBV-infected donors[14]. Additionally, many epitopes of monoclonal antibodies directed against preS1 have also been mapped such as preS1 (27-35), preS1 (72-78)[15], preS1 (30-35)[16], preS1 (19-26), preS1 (37-45)[17,18], preS1 (37-43)[19] and preS1 (32-47)[20]. Many T-cell epitopes in preS1 region have also been identified, such as preS1 (21-30), preS1 (29-48)[21], preS1 (12-21) and preS1 (94-117)[13]. On the other hand, the incorporate site and size of preS1 sequences are controversial. Some candidate vaccines integrated all preS1 sequences[22-24]; other incorporated partial sequences of preS1 such as preS1 (21-47)[25], preS1 (12-52)[26] and preS1 (1-42)[27]. So it is important to further identify the immunogenic domains in HBsAg preS1 region for the design of vaccines against HBV.

Some reports pointed out that there were no important B-cell epitopes in preS1 (1-20) domains[13,28]. In the present study, eight GST-preS1 fusion proteins overlapped in the preS1 (21-119) region were highly expressed in *E.coli* and used to identify its immunogenic domains in mice and humans by Western blot analysis and ELISA.

MATERIALS AND METHODS

Expression, purification of GST-preS1 fusion proteins

Eight overlapping fragments, preS1 (21-47), preS1 (34-59), preS1 (48-70), preS1 (60-85), preS1 (71-94), preS1 (86-109), preS1 (95-119) and preS1 (21-119) of HBV *adr* subtype were individually expressed as a fusion protein with GST. The coding sequences of these preS1 fragments were synthesized by PCR from pADR-1 using 5'- and 3'-primers and subcloned into the *Bam*HI and *Eco*RI sites of pGEX 4T-1 (Pharmacia) to yield expression plasmids. To express the GST-preS1 fusion proteins, expression plasmids were transformed into *E.coli* BL21 (gold) cells and the expression of fusion proteins was induced by 0.1 mmol/L isoprophyl-β-D-thiogalactopyranoside (IPTG) at 37 ℃ for 2 h. The induced cells were harvested and sonicated. Supernatants of the cell lysates were affinity purified by glutathione (GSH)-sepharose 4B (Sigma) column chromatography. The quantity of purified fusion proteins was measured by Lowry's method using bovine serum albumin as the standard. The procedures in detail were described in a previous study[29]. Then the cell lysates and the purified fusion proteins were subjected to 12.5% SDS-PAGE and Western blot analysis.

Immunization of mice

A group of five 7-week-old female Balb/C mice were immunized intraperitoneally with 25 μg of His-preS1 (21-119) fusion proteins[30] in 0.5 mL of complete Freund's adjuvant (CFA, Sigma) at wk 0 and boosted at wk 2, 4, 6, and 8 with a same amount of antigen in Freund's incomplete adjuvant (IFA, Sigma). The collected sera obtained at wk 0, 1, 3, 5, 7 and 9 were used to analyze the antigenicity of the above eight preS1 fusion proteins by Western blot analysis and ELISA.

Western blot analysis

After electrophoresis, electrophoretic protein bands of the expressed cell lysates were transferred to nitrocellulose membranes (Hoefer Scientific). The membranes were incubated with the mixture of five mice antisera (1∶300 dilution) collected at wk 9, then reacted with goat anti-mouse IgG peroxidase conjugates (Novagen) (1∶20 000 dilution). After being washed, the substrate solution containing DAB·4HCl (0.5 mg/mL, Amersco) and H_2O_2 (0.1 μL/mL) was added and the reaction was quenched with distilled water.

ELISA of mouse antisera

A same amount (100 ng/well) of eight preS1 fusion proteins dissolved in 15 mmol/L sodium carbonate, 35 mmol/L sodium bicarbonate buffer, pH 9.6 were coated on microtiter plates (Nunc) at 37 ℃ for 2 h. After being washed thrice with PBS-0.1% Tween 20 (PBS-T) and blocked with 2.5% bovine serum albumin in PBS at 37 ℃ for 1 h, separate mouse antisera (1:300 dilution) collected at different time points were added and incubated at 37 ℃ for 1 h. The wells were washed five times as described above, then goat anti-mouse IgG peroxidase conjugates (Novagen) (1∶20 000 dilution) were added and incubated at 37 ℃ for 1 h. The substrate solution (0.06 mg/mL TMB and 0.3 μL/mL H_2O_2 in 0.1 mol/L Na_2HPO_4-citrate buffer, pH 5.0) was added to each well and incubated at 37 ℃ for 15 min. The reaction was stopped with 2 N sulfuric acid and *A* values were measured at 450 nm in an ELISA reader. The mean *A* value from five mice antisera was plotted on the corresponding graph.

In competitive ELISA, the mouse antisera were diluted in different concentrations (Figure 3), and previously incubated with the coated antigens or other overlapping antigen (s) at a dose of 2 μg at 37 ℃ for 1 h. The antisera without antigen treatment were used as controls. The selection of coated antigens with immunogenicity depends on the results of Western blot analysis. The other experimental steps were the same as described above.

ELISA of human sera

The plate wells were coated with different preS1 fusion proteins as described above, and then washed thrice with PBS-0.5% Tween 20 (PBS-T) and blocked with 25% goat sera, 2.5% skimmed milk in PBS at 37 ℃ for 1 h. Human serum samples from 28 normal individuals, 37 acute hepatitis B patients, 106 chronic hepatitis B patients and 33 HCC patients with hepatitis B collected from Changzheng Hospital, Shanghai and East Hepatobiliary Surgery Hospital, Shanghai were diluted 1∶30 with sample buffer (25% goat sera, 2.5% skimmed milk, 10% glycerol, 0.19% EDTA in PBS-T). The plates were filled with the diluted serum samples and incubated at 37 ℃ for 1 h, then washed seven times as described above. Peroxidase conjugated goat anti-human IgG (γ-chain specific, Sigma) (1∶5 000 dilution) was added to each well and incubated at 37 ℃ for 1 h. The plates were then washed seven times with PBS-T and the substrate solution was added to react. After 15-min incubation, the reaction was stopped with 2 N sulfuric acid. *A* values were measured at 450 nm in an ELISA reader. The mean value obtained from the sera of different infection types was plotted on the corresponding graph.

In competitive ELISA, the mixture of serum samples

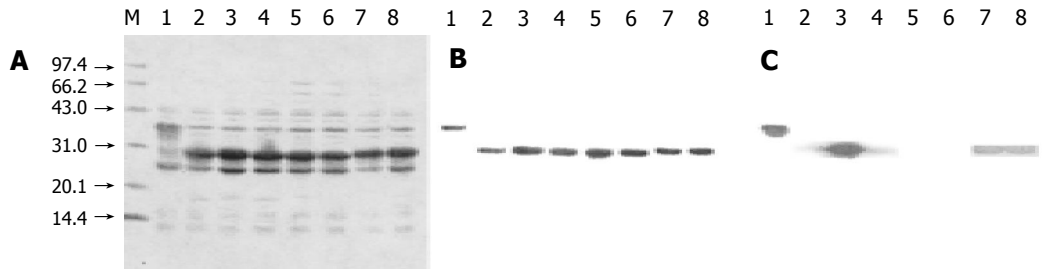

Figure 1 Expression, purification, and Western blot analysis of eight GST fusion proteins containing overlapping preS1 fragments in *E.coli* BL21 (gold). A and B: Cell lysates and purified fusion proteins subjected to 12.5% SDS-PAGE and stained with Coomassie brilliant blue. C: Protein bands on the duplicate gel of cell lysates electroblotted onto a nitrocellulose membrane for Western blot analysis with mice antisera. Lane M: Molecular weight standard. Lanes 1-8: The samples containing preS1 (21-119), preS1 (21-47), preS1 (34-59), preS1 (48-70), preS1 (60-85), preS1 (71-94), preS1 (86-109) and preS1 (95-119) in a sequent order.

from acute hepatitis B patients was used and the other procedures were similar to those in mice.

RESULTS

Expression, purification of GST-preS1 fusion proteins

After the expression plasmids were verified by sequencing, they were transformed into *E.coli* BL21 (gold). The eight overlapping preS1 fusion proteins were highly expressed in the transformed cells (Figure 1A). The supernatants of sonicated cell lysates were applied to affinity chromatography on glutathione-sepharose 4B column, and the purified fusion proteins were obtained (Figure 1B). The purities of purified fusion proteins were evaluated to be over 95% by densitometric scanning. About 50-90 mg of soluble purified proteins was obtained from 1 L of culture.

Immune response to His-preS1 (21-119) fusion protein in mice

The results of Western blot analysis (Figure 1C) showed that the immunogenic domains of preS1 (21-119) sequences in mice existed in the fragments of preS1 (21-47), preS1 (34-59) and preS1 (48-70) in the N-terminus, and in the fragments of preS1 (86-109) and preS1 (94-119) in the C-terminus, whose strips appeared obvious staining intensity. Especially, the staining intensity of preS1 (34-59) strips was much higher than that of the other preS1 fragments. While the staining intensity of preS1 (60-85) and preS1 (71-94) strips was very weak, suggesting that the five fragments in preS1 (21-119) region, especially preS1 (34-59), had strong immunogenicity, and the two fragments in the middle had little immunogenicity.

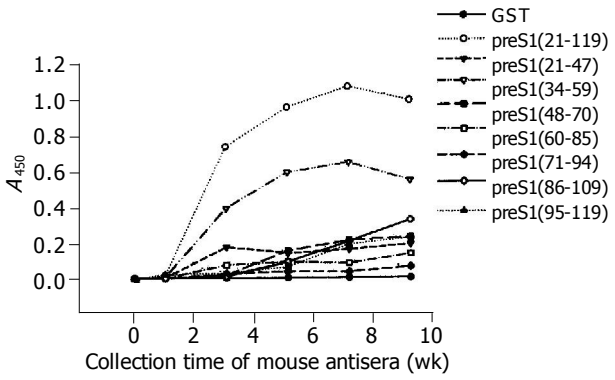

Figure 2 Immunogenicity analysis of different fragments in preS1 (21-119) region in mice by ELISA using eight overlapping GST-preS1 fusion proteins as coated antigens. The mice were immunized with His-preS1 (21-119) fusion proteins at wk 0, 2, 4, 6 and 8, and the antisera were collected the following week.

The results of ELISA as shown in Figure 2 indicated that the immunoreactivity of antisera directed against most preS1 fragments increased obviously at wk 3 and went to the utmost at wk 7. It also showed that the antigenicity of preS1 (21-119) and preS1 (34-59) decreased slightly after wk 7, while the antigenicity of the other fragments did not. The distribution and strength of immunogenicity in these fragments were in agreement with the observations in Western blot analysis. The results also demonstrated that preS1 (34-59) fragments were also the strongest in immunogenicity.

The precise immunogenic domains in preS1 (21-119) region in mice were further identified with competitive ELISA. The antigenicity of each coated antigen could be inhibited by itself, which confirmed the specificity of its corresponding antibody. The antigenicity of preS1 (21-47) could be partially inhibited by preS1 (34-59) (Figure 3A), suggesting that the two fragments, preS1 (21-33) and preS1 (34-47) had immunogenicity. The antigenicity of preS1 (34-59) could only be slightly inhibited by preS1 (21-47) or preS1 (48-70) or a mixture of them (Figure 3B), implying that there might be a conformational epitope in preS1 (34-59) region. While the antigenicity of preS1 (48-70) could be almost totally inhibited by preS1 (34-59) (Figure 3C), suggesting that there was an immunogenic domain in the part of preS1 (48-59). In addition, the antigenicity of preS1 (86-109) and preS1 (95-119) could be inhibited by each other (Figure 3D and E), implying that the immunogenic domain existed in the overlapping part, preS1 (95-109).

Detection of antibodies against overlapping preS1 fragments in the sera from HBV-infected patients

The activity of antibodies against different preS1 fragments detected from the sera of patients with different infection types is shown in Figure 4. The discrimination of HBV infection types was based on the immunological evidence of sera and clinical manifestations of cases. The results indicated that all the fragments showed stronger antigenicity against acute hepatitis B patient samples and the fragments of preS1 (34-59) also had much stronger antigenicity as in mice. In addition, the antigenicity of the fragments, preS1 (21-47),

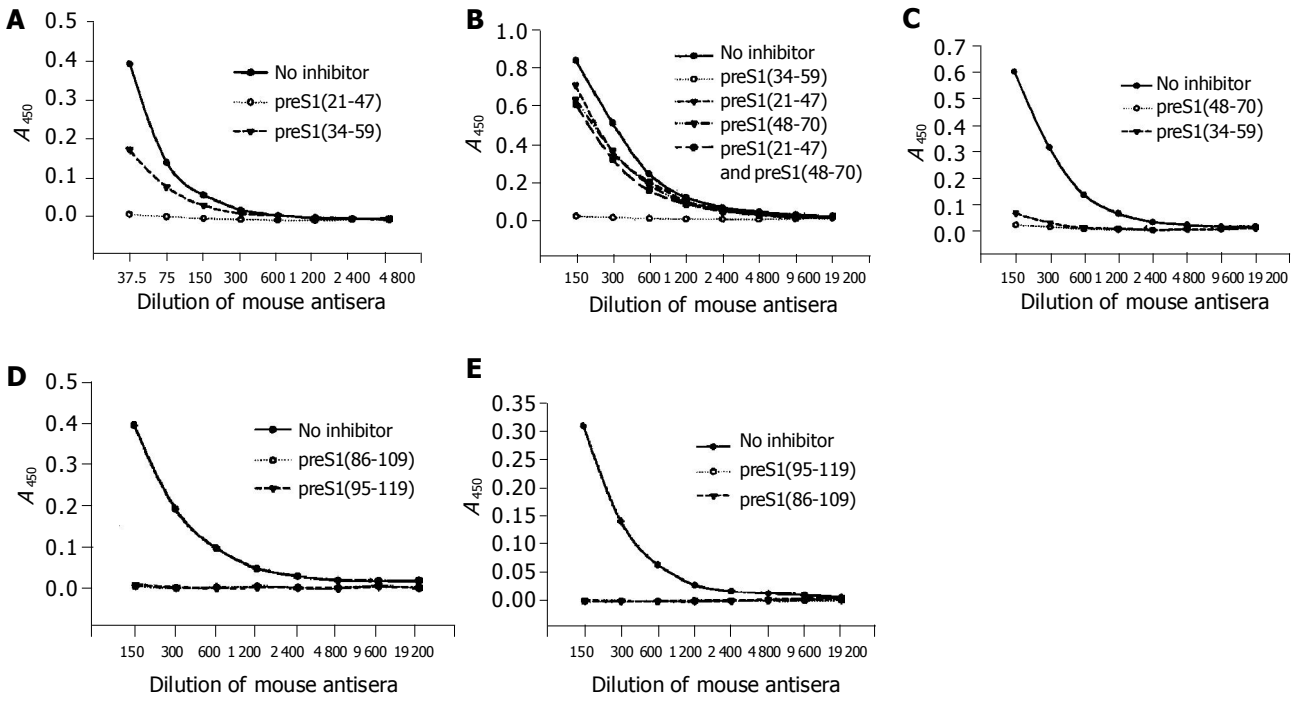

Figure 3 Identification of the precise immunogenic domains in mice by competitive ELISA. The coated antigens were the five fusion proteins containing different preS1 fragments: preS1 (21-47) (A), preS1 (34-59) (B), preS1 (48-70) (C), preS1 (86-109) (D) and preS1 (95-119) (E), respectively. The mouse antisera colleted at wk 9 were previously incubated with the coated antigens or the other overlapping antigen(s) at a dose of 2 μg, and the samples not treated with antigen(s) were used as controls.

preS1 (48-70), preS1 (86-109), preS1 (95-119), and especially preS1 (34-59), was significantly lower in chronic-phase sera (chronic hepatitis B and HCC with hepatitis B samples) than in acute-phase sera (P<0.05). However, the antigenicity of the fragments, preS1 (60-85) and preS1 (71-94), in the middle part of preS1 showed less diversity (P>0.05).

The data of competitive ELISA (Figure 5) likewise confirmed the specificity of corresponding antib-odies. It also indicated that the antigenicity of most fragments could not be chiefly inhibited by the overlapping fragment (s). With an exception, the antigenicity of preS1 (60-85) could be most inhibited by preS1 (71-94), but could not be inhibited by preS1 (48-70). The above results suggested that all the domains except for preS1 (60-70) had some immunogenicity.

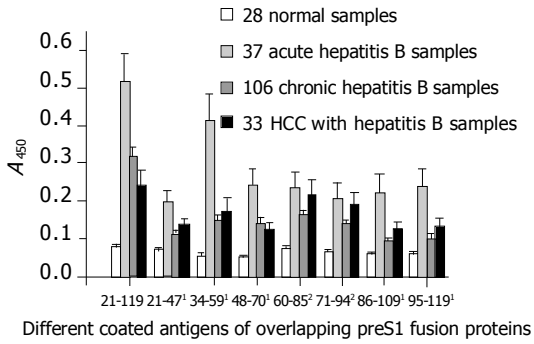

Figure 4 Detection of antigenicity (A_{450}) of the eight different preS1 fragments overlapped in preS1 (21-119) region against hepatitis B patients' serum samples with different infection types by indirect ELISA. [1]The antigenicity of the fragments, preS1 (21-47), preS1 (48-70), preS1 (86-109), preS1 (95-119), and especially preS1 (34-59), decreased significantly in chronic-phase sera (chronic hepatitis B and HCC with hepatitis B samples) in comparison with acute-phase sera (P<0.05). However, [2]the antigenicity of the fragments, preS1 (60-85) and preS1 (71-94), in the middle part showed less diversity (P>0.05). Each column represents the mean A value±SE.

DISCUSSION

Because the HBsAg preS1 region correlates with the assembly and infectivity of HBV[31-33], possesses the binding site on hepatocyte membranes[31], has abundant T-and B-cell epitopes[13] and may overcome the none-response against common vaccines containing only S region[34,35], the incorporation of preS1 region into epitope-based vaccines has been widely accepted[10,36]. While the incorporation site and size of preS1 sequences are controversial, some previous studies on the immunogenicity of preS1 region mainly focused on mice and the tested antigens in preS1 region did not overlap[13,37]. So it may acquire more information about the immunogenic domains in preS1 region if its immunogenic domains in mice and humans with overlapping preS1 fragments are simultaneously analyzed.

It has been established that small proteins could be successfully expressed in *E.coli* by fusing them with GST[38], with which the fusion proteins could be expressed mostly in soluble form and purified more easily by a simple affinity chromatography. In addition, GST did not influence the specificity of anti-preS1 antibodies[29,39]. Therefore, we selected the plasmid of pGEX 4T-1 as a vector to express the different overlapping preS1 fragments in *E.coli* and gained the satisfactory results. Then the mice were immunized by His-preS1 (21-119) fusion proteins expressed previously in

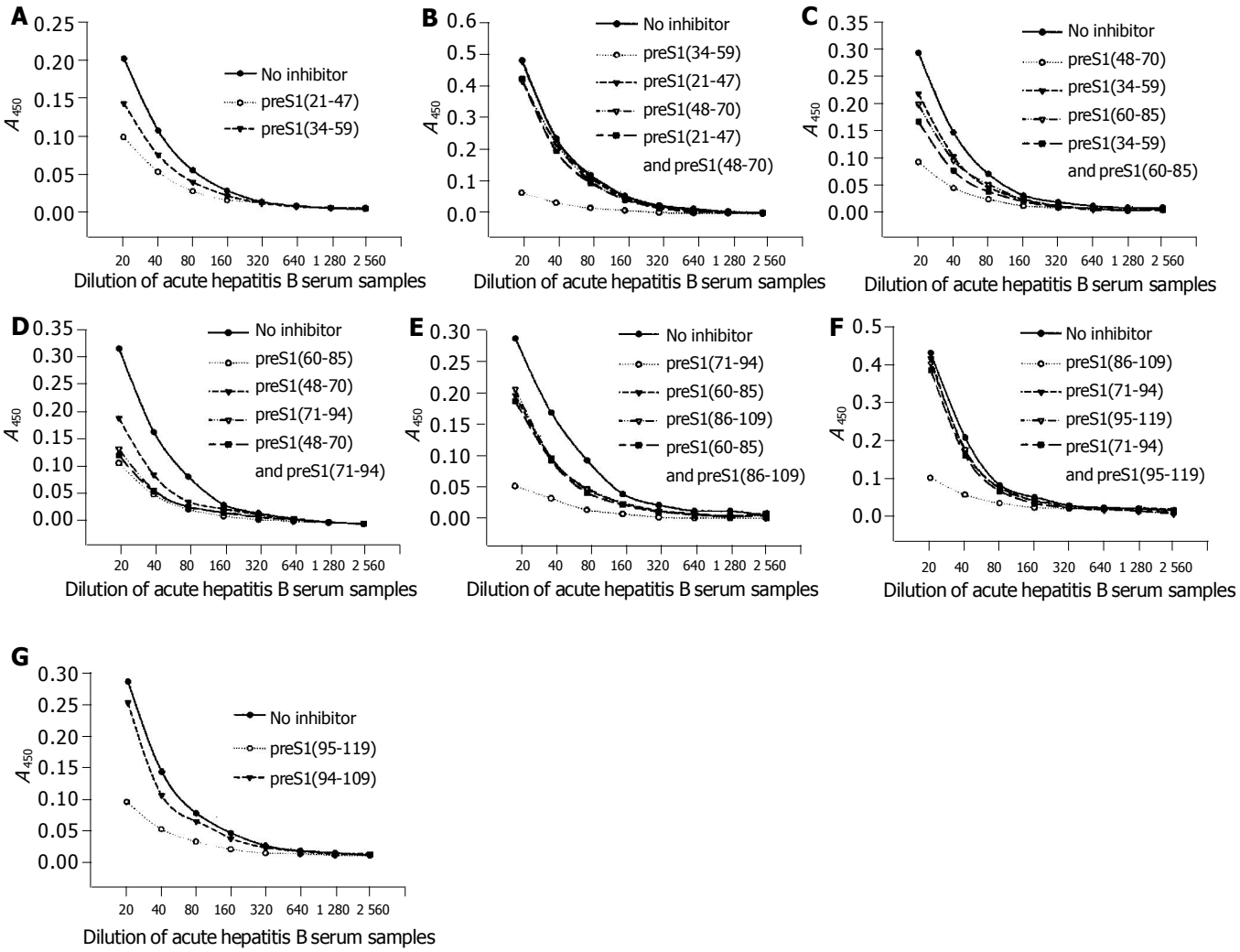

Figure 5 Identification of the precise immunogenic domains in humans by competitive ELISA. The coated antigens were the seven fusion proteins containing different preS1 fragments: preS1 (21-47) (A), preS1 (34-59) (B), preS1 (48-70) (C), preS1 (60-85) (D), preS1 (71-94) (E), preS1 (86-109) (F) and preS1 (95-119) (G), respectively. The mixture of sera samples from acute hepatitis B patients was previously incubated with the coated antigens or the overlapping antigen(s) at a dose of 2 μg, and the samples not treated with antigen(s) were used as controls.

our laboratory[30] and the anti-sera were used to identify the immunogenic domains of preS1 (21-119) region in mice by ELISA using these overlapping preS1 fusion proteins. The antigenicity of these different preS1 fragments against the sera from different HBV-infected patients was also investigated.

The results of immunogenicity analysis in mice showed that the immunogenic domains existed in preS1 (21-59) and preS1 (95-109). It is in agreement with the previous observations, which indicated that the immunogenic domains of preS1 in mice were located in preS1 (16-53) and preS1 (94-117) with the immunization of HBsAg/p43 particles[13]. A previous study also found that the immunogenicity of natural and recombinant antigens was identical[40]. However, the results in humans indicated that other fragments, such as preS1 (71-94), also had strong immunogenicity. It implies that there are more abundant immunogenic domains in preS1 region and more complex immune responses to preS1 region in humans, which might be due to the more complex MHC gene regulation of human immune responses[41]. Additionally, the antigenicity of the N-and C-terminal of the sequences of preS1 (21-119), preS1 (21-47), preS1 (48-70), preS1 (86-109), preS1 (95-119) and especially preS1 (34-59), was significantly lower in chronic-phase sera than in acute-phase sera ($P<0.05$), leading to the speculation that the antibodies against these fragments, especially preS1 (34-59), are virus-neutralizing.

On the other hand, some previous data figured out that the major epitope of preS1 region in acute-phase sera was conformational, its specific antibody was virus-precipitating and the activity was decreased later[37,40-42]. But it has not been identified. Importantly, the results here clearly showed that the fragments of preS1 (34-59) were the major immunogenic domains in mice and human immune responses to preS1 region and its antibody activity was also decreased in mice at wk 7 after immunization. Therefore, the antibody could be speculated to be virus-neutralizing, and it might be efficient to develop a promising vaccine, which incorporates these fragments into HBsAg-based recombinant vaccines.

The predictions of secondary structure and immunological properties in the preS1 (21-119) region using Lasegene software (DNASTAR Inc., Madison, WI) also supported

the above results. In conclusion, there are a great deal of turn regions and coil regions, which lack of alpha and beta regions in preS1 region. The only alpha region is located in the domain of preS1 (51-58), which may partially explain the much stronger immunogenicity of preS1 (34-59). In addition, the N-and C-terminal in preS1 (21-119) region have a strong hydrophilicity, a high antigenic index and a high surface probability, which cause the strong immunogenicity, while preS1 (60-70) has a very weak hydrophilicity, a low antigenic index and low surface probability, which cause the little immunogenicity.

ACKNOWLEDGMENTS

The authors are deeply grateful to Dr. Wen-Sheng Xue, Dr. En-Bing Xue and Dr. Xiang-Ji Luo in Changzheng Hospital, Shanghai and East Hepatobiliary Surgery Hospital, Shanghai for the collection of human sera samples.

REFERENCES

1 **Heermann KH,** Goldmann U, Schwartz W, Seyffarth T, Baumgarten H, Gerlich WH. Large surface proteins of hepatitis B virus containing the pre-s sequence. *J Virol* 1984; **52**: 396-402
2 **Ganem D,** Varmus HE. The molecular biology of the hepatitis B viruses. *Annu Rev Biochem* 1987; **56**: 651-693
3 **Beasley RP,** Hwang LY. Hepatocellular carcinoma and hepatitis B virus. *Semin Liver Dis* 1984; **4**: 113-121
4 **Malik AH,** Lee WM. Chronic hepatitis B virus infection: treatment strategies for the next millennium. *Ann Intern Med* 2000; **132**: 723-731
5 **Blumberg BS.** Hepatitis B virus, the vaccine, and the control of primary cancer of the liver. *Proc Natl Acad Sci USA* 1997; **94**: 7121-7125
6 **Lee CL,** Ko YC. Hepatitis B vaccination and hepatocellular carcinoma in Taiwan. *Pediatrics* 1997; **99**: 351-353
7 **Mahoney FJ,** Kane M. Hepatitis B vaccine. In: Plotkin S A, Orenstein W A (Eds), Vaccines. 3rd ed. *London Saunders* 1999: 158-182
8 **West DJ,** Calandra GB, Ellis RW. Vaccination of infants and children against hepatitis B. *Pediatr Clin North Am* 1990; **37**: 585-601
9 **André FE.** Overview of a 5-year clinical experience with a yeast-derived hepatitis B vaccine. *Vaccine* 1990; **8**: S74-S78; discussion S79-S80
10 **Milich DR**. Genetic and molecular basis for T- and B-cell recognition of hepatitis B viral antigens. *Immunol Rev* 1987; **99**: 71-103
11 **Milich DR.** T-and B-cell recognition of hepatitis B viral antigens. *Immunol Today* 1988; **9**: 380-386
12 **Horsfall AC,** Hay FC, Soltys AJ, Jones MG. Epitope mapping. *Immunol Today* 1991; **12**: 211-213
13 **Milich DR,** McLachlan A, Moriarty A, Thornton GB. A single 10-residue pre-S (1) peptide can prime T cell help for antibody production to multiple epitopes within the pre-S (1), pre-S (2), and S regions of HBsAg. *J Immunol* 1987; **138**: 4457-4465
14 **Park JH,** Cho EW, Lee YJ, Shin SY, Kim KL. Determination of the protective effects of neutralizing anti-hepatitis B virus (HBV) immunoglobulins by epitope mapping with recombinant HBV surface-antigen proteins. *Microbiol Immunol* 2000; **44**: 703-710
15 **Kuroki K,** Floreani M, Mimms LT, Ganem D. Epitope mapping of the PreS1 domain of the hepatitis B virus large surface protein. *Virology* 1990; **176**: 620-624
16 **Küttner G,** Kramer A, Schmidtke G, Giessmann E, Dong L, Roggenbuck D, Scholz C, Seifert M, Stigler RD, Schneider-Mergener J, Porstmann T, Höhne W. Characterization of neutralizing anti-pre-S1 and anti-pre-S2 (HBV) monoclonal antibodies and their fragments. *Mol Immunol* 1999; **36**: 669-683
17 **Ryu CJ,** Kim YK, Hur H, Kim HS, Oh JM, Kang YJ, Hong HJ. Mouse monoclonal antibodies to hepatitis B virus preS1 produced after immunization with recombinant preS1 peptide. *Hybridoma* 2000; **19**: 185-189
18 **Maeng CY,** Ryu CJ, Gripon P, Guguen-Guillouzo C, Hong HJ. Fine mapping of virus-neutralizing epitopes on hepatitis B virus PreS1. *Virology* 2000; **270**: 9-16
19 **Pizarro JC,** Vulliez-le Normand B, Riottot MM, Budkowska A, Bentley GA. Structural and functional characterization of a monoclonal antibody specific for the preS1 region of hepatitis B virus. *FEBS Lett* 2001; **509**: 463-468
20 **Petit MA,** Strick N, Dubanchet S, Capel F, Neurath AR. Inhibitory activity of monoclonal antibody F35.25 on the interaction between hepatocytes (HepG2 cells) and preS1-specific ligands. *Mol Immunol* 1991; **28**: 517-521
21 **Ferrari C,** Cavalli A, Penna A, Valli A, Bertoletti A, Pedretti G, Pilli M, Vitali P, Neri TM, Giuberti T. Fine specificity of the human T-cell response to the hepatitis B virus preS1 antigen. *Gastroenterology* 1992; **103**: 255-263
22 **Bertino JS,** Tirrell P, Greenberg RN, Keyserling HL, Poland GA, Gump D, Kumer ML, Ramsey K. A comparative trial of standard or high-dose S subunit recombinant hepatitis B vaccine versus a vaccine containing S subunit, Pre-S1, and Pre-S2 particles for revaccination of healthy adult non-responders. *J Inf Dis* 1997; **175**: 678-681
23 **Holzer GW**, Mayrhofer J, Leitner J, Blum M, Webersinke G, Heuritsch S, Falkner FG. Overexpression of hepatitis B virus surface antigens including the preS1 region in a serum-free Chinese hamster ovary cell line. *Protein Expr Purif* 2003; **29**: 58-69
24 **Kniskern PJ,** Hagopian A, Burke P, Dunn N, Emini EA, Miller WJ, Yamazaki S, Ellis RW. A candidate vaccine for hepatitis B containing the complete viral surface protein. *Hepatology* 1988; **8**: 82-87
25 **Xu X,** Li GD, Kong YY, Yang HL, Zhang Z, Cao HT, Wang Y. A modified hepatitis B virus surface antigen with the receptor-binding site for hepatocytes at its C terminus: expression, antigenicity and immunogenicity. *J Gen Virol* 1994; **75 (Pt 12)**: 3673-3677
26 **Petre J,** Rutgers T, Hauser P. Properties of a recombinant yeast-derived hepatitis B surface antigen containing S, preS2 and preS1 antigenic domains. *Arch Virol Suppl* 1992; **4**: 137-141
27 **Prange R,** Werr M, Birkner M, Hilfrich R, Streeck RE. Properties of modified hepatitis B virus surface antigen particles carrying preS epitopes. *J Gen Virol* 1995; **76 (Pt 9)**: 2131-2140
28 **Alberti A,** Gerlich WH, Heermann KH, Pontisso P. Nature and display of hepatitis B virus envelope proteins and the humoral immune response. *Springer Semin Immunopathol* 1990; **12**: 5-23
29 **Hu W,** Li F, Yang X, Li Z, Xia H, Li G, Wang Y, Zhang Z. A flexible peptide linker enhances the immunoreactivity of two copies HBsAg preS1 (21-47) fusion protein. *J Biotechnol* 2004; **107**: 83-90
30 **Wei J,** Wang YQ, Lu ZM, Li GD, Wang Y, Zhang ZC. Detection of anti-preS1 antibodies for recovery of hepatitis B patients by immunoassay. *World J Gastroenterol* 2002; **8**: 276-281
31 **Neurath AR,** Kent SB, Strick N, Parker K. Identification and chemical synthesis of a host cell receptor binding site on hepatitis B virus. *Cell* 1986; **46**: 429-436
32 **Ou JH,** Rutter WJ. Regulation of secretion of the hepatitis B virus major surface antigen by the preS-1 protein. *J Virol* 1987; **61**: 782-786
33 **Persing DH,** Varmus HE, Ganem D. Inhibition of secretion of hepatitis B surface antigen by a related presurface polypeptide. *Science* 1986; **234**: 1388-1391
34 **Neurath AR,** Kent SB, Strick N, Stark D, Sproul P. Genetic restriction of immune responsiveness to synthetic peptides

corresponding to sequences in the pre-S region of the hepatitis B virus (HBV) envelope gene. *J Med Viro*l 1985; **17**: 119-125

35 **Milich DR,** McLachlan A, Chisari FV, Kent SB, Thorton GB. Immune response to the pre-S (1) region of the hepatitis B surface antigen (HBsAg): a pre-S (1)-specific T cell response can bypass nonresponsiveness to the pre-S(2) and S regions of HBsAg. *J Immunol* 1986; **137**: 315-322

36 **Jilg W**. Novel hepatitis B vaccines. *Vaccine* 1998; **16**: s65-68

37 **Alberti A,** Cavalletto D, Chemello L, Belussi F, Fattovich G, Pontisso P, Milanesi G, Ruol A. Fine specificity of human antibody response to the PreS1 domain of hepatitis B virus. *Hepatology* 1990; **12**: 199-203

38 **Smith DB,** Johnson KS. Single-step purification of polypeptides expressed in *Escherichia coli* as fusions with glutathione *S*-transferase. *Gene* 1988; **67**: 31-40

39 **Wei J,** Liu XJ, Wang YQ, Lu ZM, Li GD, Wang Y, Zhang ZC. Development of the diagnostic immunoassay to detect anti-PreS1(21-47aa) antibody--a marker suggesting the health improvement of hepatitis B patients. *Clin Chim Acta* 2002; **317**: 159-169

40 **Heermann KH,** Kruse F, Seifer M, Gerlich WH. Immunogenicity of the gene S and Pre-S domains in hepatitis B virions and HBsAg filaments. *Intervirology* 1987; **28**: 14-25

41 **Milich DR,** Leroux-Roels GG. Immunogenetics of the response to HBsAg vaccination. *Autoimmun Rev* 2003; **2**: 248-257

42 **Cavalletto D,** Pontisso P, Belussi F, Alberti A. Fine specificity of antibodies precipitating Dane particles in hepatitis B. *J Hepatol* 1988; **7**: s19-22

Science Editor Wang XL and Li WZ **Language Editor** Elsevier HK

PO Box 2345, Beijing 100023, China
www.wjgnet.com
wjg@wjgnet.com

ELSEVIER

World J Gastroenterol 2005;11(14):2095-2100
World Journal of Gastroenterology ISSN 1007-9327

• *BASIC RESEARCH* •

Effects of emodin and baicalein on rats with severe acute pancreatitis

Xi-Ping Zhang, Zhong-Fang Li, Xiao-Gong Liu, Yong-Tao Wu, Jun-Xian Wang, Kang-Min Wang, Yi-Feng Zhou

Xi-Ping Zhang, Department of General Surgery, First People's Hospital of Hangzhou, Hangzhou 310006, Zhejiang Province, China
Zhong-Fang Li, Xiao-Gong Liu, Yong-Tao Wu, Department of General Surgery, Second Hospital of Xi'an Jiaotong University, Xi'an 710004, Shaanxi Province, China
Jun-Xian Wang, Pharmaceutical College of Xi'an Jiaotong University, Xi'an 710016, Shaanxi Province, China
Kang-Min Wang, Department of Pathology, Second Hospital of Xi'an Jiaotong University, Xi'an 710004, Shaanxi Province, China
Yi-Feng Zhou, Department of Digestion, First People's Hospital of Hangzhou, Hangzhou 310006, Zhejiang Province, China
Supported by the National Natural Science Foundation of China, No. 30171167
Correspondence to: Dr. Xi-Ping Zhang, Department of General Surgery, First People's Hospital of Hangzhou, Hangzhou 310006, Zhejiang Province, China. zxp99688@sina.com
Telephone: +86-571-86069376
Received: 2004-05-07 Accepted: 2004-06-17

Abstract

AIM: To investigate the therapeutic effects of emodin in combination with baicalein on severe acute pancreatitis (SAP) rats and to explore the mechanism of SAP.

METHODS: A total of 112 SAP rats induced by retrograde injection of 5% sodium taurocholate into the biliary-pancreatic duct, randomly assigned to a untreated group and three treated groups emodin group, combined emodin and baicalein group, and sandostatin group. Meanwhile, another 28 other rats were selected as sham operation (SO) group. There were 28 rats in each group, 8 rats were in 3 and 6 h groups respectively, and 12 rats in 12 h group. At each time-points, survival rates, ascites volumes, pathological lesion scores of pancreas tissues, serum amylase, tumor necrosis factor-α and IL-6 levels were determined as the indexes of therapeutic effects.

RESULTS: The survival rate at 12 h was significantly higher in three treated groups than in untreated group. The ascites volume at 12 h was remarkably less in combined and sandostatin groups than in emodin group, but there was no difference between combined group and sandostatin group (P>0.05). Serum amylase levels at all time-points were significantly lower in three treated groups than in untreated group. However, they had no difference among treated groups (P>0.05). Serum TNF-α were lower in three treated groups than in untreated group at all time points. Among the three treated groups, at 6 h, the TNF-α levels of combination and sandostatin groups were lower than those of emodin group. These was no difference between combined and sandostantin. Serum IL-6 concentration at 3 h were lower in combined and sandostatin groups than in untreated group, but at 6 and 12 h they were lower in all treated groups than in untreated group and the combined and sandostatin groups and in emodin group, no difference was found between combined and sandostatin groups at all time-points (P>0.05). The pathological scores of pancreas at all time points were significantly lower in three treated groups than in the untreated group, and at 6, 12 h, the scores of combined and sandostatin groups were lower than in emodin group. There was no difference between combined and sandostatin groups (P>0.05).

CONCLUSION: Combination of emodin with baicalein has significant therapeutic effects on SAP rats.

Key words: Emodin; Severe acute pancreatitis

Zhang XP, Li ZF, Liu XG, Wu YT, Wang JX, Wang KM, Zhou YF. Effects of emodin and baicalein on rats with severe acute pancreatitis. *World J Gastroenterol* 2005; 11(14): 2095-2100
http://www.wjgnet.com/1007-9327/11/2095.asp

INTRODUCTION

Severe acute pancreatitis (SAP) has high incidence of complications and high mortality. For many years, treating SAP has been difficult. Up to now, some drugs for treating SAP have been used in the clinic, especially sandostatin, an analog to somatostatin has rather excellent effects on inhibiting pancreatic excretion and preventing complications. However, it is too expensive, especially in remote poor areas. So, it is necessary to find some cheap and high effective drugs. Emodin is a main active monomer of rhubarb, which is widely used in traditional Chinese herb as laxative, is a derivative of anthraquinone (3-methyl-1,6,8-trihydroxyanthraquinone). Baicalein is a main active monomer in herb *Scutellaria baicalensis* (baikal skullcap root), and belongs to glucuronid category[1,2]. A lot of studies have confirmed[3-5] that intravenous injection of emodin has some curative effects on SAP rats. Our previous research on the treatment of SAP rat using intravenous injection of baicalein showed that baicalein could attenuate pancreatic pathological lesions and reduce SAP mortality. From Chinese traditional medicine view, the effect of complex-prescriptions is better than that of simple ones. For this reason, we investigated the curative effect of combined emodin with baicalein on SAP rats and

explored its mechanism.

MATERIALS AND METHODS

Main drugs and reagents

Sodium taurocholate purchased from Sigma Company was diluted to 5% solution before application. Emodin from Beijing Biological Products Clinical Laboratory, baicalein extracted from Baikal skullcap root by Pharmaceutical College of Xi'an Jiaotong University, China (purity>98%, HPLC), were prepared to 0.25% and 1% injection solution, respectively. The national invention patents have applied for the formula of Emodin injection solution and Baicalein injection solution. The patent numbers are 200410016809. X and 200410016810.2, respectively. Sandostatin was purchased from Novartis Pharma Company, Switzerland, and the test kit of amylase was obtained from Nanjing Jiancheng Bioengineering Institute. The test kits of TNF-α and IL-6 were purchased from Shanghai Shensu Biotech Company, China.

Experimental rats

Healthy male sanitary SD rats weighing 250-335 g were supplied by Animal Experimental Center of Shanxi Research Institute of Chinese Traditional Medicine, Shanxi Province, China. A total of 112 SAP rats induced by retrograde injection 5% sodium taurocholate into biliary-pancreatic duct, were randomly divided into an untreated group and three treated groups: emodin group combined emodin with baicalein group, and sandostatin group. Each group contained 28 SAP rats. Meanwhile another 28 rats were selected to perform exploratory laparotomy as sham operation (SO) group. The 28 rats in each group were further divided into three subgroups; postoperative 3 h (8 rats), 6 h (8 rats) and 12 h (12 rats) groups. At the above-correspondent time-points these rats were killed by cervical decapitation. Blood and pancreas tissue samples of the killed rats were studied.

Operative procedures and treatment

Before operation, the rats were fasted for 12 h, but allowed to drink water freely. They were anesthetized by 20% urethane intraperitoneal injection (0.5 mL/100 g) as routine. A thigh vein cannulation was set up, and through it NS (sodium chloride) solution was successively supplied at 1 mL/100 g/h speed. After abdomen was opened, according to the calculation of 4 mg/100 g, 5% sodium taurocholate was retrograde injected into the biliary-pancreatic duct at 10 mg/min speed to induce the SAP model. Meanwhile, exploratory laparatomy was performed on the rats in SO group and their pancreas was gently drawn, then the abdomen was closed. After that, emodin (0.25 mg/100 g/6 h), baicalein (2 mg/100 g/6 h) and sandostatin (0.2 μg/100 g/6 h) were transfused into the rats of each correspondent group.

Table 1 The standard of pathological score of pancreas

Histological changes	Classification	Score
Edema	Lobar diaphragm widen	1
	Lobar + interlobular septae widen	2
	Lobar + lobulous + interacinar septae widen	3
Infiltration of inflammatory cell	1–10 leukocyte / HPF	1
	11–20 leukocyte / HPF	2
	>20 leukocyte / HPF	3
Fat necrosis	<2 necrotic cells / per lobule	3
	3–5 necrotic cells / per lobule	5
	>5 necrotic cells / per lobule	7
Parenchymatous necrosis	Necrotic area <5% total area	3
	Necrotic area accout 5–20% total area	5
	Necrotic area>20% total area	7
Hemorrhagic focus	<2 focus / per lobule	3
	2–4 focus / per lobule	5
	>4 focus / per lobule	7

Note: HPF = 400× microscopy.

Observatory indexes and measurement methods

To observe the survival of rats at each time-point, the fluid from the peritoneal cavity was taken using absorbent cotton, weighed before and after operation, and the difference of weights (g) was converted to mL. The tissue samples were fixed in 40 g/L formaldehyde, then sliced and stained with HE. Under microscopy, the pathological lesion scores were evaluated by the double blind method, the assay standard of the scores was acted in methods of Spomam[6] (Table 1). The level of serum amylase was determined by iodine-amylum chromatometry. The serum TNF-α and IL-6 levels were assayed by ABC-ELISA.

Statistical analysis

The results were presented as mean±SD. The χ^2 test was used to compare the difference of survival rates. The difference among various groups was assessed by variance analysis, and $P<0.05$ was considered statistically significant. Computations were performed with SPSS software.

RESULTS

Survival rate

At 3 and 6 h, the rats in all groups were alive. At 12 h, the survival rates of the rats in SO group and three treated groups were 100%, and 50% in untreated group. So the survival rate was significantly higher in treated groups than in untreated group ($P<0.05$) (Table 2).

Ascites volume

The ascites volume at 3 h was not different between untreated group and treated groups ($P>0.05$). At 6 h, the ascites volume in sandostatin group was significantly less than that in untreated group ($P<0.05$). At 12 h, the volume was significantly less in three treated groups than in emodin group

Table 2 Survival rate of each group

Groups	3 h ($n=8$)	6 h ($n=8$)	12 h ($n=12$)
SO	8	8	12[a]
Untreated	8	8	6
Emodin	8	8	12[a]
Combined	8	8	12[a]
Sandostatin	8	8	12[a]

[a]$P<0.05$, *vs* the untreated group.

($P<0.01$), and it was even more significant in the combined group and sandostatin groups than in untreated group ($P<0.01$), but no difference was found between combined and sandostatin groups ($P<0.05$). However, the ascites volume in untreated and treated groups was more than that in SO group ($P<0.001$) (Table 3 and Figure 1).

Serum amylase level

The amylase levels at each time-point were lower in SO group than in all treated groups and untreated group ($P<0.001$). There was no difference among three treated groups ($P>0.05$) (Table 4 and Figure 2).

Serum TNF-α levelIL

At each time-point, TNF-α level was significantly lower in SO group than in the untreated group and all treated groups ($P<0.001$). Among treated groups at 6 h, the TNF-α levels in combined and sandostatin group was markedly lower than in emodin group ($P<0.01$), no difference was found between the combined and sandostantin groups ($P>0.05$) (Table 5 and Figure 3).

Serum IL-6 level

At each time-point, IL-6 level was significantly lower in SO group than in untreated group and all treated groups ($P<0.001$). At 3 h, the IL-6 levels in combined and sandostatin groups was lower than in untreated group ($P<0.01$). At 6 and 12 h, the IL-6 levels in three treated groups were lower than those in untreated group ($P<0.01$). No difference was found between combined and sandostatin groups at all time-points ($P>0.05$) (Table 6 and Figure 4).

Pathological lesions of pancreas

In SO group, there was no significant abnormality in pancreas at all time-points. Mild interstitial edema and inflammatory cell infiltration could be seen in some rats. But in three treated groups and the untreated group, the pathological lesions progressed gradually. However, compared with untreated group, they were obviously attenuated in three treated groups. At 12-h points, the attenuations were more remarkable.

Pathological lesion scores for pancreas

The pathological score at each time-point had no marked difference in SO group, but it was lower in the untreated group and the three treated groups ($P<0.001$), and was more significantly lower in treated groups than in untreated group at different time-points ($P<0.05$, $P<0.01$). There was no difference between combined and sandostatin groups at 6 and 12 h ($P>0.05$) (Table 7 and Figure 5).

DISCUSSION

SAP is a life-threatening disease with a high incidence of complications. Its pathogenesis has not been completely elucidated, nevertheless, experimental and clinical studies have demonstrated that a lot of factors were involved in the local and systemic complications of SAP, such as systemic inflammatory response syndrome which could lead to multiple organ failure and pancreatic necrosis, and are the major cause of deaths. Among them, an intensive systemic inflammatory response mediated by overproduction

Table 3 Ascites volume of each group (mean±SD, mL)

Groups	3 h (n = 8)	6 h (n = 8)	12 h (n = 12)
SO	1.13±0.32	1.15±0.30	1.21±0.32
Untreated	4.51±1.37	7.06±1.91	14.72±2.36
Emodin	4.15±1.32	6.90±1.58	10.54±1.86[b]
Combined	4.44±1.31	6.29±1.97	8.47±1.23[b,d]
Sandostatin	4.15±1.04	5.40±1.82[a]	8.26±1.07[b,d]

[a]$P<0.05$; [b]$P<0.01$ *vs* untreated group. [d]$P<0.01$ *vs* emodin group.

Table 4 Serum amylase level of each group (mean±SD, U/L)

Groups	3 h (n = 8)	6 h (n = 8)	12 h (n = 12)
SO	1 473.38±363.80	1 425.00±304.85	1 489.50±176.67
Untreated	4 108.50±862.24	5 059.63±326.35	5 668.17±547.07
Emodin	3 406.00±762.16[a]	4 033.38±481.53[b]	4 399.75±577.54[b]
Combined	3 524.38±637.19[a]	3 941.25±435.76[b]	4 225.50±435.70[b]
Sandostatin	3 518.50±636.9[a]	3 641.00±369.02[b]	4 255.00±605.2[b]

[a]$P<0.05$; [b]$P<0.01$ *vs* untreated group.

Table 5 Serum TNF-α levels of each group (mean±SD, pg/mL)

Groups	3 h (n = 8)	6 h (n = 8)	12 h (n = 12)
SO	53.12±6.57	60.00±8.61	62.92±10.43
Untreated	253.25±9.69	353.88±23.67	327.50±25.62
Emodin	185.13±21.35[b]	306.50±16.83[b]	249.42±29.86[b]
Combined	199.38±23.69[b]	267.50±21.04[b,d]	264.25±40.79[b]
Sandostatin	194.50±18.46[b]	269.50±26.87[b,d]	232.58±23.35[b]

[b]$P<0.01$ *vs* untreated group. [d]$P<0.01$ *vs* emodin group.

Table 6 Serum IL-6 levels of each group (mean±SD, pg/mL)

Groups	3 h	6 h	12 h
SO	72.75±13.26	65.13±13.91	69.08±12.89
Untreated	252.00±21.21	304.63±29.60	299.67±18.02
Emodin	236.25±25.06	270.63±20.85[b]	259.75±18.76[b]
Combined	217.63±22.62[b]	236.75±12.09[b,d]	224.25±22.30[b,d]
Sandostatin	214.75±24.22[b]	237.50±21.26[b,d]	212.00±18.78[b,d]

[b]$P<0.01$ *vs* untreated group. [d]$P<0.01$ *vs* emodin group.

Table 7 Pathological lesion score for pancreas of each group (mean±SD)

Groups	3 h	6 h	12 h
SO	0.50±0.53	0.88±0.64	0.83±0.48
Untreated	7.69±0.84	10.57±2.24	13.50±3.90
Emodin	6.31±1.44[b]	8.75±0.97[a]	10.67±0.86[b]
Combined	6.19±0.96[b]	6.94±0.73[a,d]	8.38±1.05[b,d]
Sandostatin	5.69±0.96[b]	6.06±1.29[a,d]	8.17±1.64[b,d]

[a]$P<0.05$; [b]$P<0.01$ *vs* untreated group. [d]$P<0.01$ *vs* emodin group.

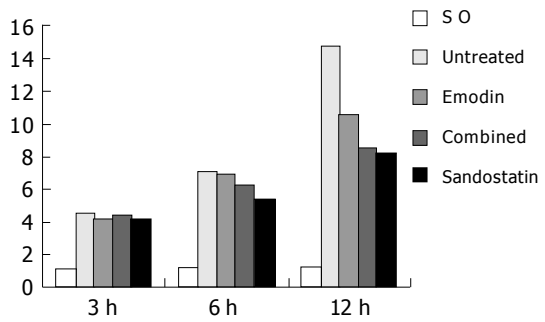

Figure 1 Ascites volume of each group.

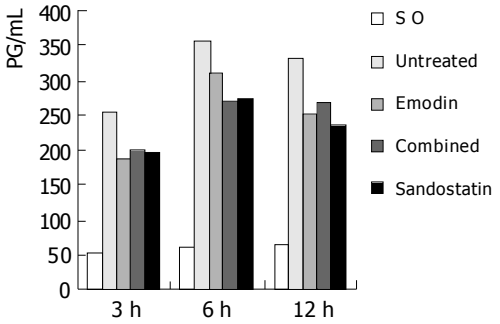

Figure 3 Serum TNF-α levels of each group.

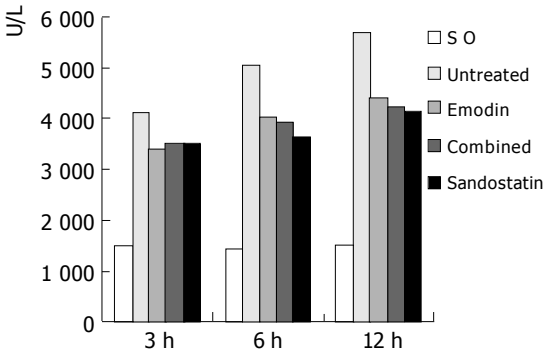

Figure 2 Serum amylase level of each group.

of proinflammatory cytokines and pancreatic autodigestion by activated trypsin plays a very important role. In addition, oxidative stress, secondary infection, endotoxemia are also risk factors. So that, blocking these pathogenetic chains should be the key measures in the treatment of SAP.

Chinese traditional medicine and herbs are the precious treasure of our country, "Qingyi decoction" (Pancreas clearance soup) is an effective traditional prescription in treatment of SAP and has the advantages of a low price and a high therapeutic effect. But during the therapeutic period, patients with SAP always need fasting and gastrointestinal decompression, so oral administration is disadvantageous[7-11]. Rhubarb and Baikal skullcap root are two key herbs in "Qingyi decoction", and emodin and baicalein are their main effective components. They can be taken in the form of an intravenous injection and their prices are low. Researches have demonstrated that both emodin and baicalein have a wide, range of pharmacodynamic effects, the effects are similar and complementary to each other in many aspects. For example, they could effectively inhibit inflammatory reaction, depress the activity of pancreatins or trypsin, antibiosis, antioxidation, scavenging free-radical and anti-thrombosis. A combination of emodin and baicalein could better block the pathogenesis of SAP on multiple levels (the pharmacodynamics of emodin and baicalein is shown in Table 8). Some studies have confirmed that intravenous injection of emodin alone can improve the

Table 8 Pharmacodynamic comparation of emodin and baicalein[12-53]

Pharmacological function	Emodin	Baicalein
Antibiosis	*Escherichia coli*, Dysentery *Bacillus. Aureus staphylococcus*	G^+,G^- bacterium, fungi, spirilla
Anti-inflammation	Inhibiting inflammatory cytokine release, restraining vascular permeability, inhibiting leukotrienes synthesis	Anti-histamin release. anti-arachidonic acid metabolism, restraining vascular permeability, anti-allergy
Immunoregulation	Enhance immunity	(−)
Inhibiting pancreatin activity	Strongly suppressive effect on multiple pancreatins	Only on trypsogen
Protecting liver	Anti-hepatofibrosis, antagonzism of liver damage by CCL_4	Anti-hepatofibrosis,
Protecting kidney	Inhibiting kidney compensative hypertrophy. restraining proliferation of kidney fibroblast, preventing and curing earlier injury of kidney on rats with diabetes	(–)
Protecting pancreas	(+)	(–)
Cholagog	(+)	(–)
Diuresis	(+)	(+)
Antioxidation	(+)	(+)
Scavenging free-radicals	(+)	(+)
Anti-thrombosis	(+)	(+)
Circulatory system	Dilative effect on multiple blood vessel, depressing proliferation of vascular smooth muscle cell	Double effects of vasodilatation and vasoconstriction
Gastrointestinal tract	Double regulation of isolated intestine, anti-gastric ulcer,reducing gastric acid and pepsin, purgate	Curative effect on acute and chronic gastroenteritis
Anti-endotoxemia	(+)	(+)
Fever relieving	(–)	(+)

"+" for positive pharmacological action; "–" for negative pharmacological action.

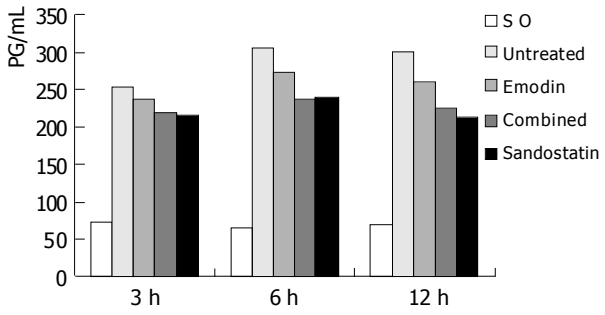

Figure 4 The serum IL-6 levels of each group.

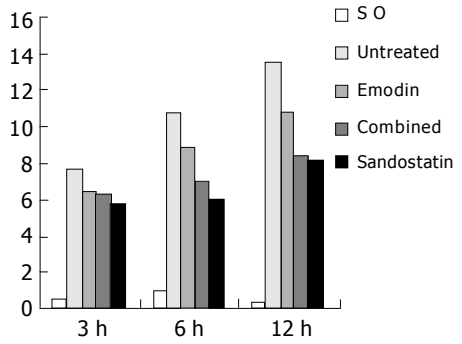

Figure 5 Pathological lesion score for pancreas of each group.

prognosis and decrease the mortality of SAP in rats[3-5]. Whether combined emodin with baicalein can further enhance SAP curative effect, and cut down mortality remains to be studied.

Our results showed that intravenous injection of emodin alone could significantly decrease the serum level of proinflammatory cytokines such as TNF-α, IL-6, and serum amylase concentration in SAP rat, and combination of emodin with baicalein further reduced the TNF-α and IL-6 levels. It indicated that the combination had better effect on blocking important factors of pathogenesis of SAP. At the same time, the combined group showed better therapeutic effect on reducing ascites volume and attenuating pancreatic pathological lesions than those of emodin alone. Sandostatin is considered to be one of the best drugs in the treatment of SAP. However, our results also showed that the therapeutic effect of a combination of emodin with bacalein was similar to that on SAP rats. Emodin and baicalein are easy to be extracted, isolated and identified, so they show an excellent prospect in the development of some new drugs for treating SAP.

In conclusion, the therapeutic effect of a combination of emodin with baicalein on SAP rats is better than emodin alone, and is worthy to be studied further.

REFERENCES

1 **Zhang XP,** Li ZF. General situation in pharmacological studies on Emodin. *Zhongguo Yaolixue Tongbao* 2003; **19**: 851-854
2 **Zhang XP,** Li ZF, Liu XG. Statusquo in the pharmacological studies on Baicalein. *Zhongguo Yaolixue Tongbao* 2001; **17**: 711-713
3 **Wu JX,** Xu JY, Yuan YZ. Effects and mechanism of emodin and sandostatin on pancreatic ischemia in acute haemorrhagic necrotizing pancreatitis. *Zhongguo Zhongxiyi Jiehe Zazhi* 1997; **17**: 356-359
4 **Wu JX,** Xu JY, Yuan YZ. Effectes of emodin and sandostatin on eicosanoid metabolism in acute hamorrhagic necrotizing pancreatitis in rats. *Zhonghua Shiyan Waike Zazhi* 1997; **14**: 215-216
5 **Wu JX,** Xu JY, Yuan YZ. Effect of emodin and sandostatin on metabolism of eicosanoids in acute necrotizing pancreatitis. *World J Gastroenterol* 2000; **6**: 293-294
6 **Spormann H,** Sokolowski A, Letko G. Effect of temporary ischemia upon development and histological patterns of acute pancreatitis in the rat. *Pathol Res Pract* 1989; **184**: 507-513
7 **Li YY,** Gao ZF, Dui DH. Therapeutic effect of qingyi decoction and tetrandrine in treating severe acute pancreatitis in miniature pigs and serum drug level determination. *Zhongguo Zhongxiyi Jiehe Zazhi* 2003; **23**: 832-836
8 **Wen QP,** Chen HL, Guan FL. Effect of qingyi decoction on rats with acute lung injury caused by severe acute pancreatitis. *Zhongguo Zhongxiyi Jiehe Waike Zazhi* 2003; **9**: 302-306
9 **Yao GQ,** Wu XZ. Clinical study of treatment of severe acut pancreatitis with qingyi decoction. *Zhongguo Zhongxiyi Jiehe Waike Zazhi* 1997; **3**: 244-246
10 **Wu CT,** Li ZL, Huang XC, Zhang ZL. Effect of Chinese medicine "QingYiTang" and bifidobacterium mixture on intestinal bacterial translocation following acute necrotizing pancceatitis. *Shijie Huanren Xiaohua Zazhi* 1999; **7**: 525-528
11 **Li JJ,** Yang XJ, Wei MX. The effect of Qingyitang on gastrointestinal motility in rats with acute Pancreatitis.*Nanjing Yikedaxue Xuebao* 2002; **22**: 223-225
12 **Miyamoto K,** Katsuragi T, Abdu P, Furukawa T. Effects of baicalein on prostanoid generation from the lung and contractile responses of the trachea in guinea pig. *Am J Chin Med* 1997; **25**: 37-50
13 **Shieh DE,** Liu LT, Lin CC. Antioxidant and free radical scavenging effects of baicalein, baicalin and wogonin. *Anticancer Res* 2000; **20**: 2861-2865
14 **Gao Z,** Huang K, Yang X, Xu H. Free radical scavenging and antioxidant activities of flavonoids extracted from the radix of Scutellaria baicalensis Georgi. *Biochim Biophys Acta* 1999; **1472**: 643-650
15 **Gao D,** Tawa R, Masaki H, Okano Y, Sakurai H. Protective effects of baicalein against cell damage by reactive oxygen species. *Chem Pharm Bull (Tokyo)* 1998; **46**: 1383-1387
16 **Shao ZH,** Li CQ, Vanden Hoek TL, Becker LB, Schumacker PT, Wu JA, Attele AS, Yuan CS. Extract from Scutellaria baicalensis Georgi attenuates oxidant stress in cardiomyocytes. *J Mol Cell Cardiol* 1999; **31**: 1885-1895
17 **Lee MJ,** Wang CJ, Tsai YY, Hwang JM, Lin WL, Tseng TH, Chu CY. Inhibitory effect of 12-O-tetradecanoylphorbol-13-acetate-caused tumor promotion in benzo[a]pyrene-initiated CD-1 mouse skin by baicalein. *Nutr Cancer* 1999; **34**: 185-191
18 **Chang CH,** Lin CC, Yang JJ, Namba T, Hattori M.Anti-inflammatory effects of emodin from ventilago leiocarpa. *Am J Chin Med* 1996; **24**: 139-142
19 **Qi H.** Anti-inflammatory effects of emodin. *Zhongcaoyao Zazhi* 1995; **30**: 522-524
20 **Goel RK,** Das Gupta G, Ram SN, Pandey VB. Antiulcerogenic and anti-inflammatory effects of emodin, isolated from Rhamnus triquerta wall. *Indian J Exp Biol* 1991; **29**: 230-232
21 **Jiao JJ,** Wen FH, Hu P. Effect of emodin on the synthesis of LTB_4 by peritoneal mecrophages in rats. *Tianjing Yikedaxue Xuebao* 1996; **2**: 11-13
22 **Kuo YC,** Tsai WJ, Meng HC, Chen WP, Yang LY, Lin CY. Immune reponses in human mesangial cells regulated by emodin from Polygonum hypoleucum Ohwi. *Life Sci* 2001; **68**: 1271-1286
23 **Kuo YC,** Meng HC, Tsai WJ. Regulation of cell proliferation, inflammatory cytokine production and calcium mobilization in primary human T lymphocytes by emodin from Polygonum

hypoleucum Ohwi. *Inflamm Res* 2001; **50**: 73-82
24 **Wang WJ,** Wu XZ, Yao Z, Li HQ. The influence of emodin and danshensu on monocyte's secretion of inflammatory cytokines. *Zhongguo Mianyixue Zazhi* 1995; **11**: 370-372
25 **Zhan YT,** Wei HS, Wang ZR, Huang X, Xu QF, Li DG. Experimental study on the protective effect of emodin on rat's liver injury induced by CCl_4. *Zhongguo Zhongyiyao Keji* 2000; **7**: 30-31
26 **Lin CC,** Chang CH, Yang JJ, Namba T, Hattori M. Hepatoprotective effects of emodin from Ventilago leiocarpa. *J Ethnopharmacol* 1996; **52**: 107-111
27 **Zhan Y,** Li D, Wei H, Wang Z, Huang X, Xu Q, Lu H. Emodin on hepatic fibrosis in rats. *Chin Med J (Engl)* 2000; **113**: 599-601
28 **Zhan YT,** Li DG, Wei HS, Wang ZR, Huang X, Li ZD, Xu QF, Lu HM. Effect of emodin on development of hepatic fibrosis in rats. *Zhongguo Zhongxiyi Jiehe Waike Zazhi* 2000; **20**: 276-278
29 **Liu GX,** Ye RG, Tan ZM, Zhong WQ, Yang YM, Zhang GQ, Fang JA. Effect of emosin on fibroblast in lupus nephritis. *Zhongguo Shiyan Linchuang Mianyixue Zazhi* 1999; **11**: 24-27
30 **Zhan Y,** Wei H, Wang Z, Huang X, Xu Q, Li D, Lu H. Effects of emodin on hepatic fibrosis in rats. *Zhonghua Ganzangbing Zazhi* 2001; **9**: 235-236
31 **Liu GX,** Ye RG, Tan ZM, Zhong WQ, Yang YM, Zhang GQ, Fang JA. Effect of emodin on fibroblasts in lupus nephritis. *Zhongguo Zhongxiyi jiehe Zazhi* 2000; **20**: 196-198
32 **Ning Y,** Wang J, Qu S. Effect of emodin on human kidney fibroblast proliferation. *Zhongguo Zhongxiyi Jiehe Zazhi* 2000; **20**: 105-106
33 **Yang JW,** Li LS, Hu WX, Xu RJ. Inhibitory effect of emodin on compensatory renal hypertrophy in rats. *Zhongguo Yaolixue Tongbao* 1994; **10**: 224-227
34 **Jin ZH,** Ma DL, Lin XZ. Study on effect of emodin on the isolated intestinal smooth muscle of guinea pigs. *Zhongguo Zhongxiyi Jiehe Zazhi* 1994; **14**: 429-431
35 **Zhen F,** Li LS, Liu ZH, Zhou H, Liang LQ. The effects of emodin on cellular proliferation and c-myc prctooncogene and TGF-β gene expressions in renal tubular cells. *Zhongguo Yaolixue Tongbao* 1994; **10**: 375-378
36 **Dai CS,** Liu ZH, Chen HP, Zhou H, Wang JP, Li LS. Combined tretment of triptolide and emodin inhibits the progression of anti-GBM nephritis in rats. *Shenzangbing Yu Touxi Shenyizhi Zazhi* 2000; **9**: 117-123
37 **Nakamura N,** Hayasaka S, Zhang XY, Nagaki Y, Matsumoto M, Hayasaka Y, Terasawa K. Effects of baicalin, baicalein, and wogonin on interleukin-6 and interleukin-8 expression, and nuclear factor-kappab binding activities induced by interleukin-1beta in human retinal pigment epithelial cell line. *Exp Eye Res* 2003; **77**: 195-202
38 **Shen YC,** Chiou WF, Chou YC, Chen CF. Mechanisms in mediating the anti-inflammatory effects of baicalin and baicalein in human leukocytes. *Eur J Pharmacol* 2003; **465**: 171-181
39 **Hong T,** Jin GB, Cho S, Cyong JC. Evaluation of the anti-inflammatory effect of baicalein on dextran sulfate sodium-induced colitis in mice. *Planta Med* 2002; **68**: 268-271
40 **Shao ZH,** Vanden Hoek TL, Qin Y, Becker LB, Schumacker PT, Li CQ, Dey L, Barth E, Halpern H, Rosen GM, Yuan CS. Baicalein attenuates oxidant stress in cardiomyocytes. *Am J Physiol Heart Circ Physiol* 2002; **282**: H999-H1006
41 **Nakahata N,** Kutsuwa M, Kyo R, Kubo M, Hayashi K, Ohizumi Y. Analysis of inhibitory effects of scutellariae radix and baicalein on prostaglandin E2 production in rat C6 glioma cells. *Am J Chin Med* 1998; **26**: 311-323
42 **Butenko IG,** Gladtchenko SV, Galushko SV. Anti-inflammatory properties and inhibition of leukotriene C4 biosynthesis *in vitro* by flavonoid baicalein from Scutellaria baicalensis georgy roots. *Agents Actions* 1993; **39 Spec No**: C49-C51
43 **Miyamoto K,** Katsuragi T, Abdu P, Furukawa T. Effects of baicalein on prostanoid generation from the lung and contractile responses of the trachea in guinea pig. *Am J Chin Med* 1997; **25**: 37-50
44 **Inoue T,** Jackson EK. Strong antiproliferative effects of baicalein in cultured rat hepatic stellate cells. *Eur J Pharmacol* 1999; **378**: 129-135
45 **Shieh DE,** Liu LT, Lin CC. Antioxidant and free radical scavenging effects of baicalein, baicalin and wogonin. *Anticancer Res* 2000; **20**: 2861-2865
46 **Gao Z,** Huang K, Yang X, Xu H. Free radical scavenging and antioxidant activities of flavonoids extracted from the radix of Scutellaria baicalensis Georgi. *Bichim Biophys Acta* 1999; **1472**: 643-650
47 **Gao D,** Tawa R, Masaki H, Okano Y, Sakurai H. Protective effects of baicalein against cell damage by reactive oxygen species. *Chem Pharm Bull (Tokyo)* 1998; **46**: 1383-1387
48 **Shao ZH,** Li CQ, Vanden Hoek TL, Becker LB, Schumacker PT, Wu JA, Attele AS, Yuan CS. Extract from Scutellaria baicalensis Georgi attenuates oxidant stress in cardiomyocytes. *J Mol Cell Cardiol* 1999; **31**: 1885-1895
49 **Kimura Y,** Yokoi K, Matsushita N, Okuda H. Effects of flavonoids isolated from scutellariae radix on the production of tissue-type plasminogen activator and plasminogen activator inhibitor-1 induced by thrombin and thrombin receptor agonist peptide in cultured human umbilical vein endothelial cells. *J Pharm Pharmacol* 1997; **49**: 816-822
50 **Chen ZY,** Su YL, Lau CW, Law WI, Huang Y. Endothelium-dependent contraction and direct relaxation induced by baicalein in rat mesenteric artery. *Eur J Pharmacol* 1999; **374**: 41-47
51 **Huang HC,** Wang HR, Hsieh LM. Antiproliferative effect of baicalein, a flavonoid from a Chinese herb, on vascular smooth muscle cell. *Eur J Pharmacol* 1994; **251**: 91-93
52 **Kimura Y,** Matsushita N, Okuda H. Effects of baicalein isolated from Scutellaria baicalensis on interleukin 1 beta- and tumor necrosis factor alpha-induced adhesion molecule expression in cultured human umbilical vein endothelial cells. *J Ethnopharmacol* 1997; **57**: 63-67
53 **Kimura Y,** Matsushita N, Yokoi-Hayashi K, Okuda H. Effects of baicalein isolated from Scutellaria baicalensis Radix on adhesion molecule expression induced by thrombin and thrombin receptor agonist peptide in cultured human umbilical vein endothelial cells. *Planta Med* 2001; **67**: 331-334

Science Editor Wang XL and Li WZ **Language Editor** Elsevier HK

PO Box 2345, Beijing 100023, China
www.wjgnet.com
wjg@wjgnet.com

ELSEVIER

World J Gastroenterol 2005;11(14):2101-2108
World Journal of Gastroenterology ISSN 1007-9327

• *BASIC RESEARCH* •

Chromic-P32 phosphate treatment of implanted pancreatic carcinoma: Mechanism involved

Lu Liu, Guo-Sheng Feng, Hong Gao, Guan-Sheng Tong, Yu Wang, Wen Gao, Ying Huang, Cheng Li

Lu Liu, Yu Wang, Wen Gao, Ying Huang, Cheng Li, Institute of Nuclear Medicine Technology of Southeast University, Nanjing 210009, Jiangsu Province, China
Guo-Sheng Feng, Hong Gao, Guan-Sheng Tong, Beijing Railway General Hospital, Beijing 100038, China
Supported by the Jiangsu Province Public Health Bureau Foundation, No. H200117, and Jiangsu Science Technology Foundation, No. 2000004
Correspondence to: Dr. Lu Liu, Institute of Nuclear Medicine Technology of Southeast University, 87 Dingjiaqiaolu, Nanjing 210009, Jiangsu Province, China. luliuzhou@sina.com
Telephone: +86-25-83272557 Fax: +86-25-83426368
Received: 2004-03-18 Accepted: 2004-04-13

Abstract

AIM: To study the effects of chromic-P32 phosphate (^{32}P colloids) interstitial administration in Pc-3 implanted pancreatic carcinoma, and investigate its anticancer mechanism.

METHODS: Ninety-eight tumor bearing nude mice were killed at different time points after the injection of ^{32}P colloids to the tumor core with observed radioactivity. The light microscopy, transmission electron microscopy (TEM) and immuno-histochemistry and flow cytometry were used to study the rates of tumor cell necrosis, proliferating cell nuclear antigen index, the micro vessel density (MVD). The changes of the biological response to the lymphatic transported ^{32}P colloids in the inguinal lymph node (ILN) were dynamically observed, and the percentage of tumor cell apoptosis, and Apo2.7, caspase-3, Bcl-2, Bax-related gene expression were observed too.

RESULTS: The half-life of effective medication is 13 d after injection of ^{32}P colloids to the tumor stroma, in 1-6 groups, the tumor cell necrosis rates were 20%, 45%, 65%, 70%, 95% and 4%, respectively (F = 4.14-105.36, P<0.01). MVD were 38.5±4.0, 28.0±2.9, 17.0±2.9, 8.8±1.5, 5.7±2.3 and 65.0±5.2 (t = 11.9-26.1, P<0.01), respectively. Under TEM fairly differentiated Pc-3 cells were found. Thirty days after medication, tumors were shrunk and dried with scabs detached, and those in control group increased in size prominently with plenty of hypodermic blood vessels. In all animals the ILN were enlarged but in medicated animals they appeared later and smaller than those in control group. The extent of irradiative injury in ILN was positively correlated to the dosage of medication. Typical tumor cell apoptosis could be found under TEM in animals with intra-tumoral injection of low dosed ^{32}P colloids. The peak of apoptosis occurred in 2.96 MBq group and 24 h after irradiation. In the course of irradiation-induced apoptosis, the value of Bcl-2/Bax was down regulated; Apo2.7 and caspase-3 protein expression were prominently increased dose dependently.

CONCLUSION: ^{32}P colloids intra-tumor injection having prominent anticancer effectiveness may reveal the ability of promoting cell differentiation. The low dose ^{32}P colloids may induce human pancreatic carcinoma Pc-3 implanted tumor cell apoptosis; Apo2.7, caspase-3, Bcl-2 and Bax protein participated in regulating the process of irradiation induced cell apoptosis.

Key words: Chromic-P32 phosphate; Pancreatic carcinoma

Liu L, Feng GS, Gao H, Tong GS, Wang Y, Gao W, Huang Y, Li C. Chromic-P32 phosphate treatment of implanted pancreatic carcinoma: Mechanism involved. *World J Gastroenterol* 2005; 11(14): 2101-2108
http://www.wjgnet.com/1007-9327/11/2101.asp

INTRODUCTION

High malignant pancreatic carcinoma mostly not diagnosed until in medium or late stage with the mortality remains high. Measures in clinical treatment of tumors have greatly advanced as the development of new preparations in cell growth inhibition, gene therapy, ^{125}I seeds, sustained release chemotherapy seeds, *etc.*, but a great deal of problems remain in the treatment of most solid tumor. The effectiveness of radioactive nuclide has not been fully recognized yet among the measures of conservative therapy. The aim of this study was to observe the biological distribution of chromic-P32 phosphate ($Cr^{32}PO_4$, ^{32}P colloids) in tumor and regional lymph nodes, as well as its anticancer effect and the dose/time-dependent relationship after intra-tumoral injection of ^{32}P colloids to treat the human pancreatic carcinoma cell (Pc-3) bearing models, and to explore its mechanism. Based on this experiment we further studied the effect of low dose ^{32}P colloids on inducing apoptosis of transplanted Pc-3 cell in nude mice, and exploring its possible mechanism.

MATERIALS AND METHODS

Materials

Medicine Medical ^{32}P colloids were provided by Zhonghe Gaotong Isotope Co Ltd. Colloid particles 20-50 nm in

diameter had stable property, specific radioactivity ratio 222-370 MBq/mL, radiochemical purity ⩾98%, pH 6.0-8.0, ^{32}P physical half-life 14.28 d, pure β-emitter, β ray mean energy 0.695 MeV (maximum energy 1.711 MeV), penetrating distance in soft tissue 3-4 mm on average.

Animal models After culturing and multiplying the human pancreatic carcinoma cell, Pc-3 2×10^6 cells were planted into each of the 10 BALB/c-nu/nu nude mice (male, mean body weight 20 g, 6-wk old, from Experimental Center, Shanghai Institute of Oncology, as in all of the following experiments) on the dorsum hypodermically. About 10 d after implantation, the tumor mass attained the diameter of 1.0 cm, the animals were killed by cervical dislocation. Under aseptic condition the tumor mass was dissected and sliced into pieces of 2.0 mm in diameter, rinsed in RPMI 1640 solution (no bovine serum) then the tumor tissue was implanted into the right axilla of 93 BALB/c-nu/nu nude mice subcutaneously. The animals were to be used in experiment as the tumor grew to 0.8-1.0 cm in diameter after 10 d.

Experiment and grouping Forty-eight tumor bearing nude mice were randomly allocated into eight groups, six mice in each group. ^{32}P colloids in 3.7, 7.4, 14.8, 18.5, 29.6 and 0 (cold colloid as control) MBq, in the volume of 0.05-0.1 mL, were injected respectively to 1st-6th groups, then killed at the 14th d after medication. The 7th and 8th groups, 14.8 MBq and placebo were medicated respectively and bred for 30 d on average (maximum 40 d). Fifty tumor bearing nude mice were randomly allocated into 10 groups (n = 5). To the mice in 9th-14th groups ^{32}P colloids of 0.37, 0.74, 1.48, 2.96, 5.92 and 0 MBq, were injected respectively, and then killed 24 h after medication. ^{32}P colloids 1.48 MBq were injected to animals in 15th-19th group and then killed at 6, 12, 24, 36, and 48 h after medication respectively. Groups 11 and 17 were the same group. From the resected tumor masses the percentage of tumor cell apoptosis and necrosis, the changes in ultra structure and Apo2.7, caspase-3, Bcl-2, Bax-related gene expression were observed.

Methods

Estimation of the half-life of effectiveness In groups two and seven, the radioactivity counts on tumor surface were measured daily by ZC-201 surveying instrument with probe at fixed spatial geometric position, 6 cm above the tumor surface for 10 s, mean value of three measurements taken as the final value. Consecutive measurement was done for 14 and 28 d respectively (n = 12 before 14 d, n = 6 after 14 d). The effective half-life of intra-tumoral injection of ^{32}P was calculated.

Pathological observation In 1st-8th groups, the tumor mass and bilateral inguinal lymph nodes (ILN) were dissected, sampled in several sites from each tissue, two pieces of tumor and normal tissues without necrosis under naked eye, 1 mL^3 in size were taken, fixed in 2% glutaraldehyde, dehydrated, sliced in super-thin thickness, double stained with lead-uranium, then observed under TEM H-600. The remaining tumor or normal tissues were fixed in 10% formaldehyde immediately, embedded in paraffin then prepared for light microscopy (Olympus). The morphological changes of tumor were observed and the rate of tumor cell necrosis was calculated on 14th d. The whole course changes of bilateral groin lymph nodes in nude mice, ^{32}P colloids transported in the lymphatic ducts and influence on the changes in ILN were dynamically observed. All of the paraffin slides were made to undergo microwave retrieval with tissue antigen, and dyed with SABC method. Estimation of positive expression of mouse against human proliferating cell nuclear antigen (PCNA) was done. When brown yellow colored granules presented in the tumor cell nuclei without plasma staining, it is defined as positive expression. Method of PCNA index (PI) calculation: Firstly under low and high power microscopes suitable visual fields with plenty of tumor cells were selected, then the cell number under high power microscope counted. From 5 to 10 high power visual fields in different tissues the number of positive cells and their PI were noted. PI = number of PCNA positive cells/number of tumor cells counted×100%. Cluster of differentiation 34 (CD34) is the specific surface marker of endothelial cell in tumor blood vessels. The positive expression signifies the formation of micro blood vessels. Methods of counting the micro blood vessel were that each slide was examined blindly by two expert pathologists, 10 visual fields with micro vessel density (MVD) under low power (×100) magnification were randomly selected, then the MVD under high power magnification counted, the mean value of MVD calculated. Any yellow stained cell or cell cluster signified as one MVD value.

Estimation of cell apoptosis and necrosis by Annexin V-FITC/PI double parameters flow cytometry was prepared A piece of fresh tumor 5-8 mm in diameter was cut, rinsed with PBS solution, the single cell suspension was prepared through digestion, grinding and filtration. Annexin V-FITC 5 μL (10 μg/mL) and PI 5 μL (50 μg/mL) were added to 100 μL cell suspension, kept at room temperature (20-25 ℃), protected from light for 15 min, then assessed with flow cytometry, the data analyzed by Cellquest software program. For estimation of protein caspase-3 and Apo2.7, to each of 100 μL single cell suspension 10 μL of rabbit anti-caspase-3 polyclonal antibody and 20 μL mouse anti-Apo2.7 polyclonal antibody were added respectively, protected from light, reacted 20 min at 4 ℃, rinsed twice with PBS; diluted with 1 mL PBS; and assessed by flow cytometry with exciting wave length 488 nm. Corresponding negative control was prepared. Percentage of positive cells were acquired and analyzed by Cellquest software program. Bax, Bcl-2 protein was estimated by immuno-histochemistry. The positive expression of Bax, Bcl-2 protein was the presentation of brown granules distributed in the cytoplasm of Pc-3 cells. Two expert pathologists examined each slide blindly through randomly counting 200 clear nucleated tumor cells. The percentage of positive cell in the total cells counted was calculated, and then the mean value was taken.

Observation under electron microscopy Samples were taken from several sites of the tumor prepared routinely by the super thin slides in 0.05 μm thickness, under H-600 model transmission electron microscopy (TEM), the changes in ultra structure of the tumor cell and morphology of the apoptosis cell were observed.

Estimating the dose absorbed Based on the equation of absorbed dose in β-internal irradiation the absorbed dose was calculated[1,2]:

Table 1 Fourteen day-absorbed doses in tumor, tumor weight, tumor cell necrosis rate, MVD, PI and percentage of loosely arranged tumor cells to remaining tumor cells (n = 6)

Group	Injected dose (MBq)	Absorbed dose (Gy)	14 d tumor weight (g)	Tumor cell necrotic rate (%)	F	SNK[1]	MVD[2]	PI
6	3.7	248.7	2.16±0.15	20	4.14	A	38.5±4.0	70
7	7.4	497.4	1.60±0.12	45	33.57	B	28.0±2.9	65
8	14.8	852.7	1.13±0.10	65	44.62	C	17.0±2.9	45
9	18.5	1 147.8	0.86±0.09	70	54.93	C	8.8±1.5	20
10	29.6	2 023.4	0.30±0.05	95	105.36	D	5.7±2.3	10
11	0	–	2.84±0.17	4	–	E	65.0±5.2	92

[1]Variance analysis after conversion of tumor cell necrosis rate to square root in each group compared with 0 MBq group, F = 4.14–105.36, P<0.01, SNK test for cell necrosis rate: Same letter means no statistical difference of mean values among groups; differed letters mean the statistical difference among groups. [2]Comparison of MVD between medication and control groups, t = 11.9–26.1, P<0.01, all with prominent differences.

$$D_0=1.443\ (\Sigma \triangle_i) C_0 T_{eff}[1\text{-}e^{-(0.693/Teff)t}]\ \text{cGy} \qquad (1)$$

where C_0 means when t=0, the concentration of β radioactive nuclide in tissue (kBq/g); $\triangle_i$ is the coefficient of the balanced absorbed dose in i type ray for releasing radioactive nuclide, expressed as g·cGy/kBq·h; $\triangle_i$ of ^{32}P is 0.04; T_{eff} is the half-life of effectiveness; D_0 is the absorbed dose in tissue at t time expressed as cGy (1 Gy = 100 cGy).

Statistical analysis

Analysis of variance was conducted after the rate of tumor cell necrosis and apoptosis in different dose group was converted to its square root, when the differences revealed statistical significance; Student-Newman-Keuls' method (SNK) was employed. The value of MVD is expressed as mean value plus standard deviation (mean±SD), t -test between groups was conducted.

RESULTS

Effective half-life and absorbed dosage of ^{32}P colloids in tumor

The effective half-life of ^{32}P colloids 7.4 and 14.8 MBq groups were 12 and 14 d respectively, 13 d on average, equal to 312 h (Figure 1). The related data brought to equation (1), an equation for estimating the absorbed dose of interstitially injected ^{32}P colloids was obtained.

$$D_\beta = 19.78 C_0(1\text{-}e^{-0.002t}) \qquad (2)$$

Manifestation in morphology

General presentation Ten days after implantation of tumor cells, the tumor presented as a prominent solid nodular mass on the body surface, covered with smooth, light red colored skin. One week later, in groups 6 and 8 the tumor evidently increased in size with thinning of the superficial skin in bright and red color, in some cases ulceration on the covering skin occurred. In groups 1-5, 2-3 d after ^{32}P colloids administration, the nude mice showed slightly decreased in appetite, local swollen and redness appeared on the injection sites, vanished 24 h later. In about 3-5 d, spotted ulceration appeared on tumor surface. At beginning tumor growth in therapeutic groups were comparatively slower than those in control group, after 7 d, ecchymosis appeared on the tumor surface, followed by cystic change of the tumor, rupture and bleeding took place, gradually shrunk and finally healed with scab. In groups 4, 5 and 7, 10-14 d after medication, scattered small petechiae appeared on the dorsum of six nude mice, in group 7 about 20 d later the petechiae diminished gradually, tumor size decreased then dried and the scab shed.

Light microscopy and immuno-histochemistry Animals in groups 1-6 were executed on 14th d, the weight of tumor, macroscopically average absorbed dosage in tumor tissues, rate of tumor cell necrosis, value of MVD and PI are shown in Table 1. The Pc-3 cells of control group 11 were densely arranged with plenty of blood vessels. In medication groups there revealed necrosis in different extents, or some loosely arranged tumor cells remained. In low dose groups there were remaining actively proliferated tumor cells and lymphocyte infiltration; and in high dose group, most of the tumor cells damaged instead by fibrotic connective tissues. In medicated nude mice their tissues of main viscera such as liver, lung, spleen, *etc.,* were essentially normal, but in one case of group 5, epithelial anaphase and pearl formation occurred.

Results of CD34 and PCNA assay were shown in Figure 2. In control group CD34 was highly expressed, the tumor field showed plenty of stained micro-vessels, and poly-nucleated, deep brown yellow colored PCNA tumor cells; in medication groups, CD34 expression lowered prominently, tumor cells loosely arranged with scanty of micro-vessels stained or micro-vessels were not found. Only a few PCNA cell had nuclei stained light brown-yellow.

Transmission electron microscopy In control group the characteristic presentation of actively growing tumor cell was: large nuclei, poly-nucleoli, scanty cytoplasm, and some nuclear division might be found. There were few microvilli on the cell surface, bridging the connection between the neighboring cells with formation of pseudo-lumen. In medication groups with differences in absorbed dosages their presentations were: (1) Large numbers of necrotic Pc-3 tumor cells, breaking down into debris, a lot of vacuoles in the cytoplasm, in some cells only the contour of nucleus remained. Some apoptotic tumor cells could be found accompanied with shrunken and broken nuclei, bleeding in interstitium, many neutrocytes infiltrated between the necrosed cells, many collagen fibers and fibroblasts presented in the interstitium. (2) The remaining tumor cells showed swollen mitochondria, distension of endoplasmic reticulum with many lipid droplets, collagen fiber hyperplasia, bleeding and inflammatory cell infiltration in the interstitium. (3) Tumor cells have small nuclei and plenty of cytoplasm in

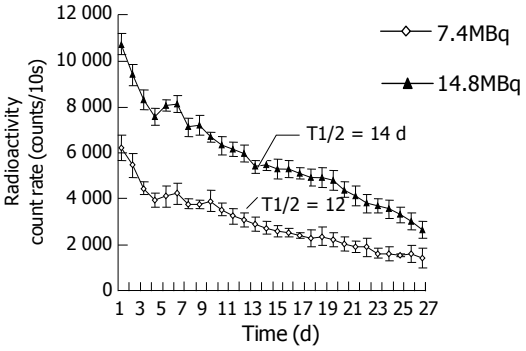

Figure 1 Effective half-life in ^{32}P colloids 7.4 and 14.8 MBq injected group averaged 13 d.

which were presented many mitochondria and free ribosomes, many microvilli on the cell surface. (4) Some tumor cells were well-differentiated (Figure 3), some glandular lumen-like structure presented between the cells, many long microvilli presented on the cell surface. (5) No tumor cells were found in dry scab of the tumor debris, and in the muscular tissue around the tumor there were longitudinal myocomma, neutrocytes in interstitial tissue, and normal nervous structure.

Influence of ^{32}P colloids on ILN (Figure 4) Twelve days after medication bilateral superficial ILN were palpable, while in control group the ILN were palpable 6 d earlier than those in medication group. The characteristics of swelling of ILN were control group>medicated mice, low dose group>high dose group. Under light microscope, lymphocytes uniformly distributed in ILN of group 6 (control group), manifested as normal glandular tissue without abnormalities in lipid tissue and blood vessels; in groups 1-5 the changes in ILN are positively correlated to the dosage of medication. Many plasma cells (rich in rough endoplasmic reticulum) in ILN of groups 1 and 2, showed chronic lymphadenitis; in groups 1-4, apoptotic cells could be found in connective tissue and endothelium of lymph sinus, and lymphocytes loosely distributed in group 5. The vital and denatured Pc-3 cells were found in ILN of control and medicated mice respectively.

Low dose irradiation induced apoptosis

Percentages of apoptosis and necrosis of tumor cells (Tables 2 and 3) In the dose range 0.37-5.92 MBq apoptosis rate tended to increase with the increase of dose absorbed, similar tendency occurred in necrotic rate. The apoptosis rate of the same dose (1.48 MBq) group gradually increased in the time range 6-24 h along with the prolongation of time, attained the peak at 24 h without evident plateau, and then tending to decrease. There were statistically significant differences in rates of cell apoptosis and necrosis between each dosage group and the control group. As compared with group 14, in groups 9-13 the expression of Pc-3 cell Apo2.7 protein and caspase-3 enhanced prominently, and increased along the increase of absorbed dose, existed a dose-response dependent relationship, the correlation coefficient r are 0.774 and 0.768 ($n = 30$, $P<0.01$); Bcl-2/Bax ratio is evidently lower than that of control group ($F = 35.95$, $P<0.01$).

Transmission electron microscopy Normal Pc-3 cell was round in shape with large nucleus and several nucleoli, scanty cytoplasm, chromatin evenly distributed in the cell. The ultra

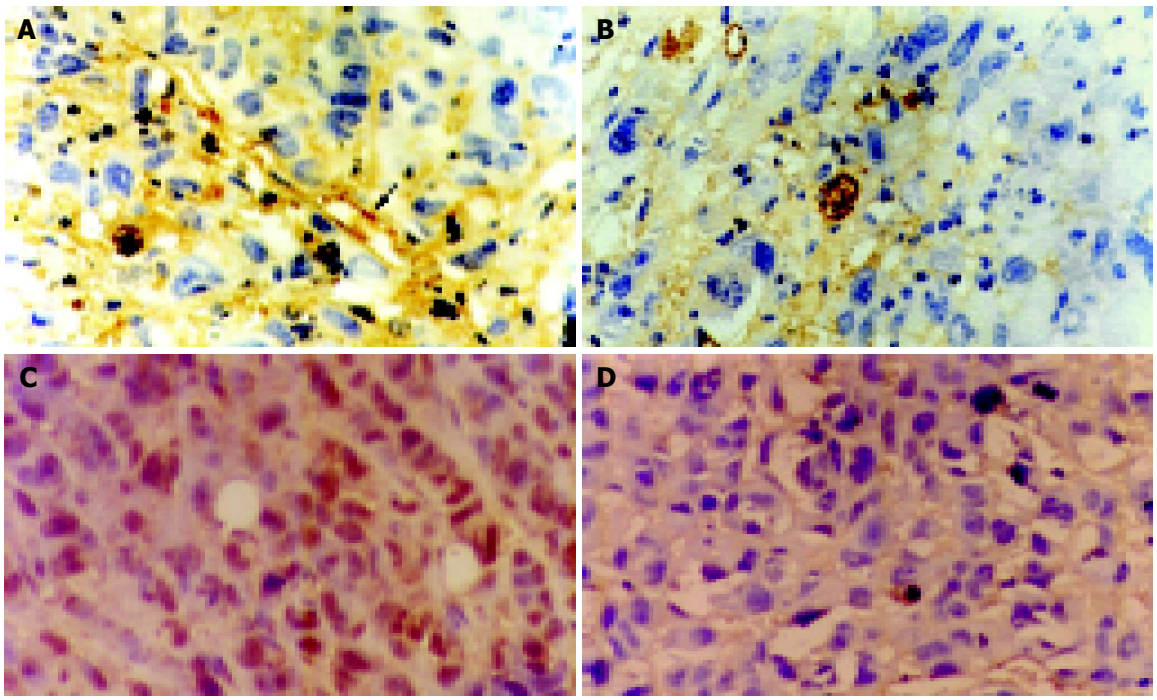

Figure 2 Results of immuno-histochemistry assay of CD34 expression in Pc-3. A: Plenty of stained and densely arranged micro-vessels in tumor field (arrow); B: After medication the tumor cells loosely arranged in tumor field with scanty of micro-vessels stained or no micro-vessels (SABC ×400); PCNA expression in Pc-3. C: In control site, tumor cells were densely arranged with poly nuclei stained in deep brown yellow; D: In each of the dosed sites loosely arranged tumor cells merely with few nuclei stained in light brown yellow color (SABC ×400).

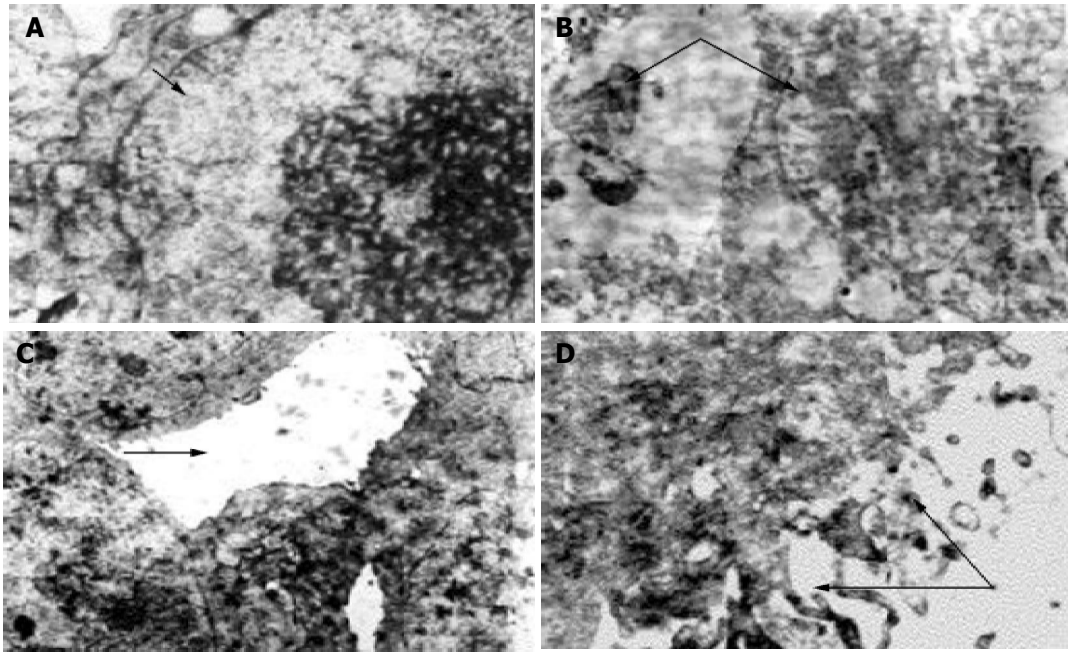

Figure 3 TEM shows the changes in Pc-3 tumor cell; A: Tumor cells (arrow) in control group grew vividly with large nuclei and some nucleoli ($12\times10^3\times1.2$); B: Tumor cells (arrow) were damaged, only the contour of nucleus remained (6×10^3); C: A few remaining tumor cells arranged as a glandular lumen (arrow) with small nucleoli ($8\times10^3\times1.2$); D: At low dose point, well differentiated Pc-3 cell with small nucleoli, plenty of euchromatin, many long micro-villi on cell surface (arrow), glandular lumens interplaced between the cells having the tendency of exocrine formation ($15\times10^3\times1.2$).

structure unchanged, neither apoptosis nor necrosis was found in Pc-3 cell when the absorbed dose 2.89±0.20 Gy. Apoptosis cell and some necrotic picture could be found at absorbed dose 5.78±0.25 Gy (Figure 5). A great number of Pc-3 cells necrosed when absorbed dose 46.23±4.20 Gy. The characteristics of apoptosis cells were the volume of cell nucleus diminished, chromatin densely aggregated at periphery, vacuoles presented on some cell membrane, encapsulated plasmid and debris formed apoptosis body, structure of cell membrane and organelle remained intact. The characteristics of necrosed cells were condensed, ruptured or lyzed nucleus, prominently swollen mitochondria, broken cristae or vacuolation, rupture of cell membrane, and damaged organelle.

DISCUSSION

Anticancer effect of ^{32}P colloids and its mechanism

After interstitial injection of $^{99}Tc^{m}$-sulfur colloids, the mechanism

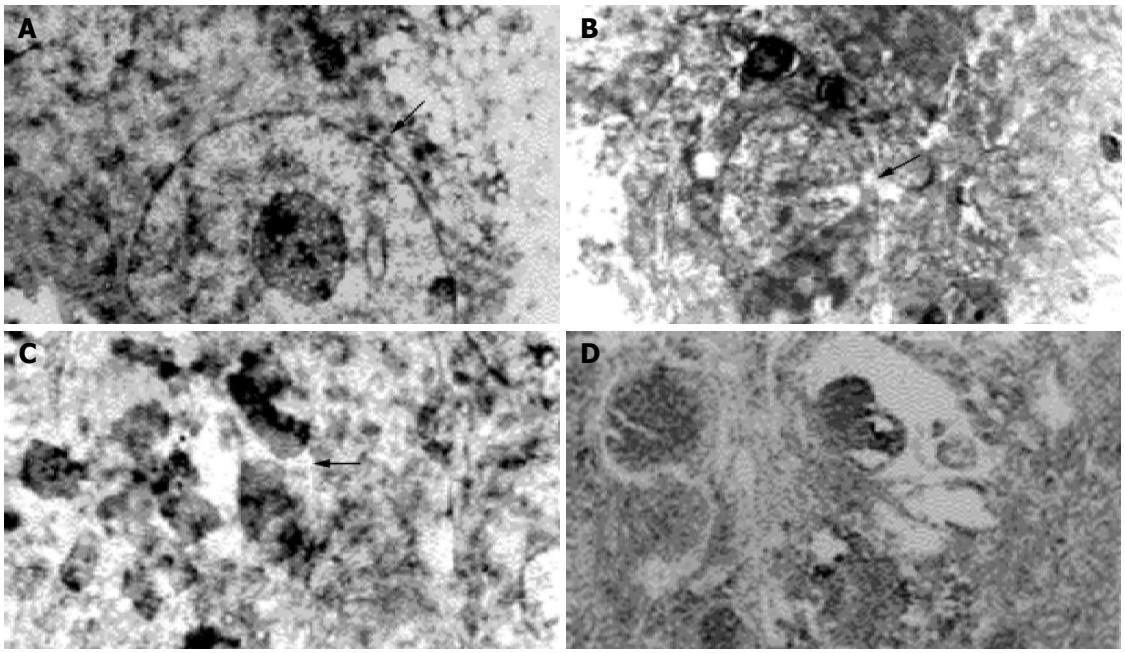

Figure 4 Transmission electron microscopy of ILN A: Metastatic Pc-3 cells (arrow) in lymphatic tissue of control group (4×10^3); B: After ^{32}P colloids irradiation apoptotic cells (arrow) in the connective tissue and endothelium of lymphatic sinuses (2.5×10^3); C: Denatured tumor cells (arrow) after medication ($5\times10^3\times1.2$); D: ILN under light microscope: lymphatic tissue recovered to normal 4 wk after medication (HE ×400).

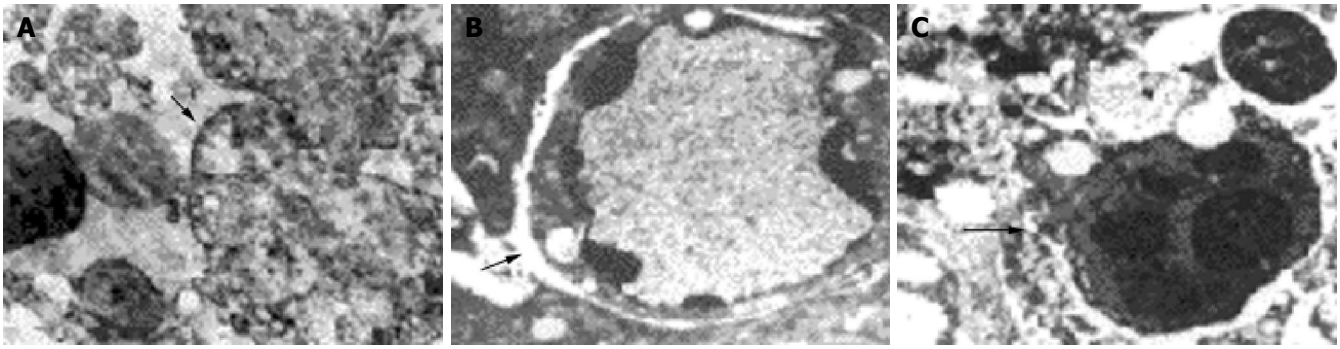

Figure 5 Results of TEM: A: Cell necrosis, breaking into debris (arrow) (10×10^3); B: Early apoptosis (arrow). Chromatin aggregated at periphery ($10\times10^3\times1.2$); C: Medium stage of apoptosis (arrow) showing nucleus shrunk and broken ($10\times10^3\times1.2$).

of their transportation in the regional lymphatic system has been applied to locate the pioneer lymph nodes in breast cancer[3]. Some authors have reported that phosphous-32 chromic phosphate in conjunction with platinum analog chemotherapy intraperitoneal injection for treatment of disseminated ovarian cancer in 30 cases the survival rate at 3 year was 63%[4]. In the recent years, some preliminary reports on the treatment of refractory malignant solid tumors or metastatic tumors have been published[5-8].

Radioactive nuclide internal irradiation in treating tumor has the character of continuity of radiation effective time and accumulation of response. ^{32}P in a pure β-emitter by its direct or indirect effects of radioactive ionization destroys tumor cell membrane and structure of organelle membrane, leading to cell necrosis or apoptosis, finally inhibiting the proliferation of tumor cells. It was confirmed that: (1) the positive correlation of dose-response and time-response existed in the rates of tumor cell necrosis. Reciprocal relationship occurred between PI value and absorbed dose of tumor, suggesting PCNA of Pc-3 cell under the effect of ^{32}P β ray, participating in DNA synthesis, is directly or indirectly inhibited, thereby the DNA synthesis and cell proliferation suppressed. (2) In low dosage group, the morphological characters of highly differentiated pancreatic carcinoma were observed. This is the phenomenon similar to ^{32}P glass micro sphere interventional treatment of liver cancer[9] Further improved that irradiation in suitable dosage has the effect of inducing differentiation on tumor cells. (3) Neogenesis of blood vessel in tumor is one of the important premises in growth, infiltration and metastasis of malignant tumor. Quantitative analysis of CD34 expression in Pc-3 tumor tissue revealed MVD in treating groups was prominently lower than that of control group, and existed dose-response relationship with the absorbed dose, this suggests ^{32}P colloids may inhibit the angiopoiesis of tumor by blocking the blood vessels in the lesions and their surroundings thus suppressing growth of Pc-3 cell and blood-borne metastasis, leading to death of tumor cells.

Lymphatic metastasis is the main manner of early metastasis in most malignant tumors. ^{32}P colloids intratumoral injection is superior to other radionuclide preparations such as seeds[10] and microsphere[11-13], with the advantage of treating solid tumor as well as the early lymphatic metastasis at the same time. This study confirmed that: (1) In early implanted tumor, even with intact capsule, lymphatic metastasis already occurred. After the effect of ^{32}P irradiation on ILN the tumor cells denatured and died. This explained the transport route of colloids in local lymphatic system after interstitial medication was basically similar to the dispersion route of primary tumor by the lymphatic ducts. (2) In medicated mice, the occurrence of ILN swelling was later in time and smaller in size than that in control; the extent of ILN swelling in medicated mice was reciprocally related to the dosage. This showed ^{32}P had certain abilities of inhibiting the progress of lymphatic metastasis and exerting pursuing effects on occult metastatic foci in lymphatic drainage area of neighboring tumor. (3) The degree of irradiative injury to ILN became more severe with the increasing of ^{32}P colloids activity injected to the tumor, after 4 wk the tissues repaired to normal. This explained the positive correlation between ^{32}P

Table 2 Absorbed dose, rates of Pc-3 cell apoptosis and necrosis, percentages of Apo2.7 and caspase-3 positive expression (%) and Bcl-2/Bax value in different activity groups

Group (n = 5)	Radioactivity (MBq)	Tumor absorbed dose (Gy)	Pc-3 cell apoptosis rate (%)	SNK	Pc-3 cell necrosis rate (%)	SNK	Apo2.7 positive (%)	Caspase-3 positive (%)	Bcl-2/Bax
14	0	0.00±0.00	0.67±0.15	A	1.8±0.5	A	4.9±1.8	7.69±1.5	2.07±0.85
9	0.37	2.89±0.20	10.09±1.84	B	2.2±0.6	B	8.3±2.4	10.43±2.6	1.64±0.62
10	0.74	5.78±0.25	17.36±4.33	C	6.0±1.1	B	13.6±2.3	13.46±2.9	1.02±0.52
11	1.48	11.56±1.29	21.85±3.04	D	11.7±0.5	C	15.0±3.2	14.92±4.1	0.81±0.32
12	2.96	23.12±3.12	33.67±3.69	E	13.1±1.0	D	16.3±3.1	18.68±4.6	0.37±0.12
13	5.92	46.23±4.20	27.76±4.09	F	23.4±2.6	D	27.3±4.9	25.57±5.3	0.07±0.03

Variance analysis after conversion of tumor cell apoptosis and necrosis rate to square root: cell apoptosis rate, F = 178.12, P<0.001, statistical difference between groups; Cell necrosis rate, F = 249.27, P<0.001, statistical difference between groups, if the variance analysis of the mean Pc-3 apoptosis and necrosis rate showed statistical differences, Student–Newman–Keuls' method was employed.

Table 3 Rates of absorbed dose and Pc-3 apoptosis on same dosage (1.48 MBq) but between different time groups

Group (n = 3)	Time (h)	Tumor absorbed dose (Gy)	Pc-3 apoptosis rate[1] (%)	SNK
15	6	7.25±2.58	10.00±3.02	A
16	12	13.73±2.43	17.93±2.24	B
17	24	24.82±5.14	33.85±4.54	C
18	36	46.06±8.55	27.85±3.04	D
19	48	47.43±11.60	18.41±5.40	E

[1]Variance analysis after conversion of tumor cell apoptosis rate to square root: F = 87.76, P<0.001 statistical difference between groups.

colloids in ILN and the injected activity in tumor; irradiated injury to ILN was reversible after interstitial medication to tumor. (4) After the tumor mass received different irradiation doses, the picture of cell apoptosis was found in the sinus of ILN, suggesting irradiation at low dose had the effect of inducing apoptosis in actively proliferating cells. ^{32}P colloids exerted influence on the morphology of ILN suggesting this therapeutical measure not only affects the primary tumor lesion but also prevention and treatment of tumor with occult lymphatic metastasis.

Gene regulating mechanism of low dose irradiation induced apoptosis

The conception of ionized irradiation in inducing cell apoptosis received increasingly great concern. We have studied the gene regulating mechanism of low dose interstitial injection of ^{32}P colloids in inducing apoptosis of implanted human pancreatic carcinoma Pc-3 cells in nude mice. The experience confirmed: (1) After β ray 3-50 Gy internal irradiation for 6-48 h, apoptotic cells were found in Pc-3 cells, indicating these tumor cells are irradiation susceptible cells, sensitive to low dose irradiation. Based on the differences of sensitivity of tumor and normal tissues in inducing apoptosis, we might selectively induce cell apoptosis with low dose irradiation, eliminating the tumor cells, at the same time protecting normal cells[14], minimizing the adverse injury in internal irradiation therapy. (2) When the absorbed dose was at 2.89±0.20 to 23.12±3.12 Gy, the increase of percentage in cell apoptosis was parallel to the increase of dosage, this conclusion coincides with *in vitro* or other experiments[15]. As the absorbed dose increased continuously to 46.23±4.20 Gy, the apoptosis rate was prominently lower than that of low dosage group, there was clearly dose-response relationship between them, and the cell necrosis rate was positively correlated to the absorbed dose. The changes of apoptosis and necrosis are related to the intensity of injury and the continuity of stimuli, suggesting the onset of apoptosis and necrosis and their regulating mechanism are related to the time and intensity thresholds of the external injury. (3) The irradiation induced cell apoptosis was related to regulation of several genes, in which the closely related genes are p53, Bcl-2 and Bax, *etc*. Gene Bcl-2 is a kind of apoptosis inhibiting gene, gene Bax is a kind of apoptosis promoting gene, introduction of Bax gene may accelerate cell apoptosis, and mutation of gene Bax may inhibit apoptosis. Gene Bcl-2/Bax gave important effects on regulating cell apoptosis. Generally the ratio of Bcl-2/Bax decides whether the cell is apoptosis or not[16]. The results of this experiment showed that in the process of β radiation induced apoptosis of Pc-3 cells, genes Bcl-2 and Bax participated in regulation, prominently down regulation of Bcl-2/Bax ratio. This injury of DNA molecule resulted from ionized irradiation, activated p53 exerted transcription effect to activate Bax gene, and elevate Bax mRNA and protein expression, forming Bax homologous dimerism polymer. The ratio of Bcl-2/Bax lowered, cell apoptosis was induced. (4) Recent study discovered that mitochondria event was the key event in cell apoptosis; the most important process was the activation of caspase proteinase family. Caspase-3 is the most important responsive caspase in the family, responsible for the cleavage of all or part of the proteinase in the process of cell apoptosis, after activation of caspase cells will irreversibly progress to apoptosis[17,18]. In this experiment we found that caspase-3 protein expression was prominently increased after the action of ^{32}P colloids; it confirmed the mechanism of initiating apoptosis by the action of ^{32}P colloids. (5) Apo2.7 protein is a new quantitative marker of cell apoptosis, reacting with the membranous protein of 38 ku mitochondria, and denoting in early stage of cell apoptosis related to molecular cascade of cell apoptosis[19]. From the results of this experiment, Apo2.7 protein expression was evidently enhanced, and showed dose-response relation with the absorbed dose. (6) Cell apoptosis is a very complicated biological process involving multiple regulating genes and signal transmitting paths. Different dose of irradiation induced cell apoptosis underwent different mechanisms, but the same dose of irradiation might have several pathways to arouse apoptosis. In this experiment it was found that at a particular time point (24 h), following the increase of absorbed dose in tumor, the expression of apoptosis related gene was up-regulated (caspase-3, Apo2.7) or down-regulated (Bcl-2/Bax), the rate of apoptosis did not raise when the absorbed dose increased, but decreased in the high dose group. It is possible other than the above mentioned regulating genes, some unknown apoptosis regulating genes participated in this process, which needs to be further studied.

Absorbed dose in tumor and toxic side effects

Biological distribution of ^{32}P colloids greatly influenced absorbed dose in tumor and the toxic side effects. This study[20] confirmed that: radioactive nuclides after interstitial injection of ^{32}P colloids, are mainly condensed in the tumor mass with prolonged duration, and the amount distributed in the organs other than tumor was very less. This study confirmed that the effective half-life of ^{32}P colloids in tumor is nearly the same to its physical half-life. The characteristic curve of radioactivity counting rate on tumor surface manifested as: within 4 d after injection the radioactivity decreased exponentially, then 2 d later raised again, presented as a small peak in the curve, followed by a tendency of continuously gradual decline. After interstitial medication of ^{32}P colloids, they were engulfed and transported by phagocytes through the lymphatic circulation to the drained lymph nodes or micro-vessels, and finally attained by the tumor tissue rich in blood supply, the circulation was repeated continuously, the total body radioactivity decreased concomitantly with elapse of time and excretion, the radioactivity decreased rapidly in normal tissues and organs, while in the tumor

mass the ratio of its radioactivity to the total activity of whole body was continuously elevated. Therefore T/N ratio was high, signifying the irradiative dose was highly acquired by the tumor, scarcely distributed to other parts of the body. In this experiment we found that under the condition of high dose ionized irradiation, coagulative necrosis happened in Pc-3 cells with fair tumor inhibition response, but scattered small petechiae presented on the dorsum of six experimental nude mice and some mice getting emaciated distinctly. Morphological examination revealed fibrotic changes in lung, anaplasia in the epiderma covering the tumor. As the absorbed dose was ≤853 Gy, it attained ideal anti-cancer effectiveness, no general toxic side effects were found in the experimental animals. Therefore it is important to choose the suitable dose of interstitial medication, so as to attain the maximum effect on tumor cells and minimize irradiative injury to other tissues and organs as far as possible.

REFERENCES

1 **Tang ZY.** Modern Oncology. 2nd Ed. Shanghai: *Shanghai University of Medical Science Press* 2000: 1132-1134
2 **Qin MX,** Diao GP. Clinical Interventional Nuclear Medicine. 1st Ed. *Tianjin Scientific Technology Press* 1996: 11-13
3 **Shen K,** Nirmal L, Han Q, Wu J, Lu J, Zhang J, Liu G, Shao Z, Shen Z. Sentinel lymph node biopsy in breast cancer. *Zhonghua Waike Zazhi* 2002; **40**: 347-350
4 **Pattillo RA,** Collier BD, Abdel-Dayem H, Ozker K, Wilson C, Ruckert AC, Hamilton K. Phosphorus-32-chromic phosphate for ovarian cancer: I. Fractionated low-dose intraperitoneal treatments in conjunction with platinum analog chemotherapy. *J Nucl Med* 1995; **36**: 29-36
5 **Dempke W,** Firusian N. Treatment of malignant pericardial effusion with ^{32}P-colloid. *Br J Cancer* 1999; **80**: 1955-1957
6 **Firusian N,** Dempke W. An early phase II study of intratumoral P-32 chromic phosphate injection therapy for patients with refractory solid tumors and solitary metastases. *Cancer* 1999; **85**: 980-987
7 **Order SE,** Siegel JA, Principato R, Zeiger LE, Johnson E, Lang P, Lustig R, Wallner PE. Selective tumor irradiation by infusional brachytherapy in nonresectable pancreatic cancer: a phase I study. *Int J Radiat Oncol Biol Phys* 1996; **36**: 1117-1126
8 **Order SE,** Court WS. Models of clinical infusional brachytherapy. *Int J Radiat Oncol Biol Phys* 2001; **50**: 279
9 **Liu L,** Jiang Z, Teng GJ, Song JZ, Zhang DS, Guo QM, Fang W, He SC, Guo JH. Clinical and experimental study on regional administration of phosphorus-32 glass microspheres in treating hepatic carcinoma. *World J Gastroenterol* 1999; **5**: 492-505
10 **Zelefsky MJ,** Hollister T, Raben A, Matthews S, Wallner KE. Five-year biochemical outcome and toxicity with transperineal CT-planned permanent I-125 prostate implantation for patients with localized prostate cancer. *Int J Radiat Oncol Biol Phys* 2000; **47**: 1261-1266
11 **Liu L,** Teng GJ, Jiang Z, He SC, Xie SL, Wu LS, Song FJ, Guo JH, Fang W, Zhao CG, Huang WH. Preliminary clinical application of phosphorus-32 glass microspheres in interventional treating hepatocellular carcinoma. *Hejishu* 2000; **23**: 316-322
12 **Liu L,** Teng GJ, Zhang DS, Song JZ, He SC, Guo JH, Fang W. Toxicology of intrahepatic arterial administration of interventional phosphorus-32 glass microspheres to domestic pigs. *Chinese Med J* 1999; **112**: 632-636
13 **Nijsen F,** Rook D, Brandt C, Meijer R, Dullens H, Zonnenberg B, de Klerk J, van Rijk P, Hennink W, van het Schip F. Targeting of liver tumour in rats by selective delivery of holmium-166 loaded microspheres: a biodistribution study. *Eur J Nucl Med* 2001; **28**: 743-749
14 **Fan ZP.** Ionized radiation and cell apoptosis. *Haijun Yixue Zazhi* 2000; **21**: 83-85
15 **Akagi Y,** Ito K, Sawada S. Radiation-induced apoptosis and necrosis in Molt-4 cells: a study of dose-effect relationships and their modification. *Int J Radiat Biol* 1993; **64**: 47-56
16 **Lee JU,** Hosotani R, Wada M, Doi R, Kosiba T, Fujimoto K, Miyamoto Y, Tsuji S, Nakajima S, Nishimura Y, Imamura M. Role of Bcl-2 family proteins (Bax,Bcl-2 and Bcl-X) on cellular susceptibility to radiation in pancreatic cancer cells. *Eur J Cancer* 1999; **35**: 1374-1380
17 **Kirsch DG,** Doseff A, Chau BN, Lim DS, de Souza-Pinto NC, Hansford R, Kastan MB, Lazebnik YA, Hardwick JM. Caspase-3-dependent cleavage of Bcl-2 promotes release of cytochrome c. *J Biol Chem* 1999; **274**: 21155-21161
18 **Thornberry NA,** Lazebnik Y. Caspases: enemies within. *Science* 1998; **281**: 1312-1316
19 **Zhang C,** Ao Z, Seth A, Schlossman SF. A mitochondrial membrane protein defined by a novel monoclonal antibody is preferentially detected in apoptotic cells. *J Immunol* 1996; **157**: 3980-3987
20 **Gao W,** Liu L, Yin QH, Wang ZZ, Wang Y, Duan MH, Huang Y, Zhang DS, Li C. Biodistribution pharmacokinetics and toxic effect of P-32 chromic phosphate colloids interstitially injected into human pancreatic cancer (Pc-3) bearing nude mice. *Zhonghua Fangsheyixue Yu Fanghuzazhi* 2004; **24**: 23-25

Science Editor Zhu LH and Li WZ **Language Editor** Elsevier HK

PO Box 2345, Beijing 100023, China
www.wjgnet.com
wjg@wjgnet.com

ELSEVIER

World J Gastroenterol 2005;11(14):2109-2116
World Journal of Gastroenterology ISSN 1007-9327

• *BASIC RESEARCH* •

Expression profiling suggests a regulatory role of gallbladder in lipid homeostasis

Zuo-Biao Yuan, Tian-Quan Han, Zhao-Yan Jiang, Jian Fei, Yi Zhang, Jian Qin, Zhi-Jie Tian, Jun Shang, Zhi-Hong Jiang, Xing-Xing Cai, Yu Jiang, Sheng-Dao Zhang, Gang Jin

Zuo-Biao Yuan, Tian-Quan Han, Zhao-Yan Jiang, Jian Fei, Yi Zhang, Jian Qin, Zhi-Jie Tian, Jun Shang, Zhi-Hong Jiang, Xing-Xing Cai, Yu Jiang, Sheng-Dao Zhang, Gang Ji, Department of Surgery, Ruijin Hospital, Shanghai Second Medical University, Shanghai Institute of Digestive Surgery, Shanghai 200025, China
Supported by the National Natural Science Foundation of China, No. 30271272, and the Foundation of Chinese National Human Genome Center at Shanghai, No. CHCS-99M-06
Co-first-authors: Gang Jin
Correspondence to: Tian-Quan Han, Department of Surgery, Ruijin Hospital, Shanghai Second Medical University, No.197, Ruijin 2nd Rd, Shanghai 200025, China. digsurgrj@yahoo.com.cn
Telephone: +86-21-64373909 Fax: +86-21-64373909
Received: 2004-04-04 Accepted: 2004-05-24

Abstract

AIM: To examine expression profile of gallbladder using microarray and to investigate the role of gallbladder in lipid homeostasis.

METHODS: ^{33}P-labelled cDNA derived from total RNA of gallbladder tissue was hybridized to a cDNA array representing 17 000 cDNA clusters. Genes with intensities $\geqslant$2 and variation <0.33 between two samples were considered as positive signals with subtraction of background chosen from an area where no cDNA was spotted. The average gray level of two gallbladders was adopted to analyze its bioinformatics. Identified target genes were confirmed by touch-down polymerase chain reaction and sequencing.

RESULTS: A total of 11 047 genes expressed in normal gallbladder, which was more than that predicted by another author, and the first 10 genes highly expressed (high gray level in hybridization image), e.g., ARPC5 (2 225.88±90.46), LOC55972 (2 220.32±446.51) and SLC20A2 (1 865.21±98.02), were related to the function of smooth muscle contraction and material transport. Meanwhile, 149 lipid-related genes were expressed in the gallbladder, 89 of which were first identified (with gray level in hybridization image), e.g., FASN (11.42±2.62), APOD (92.61±8.90) and CYP21A2 (246.11±42.36), and they were involved in each step of lipid metabolism pathway. In addition, 19 of those 149 genes were gallstone candidate susceptibility genes (with gray level in hybridization image), e.g., HMGCR (10.98±0.31), NPC1 (34.88±12.12) and NR1H4 (16.8±0.65), which were previously thought to be expressed in the liver and/or intestine tissue only.

CONCLUSION: Gallbladder expresses 11 047 genes and takes part in lipid homeostasis.

Key words: Gallbladder; Microarray; Gene expression; Lipid homeostasis

Yuan ZB, Han TQ, Jiang ZY, Fei J, Zhang Y, Qin J, Tian ZJ, Shang J, Jiang ZH, Cai XX, Jiang Y, Zhang SD, Jin G. Expression profiling suggests a regulatory role of gallbladder in lipid homeostasis. *World J Gastroenterol* 2005; 11(14): 2109-2116
http://www.wjgnet.com/1007-9327/11/2109.asp

INTRODUCTION

Cholesterol cholelithiasis is an extremely common, economically significant digestive disease that affects some 10-15% of the global population[1]. Gallstone is also the main cause of gallbladder carcinoma, biliary pancreatitis and iatrogenic lesions of the biliary tract. It has been reported that the USA spends 8-10 billion dollars on gallstone disease annually[2]. It was suggested from the data in the late 1980s that about 5.6% of the population in China was affected with gallstones[3], and the incidence may be increased in recent years. The patients with gallstone-related diseases hospitalized in the surgical department of our hospital accounted for 47% in 2001. Clearly, it is an important disease that deserves more attention.

Cholesterol saturated bile secreted by the liver is the prerequisite of gallstone formation, so liver is the place of lipid metabolism and becomes the focus of study. However, gallbladder is the place of stone formation and its relationship with lipid metabolism has been seldom investigated. Furthermore, the molecular mechanisms of gallstone formation in gallbladder-related with lipid metabolism are far from clear. Only about 40 genes (including gallstone susceptible gene loci) have been identified presently, and most of the previous studies were based on the changes in a single gene. Obviously, a total list of genes expressed in the gallbladder should be identified. The relatively new advent of cDNA array technology has provided a powerful method for large-scale expression profiling[4], and has led to the elucidation of a number of regulatory pathways involved in complex biological processes especially in tumor-related areas[5]. In this study, we used a powerful tool to examine expression profile of gallbladder and to investigate the role of gallbladder in lipid homeostasis. This would build a basis for understanding the physiological function of gallbladder, especially the mechanism of gallstone formation.

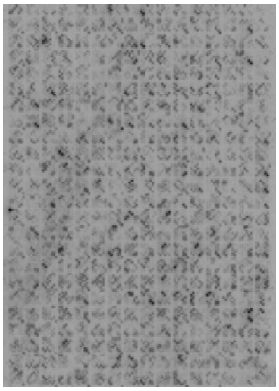

Figure 1 Half of an array hybridization image from a normal gallbladder sample.

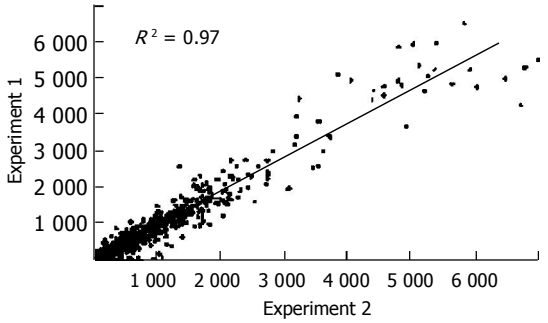

Figure 2 Scatterplot of two independent cDNA array analyses of the same sample. Each point stands for a gene or cDNA cluster, with the *X* coordinate representing the gene expression level in one test and the *Y* representing the value of the other test. An R^2 of 0.97 indicates high reproducibility of the cDNA array assay.

MATERIALS AND METHODS

cDNA array construction

cDNA clones were derived from liver and hepatocarcinoma cell lines, isolated from hypothalamus-pituitary-adrenal libraries[6] or purchased from Research Genetics (Huntsville, AL, USA). The assembled cDNA array contained 17 000 cDNA clones (representing the same number of independent cDNA clusters), of which 7 565 clusters were homologous to those found in the UniGene Database. All cDNA fragments were amplified and verified by electrophoresis. The average length of the cDNA fragments was -1 kb. PCR products were precipitated in isopropanol, redissolved in 10 μL of denaturing buffer (1.5 mol/L NaCl, 0.5 mol/L NaOH), and spotted on two 8×12-cm Hybond-N nylon membranes (Amersham Pharmacia, Buckinghamshire, UK) with an arrayer (BioRobotics, Cambridge, UK). Each spot carried -100 nL in volume and was 0.4 mm in diameter each cDNA fragment was placed in two different spots (double-offset). Lambda phage and pUC18 vector DNAs were spotted as negative controls.

Hybridization intramembrane control

Eight housekeeping genes were used as hybridization intramembrane controls (HIC): ribosomal protein S9 (RPS9), β-actin (ACTB), glyceraldehyde-3-phosphate dehydrogenase, hypoxanthine phosphoribosyltransferase 1, M_r 23 000 highly basic protein (RPL13A), ubiquitin C, phospholipase A2, and ubiquitin thiolesterase (UCHL1). These were evenly distributed in 12 places each per 8×12-cm array. Hybridization data was considered invalid if among the 12 spots representing the same gene, the intensity of the darkest spot exceeded 1.5-fold that of the weakest spot.

Clinical samples

Normal gallbladders were removed within 4 h postmortem from two adult males (aged 25 and 20 years, respectively) who died in traffic accidents. The Institute of Biomedical Science, Shanghai Second Medical University, approved the study, and all samples were obtained with informed consent. Tissues were frozen in liquid nitrogen immediately after separation, and kept frozen until used.

RNA extraction and probe preparation

Total RNA was extracted using a standard TRIzol RNA isolation protocol (Life Technologies, Inc., Grand Island, NY, USA). Poly (A)+ mRNA was then isolated from total RNA using a poly (dT) resin (Qiagen, Hilden, Germany). Approximately 1-2 μg of mRNA was labeled in a reverse transcription reaction in the presence of 200 μCi [α-^{33}P] deoxyadenosine 5'-triphosphate (DuPont NEN, Boston, MA, USA) using Moloney murine leukemia virus reverse transcriptase as per the manufacturer's instructions (Promega Corp., Madison, WI, USA).

Hybridization and image processing

Prehybridization was carried out in 20 mL of prehybridization solution (6× SSC, 0.5% SDS, 5× Denhardt's, and 100 μg/mL denatured salmon sperm DNA) at 68 ℃ for 3 h. Overnight hybridization with the ^{33}P-labeled cDNA in 6 mL of hybridization solution (6× SSC, 0.5% SDS, and 100 μg/mL salmon sperm DNA) was followed by stringent washing (0.1× SSC and 0.5% SDS at 65 ℃ for 1 h). Membranes were exposed to phosphor screens overnight and scanned using an FLA-3000A Plate/Fluorescent Image Analyzer (Fuji Photo Film, Tokyo, Japan). The radioactive intensity of each spot was linearly digitalized to 65 536 gray-grade in a pixel size of 50 μm in an Image Reader, and recorded with Array Gauge software (Fuji).

Data collection and analysis

After subtraction of background values (3±3) measured in an area where no cDNA was spotted, genes with intensities ⩾2 were considered positive signals; this ensured that positives were distinguished from the background with a statistical confidence of >99.9%. Normalization among arrays was based on the sum of background-subtracted signals from all genes on the membrane[7]. The average hybridization intensities of two gallbladders were adopted to analyze the bioinformatics.

Touchdown reverse transcription polymerase chain reaction

For most of the genes, mRNA levels in the gallbladder samples were too low to be detected by standard dot blot and hybridization *in situ*, or even by conventional PCR, we used touch-down PCR to confirm the array hybridization results. All PCR products were verified by sequencing to avoid false positives.

Table 1 The top 10 highly expressed genes in normal gallbladder tissue

Name of gene	Symbol	Gray level (mean±SD)
Breakpoint cluster region protein, uterine leiomyoma, 2	BCRP2	2 738.74±23.23
Actin-related protein 2/3 complex, subunit 5 (16 ku)	ARPC5	2 225.88±90.46
Eukaryotic translation initiation factor 4A, isoform 1	EIF4A1	2 223.86±274.74
Mitochondrial carrier family protein	LOC55972	2 220.32±446.51
Solute carrier family 20 (phosphate transporter), member 2	SLC20A2	1 865.21±98.02
Cytochrome b5 reductase 1 (B5R.1)	LOC51706	1 851.01±298.45
ADP-ribosylation factor 1	ARF1	1 844.63±353.31
FERM, RhoGEF (ARHGEF) and pleckstrin domain protein 1 (chondrocyte-derived)	FARP1	1 654.95±126.85
Proteasome (prosome, macropain) activator subunit 2 (PA28 beta)	PSME2	1 635.33±148.15
cAMP responsive element binding protein-like 1	CREBL1	1 579.36±71.68

RESULTS

Establishment of cDNA array system

Human cDNA clones randomly picked from cDNA libraries were terminally sequenced and compared with the Unigene database prior to their use in creating a cDNA array representing 17 000 genes or cDNA clusters (Figure 1). The reproducibility of the cDNA array analysis was evaluated in multiple replicated tests in which cDNA probes independently generated from the same mRNA sample were hybridized to different replicates of the cDNA arrays. The results from these experiments were almost perfectly concordant with a scatterplot R^2 (the square of the Pearson correlation coefficient, which measures similarity in gene expression patterns) of 0.97-0.98 (Figure 2). Of the 17 000 genes, only 0.2% showed >two-fold differences in their expression levels across different measurements. This showed that the cDNA array system was highly reproducible.

Gene list expressed in the gallbladder

In our work, a catalog of genes expressed in the human gallbladder was identified by cDNA array hybridization. The radio-intensities of corresponding spots on two parallel arrays were averaged. If the value was >2 and the variation <0.33 between the two samples, the signal was considered efficient. Of the 17 000 genes tested, a total of 11 047 genes were expressed in human normal gallbladder tissue, which is more than the number of 3 754 predicted by Lewis[8].

Top 10 genes expressed in the gallbladder

The 10 most highly expressed genes are listed in Table 1, and the top 3 breakpoint cluster region protein, uterine leiomyoma, 2; actin-related protein 2/3 complex, subunit 5 (16 ku) and eukaryotic translation initiation factor 4A, isoform 1, respectively.

Lipid metabolism-related genes and gallstone candidate genes in gallbladder

Totally 149 lipid metabolism-related genes were expressed in the gallbladder (Table 2). Eighty-three of them were identified for the first time in gallbladder (results after searching Unigene and Pubmed). Lammert *et al* have listed 45 possible gallstone candidate genes based on previous knowledge, 24 of which were assembled in our array, and 19 of these 24 genes were lipid-related genes and expressed in the gallbladder. We selected four lipid-related genes randomly, and by touchdown reverse transcription polymerase chain reaction (RT-PCR) and sequencing, confirmed the results in cDNA array (Figure 3).

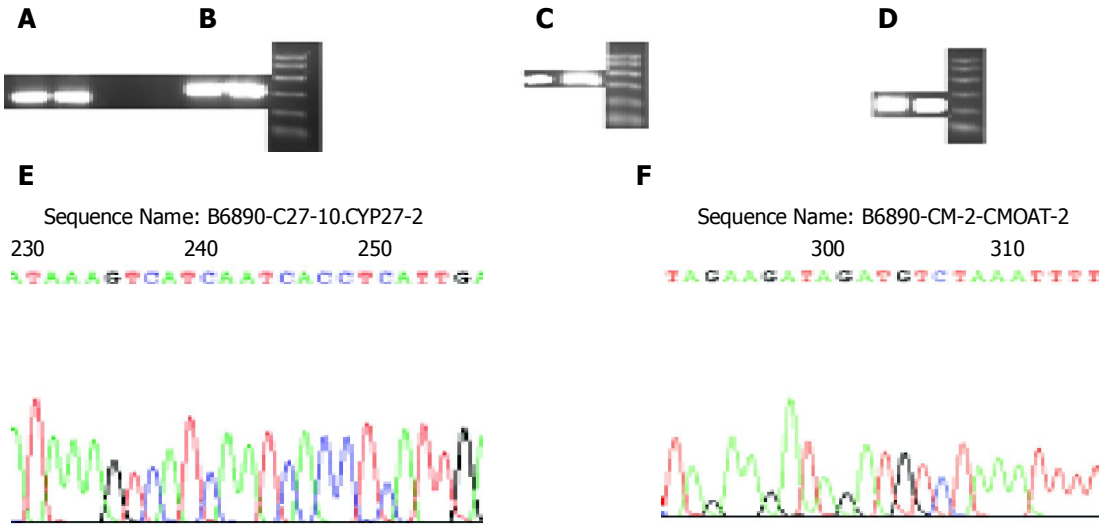

Figure 3 RT-PCR and sequencing confirmation of genes that were expressed in the gallbladder. RT-PCR electrophoresis result: A: CYP27A1 (320 bp); B: NR1H4(352 bp); C: CMOAT(353 bp); D: AKR1C3(240 bp). Sequencing result of PCR product: E: CYP27A1; F: CMOAT.

Table 2 Lipid-related genes expressed in normal gallbladder

GenBank ID	Gene name	Symbol	Reported or not	Gray level (mean±SD)
NM_000859	3-Hydroxy-3-methylglutaryl-Coenzyme A reductase[2]	HMGCR	P[3]	10.98±0.31
U66669	3-hydroxyisobutyryl-Coenzyme A hydrolase	HIBCH		11.17±0.09
U29344	Fatty acid synthase	FASN		11.42±2.62
AA460901	ATPase, aminophospholipid transporter-like, Class I, type 8A, member 2	ATP8A2		11.53±1.08
BE730527	Lipase protein	LOC57406	P[3]	11.58±0.85
AL043165	Homolog of mouse transient receptor potential-phospholipase C-interacting kinase CHaK; hypothetical protein FLJ20117	LTRPC7		11.59±0.69
U22662	Nuclear receptor subfamily 1, group H, member 3[2]	NR1H3		11.77±0.85
M14564	Cytochrome P450, subfamily XVII (steroid 17-alpha-hydroxylase), adrenal hyperplasia	CYP17		12.06±1.35
M93107	3-Hydroxybutyrate dehydrogenase (heart, mitochondria)	BDH	P[3]	12.10±2.22
NM_019844	Solute carrier family 21 (organic anion transporter), member 8[2]	SLC21A8	P[3]	12.14±0.77
AK000184	Acid sphingomyelinase-like phosphodiesterase	ASM3A		12.22±0.65
±X04506	±Apolipoprotein B (including Ag(x) antigen)	APOB	U[1]	12.23±1.17
X87176	Hydroxysteroid (17-beta) dehydrogenase 4	HSD17B4	U[1]	12.25±0.57
AF095703	L-3-hydroxyacyl-Coenzyme A dehydrogenase, short chain	HADHSC		12.37±1.66
AW022180	ESTs, weakly similar to S14747 sphingomyelin phosphodiesterase [*H. sapiens*]			12.39±2.40
U32576	Apolipoprotein C-IV	APOC4	U[1]	12.58±0.28
AI133376	Human DNA sequence from clone RP11-16L21 on chromosome 9. Contains the gene for NADP-dependent leukotriene B4 12-hydroxydehydrogenase, the gene for a novel DnaJ domain protein similar to Drosophila, *C. elegans* and Arabidopsis predicted proteins, the GNG10			12.75±1.64
AV658073	Homolog of mouse transient receptor potential-phospholipase C-interacting kinase CHaK; hypothetical protein FLJ20117	LTRPC7		12.83±1.45
X03635	Estrogen receptor 1	ESR1		12.83±0.34
AF165514	Hydroxysteroid (17-beta) dehydrogenase 7	HSD17B7	P[3]	12.99±0.56
NM_018557	Low density lipoprotein-related protein 1B (deleted in tumors)	LRP1B		13.06±0.29
U22526	Lanosterol synthase (2,3-oxidosqualene-lanosterol cyclase)	LSS		13.14±0.70
X83618	3-Hydroxy-3-methylglutaryl-Coenzyme A synthase 2 (mitochondrial)	HMGCS2	P[3]	13.34±0.03
D14662	Anti-oxidant protein 2 (non-selenium glutathione peroxidase, acidic calcium-independent phospholipase A2)	KIAA0106	U[1]	13.40±0.78
M62839	Apolipoprotein H (beta-2-glycoprotein I)	APOH		13.49±0.20
Z99716	Sterol regulatory element binding transcription factor 2[2]	SREBF2	P[3]	13.53±2.31
AF126799	Fatty acid desaturase 2	FADS2		13.62±2.16
AV662152	EST, moderately similar to LPHUC1 apolipoprotein C-I precursor [*H. sapiens*]			13.63±1.57
M37238	Phospholipase C, gamma 2 (phosphatidylinositol-specific)	PLCG2	P[3]	13.79±2.16
AF129756	Apolipoprotein M G3A			13.90±0.29
AW873435	Lipase A, lysosomal acid, cholesterol esterase (Wolman's disease)	LIPA		13.98±1.71
U09117	Phospholipase C, delta 1	PLCD1	P[3]	14.06±0.58
AC007954	Glutathione transferase zeta 1 (maleylacetoacetate isomerase)	GSTZ1		14.13±0.76
AA706930	Fatty acid binding protein 1, liver	FABP1	U[1]	14.19±0.25
AB011153	Phosphoinositide-specific phospholipase C-beta 1	PLCB1		14.65±2.22
AF038440	Phospholipase D2	PLD2		14.66±5.01
N42553	Homolog of mouse transient receptor potential-phospholipase C-interacting kinase CHaK; hypothetical protein FLJ20117	LTRPC7		14.68±2.50
AL110209	LCAT-like lysophospholipase	LLPL		14.88±2.24
X13916	Low density lipoprotein-related protein 1 (alpha-2-macroglobulin receptor) [2]	LRP1		14.91±1.56
AI955289	ESTs, weakly similar to DXHUBH 11beta-hydroxysteroid dehydrogenase [*H.sapiens*]			14.96±1.66
AF077046	Ganglioside expression factor 2	GEF-2		15.11±1.98
Z34975	Low density lipoprotein receptor defect C complementing	LDLC		15.18±2.11
BE271295	Group XII secreted phospholipase A2	PLA2G12		15.64±1.27
U49248	ATP-binding cassette, sub-family C (CFTR/MRP), member 2[2]	ABCC2	U[1]	15.78±0.45
N78156	Homolog of yeast long chain polyunsaturated fatty acid elongation enzyme 2	HELO1		15.95±5.40
AB016247	Sterol-C5-desaturase (fungal ERG3, delta-5-desaturase)-like	SC5DL	P[3]	16.09±3.33
NM_000954	Prostaglandin D2 synthase (21 ku, brain)	PTGDS		16.19±3.18
U60205	Sterol-C4-methyl oxidase-like	SC4MOL		16.22±1.29
AA557324	ESTs, weakly similar to fatty acid omega-hydroxylase [*H.sapiens*]			16.31±2.98
X66435	3-Hydroxy-3-methylglutaryl-Coenzyme A synthase 1 (soluble)	HMGCS1	P[3]	16.46±2.32
AL117352	Human DNA sequence from clone RP5-876B10 on chromosome 1q42.12-43. Contains the 3' end of the GNPAT gene for glyceronephosphate O-acyltransferase (DHAPAT, DAPAT, dihydroxyacetone phosphate acyltransferase, EC 2.3.1.42), the gene for a novel protein (ortho)			16.74±0.16
BE737965	Caveolin 1, caveolae protein, 22 ku[2]	CAV1		16.74±2.50

U68233	Nuclear receptor subfamily 1, group H, member 4**	NR1H4		16.80±0.65
AF035284	Fatty acid desaturase 1	FADS1	U[1]	16.82±0.92
X04898	Apolipoprotein A-II	APOA2	U[1]	16.96±2.01
AL031295	Lysophospholipase II	LYPLA2	P[3]	17.01±0.19
AL031295	3-Hydroxymethyl-3-methylglutaryl-Coenzyme A lyase (hydroxymethylglutaricaciduria)	HMGCL		17.01±0.19
M55150	Fumarylacetoacetate hydrolase (fumarylacetoacetase)	FAH		17.41±2.04
M31210	Endothelial differentiation, sphingolipid G-protein-coupled receptor, 1	EDG1		17.56±0.62
BE395256	Lanosterol synthase (2,3-oxidosqualene-lanosterol cyclase)	LSS		17.63±1.71
NM_000483	Apolipoprotein C-II	APOC2	U[1]	17.71±1.70
L76465	Hydroxyprostaglandin dehydrogenase 15-(NAD)	HPGD		17.86±0.79
S68287	Aldo-keto reductase family 1, member C4 (chlordecone reductase; 3-alpha hydroxysteroid dehydrogenase, type I; dihydrodiol dehydrogenase 4)	AKR1C4	P[3]	18.11±2.89
M54927	Proteolipid protein 1 (Pelizaeus-Merzbacher disease, spastic paraplegia 2, uncomplicated)	PLP1	P[3]	18.21±1.67
BE714757	Lipase A, lysosomal acid, cholesterol esterase (Wolman's disease)	LIPA		18.26±2.02
AJ238243	Phospholipase A2-activating protein	PLAA		18.73±3.07
AF077820	Low density lipoprotein receptor-related protein 5	LRP5		18.98±2.79
AL031778	Apolipoprotein B mRNA editing enzyme, catalytic polypeptide-like 2	APOBEC2	P[3]	19.21±3.45
AC004770	Fatty acid desaturase 1	FADS1	U[1]	19.22±9.65
AC004770	Fatty acid desaturase 3	FADS3		19.22±9.65
AA280051	Fatty acid binding protein 1, liver	FABP1	U[1]	19.81±3.80
X67698	Niemann–Pick disease, type C2 gene	NPC2		20.53±1.84
AL049748	Apolipoprotein L, 5	APOL5		20.61±0.01
X51416	Estrogen-related receptor alpha	ESRRA		20.63±1.82
AF065215	Phospholipase A2, group IVB (cytosolic)	PLA2G4B	P[3]	20.71±3.25
AB006746	Phospholipid scramblase 1	PLSCR1	U[1]	21.33±0.62
M59979	Prostaglandin-endoperoxide synthase 1 (prostaglandin G/H synthase and cyclooxygenase)	PTGS1	P[3]	21.55±0.74
X02162	Apolipoprotein A-I	APOA1	U[1]	21.70±0.75
AF079167	Oxidised low density lipoprotein (lectin-like) receptor 1	OLR1	P[3]	22.12±7.75
U55764	Sulfotransferase, estrogen-preferring	STE		22.15±2.72
J03459	Leukotriene A4 hydrolase	LTA4H		22.32±4.28
U03090	Phospholipase A2, group V	PLA2G5	P[3]	22.88±2.74
M76665	Hydroxysteroid (11-beta) dehydrogenase 1	HSD11B1	P[3]	22.98±3.71
NM_016108	Androgen induced protein	AIG-1	P[3]	23.02±3.33
AV651650	ESTs, highly similar to AF237982 1 oxysterol 7 alpha-hydroxylase [*H.sapiens*]			23.62±0.57
U11313	Sterol carrier protein 2[2]	SCP2	U[1]	23.92±0.18
NM_001645	Apolipoprotein C-I	APOC1	U[1]	25.02±12.59
X54741	Cytochrome P450, subfamily XIB (steroid 11-beta-hydroxylase), polypeptide 2	CYP11B2		25.13±3.81
X01388	Apolipoprotein C-III	APOC3		25.17±4.82
R98624	Bile acid Coenzyme A: amino acid *N*-acyltransferase (glycine *N*-choloyltransferase)	BAAT	P[3]	25.26±16.74
U93305	Proteolipid protein 2 (colonic epithelium-enriched)	PLP2	P[3]	25.41±2.44
U67963	Lysophospholipase-like	HU-K5		26.75±5.28
D86096	Prostaglandin E receptor 3 (subtype EP3)	PTGER3	P[3]	26.79±0.19
AL022398	Hydroxysteroid (11-beta) dehydrogenase 1	HSD11B1		26.82±8.70
X76488	Lipase A, lysosomal acid, cholesterol esterase (Wolman's disease)	LIPA		27.10±11.84
AF019225	Apolipoprotein L	APOL1	U[1]	28.12±1.76
AL034374	Homolog of yeast long chain polyunsaturated fatty acid elongation enzyme 2	HELO1		28.76±4.09
AI675602	EST, moderately similar to I65981 fatty acid omega-hydroxylase [*H.sapiens*]			28.85±13.77
U89281	Oxidative 3 alpha hydroxysteroid dehydrogenase; retinol dehydrogenase; 3-hydroxysteroid epimerase	RODH		29.09±7.19
AL022318	Phorbolin (similar to apolipoprotein B mRNA editing protein)	DJ742C19.2		29.26±5.26
X07228	Lipase, hepatic	LIPC	P[3]	30.57±4.34
AL031230	Glycosylphosphatidylinositol specific phospholipase D1	GPLD1		30.88±1.21
AA128778	Tissue factor pathway inhibitor (lipoprotein-associated coagulation inhibitor)	TFPI		32.76±0.09
Z99390	L-3-hydroxyacyl-Coenzyme A dehydrogenase, short chain	HADHSC		33.87±0.98
AF002020	Niemann–Pick disease, type C1[2]	NPC1		34.88±12.12
X55764	Cytochrome P450, subfamily XIB (steroid 11-beta-hydroxylase), polypeptide 1	CYP11B1		34.95±1.61
L34081	Bile acid Coenzyme A: amino acid *N*-acyltransferase (glycine N-choloyltransferase)	BAAT	P[3]	37.8±3.91
AF002668	Degenerative spermatocyte (homolog Drosophila; lipid desaturase)	DEGS		37.93±4.50
AF034544	7-Dehydrocholesterol reductase	DHCR7		38.05±2.80
D82073	Prostaglandin D2 synthase, hematopoietic	PGDS		38.83±13.58
Z37986	Emopamil-binding protein (sterol isomerase)	EBP		41.25±12.24
L21934	Sterol O-acyltransferase (acyl-Coenzyme A: cholesterol acyltransferase) 1	SOAT1	P[3]	44.08±1.76
L21934	Sterol O-acyltransferase (acyl-Coenzyme A: cholesterol acyltransferase) 1[2]	SOAT1	P[3]	44.08±1.76

M12792	Cytochrome P450, subfamily XXIA (steroid 21-hydroxylase, congenital adrenal hyperplasia), polypeptide 2	CYP21A2		44.19±7.57
L07077	Enoyl-Coenzyme A, hydratase/3-hydroxyacyl Coenzyme A dehydrogenase	EHHADH		45.78±6.21
BE566894	Human DNA sequence from clone RP11-16L21 on chromosome 9. Contains the gene for NADP-dependent leukotriene B4 12-hydroxydehydrogenase, the gene for a novel DnaJ domain protein similar to Drosophila, *C. elegans* and Arabidopsis predicted proteins, the GNG10		U[1]	47.45±1.75
NM_016371	Hydroxysteroid (17-beta) dehydrogenase 7	HSD17B7		48.38±6.73
AF151638	Phosphatidylcholine transfer protein[2]	PCTP	P[3]	53.38±6.96
M12529	Apolipoprotein E[2]	APOE	P[3]	53.51±9.77
AL034369	Human DNA sequence from clone 149D17 on chromosome Xq22.2-23. Contains part of a PLRP2 (PNLIPRP2, pancreatic lipase-related protein 2 Precursor, EC 3.1.1.3) LIKE gene and 5' exons of the COL4A5 and alternatively spliced COL4A6 genes for Collagen, type IV,			54.46±5.61
M22430	Phospholipase A2, group IIA (platelets, synovial fluid)	PLA2G2A	P[3]	58.57±9.02
AK000339	Long-chain fatty acid Coenzyme A ligase 5	FACL5	U[1]	58.82±3.86
NM_013389	NPC1 (Niemann–Pick disease, type C1, gene)-like 1	NPC1L1	U[1]	59.9±13.58
M63959	Low density lipoprotein-related protein-associated protein 1 (alpha-2-macroglobulin receptor-associated protein 1)[2]	LRPAP1	U[1]	60.24±6.70
AF263613	Intracellular membrane-associated calcium-independent phospholipase A2 gamma	IPLA2(GAMMA)		60.96±13.23
Z29481	3-Hydroxyanthranilate 3,4-dioxygenase	HAAO		62.47±0.09
D38081	Thromboxane A2 receptor	TBXA2R		66.03±19.67
X71973	Glutathione peroxidase 4 (phospholipid hydroperoxidase)	GPX4		69.27±12.44
AW662196	Apolipoprotein L, 2	APOL2	P[3]	79.49±5.89
AI590076	3-Hydroxy-3-methylglutaryl-Coenzyme A synthase 1 (soluble)	HMGCS1	P[3]	83.08±4.33
AL022398	*Homo sapiens* DNA sequence from PAC 434O14 on chromosome 1q32.3.-41. Contains the HSD11B1 gene for hydroxysteroid (11-beta) dehydrogenase 1, the ADORA2BP adenosine A2b receptor LIKE pseudogene, the IRF6 gene for Interferon Regulatory Factor 6 and two novel			85.30±14.15
AL022394	Phospholipase C, gamma 1 (formerly subtype 148)	PLCG1	P[3]	85.54±21.21
Z82215	Apolipoprotein L	APOL1	U[1]	89.89±16.36
J02611	Apolipoprotein D	APOD		92.61±8.90
U19487	Prostaglandin E receptor 2 (subtype EP2), 53 ku	PTGER2	P[3]	95.40±18.27
X59812	Cytochrome P450, subfamily XXVIIA (steroid 27-hydroxylase, cerebrotendinous xanthomatosis), polypeptide 1[2]	CYP27A1	P[3]	100.70±10.81
AF070675	Apolipoprotein L, 3	APOL3	U[1]	105.58±12.73
U00968	Sterol regulatory element binding transcription factor 1[2]	SREBF1	P[3]	107.4±8.65
AB018580	Aldo-keto reductase family 1, member C3 (3-alpha hydroxysteroid dehydrogenase, type II) [2]	AKR1C3	P[3]	110.69±31.00
X98332	Solute carrier family 22 (organic cation transporter), member 1[2]	SLC22A1	P[3]	112.02±22.09
M10617	Fatty acid binding protein 1, liver[2]	FABP1	U[1]	117.5±11.59
L11702	Glycosylphosphatidylinositol specific phospholipase D1	GPLD1		149.16±33.78
X06290	Lipoprotein, Lp(a)	LPA	P[3]	156.94±26.59
X14723	Clusterin (complement lysis inhibitor, SP-40,40, sulfated glycoprotein 2, testosterone-repressed prostate message 2, apolipoprotein J)	CLU	U[1]	163.92±11.19
BE018577	3-Hydroxy-3-methylglutaryl-Coenzyme A synthase 1 (soluble)	HMGCS1	P[3]	169.72±16.05
U23942	Cytochrome P450, 51 (lanosterol 14-alpha-demethylase)	CYP51		219.74±47.13
AL049547	Cytochrome P450, subfamily XXIA (steroid 21-hydroxylase, congenital adrenal hyperplasia), polypeptide 2	CYP21A2		246.11±42.36
AF081281	Lysophospholipase I	LYPLA1	P[3]	348.56±34.15
L40802	Hydroxysteroid (17-beta) dehydrogenase 2	HSD17B2		396.94±5.65

[1]U: Genes expressed in the gallbladder through searching Unigene Database; [2]Gallstone candidate genes; [3]P: Genes expressed in the gallbladder suggested by previous report.

DISCUSSION

A cDNA array representing 17 000 human genes or cDNA clusters was established. Compared with the cDNA array without hybridization intra membrane controls, the HIC in the cDNA array system significantly contributed to the evenness of hybridization among different parts of the array membrane and therefore improved the reliability of the array analysis (data not shown). Replicated examinations of the same sample indicated that only 0.2-0.3% of the genes spotted or 0.5% informative genes, might be false-positive signals. Because we chose the genes that were lower than 0.33 in the variation of average on two samples, the possibilities of false-positives were remote.

Totally 11 047 genes were expressed in the gallbladder, which is almost thrice the number of 3 754 predicted by Lewis. The results remind us the importance of the role of gallbladder in the human body.

So far, two measures can be used to study gene expression profile, namely constructing a cDNA library following sequencing or thorough cDNA array. The former is a

labor-consuming and accurate work, but it needs complex procedures, and can be affected by many factors, thus, it is not so sensitive. On the contrary, cDNA array is a high-throughput and relatively less expensive technology.

The top 10 highly expressed genes with a clear function are displayed in Table 1, they are: BCRP2: breakpoint cluster region protein, uterine leiomyoma, 2; ARPC5: actin-related protein 2/3 complex, subunit 5 (16 ku); EIF4A1: eukaryotic translation initiation factor 4A, isoform 1; LOC55972: mitochondrial carrier family protein; SLC20A2: solute carrier family 20 (phosphate transporter), member 2; LOC51706: cytochrome b5 reductase 1 (B5R.1); ARF1: ADP-ribosylation factor 1; FARP1: FERM, RhoGEF (ARHGEF) and pleckstrin domain protein 1 (chondrocyte-derived); PSME2: proteasome (prosome, macropain) activator subunit 2 (PA28 beta); CREBL1: cAMP responsive element binding protein-like 1. Their functions are associated with smooth muscle contraction and material transport, thus, they may participate in the contraction and concentration of gallbladder bile[9-16].

The human body contains both exogenous and endogenous cholesterol. Exogenous cholesterol comes from diet while the endogenous is synthesized inside the body by liver cells. Excess total cholesterol in the plasma will eventually become deposited on the arterial walls, leading to atherosclerosis[17]. High-density lipoprotein is the only lipoprotein that can transport cholesterol to the liver for degradation; this is called reverse cholesterol transport[18]. Liver cells catalyze cholesterol into bile acid, which is secreted into the biliary tract. Supersaturated cholesterol remains in the gallbladder bile, and can result in the formation of cholesterol monohydrate crystals, and finally gallstones[19]. Normally, the gallbladder epithelium absorbs high amounts of biliary cholesterol and phosphatidylcholine in a proportion determined by their molar ratio in the bile entering the lumen. This physiological lipid absorption continuously reduces biliary cholesterol molar percentage in the gallbladder, thus avoiding crystal precipitation. In contrast, gallbladder epithelium in patients affected with cholesterol gallstone disease may be hyperplastic and/or hypertrophic, and consistently absorbs cholesterol and phosphaticylcholine less efficiently, leading to a higher likelihood of cholesterol crystal precipitation[20]. A number of lipid metabolism genes or proteins are reportedly expressed in gallbladder tissue, including scavenger receptor class B type I(SR-BI)[21], Apo B[22], acyl-coA: cholesterol acyltransferase (Soat1)[23], sodium-dependent bile acid transporter and organic anion transporting polypeptide(Oatp1)[24], and the multidrug resistance protein (MRP)[25]. However, most of the lipid metabolism-related genes we identified in this study (Table 2) have not previously been reported in the gallbladder. From our results, we hypothesize that supersaturated lipids in bile lead to impaired regulation of the buffering ability of the gallbladder, resulting in the formation of gallstones. In our previous work, we observed that high cholesterol diet decreased the expression of cholecystokinin-A receptor in guinea pig, which led to the formation of gallstone[26]. Usually, it is nucleation factors or impaired motility of gallbladder that results in the formation of gallstone[27]. However, we found 19 lipid metabolism-related genes expressed in the gallbladder in our previous research[28,29], and currently a total of 149 lipid metabolism-related genes were expressed in the gallbladder, and most of them were firstly identified (83 genes), thus, we think it is necessary to consider the regulation ability of gallbladder in lipid homeostasis while we study the mechanism of gallstone formation.

Lammert *et al*[2] collected 45 possible candidate genes in gastroenterology. Twenty-four of the 45 genes were included in our array, and 21 of them were expressed in the gallbladder. Among the 21 genes, 19 genes were lipid-related genes, and they can be divided into five groups: lipid regulatory enzymes, lipoprotein receptors and related proteins, intracellular lipid transporters, membrane lipid transporters and lipid regulatory transcription factors. Previously those genes were believed to be expressed in the liver and/or intestinal cells only, not in gallbladder, and they could not be searched in Unigene and Pubmed for their association with gallbladder except LRPAP1[30], FABP1[31], SCP2 and ABCC2[32]. It is well known that lipid metabolism has a close relationship with liver, but we found those genes were expressed in the gallbladder, too, suggesting gallbladder takes part in both digestion and lipid homeostasis. Those genes of patients with gallstones expressed in the gallbladder are involved in each step of gallstone formation, thus, if we study the differentially expressed genes between normal and gallstone affected gallbladder by cDNA hybridization, we may find some valuable gallstone-related genes.

In summary, we established a cDNA array and identified a catalog of genes expressed in normal gallbladder tissue, the number is greater than previous predictions. In addition, we identified the expression of 139 lipid metabolism-related genes, eighty-three of them were first discovered, suggesting that the gallbladder takes part in lipid homeostasis.

ACKNOWLEDGMENTS

The authors thank Professor Ji Zhang at the Shanghai Institute of Biology Science, Academy of China, and all members of the Shanghai Institute of Digestive Surgery for their constructive discussions and encouragement.

REFERENCES

1 **Kratzer W**, Mason RA, Kachele V. Prevalence of gallstones in sonographic surveys worldwide. *J Clin Ultrasound* 1999; **27**: 1-7

2 **Lammert F**, Carey MC, Paigen B. Chromosomal organization of candidate genes involved in cholesterol gallstone formation: a murine gallstone map. *Gastroenterology* 2001; **120**: 221-238

3 **Zhang SD**, Han TQ. Epidemiology of cholelithiasis. In: ZQ Huang. ed. Current Biliary Surgery. Shanghai: Shanghai Press of Science and Technology Documents 1998: 249-260

4 **Young RA**. Biomedical discovery with DNA arrays. *Cell* 2000; **102**: 9-15

5 **Zhou J**, Zhao LQ, Xiong MM, Wang XQ, Yang GR, Qiu ZL, Wu M, Liu ZH. Gene expression profiles at different stages of human esophageal squamous cell carcinoma. *World J Gastroenterol* 2003; **9**: 9-15

6 **Xu L**, Hui L, Wang S, Gong J, Jin Y, Wang Y, Ji Y, Wu X, Han Z, Hu G. Expression profiling suggested a regulatory role of liver-enriched transcription factors in human hepatocellular carcinoma. *Cancer Res* 2001; **61**: 3176-3181

7 **Zhang QH**, Ye M, Wu XY, Ren SX, Zhao M, Zhao CJ, Fu G, Shen Y, Fan HY, Lu G, Zhong M, Xu XR, Han ZG, Zhang JW,

Tao J, Huang QH, Zhou J, Hu GX, Gu J, Chen SJ, Chen Z. Cloning and functional analysis of cDNAs with open reading frames for 300 previously undefined genes expressed in CD34+ hematopoietic stem/progenitor cells. *Genome Res* 2000; **10**: 1546-1560

8 **Lewis R**. Human genetics concepts and applications, 3rd edition. Ohio: *WCB McGraw-Hill* 1999: 16-20

9 **Welch MD**, DePace AH, Verma S, Iwamatsu A, Mitchison TJ. The human Arp2/3 complex is composed of evolutionarily conserved subunits and is localized to cellular regions of dynamic actin filament assembly. *J Cell Biol* 1997; **138**: 375-384

10 **Chen D**, Xu W, He P, Medrano EE, Whiteheart SW. Gaf-1, a gamma -SNAP-binding protein associated with the mitochondria. *J Biol Chem* 2001; **276**: 13127-13135

11 **Chittenden T**. BH3 domains: intracellular death-ligands critical for initiating apoptosis. *Cancer Cell* 2002; **2**: 165-166

12 **Marobbio CM**, Vozza A, Harding M, Bisaccia F, Palmieri F, Walker JE. Identification and reconstitution of the yeast mitochondrial transporter for thiamine pyrophosphate. *EMBO J* 2002; **21**: 5653-5661

13 **Kozak SL**, Siess DC, Kavanaugh MP, Miller AD, Kabat D. The envelope glycoprotein of an amphotropic murine retrovirus binds specifically to the cellular receptor/phosphate transporter of susceptible species. *J Virol* 1995; **69**: 3433-3440

14 **Lehnerer M**, Schulze J, Bernhardt R, Hlavica P. Some properties of mitochondrial adrenodoxin associated with its nonconventional electron donor function toward rabbit liver microsomal cytochrome P450 2B4. *Biochem Biophys Res Commun* 1999; **254**: 83-87

15 **Rumenapp U**, Geiszt M, Wahn F, Schmidt M, Jakobs KH. Evidence for ADP-ribosylation-factor-mediated activation of phospholipase D by m3 muscarinic acetylcholine receptor. *Eur J Biochem* 1995; **234**: 240-244

16 **Koyano Y**, Kawamoto T, Shen M, Yan W, Noshiro M, Fujii K, Kato Y. Molecular cloning and characterization of CDEP, a novel human protein containing the ezrin-like domain of the band 4.1 superfamily and the Dbl homology domain of Rho guanine nucleotide exchange factors. *Biochem Biophys Res Commun* 1997; **241**: 369-375

17 **Francis GA**, Annicotte JS, Auwerx J. PPAR agonists in the treatment of atherosclerosis. *Curr Opin Pharmacol* 2003; **3**: 186-191

18 **Brewer HB**, Santamarina-Fojo S. New insights into the role of the adenosine triphosphate-binding cassette transporters in high-density lipoprotein metabolism and reverse cholesterol transport. *Am J Cardiol* 2003; **91**: 3E-11E

19 **Portincasa P**, Moschetta A, Calamita G, Margari A, Palasciano G. Pathobiology of cholesterol gallstone disease: from equilibrium ternary phase diagram to agents preventing cholesterol crystallization and stone formation. *Curr Drug Targets Immune Endocr Metabol Disord* 2003; **3**: 67-81

20 **Corradini SG**, Liguori F. Recent studies on the pathogenesis of cholelithiasis: the role of the gallbladder epithelium. *Recenti Prog Med* 2001; **92**: 471-476

21 **Johnson MS**, Svensson PA, Boren J, Billig H, Carlsson LM, Carlsson B. Expression of scavenger receptor class B type I in gallbladder columnar epithelium. *J Gastroenterol Hepatol* 2002; **17**: 713-720

22 **Ivanchenkova RA**, Sviridov AV, Kuznetsov NA, Dadvani SA, Grachev SV. Immunomorphologic detection of apoprotein B antigenic determinants in the gallbladder wall in cholesterosis and cholelithiasis. *Khirurgiia (Mosk)* 2001; **12**: 19-24

23 **Stromsten A**, von Bahr S, Bringman S, Saeki M, Sahlin S, Bjorkhem I, Einarsson C. Studies on the mechanism of accumulation of cholesterol in the gallbladder mucosa. Evidence that sterol 27-hydroxylase is not a pathogenetic factor. *J Hepatol* 2004; **40**: 8-13

24 **Chignard N**, Mergey M, Veissiere D, Parc R, Capeau J, Poupon R, Paul A, Housset C. Bile acid transport and regulating functions in the human biliary epithelium. *Hepatology* 2001; **33**: 496-503

25 **Scheffer GL**, Kool M, de Haas M, de Vree JM, Pijnenborg AC, Bosman DK, Elferink RP, van der Valk P, Borst P, Scheper RJ. Tissue distribution and induction of human multidrug resistant protein 3. *Lab Invest* 2002; **82**: 193-201

26 **Shuai J**, Zhang SD, Han TQ, Jiang Y, Jiang ZH, Cai XX. Study of gene expression and affect factors to cholecystokinin A receptor in the early formation stage of gallstone in guinea pig. *Natl Med J China* 1999; **79**: 392-393

27 **Shuai J**, Zhang S, Han T, Jiang Y, Lei R, Chen S. Correlation between gene expression of CCK-A receptor and gallbladder emptying in gallstone patients. *Zhonghua Waike Zazhi* 1999; **37**: 292-294

28 **Yuan ZB**, Han TQ, Jiang ZY. Gene expression profile of human gallbladder. *J Surg Concepts Practice* 2003; **8**: 103-106

29 **Yuan ZB**, Han TQ, Jiang ZY. Profiling the adult human gallbladder and familial gallstone transcriptomes: Analysis by cDNA array hybridization. In Falk Symposium No 139: gallstones: pathogenesis and treatment. 49

30 **Schwarz HP**, Schlokat U, Mitterer A, Varadi K, Gritsch H, Muchitsch EM, Auer W, Pichler L, Dorner F, Turecek PL. Recombinant von Willebrand factor-insight into structure and function through infusion studies in animals with severe von Willebrand disease. *Semin Thromb Hemost* 2002; **28**: 215-226

31 **Borchers T**, Hohoff C, Buhlmann C, Spener F. Heart-type fatty acid binding protein - involvement in growth inhibition and differentiation. *Prostaglandins Leukot Essent Fatty Acids* 1997; **57**: 77-84

32 **Rost D**, Konig J, Weiss G, Klar E, Stremmel W, Keppler D. Expression and localization of the multidrug resistance proteins MRP2 and MRP3 in human gallbladder epithelia. *Gastroenterology* 2001; **121**: 1203-1208

Science Editor Zhu LH and Guo SY **Language Editor** Elseiver HK

PO Box 2345, Beijing 100023, China
www.wjgnet.com
wjg@wjgnet.com

ELSEVIER

World J Gastroenterol 2005;11(14):2117-2123
World Journal of Gastroenterology ISSN 1007-9327

• *BASIC RESEARCH* •

β-catenin up-regulates the expression of cyclinD1, c-myc and MMP-7 in human pancreatic cancer: Relationships with carcinogenesis and metastasis

Yu-Jun Li, Zhi-Min Wei, Yun-Xiao Meng, Xiang-Rui Ji

Yu-Jun Li, Zhi-Min Wei, Yun-Xiao Meng, Xiang-Rui Ji, Department of Pathology, The Affiliated Hospital of Medical College, Qingdao University, Qingdao 266003, Shandong Province, China
Supported by the Foundation of Shandong Education Committee, No. 03K02
Correspondence to: Dr. Yu-Jun Li, The Affiliated Hospital of Medical College, Qingdao University, 16 Jiangsu Road, Qingdao 266003, Shandong Province, China. yujun-Li66@yahoo.com
Telephone: +86-532-2911533
Received: 2004-03-11 Accepted: 2004-05-29

Abstract

AIM: To investigate whether abnormal expression of β-catenin in conjunction with overexpression of cyclinD1, c-myc and matrix metalloproteinase-7 (MMP-7) correlated with the carcinogenesis, metastasis and prognosis of pancreatic cancer, and to analyze the relationship of β-catenin expression with cyclinD1, c-myc and MMP-7 expression.

METHODS: Using immunohistochemistry, we examined the expression of β-catenin, cyclinD1, c-myc and MMP-7 in 47 pancreatic adenocarcinoma tissues, 12 pancreatic intraepithelial neoplasia (PanIN) and 10 normal pancreases, respectively. Proliferation cell nuclear antigen was also tested as the index of proliferative activity of pancreatic cancer cells.

RESULTS: In 10 cases of normal pancreatic tissues, epithelial cells showed equally strong membranous expression of β-catenin protein at the cell-cell boundaries, but the expression of cyclinD1, c-myc and MMP-7 was negative. The expression of β-catenin, cyclinD1, c-myc and MMP-7 in PanIN and pancreatic adenocarcinoma tissues had no significant difference [6/12 and 32/47 (68.1%), 6/12 and 35/47 (74.5%), 5/12 and 33/47 (70.2%), 7/12 and 30/47 (63.8%), respectively]. The abnormal expression of β-catenin was significantly correlated to metastasis and one-year survival rate of pancreatic cancer, but had no relation with size, differentiation and cell proliferation. The expression of cyclinD1 was correlated with cell proliferation and extent of differentiation, but not with size, metastasis and one-year survival rate of the pancreatic cancer. The expression of c-myc was not correlated with size, extent of differentiation, metastasis and 1-year survival rate, but closely with cell proliferation of pancreatic cancer. The overexpression of MMP-7 was significantly associated with metastasis and 1-year survival rate of pancreatic cancer, but not with size, extent of differentiation and cell proliferation. There was a highly significant positive association between abnormal expression of β-catenin and overexpression of cyclinD1, c-myc and MMP-7 not only in PanIN (r = 1.000, 0.845, 0.845), but also in pancreatic cancer (r = 0.437, 0.452, 0.435).

CONCLUSION: The abnormal expression of β-catenin plays a key role in the carcinogenesis and progression of human pancreatic carcinoma by up-regulating the expression of cyclinD1, c-myc and MMP-7, resulting in the degradation of extracellular matrix and uncontrolled cell proliferation and differentiation. β-catenin abnormal expression and MMP-7 overexpression may be considered as two useful markers for determining metastasis and prognosis of human pancreatic cancer.

Key words: cyclinD1; c-myc; MMP-7

Li YJ, Wei ZM, Meng YX, Ji XR. β-catenin up-regulates the expression of cyclinD1, c-myc and MMP-7 in human pancreatic cancer: Relationships with carcinogenesis and metastasis. *World J Gastroenterol* 2005; 11(14): 2117-2123
http://www.wjgnet.com/1007-9327/11/2117.asp

INTRODUCTION

β-catenin is a multifunctional cytoplasmic protein. It links E-cadherin and α-catenin to cytoskeleton constituting E-cadherin-catenin complex to maintain normal epithelial polarity and intercellular adhesion, and regulate cellular differentiation and proliferation[1-4]. Reduction and loss of β-catenin or other molecules might disrupt stability and integrity of the E-cadherin-catenin complex and disturb cellular adhesive junction, resulting in cell proliferation, invasion and metastasis of tumor[5-9]. Our previous study has found that abnormal expression of E-cadherin and α, β-catenin significantly correlated with differentiation, lymph node and liver metastasis of pancreatic cancer[10]. Recently, β-catenin has been found as an important member in the Wnt signaling pathway, which is conserved in various organisms from worms to mammals, and plays important roles in cellular development, proliferation and differentiation[11-14]. In the absence of Wnt signals, β-catenin is sequestered in a complex with the adenomatous polyposis coli tumor suppressor, AXIN, and a serine threonine glycogen synthetase kinase-

3β (GSK-3β), enabling phosphorylation and degradation of free β-catenin by the ubiquitin-proteasome system[11-14]. Thus, in normal epithelial cells, levels of free cytosolic β-catenin are low. During embryogenesis and activation of the Wnt signaling pathway, phosphorylation by GSK-3β is inhibited, and β-catenin accumulates in the cytosol at high levels, binds to cytosolic T cell-factor/lymphoid-enhancer-factor (Tcf/Lef) transcription factors, and the resulting complex is shuttled to the nucleus, leading to activation of target genes expression[14-16]. Recent studies have demonstrated that cyclinD1, c-myc and MMP-7 were important target genes of Wnt signaling pathway and overexpression of them was highly associated with accumulation of β-catenin and mutational defects of the Wnt signaling pathway in numerous tumor types[17-23], but there were only few reports in pancreatic cancer, and the results were conflicting[7,23-28].

To investigate the role of the Wnt signaling pathway in carcinogenesis and progression of pancreatic cancer, we detected expression of β-catenin, cyclinD1, c-myc and MMP-7 in normal pancreas, pancreatic intraepithelial neoplasia (PanIN) and pancreatic adenocarcinoma by immunohistochemistry.

MATERIALS AND METHODS

Patients and specimens

Forty-seven specimens of pancreatic carcinomas were collected from the Department of Pathology, Affiliated Hospital of Medical College, Qingdao University from 1995 to 1999. These included 29 male and 18 female patients with a mean age of 56.7 years (range 27-75 years). No patient received radiotherapy or chemotherapy before surgery. The tumor size was divided into three groups: smaller than 3 cm in diameter in 9 patients, 3-5 cm in 15 patients and larger than 5 cm in 23. Histologically, all cases were infiltrative ductal adenocarcinoma. According to the Modified Kloppel Histological Grading System[29], 10 cases were in grade I (well differentiated), 16 in grade II (moderately differentiated) and 21 in grade III (poorly differentiated). Twenty-five cases were with local and distant lymph node metastases, and 22 without metastasis. All patients were followed up for more than 1 year; 13 patients survived more than 12 mo and 34 patients died within 12 mo. The one-year survival rate was 27.6%. Twelve of 47 cases of pancreatic carcinoma tissues had regions containing identifiable PanIN lesions (all cases were PanIN-2). Ten normal adult pancreatic tissues were obtained from healthy young men who died of traffic accidents.

Immunohistochemistry

All specimens were fixed in 100 mL/L neutral formalin for 24-48 h, embedded by paraffin, and cut into 4-μm thick sections for immunohistochemical staining. PicTure™ method was used (Zymed, USA) as well as the following antibodies: β-catenin monoclonal antibody (diluted 1:100, Sigma, USA); cyclinD1, c-myc and MMP-7 monoclonal antibodies (ready for use, Zymed, USA); proliferation cell nuclear antigen (PCNA) monoclonal antibody (ready for use, Dako, USA) respectively. Before staining, the sections were pretreated with microwave (4 min×4 min at 900 W) in 0.1 mol/L citrate buffer for antigen retrieval. DAB was used for chromogen. PBS was substituted for primary antibodies as negative control.

Evaluation of immunohistochemical staining

The slides were reviewed by two independent observers who had no knowledge of patients' outcome. The positive staining of β-catenin appeared in brown, and was located in the cell membrane. Staining grade was based on the method described by Jawhari *et al*[30]: 0 score: no expression; 1 score: expression in cytoplasm; 2 scores: decreased expression; 3 scores: expression in cell membrane, namely normal expression. A score of 0-2 was abnormal expression. The expression of cyclinD1 and c-myc was stained in nucleus. A semi-quantitative evaluation was used to determine positive expression of cells by viewing 10 high power fields (×400)[31]: negative (-), cells were stained less than 10%; mildly positive, cells were stained at 11-25%; moderately positive, cells were stained at 26-50%; strongly positive, cells were stained over 50%. And we regarded the last three grades as positive (+, or overexpression). Positive immunostaining of MMP-7 was predominantly localized in cytoplasm. The slides were regarded as negative (-), and positive (+, or overexpression) if the count of positive cells was less than 20% and exceeded 20%. The positive staining of PCNA was located in the nuclei of pancreatic cancer cells with brown-yellow granules. The expression of PCNA was classified into four grades according to the count of positive cells, as follows[32]: 1, less than 25%; 2, between 26 and 50%; 3, between 51 and 75%; 4, more than 76%. Grades 1 and 2 were defined as low proliferative activity, and grades 3 and 4 were defined as high proliferative activity.

Statistical analysis

Statistical analysis was performed using the χ^2 test or Fisher's exact test and Spearman rank correlation coefficient analysis. $P<0.05$ was considered significant.

RESULTS

Expression of β-catenin, cyclinD1, c-myc and MMP-7 in normal pancreas, PanIN and pancreatic carcinoma tissues

The immunoreactivity of β-catenin was expressed by normal ductal and acinar cells with strong membranous staining at the intercellular border in 10 cases of adult normal pancreases. The rates of abnormal expression of β-catenin in pancreatic carcinoma and PanIN tissues were 68.1% (32/47) and 6/12 ($\chi^2 = 0.689$, $P>0.05$). The expression of β-catenin in most cases was in cytoplasm, whereas membranous staining reduced or disappeared (Figures 1A-C). The positive staining of cyclinD1 and c-myc was located in the nucleus (Figures 2A-D), and was not detected in 10 normal tissues of the pancreas. The positive rates of cyclinD1 and c-myc in pancreatic carcinoma and PanIN tissues were 74.5% (35/47) and 6/12 ($\chi^2 = 0.213$, $P>0.05$), 70.2% (33/47) and 5/12 ($P = 1.000$, $P>0.05$), respectively. Positive immunostaining of MMP-7 was predominantly localized in cytoplasm (Figures 3A-C), and it was detected in 30 (63.8%) of the 47 tumor tissues and 7 of the 12 PanIN tissues ($\chi^2 = 0.124$, $P>0.05$), but not in any of the normal pancreases.

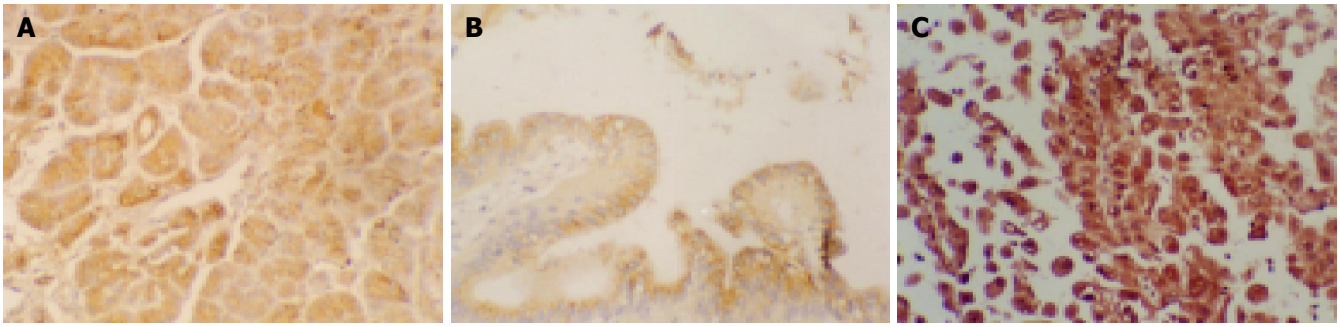

Figure 1 Immunohistochemical PicTure™ staining. A: Immunoreactivity of β-catenin was expressed by normal ductal and acinar cells with strong membranous staining at intercellular border, ×100; B and C: Immunoreactivity of β-catenin was mainly located in cytoplasm of PanIN and pancreatic cancer cells, ×200.

Expression of PCNA in pancreatic carcinoma tissues

The positive staining of PCNA was located in the nuclei of pancreatic cancer cells with brown-yellow granules (Figures 3A-C). There were 6 cases of grade 1, 13 cases of grade 2, 16 cases of grade 3 and 12 cases of grade 4 in 47 cases of pancreatic cancer. Low proliferative activity was in 19 cases (grades 1 and 2) and high proliferative activity in 28 cases (grades 3 and 4).

Relationships between expression of β-catenin, cyclinD1, c-myc and MMP-7 and clinicopathologic characteristics of pancreatic carcinoma

The abnormal expression of β-catenin was significantly correlated to metastasis and 1-year survival rate of pancreatic cancer (χ^2 = 6.23, 5.50; P<0.05), but had no relation with tumor size, histological grade and cell proliferation (P = 0.981, χ^2 = 3.51, 1.17; all P>0.05). The overexpression of cyclinD1 was correlated with cell proliferation and histological grade (P = 0.006, χ^2 = 6.19; P<0.05), but not with size, metastasis and one-year survival rate of the pancreatic cancer (χ^2 = 0.01, 0.86, 0.78; all P>0.05). The overexpression of c-myc was not correlated with size, histological grade, metastasis and survival rate (P = 1.000, 0.208; χ^2 = 0.90, 1.35; all P>0.05), but closely related with cell proliferation of pancreatic cancer (χ^2 = 4.17; P<0.05). The overexpression of MMP-7 was significantly associated with metastasis and survival rate of pancreatic cancer (χ^2 = 6.05, 6.61; both P<0.05), but not with size, histological grade and cell proliferation (χ^2 = 0.40, 0.74, 1.34; all P>0.05) (Table 1).

Relationships between abnormal expression of β-catenin and overexpression of cyclinD1, c-myc and MMP-7 in PanIN

In PanIN, β-catenin abnormal expression rates in tumor tissues of cyclinD1, c-myc and MMP-7 overexpression group were 6/6, 5/6, 6/6, and β-catenin normal expression rates in tumor tissues of cyclinD1, c-myc and MMP-7 negative expression group were 6/6, 6/6 and 5/6, respectively. There was a highly significant positive association between abnormal expression of β-catenin and overexpression of

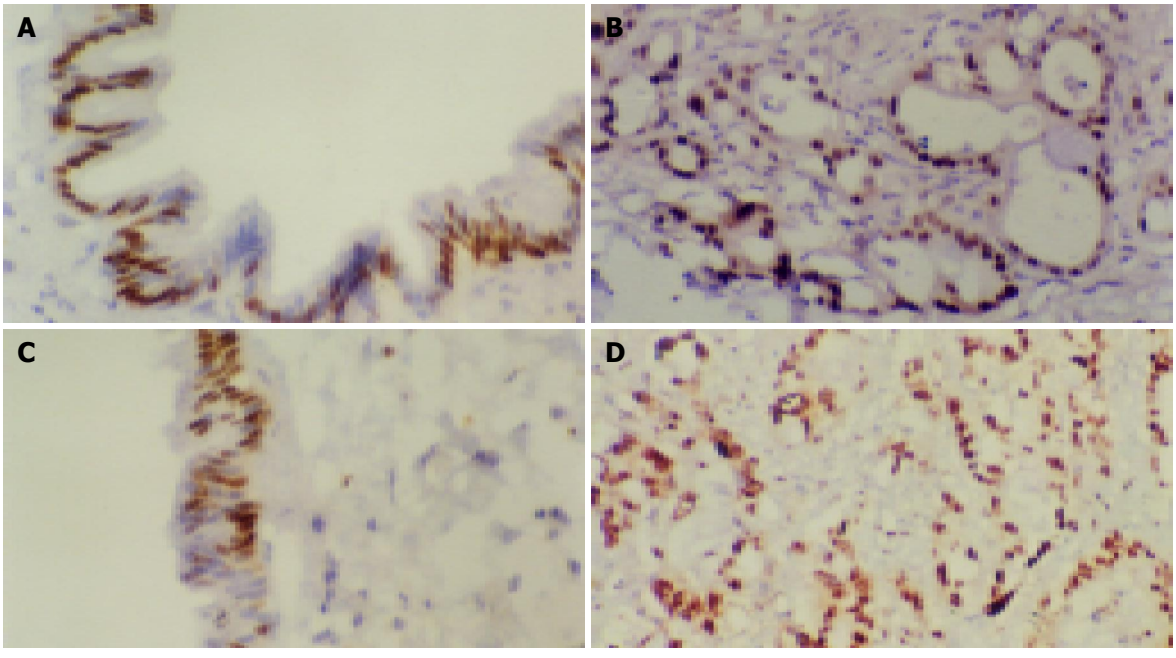

Figure 2 Immunohistochemical PicTure™ staining. A and B: CyclinD1 expression was in the nuclei of PanIN and pancreatic cancer cells, ×200; C and D: c-myc expression located in the nuclei of PanIN and pancreatic cancer cells, ×200.

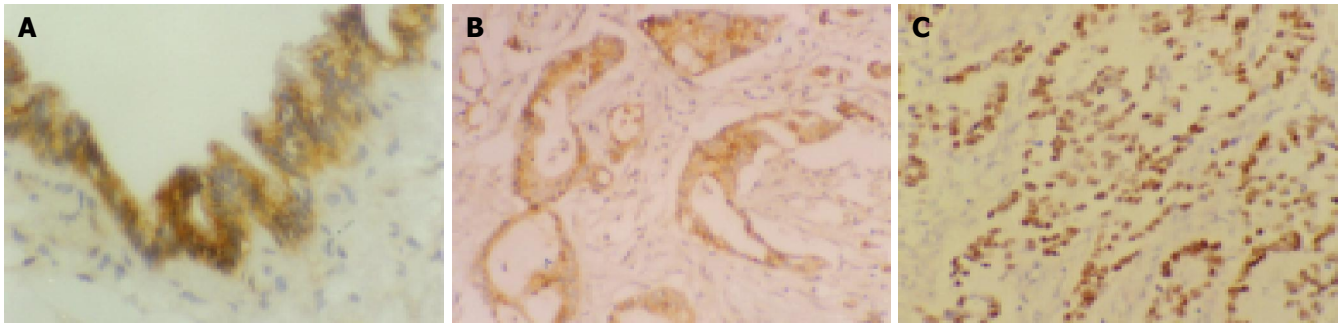

Figure 3 Immunohistochemical PicTure™ staining. A and B: The expression of MMP-7 was mainly located in cytoplasm of PanIN and pancreatic cancer cells, ×200. C: Expression of PCNA protein was located in the nuclei of pancreatic cancer cells with brown-yellow granules, ×200.

cyclinD1, c-myc and MMP-7 in PanIN (P = 0.002, 0.015, 0.015; r = 1.000, 0.845, 0.845) (Table 2).

Relationships between abnormal expression of β-catenin and overexpression of cyclinD1, c-myc and MMP-7 in pancreatic carcinomas

As summarized in Table 3, β-catenin abnormal expression rates in cancer tissues of cyclinD1, c-myc and MMP-7 overexpression group were 87.5%, 84.7%, 78.1%, and β-catenin normal expression rates in cancer tissues of cyclinD1, c-myc and MMP-7 negative expression group were 8/15, 9/15 and 10/15, respectively. There was a close positive and significant association between abnormal expression of β-catenin and overexpression of cyclinD1, c-myc and MMP-7 in pancreatic cancer (χ^2 = 6.94, 7.61, 8.87; r = 0.437, 0.452, 0.435; all P<0.05).

DISCUSSION

In addition to its role in regulating intercellular adhesion, β-catenin has a critical role in the highly conserved Wnt signaling pathway. Mutations of β-catenin and aberrant expression of its protein have been identified in a number of different types of human cancers, and implicated in tumor invasion and metastasis[33-35]. However, reports regarding the expression of β-catenin in human pancreatic cancer are very few, and the results are controversial. Gerdes *et al*[27], reported that intracellular accumulation of β-catenin was not observed in any of the 40 pancreatic adenocarcinomas, and neither 78 pancreatic adenocarcinomas nor 14 pancreatic cancer cell lines had mutations in exon 3 of the β-catenin gene. Thus, Wnt-β-catenin pathways did not appear to be common targets of genetic alterations in pancreatic carcinogenesis. But most researchers[17,24,25] found that alterations in β-catenin expression were common in pancreatic cancer and correlated with loss of tumor differentiation, metastasis and prognosis. In our study, we found that the expression of β-catenin was located in normal ductal and acinar cells with strong membranous staining in adult normal pancreases, but in most cases of pancreatic carcinomas was in cytoplasm and membranous staining reduced or disappeared, and the abnormal expression rates of β-catenin in pancreatic carcinoma and PanIN tissues were 68.1% and 6/12 (P>0.05), and abnormal β-catenin was correlated with metastasis and survival time of pancreatic cancer. These data suggest that the abnormal expression of β-catenin plays an important role in the process of pancreatic tumorigenesis and metastasis, and may be considered as a valuable marker for early diagnosis and prognosis of pancreatic cancer.

CyclinD1 and c-myc are critical genes involved in cell proliferation and differentiation. As two target genes of Wnt signaling pathway, the amplification and/or overexpression of cyclinD1 and c-myc in tumor cells are extremely common, indicating that their activation may be essential during carcinogenesis[36-40]. To date, only few data on the biological significance and prognostic value of cyclinD1 and c-myc overexpression have been reported in pancreatic cancer. Several investigators[41-44] have reported that cyclinD1 overexpression was detected in pancreatic carcinoma and PanIN, whereas normal human pancreas stained negative, and its overexpression was associated with tumor stage, cell proliferating activity, differentiation, perineural invasion, lymph node metastasis and poor prognosis of pancreatic adenocarcinoma. Schleger *et al*[45], recently have shown that c-myc activation was detected in some high-grade PanIN lesions, and its overexpression was common in pancreatic cancer, and significantly associated with poor tumor differentiation, but not with tumor stage or metastasis. So

Table 1 Relationships between expression of β-catenin, cyclinD1, c-myc and MMP-7 and clinicopathologic characteristics of pancreatic cancer

Parameter	*n*	β-catenin		c-myc		cyclinD1		MMP-7	
		Normal	Abnormal	+	–	+	–	+	–
Mass size (cm)									
<3	9	3	6	6	3	6	3	6	3
3–5	15	4	11	11	4	10	5	10	5
>5	23	8	15	16	7	19	4	14	9
Histological grade									
I	10	4	6	5	5	4	6	7	3
II	16	6	10	11	5	12	4	11	5
III	21	5	16	17	4	19[a]	2	12	9
Proliferation degree									
High	28	6	22	23	5	25	3	16	12
Low	19	9	10	10[c]	9	10[c]	9	14	5
Metastasis									
Positive	25	4	21	19	6	20	5	20	5
Negative	22	11[e]	11	14	8	15	7	10[e]	12
Survival time (yr)									
>1	13	8	5	8	5	9	4	4	9
≤1	34	7[g]	27	25	9	26	8	26[g]	8

[a]P<0.05 *vs* grade I; [c]P<0.05 *vs* high proliferation degree; [e]P<0.05 *vs* positive metastases. [g]P<0.05 *vs* >1 year.

Table 2 Relationships between expression of β-catenin and cyclinD1, c-myc and MMP-7 in PanIN

β-catenin	*n*	cyclinD1		c-myc		MMP-7	
		+	–	+	–	+	–
Normal	6	0	6	0	6	1	5
Abnormal	6	6	0	5	1	6	0

P = 0.002, 0.015, 0.015; r = 1.000, 0.845, 0.845.

Table 3 Relationships between expression of β-catenin and cyclinD1, c-myc and MMP-7 in pancreatic carcinomas

β-catenin	*n*	CyclinD1 (%)		c-myc (%)		MMP-7 (%)	
		+	–	+	–	+	–
Normal	15	7	8	6	9	5	10
Abnormal	32	28 (87.5)	4	27 (84.5)	5	25 (78.1)	7

χ^2 = 6.94, 7.61, 8.87; r = 0.437, 0.452, 0.435; P<0.05.

they considered that c-myc activation was involved in early stages of development and progression of pancreatic neoplasia, rather than in late stages of local spread and lymph node metastasis of invasive adenocarcinoma. In the present study, we found that cyclinD1 and c-myc overexpression was detected in 35 and 33 of 47 cases of pancreatic carcinoma, 6 and 5 of 12 PanIN tissues, respectively, but not in 10 normal pancreases. Both proteins' overexpression was significantly correlated with cell proliferation activity and degree of differentiation, but not with size, metastasis or one-year survival rate of the pancreatic cancer. These results suggest that cyclinD1 and c-myc overexpression plays an important role in pancreatic carcinogenesis, but does not affect tumor progression independently. Masuda *et al*[46], have also reported that overexpression of cyclinD1 was not associated with the presence of nodal metastasis and clinical stage in head and neck squamous cell carcinoma.

Degradation of the extracellular matrix mediated by matrix metalloproteinases (MMPs) is a crucial mechanism during tumor invasion and metastasis. They are necessary to create a microenvironment supporting the growth of primary tumor and metastasis[47]. Unlike the majority of MMPs family members, MMP-7 mRNA and protein are expressed not only in the epithelium of premalignant lesions in multiple glandular tissues[48] but also in the tumor cells, and associated with tumor progression of colorectal[49], gastric[50] and hepatic carcinomas[51]. In contrast to these gastrointestinal cancers, there has been little information on the significance of MMP-7 expression in pancreatic carcinoma. Some researchers[52-54] have found that expression of MMP-7 mRNA and protein was significantly correlated with infiltrating growth pattern, lymph node and liver metastasis, TNM stage, postoperative recurrence and survival time of pancreatic carcinoma. Crawford *et al*[55], have shown that MMP-7 was expressed in the majority of human pancreatic adenocarcinomas and PanIN, but was never detected in the normal pancreas. In our study, we also found that 10 normal pancreases did not express MMP-7, but 63.8% pancreatic adenocarcinoma tissues and 7/12 PanIN lesions showed MMP-7 positive expression. Moreover, overexpression of MMP-7 was significantly associated with metastasis and survival time of pancreatic cancer, but not with tumor size, cell proliferation activity and degree of differentiation. These results suggest that MMP-7 plays a key role not only in the earlier stages of pancreatic tumorigenesis, but also in the progression of pancreatic carcinoma, and thereby contributes to a poor prognosis.

As an effector of the Wnt signaling pathway, β-catenin is able to bind to Tcf/Lef transcription factors, and subsequently activate target genes[14-16]. Recently studies demonstrated that cyclinD1, c-myc and MMP-7 were important target genes of Wnt signaling pathway[16-18]. Immunohistochemical studies confirmed that overexpression of cyclinD1, c-myc and MMP-7 was highly associated with accumulation of β-catenin and mutational defects of the Wnt signaling pathway in numerous tumor types[17,19-22]. For instance, a strong correlation was reported between β-catenin deregulation and cyclinD1 and MMP-7 expression in primary colorectal tumors[56,57]. Brabletz *et al*[20], also found a tight correlation between nuclear β-catenin accumulation and c-myc expression in colorectal adenomas, although neither feature correlated with grade of dysplasia or proliferative activity. Zhai *et al*[17], found that nuclear accumulation of β-catenin was highly associated with overexpression of cyclinD1 and MMP-7, but not with c-myc overexpression in ovarian endometrioid adenocarcinomas. In pancreatic carcinomas, only one literature[26] reported that β-catenin might be involved in the tumorigenesis of pancreatic cancer and exhibited its effects mainly by the transactivation of cyclinD1. In this study, we examined the expression of β-catenin, cyclinD1, c-myc and MMP-7 in pancreatic carcinomas and PanIN, and confirmed that there was a highly significant positive association between abnormal expression of β-catenin and overexpression of cyclinD1, c-myc and MMP-7 not only in PanIN (r = 1.000, 0.845, 0.845), but also in pancreatic cancer (r = 0.437, 0.452, 0.435). It can be inferred from our findings that the abnormal expression of β-catenin plays a key role in the carcinogenesis and progression of human pancreatic carcinoma by up-regulating the expression of cyclinD1, c-myc and MMP-7, resulting in the degradation of extracellular matrix and uncontrolled cell proliferation and differentiation.

REFERENCES

1 **Wijnhoven BP,** Dinjens WN, Pignatelli M. E-cadherin-catenin cell-cell adhesion complex and human cancer. *Br J Surg* 2000; **87**: 992-1005

2 **Yagi T,** Takeichi M. Cadherin superfamily genes: functions, genomic organization, and neurologic diversity. *Genes Dev* 2000; **14**: 1169-1180

3 **Ivanov DB**, Philippova MP, Tkachuk VA. Structure and functions of classical cadherins. *Biochemistry (Mosc)* 2001; **66**: 1174-1186

4 **Jawhari AU,** Farthing MJ, Pignatelli M. The E-cadherin/epidermal growth factor receptor interaction: a hypothesis of reciprocal and reversible control of intercellular adhesion and cell proliferation. *J Pathol* 1999; **187**: 155-157

5 **Bremnes RM,** Veve R, Hirsch FR, Franklin WA. The E-cadherin cell-cell adhesion complex and lung cancer invasion, metastasis, and prognosis. *Lung Cancer* 2002; **36**: 115-124

6 **Berx G,** Van Roy F. The E-cadherin/catenin complex: an important gatekeeper in breast cancer tumorigenesis and malignant progression. *Breast Cancer Res* 2001; **3**: 289-293

7 **Julkunen K,** Makinen K, Karja V, Kosma VM, Eskelinen M. alpha-, beta- and chi-catenin expression in human pancreatic cancer. *Anticancer Res* 2003; **23**: 5043-5047
8 **Song BJ,** Park YJ, Kim HS, Kim CN, Chang SH. Expression of beta-catenin and E-cadherin in early gastric cancer: correlation with clinicopathologic parameters. *Korean J Gastroenterol* 2004; **43**: 82-89
9 **Tanaka N,** Odajima T, Ogi K, Ikeda T, Satoh M. Expression of E-cadherin, alpha-catenin, and beta-catenin in the process of lymph node metastasis in oral squamous cell carcinoma. *Br J Cancer* 2003; **89**: 557-563
10 **Li YJ,** Ji XR. Relationship between expression of E-cadherin-catenin complex and clinicopathologic characteristics of pancreatic cancer. *World J Gastroenterol* 2003; **9**: 368-372
11 **Polakis P.** Wnt signaling and cancer. *Genes Dev* 2000; **14**: 1837-1851
12 **Peifer M,** Polakis P. Wnt signaling in oncogenesis and embryogenesis - a look outside the nucleus. *Science* 2000; **287**: 1606-1609
13 **Morin PJ.** beta-catenin signaling and cancer. *Bioessays* 1999; **21**: 1021-1030
14 **Kikuchi A.** Regulation of beta-catenin signaling in the Wnt pathway. *Biochem Biophys Res Commun* 2000; **268**: 243-248
15 **Hovanes K,** Li TW, Munguia JE, Truong T, Milovanovic T, Lawrence Marsh J, Holcombe RF, Waterman ML. Beta-catenin-sensitive isoforms of lymphoid enhancer factor-1 are selectively expressed in colon cancer. *Nat Genet* 2001; **28**: 53-57
16 **Wong NA,** Pignatelli M. Beta-catenin-a linchpin in colorectal carcinogenesis? *Am J Pathol* 2002; **160**: 389-401
17 **Zhai Y,** Wu R, Schwartz DR, Darrah D, Reed H, Kolligs FT, Nieman MT, Fearon ER, Cho KR. Role of beta-catenin/T-cell factor-regulated genes in ovarian endometrioid adenocarcinomas. *Am J Pathol* 2002; **160**: 1229-1238
18 **Hatsell S,** Rowlands T, Hiremath M, Cowin P. Beta-catenin and Tcfs in mammary development and cancer. *J Mammary Gland Biol Neoplasia* 2003; **8**: 145-158
19 **Saeki H,** Tanaka S, Sugimachi K, Kimura Y, Miyazaki M, Ohga T, Sugimachi K. Interrelation between expression of matrix metalloproteinase 7 and beta-catenin in esophageal cancer. *Dig Dis Sci* 2002; **47**: 2738-2742
20 **Brabletz T,** Jung A, Dag S, Reu S, Kirchner T. beta-Catenin induces invasive growth by activating matrix metalloproteinases in colorectal carcinoma. *Verh Dtsch Ges Pathol* 2000; **84**: 175-181
21 **Yamazaki K,** Hanami K, Nagao T, Asoh A, Sugano I, Ishida Y. Increased cyclin D1 expression in cancer of the ampulla of Vater: relevance to nuclear beta catenin accumulation and k-ras gene mutation. *Mol Pathol* 2003; **56**: 336-341
22 **Cui J,** Zhou X, Liu Y, Tang Z, Romeih M. Alterations of beta-catenin and Tcf-4 instead of GSK-3beta contribute to activation of Wnt pathway in hepatocellular carcinoma. *Chin Med J (Engl)* 2003; **116**: 1885-1892
23 **Lowy AM,** Fenoglio-Preiser C, Kim OJ, Kordich J, Gomez A, Knight J, James L, Groden J. Dysregulation of beta-catenin expression correlates with tumor differentiation in pancreatic duct adenocarcinoma. *Ann Surg Oncol* 2003; **10**: 284-290
24 **Joo YE,** Rew JS, Park CS, Kim SJ. Expression of E-cadherin, alpha- and beta-catenins in patients with pancreatic adenocarcinoma. *Pancreatology* 2002; **2**: 129-137
25 **Karayiannakis AJ,** Syrigos KN, Polychronidis A, Simopoulos C. Expression patterns of alpha-, beta- and gamma-catenin in pancreatic cancer: correlation with E-cadherin expression, pathological features and prognosis. *Anticancer Res* 2001; **21**: 4127-4134
26 **Qiao Q,** Ramadani M, Gansauge S, Gansauge F, Leder G, Beger HG. Reduced membranous and ectopic cytoplasmic expression of beta -catenin correlate with cyclin D1 overexpression and poor prognosis in pancreatic cancer. *Int J Cancer* 2001; **95**: 194-197
27 **Gerdes B,** Ramaswamy A, Simon B, Pietsch T, Bastian D, Kersting M, Moll R, Bartsch D. Analysis of beta-catenin gene mutations in pancreatic tumors. *Digestion* 1999; **60**: 544-548
28 **Caca K,** Kolligs FT, Ji X, Hayes M, Qian J, Yahanda A, Rimm DL, Costa J, Fearon ER. Beta- and gamma-catenin mutations, but not E-cadherin inactivation, underlie T-cell factor/lymphoid enhancer factor transcriptional deregulation in gastric and pancreatic cancer. *Cell Growth Differ* 1999; **10**: 369-376
29 **Giulianotti PC,** Boggi U, Fornaciari G, Bruno J, Rossi G, Giardino D, Di Candio G, Mosca F. Prognostic value of histological grading in ductal adenocarcinoma of the pancreas. Kloppel vs TNM grading. *Int J Pancreatol* 1995; **17**: 279-289
30 **Jawhari A,** Jordan S, Poole S, Browne P, Pignatelli M, Farthing MJ. Abnormal immunoreactivity of the E-cadherin-catenin complex in gastric carcinoma: relationship with patient survival. *Gastroenterology* 1997; **112**: 46-54
31 **Barnes DM,** Dublin EA, Fisher CJ, Levison DA, Millis RR. Immunohistochemical detection of p53 protein in mammary carcinoma: an important new independent indicator of prognosis? *Hum Pathol* 1993; **24**: 469-476
32 **Li YJ,** Meng YX, Ji XR. Relationship between expressions of E-cadherin and alpha-catenin and biological behaviors of human pancreatic cancer. *Hepatobiliary Pancreat Dis Int* 2003; **2**: 471-477
33 **Wong SC,** Lo ES, Lee KC, Chan JK, Hsiao WL. Prognostic and diagnostic significance of beta-catenin nuclear immunostaining in colorectal cancer. *Clin Cancer Res* 2004; **10**: 1401-1408
34 **Chesire DR,** Isaacs WB. Beta-catenin signaling in prostate cancer: an early perspective. *Endocr Relat Cancer* 2003; **10**: 537-560
35 **Iwaya K,** Ogawa H, Kuroda M, Izumi M, Ishida T, Mukai K. Cytoplasmic and/or nuclear staining of beta-catenin is associated with lung metastasis. *Clin Exp Metastasis* 2003; **20**: 525-529
36 **Yamamoto H,** Ochiya T, Takeshita F, Toriyama-Baba H, Hirai K, Sasaki H, Sasaki H, Sakamoto H, Yoshida T, Saito I, Terada M. Enhanced skin carcinogenesis in cyclin D1-conditional transgenic mice: cyclin D1 alters keratinocyte response to calcium-induced terminal differentiation. *Cancer Res* 2002; **62**: 1641-1647
37 **Chung DC,** Brown SB, Graeme-Cook F, Seto M, Warshaw AL, Jensen RT, Arnold A. Overexpression of cyclin D1 occurs frequently in human pancreatic endocrine tumors. *J Clin Endocrinol Metab* 2000; **85**: 4373-4378
38 **Evan GI,** Littlewood TD. The role of c-*myc* in cell growth. *Curr Opin Genet Dev* 1993; **3**: 44–49
39 **Nesbit CE,** Tersak JM, Prochownik EV. MYC oncogenes and human neoplastic disease. *Oncogene* 1999; **18**: 3004–3016
40 **Abba MC,** Laguens RM, Dulout FN, Golijow CD. The c-myc activation in cervical carcinomas and HPV 16 infections. *Mutat Res* 2004; **557**: 151-158
41 **Poch B,** Gansauge F, Schwarz A, Seufferlein T, Schnelldorfer T, Ramadani M, Beger HG, Gansauge S. Epidermal growth factor induces cyclin D1 in human pancreatic carcinoma: evidence for a cyclin D1-dependent cell cycle progression. *Pancreas* 2001; **23**: 280-287
42 **Ito Y,** Takeda T, Wakasa K, Tsujimoto M, Matsuura N. Expression and possible role of cyclin D3 in human pancreatic adenocarcinoma. *Anticancer Res* 2001; **21**: 1043-1048
43 **Biankin AV,** Kench JG, Morey AL, Lee CS, Biankin SA, Head DR, Hugh TB, Henshall SM, Sutherland RL. Overexpression of p21(WAF1/CIP1) is an early event in the development of pancreatic intraepithelial neoplasia. *Cancer Res* 2001; **61**: 8830-8837
44 **Kornmann M,** Ishiwata T, Itakura J, Tangvoranuntakul P, Beger HG, Korc M. Increased cyclin D1 in human pancreatic cancer is associated with decreased postoperative survival. *Oncology* 1998; **55**: 363-369
45 **Schleger C,** Verbeke C, Hildenbrand R, Zentgraf H, Bleyl U. c-MYC activation in primary and metastatic ductal adenocarcinoma of the pancreas: incidence, mechanisms, and clinical significance. *Mod Pathol* 2002; **15**: 462-469
46 **Masuda M,** Suzui M, Yasumatu R, Nakashima T, Kuratomi Y, Azuma K, Tomita K, Komiyama S, Weinstein IB. Constitutive activation of signal transducers and activators of transcription 3 correlates with cyclin D1 overexpression and may

provide a novel prognostic marker in head and neck squamous cell carcinoma. *Cancer Res* 2002; **62**: 3351-3355

47 **Chakraborti S,** Mandal M, Das S, Mandal A, Chakraborti T. Regulation of matrix metalloproteinases: an overview. *Mol Cell Biochem* 2003; **253**: 269-285

48 **Powell WC**, Matrisian LM. Complex roles of matrix metalloproteinases in tumor progression. *Curr Top Microbiol Immunol* 1996; **213**(Pt 1): 1-21

49 **Leeman MF,** Curran S, Murray GI. New insights into the roles of matrix metalloproteinases in colorectal cancer development and progression. *J Pathol* 2003; **201**: 528-534

50 **Huachuan Z,** Xiaohan L, Jinmin S, Qian C, Yan X, Yinchang Z. Expression of matrix metalloproteinase-7 involving in growth, invasion, metastasis and angiogenesis of gastric cancer. *Chin Med Sci J* 2003; **18**: 80-86

51 **Yamamoto H,** Itoh F, Adachi Y, Fukushima H, Itoh H, Sasaki S, Hinoda Y, Imai K. Messenger RNA expression of matrix metalloproteinases and tissue inhibitors of metalloproteinases in human hepatocellular carcinoma. *Jpn J Clin Oncol* 1999; **29**: 58–62

52 **Nakamura H,** Horita S, Senmaru N, Miyasaka Y, Gohda T, Inoue Y, Fujita M, Meguro T, Morita T, Nagashima K. Association of matrilysin expression with progression and poor prognosis in human pancreatic adenocarcinoma. *Oncol Rep* 2002; **9**: 751-755

53 **Fukushima H,** Yamamoto H, Itoh F, Nakamura H, Min Y, Horiuchi S, Iku S, Sasaki S, Imai K. Association of matrilysin mRNA expression with K-ras mutations and progression in pancreatic ductal adenocarcinomas. *Carcinogenesis* 2001; **22**: 1049-1052

54 **Yamamoto H,** Itoh F, Iku S, Adachi Y, Fukushima H, Sasaki S, Mukaiya M, Hirata K, Imai K. Expression of matrix metalloproteinases and tissue inhibitors of metalloproteinases in human pancreatic adenocarcinomas: clinicopathologic and prognostic significance of matrilysin expression. *J Clin Oncol* 2001; **19**: 1118-1127

55 **Crawford HC,** Scoggins CR, Washington MK, Matrisian LM, Leach SD. Matrix metalloproteinase-7 is expressed by pancreatic cancer precursors and regulates acinar-to-ductal metaplasia in exocrine pancreas. *J Clin Invest* 2002; **109**: 1437-1444

56 **Brabletz T,** Jung A, Dag S, Hlubek F, Kirchner T. beta-catenin regulates the expression of the matrix metalloproteinase-7 in human colorectal cancer. *Am J Pathol* 1999; **155**: 1033-1038

57 **Utsunomiya T,** Doki Y, Takemoto H, Shiozaki H, Yano M, Sekimoto M, Tamura S, Yasuda T, Fujiwara Y, Monden M. Correlation of beta-catenin and cyclin D1 expression in colon cancers. *Oncology* 2001; **61**: 226-233

Science Editor Zhu LH **Language Editor** Elsevier HK

PO Box 2345, Beijing 100023, China
www.wjgnet.com
wjg@wjgnet.com

ELSEVIER

World J Gastroenterol 2005;11(14):2124-2129
World Journal of Gastroenterology ISSN 1007-9327

• *BASIC RESEARCH* •

Effects of total glucosides of peony on immunological hepatic fibrosis in rats

Hua Wang, Wei Wei, Ni-Ping Wang, Cheng-Yi Wu, Shang-Xue Yan, Li Yue, Ling-Ling Zhang, Shu-Yun Xu

Hua Wang, Wei Wei, Ni-Ping Wang, Cheng-Yi Wu, Shang-Xue Yan, Li Yue, Ling-Ling Zhang, Shu-Yun Xu, Institute of Clinical Pharmacology, Anhui Medical University, Hefei 230032, Anhui Province, China
Supported by the National High Technology Research and Development Program of China (863 Program), No. 2002AA2Z3235
Correspondence to: Professor Wei Wei, Institute of Clinical Pharmacology, Anhui Medical University, Hefei 230032, Anhui Province, China. wwei@ahmu.edu.cn
Telephone: +86-551-5161208 Fax: +86-551-5161208
Received: 2004-04-19 Accepted: 2004-05-29

Abstract

AIM: To study the effects of *total glucosides of peony* (TGP) on immunological hepatic fibrosis induced by human albumin in rats.

METHODS: Sixty adult male Sprague-Dawley rats were randomly divided into: Normal group, model group, TGP (60 and 120 mg/kg) treatment groups and colchicines (0.1 mg/kg) treatment group. On the day before the rats were killed, those in TGP or colchicine groups received TGP or colchicine as above from the first day of tail vein injection of human albumin. The rats in normal and model groups were only administered with the same volume of vehicle. At the end of the 16th wk, rats in each group were killed. Blood and tissue specimens were taken. Levels of alanine aminotransferase (ALT), aspartate aminotransferase (AST), nitric oxide (NO), content of malondialdehyde (MDA), activity of superoxide dismutase (SOD) and glutathione peroxidase (GSH-px), were measured by biochemical methods. Serum procollagen type III (PC III) and laminin (LN) were determined by radioimmunoassay. Liver collagen level was determined by measuring hydroxyproline content in fresh liver samples. Hepatic tissue sections were stained with hematoxylin-eosin and examined under a light microscope.

RESULTS: Histological results showed that TGP improved the human albumin-induced alterations in the liver structure, alleviated lobular necrosis and significantly lowered collagen content. The antifibrotic effect of TGP was also confirmed by decreased serum content of LN and PCIII in TGP-treated group. Moreover, the treatment with TGP effectively reduced the hydroxyproline content in liver homogenates. However, the level of ALT and AST increased in fibrotic rat but had no significance compared with normal control, whereas the ratio of A/G decreased without significance. TGP had no effect on level of ALT, AST and the ratio of A/G. Furthermore, TGP treatment significantly blocked the increase in MDA and NO, associated with a partial elevation in liver total antioxidant capacity including SOD and GSH-px.

CONCLUSION: TGP has beneficial effects on hepatic fibrosis in rats by inhibition of collagen synthesis and decreasing oxidative stress.

Key words: Total glucosides of peony; Hepatic fibrosis; Rat; Oxidative stress

Wang H, Wei W, Wang NP, Wu CY, Yan SX, Yue L, Zhang LL, Xu SY. Effects of total glucosides of peony on immunological hepatic fibrosis in rats. *World J Gastroenterol* 2005; 11(14): 2124-2129
http://www.wjgnet.com/1007-9327/11/2124.asp

INTRODUCTION

Hepatic fibrosis is traditionally defined as a progressive pathological process involving multiple cellular and molecular events that lead ultimately to deposition of excess matrix proteins in the extracellular space[1-3]. Chronic injury leading to fibrosis in liver occurs in response to a variety of insults, including viral hepatitis (especially hepatitis B in China), alcohol abuse, drugs, metabolic diseases, *etc.* When this injury process is combined with ineffective regeneration and repair, there is increasing distortion of the normal liver architecture, and the end result is cirrhosis. Current evidence indicates that hepatic fibrosis even cirrhosis is dynamic and can be bidirectional (involving phases of progression and regression)[4,5]. Thus, efforts to understand fibrosis focus primarily on events that lead to the early accumulation of scar in hopes of identifying therapeutic targets to slow its progression. Unfortunately, no effective hepatic antifibrotic therapies are available. Antifibrotic strategies might therefore be usefully targeting towards either reducing matrix synthesis or increasing matrix degradation[6,7].

Paeonia lactiflora pall root, a traditional Chinese herb, has been used to relieve the pain and been a component of effective prescriptions for treatment of liver disease[8]. The *total glucosides of peony* (TGP), a powder substance extracted from *Paeonia lactiflora* pall root, were composed of peoniflorin, hydroxypeoniflorin, peonin, albiflorin, benzoylpeoniflorin, *etc.* Peoniflorin, accounting for some 90%, is a main effective component of TGP. TGP have been recognized as the valuable traditional herbs used in the treatment of rheumatoid arthritis (RA), systemic lupus erythematosus (SLE) and

hepatitis with a long history in traditional Chinese medicine[9-11]. The anti-inflammatory, anti-oxidative, anti-hepatic injury and immunoregulatory activities without evident toxic or side-effects of TGP have been extensively proved in our laboratory for many years[12-16]. These observations have led to an interest in the potential role of TGP as an antifibrotic agent.

The present study was designed to evaluate whether treatment with TGP exerts any beneficial effect on liver histopathology and liver function in an experimental model of immunological hepatic fibrosis, and the mechanism of its part were also investigated.

MATERIALS AND METHODS

Animal experiments and drug treatment

Sixty adult male Sprague-Dawley rats, weighing 120-150 g [provided by Shanghai BK Experimental Animal Center (Grade II, Certificate No D-65)] were employed in the study. The rats were randomly divided into five groups. A rat model of hepatic fibrosis was produced by immunologically attacking with human albumin, using the method introduced by Wang *et al*[17]. Ten male Sprague-Dawley rats were regarded as normal group. The other fifty healthy rats were randomly divided into four groups including model group, TGP (60 and 120 mg/kg) treated group and colchicines (0.1 mg/kg) treatment group with the experimental attacking as follows.

All rats were injected with 0.5 mL human albumin diluted with normal saline (0.5 mL equals 4 mg human albumin) and the same quantity of an incomplete Freund's adjuvant, once every 14 d for the first two times, then once every 10 d, twice. Ten days after the last injection, serum antibody was measured. Rats with positive serum antibody were chosen for experiment through tail vein injection of human albumin, twice a week, 2.5 mg each in the first week, with a gradual increase of 0.5 mg once each to 4.5 mg eventually, and this dose was maintained for 2 mo. All animals were killed under anesthesia with ether. Blood sample was collected from femoral arteries and veins, centrifuged (3 000 r/min for 10 min), and the serum stored at 4 ℃ until analysis. After this, the liver was quickly washed in situ with ice-cold isotonic saline, removed, and divided into two portions, one was for histological examination, the other immediately frozen in liquid nitrogen.

In this experiment, the animals were divided into five groups randomly which included normal group, model group, TGP (60 and 120 mg/kg) treatment groups and colchicines (0.1 mg/kg) treatment group. The rats in TGP or colchicine groups received TGP or colchicine as above using an 18-gauge stainless steel animal feeding needle from the first day of tail vein injection of human albumin to the day prior to killing the rats. The rats in normal and model groups were fed the same volume of vehicle.

Histopathological examination

Liver tissue sections were fixed in 4 g/L formaldehyde saline and embedded in paraffin. HE staining was performed according to the standard procedure. Histological grade of hepatic fibrosis was determined by a semi-quantitative method based on the criteria of the Knodell index, scoring as the following[18,19], no fibrosis: normal liver and absence of fibrosis; I, perivenular and/or pericellular fibrosis: A few collagen fibrils extended from the central vein and portal tract; II, septal fibrosis: collagen fibrils extension was apparent but had not yet encompassed the whole lobule; III, incomplete cirrhosis: collagen fibrils extended into and encompassed the whole lobule; IV, complete cirrhosis: diffuse extension of collagen fibrils and pseudo-lobule formed. Two pathologists who had no knowledge of their sources examined the stained slides independently. Each sample was observed at 100×magnification and every specimen was analyzed containing a centrilobular vein. The degree of fibrosis was expressed as the mean of 10 different fields in each slide.

Analysis of liver function

The serum activity of aspartate aminotransferase (AST) and alanine aminotransferase (ALT) and the bilirubin concentration were estimated by commercially available kits (Nanjing Jiancheng Institute of Biotechnology, China). Protein concentration was measured according to Lowry *et al*, using serum bovine albumin as standard and then the ratio of albumin and globulin (A/G) was calculated.

Measurement of NO, LN and PC III in serum

Nitric oxide (NO) content in serum was measured by a microplate assay using Griess reagent, which produces a chromophore with the nitrite[20]. The serum levels of procollagen type III (PC III) and laminin(LN) were determined by radioimmunoassays (Shanghai Navy Medical Institute, China). The operations were performed according to the manufacturer's instructions.

Measurement of MDA, SOD and GSH-px level in liver homogenates

Livers were thawed, weighed and homogenized with Tris-HCl (5 mmol/L containing 2 mmol/L EDTA, pH 7.4). Homogenates were centrifuged (1 000 r/min, 10 min, 4 ℃) and the supernatant was used immediately for the assays of MDA,GSH-px and SOD. They were determined following the kit instructions. In brief, MDA in liver tissue was determined by the thiobarbituric acid method[21]. The assays for total SOD and GSH-px were based on their ability to inhibit the oxid-ation of oxyamine by the xanthine-xanthine oxidase system.

Measurement of hydroxyproline content in liver

Liver collagen concentration was determined by measuring hydroxyproline content in fresh liver samples using a modif-ication of the method of Jamall *et al*[22,23], after digestion with acid, as previously reported. Briefly, liver samples were homogenized and hydrolyzed in 6 N HCl at 110 ℃ for 18 h. After filtration of the hydrolysate through a 0.45-mm milli-pore filter, chloramine T was added to a final concent-ration of 2.5 mmol/L. The mixture was then treated with 410 mmol/L paradi-methyl-amino-benzaldehyde and incub-ated at 60 ℃ for 30 min. After cooling to room temper-ature, samples were read spectrophotometrically at 560 nm against a reagent blank containing no tissue and compared with a standard curve of known amount of hydroxyproline. The hydroxyproline content of the liver was expressed as mg/g wet weight.

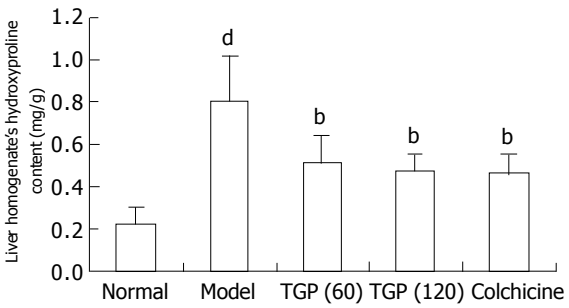

Figure 1 Effects of TGP on contents of hydroxyproline of human albumin-induced fibrotic liver in rats (n = 8, mean±SD) $^{b}P<0.01$ *vs* model group; $^{d}P<0.01$ *vs* normal control group.

Statistical analysis

mean±SD were calculated for quantitative data. Significant differences between means were evaluated by analyses of variance and in the case of significance, frequency data were compared using Ridit procedure. A difference was considered significant at $P<0.05$.

RESULTS

Effect of TGP on liver function of immunological hepatic fibrosis

In model group, the level of ALT and AST increased but had no significant difference compared with normal group, whereas the ratio of A/G decreased also with no significant difference. Transaminase activities in TGP or colchicine treated group tended to decrease, whereas the ratio of A/G had an increasing tendency and both had no significance compared with model group (Table 1).

Effect of TGP on hydroxyproline content in liver homogenates

Hepatic fibrosis was quantified by the measurement of hepatic hydroxyproline. It was found that the hydroxyproline content of the model group was significantly higher than that of the normal group. Treatment with TGP or colchicine effectively prevented the immunological hepatic fibrosis induced by human albumin by reducing the hydroxyproline content in liver homogenates (Figure 1).

Histological results

From Table 2, we can see the significant difference of pathologic grading between the normal and model groups. The pathologic grading was significantly decreased in TGP or colchicine treated group.

As shown in Figure 2, the structure of liver tissues was normal in control group (Figure 2A). In liver tissues from rats with immunological hepatic fibrosis, hyperplasia of the lattice fibers and collagenous fibers was observed in portal area and extended outwards. Hyperplasia surrounding the central vein observed was distributed along hepatic sinuses and associated with each other. The hepatic lobules were encysted and separated by collagen bundles. The normal structure of lobules was destroyed and pseudolobules formed. Infiltration of small numbers of inflammatory cells was found around the portal area and central vein (Figure 2B). TGP alleviated lobular necrosis and significantly lowered collagen content. The structure of liver tissues was almost normal (Figure 2C). In colchicine-treated group, hyperplasia of the lattice fibers and collagenous fibers was also observed in portal area, but they were alleviated compared with model group (Figure 2D).

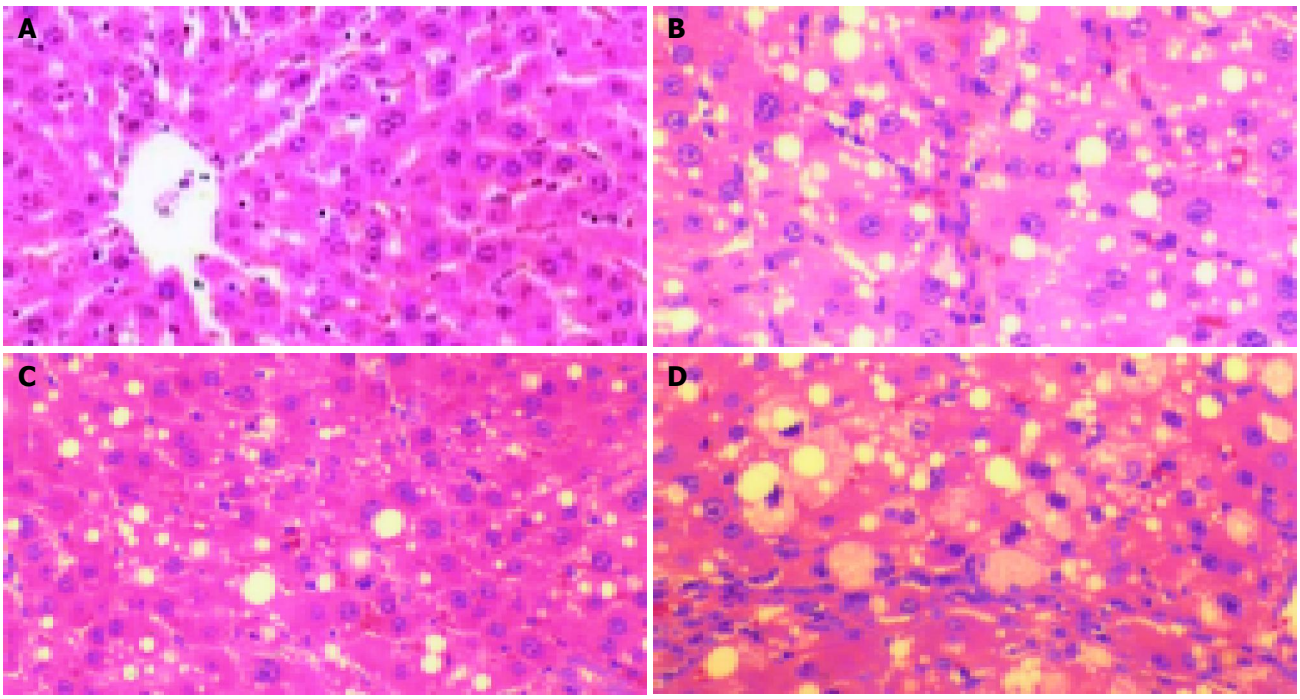

Figure 2 Histological results of tissues stained with HE under light microscope. A: Normal group; B: Model group; C: TGP-treated group; D: Colchicine-treated group.

Table 1 Effect of TGP on serum ALT, AST activities and A/G value in immunological hepatic fibrosis rat induced by human albumin. (n = 8, mean±SD)

Groups	Doses (mg/kg)	ALT (U/L)	AST (U/L)	A/G
Normal	–-	54.63±22.50	61.47±27.81	1.17±0.31
Model	–-	78.79±15.03	94.51±37.30	0.90±0.19
TGP	60	75.67±22.50	82.25±17.33	0.92±0.21
	120	70.61±24.62	75.43±26.94	0.96±0.17
Colchicine	0.1	77.71±27.64	78.99±22.24	0.93±0.18

Table 3 Effect of TGP on plasma LN and PC III level in immunological hepatic fibrosis rat induced by human albumin. (n = 8, mean±SD)

Groups	Doses (mg/kg)	LN (μg/L)	PC III (μg/L)
Normal	---	106.9±25.4	74.4±25.9
Model	---	228.0±76.2[d]	294.1±99.2[d]
TGP	60	142.1±39.8[a]	174.7±69.5
	120	127.1±26.8[b]	148.5±68.6[a]
Colchicine	0.1	112.6±27.7[b]	121.6±32.6[b]

[a]P<0.05, [b]P<0.01 *vs* model group; [d]P<0.01 *vs* normal control group.

Effect of TGP on serum LN and PC III

As expected, serum levels of LN and PC III, the surrogate markers of liver fibrogenesis, increased significantly in hepatic fibrotic rats in model group. However, in TGP-treated group they were lower compared with model group. These data confirmed the histological findings that TGP could inhibit hepatic fibrogenesis (Table 3).

Effect of TGP on MDA content and SOD, GSH-px activities in liver homogenates

Hepatic lipid peroxidation, measured as thiobarbituric acid reactive substance (MDA), was significantly increased in fibrotic rats while liver SOD and GSH-px activities decreased. TGP treatment significantly blocked the increase in MDA and was associated with a partial elevation in liver total antioxidant capacity including SOD and GSH-px (Table 4). In colchicine-treated group, only MDA content was lower than model group.

Effect of TGP on NO production in serum

As shown in Figure 3, when the rats were challenged with human albumin, the level of NO was elevated significantly. TGP obviously decreased the NO level while colchicine had no effect.

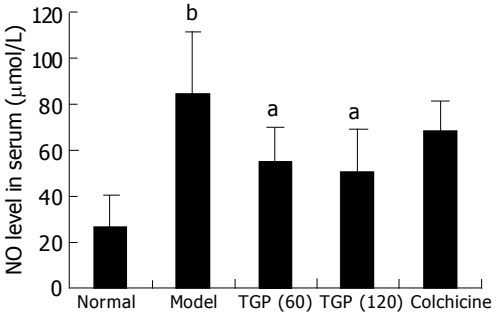

Figure 3 Effects of TGP on NO level in immunological hepatic fibrotic rats (n = 8, mean±SD), [a]P<0.05 *vs* model group; [b]P<0.01 *vs* normal control group.

DISCUSSION

Hepatic fibrosis is the common consequence of chronic liver injury of any etiology. Advanced hepatic fibrosis disrupts the normal liver architecture, causing hepatocellular dysfunction and portal hypertension. It is of great significance to search for effective ways to inhibit fibrogenesis and prevent the development of cirrhosis[24]. Unfortunately, no effective hepatic antifibrotic therapies are available. Colchicine has been commonly used for anti-fibrosis, but its side effect is severe and its clinical application is limited. Medicinally useful plants including traditional Chinese herbs are well known for their cheap prices and negligible side effects and have particular potential in the treatment of hepatic fibrosis[25,26]. In this study we firstly established the animal model of immunological hepatic fibrosis. The histological results showed that the normal structure of lobules was destroyed and pseudolobules formed, which were similar to the pathology of chemical hepatic fibrosis induced by long-term administration of carbon tetrachloride. Moreover, LN and PC III are known to be good serum markers of hepatic fibrogenesis, thus the increased hydroxyproline content in liver and serum LN and PC III also confirmed the hepatic fibrogenesis in rats. Unlike the severe hepatocyte necrosis and inflammation induced by CCl_4 toxicity, the ALT or AST released from hepatocytes did not increase and less immigration of inflammatory cells in liver indicated the mild inflammation in rat with immunological hepatic fibrosis induced by human albumin. Those results are in accordance with the findings of immunological hepatic fibrogenesis[17]. The present study demonstrated that administration of TGP was effective in

Table 2 Effect of TGP on the pathologic grading of immunological hepatic fibrosis rat induced by human albumin. (n = 10, mean±SD)

Group	Dose (mg/kg)	Pathologic grading of hepatic fibrosis					P
		0	I	II	III	IV	
Normal	–	10	0	0	0	0	–
Model	–	0	0	3	3	4	0.000[d]
TGP	60	0	2	5	2	1	0.043[a]
	120	0	4	4	2	0	0.006[b]
Colchicine	0.1	0	3	4	3	0	0.016[a]

[a]P<0.05, [b]P<0.01 *vs* model group; [d]P<0.01 *vs* normal control group.

Table 4 Effects of TGP on MDA levels, SOD and GSH-px activities liver homogenates in of immunological hepatic fibrotic rats (n = 10, mean±SD)

Groups	Doses (mg/kg)	MDA (nmol/mg pr)	SOD (U/mg pr)	GSH-Px (U/mg pr)
Normal	-	1.88±0.73	142.33±41.00	101.00±28.70
Model	-	4.34±1.12[d]	81.95±26.48[d]	50.64±15.28[d]
TGP	60	2.41±0.85[b]	116.95±32.18	73.70±16.60
	120	2.21±0.89[b]	136.53±36.15[a]	83.64±26.16[a]
Colchicine	0.1	3.02±0.68[a]	101.19±44.47	69.80±23.65

[a]P<0.05, [b]P<0.01 *vs* model group; [d]P<0.01 *vs* normal control group.

treating hepatic fibrosis in rats based on both histological examination and functional analysis. The results obtained provide a basis for further studies on the potentially protective effect of TGP on liver function in cirrhotic patients.

Increasing experimental evidence suggests that reactive oxygen species (ROS) such as H_2O_2, $O^{\cdot}_2^-$, and OH•, are implicated in the development and pathological progress of hepatic fibrosis[27-30]. Under normal conditions, low amounts of ROS are produced as by-products of the aerobic respiration. At high doses, ROS are noxious to the cells leading to impaired metabolic functions, growth inhibition, and ultimately cell death. Cells therefore employ several antioxidant enzyme systems to maintain low levels of ROS, which plays a key role in hepatic fibrosis[29]. Increased ROS and resulting oxidative stress are commonly detected in livers from patients with alcohol abuse, hepatitis C virus infection, iron overload, or chronic cholestasis, as well as in most types of experimental liver fibrogenesis[31]. Oxidative stress, in particular, lipid peroxidation, induces collagen synthesis. It also acts as a signaling mediator for transforming growth factor (TGF)-β, and plays a major role in hepatic fibrosis. Hepatic stellate cells produce and respond to TGF-β in an autocrine manner with increased collagen expression. Consequently, antioxidants, particularly those of plant origin, have emerged as potent antifibrotic agents. Previous and recent findings on the antifibrotic potential of plant-derived antioxidants could attenuate hepatic fibrosis in rodents and may exert beneficial effects in patients with chronic liver diseases.

Our previous study showed that TGP attenuated inflammation and ROS and TGP inhibited hydrogen peroxide (H_2O_2) were released from peritoneal macrophages in adjuvant arthritis (AA) rats[15]. It was also found that treatment of AA rats with TGP (50 mg/kg) ig (14-28 d) could counteract the elevated level of MDA and NO and the lowered activities of SOD and GSH-px. The hemolytic action of H_2O_2 is related to the induction of lipid perox-idation and glutathione depletion in human erythrocytes. TGP (0.5-2.5 mg/L) could significantly inhibit hemolysis, lipid peroxidation, and glutathione depletion induced by H_2O_2. *In vitro*, TGP could scavenge OH· and $O^{\cdot}_2^-$[9-15]. In the experimental model of human albumin-induced fibrosis, hepatic injury occurs with an increased generation of ROS that causes lipid peroxidation. In addition to being a product of lipid peroxidation, oxidative stress may result from deran-gement of antioxidant defenses including SOD and decr-eased GSH-px activities. Inverse correlations between antioxidant enzymes and pathology scores and/or lipid pero-xidation have been found in rats with CCl_4-induced cirrhosis, biliary obstruction, or alcoholic liver disease[30-32]. Beneficial effects and diminished hepatic fibrosis by TGP may be partially related to the preservation of antioxidant enzymes defenses and reduction of lipid peroxidation, but colchicine treatment only significantly inhibited malondialdehyde[33]. Changes in nitric oxide (NO) production may also play a role in the TGP-induced prevention of liver damage in cirrhotic rats. NO has been shown to react with superoxide generating the strong oxidant peroxynitrite, which can initiate lipid peroxidation or cause a direct inhibition of the mitoch-ondrial respiratory chain[34]. TGP was found to inhibit prod-uction of NO in this human albumin induced immun-ological hepatic fibrotic rats.

In conclusion, TGP could greatly retard the progression of experimental immunological hepatic fibrosis through inhibition of collagen synthesis and decreasing oxidative stress. Therefore, it is a potentially new antifibrotic drug for clinical application.

REFERENCES

1 **Dai WJ**, Jiang HC. Advances in gene therapy of liver cirrhosis: a review. *World J Gastroenterol* 2001; **7**: 1-8
2 **Friedman SL**. Seminars in medicine of the Beth Israel Hospital, Boston. The cellular basis of hepatic fibrosis. Mechanisms and treatment strategies. *N Engl J Med* 1993; **328**: 1828-1835
3 **Friedman SL**. Molecular regulation of hepatic fibrosis, an integrated cellular response to tissue injury. *J Biol Chem* 2000; **275**: 2247-2250
4 **Mann DA**, Smart DE. Transcriptional regulation of hepatic stellate cell activation. *Gut* 2002; **50**: 891-896
5 **Bonis PA**, Friedman SL, Kaplan MM. Is liver fibrosis reversible? *N Engl J Med* 2001; **344**: 452-454
6 **Albanis E**, Friedman SL. Hepatic fibrosis. Pathogenesis and principles of therapy. *Clin Liver Dis* 2001; **5**: 315-334, v-vi
7 **Yang XB**, Huang ZM, Wang JH. The drug therapy of liver fibrosis. *Shijie Huaren Xiaohua Zazhi* 2002; **10**: 956-957
8 **Dai LM**, Chen MZ, Xu SY. Protective effects of total glucocides of paeony on experimental hepatitis. *Zhongguo Yaolixue Tongbao* 1993; **9**: 449-453
9 **Wang B**, Yao YY, Zhou AW, Ge ZD, Chen MZ, Xu SY. Protective effect of total glucosides of paeony on joint damage in adjuvant arthritis rats. *Zhongguo Yaolixue Yu Dulixue Zazhi* 1996; **10**: 211-214
10 **Wang B**, Yao YY, Zhou AW, Chen MZ, Xu SY. Study on immunomodulatory effect of total glucosides of paeony and its relationship with nitric oxide in adjuvant arthritis rats. *Zhongguo Mianyixue Zazhi* 1996; **12**: 104-106
11 **Zhou LL**, Wei W, Shen YX, Xu SY. The effects of TGP on CJ-S131-induced systemic lupus erythematosus-like model in mice. *Zhongguo Yaolixue Tongbao* 2002; **18**: 175-177
12 **Xu SY**, Shen YX, Xu DJ, Wei W, Liang JS. Effects of total glucosides of paeony and moutan cortex on the function of pineal gland in inflammatory-immune regulation in rats. *Zhongguo Yaolixue Yu Dulixue Zazhi* 1994; **8**: 161-165
13 **Wei W**, Liang JS, Zhou AW, Chen MZ, Xu SY. Effects of total glucosides of paeony on interleukin 2 production. *Zhongguo Yaolixue Tongbao* 1989; **5**: 176-179
14 **Ge ZD**, Wei W, Shen YX, Wang B, Ding CH, Zhou AW, Zhang AP, Xu SY. Effects of paeoniflorin, total glucosides of paeony removed paeoniflorin on interleukin 2 production by splenic lymphocytes form adjuvant arthritic rats. *Anhui Yike Daxue Xuebao* 1996; **31**: 4-6
15 **Gao BB**, Dai LM, Xu SY. The scavenging activities of TGM and TGP on free radicals. *Suifang Yixueyuan Xuebao* 1996; **18**: 43-46
16 **Wang B**, Chen MZ, Xu SY. Regulatory mechanism of total glucosides of paeony on tumor necrosis factor production by peritoneal macrophages in rats. *Zhongguo Yaolixue Tongbao* 1997; **13**: 255-257
17 **Wang BE**, Wang ZF, Yin WY, Huang SF, Li JJ. Study on experimental immunity model of hepatic fibrosis. *Zhonghua Yixue Zazhi* 1998; **69**: 503-505
18 **Desmet VJ**, Gerber M, Hoofnagle JH, Manns M, Scheuer PJ. Classification of chronic hepatitis: diagnosis, grading and staging. *Hepatology* 1994; **19**: 1513-1520
19 **Chevallier M**, Guerret S, Chossegros P, Gerard F, Grimaud JA. A histological semiquantitative scoring system for evaluation of hepatic fibrosis in needle liver biopsy specimens: comparison with morphometric studies. *Hepatology* 1994; **20**: 349-355
20 **Kiechle FL**, Malinski T. Nitric oxide. Biochemistry, pathophysiology, and detection. *Am J Clin Pathol* 1993; **100**:

567-575
21 **Gavino VC**, Miller JS, Ikharebha SO, Milo GE, Cornwell DG. Effect of polyunsaturated fatty acids and antioxidants on lipid peroxidation in tissue cultures. *J Lipid Res* 1981; **22**: 763-769
22 **Jamall IS**, Finelli VN, Que Hee SS. A simple method to determine nanogram levels of 4-hydroxyproline in biological tissues. *Anal Biochem* 1981; **112**: 70–75
23 **Fort J**, Pilette C, Veal N, Oberti F, Gallois Y, Douay O, Rosenbaum J, Cales P. Effects of long-term administration of interferon alpha in two models of liver fibrosis in rats. *J Hepatol* 1998; **29**: 263–270
24 **Friedman SL**. Liver fibrosis-from bench to bedside. *J Hepatol* 2003; **38** Suppl 1: S38-S53
25 **Shimizu I**, Ma YR, Mizobuchi Y, Liu F, Miura T, Nakai Y, Yasuda M, Shiba M, Horie T, Amagaya S, Kawada N, Hori H, Ito S. Effects of Sho-saiko-to, a Japanese herbal medicine, on hepatic fibrosis in rats. *Hepatology* 1999; **29**: 149-160
26 **Li BS**, Wang J, Zhen YJ, Liu JX, Wei MX, Sun SQ, Wang SQ. Experimental study on serum fibrosis markers and liver tissue pathology and hepatic fibrosis in immuno-damaged rats. *Shijie Huaren Xiaohua Zazhi* 1999; **7**: 1031-1034
27 **Apte M**. Oxidative stress: does it initiate hepatic stellate cell activation or only 'perpetuate' the process? *J Gastroenterol Hepatol* 2002; **17**: 1045-1048
28 **Serviddio G**, Pereda J, Pallardo FV, Carretero J, Borras C, Cutrin J, Vendemiale G, Poli G, Vina J, Sastre J. Ursodeoxycholic acid protects against secondary biliary cirrhosis in rats by preventing mitochondrial oxidative stress. *Hepatology* 2004; **39**: 711-720
29 **Muriel P**, Moreno MG. Effects of silymarin and vitamins E and C on liver damage induced by prolonged biliary obstruction in the rat. *Basic Clin Pharmacol Toxicol* 2004; **94**: 99-104
30 **Lu G**, Shimizu I, Cui X, Itonaga M, Tamaki K, Fukuno H, Inoue H, Honda H, Ito S. Antioxidant and antiapoptotic activities of idoxifene and estradiol in hepatic fibrosis in rats. *Life Sci* 2004; **74**: 897-907
31 **Pietrangelo A**. Iron-induced oxidant stress in alcoholic liver fibrogenesis. *Alcohol* 2003; **30**: 121-129
32 **Gebhardt R**. Oxidative stress, plant-derived antioxidants and liver fibrosis. *Planta Med* 2002; **68**: 289-296
33 **Das D**, Pemberton PW, Burrows PC, Gordon C, Smith A, McMahon RF, Warnes TW. Antioxidant properties of colchicine in acute carbon tetrachloride induced rat liver injury and its role in the resolution of established cirrhosis. *Biochim Biophys Acta* 2000; **1502**: 351-362
34 **Koruk M**, Aksoy H, Akcay F, Onuk MD. Antioxidant capacity and nitric oxide in patients with hepatic cirrhosis. *Ann Clin Lab Sci* 2002; **32**: 252-256

Science Editor Zhu LH and Li WZ **Language Editor** Elsevier HK

PO Box 2345, Beijing 100023, China
www.wjgnet.com
wjg@wjgnet.com

ELSEVIER

World J Gastroenterol 2005;11(14):2130-2135
World Journal of Gastroenterology ISSN 1007-9327

• *BASIC RESEARCH* •

Effects of STI571 and p27 gene clone on proliferation and apoptosis of K562 cells

Wei Wang, Li-Bo Yao, Xin-Ping Liu, Qi Feng, Zhen-Chuan Shang, Yun-Xin Cao, Bing-Zhong Sun

Wei Wang, Qi Feng, Zhen-Chuan Shang, Bing-Zhong Sun, Department of Hematology, Xijing Hospital, The Fourth Military Medical University, Xi'an 710032, Shaanxi Province, China
Li-Bo Yao, Xin-Ping Liu, Department of Biochemistry and Molecular Biology, The Fourth Military Medical University, Xi'an 710032, Shaanxi Province, China
Yun-Xin Cao, Department of Immunology, The Fourth Military Medical University, Xi'an 710032, Shaanxi Province, China
Supported by the National Natural Science Foundation of China, No. 39770336
Correspondence to: Bing-Zhong Sun, Department of Hematology, Xijing Hospital, The Fourth Military Medical University, Xi'an 710032, Shaanxi Province, China. hematol@fmmu.edu.cn
Telephone: +86-29-83375615
Received: 2004-02-27 Accepted: 2004-04-20

Abstract

AIM: To investigate the combined effect of STI571 and p27 gene clone on the regulation of proliferation, cell cycle and apoptosis of K562 cell line.

METHODS: p27 gene was obtained by RT-PCR, and its sequence was approved to be correct. Then p27-pcDNA3.1 vector was constructed and transfected into K562 cell line. p27-pcDNA3.1-K562 cell clone was screened by G418 after transfection, p27 protein was identified by Western blot. MTT was used to detect the survival rate of the cell. Flow cytometry was used to detect cell cycle and apoptosis index.

RESULTS: The expression of p27 protein could be detected by Western blot in p27-pcDNA3.1-K562 cells. A strong inhibition of cell proliferation was observed in p27-pcDNA3.1 -K562 cells as compared with that of the control (pcDNA3.1 -K562 cells). The cells at G0/G1 phase were significantly increased, and cells at S phase were greatly declined. The apoptosis index was increased greatly after p27-pcDNA3.1-K562 cells were treated with STI571, and survival rate of the cell was markedly declined (0.35-0.58, $P<0.05$-0.048 *vs* STI571-K562 cell, 0.35-0.72, $P<0.01$-0.001 *vs* p27-K562 cell).

CONCLUSION: p27 and STI571 have a synergistic action on inhibition of proliferation and induction of apoptosis on K562 cells.

Key words: STI571; p27; Gene clone

Wang W, Yao LB, Liu XP, Feng Q, Shang ZC, Cao YX, Sun BZ. Effects of STI571 and p27 gene clone on proliferation and apoptosis of K562 cells. *World J Gastroenterol* 2005; 11 (14): 2130-2135
http://www.wjgnet.com/1007-9327/11/2130.asp

INTRODUCTION

STI571, a tyrosine kinase inhibitor used in clinic, can inhibit the tyrosine kinase of P210 protein encoded by BCR-ABL (Breakpoint cluster region and Abelson leukemia virus oncogene) fusion gene with a high selectivity[1,2]. Only the tyrosine kinase of platelet-derived growth factor[3,4] is inhibited at a similarly low concentration. This activity is believed essential for malignant transformation[5]. So it has an optimal therapeutic action on K562 cell line and sets up an epoch era in molecular targeted therapy. But multidrug resistance, recurrence and poor curative effect to acute phase cells were its major problems[6-8]. So combined therapy should be a new direction for future therapeutic development. p27 is an important member of the cyclin-dependent kinase inhibitor family and has been reported as a tumor suppressor gene[9,10], and its deletion, mutation or down-regulation play an important role in tumorigenesis[11,12]. So combined treatment of p27 and STI571 may exert an obvious therapeutic effect on K562 cells.

MATERIALS AND METHODS

Materials

STI571 was kindly provided by Novartis Company (Basel, Switzerland). A 1.0 mmol/L stock solution of STI571 in distilled water was prepared, filtrated and sterilized. pcDNA3.1 eukaryote expression plasmid was purchased from Invitrogen Company. *E.coli* JM109 cell strain was kindly provided by Biochemistry and Molecular Biology Laboratory of The Fourth Military Medical University (Xi'an, China). Digestion enzymes *Eco*RI and *Hind*III, Taq DNA, reverse transcriptase, and T4 ligase were purchased from Santa Cruz or Sangon Company. TRIzol RNA reagent and DNA purifying reagent were from Invitrogen Company. Mouse monoclonal antibody against p27 and goat anti-mouse antibody were purchased from Santa Cruz Company.

Cell culture

K562 cells (containing BCR-ABL fusion gene, expressing P210 protein[13]) were grown in RPMI1640 medium supplemented with 10 mL/L fetal calf serum, penicillin, streptomycin, and L-glutamine, at 37 ℃ in an incubator containing 50 mL/L CO_2.

Primer sequences to amplify p27 gene

Upstream primer (5'GTAAGCTTATGTCAAACGT-GCGAGTGTCTA3') and downstream primer (5'TGGAA-TTCTTACGTTTGACGTCTTCTGAGG3') were used to amplify p27 gene. The sequences of upstream and downstream primers contained restriction sites of *Hind*III and *Eco*RI (restriction endonuclease) respectively in order to digest PCR products or vectors. The PCR product of these primers was about 600 bp in length.

RT-PCR

Total RNA was extracted from peripheral blood mononuclear cells (PMC) with TRIzol reagent following the manufacturer's instructions. Then 2.0 μg of total RNA was reverse transcribed with M-Mulv reverse transcriptase and oligo(dT). PCR reaction mixture (25 μL) containing 0.2 μg of cDNA, 0.5 μL of 10 mmol/L dNTP, 10 pmoL of each primer and 1 U Taq polymerase was subjected to 30 amplification cycles, each cycle consisting of denaturation at 94 ℃ for 45 s, annealing at 55 ℃ for 40 s, and extension at 72 ℃ for 1 min. An additional extension at 72 ℃ for 30 min was performed. PCR products were electrophoresed on 1% agarose gels and stained with ethidium bromide (EB). Photographs of EB-stained gels were taken.

Southern blot analysis

Total RNA was extracted from PMC and K562 cells respectively, and reverse transcribed into cDNA, and quantified by absorbance at 260 nm, then 20 μg of cDNA was electrophoresed on 0.8% alkalescence agarose gels. DNA was transferred to Hybond-N membranes and subjected to Southern blotting. DNA was fixed in Hybond-N membranes by ultraviolet irradiation. Hybridized membranes were wetted with 6× SSC, and then pre-hybridized for 3 h at 68 ℃. Then denaturalized probes were joined and hybridized with DNA overnight at 68 ℃. Hybridized membranes were washed with 2× SSC/0.1% SDS and 0.2× SSC/0.1% SDS twice and reserved at -70 ℃ for 5-7 d. p27 was detected by hybridization with its respective full-length ^{32}P-labeled PMC cDNA probes and imaged by autoradiography[14].

Purification of PCR products from gel

After PCR products were separated by electrophoresis, positive agarose gels were sliced, and then PCR products were purified and call backed using a DNA purifying kit, and deposited by ethanol.

T vector ligation and DNA sequence test

Reaction mixture contained 5 μL of purified DNA, 1 μL of T vector, and 4 μL of rapid ligation fluid. After being incubated at 16 ℃ for 4 h, the mixture was transduced into JM109 cell strain. The transduced cells were detected by staining with 5-bromo-4 chloro-3 indolyl β-D-galactopyranosides (X-gal). A white positive clone was chosen and sent to Sagon Company to test its sequence.

Construction of K562-p27-pcDNA3.1 cell line

pcDNA3.1 and T-p27 vectors were digested with *Hind*III and *Eco*RI. Then pcDNA plasmid and p27 were ligated with T4 ligase. After pcDNA-p27 vector was transduced into JM109 strain, the positive clones were used to pick-up plasmids, which were transfected into K562 cells with lipofectine as previously described. After 48 h, the cells were cultured in RPMI1640 medium containing G418 (500 mL/L) for 28 d to select the stably transfected positive clones[15] (pcDNA3.1-p27-K562 cell clone).

Western blot analysis

Western blot extracts were prepared by lysing K562 cells with lysis buffer[16] (20 mmol/L HEPES, pH 7.9, 150 mmol/L NaCl, 1.0 mmol/L $MgCl_2$, 5 mmol/L EDTA, pH 8, 0.1% nonidet P-40, 0.5% sodium deoxycholate, 0.1% SDS, 50 mmol/L NaF, 5 mmol/L sodium orthovanadate) on ice for 20 min. Fifty micrograms of lysate was separated by SDS-polyacrylamide gel electrophoresis, transferred onto nitrocellulose membranes, and specific proteins were recognized by mouse moloclonal antibody against p27 and cyclin-E. Membranes were incubated for 1 h at room temperature with mouse moloclonal antibody against p27 and cyclin-E. After three washes in TBS-T (Tris 10 mmol/L, NaCl 50 mmol/L, Tween 0.005%, pH 8.0), membranes were incubated for 1 h at room temperature with goat anti-mouse IgG horseradish peroxidase-linked at 1/3 000 final dilution. After three washes in TBS-T, membranes were revealed with the enhanced chemiluminescent detection system[17] (Pierce Biotech).

MTT assay

Cells (5×10^4/L) were put in each well of a 96-well plate, and divided into p27 group, STI571 group, p27 and STI571 group. Each group had six different concentrations of cells, and each concentration of cells was put in three wells to calculate the average value. The cells were cultured for 5 d and the cells were calculated everyday to determine the growth inhibition and survival rate of the cells.

Flow cytometry analysis

After p27-pcDNA vector was transfected into K562 cells, the cells were treated with STI571. After 48 h, the cells were collected by centrifugation, washed twice with phosphate-buffered saline, and permeabilized in 70 mL/L ethanol (-20 ℃). The permeabilized cells were incubated with 50 μg/mL of propidium iodide, 0.1 μg/mL of Rnase A, 0.1% Nonidet P-40, and 50 μg/mL trisodium citrate for 30 min prior to analysis using a Becton Dickinson FACSort analyzer.

Statistical analysis

One-way ANOVA was used to compare the data between groups, and Dunnett's *t* test was used to compare the data within each group by using SPSS11.0 statistic software.

RESULTS

p27 gene amplified by RT-PCR

The complete cDNA sequence of p27 gene was amplified from PMC by RT-PCR to construct p27-pcDNA3.1 recombinant vector, and RT-PCR products were electrophoresed in 1% agarose gels and stained with EB. The amplified DNA fragments (about 600 bp) were completely

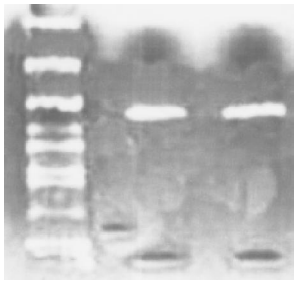

Figure 1 p27 gene amplified from PMC and K562 by RT-PCR. Lane1: DGL2000 DNA marker, Lane2: P27 gene amplified from peripheral-blood mononuclear cells (about 750 bp), and lane3: P27 gene amplified from K562 cells.

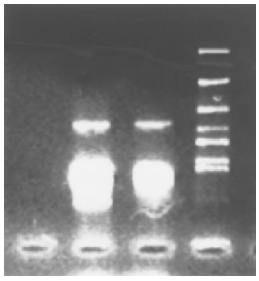

Figure 3 Digestion pattern of P27-pcDNA3.1 vector with *EcoRI* and *HindIII*. Lane1: Digestion pattern of P21-K562-pcDNA3.1 vector (about 600 bp); Lane2: Digestion pattern of P21-PMC-pcDNA3.1 vector (about 600 bp); and lane3: DGL2000 DNA marker.

consistent with p27 gene full-length cDNA. Meanwhile a DNA fragment (about 600 bp) was amplified from K562 cells using the same primers (Figure 1).

Detection of p27 gene by Southern blot

p27 gene deletion in K562 cells was proved by Southern blot (Figure 2).

Plasmid reconstruction

The complete cDNA sequence of p27 gene amplified from PMC and pcDNA3.1 vector was digested with *Hind*III and *Eco*RI, and ligated with T4 ligase, and the recombinant p27-pcDNA3.1 vector was constructed. The recombinant vector was digested with *Hind*III and *Eco*RI. The size of digested DNA fragments was completely consistent with p27 gene full-length cDNA (Figure 3).

p27 gene sequence analysis

p27 gene amplified from PMC was ligated with PUC18-T vector to test p27 gene sequence, and the result proved that its sequence was correct with the designed p27 gene sequence (Figure 4A). Meanwhile the tested sequence of DNA fragments amplified from K562 cells was absolutely incorrect with p27 gene (Figure 4B). That means it was a non-specific amplification. Thus p27 gene deletion in K562 cells was proved.

Establishment of K562-p27-pcDNA3.1 cell line expressing p27 protein

After p27-pcDNA3.1 recombinant vector was stably transfected into K562 cells by using lipofectine for 2 wk, a cell line stably expressing p27 protein was established. In this cell line, p27 protein expression was proved by Western blot, whereas cyclin-E protein expression was decreased. Protein quantity analysis was performed by Lowry's method, and β-actin was used as an internal control (Figure 5).

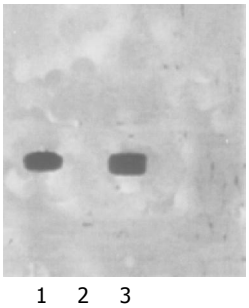

Figure 2 p27 gene deletion in K562 cells proved by Southern blot. Lane1: Positive (P27 gene probe hybridized with PMC), lane2: Negative (P27 gene probe hybridized with K562 cells), and lane3: Positive (P27 gene probe hybridized with stomach tissue).

Cell cycle and apoptosis by flow cytometry

The number of S phase cells was increased in the control K562 cells. The percentage of cells was 30.2% in G1 phase, 57.4% in S phase and 12.3% in G2/M phase. After p27-pcDNA3.1 recombinant vector was transfected into K562 cells, the percentage of S phase cells was significantly decreased, while the percentage of G1 phase cells was increased apparently, indicating that p27 gene could inhibit K562 cell proliferation and decrease S phase cells by cell cycle arresting in G1 phase. When K562 cells were treated with STI571 for 48 h (>0.5 μmol/L), apoptosis apex could be observed in flow cytometry map, and it increased with the increase of STI571 concentration. STI571 could induce apoptosis in a dose-dependent manner. In control K562 cells, apoptosis apex was not observed when the concentration of STI571 was 0.25 μmol/L. But in K562-p27-pcDNA3.1 cells, apoptosis apex (32.4%) was observed when treated with the same concentration of STI571 (0.25 μmol/L) for 48 h, and the percentage of S phase cells was decreased apparently, suggesting the synergistic action of p27 and STI571 on induction of apoptosis and inhibition of proliferation of K562 cells (Figure 6).

Cell growth analysis

MTT assay showed that K562 cells proliferated rapidly and the population doubling time was about 18-24 h. Little change was found in growth rate when control pcDNA3.1 vector was transfected into K562 cells, but the growth rate of K562 cells transfected with p27-pcDNA3.1 was apparently slower than that of the control K562 cells, and the population doubling time was about 48-60 h, indicating that p27 protein could inhibit K562 cell proliferation. STI571 could also apparently inhibit K562 cell proliferation, and the cell survival rate declined in a time-dependent manner. When p27-pcDNA3.1-K562 cells were treated with STI571, the cell survival rate was markedly decreased compared to K562 cells treated with STI571 or p27-pcDNA3.1-K562 cells, suggesting that p27 and STI571 had a synergistic action on inhibiting K562 cell proliferation (Figure 7).

Hind III

A attcgatgta gttgcctgca ggtcgactct agaggatccc ctgt**AAGCTT**atgtc aaacgtgcga
gtgtctaacg ggagccctag cctggagcgg atggacgcca ggcaggcgga gcaccccaag
ccctcggcct gcaggaacct cttcggcccg gtggaccacg aagagttaac ccgggacttg
gagaagcact gcagagacat ggaagaggcg agccagcgca agtggaattt cgattttcag
aatcacaaac ccctagaggg caagtacgag tggcaagagg tggagaaggg cagcttgccc
gagttctact acagaccccc gcggcccccc aaaggtgcct gcaaggtgcc ggcgcaggag
agccaggatg tcagcgggag ccgcccggcg gcgcctttaa ttggggctcc ggctaactct
gaggacacgc atttggtgga cccaaagact gatccgtcgg acagccagac ggggttagcg
gagcaatgcg caggaataag gaagcgacct gcaaccgacg attcttctac tcaaaacaaa
agagccaaca gaacagaaga aaatgtttca gacggttccc caaatgccgg ttctgtggag
cagacgccca agaagcctgg cctcagaaga cgtcaaacgt aa**GAATTC**ac cagggta
aaagaagcgattct

EcoR I

EcoR I

B tgccaagctt gcatgcctgc aggtcgactc tagaggatcc ccttg**GAATTC**ttaactact
agacaatct tgaaaacgga agcaatcact tgcaatcttc cacacagtat tgttgggagt
ggactgagca gtcagcagga agttctggtt gaagaaatgt tgtttgtttc catcaaactt
cacagttcca ctggtcacaa caagaactgt agtttgggac tgagttgctt gcgcatgaac
tggttggcaa tctaacatat tgacctggaa ctcactagaa ggcaatgtgt caaaaaatt
atttagggca tccagccctg aaacagcatt tccattccat attaaggtgg ccttgtccag
atacagcctg gttagt gccc gtcttctttt atccattgtc tcatagtaaa tattgacaaa ctcctcagca
gctctacatg cctgatctac

Hind III

ataagtttta aaatccagag acgtggccat **AAGCTT**acag ggtaccgagc tcgaattcgt
aatcatggtc atagctgttt cctgtgtgaa attgttatcc gctcacaatt ccacacaaca
tacgagccgg aagcataaag tgtaaagcct ggggtgccta atgagtgagc taactcacat
taattgcgtt gcgctcactg gccgcttcca gtcgggaaaa ctgtcgtgcc agctgcatta atgaatc

Figure 4 Gene sequences in p27-PMC-pcDNA3.1 vector (A) p27-K562-pcDNA3.1 vector (B).

DISCUSSION

p27 gene is a member of CDK-interacting protein/kinase inhibitor protein family, and could combine with cyclin-E/CDK2 or cyclin-D/CDK4 to inhibit its kinase activity[18,19]. We constituted a p27-pcDNA3.1 vector and transfected it into K562 cell line and found that the growth rate of p27-pcDNA3.1-K562 cells was apparently lower than that of control K562 cells. Cell cycle analysis indicated that transfected cells were arrested in G0/G1 phase, Western blot analysis showed that cyclin-E protein expression was decreased, suggesting that p27 gene mainly inhibits cyclin-E/CDK2 activity leading to the arrest of K562 cells in G0/G1 phase. Cells could not get across the G1/S checkpoint[20] to enter S phase. As replication of DNA is in S phase, so the decrease

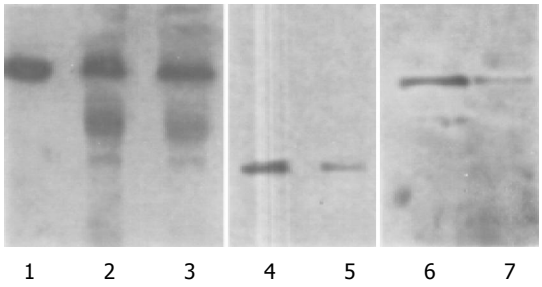

Figure 5 Expressions of p27 and cyclin-E protein observed by Western blot 1: positive control of β-actin; 2: control of β-actin in K562 cells; 3: β-actin in p27-pcDNA3.1-K562 cells; 4: Positive control of p27; 5: positive expression of p27 in P27-pcDNA3.1-K562 cells; 6: positive expression of cyclin-E in K562 cells; 7: decrease of cyclin-E in P27-pcDNA3.1-K562 cells.

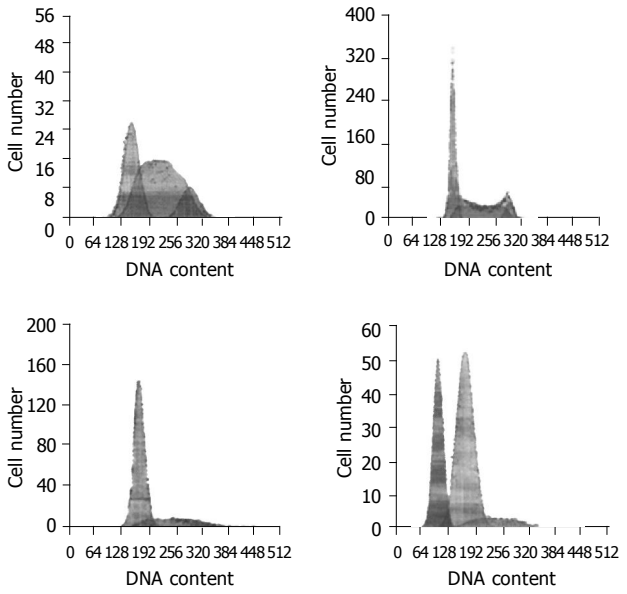

Figure 6 Cell cycle and apoptosis of K562 affected by STI571 and P27 1: Cell cycle of control K562 cells; 2: Cell cycle of K562 cells affected by P27; 3: Cell cycle of K562 cell affected by 0.25 μmol/L STI571; and 4: Cell cycle and apoptosis of K562 cells affected by STI571 and P27.

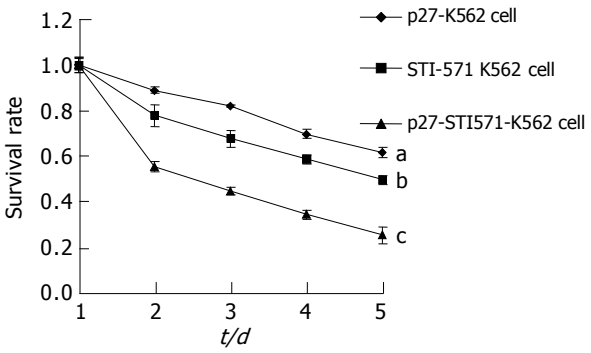

Figure 7 Cell survival rate of K562 cell affected by p27 and STI571. The presented values were mean±SE, $n = 3$; $^aP<0.05$ (between groups), $^bP<0.01$ *vs* p27-k562 cell, and $^cP<0.05$ *vs* STI571-k562 cell.

of DNA replication inhibited cell growth. p27 and STI571 showed a synergistic action on inhibition of cell proliferation, and the mechanism might be associated with the cell cycle regulating function of STI571. Deininger[21] and Jonuleit[22] discovered that STI571 could down-regulate cyclin-E and cyclin-D and make over-expression of S phase cells return to normal level.

Our experiments demonstrated that p27 combined with STI571 had a synergistic action on induction of apoptosis of K562 cells. There are different opinions on the apoptosis induction by p27. Eymin[23] found that p27 could inhibit apoptosis induced by drugs because leukemia cells could induce hydrolysis of p27 and the hydrolytic products, p23 and p15 had an inhibition function on apoptosis. Barata[24] found that over-expression of p27 could inhibit Bcl-2 expression induced by IL-7, thereby inducing apoptosis of leukemia cells. Patel[25] found that adenovirus-mediated p27 transfection could induce apoptosis of many cancer cell lines, and the results of Schreiber[26] and Craig[27] were similar. So whether p27 promotes or inhibits apoptosis depends on its hydrolytic state, cell types and states. The maladjusted relation of BCR-ABL and p27 plays an important role in the progress of K562 cells. Parada[28] found that BCR-ABL could downregulate p27 protein expression and mRNA level, mainly by inhibiting the phosphatidylinostiol-3-kinase (PI_3K) signal pathway and by decreasing the degradation of p27. STI571 could inhibit the expression of some cyclins such as cyclin-D, cyclin-A, cyclin-E, which could relieve the inhibition function of cyclins to p27[29]. So p27 gene transfected into K562 cells not only could reconstruct the regulation of cell cycle pathways, but also strengthen the apoptosis-inducing function of p27 after combining with STI571, suggesting that p27 and STI571 has a synergistic action on apoptosis induction.

p27 gene clone combined with STI571 can not only inhibit cell proliferation and induce apoptosis, but also induce cell differentiation as shown by Fang[30] and Caslini[31] independently. STI571 and p27 gene used in combination may have an important therapeutic significance.

REFERENCES

1 **Buchdunger E,** Zimmermann J, Mett H, Meyer T, Muller M, Druker BJ, Lydon NB. Inhibition of the Abl protein-tyrosine kinase *in vitro* and *in vivo* by a 2-phenylaminopyrimidine derivative. *Cancer Res* 1996; **56**: 100-104

2 **Druker BJ,** Tamura S, Buchdunger E, Ohno S, Segal GM, Fanning S, Zimmermann J, Lydon NB. Effects of a selective inhibitor of the Abl tyrosine kinase on the growth of Bcr-Abl positive cells. *Nat Med* 1996; **2**: 561-566

3 **Carroll M,** Ohno-Jones S, Tamura S, Buchdunger E, Zimmermann J, Lydon NB, Gilliland DG, Druker BJ. CGP 57148, a tyrosine kinase inhibitor, inhibits the growth of cells expressing BCR-ABL, TEL-ABL, and TEL-PDGFR fusion proteins. *Blood* 1997; **90**: 4947-4952

4 **McGary EC,** Onn A, Mills L, Heimberger A, Eton O, Thomas GW, Shtivelband M, Bar-Eli M. Imatinib mesylate inhibits platelet-derived growth factor receptor phosphorylation of melanoma cells but does not affect tumorigenicity *in vivo*. *J Invest Dermatol* 2004; **122**: 400-405

5 **Lugo TG,** Pendergast AM, Muller AJ, Witte ON. Tyrosine kinase activity and transformation potency of bcr-abl oncogene products. *Science* 1990; **247**: 1079-1082

6 **le Coutre P,** Tassi E, Varella-Garcia M, Barni R, Mologni L, Cabrita G, Marchesi E, Supino R, Gambacorti-Passerini C. Induction of resistance to the Abelson inhibitor STI571 in human leukemic cells through gene amplification. *Blood* 2000; **95**: 1758-1766

7 **Hofmann WK,** Komor M, Hoelzer D, Ottmann OG. Mechanisms of resistance to STI571 (Imatinib) in Philadelphia-chromosome positive acute lymphoblastic leukemia. *Leuk Lymphoma* 2004; **45**: 655-660

8 **Druker BJ,** Sawyers CL, Kantarjian H, Resta DJ, Reese SF, Ford JM, Capdeville R, Talpaz M. Activity of a specific inhibitor of the BCR-ABL tyrosine kinase in the blast crisis of chronic myeloid leukemia and acute lymphoblastic leukemia with the Philadelphia chromosome. *N Engl J Med* 2001; **344**: 1038-1042

9 **Fero ML,** Randel E, Gurley KE, Roberts JM, Kemp CJ. The murine gene p27Kip1 is haplo-insufficient for tumour suppression. *Nature* 1998; **396**: 177-180

10 **Koh TY,** Park SW, Park KH, Lee SG, Seol JG, Lee DW, Lee CT, Heo DS, Kim KH, Sung MW. Inhibitory effect of p27KIP1 gene transfer on head and neck squamous cell carcinoma cell lines. *Head Neck* 2003; **25**: 44-49

11 **Piva R,** Cancelli I, Cavalla P, Bortolotto S, Dominguez J, Draetta GF, Schiffer D. Proteasome-dependent degradation of p27/kip1 in gliomas. *J Neuropathol Exp Neurol* 1999; **58**: 691-696

12 **Hoos A,** Nissan A, Stojadinovic A, Shia J, Hedvat CV, Leung DH, Paty PB, Klimstra D, Cordon-Cardo C, Wong WD. Tissue microarray molecular profiling of early, node-negative adenocarcinoma of the rectum: a comprehensive analysis. *Clin Cancer Res* 2002; **8**: 3841-3849

13 **Kawano T,** Horiguchi-Yamada J, Saito S, Iwase S, Furukawa Y, Kano Y, Yamada H. Ectopic cyclin D1 expression blocks STI571-induced erythroid differentiation of K562 cells. *Leuk Res* 2004; **28**: 623-629

14 **Hehlmann R,** Hochhaus A, Berger U, Reiter A. Current trends in the management of chronic myelogenous leukemia. *Ann Hematol* 2000; **79**: 345-354

15 **Amarante-Mendes GP,** Jascur T, Nishioka WK, Mustelin T, Green DR. Bcr-Abl-mediated resistance to apoptosis is independent of PI 3-kinase activity. *Cell Death Differ* 1997; **4**: 548-554

16 **Amarante-Mendes GP,** Naekyung Kim C, Liu L, Huang Y, Perkins CL, Green DR, Bhalla K. Bcr-Abl exerts its antiapoptotic effect against diverse apoptotic stimuli through blockage of mitochondrial release of cytochrome C and activation of caspase-3. *Blood* 1998; **91**: 1700-1705

17 **Li J,** Kleeff J, Guo J, Fischer L, Giese N, Buchler MW, Friess H. Effects of STI571 (gleevec) on pancreatic cancer cell growth. *Mol Cancer* 2003; **2**: 32

18 **Polyak K,** Lee MH, Erdjument-Bromage H, Koff A, Roberts JM, Tempst P, Massague J. Cloning of p27Kip1, a cyclin-dependent kinase inhibitor and a potential mediator of extracellular antimitogenic signals. *Cell* 1994; **78**: 59-66

19 **Russo AA,** Jeffrey PD, Patten AK, Massague J, Pavletich NP.

Crystal structure of the p27Kip1 cyclin-dependent-kinase inhibitor bound to the cyclin A-Cdk2 complex. *Nature* 1996; **382**: 325-331

20 **Pommier Y,** Kohn KW. Cell cycle and checkpoints in oncology: new therapeutic targets. *Med Sci (Paris)* 2003; **19**: 173-186

21 **Deininger MW,** Vieira S, Mendiola R, Schultheis B, Goldman JM, Melo JV. BCR-ABL tyrosine kinase activity regulates the expression of multiple genes implicated in the pathogenesis of chronic myeloid leukemia. *Cancer Res* 2000; **60**: 2049-2055

22 **Jonuleit T,** Peschel C, Schwab R, van der Kuip H, Buchdunger E, Fischer T, Huber C, Aulitzky WE. Bcr-Abl kinase promotes cell cycle entry of primary myeloid CML cells in the absence of growth factors. *Br J Haematol* 1998; **100**: 295-303

23 **Eymin B,** Sordet O, Droin N, Munsch B, Haugg M, Van de Craen M, Vandenabeele P, Solary E. Caspase-induced proteolysis of the cyclin-dependent kinase inhibitor p27Kip1 mediates its anti-apoptotic activity. *Oncogene* 1999; **18**: 4839-4847

24 **Barata JT,** Cardoso AA, Nadler LM, Boussiotis VA. Interleukin-7 promotes survival and cell cycle progression of T-cell acute lymphoblastic leukemia cells by down-regulating the cyclin-dependent kinase inhibitor p27 (kip1). *Blood* 2001; **98**: 1524-1531

25 **Patel SD,** Tran AC, Ge Y, Moskalenko M, Tsui L, Banik G, Tom W, Scott M, Chen L, Van Roey M, Rivkin M, Mendez M, Gyuris J, McArthur JG. The p53-independent tumoricidal activity of an adenoviral vector encoding a p27-p16 fusion tumor suppressor gene. *Mol Ther* 2000; **2**: 161-169

26 **Schreiber M,** Muller WJ, Singh G, Graham FL. Comparison of the effectiveness of adenovirus vectors expressing cyclin kinase inhibitors p16INK4A, p18INK4C, p19INK4D, p21 (WAF1/CIP1) and p27KIP1 in inducing cell cycle arrest, apoptosis and inhibition of tumorigenicity. *Oncogene* 1999; **18**: 1663-1676

27 **Craig C,** Wersto R, Kim M, Ohri E, Li Z, Katayose D, Lee SJ, Trepel J, Cowan K, Seth P. A recombinant adenovirus expressing p27Kip1 induces cell cycle arrest and loss of cyclin-Cdk activity in human breast cancer cells. *Oncogene* 1997; **14**: 2283-2289

28 **Parada Y,** Banerji L, Glassford J, Lea NC, Collado M, Rivas C, Lewis JL, Gordon MY, Thomas NS, Lam EW. BCR-ABL and interleukin 3 promote haematopoietic cell proliferation and survival through modulation of cyclin D2 and p27Kip1 expression. *J Biol Chem* 2001; **276**: 23572-23580

29 **Jonuleit T,** van der Kuip H, Miething C, Michels H, Hallek M, Duyster J, Aulitzky WE. Bcr-Abl kinase down-regulates cyclin-dependent kinase inhibitor p27 in human and murine cell lines. *Blood* 2000; **96**: 1933-1939

30 **Fang G,** Kim CN, Perkins CL, Ramadevi N, Winton E, Wittmann S, Bhalla KN. CGP57148B (STI-571) induces differentiation and apoptosis and sensitizes Bcr-Abl-positive human leukemia cells to apoptosis due to antileukemic drugs. *Blood* 2000; **96**: 2246-2253

31 **Caslini C,** Shilatifard A, Yang L, Hess JL. The amino terminus of the mixed lineage leukemia protein (MLL) promotes cell cycle arrest and monocytic differentiation. *Proc Natl Acad Sci USA* 2000; **97**: 2797-2802

Science Editor Wang XL, Kumar M and Guo SY **Language Editor** Elsevier HK

PO Box 2345, Beijing 100023, China
www.wjgnet.com
wjg@wjgnet.com

ELSEVIER

World J Gastroenterol 2005;11(14):2136-2141
World Journal of Gastroenterology ISSN 1007-9327

• *BASIC RESEARCH* •

Hepatic preconditioning of doxorubicin in stop-flow chemotherapy: NF-κB/IκB-α pathway and expression of HSP72

Hui Lu, Zheng-Gang Zhu, Xue-Xin Yao, Ren Zhao, Chao Yan, Yi Zhang, Bing-Ya Liu, Hao-Ran Yin, Yan-Zhen Lin

Hui Lu, Chao Yan, Yi Zhang, Bing-Ya Liu, Shanghai Institute of Digestive Surgery, Rujin Hospital, Shanghai Second Medical University, Shanghai 200025, China
Zheng-Gang Zhu, Xue-Xin Yao, Ren Zhao, Hao-Ran Yin, Yan-Zhen Lin, Department of General Surgery, Rujin Hospital, Shanghai Second Medical University, Shanghai 200025, China
Supported by the Shanghai Bureau of Health, 99ZDII003
Correspondence to: Dr. Hui Lu, Shanghai Institute of Digestive Surgery, Rujin Hospital, Shanghai Second Medical University, No. 197, Ruijin Road II, Shanghai 200025, China. luhui75@yahoo.com.cn
Telephone: +86-21-64370045-611006
Received: 2004-03-15 Accepted: 2004-04-05

Abstract

AIM: To provide hepatic protection through administration of doxorubicin before stop-flow chemotherapy (SFC) and to investigate the expression of heat shock protein 72 (HSP72) and role of nuclear factor kappa B (NF-κB) in this effect.

METHODS: The hepatic preconditioning of doxorubicin was established in a porcine model by injection of doxorubicin (1 mg/kg) before SFC. The experimental animals were randomized into two groups: groups receiving doxorubicin (DOX) and normal saline (NS). Serial serum and tissue samples were taken from both groups to evaluate the protection of doxorubicin. Western blot and immunoprecipitation were applied to detect the expression of HSP72, NF-κB p65 protein, inhibitor κB-α (IκB-α) and phosphorylated IκB-α as well. The expression of tumor necrosis factor α (TNF-α) was estimated by semiquantitative RT-PCR. And the extent of the hepatic injury was estimated with the level of serum aminotransferases.

RESULTS: An abundance production of HSP72 in porcine liver was observed after 24 h of intravenous administration of doxorubicin, but without any change in the expression of NF-κB p65 subunit in cytoplasm. NF-κB p65 subunit accumulated in nuclei at the end of SFC and reached its highest level at 30 min after the restoration of the abdominal circulation and decreased gradually during the 6 h after SFC in NS group, while there was little change in DOX group. There was also a slight decrease of IκB-α at 30 min after the restoration of the abdominal circulation in NS group accompanying with the appearance of phosphorylated IκB-α. The expression of TNF-α was significantly higher in NS group than that in DOX group (average 1.40±0.17 *vs* 0.62±0.22, $P<0.01$) at serial time points after SFC. Serum ALT and AST levels of NS group were higher after 24 h than those of DOX group (93.2±7.8 IU/L *vs* 53.3±13.9 IU/L, 217.0±29.4 IU/L *vs* 155.0±15.6 IU/L for ALT and AST respectively, $P<0.05$) and after 48 h than those of DOX group (66.6±18.1 IU/L *vs* 43.3±16.7 IU/L, 174.4±21.3 IU/L *vs* 125.7±10.5 IU/L for ALT and AST respectively, $P<0.05$).

CONCLUSION: Doxorubicin renders the liver to be tolerant to the hepatic influence in SFC in a porcine model through the NF-κB/IκB-α pathway with the expression of HSP72.

Key words: SFC; NF-κB

Lu H, Zhu ZG, Yao XX, Zhao R, Yan C, Zhang Y, Liu BY, Yin HR, Lin YZ. Hepatic preconditioning of doxorubicin in stop-flow chemotherapy: NF-κB/IκB-α pathway and expression of HSP72. *World J Gastroenterol* 2005; 11(14): 2136-2141
http://www.wjgnet.com/1007-9327/11/2136.asp

INTRODUCTION

Although the surgical excision is currently the most ideal treatment for abdominal cancer, its application in the management of malignant disorders in the advanced stage is limited. The severe untoward effects, however, preclude the administration of high-dose chemotherapeutic drugs systematically. So it is rationale to perform regional chemotherapies to increase the local tumor cells' exposure to the chemotherapeutic agents and obviate the toxic effect on other organs and tissues. As one of the newly developed means of regional chemotherapies, the stop-flow chemotherapy (SFC) procedure blocks the blood supply of tumor bearing tissues with inflated balloons and provides higher local concentration of chemotherapeutic medicines than intra-arterial and intravenous drugs injection[1-4].

Taking the entire abdominal cavity as target territory, the clinical trial of SFC in the treatment of upper digestive tract cancer is rather optimistic; however, some modifications are indicated, especially the protection of some vital organs, such as liver, kidney and pancreas, which are subjected to hypoxia and chemotherapeutic agents during the process. The liver, which is highly sensitive to short period of hypoxia, may suffer from another injury upon re-oxygenation. It has been suggested that the ischemic/reperfusion injury is initialized by over production of active oxygen species upon re-exposure to the oxygen. The oxygen stress will impair the balances among members of NF-κB family and increase the expression of various inflammatory factors, such as TNF-α and IL-1β[5-10], which propagate the inflammatory

response and cause sequestration of polymorphonuclear neutrophils in liver. And there are abundant evidences supporting that ischemia/reperfusion injury can be alleviated by interfering the activation of NF-κB in various organs including liver[11-13].

Thus we propose that the hepatic influence caused by SFC should be related to the activation of NF-κB and inhibition of this activation through induction of HSP72 via intravenous administration of doxorubicin can mitigate this influence.

MATERIALS AND METHODS

Materials

Stop-flow balloon catheters and Gambro roller were purchased from PfM (Germany). TRIzol reagent was purchased from Invitrogen Life Technologies (USA). Reverse transcription system was from Promega (USA). BCA Protein Assay Reagents and Seize X Immunoprecipitation Kit were from Pierce (USA). All antibodies were purchased from Santa Cruz (USA).

Animals and grouping

Healthy female hybrid prepubertal pigs weighing 25.0±4.4 kg were employed in accordance with the guideline for animal research and were approved by the Ethical and Research Committee of the hospital. Twelve pigs were randomized into two groups, six animals in each. Animals in preconditioning and SFC group (DOX group) were anesthetized with an intramuscular injection of ketamine hydrochloride and doxorubicin (DOX) 1 mg/kg was then injected through peripheral veins. After recovery for 24 h, animals were subjected to SFC as described below. Meanwhile, animals in SFC group (normal saline (NS) group) were the same as in DOX group, but were injected with NS instead of DOX.

Stop-flow chemotherapy procedure

After overnight fast, all animals were subject to intravenous anesthesia with orotracheal intubation and controlled mechanic ventilation. A midline incision was performed. The abdominal aorta and inferior vena cava were exposed and separated about 2-3 cm. After systemic heparinization with 0.75 mg/kg of heparin, the abdominal aorta and inferior vena cava were clamped by Satinsky clamps just above the aortic and venous bifurcation. Then two small incisions were made above the clamp sites of the abdominal aorta and inferior vena cava, respectively. The isolation of abdomen was achieved by insertion of two 3-lumen stop-flow balloon catheters (PfM, Cologne, Germany) into the abdominal aorta and inferior vena cava respectively. The balloons were positioned above the celiac axis and hepatic venous under fluoroscopic control and filled with NS. As soon as the inflation of balloons, mitomycin C was perfused through an extra-corporeal circuit connected to both catheters at the dosage of 0.2 mg/kg, the Gambro roller (PfM, Cologne, Germany) was then started and the flow rate was adjusted at about 100 mL/min. No oxygen was added to this extra-corporeal circuit. After a total of 20-min hypoxic perfusion, the circulation to abdomen was restored by deflation of the balloons in aorta and inferior vena cava. The catheters were extracted after a brief stabilization period and the incisions were sutured. The circulation of hind legs was recovered by unclamping the Satinsky clamps. After the biopsies of liver tissue and blood samples were taken, the abdominal cavity was lavaged and the incision was sutured.

The hepatic biopsies were collected before, at the end of SFC and at 30 min, 3 and 6 h following the restoration of the abdominal circulation. Hepatic biopsy's sites were rotated randomly, but were in all cases as remote from each other as possible. The liver tissues were frozen immediately in liquid nitrogen and stored at -80 ℃ until analyzed. Peripheral blood samples were taken before, at the end of SFC and at 30 min, 3, 6, 24, 48 h and 7 d following the restoration of the abdominal circulation. Blood samples were centrifuged at 4 000 r/min immediately after taken from peripheral veins. Serum was separated and stored in aliquots at -80 ℃ until analyzed. All animals were killed at d 7 after SFC.

Semiquantitative RT-PCR

Total RNA was extracted using TRIzol reagent (Invitrogen, USA) from stored liver tissues at each given time point and 2 μg of it was reversely transcribed to complementary DNA (cDNA) using a reverse transcription system according to the manufacturer's guide (Promega, USA). An aliquot of 1 μL of cDNA products was amplified using specific primers for TNF-α and β-actin as described below. And housekeeping gene (β-actin) was amplified as internal control to verify the equal loading of RNA and cDNA in the reverse transcription and PCR creations.

PCR primers were as follows: TNF-α sense, 5'-atcggc-ccccagaaggaagag-3' and TNF-α antisense, 5'-gatggcagagag-gaggttgac-3' to give a 351-bp product; β-actin sense, 5'-ggacttcgagcaggagatgg-3' and antisense, 5'-gcaccgtgttgg-cgtagagg-3' to give a 233-bp product. All primers spanned at least one intron of genomic DNA. Eight microliters of each PCR products were electrophoresed in a 2% agarose gel and stained with ethidium bromide. The intensities of the specific bands were analyzed to determine whether the differences were statistically significant.

Preparing for cytoplasmic and nuclear extracts

Frozen liver tissues were homogenized in 1 mL of homogenization buffer A [10 nmol/L HEPES (pH 7.9), 1.5 mmol/L $MgCl_2$, 10 mmol/L KCl, 0.5 mmol/L DTT, 0.2 mmol/L PMSF, 0.1 mmol/L EDTA] on ice. The homogenates were incubated for 15 min on ice and centrifuged at 14 000 *g* for 15 min. The supernatants were stored at -80 ℃ as cytoplasmic extracts. The pellet was further suspended in ice-cold buffer B [20 mmol/L HEPES (pH 7.9), 1.5 mmol/L $MgCl_2$, 10 mmol/L KCl, 0.42 mol/L NaCl, 25% glycerol, 0.5 mmol/L DTT, 0.2 mmol/L PMSF, 0.2 mmol/L EDTA] and incubated for 30 min on ice with frequent vortex. After the suspensions were centrifuged at 14 000 *g* for 15 min, the supernatants were collected as nuclear extracts in aliquots and stored at -80 ℃.

Western blot and immunoprecipitation/Western blot analysis

Western blot was applied to determine the expression of

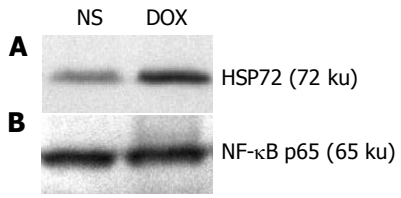

Figure 1 Western blot analysis of HSP72 (A) and NF-κB p65 subunit (B) in liver cytoplasmic extracts before SFC in NS and DOX groups.

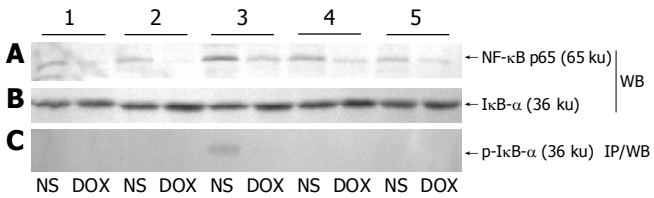

Figure 2 Western blot analysis of NF-κB presentation (A) in liver nuclear extracts, IκB-α expression (B) and immunoprecipitation/ Western blot analysis of p-IκB-α expression (C) in liver cytoplasmic extracts at different time points, i.e. before SFC, at the end of SFC (20 min), 30 min after the restoration of the abdominal circulation, 3 h after the restoration of the abdominal circulation, 6 h after the restoration of the abdominal circulation. WB, Western blot, IP, Immunoprecipitation.

HSP72, NF-κB p65 subunit and I-κBα in liver tissues. In brief, the protein contents of cytoplasmic and nuclear extracts were measured by a BCA protein assay (Pierce, USA), and 100 μg per lane was separated on a denaturing 10% SDS-PAGE gel (Laemmli). The proteins were then transferred to a nitrocellulose membrane (Hybond™-C, Amersham, UK) using a semi-dry transfer system (BioRad, USA). The membrane was stained by Ponceau S to check for the efficiency of transfer and subsequently blocked by 2% BSA for 1 h at room temperature. Membrane was then washed thrice for 5 min in TBS and then incubated for 2 h at room temperature with polyclonal goat anti-HSP72 antibody, polyclonal rabbit anti-p65 antibody, and polyclonal rabbit anti-IκB-α antibody in TBS. The membrane was washed thrice for 10 min in TBS and incubated with an appropriate secondary antibody (anti-goat or anti-rabbit) coupled to alkaline phosphatase in TBS. After the membrane was washed thrice for 10 min, it was developed with NBT/ BICP staining kit (Sino-American, China) according to the manufacturer's protocol.

The immunoprecipitation was performed using a commercial immunoprecipitation kit (Pierce, USA) according to the manufacturer's guide. After immunoprecipitation, the products were analyzed by Western blot as described above. An antibody, polyclonal rabbit anti-p-IκB-α antibody, special for phosphorylated inhibitor κB-α (IκB-α) was applied to detect the phosphorylated IκB-α.

Serum aspartate aminotransferase (AST) and alanine aminotransferase (ALT) assay

ALT and AST were determined according to the manufacturer's protocols. The serum levels of ALT and AST in serum were analyzed to determine whether the differences were statistically significant.

Statistical methods

Experimental results were expressed as mean±SD. SPSS statistical package was applied. Statistical comparisons were made using a general linear model (SNK). *P* value less than 0.05 was considered statistically significant.

RESULTS

The expression of HSP72 and NF-κB p65 subunit after intravenous administration of doxorubicin

After 24 h intravenous administration of doxorubicin (1 mg/kg), we observed a substantial production of HSP72 in liver tissue (Figure 1A, lane 2), whereas there was a minor expression in liver in NS group (Figure 1A, lane 1). But there was no observed change in the expression of cytoplasmic NF-κB p65 subunit between NS group and DOX group (Figure 1B), suggesting that administration of doxorubicin could induce the expression of HSP72 in liver and did not alter that of NF-κB p65 subunit in porcine liver.

The presence of NF-κB p65 subunit in nuclear and the phosphorylation of IκB-α

The dynamic change of NF-κB p65 subunit presenting in hepatic tissue nuclear extracts is shown in Figure 2A. The p65 subunit of NF-κB was absent in the nuclei in both NS and DOX groups. But it began to accumulate in nuclei at the end of SFC in NS group, reached its highest level in 30 min after the restoration of abdominal circulation and then decreased gradually. Compared with NS group, there was little change of p65 subunit in DOX group at corresponding time points. Thus we investigated the IκB-α level in cytoplasm at these time points and tried to figure out the relationship between NF-κB p65 and its inhibitor. A slight decrease of IκB-α in cytoplasm was noticed at 30 min after the restoration of the abdominal circulation and then recovered at following time points in NS group. In contrast to this, IκB-α level in DOX group remained constant during SFC (Figure 2B). Then we performed immunoprecipitation to evaluate the phosphorylation course of IκB-α during and after SFC procedure. The phosphorylated IκB-α solely appeared at 30 min after the restoration of the abdominal circulation in cytoplasm in NS group, which was consistent with the slight decrease of IκB-α (Figure 2C).

Transcription of TNF-α mRNA

The transcriptional activity of NF-κB downstream gene, TNF-α, was evaluated by semiquantitative RT-PCR (Figure 3).

According to the difference of activated NF-κB between NS and DOX groups, the transcriptional activity of TNF-α mRNA in DOX group was significantly lower than that in NS group at different time points (average 1.40 *vs* 0.62 for NS *vs* DOX respectively, $P<0.01$).

Serum level of ALT and AST

The serum level of ALT and AST of NS group was significantly higher than that of DOX group at 24 and 48 h after SFC ($P<0.05$, Figure 4).

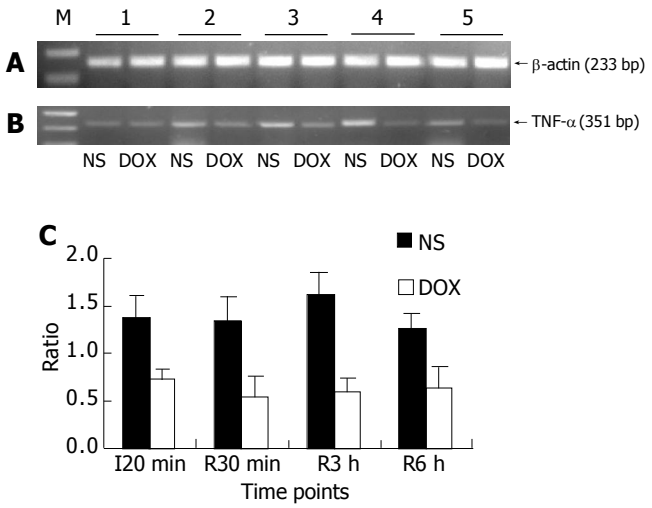

Figure 3 Semiquantitive RT-PCR analysis of β-actin (A) as an internal control and TNF-α mRNA (B) expression in liver tissues at different time points, i.e., before SFC, at the end of SFC (20 min), 30 min after the restoration of the abdominal circulation, 3 h after the restoration of the abdominal circulation, 6 h after the restoration of the abdominal circulation, and the ratio between the expression of TNF-α mRNA at different time points and the expression of TNF-α mRNA (C).

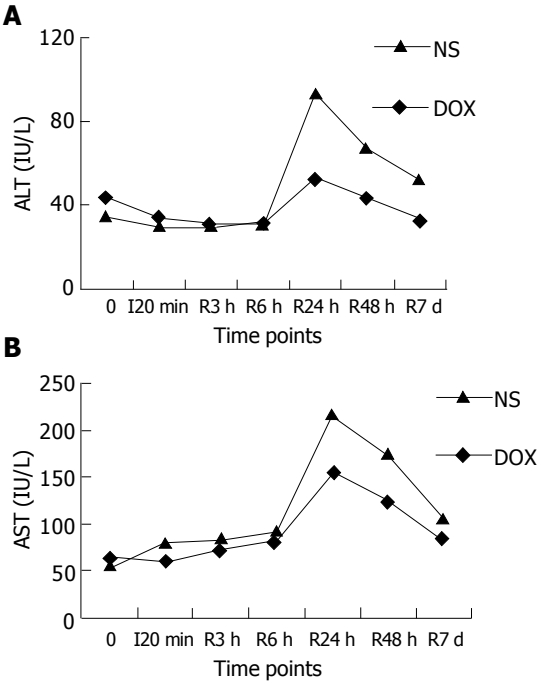

Figure 4 Serum level of ALT (A) and AST (B) at different time points before and after SFC respectively, 0, before SFC, I20 min, at the end of SFC (20 min), R3h, 3 h after the restoration of the abdominal circulation, R6 h, 6 h after the restoration of the abdominal circulation, R24 h, 24 h after the restoration of the abdominal circulation, R48 h, 48 h after the restoration of the abdominal circulation, R7d, 7 d after the restoration of the abdominal circulation.

DISCUSSION

Although a lot of work has been done in hepatic ischemia/reperfusion injury, little is known at such a particular situation that liver was under hypoxia and low-flow but not no-flow in SFC procedure. We have previously shown a mild and reversible hepatic influence[4], and there was a mild elevation in serum aminotransferases within 48 h after SFC procedure. The purpose of this study was to investigate the role of NF-κB pathway during SFC and tried to alleviate this influence through pharmacologically hepatic preconditioning by administration of doxorubicin before SFC procedure and further investigate the potential mechanism of this effect.

With regard to the activation of nuclear factor kappa B (NF-κB) p65 subunit, the presence of p65 protein was investigated in both hepatic cytoplasmic and nuclear extracts. We first examined the expression of cytoplasmic p65 subunit obtained from liver before SFC procedure and there was no difference between two groups (Figure 1B). It means that the expression of p65 subunit was not affected by the administration of doxorubicin before SFC procedure. However, there was a significant change of p65 subunit in nuclei during and after SFC procedure between NS and DOX groups. It was that in NS group, the p65 subunit in hepatic nuclear extract accumulated gradually from the end of SFC and reached its highest level in 30 min after the restoration of the abdominal circulation and then decreased in the following 6 h after SFC procedure, while there was only a little change in DOX group during the same time period. Meanwhile, we also observed a slight decrease of IκB-α and the appearance of phosphorylated IκB-α in cytoplasm at 30 min after the restoration of the abdominal circulation in NS group when compared with DOX group at that time point. NF-κB was first thought to be primarily a lymphocyte and macrophage transcription factor, but it now has been demonstrated in various tissues and organs including liver, in which it responds to hypoxia and re-oxygenation and is involved in immune and inflammatory responses. Cells must retain their NF-κB proteins in cytoplasm from activating gene transcription wantonly by means of NF-κB inhibitors such as IκB family. Once cells receive an appropriate stimulus such as pro-inflammatory cytokines, metal ions, and reactive oxygen species as well, the IκB kinase (IKK) complexes become active and phosphorylate the IκB inhibitors. The most common active dimer of NF-κB is composed of p50 and p65, in which p65 is a transcription-activating subunit and p50 contributes to the binding of specific DNA sequence[10]. The activated NF-κB promotes transcriptional activity of pro-inflammatory genes like TNF-α. We then investigated the mRNA level of TNF-α in liver tissues at the same time points and observed an elevated transcriptional activity of TNF-α after the restoration of the abdominal circulation in NS group, but there was a little change of it in DOX group. This difference is compatible with the activation pattern of NF-κB in NS and DOX groups respectively. TNF-α is one of the key pro-inflammatory cytokines that play a pivotal role in augmenting the inflammatory response in hepatic ischemia/reperfusion injury. The extent of hepatic ischemia/reperfusion injury was limited via applying anti-TNF-α mono-antibody or ischemic preconditioning to restrain the production or activity of TNF-α[14,15]. Teoh[16] proved that the hepatic ischemia/reperfusion injury in TNF-α knock-out mice was suppressed during both the early (2 h) and late (24 h) phases of ischemia/reperfusion injury. In our model, the inhibition of NF-κB

was also followed by the inhibition of transcriptional activity of TNF-α. Furthermore, we also observed a significant change in the serum level of ALT and AST between NS and DOX groups. The serum level of aminotransferases in NS group significantly increased within 48 h and the peak value of ALT in NS group almost doubled at 24 h after SFC when compared with that of DOX group. These results indicate that NF-κB/IκB-α pathway acts quickly to the hypoxia/re-oxygenation in liver caused by SFC procedure and cause the following inflammatory response. Administration of doxorubicin preceding SFC procedure protects the liver from this insult by the inhibition of the activity of NF-κB through stabilization of IκB-α.

The remaining paradoxical phenomenon is how doxorubicin, a potential deleterious agent to liver, provides protection for liver in SFC procedure. Interestedly, we observed obvious expression of HSP72 protein in porcine liver after 24 h of the administration of doxorubicin via peripheral venous when compared with injection of NS, which is consistent with the work of Kume[17]. If administrated intravenously, doxorubicin accumulates in liver and is reductively metabolized to semiquinone radical intermediate participating in the formation of reactive oxygen species[18]. Because of the enterohepatic circulation of doxorubicin and its metabolites, there might be appreciable reactive oxygen species triggering oxidant stress and might induce the production of another stress reaction protein that is heat shock protein (HSP) family. HSP72 is the inducible member of HSP70 family, the other is constitutively expressed, HSP73. As a molecular chaperon, HSP72 serves as preventing the aggregation and misfolding of proteins. In addition, it also assists in the folding of newly synthesized proteins, translocating proteins to appropriate organs. Induction of HSP72 pharmacologically or through heat shock preconditioning renders liver to be tolerant to ischemia/reperfusion injury[13,17,19]. It has been speculated that binding of HSP72 and NF-κB/IκB-α may contribute to block the activation of NF-κB, and Shimizu *et al*[20], has reported the formation of complex of HSP72-IκB-α in the model of myocardial infarct. Another hypothesis is that it is the activity of IKK that is inhibited after the induction of HSP72[21-23].

Combination NF-κB/IκB-α with the expression of HSP72 in our animal model of SFC, administration of doxorubicin before SFC did not down-regulate the expression of p65 subunit in liver, and the inhibitory effect of NF-κB is blunted at the phosphorylation and degradation of IκB-α. Our results are in agreement with those studies showing that NF-κB/IκB-α pathway can be blocked by various stimuli[13,21,22,24]. Further work in the interaction between HSP72 and NF-κB/IκB-α is needed to elucidate the exact role of HSP72 in pharmacological preconditioning of doxorubicin in SFC.

In conclusion, we have revealed the role of NF-κB/IκB-α pathway in the model of abdominal SFC. Our study also shows that doxorubicin is not only beneficial to patients with advanced abdominal cancer, but also can interfere with the activation of NF-κB through stabilizing the IκB-α probably by inducing HSP72 in liver. The understanding of doxorubicin in pharmacological hepatic preconditioning sheds light on a new approach to prevent the hepatic influence in SFC and makes this new chemotherapy feasible in clinical practice.

REFERENCES

1 **Averbach AM,** Stuart OA, Sugarbaker TA, Stephens AD, Fernandez-Trigo V, Shamsa F, Sugarbaker PH. Intraaortic stop-flow infusion: pharmacokinetic feasibility study of regional chemotherapy for unresectable gastrointestinal cancers. *Ann Surg Oncol* 1995; **2**: 325-331

2 **Turk PS,** Belliveau JF, Darnowski JW, Weinberg MC, Leenen L, Wanebo HJ. Isolated pelvic perfusion for unresectable cancer using a balloon occlusion technique. *Arch Surg* 1993; **128**: 533-538; discussion 538-539

3 **Guadagni S,** Fiorentini G, Palumbo G, Valenti M, Russo F, Cantore M, Deraco M, Vaglini M, Amicucci G. Hypoxic pelvic perfusion with mitomycin C using a simplified balloon-occlusion technique in the treatment of patients with unresectable locally recurrent rectal cancer. *Arch Surg* 2001; **136**: 105-112

4 **Yao XX,** Zhu ZG, Zhao R, Su J, Zhou S, Yu BW, Yin HR, Lin YZ. The influence of Stop-flow chemotherapy on the abdominal visceral function of swine. *J Surg Concepts Pract* 2003; **8**: 223-225

5 **Bronk SF,** Gores GJ. Efflux of protons from acidic vesicles contributes to cytosolic acidification of hepatocytes during ATP depletion. *Hepatology* 1991; **14**: 626-633

6 **Gasbarrini A,** Borle AB, Farghali H, Bender C, Francavilla A, Van Thiel D. Effect of anoxia on intracellular ATP, Na+i, Ca2+i, Mg2+i, and cytotoxicity in rat hepatocytes. *J Biol Chem* 1992; **267**: 6654-6663

7 **Lentsch AB,** Kato A, Yoshidome H, McMasters KM, Edwards MJ. Inflammatory mechanisms and therapeutic strategies for warm hepatic ischemia/reperfusion injury. *Hepatology* 2000; **32**: 169-173

8 **Zhu XH,** Qiu YD, Shen H, Shi MK, Ding YT. Effect of matrine on Kupffer cell activation in cold ischemia reperfusion injury of rat liver. *World J Gastroenterol* 2002; **8**: 1112-1116

9 **Shakhov AN,** Collart MA, Vassalli P, Nedospasov SA, Jongeneel CV. Kappa B-type enhancers are involved in lipopolysaccharide-mediated transcriptional activation of the tumor necrosis factor alpha gene in primary macrophages. *J Exp Med* 1990; **171**: 35-47

10 **Baeuerle PA,** Henkel T. Function and activation of NF-kappa B in the immune system. *Annu Rev Immunol* 1994; **12**: 141-179

11 **Vos IH,** Govers R, Grone HJ, Kleij L, Schurink M, De Weger RA, Goldschmeding R, Rabelink TJ. NFkappaB decoy oligodeoxynucleotides reduce monocyte infiltration in renal allografts. *FASEB J* 2000; **14**: 815-822

12 **Kis A,** Yellon DM, Baxter GF. Role of nuclear factor-kappa B activation in acute ischaemia-reperfusion injury in myocardium. *Br J Pharmacol* 2003; **138**: 894-900

13 **Uchinami H,** Yamamoto Y, Kume M, Yonezawa K, Ishikawa Y, Taura K, Nakajima A, Hata K, Yamaoka Y. Effect of heat shock preconditioning on NF-kappaB/I-kappaB pathway during I/R injury of the rat liver. *Am J Physiol Gastrointest Liver Physiol* 2002; **282**: G962-G971

14 **Iwasaki Y,** Tagaya N, Hattori Y, Yamaguchi K, Kubota K. Protective effect of ischemic preconditioning against intermittent warm-ischemia-induced liver injury. *J Surg Res* 2002; **107**: 82-92

15 **Ben-Ari Z,** Hochhauser E, Burstein I, Papo O, Kaganovsky E, Krasnov T, Vamichkim A, Vidne BA. Role of anti-tumor necrosis factor-alpha in ischemia/reperfusion injury in isolated rat liver in a blood-free environment. *Transplantation* 2002; **73**: 1875-1880

16 **Teoh N,** Field J, Sutton J, Farrell G. Dual role of tumor necrosis factor-alpha in hepatic ischemia-reperfusion injury: studies in tumor necrosis factor-alpha gene knockout mice. *Hepatology* 2004; **39**: 412-421

17 **Kume M,** Yamamoto Y, Yamagami K, Ishikawa Y, Uchinami H, Yamaoka Y. Pharmacological hepatic preconditioning: involvement of 70-kDa heat shock proteins (HSP72 and HSP73)

in ischaemic tolerance after intravenous administration of doxorubicin. *Br J Surg* 2000; **87**: 1168-1175

18 **Gewirtz DA.** A critical evaluation of the mechanisms of action proposed for the antitumor effects of the anthracycline antibiotics adriamycin and daunorubicin. *Biochem Pharmacol* 1999; **57**: 727-741

19 **Fudaba Y,** Ohdan H, Tashiro H, Ito H, Fukuda Y, Dohi K, Asahara T. Geranylgeranylacetone, a heat shock protein inducer, prevents primary graft nonfunction in rat liver transplantation. *Transplantation* 2001; **72**: 184-189

20 **Shimizu M,** Tamamori-Adachi M, Arai H, Tabuchi N, Tanaka H, Sunamori M. Lipopolysaccharide pretreatment attenuates myocardial infarct size: A possible mechanism involving heat shock protein 70-inhibitory kappaBalpha complex and attenuation of nuclear factor kappaB. *J Thorac Cardiovasc Surg* 2002; **124**: 933-941

21 **Roussel RR,** Barchowsky A. Arsenic inhibits NF-kappaB-mediated gene transcription by blocking IkappaB kinase activity and IkappaBalpha phosphorylation and degradation. *Arch Biochem Biophys* 2000; **377**: 204-212

22 **Yoo CG,** Lee S, Lee CT, Kim YW, Han SK, Shim YS. Anti-inflammatory effect of heat shock protein induction is related to stabilization of I kappa B alpha through preventing I kappa B kinase activation in respiratory epithelial cells. *J Immunol* 2000; **164**: 5416-5423

23 **Kohn G,** Wong HR, Bshesh K, Zhao B, Vasi N, Denenberg A, Morris C, Stark J, Shanley TP. Heat shock inhibits tnf-induced ICAM-1 expression in human endothelial cells via I kappa kinase inhibition. *Shock* 2002; **17**: 91-97

24 **Kiemer AK,** Gerbes AL, Bilzer M, Vollmar AM. The atrial natriuretic peptide and cGMP: novel activators of the heat shock response in rat livers. *Hepatology* 2002; **35**: 88-94

Science Editor Zhang JZ, Guo SY and Ma JY **Language Editor** Elsevier HK

PO Box 2345, Beijing 100023, China
www.wjgnet.com
wjg@wjgnet.com

ELSEVIER

World J Gastroenterol 2005;11(14):2142-2147
World Journal of Gastroenterology ISSN 1007-9327

• *CLINICAL RESEARCH* •

Value of CT in the diagnosis and management of gallstone ileus

Chih-Yung Yu, Chang-Chyi Lin, Rong-Yaun Shyu, Chung-Bao Hsieh, Hurng-Sheng Wu, Yeu-Sheng Tyan, Jen-I Hwang, Chang-Hsien Liou, Wei-Chou Chang, Cheng-Yu Chen

Chih-Yung Yu, Chang-Hsien Liou, Wei-Chou Chang, Cheng-Yu Chen, Department of Radiology, Tri-Service General Hospital, National Defense Medical Center, Taipei, Taiwan, China
Chang-Chyi Lin, Rong-Yaun Shyu, Department of Internal Medicine, Tri-Service General Hospital, National Defense Medical Center, Taipei, Taiwan, China
Chung-Bao Hsieh, Department of Surgery, Tri-Service General Hospital, National Defense Medical Center, Taipei, Taiwan, China
Hurng-Sheng Wu, Department of Surgery, Show-Chwan Memorial Hospital, Changhua, Taiwan, China
Yeu-Sheng Tyan, Department of Radiology, Chung Shan Medical University Hospital, Taichung, Taiwan, China
Jen-I Hwang, Department of Radiology, Taichung Veterans General Hospital, Taichung, Taiwan, China
Correspondence to: Dr. Chih-Yung Yu, Department of Radiology, Tri-Service General Hospital, National Defense Medical Center, No 325, Sec. 2, Cheng-Gung Road, 114 Nei-Hu, Taipei, Taiwan, China. jefcyyu@ms24.hinet.net
Telephone: +886-2-87927247 Fax: +886-2-87927245
Received: 2004-09-21 Accepted: 2004-11-29

Abstract

AIM: To retrospectively establish the diagnostic criteria of gallstone ileus on CT, and to prospectively apply these criteria to determine the diagnostic accuracy of CT to confirm or exclude gallstone ileus in patients who presented with acute small bowel obstruction (SBO). Another purpose was to ascertain whether the size of ectopic gallstones would affect treatment strategy.

METHODS: Fourteen CT scans in cases of proved gallstone ileus were evaluated retrospectively by two radiologists for the presence or absence of previously reported CT findings to establish the diagnostic criteria. These criteria were applied in a prospective contrast enhanced CT study of 165 patients with acute SBO, which included those 14 cases of gallstone ileus. The hard copy images of 165 CT studies were reviewed by a different group of two radiologists but without previous knowledge of the patient's final diagnosis. All CT data were further analyzed to determine the diagnostic accuracy of gallstone ileus when using CT in prospective evaluation of acute SBO. The size of ectopic gallstone on CT was correlated with the clinical course.

RESULTS: The diagnostic criteria of gallstone ileus on CT were established retrospectively, which included: (1) SBO; (2) ectopic gallstone; either rim-calcified or total-calcified; (3) abnormal gall bladder with complete air collection, presence of air-fluid level, or fluid accumulation with irregular wall. Prospectively, CT confirmed the diagnosis in 13 cases of gallstone ileus with these three criteria. Only one false negative case could be identified. The remaining 151 patients are true negative cases and no false positive case could be disclosed. The overall sensitivity, specificity and accuracy of CT in diagnosing gallstone ileus were 93%, 100%; and 99%, respectively. Surgical exploration was performed in 13 patients of gallstone ileus with ectopic stones sized larger than 3 cm. One patient recovered uneventfully following conservative treatment with an ectopic stone sized 2 cm in the long axis.

CONCLUSION: Contrast enhanced CT imaging offered crucial evidence not only for the diagnosis of gallstone ileus but also for decision making in management strategy.

Key words: CT; Gallstone ileus

Yu CY, Lin CC, Shyu RY, Hsieh CB, Wu HS, Tyan YS, Hwang JI, Liou CH, Chang WC, Chen CY. Value of CT in the diagnosis and management of gallstone ileus. *World J Gastroenterol* 2005; 11(14): 2142-2147
http://www.wjgnet.com/1007-9327/11/2142.asp

INTRODUCTION

Gallstone ileus resulted from recurrent attacks of cholecystitis and erosion of gallstone through adjacent duodenal wall into small intestine, which may lead to bowel obstruction. It accounts for 1-2% per cent of mechanical small bowel obstruction (SBO). In geriatric population, the incidence could be as high as 25%[1].

Gallstone ileus presented a challenging surgical dilemma clinically. Misdiagnosis is common and it also carries a significant rate of complications with a mortality rate ranging from 12% to 27% in most series reported[2]. High morbidity and mortality rate could be attributed to delayed diagnosis, senile patient, and coexisting concomitant medical disease. Early diagnosis is therefore pivotal to improve morbidity, mortality and post-operative complications.

Traditionally, plain abdominal radiography remained a mainstay for the assessment of SBO. However, the sensitivity of plain film varies from 40% to 70% in diagnosing gallstone ileus[3,4].

Recent literatures have shown that ultrasonography (US) was more helpful in diagnosing gallstone ileus than plain abdominal radiography[5,6]. But the sensitivity of detection rate in a large-scale US study was 74% at best[6].

Most case reports on CT had also proven its value for

diagnosing gallstone ileus[7-11] but still lack prospective study in large patient population thus far to verify the diagnostic accuracy if clinician chooses CT to evaluate acute SBO.

The aim of the present article is to retrospectively establish CT diagnostic criteria of gallstone ileus, and to prospectively apply these criteria to determine the diagnostic accuracy of CT to confirm or exclude gallstone ileus in patients who presented with acute SBO.

Advantages and limitations of different CT protocols were also assessed from our findings and previous reports to verify whether oral or IV contrast administration post any helpful in patients with suspected gallstone ileus and other etiology of SBO.

Another aim of this work is to determine whether the size of ectopic gallstones would affect treatment strategy.

MATERIALS AND METHODS

Patients

From our radiology database between November 1994 and 2002, 14 patients of gallstone ileus were identified for inclusion in this study. There were nine women and five men with mean age of 74 years (range 38-94 years). Ten patients were older than 70 years. All patients were documented by surgery (n = 13) or by classic CT criteria with spontaneous recovery after conservative treatment (n = 1). The CT images were evaluated retrospectively with two board-certified radiologists (CYY, CHL) for published or unpublished CT findings to establish the diagnostic criteria.

During the same period, 151 consecutive patients with other etiology of acute SBO were included in this study. There were 82 males and 69 females with mean age of 63 years (range 20-89 years). Acute SBO was suspected by the clinical symptoms and plain abdominal radiography. The final diagnosis was established by surgery (n = 128), clinical follow up (n = 21), and US-guide aspiration and drainage (n = 2). The etiology of clinical follow up patients included adhesive band (n = 19) and intramural hematoma (n = 2). Adhesive band was inferred from CT when no mass or other abnormality was noted around the site of obstruction. Intramural hematoma of small intestine following blunt abdominal injury was also inferred from CT on the basis of demonstration of transition zone with a focal homogeneous wall thickening and higher attenuation than the adjacent normal bowel wall. The clinical symptom of all these patients showed complete resolution within 2 wk.

Methods

All patients accepted CT examination and the hardware included either a conventional CT (Somatom Hi-Q, Simens Medical System, Germany) or a spiral CT (Somatom plus-4, Siemens Medical System, Germany). Oral contrast material was administered with 2% iodinated water-soluble contrast medium at least 1 h before scanning if patient could tolerate. One hundred milliliters of 60% iodinated nonionic or ionic IV contrast was delivered by a power injector or by hand injection at a rate of 2 cm^3/s if patient showed no history of contrast allergy or renal function impairment. No rectal contrast was given simultaneously. Scanning was performed in the craniocaudal direction, beginning at the dome of the right hemidiaphragm to the symphysis pubis.

In gallstone ileus patients group, only one patient did not accept IV contrast due to renal function impairment. Oral contrast was given to six patients, who presented with intestinal obstruction; however, clinical symptom still could tolerate oral contrast.

In the rest of SBO patients group, 151 patients accepted IV contrast and only 32 patients received oral contrast administration.

CT images were obtained at portal venous phase (70 s after contrast injection). A beam collimation of 8 mm, pitch 1.5, and reconstructed at 8 mm intervals were used in spiral CT. Conventional CT used 10 mm slice thickness and 10 mm table incremental scan.

The hard copy images of 165 CT studies were reviewed retrospectively by a different group of two board-certified radiologists (YST, JIH), whom were blinded to the final diagnosis. All CT data were further analyzed to determine the diagnostic accuracy of gallstone ileus when using CT in prospective evaluation acute SBO.

RESULTS

The etiology of SBO in our 165 patients is described in Table 1. Detailed plain film, CT findings, and clinical data of these 14 patients of gallstone ileus are listed in Table 2. Duration of symptom onset prior to admission in patients with gallstone ileus varied from 1 to 5 d. Time interval between admission and CT was less than 24 h. The time lag between CT and operation was also less than 24 h. Plain abdominal radiography was taken routinely on admission and only five patients matched the full criteria of Rigler's triad (5/14 = 36%). In the individual criterion analysis, pneumobilia presented on plain film of five cases (5/14 = 36%)

Table 1 Causes of SBO in 165 patients

Cause of SBO	Number of patients
Gallstone ileus	14
Phytobezoar	7
Intussusception	13
Inguinal hernia	10
Spigelian hernia	7
Obturator hernia	3
Transmesosigmoid hernia	1
Appendicitis	6
Perforated appendicitis	4
Periappendiceal abscess	2 (2[1])
Diverticulitis with rupture	2
Ischemic bowel disease	5
Eosinophilic enteritis	1
Intramural hematoma	3 (2[2])
Adhesive band	57 (19[2])
Malignant lymphoma	3
Adenocarcinoma of jejunum	1
Adenocarcinoma of ileum	1
Adenocarcinoma of ileo-cecal valve	9
Adenocarcinoma of ascending colon	17
Adenocarcinoma of hepatic flexure colon	2

Numbers in parenthesis refer to numbers of cases whose final diagnosis was determined either by [1]US-Guide aspiration drainage or [2]clinical follow up.

Figure 1 Ectopic gallstone (arrow) showed totally calcified component (A) and rim-calcified component (B).

and on CT of seven cases (7/14 = 50%). Mechanical SBO was suggested by plain film (n = 10, 10/14 = 71%) and by clinical symptoms (n = 4). These latter four patients demonstrated massive fluid accumulation within bowel lumen, which made invaluable of plain film. Ectopic gallstone could be diagnosed using plain film on six patients (6/14 = 43%).

The diagnostic criteria of gallstone ileus on CT were established retrospectively, which included: (1) SBO (n = 14); (2) ectopic gallstone; either rim-calcified (n = 9) (Figure 1A) or total-calcified (n = 5) (Figure 1B); (3) abnormal gall bladder with complete air collection (n = 9) (Figure 2A), presence of air-fluid level (n = 3) (Figure 2B), or fluid accumulation with irregular wall (n = 2) (Figure 2C).

All three criteria were utilized in a prospective evaluation of 165 patients with acute SBO. Gallstone ileus was confirmed pre-operatively with CT in 13 cases. Only one false negative case could be identified and it showed less calcification in the rim-calcified ectopic gallstone, which rendered poor differentiation from the enhanced small bowel wall with similar density and without clear space between each other (Figure 3).

No false positive case could be disclosed, which means positive predictive value is 100%. The remaining 151 patients are true negative cases. The overall sensitivity, specificity and accuracy of CT to diagnosing gallstone ileus was 93% (13/14), 100% (151/151); and 99% (164/165), respectively.

Two low sensitivity CT findings also could be identified in our study, which included cholecystoduodenal fistula (n = 3) and wall thickening (>1 cm) of the second portion duodenum (n = 3) (Figure 4). The latter three patients had symptom onset duration that lasted less than 1 d with leukocytosis over 20.00×10^9/L and ascites (Table 2).

Another low sensitivity finding on CT showed segmental edematous wall thickening (>1 cm) over ileum, just prior to the transition zone (n = 2) (Figures 5A and B). During operation, peal formation and edematous change could be identified. However, there was a lack of evidence of perforation or ischemia in these patients, who recovered uneventfully following surgery.

The size of ectopic gallstone by CT imaging showed to be larger than 3 cm in 13 cases. All of them accepted surgical intervention. Only one patient achieved spontaneous recovery following conservative treatment, which presented with an ovoid ectopic gallstone sized 2 cm in the long axis (Figure 6).

DISCUSSION

Clinical manifestation and plain abdominal radiographic findings of gallstone ileus are rarely specific, often similar to other causes of mechanical SBO, and more than one-

Table 2 Plain film, CT findings and clinical data in 14 cases of gallstone ileus

Case	1	2	3	4	5	6	7	8	9	10	11	12	13	14
Plain film														
Pneumobilia	–	–	+	–	+	–	+	–	+	+	–	–	–	–
Gas in gall bladder fossa	–	–	–	–	–	+	–	–	–	–	–	–	–	+
Small bowel obstruction	–	–	+	+	+	+	+	+	+	+	+	+	–	–
Ectopic gallstone	+	–	–	+	+	+	+	–	–	+	–	–	–	–
CT														
Pneumobilia	–	–	+	+	+	–	+	–	+	+	–	–	+	–
Gall bladder content	Air	Fluid	Air	Air	Air-fluid	Air	Air-fluid	Air	Air	Air	Air	Air	Fluid	Air-fluid
Small bowel obstruction	+	+	+	+	+	+	+	+	+	+	+	+	+	+
Ectopic gallstone	TC	RC	RC	TC	TC	RC	TC	RC	RC	TC	RC	RC	RC	RC
Other CT findings														
Cholecysto-duodenal fistula	–	–	–	+	–	+	–	–	–	+	–	–	–	–
Thickened duodenum (>1cm)	+	+	+	–	–	–	–	–	–	–	–	–	–	–
Ascites	+	+	+	+	+	+	–	+	–	+	–	–	–	–
Thickened small intestine (>1cm)	–	+	–	–	–	+	–	–	–	–	–	–	–	–
Clinical data														
Symptom onset duration (d)	1	1	1	2	3	3	3	4	5	5	5	5	5	5
WBC($\times10^9$/L) upon admission	24.70	24.50	21.70	16.50	13.90	13.50	12.40	10.25	10.90	5.30	7.30	6.60	9.50	8.30

+: Presence, –: absence TC: total-calcified, RC: rim-calcified.

Figure 2 Diseased gallbladder (arrow) was replaced by gas (A); mixed air and fluid (B); and fluid with irregular wall (C).

third of patients presented no history of biliary symptoms [12]. Several case reports have shown accuracy of CT in the diagnosis of gallstone ileus[7-11]. However, larger patient population is needed to establish the diagnostic CT criteria and to verify the diagnostic accuracy if clinician chooses CT to evaluate acute SBO. Based on our study, the diagnostic CT criteria include: (1) SBO; (2) ectopic gallstone; either rim-calcified or total-calcified; (3) abnormal gall bladder with complete air collection, presence of air-fluid level, or fluid accumulation with irregular wall. Our study also demonstrated that contrast enhanced CT have high sensitivity (93%), specificity (100%), and accuracy (99%) to diagnose gallstone ileus in patients who presented with acute SBO.

Gallstone ileus takes an insidious course, presented symptoms of intermittent intestinal obstruction. Duration of symptoms prior to admission was varied from 6 h to 22 d[2,7]. The longest in our series is 5 d. Duration from admission to operation ranged from 5 h to 14 d and overall mortality rate was 19%[2,7,12-14]. According to these reports, delayed diagnosis plus concomitant geriatric disease could lead to severe complications, including fatality. All of our patients had CT study within 24 h upon admission, which made early diagnosis possible. Therefore, we were not able to observe classical tumbling phenomenon in any of our cases. All of our patients showed full recovery and the key issue here is to be able to obtain prompt diagnosis with CT imaging and early surgical intervention.

The classic Rigler's triad for diagnosis of gallstone ileus on plain abdominal radiography was reported to be present about 30-35% cases[1,15]. In our study, only 36% cases (5/14) presented full criteria.

When single criterion was used for evaluation, pneumobilia could be detected on plain film in five patients (5/14 = 36%) and on CT in seven patients (7/14 = 50%). The rare incidence may be secondary to persistent obstruction of cystic duct even with cholecystoduodenal fistula presence to decompress the gallbladder.

Air collection within the gall bladder can be easily misdiagnosed and misinterpreted as colon gas by plain film alone. However, CT could easily detect complete air collection, air-fluid level, or fluid accumulation with irregular wall within the diseased gall bladder in all fourteen cases of our study.

Only six cases with ectopic gallstones could be identified by plain film but CT picked up 13 cases. Possible etiology for this limitation of plain film may be related that ectopic gallstone superimposed with bony structures or fluid-filled bowel, obscured by obesity, or lack of identifiable calcification.

Recent works suggested that CT has high sensitivity and accuracy for pre-operative evaluation of patient with suspected intestinal obstruction or acute abdomen[16-19]. The promptness and capability of contrast-enhanced CT to reveal the cause of SBO and acute abdomen makes it essential for emergency use[20].

When dealing with CT, the first issue is whether oral water-soluble contrast is needed in SBO evaluation? In CT evaluation of high grade obstruction, oral contrast administration should be prohibited on account of: (1) vomiting always precluding excessive fluid intake; (2) suffocation likely while patient changes position from sitting to supine if excessive fluid accumulation within the stomach; (3) existing intestinal fluid offered natural negative contrast effect to differentiate the location and wall thickness of the transition zone[19]. However, if patient posed with partial intestinal obstruction or intermittent high grade obstruction as in cases of gallstone ileus, oral contrast could be used to further dilate the proximal small intestine, which allows better evaluation of the transition zone[3].

Rim-or totally calcified ectopic gallstone could be easily detected by CT without oral contrast administration. But based on our study (n = 6) and previous reports[10], oral contrast administration may not interfere with the diagnosis of ectopic gallstone because: (1) most oral contrast did not reach the transition zone due to obstruction; (2) diluted oral contrast consists of relatively low density as compared to the high density of rim or totally calcified stone.

Non-enhanced (free IV) CT can serve as a diagnostic imaging tool to prompt identification of ectopic gallstone despite the presence of any degree of calcification, based on our study (n = 1) and previous reports[8-11]. It also offers two advantages: (1) no risk of contrast allergy, and (2) routine application to all patient population, including those with renal function impairment.

Contrast-enhanced CT, on the other hand, is more difficult to identify rim-calcified stone than total calcified ones. Rim-calcified component would be easily missed as normal bowel wall appears without clear space in-between to separate each other. In addition, less calcification in ectopic rim-calcified gallstone could be neglected when equal enhancement is achieved in the small bowel wall[7,21,22]. Only one false negative case could be identified in our study and

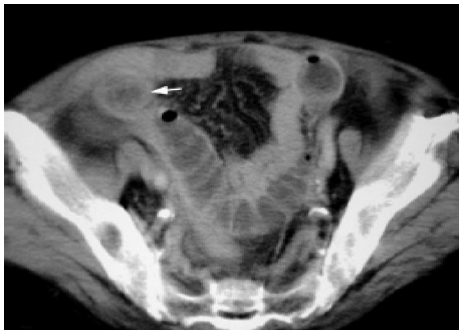

Figure 3 False negative case showed poor differentiation between less calcified rim of the ectopic gallstone (arrow) and the enhanced bowel wall (case 8).

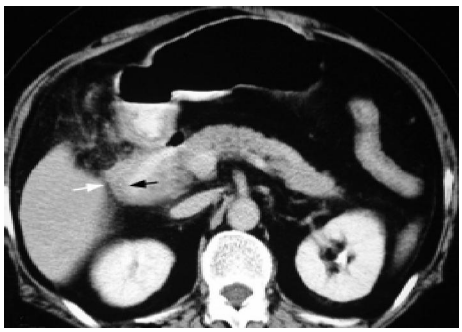

Figure 4 Axial contrast enhanced CT delineated wall thickening (between arrows) of duodenum second portion >1 cm (case 3).

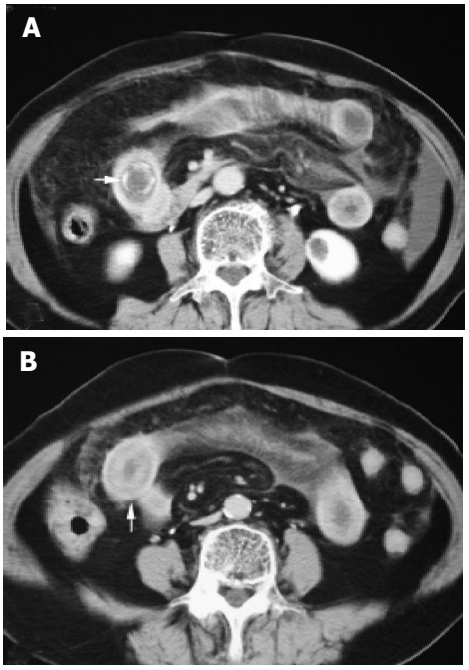

Figure 5 Axial contrast enhanced CT showed rim-calcified ectopic gallstone in the proximal ileum (A). CT section located 3 cm caudal to (A) reveal segmental edematous wall thickening of small intestine (arrow) proximal to transition zone, which indicated transient ischemic change secondary to bowel obstruction (B) (case 2).

Figure 6 Rim-calcified ectopic stone (arrow) sized 2 cm in the long axis with SBO but evacuated spontaneously following conservative treatment (case 9).

the remaining 13 could be diagnosed well before operation.

Intravenous contrast material is valuable for improved detection of edema, inflammation, and ischemia of the small intestine[19]. Therefore contrast enhanced CT may help to establish alternate diagnosis of SBO and to predict the presence of complications. In our study, edematous wall thickening of the small intestine prior to transition zone could be clearly identified by CT in two cases and it was proved to be transient ischemic change from distended bowel loops.

Another two low sensitivity CT findings, cholecystoduodenal fistula and wall thickening of duodenum second portion, also could be clearly identified by contrast-enhanced CT. These two findings existed concomitantly in a previous report[7] but our result did not. Previous report did not define the criteria of thickening duodenum or offer any graphic evidence for this finding. Wall thickening of the duodenum second portion in our study correlated well with symptom onset duration less than 24 h, leukocytosis over 20.00×10^9/L, and ascites, which were suggestive of acute inflammatory process in progress. However, the presence of cholecystoduodenal fistula did not parallel with the acute inflammatory status in our study and it may well be due to pressure generated by incomplete evacuation of the gallbladder contents and/or high-grade SBO persistent but we can only hypothesize this for lack of direct evidence.

Accurate diagnosis of the location and etiology of small-bowel obstruction is essential for therapeutic planning[20]. Precision surgical incision for gallstone ileus with open or laparoscopic enterolithotomy need detailed anatomical correlation[23,24]. Previous report suggested primary surgical intervention is mandatory for all cases with gallstone ileus[13]. But one patient in our series demonstrated spontaneous recovery and his ectopic gallstone size was 2 cm in long axis, which others also witnessed[11]. It is the second case in the literature to validate conservative treatment was also effective in the management of gallstone ileus[11]. Then, we proposed that when prospective CT estimation of ectopic gallstone sized less than 2 cm in size, patients should receive conservative treatment with constant monitoring of vital signs until complete clinical recuperation. If conservative measures affected resolution of gallstone ileus accordingly, better prognosis could be achieved especially in elderly and debilitating patients.

In conclusion, contrast enhanced CT evaluation of acute SBO offers prompt and rapid diagnosis of gallstone ileus before operation. CT also has the capability to estimate the

size of ectopic gallstone, which rendering decision making in management strategy.

REFERENCES

1 **Hudspeth AS,** McGuirt WF. Gallstone ileus. A continuing surgical problem. *Arch Surg* 1970; **100**: 668-672
2 **Clavien PA,** Richon J, Burgan S, Rohner A. Gallstone ileus. *Br J Surg* 1990; **77**: 737-742
3 **Maglinte DD,** Reyes BL, Harmon BH, Kelvin FM, Turner WW, Hage JE, Ng AC, Chua GT, Gage SN. Reliability and role of plain film radiography and CT in the diagnosis of small-bowel obstruction. *AJR Am J Roentgenol* 1996; **167**: 1451-1455
4 **Shrake PD,** Rex DK, Lappas JC, Maglinte DD. Radiographic evaluation of suspected small bowel obstruction. *Am J Gastroenterol* 1991; **86**: 175-178
5 **Lasson A,** Loren I, Nilsson A, Nirhov N, Nilsson P. Ultrasonography in gallstone ileus: a diagnostic challenge. *Eur J Surg* 1995; **161**: 259-263
6 **Ripolles T,** Miguel-Dasit A, Errando J, Morote V, Gomez-Abril SA, Richart J. Gallstone ileus: increased diagnostic sensitivity by combining plain film and ultrasound. *Abdom Imaging* 2001; **26**: 401-405
7 **Swift SE,** Spencer JA. Gallstone ileus: CT findings. *Clin Radiol* 1998; **53**: 451-454
8 **Grumbach K,** Levine MS, Wexler JA. Gallstone ileus diagnosed by computed tomography. *J Comput Assist Tomogr* 1986; **10**: 146-148
9 **Leen GL,** Finlay M. CT diagnosis of gall stone ileus. *Acta Radiol* 1990; **31**: 497-498
10 **Lobo DN,** Jobling JC, Balfour TW. Gallstone ileus: diagnostic pitfalls and therapeutic successes. *J Clin Gastroenterol* 2000; **30**: 72-76
11 **Ihara E,** Ochiai T, Yamamoto K, Kabemura T, Harada N. A case of gallstone ileus with a spontaneous evacuation. *Am J Gastroenterol* 2002; **97**: 1259-1260
12 **Kurtz RJ,** Heimann TM, Beck AR, Kurtz AB. Patterns of treatment of gallstone ileus over a 45-year period. *Am J Gastroenterol* 1985; **80**: 95-98
13 **Syme RG.** Management of gallstone ileus. *Can J Surg* 1989; **32**: 61-64
14 **Reisner RM,** Cohen JR. Gallstone ileus: a review of 1001 reported cases. *Am Surg* 1994; **60**: 441-446
15 **Rigler LG,** Borman CN, Noble JF. Gallstone obstruction. Pathogenesis and roentgen manifestations.. *JAMA* 1941; **117**: 1753-1759
16 **Megibow AJ,** Balthazar EJ, Cho KC, Medwid SW, Birnbaum BA, Noz ME. Bowel obstruction: evaluation with CT. *Radiology* 1991; **180**: 313-318
17 **Fukuya T,** Hawes DR, Lu CC, Chang PJ, Barloon TJ. CT diagnosis of small-bowel obstruction: efficacy in 60 patients. *AJR Am J Roentgenol* 1992; **158**: 765-769; discussion 771-772
18 **Siewert B,** Raptopoulos V, Mueller MF, Rosen MP, Steer M. Impact of CT on diagnosis and management of acute abdomen in patients initially treated without surgery. *AJR Am J Roentgenol* 1997; **168**: 173-178
19 **Balthazar EJ.** George W. Holmes Lecture. CT of small-bowel obstruction. *AJR Am J Roentgenol* 1994; **162**: 255-261
20 **Maglinte DD,** Balthazar EJ, Kelvin FM, Megibow AJ. The role of radiology in the diagnosis of small-bowel obstruction. *AJR Am J Roentgenol* 1997; **168**: 1171-1180
21 **Machi J,** Ikeda A, Yarofalir J, Yahara T, Miki N. Gallstone ileus with cholecystoduodenal fistula. *Am J Surg* 2002; **183**: 56-57
22 **Abou-Saif A,** Al-Kawas FH. Complications of gallstone disease: Mirizzi syndrome, cholecystocholedochal fistula, and gallstone ileus. *Am J Gastroenterol* 2002; **97**: 249-254
23 **Kasahara Y,** Umemura H, Shiraha S, Kuyama T, Sakata K, Kubota H. Gallstone ileus. Review of 112 patients in the Japanese literature. *Am J Surg* 1980; **140**: 437-440
24 **Allen JW**, McCurry T, Rivas H, Cacchione RN. Totally laparoscopic management of gallstone ileus. *Surg Endosc* 2003; **17**: 352

Science Editor Guo SY **Language Editor** Elsevier HK

PO Box 2345, Beijing 100023, China
www.wjgnet.com
wjg@wjgnet.com

ELSEVIER

World J Gastroenterol 2005;11(14):2148-2153
World Journal of Gastroenterology ISSN 1007-9327

• *CLINICAL RESEARCH* •

Clinical significance of hepatic derangement in severe acute respiratory syndrome

Henry Lik-Yuen Chan, Ambrose Chi-Pong Kwan, Ka-Fai To, Sik-To Lai, Paul Kay-Sheung Chan, Wai-Keung Leung, Nelson Lee, Alan Wu, Joseph Jao-Yiu Sung

Henry Lik-Yuen Chan, Wai-Keung Leung, Nelson Lee, Alan Wu, Joseph Jao-Yiu Sung, Department of Medicine and Therapeutics, Chinese University of Hong Kong, Hong Kong SAR, China
Ambrose Chi-Pong Kwan, Sik-To Lai, Department of Medicine, Princess Margaret Hospital, Hong Kong SAR, China
Ka-Fai To, Department of Anatomical and Cellular Pathology, Chinese University of Hong Kong, Hong Kong SAR, China
Paul Kay-Sheung Chan, Department of Microbiology, Chinese University of Hong Kong, Hong Kong SAR, China
Correspondence to: Joseph Jao-Yiu Sung, Department of Medicine and Therapeutics, 9/F Prince of Wales Hospital, Shatin, Hong Kong SAR, China. joesung@cuhk.edu.hk
Telephone: +852-26323132 Fax: +852-26451699
Received: 2004-07-26 Accepted: 2004-09-19

Abstract

AIM: Elevation of alanine aminotransferase (ALT) level is commonly seen among patients suffering from severe acute respiratory syndrome (SARS). We report the progression and clinical significance of liver derangement in a large cohort of SARS patient.

METHODS: Serial assay of serum ALT was followed in patients who fulfilled the WHO criteria of SARS. Those with elevated ALT were compared with those with normal liver functions for clinical outcome. Serology for hepatitis B virus (HBV) infection was checked. Adverse outcomes were defined as oxygen desaturation, need of intensive care unit (ICU) and mechanical ventilation and death.

RESULTS: Two hundred and ninety-four patients were included in this study. Seventy (24%) patients had elevated serum ALT on admission and 204 (69%) patients had elevated ALT during the subsequent course of illness. Using peak ALT >5×ULN as a cut-off and after adjusting for potential confounding factors, the odds ratio of peak ALT >5× ULN for oxygen desaturation was 3.24 (95%CI 1.23-8.59, P = 0.018), ICU care was 3.70 (95%CI 1.38-9.89, P = 0.009), mechanical ventilation was 6.64 (95%CI 2.22-19.81, P = 0.001) and death was 7.34 (95%CI 2.28-24.89, P = 0.001). Ninety-three percent of the survived patients had ALT levels normalized or were on the improving trend during follow-up. Chronic hepatitis B was not associated with worse clinical outcomes.

CONCLUSION: Reactive hepatitis is a common complication of SARS-coronavirus infection. Those patients with severe hepatitis had worse clinical outcome.

Key words: SARS; Hepatitis; Hepatitis B virus; Coronavirus

Chan HLY, Kwan ACP, To KF, Lai ST, Chan PKS, Leung WK, Lee N, Wu A, Sung JJY. Clinical significance of hepatic derangement in severe acute respiratory syndrome. *World J Gastroenterol* 2005; 11(14): 2148-2153
http://www.wjgnet.com/1007-9327/11/2148.asp

INTRODUCTION

Severe acute respiratory syndrome (SARS) is caused by a novel coronavirus (SARS-coronavirus, SARS-CoV) infecting primarily the lung and the enteric tract[1-9]. Up to August 2003, there were 8 422 reported cases worldwide and 916 cases died of this condition[10]. Although the outbreak of SARS is currently under control, the source of SARS-CoV has not been identified and the threat of SARS returning in winter persists.

Case series in Hong Kong and Toronto indicated that SARS is not merely a respiratory disease. Diarrhea and bleeding diathesis had also been reported in patients infected by SARS-CoV[11,12]. In our previous report, SARS-CoV was found in biopsy of small intestine and colon of patients with diarrhea[11]. Deranged liver functions were reported in 22-56% of patients at the time of hospital admission[13-17]. In a previous study, it has also been suggested that co-infection with hepatitis B virus (HBV) is associated with more severe respiratory disease[18]. The cause of impaired liver function, its clinical implication and association with HBV co-infection have not been fully explored.

In this study, we follow the natural course of hepatic involvement in SARS. The impact of liver derangement and chronic HBV infection on the clinical outcome of SARS patients is revisited.

MATERIALS AND METHODS

Patients

Patients in the present study were collected from a university medical center (Prince of Wales Hospital) and a community hospital (Princess Margaret Hospital) designated to look after SARS patients during the outbreak in Hong Kong. All patients fulfilled the case definitions of SARS by the World Health Organization, i.e., temperature above 38 ℃, difficulty in breathing and cough, pneumonic changes on chest X-ray or high-resolution computed tomography, and contact history with SARS patients[19]. All patients were initially treated with empirical antibiotics including cefotaxime and

clarithromycin (or levofloxacin) to cover common pathogens causing community-acquired pneumonia. Oseltamivir (Tamiflu) was also given to treat possible influenza infection when little was known about SARS during the early phase of the outbreak. If fever persisted for more than 48 h, all patients received corticosteroids and ribavirin treatment. The choice of corticosteroids was intravenous hydrocortisone 100 mg every 8 h or oral prednisolone 1 mg/kg body weight per day. Ribavirin was given at 400 mg every 8 h intravenously or 1 200 mg thrice a day orally. Pulse intravenous methylprednisolone (500-1 000 mg/d), up to a maximum dose of 3 g, was given when there were signs of radiological or clinical deterioration. Patients, with oxygen saturation that fell below 90% at room air, were offered supplementary oxygen through nasal cannula. Those who required more than 4 L/min oxygen would be transferred to intensive care unit (ICU) for close monitoring. Mechanical ventilation by CPAP was implemented, when patients could not achieve 90% oxygen saturation despite receiving 5 L/min oxygen or more. All patients were kept in hospital for monitoring for at least 3 wk before discharge. Liver enzymes were checked every 1-3 d during hospital stay, on discharge and on follow-up visits. Clinical outcomes were assessed at least 8 wk after the admission of patients.

Serological assays

The level of anti-coronavirus IgG antibody was measured by immunofluorescence assay. Paired sera from acute (taken within 7 d after the onset of fever) and convalescent (taken 14-21 d after the onset of fever) blood samples were tested at serial two-fold dilutions starting from 1:40. Positive serological evidence of coronavirus infection was defined as either having a seroconversion or $\geqslant$four-fold rise in antibody titer. Hepatitis B surface antigen (HBsAg) and hepatitis C antibodies (anti-HCV) were tested by commercially available enzyme-linked immunosorbent assay kits (Abbott GmBH Diagnostika, Wiesbaden-Delkenheim, Germany). Hepatitis B e antigen (HBeAg) and antibodies to hepatitis B e antigen (anti-HBe) were measured by ELISA (Sanofi Diagnostics, Pasteur, France).

Data analysis

Continuous variables were expressed as mean±SD for normal distribution data and median (range) if the distribution was skewed. Statistical analysis was performed by SPSS (version 11.0, Chicago). Categorical variables were compared by χ^2 test and continuous variables by Student's *t* test or Mann-Whitney *U* test as appropriate. Adverse clinical outcomes were defined as need of oxygen desaturation requiring oxygen supplementation, ICU admission, mechanical ventilation, liver decompensation and mortality. Liver decompensation was defined as development of hepatic encephalopathy associated with elevated serum bilirubin (>51 mmol/L) and prolonged prothrombin time (>16 s). As the reference ranges of alanine aminotransferase (ALT) levels were different between the two hospitals, ALT levels were expressed as folds of increase above the upper limit of normal (ULN) in individual laboratories. The relationships of peak ALT levels and various adverse clinical outcomes were compared by receiver operator characteristic curve. Baseline clinical characteristics with a *P* value <0.1 for adverse clinical outcomes on comparing patients with high peak ALT levels vs. those with lower ALT levels were adjusted by multivariate logistic regression analysis. All statistical tests were two-sided. *P* value <0.05 was statistically significant.

RESULTS

Clinical characteristics

Two hundred and ninety-four patients including 126 male (43%) and 168 female were included in this study. The median age of this cohort was 36 years, range 12-83 years. Two hundred and forty-three patients had paired blood samples checked for SARS-CoV serology and all had positive results. These patients were admitted on the third (range 0-11) day after the onset of fever. Thirty (10%) patients were found to have positive HBsAg and 214 patients had negative HBsAg. In 50 cases, HBsAg status was not checked during hospitalization. All patients in the Prince of Wales cohort had negative anti-HCV antibodies, and 7 of 12 HBV-infected patients had positive HBeAg. Anti-HCV and HBeAg status were not routinely monitored in the Princess Margaret Hospital cohort. Lamivudine (100 mg/d) was commenced in 20 of the 30 chronic hepatitis B patients on or before the commencement of corticosteroid treatment and was continued thereafter. Two chronic hepatitis B infected patients had co-existing liver cirrhosis. One of them had inoperable multi-focal hepatocellular carcinoma and the other was admitted for bleeding esophageal variceal. Forty-one (14%) patients had other co-morbid illnesses including hypertension (12), diabetes mellitus (5), end-stage renal failure (2), chronic rheumatic heart disease (2), ischemia heart disease (2), sick sinus syndrome (1), atrial fibrillation (1), asthma (1), chronic obstructive airway disease (1), bronchiectasis (1), old pulmonary tuberculosis (1), previous cerebrovascular accident (1), autism (1) and pregnancy (1).

Overall, 141 (48%) patients had oxygen desaturation, 50 (17%) required admission to ICU, 33 (11%) patients required mechanical ventilation, and 27 (9%) patients died. None of the patients developed liver decompensation after contracting SARS. All mortalities were due to respiratory failure related to SARS with or without sepsis and multi-organ failure. The outcome of the studied cohort is summarized in Figure 1.

Liver enzyme derangement on admission

Seventy (24%) patients, including 15 chronic hepatitis B-infected patients, had elevated ALT levels on admission. The median ALT levels on admission was 0.55 (0.16-26.09) times upper limit of laboratory normal. The proportion of patients with different ALT levels, serum bilirubin and prothrombin time on admission are shown in Figure 2. Two chronic hepatitis B infected patients were admitted with icteric flare-up of chronic hepatitis B on lamivudine treatment and contracted SARS during their hospital stay. They had elevated serum bilirubin to more than 150 mmol/L and one of them had prolonged prothrombin time to 17 s. All other patients who had elevated ALT levels had normal

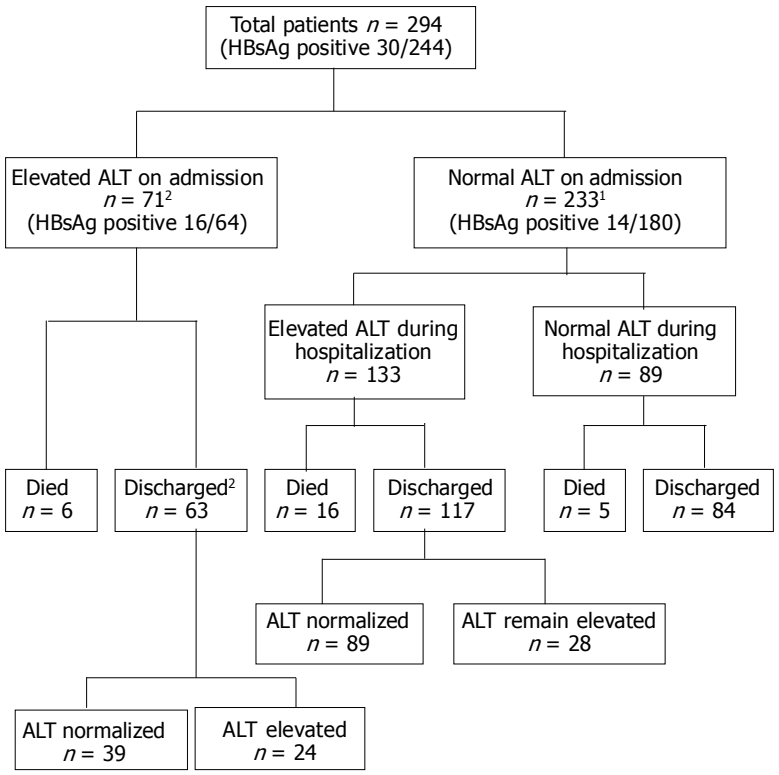

Figure 1 Clinical outcomes of patients included in the study. ALT, alanine aminotransferase. [1]One patient did not have serial ALT results. [2]Two patients did not have follow-up ALT results after discharge.

serum bilirubin levels and had no evidence of hepatic decompensation.

Progression of liver derangement on follow-up

During the course of illness, 204 (69%) patients, including 23 HBsAg-positive patients, had elevated ALT levels. Majority of patients had ALT levels elevated at day 5-7 from fever onset and ALT peaked at the end of second week (Figure 3). The median peak ALT levels was 1.53 (0.28-316.25) times ULN. The proportion of patients with different peak ALT levels, serum bilirubin and prothrombin time are shown in Figure 2. Twenty-eight (9.5%) patients had ALT raised to over 5× ULN; among them 7 patients had elevated serum bilirubin (median 83 mmol/L, range 48-231 mmol/L) and 10 patients had elevated prothrombin time (median 20 s, range 14-56 s). Among the 138 patients in the Prince of Wales Hospital cohort, the median peak alkaline phosphatase (ALP) level was 0.78 (range 0.31-19.38) times ULN and 40 (29%) patients had experienced elevated ALP during the course of illness. None of these patients developed hepatic encephalopathy. Seven of the 28 (25%) patients died of SARS and multi-organ failure. On the other hand, only 5 of 89 (6%) patients who had persistently normal ALT died.

The area under the receiver operator characteristic curve of peak ALT for oxygen desaturation, need of ICU care, mechanical ventilation and mortality were 0.70 (95%CI 0.64-0.75; $P<0.001$), 0.72 (95%CI 0.65-0.79; $P<0.001$), 0.71 (95%CI 0.62-0.80, $P<0.001$) and 0.65 (95%CI 0.54-0.76,

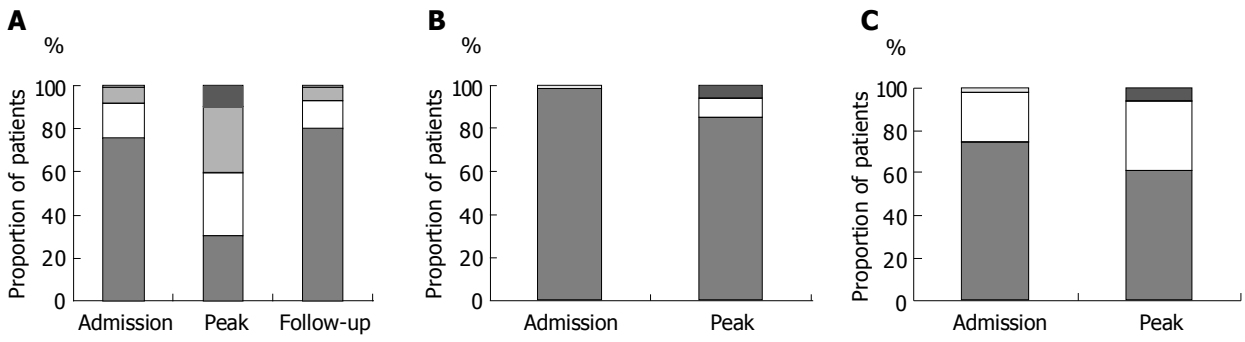

Figure 2 A: Proportion of patients with different ALT levels at initial visit (n = 294), at peak ALT (n = 293; 1 missing data) and on last follow-up (n = 264; 27 patients died, 3 missing data). ALT normal■, 1–2× ULN□, 2–5× ULN■, >5× ULN■. B: Proportion of patients with different serum bilirubin levels at initial visit (n = 294) and at peak bilirubin (n = 293, 1 missing data). <35 μmol/L■, 35–51 μmol/L□, >51 μmol/L■. C: Proportion of patients with different prothrombin time at initial visit (n = 293, one missing data) and at peak prothrombin time (n = 283, 11 missing data). <12 s■, 12–16 s□, >16 s■.

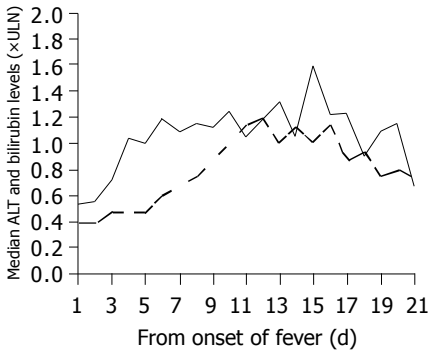

Figure 3 Median ALT and serum bilirubin levels of patients admitted to Prince of Wales Hospital (n = 138) from the day of fever onset to day 21 at hospital discharge. Both ALT and bilirubin levels were expressed as folds of ULN. Only patients who had at least one elevated ALT level during admission were included (n=104). ULN, upper limit of laboratory normal; solid line, serum ALT; broken line, serum bilirubin.

P = 0.011), respectively. Using the coordinate of peak ALT >5× ULN, the sensitivity and specificity for any adverse outcomes were 15-27% and 93-95% respectively. Patients who had peak ALT over 5× ULN had significant male predominance, more co-existing co-morbid conditions, more chronic hepatitis B patients and marginally higher serum creatinine levels as compared to those who had lower peak ALT levels (Table 1). Using peak ALT >5×ULN as a cut-off and after adjusting these potential confounding factors, the odds ratio of peak ALT >5×ULN for oxygen desaturation was 3.24 (95%CI 1.23-8.59, P = 0.018), ICU care was 3.70 (95%CI 1.38-9.89, P = 0.009), mechanical ventilation was 6.64 (95%CI 2.22-19.81, P = 0.001) and death was 7.34 (95%CI 2.28-24.89, P = 0.001).

Excluding 27 patients who died and 3 patients who had no follow-up ALT results, 84 of 264 (32%) patients had persistently normal ALT levels during the entire course of illness. Among the 180 patients who had elevated ALT levels, 128 (71%) had ALT subsequently normalized and 37 (21%) patients had ALT on downward trend at the last follow-up visit. The remaining 8% of patients still had elevated ALT levels on the last follow-up.

Co-infection with hepatitis B virus

Two of the 30 HBsAg-positive patients died despite lamivudine treatment. One patient was admitted for icteric flare-up of chronic hepatitis B and the other had liver cirrhosis admitted for esophageal variceal bleeding. Both patients acquired SARS during their hospital stay. Seven patients had persistently normal ALT levels throughout the admission and follow-up visits (six were on lamivudine). Twenty-one HBsAg-positive patients had elevated ALT during the SARS illness. Among them, 10 patients (6 on lamivudine) had transient elevation of ALT which subsequently returned to normal levels, 8 (5 on lamivudine) had declining levels of ALT and 3 patients (1 on lamivudine) had persistently elevated ALT levels. In this series, co-infection with viral hepatitis B was not associated with higher peak ALT level, increased risk of oxygen desaturation, ICU admission, mechanical ventilation or mortality (Table 2).

Table 1 Univariate analysis of baseline clinical characteristics among patients with peak ALT levels >5× ULN *vs* with patients with peak ALT levels ≤5× ULN

	Peak ALT >5× ULN	Peak ALT ≤5× ULN	*P*
Number of patients	28	265	
Age (yr)	40±14	39±15	0.68
Male	17 (61%)	109 (41%)	<0.001
Co-morbid	4 (14%)	37 (14%)	0.002
Hemoglobin (g/dL)	13.4±2.1	13.4 ±1.5	0.94
White cell count (×10^9/L)	5.3±2.3	5.0±2.0	0.49
Neutrophil (×10^9/L)	4.2±1.9	3.8±1.9	0.30
Lymphocyte (×10^9/L)	0.8±0.5	0.8±0.5	0.90
Platelet (×10^9/L)	146±53	151±53	0.64
Creatinine (μmol/L)	83 (48–1 318)	79 (43–214)	0.09
HBsAg	6/25 (24%)	24/218 (11%)	<0.001
Oxygen supplementation	21 (75%)	120 (45%)	<0.001
ICU care	11 (39%)	39 (15%)	<0.001
Mechanical ventilation	9 (32%)	24 (9%)	0.012
Death	7 (25%)	20 (8%)	0.017

Table 2 Clinical outcome of patients with and without chronic hepatitis B

	HBsAg positive	HBsAg negative	*P*
Number of patients	30	214	
Peak ALT (×ULN)	2.2 (0.6–26.1)	1.5 (0.3–316.3)	0.16
Oxygen supplementation	17 (57%)	104 (49%)	0.68
ICU care	5 (17%)	30 (14%)	0.70
Mechanical ventilation	3 (10%)	19 (9%)	0.84
Death	2 (7%)	14 (7%)	0.98

DISCUSSION

Although SARS is primarily a pulmonary disease, liver derangement was commonly observed[13-17]. In this study, approximately a quarter of patients had elevated ALT on admission, and a further 45% of patients who had normal ALT on admission had ALT elevation during the course of illness. In a majority of patients ALT levels started to elevate towards the end of first week and peak at the end of second week. High peak ALT level appears to be an independent predictor of more severe illness and worse clinical outcome. Most patients however had transient elevation of ALT, which normalize spontaneously with the recovery of SARS.

The underlying cause for ALT elevation was uncertain but several mechanisms were worth considering. Direct pathogenic effect of SARS-CoV on the liver is unlikely due to the failure of identification of SARS-CoV or specific hepatitis features in the liver at autopsy in previous reports[20-23]. Elevated ALT might be related to the prescribed medications including antibiotics and high dose ribavirin. As a quarter of patients had elevated ALT levels on admission well before the prescription of drugs, drug treatment should not be the cause of liver enzyme derangement in these patients. Furthermore, many patients had ALT >5× ULN. This is exceedingly rare with antibiotic and ribavirin given at these dosages[24]. Although chronic hepatitis C virus infection has only been excluded in about half of the cases in this series (the Prince of Wales Hospital cohort), the prevalence of chronic hepatitis C is very low among the general population in Hong Kong.

We believe that the elevation of liver enzyme is a reactive response towards SARS-CoV infection[25]. The hepatic acute phase response involving cytokine release from inflammatory cells is a defense reaction of the body against the causative agent to protect the vital functions of the liver[26]. The liver enzyme elevation in SARS is not typical of cholestasis secondary to sepsis as majority of patients did not have accompanied elevation of ALP. This is usually a transient reaction and therefore majority of patients have ALT levels returned to normal after recovery.

Although SARS-CoV is not a direct cause of liver injury, results from this study indicated that gross liver enzyme elevation, as indicated by high peak ALT levels, is an independent factor associated with poor clinical outcome. Peak ALT over 5×ULN increased the risk of mortality by seven-folds. Although age and co-morbid illnesses had been found to have significant negative impact on prognosis in SARS[6,13,18,27], in this study, the age of patients did not differ significantly between those with high or low peak ALT levels. Baseline ALT levels have not been found to be associated with any adverse clinical outcome in the past probably because of the delayed elevation of ALT levels in most patients. In fact most immunological damage of SARS in the lungs occurred in the second week of the illness[12,28]. The level of ALT elevation may reflect the severity of acute phase response, which in turn may reflect the severity of tissue damage in SARS[17]. We believe that the elevated ALT can serve as a surrogate marker to predict the clinical outcome of SARS.

We did not find any difference in various adverse clinical outcomes among chronic hepatitis B patients as compared to the HBsAg-negative patients. In our cohort, 16 (53%) chronic hepatitis B patients had elevated ALT levels upon admission and two of them suffered from icteric flare-up of hepatitis. Perhaps those patients who suffered from severe flare-up of hepatitis or decompensated liver cirrhosis might have a higher risk of mortality[29]. Lamivudine was not prescribed to one-third of the patients but none of them died or developed hepatic decompensation.

In conclusion, we found that elevation of transaminase is a very common feature in SARS. The ALT elevation is usually transient and likely to be reactive in nature. Co-infection with HBV in the absence of liver cirrhosis or reactivated hepatitis does not affect the natural course of the disease.

REFERENCES

1 **Ksiazek TG**, Erdman D, Goldsmith CS, Zaki SR, Peret T, Emery S, Tong S, Urbani C, Comer JA, Lim W, Rollin PE, Dowell SF, Ling AE, Humphrey CD, Shieh WJ, Guarner J, Paddock CD, Rota P, Fields B, DeRisi J, Yang JY, Cox N, Hughes JM, LeDuc JW, Bellini WJ, Anderson LJ. A novel coronavirus associated with severe acute respiratory syndrome. *N Engl J Med* 2003; **348**: 1953-1966

2 **Drosten C**, Gunther S, Preiser W, van der Werf S, Brodt HR, Becker S, Rabenau H, Panning M, Kolesnikova L, Fouchier RA, Berger A, Burguiere AM, Cinatl J, Eickmann M, Escriou N, Grywna K, Kramme S, Manuguerra JC, Muller S, Rickerts V, Sturmer M, Vieth S, Klenk HD, Osterhaus AD, Schmitz H, Doerr HW. Identification of a novel coronavirus in patients with severe acute respiratory syndrome. *N Engl J Med* 2003; **348**: 1967-1976

3 **Peiris JS**, Lai ST, Poon LL, Guan Y, Yam LY, Lim W, Nicholls J, Yee WK, Yan WW, Cheung MT, Cheng VC, Chan KH, Tsang DN, Yung RW, Ng TK, Yuen KY. Coronavirus as a possible cause of severe acute respiratory syndrome. *Lancet* 2003; **361**: 1319-1325

4 **Marra MA**, Jones SJ, Astell CR, Holt RA, Brooks-Wilson A, Butterfield YS, Khattra J, Asano JK, Barber SA, Chan SY, Cloutier A, Coughlin SM, Freeman D, Girn N, Griffith OL, Leach SR, Mayo M, McDonald H, Montgomery SB, Pandoh PK, Petrescu AS, Robertson AG, Schein JE, Siddiqui A, Smailus DE, Stott JM, Yang GS, Plummer F, Andonov A, Artsob H, Bastien N, Bernard K, Booth TF, Bowness D, Czub M, Drebot M, Fernando L, Flick R, Garbutt M, Gray M, Grolla A, Jones S, Feldmann H, Meyers A, Kabani A, Li Y, Normand S, Stroher U, Tipples GA, Tyler S, Vogrig R, Ward D, Watson B, Brunham RC, Krajden M, Petric M, Skowronski DM, Upton C, Roper RL. The Genome sequence of the SARS-associated coronavirus. *Science* 2003; **300**: 1399-1404

5 **Rota PA**, Oberste MS, Monroe SS, Nix WA, Campagnoli R, Icenogle JP, Penaranda S, Bankamp B, Maher K, Chen MH, Tong S, Tamin A, Lowe L, Frace M, DeRisi JL, Chen Q, Wang D, Erdman DD, Peret TC, Burns C, Ksiazek TG, Rollin PE, Sanchez A, Liffick S, Holloway B, Limor J, McCaustland K, Olsen-Rasmussen M, Fouchier R, Gunther S, Osterhaus AD, Drosten C, Pallansch MA, Anderson LJ, Bellini WJ. Characterization of a novel coronavirus associated with severe acute respiratory syndrome. *Science* 2003; **300**: 1394-1399

6 **Yeh SH**, Wang HY, Tsai CY, Kao CL, Yang JY, Liu HW, Su IJ, Tsai SF, Chen DS, Chen PJ. Characterization of severe acute respiratory syndrome coronavirus genomes in Taiwan: molecular epidemiology and genome evolution. *Proc Natl Acad Sci USA* 2004; **101**: 2542-2547

7 **Chim SS**, Tsui SK, Chan KC, Au TC, Hung EC, Tong YK, Chiu RW, Ng EK, Chan PK, Chu CM, Sung JJ, Tam JS, Fung KP, Waye MM, Lee CY, Yuen KY, Lo YM. Genomic characterisation of the severe acute respiratory syndrome coronavirus of Amoy Gardens outbreak in Hong Kong. *Lancet* 2003; **362**: 1807-1808

8 **Nicholls JM**, Poon LL, Lee KC, Ng WF, Lai ST, Leung CY, Chu CM, Hui PK, Mak KL, Lim W, Yan KW, Chan KH, Tsang NC, Guan Y, Yuen KY, Peiris JS. Lung pathology of fatal severe acute respiratory syndrome. *Lancet* 2003; **361**: 1773-1778

9 **Chan HL**, Tsui SK, Sung JJ. Coronavirus in severe acute respiratory syndrome (SARS). *Trends Mol Med* 2003; **9**: 323-325

10 World Health Organization. Summary table of SARS cases by country, 1 November 2002 - 7 August 2003. http://www.who.int/csr/sars/country/2003_08_15/en/

11 **Leung WK**, To KF, Chan PK, Chan HL, Wu AK, Lee N, Yuen KY, Sung JJ. Enteric involvement of severe acute respiratory syndrome-associated coronavirus infection. *Gastroenterology* 2003; **125**: 1011-1017

12 **Wong RS**, Wu A, To KF, Lee N, Lam CW, Wong CK, Chan PK, Ng MH, Yu LM, Hui DS, Tam JS, Cheng G, Sung JJ. Haematological manifestations in patients with severe acute respiratory syndrome: retrospective analysis. *BMJ* 2003; **326**: 1358-1362

13 **Lee N**, Hui D, Wu A, Chan P, Cameron P, Joynt GM, Ahuja A, Yung MY, Leung CB, To KF, Lui SF, Szeto CC, Chung S, Sung JJ. A major outbreak of severe acute respiratory syndrome in Hong Kong. *N Engl J Med* 2003; **348**: 1986-1994

14 **Booth CM**, Matukas LM, Tomlinson GA, Rachlis AR, Rose DB, Dwosh HA, Walmsley SL, Mazzulli T, Avendano M, Derkach P, Ephtimios IE, Kitai I, Mederski BD, Shadowitz SB, Gold WL, Hawryluck LA, Rea E, Chenkin JS, Cescon DW, Poutanen SM, Detsky AS. Clinical features and short-term outcomes of 144 patients with SARS in the greater Toronto area. *JAMA* 2003; **289**: 2801-2809

15 **Poutanen SM**, Low DE, Henry B, Finkelstein S, Rose D, Green K, Tellier R, Draker R, Adachi D, Ayers M, Chan AK, Skowronski DM, Salit I, Simor AE, Slutsky AS, Doyle PW, Krajden M, Petric M, Brunham RC, McGeer AJ. Identification of

severe acute respiratory syndrome in Canada. *N Engl J Med* 2003; **348**: 1995-2005
16 **Choi KW**, Chau TN, Tsang O, Tso E, Chiu MC, Tong WL, Lee PO, Ng TK, Ng WF, Lee KC, Lam W, Yu WC, Lai JY, Lai ST. Outcomes and prognostic factors in 267 patients with severe acute respiratory syndrome in Hong Kong. *Ann Intern Med* 2003; **139**: 715-723
17 **Wong WM**, Ho JC, Ooi GC, Mok T, Chan J, Hung IF, Ng W, Lam YM, Tam WO, Wong BC, Wong PC, Ho PL, Lai CL, Lam WK, Lam SK, Tsang KW. Temporal patterns of hepatic dysfunction and disease severity in patients with SARS. *JAMA* 2003; **290**: 2663-2665
18 **Peiris JS,** Chu CM, Cheng VC, Chan KS, Hung IF, Poon LL, Law KI, Tang BS, Hon TY, Chan CS, Chan KH, Ng JS, Zheng BJ, Ng WL, Lai RW, Guan Y, Yuen KY. Clinical progression and viral load in a community outbreak of coronavirus-associated SARS pneumonia: a prospective study. *Lancet* 2003; **361**: 1767-1772
19 World Health Organization. Case definition for surveillance of severe acute respiratory syndrome (SARS). http://www.who.int/csr/sars/caedefinition/en (accessed August 29, 2003)
20 **MacPhee PJ**, Dindzans VJ, Fung LS, Levy GA. Acute and chronic changes in the microcirculation of the liver in inbred strains of mice following infection with mouse hepatitis virus type 3. *Hepatology* 1985; **5**: 649-660
21 **Levy GA**, MacPhee PJ, Fung LS, Fisher MM, Rappaport AM. The effect of mouse hepatitis virus infection on the microcirculation of the liver. *Hepatology* 1983; **3**: 964-973
22 **Chan HL**, Leung WK, To KF, Chan PK, Lee N, Wu A, Tam JS, Sung JJ. Retrospective analysis of liver function derangement in severe acute respiratory syndrome. *Am J Med* 2004; **116**: 566-567
23 **Zhang JZ**. Severe acute respiratory syndrome and its lesions in digestive system. *World J Gastroenterol* 2003; **9**: 1135-1138
24 Investigator Brouchure. Ribavirin (SCH 18908). A nucleoside analogue, broad-spectrum antiviral agent for the oral treatment of chronic hepatitis C in combination with INTRON A (interferon alfa-2b recombinant [SCH 30500]. Schering Plough 1997
25 **Ding Y**, Wang H, Shen H, Li Z, Geng J, Han H, Cai J, Li X, Kang W, Weng D, Lu Y, Wu D, He L, Yao K. The clinical pathology of severe acute respiratory syndrome (SARS): a report from China. *J Pathol* 2003; **200**: 282-289
26 **Buschenfelde KHM**, Gerken G. Immune mechanisms in the production of liver diseases. In Zakin D and Boyer TD ed: Hepatology. A Textbook of Liver Diseases, ed 4. Philadelphia, *Saunders* 2003: 1127-1163
27 **Donnelly CA**, Ghani AC, Leung GM, Hedley AJ, Fraser C, Riley S, Abu-Raddad LJ, Ho LM, Thach TQ, Chau P, Chan KP, Lam TH, Tse LY, Tsang T, Liu SH, Kong JH, Lau EM, Ferguson NM, Anderson RM. Epidemiological determinants of spread of causal agent of severe acute respiratory syndrome in Hong Kong. *Lancet* 2003; **361**: 1761-1766
28 **Wu KL**, Lu SN, Changchien CS, Chiu KW, Kuo CH, Chuah SK, Liu JW, Lin MC, Eng HL, Chen SS, Lee CM, Chen CL. Sequential changes of serum aminotransferase levels in patients with severe acute respiratory syndrome. *Am J Trop Med Hyg* 2004; **71**: 125-128
29 **Hui AY**, Chan HL, Liew CT, Chan PK, To KF, Chan CP, Sung JJ. Fatal outcome of SARS in a patient with reactivation of chronic hepatitis B. *Am J Med* 2003; **115**: 334-336

Science Editor Guo SY **Language Editor** Elsevier HK

PO Box 2345, Beijing 100023, China
www.wjgnet.com
wjg@wjgnet.com

ELSEVIER

World J Gastroenterol 2005;11(14):2154-2156
World Journal of Gastroenterology ISSN 1007-9327

• *BRIEF REPORTS* •

Systemic immune responses to oral administration of recombinant attenuated *Salmonella typhimurium* expressing *Helicobacter pylori* urease in mice

Xiao-Feng Liu, Jia-Lu Hu, Qi-Zheng Quan, Zi-Qin Sun, Yao-Jun Wang, Feng Qi

Xiao-Feng Liu, Qi-Zheng Quan, Zi-Qin Sun, Yao-Jun Wang, Feng Qi, Department of Gastroenterology, General Hospital of Jinan Military Command Area, Jinan 250031, Shandong Province, China
Jia-Lu Hu, Institute of Gastroenterology, Xijing Hospital, Fourth Military Medical University, Xi'an 710032, Shaanxi Province, China
Correspondence to: Dr. Xiao-Feng Liu, Department of Gastroenterology, General Hospital of Jinan Military Command Area, Jinan 250031, Shandong Province, China. liuxf0531@21cn.com
Telephone: +86-531-6732012
Received: 2003-04-12 Accepted: 2003-05-19

Abstract

AIM: To evaluate whether attenuated *Salmonella typhimurium* producing *Helicobacter pylori* (*H pylori*) urease subunit B (UreB) could induce systemic immune responses against *H pylori* infection.

METHODS: Attenuated *S. typhimurium* SL3261 was used as a live carrier of plasmid pTC01-UreB, which encodes recombinant *H pylori* UreB protein. Balb/c mice were given oral immunization with two doses of SL3261/pTC01-UreB at a 3-wk interval. Twelve weeks after oral immunization of mice, serum IgG antibodies were evaluated by ELISA assay. Gamma interferon (IFN-γ) and interleukin 10 (IL-10) in the supernatant of spleen cell culture were also assessed by ELISA.

RESULTS: After oral immunization of mice, serum specific IgG antibodies against UreB in vaccine group were much higher than that in PBS and native *Salmonella* SL3261 control groups (A_{450}, 0.373±0.100 *vs* 0.053±0.022, 0.142±0.039, respectively, $P<0.01$). Moreover, IFN-γ in vaccine group was on average 167.53±29.93 pg/mL, which showed a significant increase *vs* that of PBS control group (35.68±3.55 pg/mL, $P<0.01$). There was also a tremendous increase of IL-10 in vaccine group compared to PBS and SL3261 control groups (275.13±27.65 pg/mL *vs* 56.00±7.15 pg/mL, 68.02±15.03 pg/mL, respectively, $P<0.01$). In addition, no obvious side effects in mice and no change in gastric inflammation were observed.

CONCLUSION: The multiple oral immunizations with the attenuated *S. typhimurium* expressing *H pylori* UreB could induce significant systemic immune responses, suggesting it may be used as oral vaccine against *H pylori* infection.

Key words: *Helicobacter pylori*; *Salmonella typhimurium*; Vaccine; Systemic immune

Liu XF, Hu JL, Quan QZ, Sun ZQ, Wang YJ, Qi F. Systemic immune responses to oral administration of recombinant attenuated *Salmonella typhimurium* expressing *Helicobacter pylori* urease in mice. *World J Gastroenterol* 2005; 11(14): 2154-2156
http://www.wjgnet.com/1007-9327/11/2154.asp

INTRODUCTION

Helicobacter pylori (*H pylori*) is one of the most common bacteria worldwide, which infects more than 50% of the human population[1]. It is generally recognized that *H pylori* infection is a major etiological factor in chronic gastritis, peptic ulcer disease, gastric adenocarcinoma and gastric B-cell lymphoma (MALT). The current therapy, based on the use of a proton-pump inhibitor and antibiotics, is efficacious but faces many problems such as patient compliance, possible recurrence of infection, complex dosing, costs and various side effects, and most importantly, development of antibiotic resistance. These compromise widespread clinical use. As a consequence, new strategies for the prevention and eradication of *H pylori* infections are being explored. Vaccines are an attractive option, because they are both effective and economic in use. It is widely accepted that, given the worldwide prevalence of *H pylori* infection, vaccination would be a preferable strategy[2]. A number of trials indicate that attenuated *Salmonella typhimurium* strains can be used to deliver foreign antigens[3]. So, we had established recombinant attenuated *S. typhimurium* SL3261 expressing *H pylori* urease B subunit (UreB), which could elicit strong mucosal immune responses[4]. The purpose of the present study was to determine whether it could induce specific immune responses and whether it could be used as oral vaccine against *H pylori* infection.

MATERIALS AND METHODS

Animals

Four to six weeks old female Balb/c mice were purchased from the Animal Resources Center, Fourth Military Medical University, Guangzhou. The animals were fed on a commercial diet and given water ad libitum.

Bacterial strains, media, and growth

The attenuated *S. typhimurium* SL3261 (*S. typhimurium* WARY hisG 46 aroA del 407 Fusaricres, *etc.*) kindly provided by

Professor DamingRen (Institute of Genetics, Fudan University, Shanghai) were grown routinely at 37 ℃ in solid or liquid Luria medium.

Immunization of mice

Three groups of mice including controls were used as follows: (1) PBS control group was non-immunized mice that received PBS; (2) native *Salmonella* control group was mice that received attenuated *S. typhimurium* SL3261 strain; and (3) the vaccine group (SL3261/pTC01-UreB group) was mice immunized with *S. typhimurium* SL3261/pTC01-UreB. Prior to immunizations mice were left overnight without solid food and 4 h without water. One hundred microliters of 3% sodium bicarbonate were as given orally using a stainless steel catheter to neutralize the stomach pH. Immediately after stomach neutralization, mice from the PBS control group received 100 μL PBS, and mice from the *Salmonella* control group and vaccine group, received 5.0×10^9 cfu of *S. typhimurium* strain SL3261 or SL3261/pTC01-UreB, respectively, in a total volume of 100 μL. Water and food were returned to the mice after immunization. Three groups of mice were given twice oral dose treatment at a 3-wk interval.

ELISA assays

Twelve weeks after final oral immunization of mice, 150 μL of blood were collected retro-orbitally. Anti-UreB IgG antibodies in serum were detected by sandwich ELISA[5].

Cytokine measurement

Spleen cells were isolated by forcing the tissue through nylon cell strainers and resuspended in complete medium containing 15% fetal calf serum as routine method. After 48 h, the supernatant of spleen cell culture was collected. The presence of gamma interferon (IFN-γ) and interleukin 10 (IL-10) in the supernatant was detected by ELISA.

Analysis of anti-urease antibodies in mouse sera by immunoblotting

H pylori strain SS1 whole-cell lysates were analyzed by Western blotting. After SDS-PAGE, a 1:50 dilution of mouse serum in 5% non-fat milk-TBS was added to the strips[5].

Histology

Biopsy specimens from the antrum and the corpus were fixed in 10% buffered formalin, and 4-μm sections were cut. Sections were stained with HE to grade gastritis.

In vitro recombinant attenuated S. typhimurium SL3261/pTC01-UreB stability

S. typhimurium SL3261/pTC01-UreB was grown in Luria broth at 37 ℃ for 80 generations. For every 10 generations, number of chloromycetin resistant cfu was determined on LB-agar plates supplemented with 170 μg/mL chloromycetin. In the final generation, the expression of UreB protein was evaluated by Western blotting.

Statistical analysis

The differences in anti-UreB IgA and IgG antibodies as well as IFN-γ and IL-10 from immunized and non-immunized mice were evaluated using *t*-test. Differences were considered significant at *P* values <0.01.

RESULTS

Serum anti-UreB IgA antibodies in protected mice

As indicated in Table 1, the multiple oral immunizations with SL3261/pTC01-UreB could induce significant *H pylori*-specific serum IgG responses ($P<0.01$) (Table 1).

Table 1 Detection of intestinal IgA and serum IgG (A_{450}, mean±SD)

	PBS group	SL3261 group	Vaccine group
Serum IgG	0.053±0.022	0.142±0.039	0.373±0.100[b]

[b]$P<0.01$ *vs* PBS and SL3261 control groups.

Measurement of cytokine IFN-γ and IL-10

The difference in IFN-γ and IL-10 between immunized mice and non-immunized mice (PBS) was significant ($P<0.01$). Although the difference in IL-10 between mice immunized with strain SL3261 alone and strain SL3261/pTC01-UreB was also significant ($P<0.01$), there was no significant increase of IFN-γ between SL3261 group and SL3261/pTC01-UreB group (Table 2).

Table 2 Measurement of IFN-γ and IL-10 (pg/mL, mean±SD)

	PBS group	SL3261 group	Vaccine group
IFN-γ	35.68±3.55	118.74±16.84[b]	167.53±29.93[b]
IL-10	56.00±7.15	68.02±15.03	275.13±27.65[d]

[b]$P<0.01$ *vs* PBS group. [d]$P<0.01$ *vs* PBS and SL3261 groups.

Detection of anti-UreB antibodies in mice immunized with the salmonella vaccine strain

The protein of 61 ku, corresponding to UreB, was recognized by serum from the vaccine group mice. This band was not detectable in strips tested from non-immunized mice or mice immunized with *Salmonella* only. But other non-specific bands were also observed in most lanes.

Histology of mice stomach tissue

Histology showed that the grade of gastritis had no difference between the vaccine group and control groups.

Observation of general character

In the initial stage of immunization, the mice had a jaded appetite and weight loss. No diarrhea and death occurred in immunized mice.

Recombinant attenuated S. typhimurium SL3261/pTC01-UreB stability

After 80 generations of continuous culture, nearly 100% of the SL3261/pTC01-UreB bacterial colonies were chloromycetin resistant and could express UreB protein.

DISCUSSION

Since the idea of vaccine against *H pylori* infection was raised in 1990, scientists have placed emphasis on the study of *H pylori* protein vaccine. Urease is necessary for colonization of *H pylori* and expressed at high levels by all *H pylori* strains. Furthermore, because of the high immunogenicity and the high conservation (98%) between different *H pylori* strains,

the urease is regarded as a promising candidate of *H pylori* vaccine. Studies indicated that oral immunization of natural or recombinant UreB in combination with *Cholera* toxin (CT) or *Escherichia coli* labile toxin (LT) could protect mice from *H pylori* infection[6]. But in all successful vaccination protocols, mucosal adjuvants, i.e., CT or LT, are necessary. One major drawback with these bacterial adjuvants is that they are toxic in humans[7]. This restricts the use of oral protein vaccine. Thus, the development of new vaccine strategies for *H pylori* is indispensable. Live attenuated *S. typhimurium* vaccine strains expressing foreign antigens are a promising new generation of vaccines that induce remarkably strong and specific immune responses in the mammalian hosts when given by mucosal immunization routes such as the oral, nasal, rectal and vaginal routes. Moreover, live *S. typhimurium* used as vector for heterologous antigens do not require antigen purification, and they not only can protect antigen from degradation and denaturation in stomach but also express adjuvant activity that prevents induction of oral tolerance. *S. typhimurium* SL3261 is an aroA gene mutant that is invasive yet nonvirulent. Human trials indicate that attenuated *S. typhimurium* strain is well tolerated and highly immunogenic and may be useful for the delivery of foreign antigens and immunoprotection against a variety of pathogens including *H pylori*. So *S. typhimurium* SL3261 is an efficient live bacterial vector[8].

The expression of protective immunity against gut pathogens is normally dependent both on local (mucosal) and systemic mechanisms[2]. We cloned successfully the prokaryotic vector pTC01-UreB and established attenuated *S. typhimurium* SL3261/pTC01-UreB expressing UreB subunit. We have shown that the multiple oral immunizations with SL3261/pTC01-UreB could elicit significantly *H pylori*-specific mucosal IgA response[4]. The increases in serum IgG and mucosal IgA anti-UreB antibodies indicate that UreB delivered by *Salmonella* is highly immunogenic and capable of inducing specific humoral immunity and mucosal immunity.

At present, it is generally acknowledged that protective immunization has been associated with a progressive disappearance of Th1 cells and the development of a Th2 response[9]. In a recent study, Guy and coworkers showed strong Th1 and Th2 responses elicited better protection than a predominant Th2 type response only. They thought that an appropriate balance between Th1 and Th2 type responses is required to achieve complete protection[10]. SL3261/pTC01-UreB was vaccinated through the route of mucosal administration. Mucosal tissues favor the development of Th2-type responses[11]. Our results showed that there was significant increase of IFN-γ and IL-10 in SL3261/pTC01-UreB group. These suggest that SL3261/pTC01-UreB can induce strong Th1 and Th2 responses. Nevertheless, the level of IFN-γ had no difference between SL3261/pTC01-UreB group and SL3261control group. And the level of IFN-γ in SL3261 control mice was also higher than in PBS control mice. These facts demonstrate that the strong Th1 response is associated with attenuated *S. typhimurium* used as vaccine vector, because attenuated *S. typhimurium* is a kind of invasive pathogens[12].

Genetic stabilization of foreign antigen expression is a crucial step in the development of an immunogenic vaccine strain. Our data showed that there was no pTC01-UreB plasmid loss in SL3261/pTC01-UreB after 80 generations of continuous culture. Moreover, expression of UreB from *S. typhimurium* SL3261/pTC01-UreB was also obtained at different phases of growth including in the stationary phase. All these clarify that the recombinant plasmid pTC01-UreB is stable in SL3261 and has no obvious toxicity. In addition, the facts that no obvious side effects for mice and no change in gastric inflammation were observed indicate *S. typhimurium* SL3261/pTC01-UreB is safe. Our results show that the attenuated *S. typhimurium* expressing *H pylori* UreB may be used as oral vaccine against *H pylori* infection. Henceforth, we need to consummate anti- *H pylori S. typhimurium* vaccine and evaluate its effect.

REFERENCES

1 **Vandenplas Y**. *Helicobacter pylori* infection. *World J Gastroenterol* 2000; **6**: 20-31
2 **Mastroeni P**, Bowe F, Cahill R, Simmons C, Dougan G. Vaccines against gut pathogens. *Gut* 1999; **45**: 633-635
3 **Djavani M**, Yin C, Xia L, Lukashevich IS, Pauza CD, Salvato MS. Murine immune responses to mucosally delivered *Salmonella* expressing *Lassa fever virus* nucleoprotein. *Vaccine* 2000; **18**: 1543-1554
4 **Liu XF**, Hu JL, Huang JSH, Fan DM, Ren DM. Oral immunization of mice with attenuated *Salmonella typhimurium* expressing *Helicobacter pylori* urease B subunit. *Chin J Dig* 2001; **21**: 522-525
5 **Sambrook J**, Fritsch EF, Maniatis T. Molecular Cloning: A Laboatory Manual, 2nd edn. *Cold Spring Harbor Laboatory Press* 1989: 889-893
6 **Myers GA**, Ermak TH, Georgakopoulos K, Tibbitts T, Ingrassia J, Gray H, Kleanthous H, Lee CK, Monath TP. Oral immunization with recombinant *Helicobacter pylori* urease confers long-lasting immunity against *Helicobacter felis* infection. *Vaccine* 1999; **17**: 1394-1403
7 **Michetti P**, Kreiss C, Kotloff KL, Porta N, Blanco JL, Bachmann D, Herranz M, Saldinger PF, Corthesy-Theulaz I, Losonsky G, Nichols R, Simon J, Stolte M, Ackerman S, Monath TP, Blum AL. Oral immunization with urease and Escherichia coli heat-labile enterotoxin is safe and immunogenic in Helicobacter pylori-infected adults. *Gastroenterology* 1999; **116**: 804-812
8 **Kantele A**, Hakkinen M, Moldoveanu Z, Lu A, Savilahti E, Alvarez RD, Michalek S, Mestecky J. Differences in immune responses induced by oral and rectal immunizations with Salmonella typhi Ty21a: evidence for compartmentalization within the common mucosal immune system in humans. *Infect Immun* 1998; **66**: 5630-5635
9 **Czinn SJ**. What is the role for vaccination in *Helicobacter pylori*? *Gastroenterology* 1997; **113**: S149-S153
10 **Guy B**, Hessler C, Fourage S, Haensler J, Vialon-Lafay E, Rokbi B, Millet MJ. Systemic immunization with urease protects mice against *Helicobacter pylori* infection. *Vaccine* 1998; **16**: 850-856
11 **Weiner HL**. Oral tolerance: immune mechanisms and treatment of autoimmune diseases. *Immunol Today* 1997; **18**: 335-343
12 **Gomez Duarte OG**, Bumann D, Meyer TF. The attenuated *Salmonella* vaccine approach for the control of *Helicobacter pylori*-related diseases. *Vaccine* 1999; **17**: 1667-1673

Science Editor Zhu LH and Guo SY **Language Editor** Elsevier HK

PO Box 2345, Beijing 100023, China
www.wjgnet.com
wjg@wjgnet.com

ELSEVIER

World J Gastroenterol 2005;11(14):2157-2161
World Journal of Gastroenterology ISSN 1007-9327

• *BRIEF REPORTS* •

Effect of hepatitis C virus nonstructural protein NS3 on proliferation and MAPK phosphorylation of normal hepatocyte line

De-Yun Feng, Yi Sun, Rui-Xue Cheng, Xiao-Ming Ouyang, Hui Zheng

De-Yun Feng, Yi Sun, Rui-Xue Cheng, Xiao-Ming Ouyang, Hui Zheng, Department of Pathology, College of Basic Medicine, Central South University, Changsha 410078, Hunan Province, China
Supported by the National Natural Science Foundation of China, No. 30270601
Correspondence to: Dr. De-Yun Feng, Department of Pathology, College of Basic Medicine, Central South University, Changsha 410078, Hunan Province, China. dyfeng743@sohu.com
Telephone: +86-731-2650407
Received: 2003-04-08 Accepted: 2003-05-19

Abstract

AIM: To study the effect of hepatitis C virus nonstructural region 3 (HCV NS3) protein on proliferation and transformation of normal human liver cell line.

METHODS: QSG7701 cells were transfected with pRcHCNS3-5′, pRcHCNS3-3′ and pRcCMV using lipofectamine transfecting technique and selected with G418 method. Expression of HCV NS3 protein was determined by immunohistochemistry. Biologic characteristics of transfected cells were evaluated by population doubling time and soft agar assays. Activation of MAPK was analyzed using Western blot with phosphospecific monoclonal antibody against dually phosphorylated MAPK.

RESULTS: QSG7701 cells transfected with pRcHCNS3-5′ showed strong intracellular expression of HCVNS3 protein, and the positive signal was localized in cytoplasm. The expressing strength of HCVNS3 protein in pRcHCNS3-3′-transfected cells was weaker than that in pRcHCNS3-5′-transfected cells. The population doubling time in the transfected cells with pRcHCNS3-5′ (12 h) was much shorter than those with pRcHCNS3-3′, pRcCMV and normal cells (24, 26, 28 h, respectively) (P<0.01). The transfected cells with pRcHCNS3-5′ showed much more anchorage independent colonies than that in those with pRcHCNS3-3′ and pRcCMV (P<0.01). The cloning efficiencies of transfected cells with pRcHCNS3-5′, pRcHCNS3-3′, pRcCMV and controls were 33%, 1.33%, 1.46%, 1.11% respectively. The level of phosphorylated MAPK in the cells with pRcHCNS3-5′ was much higher than that in those with pRcHCNS3-3′and pRcCMV and normal cells (P<0.01).

CONCLUSION: The results suggest that (1) QSG7701 cells are a better human liver cell line for investigating the pathogenesis of HCV NS3 protein. (2) 5′ region of the HCV genome segment encoding HCV NS3 is involved in cell growth and cell phenotype. (3) HCV NS3 N-terminal peptide may up-regulate the activation of MAPK, but not affect the expression of MAPK.

Key words: HCV NS3; Cell proliferation; QSG7701 strain; Transfection; Mitogen-activated protein kinase

Feng DY, Sun Y, Cheng RX, Ouyang XM, Zheng H. Effect of hepatitis C virus nonstructural protein NS3 on proliferation and MAPK phosphorylation of normal hepatocyte line. *World J Gastroenterol* 2005; 11(14): 2157-2161
http://www.wjgnet.com/1007-9327/11/2157.asp

INTRODUCTION

Hepatitis C virus nonstructural region 3 (HCV NS3) gene, located in nucleotide 3 420-5 312, encodes HCV NS3 protein consisted of 631 amino acids. HCV NS3 protein is one of the important pathogenic HCV proteins, which was found and researched at first. Though it was reported that HCV NS3 protein probably has many kinds of potential biological effects, for example, proteinase and helicase activity, mediating cellular immune response, transactivating telomerase, regulating p53 function, and affecting protein kinase A (PKA) and signal transducers and activators of transcription (STAT) signal transduction, *etc*.[1-6]. So far the precise pathogenic mechanism of HCV NS3 protein remains unclear. Sakamuro *et al*[7], confirmed that NIH3T3 cells could be transformed by HCV NS3 protein and formed tumors in nude mice. Because NIH3T3 strain is a mouse fibroblast cell line, and its differentiation characteristics are different from human hepatocytes, NIH3T3 cell transformation experiment cannot really reflect the carcinogenesis process of HCV infection. In view of this, human hepatocyte line QSG7701 was transfected with mammalian expression plasmid pRcHCNS3, and the effect of HCV NS3 protein on human hepatocyte transformation and mitogen-activated protein kinase (MAPK) signal transduction were studied.

MATERIALS AND METHODS

Experimental materials

The mammalian expression plasmid pRcHCNS3-5′ (nucleotides 3 354-4 210, expressing HCV NS3 N-terminal peptide, Ile1020-Thr1295) and pRcHCNS3-3′ (nucleotides 4 116-5 147, expressing HCV NS3 C-terminal peptide, Phe1263-Trp1608) were the kind gifts of Professor Takegami[7]. Non-expressive plasmid pRcCMV was purchased from Sigma Company, USA. Human hepatocyte line QSG7701 was from Cytobiology

Research Institute of Shanghai. Lipofectamin™ kit and G418 were the products of GIBCO (Germany). *Xba*I and buffer were purchased from Sino-American Biotechnique Inc. (Shanghai, PR China), anti-HCV NS3 protein MAb from Boshide (Wuhan, PR China), S-P detection kit from Maxim Biotech Inc. (Fuzhou, PR China), p42/44^{MAPK} (Erk1/Erk2, Thr202/Tyr204) which were used to detect the phosphorylation of MAPK was presented by New England Biolab, USA, antibody to MAPK was purchased from Santa Cruz. PCR primers for amplifying HCV NS3-5' gene were synthesized at Shanghai Sangon (Shanghai, PR China).

Experimental groups

Untransfected QSG7701 cells, QSG7701 cells transfected with blank plasmid pRcCMV, QSG7701 cells transfected with plasmid pRcHCNS$_3$-5' and QSG7701 cells transfected with plasmid pRcHCNS3-3'.

Cell culture

QSG7701 cells were cultured and passaged in DMEM medium with 10% fetal calf serum in an incubator containing 50 mL/L CO_2 at 37 ℃.

Preparation, purification and identification of plasmids

Plasmids pRcCMV, pRcHCNS3-3' and pRcHCNS3-5' were transferred into *Escherichia coli,* which was dealt with calcium chloride respectively. The *E.coli* was cultured to amplify the three kinds of plasmid. A small amount of the plasmids was prepared from the *E.coli* to identify specificity of the plasmids. The plasmids pRcHCNS3-3' and pRcHCNS3-5' were digested with XbaI, resolved with agarose gel electrophoresis, and stained with ethidium bromide. After identification, the plasmids were massively extracted and purified for transfecting QSG7701 cells.

Transfection of QSG7701 cells

QSG7701 cells were transfected with plasmids pRcCMV, pRcHCNS3-3' or pRcHCNS3-5' respectively as described in instruction of Lipofectaminen reagent. Cells were seeded into selection medium containing G418 until G418-resistant clones were obtained. Non-transfected QSG7701 cells were used for parallel control.

To detect cDNA in stable transfectants, total genomic DNA was extracted from positive clones according to standard methods and subjected to PCR and agarose gel electrophoresis analysis. Based on published sequences, the primers, 5'-CGGGCA CGTTGTAGG CATC-3' (sense) and 5'-AACGGACGGCTTTAGGACGA-3' (antisense), were projected for amplifying the 5'-half sequence of HCV NS3 region[7]. PCR conditions were 35 cycles of three steps (at 94 ℃ for 30 s, at 57 ℃ for 30 s, at 72 ℃ for 40 s) in a 50 μL reaction mixture containing 5 μL 10× buffer, 5 μL 2 mmol/L dNTPs, 0.5 μL each primer (25 pmol/μL), 1 μL DNA, 5 U Taq DNA polymerase, and 37.5 μL distilled water. PCR products were subjected to electrophoresis on a 0.8% agarose gel for 30 min (voltage: 80 V), visualized by ethidium bromide staining.

Detection of HCV NS3 protein expression

S-P method was used to detect expression of HCV NS3 protein in the QSG7701 cells transfected with plasmids pRcHCNS3-5', pRcHCNS3-3', pRcCMV or non-transfected. PBS was used as substitutes of Mabs for blank control groups. Hepatocellular carcinoma tissues expressing HCV NS3 protein was used as a positive control.

Identification of biological behavior of QSG7701 cells

Survey of growth curve Non-transfected and transfected QSG7701 cells (6×10^4 cells per well) were inoculated and incubated in 24-well culture plates respectively, digested and counted at an interval of 24 h, and the average number of cells in 3 wells per group was counted per time. The detection was continued for 8 d. Then the population doubling time and growth curve of the cells were calculated. To get reliable results, experiments were repeated thrice.

Anchorage-independent growth test To examine the ability of G418-resistant cells to grow anchorage independently, 2×10^3 cells were suspended in 0.35% agarose containing DMEM and 10% fetal calf serum and overlaid onto a bottom layer of 0.7% agarose in culture plates (φ 60 mm). After 2 wk of culture, clones with more than 50 cells were scored and the colony formation efficiency was determined (colony formation efficiency = colony numbers/seeded cell numbers×100%). The experiments were repeated thrice.

Detection of expression and activity of MAPK

Western blot was used to detect expression and activity of MAPK. Briefly, cells (5×10^5) forming clones were inoculated in a 6-well culture plate and cultured for 24 h. The cells were incubated in free-serum medium for 24 h to make cell synchronous, then cultured in medium with 10% FCS for 5 h to stimulate cell growth. The cells were harvested and washed twice with pre-cooled PBS. Eighty microliters of lysis reagent (62.5 mmol/L Tris-HCl, 20 g/L SDS, 10% glycerol, 50 mmol/L DTT, 1 g/L bromophenol blue) was added and broken with ultrasound for 5-7 s, boiled at 95-100 ℃ for 5 min, centrifugalized at 12 000 *g* for 5 min. Twenty microliters of supernatant proteins were resolved by SDS-10% polyacrylamide gel electrophoresis. After electrophoresis, the proteins were transferred onto a nitrocellulose membrane, blocked in 5% skimmed milk for 3 h, probed with the antibody to phosphorylated p44/42 MAPK (1∶100) overnight at 4 ℃. After being washed thrice in TBS containing 0.1% Tween 20, the membrane was treated with horseradish peroxidase-conjugated anti-mouse antibody for 1 h. Protein binding was detected by chemiluminescence reagent (ECL). Then the membranes were eluted in cleaning solution at 50 ℃ for 30 min, total MAPK was detected with antibody to non-phosphorylated MAPK as described above. The bands on X-film were assayed by densitometric scanning.

Statistical analysis

Analysis of variance and *t* test were used according to SPSS 10.0.

RESULTS

Identification of plasmids

Plasmids pRcHCNS$_3$-3' and pRcHCNS$_3$-5' extracted from

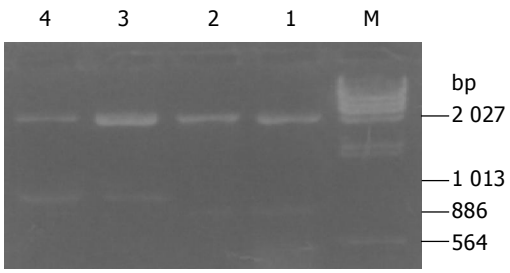

Figure 1 Agarose gel electrophoresis analysis of pRcHCN3-3' and pRcHCN3-5' digested with *Xba*I. Lane M: DNA marker (λDNA/*Hin*d III). Lanes 1 and 2: pRcHCNS3-5' plasmid, 886-bp fragment. Lanes 3 and 4: pRcHCNS3-3' plasmid, 1 031-bp fragment.

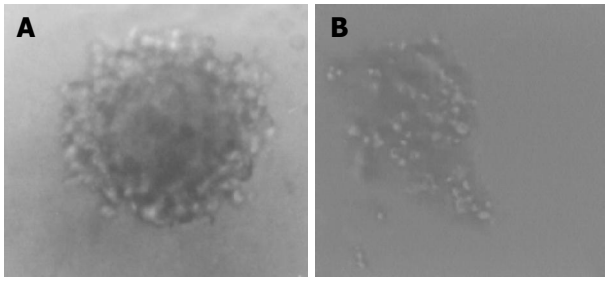

Figure 2 Clones of QSG7701 cell transfected with pRcHCNS3-5' and pRcHCN3-3' plasmid in soft agar. A: pRcHCNS3-5' transfected group. B: pRcHCNS3-3' transfected group (×100).

E.coli were digested with *Xba*I, resolved with agarose gel electrophoresis, and stained with ethidium bromide. As shown in Figure 1, electrophoresis analysis revealed that the major 866- and 1 031-bp fragments were expected from the plasmids pRcHCNS$_3$-3' and pRcHCNS$_3$-5'.

Selection and identification of positive clones

Cells transfected were seeded into selection medium containing G418. Nine pRcHCNS3-5, eight pRcHCNS3-3' and five pRcCMV positive clones were selected (Figure 2). Total genomic DNA extracted from transfected cells was amplified by PCR. As shown in Figure 3, 257-bp fragment was specifically amplified from DNA of the QSG7701 cells transfected with plasmid pRcHCNS$_3$-5', and not amplified from DNA of the QSG7701 cells transfected with plasmid pRcHCNS$_3$-3', pRcCMV and non-transfected NIH3T3 cells.

Expression of HCV NS3 protein in QSG7701 cells

Immunohistochemical staining showed that HCV NS3 protein was expressed in transfected QSG7701 cells with plasmids pRcHCNS$_3$-3' and pRcHCNS$_3$-5'. The positive signal of HCV NS3 protein was located in cytoplasm. The signal intensity of HCV NS3 protein in QSG7701 cells transfected with plasmid pRcHCNS$_3$-5' was higher than that in cells transfected with plasmid pRcHCNS$_3$-3' (Figure 4). The positive products were also found in positive control group, but not in blank and negative control groups.

Identification of biological behavior of QSG7701 cells

The growth curve of four kinds of cells was detected (Figure 5). The population doubling time of QSG7701 cells transfected with pRcHCN$_3$-5', pRcHCN$_3$-3', pRcCMV and non-transfected QSG7701 cells was 12, 24, 26, and 28 h, and the efficiency of colony formation was 33%, 1.33%, 1.46% and 1.11%, respectively. These showed that the population doubling time and colony formation efficiency of the cells transfected with pRcHCNS$_3$-5' were much shorter and higher than those of cells transfected with pRcHCNS$_3$-3', pRcCMV and non-transfected QSG7701 cells.

Detection of phosphorylated p44/42^{MAPK} in QSG7701 cells

Phosphorylation of p44/42^{MAPK} in the cells transfected with pRcHCNS$_3$-5', pRcHCNS$_3$-3', pRcCMV and non-transfected cells was detected by Western blot. The optical density of phosphorylated MAPK was 8 858±887, 5 612±656, 2 212±245, 989±188, respectively. The level of phosphorylated p44/42^{MAPK} in the cells transfected with pRcHCNS$_3$-5' was the highest (P<0.01). Expressions of total p44/42^{MAPK} in all groups were not different (12 000±1 174, 11 851±1 048, 11 321±987, 11 058±991, respectively, P>0.05, Figure 6).

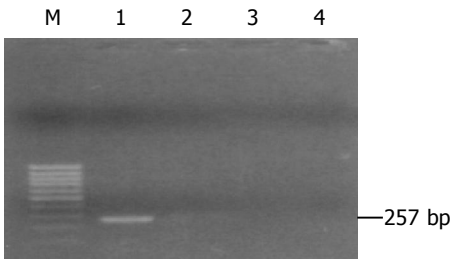

Figure 3 Identification of expression plasmid of HCNS3 protein in QSG7701 cells. Lane 1: pRcHCNS3-5'; lane 2: pRcCMV; lane 3: untransfected QSG7701 cells; lane 4: blank control.

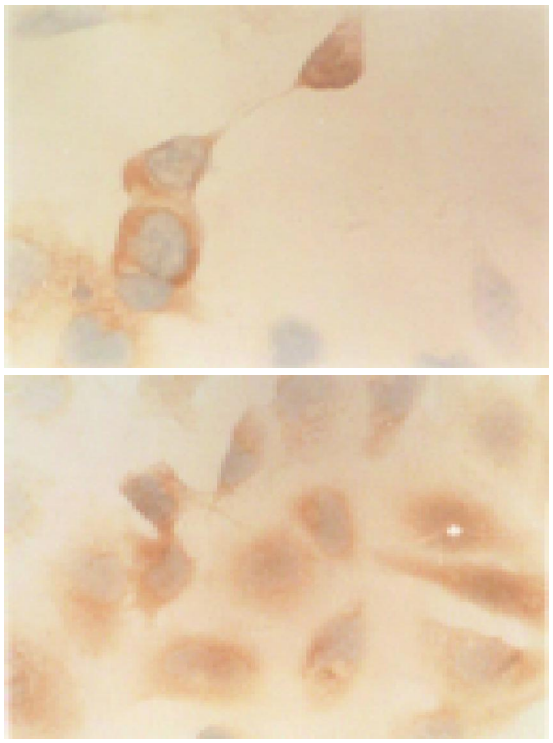

Figure 4 Expression of HCV NS3 protein in QSG77 cell transfected with pRcHCNS3-5' plasmid. The positive products were localized in cytoplasm. SP ×400.

DISCUSSION

HCV, a kind of hepatotropic virus, causes hepatopathy by specific hepatocyte-virus reaction. Its natural host cell is hepatocyte whose differentiation characteristics are different from other cells. It is very difficult to culture and passage normal hepatocytes *in vitro*. Neither could hepatocytes effectively express selection markers for eukaryotic expression plasmids and obtain stable clones, nor could be transformed successfully with HCV genes. Liver cancer cell lines are usually used as a substitute of normal hepatocytes for expressing HCV gene, but they could not be used as subject cells to identify the effect of HCV genes on cell phenotype[8]. Sakamuro *et al*[7], reported that HCV NS3 protein could transform NIH3T3 cells, and NIH3T3 cells transfected with pRcHCNS_3-5' formed tumors in nude mice. NIH3T3 cells is a mouse fibroblast line, therefore transforming NIH3T3 cells by HCV cannot really reflect the processes of infection and pathopoiesis of HCV. QSG7701 cells are an immortal normal human hepatocyte line, which were taken from liver tissue at 6 cm distance from primary liver cancer. In our experiment, QSG7701 cell line was successfully transfected with eukaryotic expression plasmids pRcHCNS_3-5', pRcHCNS_3-3'and pRcCMV, and nine clones of cells transfected with pRcHCNS_3-5', eight pRcHCNS_3-3' and five pRcCMV positive clones were obtained respectively. It was identified by immunohistochemistry that all of pRcHCNS_3-5'and pRcHCNS_3-3'positve clones expressed HCV NS3 protein. QSG7701 cells are a kind of human normal phenotype hepatocyte strains. We first used them as subject cells to study the effect of HCV on tumorigenesis and obtained satisfactory results, and built a good cell model expressing HCV NS3 protein for studying the pathogenesis of HCC related to HCV NS3 protein.

HCV is a positive-strand RNA virus which does not have reverse transcriptase activity, and thus there is no integration of viral genome or genome segments into host chromosomes. Up to now, it has been suggested that the malignant transformation of host cells may be caused by HCV expression gene products[9,10], in which HCV NS3 protein may play an essential role in hepatocarcinogenesis, but its exact mechanism is still unclear. HCV NS3 protein containing 631 amino acids is a multifunctional cytoplasmic protein whose N-terminal has proteinase activity and C-terminal helicase activity[11]. In our data, QSG7701 cells expressing HCV N3 N-terminal peptides showed the characteristics of tumor cells to a certain extent and formed tumor in nude mice (data not shown). The population doubling time was the shortest, and anchorage-independent growth ability was the strongest. Whereas, there was no difference among growth characteristics of pRcHCNS_3-3'-transfected, pRcCMV-transfected and non-transfected QSG7701 cells. The results suggest that HCVNS3 N-terminal peptide functioning as proteinase activity may play an important role during transformation of cells, which is identical with Sakamuro *et al*[7]. HCV NS3 protein might activate oncogenes and signaling transduction molecular of host cells infected by HCV[2,4,5]. Ras-Raf-MAPK signaling pathway is closely related to growth and proliferation of cells. MAPK could be activated by phosphorylation. Continuously high level of MAPK activity was a key for transformation and carcinogenesis of cells[12,13]. Our data displayed that HCVNS3 N-terminal peptide could significantly up-regulate phosphorylation of p44/42^{MAPK}, but not affect the expression of total MAPK protein. Cells expressing HCVNS3 N-terminal peptide showed significant transformation phenotype, suggesting that HCV NS3 protein may induce and promote cell transformation by activating MAPK signaling pathway.

The precise mechanism of up-regulating MAPK phosphorylation is still unclear, but it has been reported that HCV NS3 protein interfered phosphorylation of proteins and inhibited cAMP-dependent PAK signaling transduction[4]. In Ras-Raf-MAPK cascade, the interaction between Ras and Raf contact points is essential for the plasma membrane localization of Raf, which ultimately leads to kinase activation. The formation of this protein complex is negatively regulated by PKA through phosphorylation of the c-Raf-1 N-terminus. Phosphorylation of c-Raf-1 serine 43 is believed to cause a N-terminal cap structure to cover the Ras docking site and inhibit Raf activation[14-17]. HCV NS3 protein (1 487-1 500) contains a arginine-rich sequence which is highly homologous to substrate recognition site of PKA R subunit, and could mediate binding of HCV NS3 protein to PKA C subunit and result in inactivation of PKA[18]. HCV NS3 protein may activate Ras-Raf-MAPK signaling pathway through inhibiting negative regulation of PKA. Our results showed that the effect of HCVNS3 N-terminal peptide on up-regulation of MAPK activity was more significant than that of C-terminal peptide. Because HCV NS3 N-terminal peptide (nucleotides 3 354-4 210, Ile1020-Thr1295) does not contain the arginine-rich sequence (1 487-1 500), HCV NS3 protein may activate MAPK through other ways.

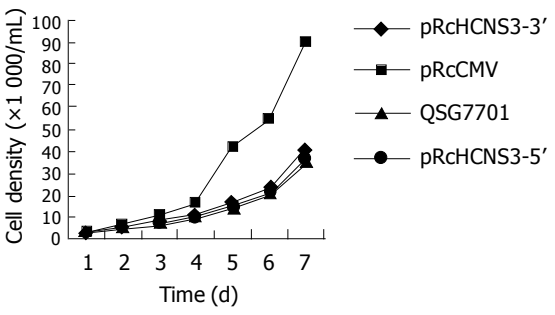

Figure 5 Growth curve of four kinds of cells.

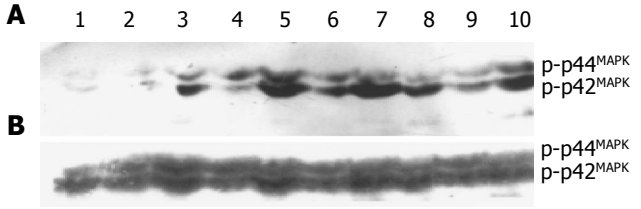

Figure 6 Western blot analysis of phosphorylated (A) and non-phosphorylated (B) MAPK in each group. Lanes 1 and 2: non-transfected group; Lanes 3 and 4: pRcCMV transfected group; Lanes 5-7: pRcHCNS3-5' transfected group; Lanes 8-10: pRcHCNS3-3' transfected group.

It was reported that HCVNS3 serine protease (nucleotides 3 356-4 080) could induce transformation of rat fibroblasts and tumor formation in nude mice. Their experiments suggested that the transformation and tumorigenesis induced by HCV NS3 serine protease were dependent on an active enzyme[19]. In conclusion, HCV NS3 N-terminal peptide expressed by QSG7701 cells transfected with pRcHCNS$_3$-5' contains the sequence coding HCV NS3 serine protease. It may need further investigation whether MAPK can be activated by serine protease of HCV NS3 N-terminal peptide, and result in proliferation and transformation of hepatocytes.

REFERENCES

1 **Suzich JA,** Tamura JK, Palmer-Hill F, Warrener P, Grakoui A, Rice CM, Feinstone SM, Collett MS. Hepatitis C virus NS3 protein polynucleotide-stimulated nucleoside triphosphatase and comparison with the related pestivirus and flavivirus enzymes. *J Virol* 1993; **67**: 6152-6158

2 **Ishido S,** Muramatsu S, Fujita T, Iwanaga Y, Tong WY, Katayama Y, Itoh M, Hotta H. Wild-type, but not mutant-type, p53 enhances nuclear accumulation of the NS3 protein of hepatitis C virus. *Biochem Biophys Res Commun* 1997; **230**: 431-436

3 **Diepolder HM,** Gerlach JT, Zachoval R, Hoffmann RM, Jung MC, Wierenga EA, Scholz S, Santantonio T, Houghton M, Southwood S, Sette A, Pape GR. Immunodominant CD4+ T-cell epitope within nonstructural protein 3 in acute hepatitis C virus infection. *J Virol* 1997; **71**: 6011-6019

4 **Borowski P,** Oehlmann K, Heiland M, Laufs R. Nonstructural protein 3 of hepatitis C virus blocks the distribution of the free catalytic subunit of cyclic AMP-dependent protein kinase. *J Virol* 1997; **71**: 2838-2843

5 **Heim MH,** Moradpour D, Blum HE. Expression of hepatitis C virus proteins inhibits signal transduction through the Jak-STAT pathway. *J Virol* 1999; **73**: 8469-8475

6 **Feng D,** Cheng R, Ouyang X, Zheng H, Tsutomu T. Hepatitis C virus nonstructural protein NS(3) and telomerase activity. *Chin Med J (Engl)* 2002; **115**: 597-602

7 **Sakamuro D,** Furukawa T, Takegami T. Hepatitis C virus nonstructural protein NS3 transforms NIH 3T3 cells. *J Virol* 1995; **69**: 3893-3896

8 **Kim DW,** Harada T, Saito I, Miyamura T. An efficient expression vector for stable expression in human liver cells. *Gene* 1993; **134**: 307-308

9 **Matsuura Y,** Harada T, Makimura M, Sato M, Aizaki H, Suzuki T, Miyamura T. Characterization of HCV structural proteins expressed in various animal cells. *Intervirology* 1994; **37**: 114-118

10 **Hino O,** Kajino K. Hepatitis virus-related hepatocarcinogenesis. *Intervirology* 1994; **37**: 133-135

11 **Shimotohno K.** Hepatitis C virus as a causative agent of hepatocellular carcinoma. *Intervirology* 1995; **38**: 162-169

12 **Okazaki K,** Sagata N. MAP kinase activation is essential for oncogenic transformation of NIH3T3 cells by Mos. *Oncogene* 1995; **10**: 1149-1157

13 **Ito Y,** Sasaki Y, Horimoto M, Wada S, Tanaka Y, Kasahara A, Ueki T, Hirano T, Yamamoto H, Fujimoto J, Okamoto E, Hayashi N, Hori M. Activation of mitogen-activated protein kinases/extracellular signal-regulated kinases in human hepatocellular carcinoma. *Hepatology* 1998; **27**: 951-958

14 **Borowski P,** Kuhl R, Laufs R, Schulze zur Wiesch J, Heiland M. Identification and characterization of a histone binding site of the non-structural protein 3 of hepatitis C virus. *J Clin Virol* 1999; **13**: 61-69

15 **Hafner S,** Adler HS, Mischak H, Janosch P, Heidecker G, Wolfman A, Pippig S, Lohse M, Ueffing M, Kolch W. Mechanism of inhibition of Raf-1 by protein kinase A. *Mol Cell Biol* 1994; **14**: 6696-6703

16 **Mischak H,** Seitz T, Janosch P, Eulitz M, Steen H, Schellerer M, Philipp A, Kolch W. Negative regulation of Raf-1 by phosphorylation of serine 621. *Mol Cell Biol* 1996; **16**: 5409-5418

17 **Marshall M.** Interactions between Ras and Raf: key regulatory proteins in cellular transformation. *Mol Reprod Dev* 1995; **42**: 493-499

18 **Borowski P,** Heiland M, Feucht H, Laufs R. Characterisation of non-structural protein 3 of hepatitis C virus as modulator of protein phosphorylation mediated by PKA and PKC: evidences for action on the level of substrate and enzyme. *Arch Virol* 1999; **144**: 687-701

19 **Zemel R,** Gerechet S, Greif H, Bachmatove L, Birk Y, Golan-Goldhirsh A, Kunin M, Berdichevsky Y, Benhar I, Tur-Kaspa R. Cell transformation induced by hepatitis C virus NS3 serine protease. *J Viral Hepat* 2001; **8**: 96-102

Science Editor Wang XL and Li WZ **Language Editor** Elsevier HK

PO Box 2345, Beijing 100023, China
www.wjgnet.com
wjg@wjgnet.com

ELSEVIER

World J Gastroenterol 2005;11(14):2162-2165
World Journal of Gastroenterology ISSN 1007-9327

• *BRIEF REPORTS* •

Clinicopathological significance of p53 and mdm2 protein expression in human pancreatic cancer

Ming Dong, Gang Ma, Wei Tu, Ke-Jian Guo, Yu-Lin Tian, Yu-Ting Dong

Ming Dong, Gang Ma, Wei Tu, Ke-Jian Guo, Yu-Lin Tian, Yu-Ting Dong, Department of Surgery, First Affiliated Hospital, China Medical University, Shenyang 110001, Liaoning Province, China
Correspondence to: Ming Dong, MD, PhD, Department of Surgery, First Affiliated Hospital, China Medical University, Shenyang 110001, Liaoning Province, China. mingdong76@yahoo.com
Telephone: +86-24-23256666-6237
Received: 2004-11-20 Accepted: 2004-12-09

Abstract

AIM: To study the clinicopathological significance of p53 and mdm2 protein expression in human pancreatic cancer.

METHODS: To investigate the expression of p53 and mdm2 in pancreatic cancer by immunohistochemistry, and the relationships between the p53 and mdm2 protein expression and clinicopathological parameters in pancreatic cancer.

RESULTS: The positive expression of p53 protein was found in 40 of 59 patients (67.8%) and that of mdm2 protein in 17 of 59 patients (28.8%). No obvious relationships were found between p53 as well as mdm2 expression and sex, tumor site, TNM staging and histological differentiation. p53 expression was increased in patients younger than 65 years old, while mdm2 had no relationship with age. The survival time of the patients with the positive expression of p53 and mdm2 proteins was obviously shorter than the other groups.

CONCLUSION: Both p53 and mdm2 presented relatively high expression in human pancreatic cancer. The overexpression of p53 and mdm2 might reflect the malignant proliferation of pancreatic cancer and their co-expression might be helpful to evaluate the prognosis of the patients with pancreatic cancer.

Key words: Pancreatic cancer; p53; mdm2; Immunohistochemistry

Dong M, Ma G, Tu W, Guo KJ, Tian YL, Dong YT. Clinicopathological significance of p53 and mdm2 protein expression in human pancreatic cancer. *World J Gastroenterol* 2005; 11(14): 2162-2165
http://www.wjgnet.com/1007-9327/11/2162.asp

INTRODUCTION

Pancreatic cancer is a gastrointestinal neoplasm with high malignancy and poor prognosis. Incidence of pancreatic cancer has shown the increasing trend in recent years, but the therapeutic efficacy is still not satisfying. That is related to the pancreas' deep location, lack of specific early symptoms, difficult early diagnosis and scarce chance of surgical resection; even for the surgical cases, the 1-, 3- and 5-year cumulative survival rates were 49.8%, 16.8% and 9.6%, respectively[1].

With the development of techniques, molecular biology research has indicated that *p53* tumor suppressor gene plays an important role in DNA transcription, cell growth and proliferation, DNA repair and various metabolic processes. *p53* abnormalities such as gene mutation and depletion can lead to the altered intracellular signal transduction pathways as well as loss of the regulation of cell growth, apoptosis, and DNA repair, which are responsible for carcinogenesis. Previous report showed that *p53* gene mutation rate in pancreatic cancer is as high as 50-70%[2,3]. p53 protein expression and gene mutation may indicate the prognosis of pancreatic cancer, and their expression level might be useful in the determination of surgical therapy outcome and clinical prognosis[4]. But, controversy still remains in this point at present. mdm2, murine double minute gene 2, is an oncogene (the corresponding human homologous gene is *hdm2*). mdm2 protein (homologous protein in human is called hdm2 protein) can be combined with p53 to inhibit p53 function of growth supervision, leading to cell overgrowth into tumor. Therefore, we detected the expression of p53 and mdm2 in primary invasive ductal carcinoma (IDC) of the pancreas by immunohistochemistry, analyzed their relationships to clinicopathological parameters and then investigated the influence on the biological activity of pancreatic cancer.

MATERIALS AND METHODS

Tissue samples

Fifty-nine well-documented surgically resectable specimens of IDCs of the pancreas were obtained in The First Affiliated Hospital of China Medical University from May 1978 to May 1997. During this period, the main method for treating pancreatic cancer was standard pancreatioduodenectomy, although the diagnostic procedure has relatively improved. The specimens were processed routinely by 40 g/L formaldehyde fixation and paraffin-embedment. All the cases were confirmed as IDCs of the pancreas pathologically. There were 21 male cases and 38 female cases. Ages of the patients ranged from 23 to 76 years old (47 cases <65 years old; 12 cases ⩾65 years old). Based on TNM staging standard established by International Union Against Cancer

(UICC), 4 patients were in stage I, 8 were in stage II, 42 were in stage III, and 5 were in stage IV. Differentiation degree: 19 cases were well differentiated, 21 cases moderately differentiated and 19 cases poorly differentiated. Average survival time after surgery was 11.2 mo and still two cases survived at the end of follow-up. Because a few cases were performed with radical pancreatioduodenectomy, we did not analyze specially the effect of this style of operation on prognosis of the patients. In addition, five patients in stage IV underwent standard pancreatioduodenectomy from achievement data, but not vascular excision. Because we cannot get whether these tumor margins were checked in operation note or not, it is different to evaluate the effect free of tumor margins on prognosis.

Immunohistochemical staining

Immunostaining was performed using the streptavidin-biotin technique (SAB method). p53 monoclonal antibody (Ab-6) and mdm2 (Ab-1) were purchased from Dako Company. According to the manufacturer's instruction, antibody dilutions at various working concentration were prepared: p53 (Ab-6), 1:20; mdm2 (Ab-1), 1:100.

The 4-μm sections were deparaffinized with xylene thrice for 3-5 min each, dehydrated in a gradient series of alcohol thrice (100%, 95% and 45% alcohol), and rinsed by PBS. Each section was covered with 0.3% peroxyacetic acid for 15 min to block endogenous peroxidase activity, microwaved for antigen retrieval (800 W, 5 min×3 min), and cooled in the room temperature for 40 min. Non-specific binding sites were blocked by 10% normal rabbit serum for 10 min. These sections were first incubated with primary antibody for 2 h at room temperature, and then rinsed twice with PBS. This is followed by incubation with a secondary antibody for 15 min at 37 ℃ as well as another rinsed twice with PBS. Slides were then treated with streptavidin-peroxidase reagent for 10 min and rinsed with PBS twice. The sections were visualized with 3,3'-diaminobenzidine (DAB) for 5 min, counterstained with hematoxylin and mounted for observation under microscope.

Evaluation of immunohistochemical analysis

Nuclear staining of p53 and mdm2 protein was shown as brown granules (Figure 1). Positive result was defined as 10% or more than 10% of the tumor cells showing positive staining.

Statistical analysis

SAS 8.0 was used. p53 and mdm2 interaction as well as their correlations with clinicopathological parameters was performed by χ^2 test. Group comparison was analyzed by analysis of variance. Statistical analyses for cumulative survival rate, survival time difference and multiplicity were performed using Kaplan-Meier method, log-rank test and Cox proportional hazards model, respectively. Significant differences were accepted at $P<0.05$.

RESULTS

p53 and mdm2 protein expression in pancreatic cancer

p53 protein expression rate was 67.8% (40/59); but mdm2 protein expression rate was 28.8% (17/59). p53 and mdm2 protein expression rate did not correlate with sex, tumor site, TNM staging and differentiation rate. p53 expression was relatively high among the group with age <65 years old ($\chi^2 = 4.711$, $P<0.05$). There was no relationship between mdm2 expression and age (Table 1).

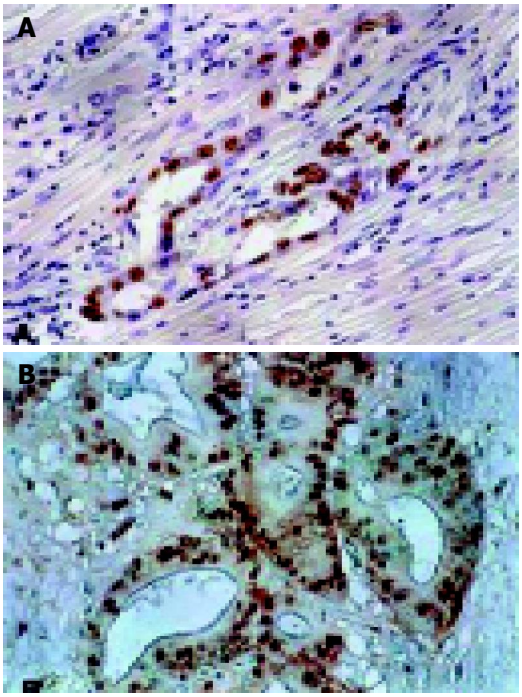

Figure 1 p53 and mdm2 staining in primary IDC of the pancreas (original magnification, ×200). A: p53 staining was seen in the majority of tumor cell nuclear; B: mdm2 staining was found in tumor cell nuclear.

Table 1 Correlation between p53 and mdm2 expression and clinicopathological parameters

Parameters		No. of patients (n = 59)	Number expressing (%)	
			p53(+) (n = 40)	mdm2(+) (n = 17)
Gender	Male	38	25 (65.8)	10 (26.3)
	Female	21	15 (71.4)	7 (33.3)
Age (yr)	<65	47	35 (74.5)	13 (27.7)
	⩾65	12	5 (41.7)	4 (33.3)
Site	Head	52	34 (65.4)	16 (30.8)
	Body/tail	7	6 (85.7)	1 (14.3)
TNM stage	I	4	2 (50)	0 (0)
	II	8	4 (50)	0 (0)
	III	42	34 (81)	15 (35.7)
	IV	5	4 (80)	2 (40)
Grade	Well	19	14 (73.7)	4 (21.1)
	Moderate	21	12 (57.1)	9 (42.9)
	Poor	19	14 (73.7)	4 (21.1)

Correlation between the p53 and mdm2 protein expression

p53 expression rate was 88.2% (15/17) in the mdm2 expression positive cases, and 59.5% (25/42) in the mdm2 expression negative cases, indicating that there was correlation between the p53 and mdm2 protein expression ($\chi^2 = 4.57$, $P = 0.0325$).

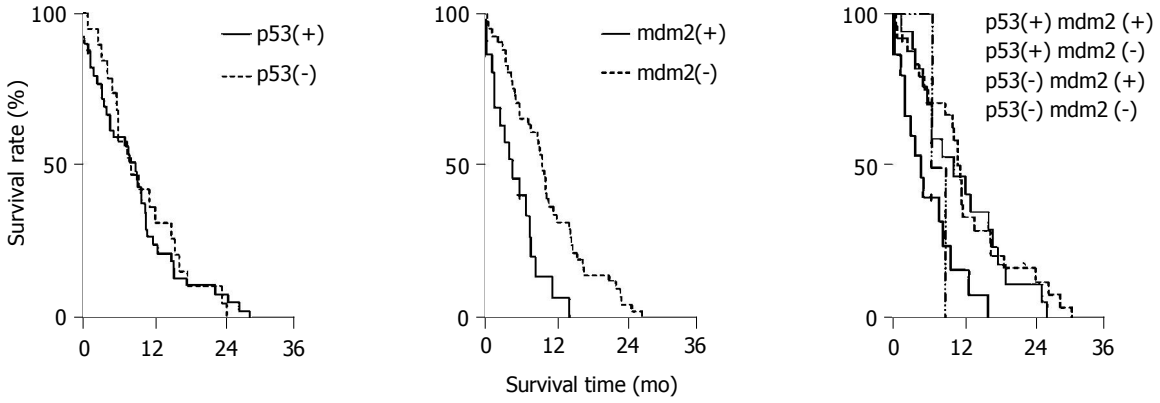

Figure 2 Survival curves with Kaplan–Meier method was applied in analyzing the influence of p53, mdm2 and their combined expression on post-surgical survival time.

Relationship between the p53 and mdm2 protein expression and prognosis

As shown in Table 2, median survival time of p53(+) and mdm2(+) group was 7.4 mo, p53(+) and mdm2(-) group 13.5 mo, p53(-) and mdm2(+) group 9.2 mo, p53(-) and mdm2(-) group 12.8 mo. Kaplan–Meier method was used for analyzing cumulative survival rate (Figure 2). Group comparison was analyzed by log-rank test, indicating that the median survival time of various groups had significant difference ($\chi^2 = 11$, $P<0.05$). p53(+) and mdm2(+) group had shorter survival time as compared with other groups.

Cox proportional hazards model was applied in multifactor analysis (p53, mdm2, clinicopathological parameters and survival time after surgery), indicating various factors such as sex, age, tumor site, TNM staging, differentiation rate, and p53 had no correlation with survival time after surgery, but mdm2 was an exception ($P<0.05$, Table 3).

Table 2 Correlation between p53 and mdm2 expression and prognosis

Protein expression	No. of patients	Median survival (mo)
p53(+)	40	6.2
p53(–)	19	10.3
mdm2(+)	17	6.8
mdm2(–)	42	12.1
p53(+)mdm2(+)	15	7.4[1]
p53(+)mdm2(–)	25	13.5[1]
p53(–)mdm2(+)	2	9.2[1]
p53(–)mdm2(–)	17	12.8[1]

[1]Group comparison was performed by log-rank test ($\chi^2 = 11$, $P = 0.012$).

Table 3 Correlation between various factors and survival time by Cox proportional hazards model (dependent variable, mo; censoring variable, death due to pancreatic cancer)

Variable	Parameter estimate (SE)	Conditional risk ratio (95% confidence limits)	P (χ^2)
mdm2	0.969 (0.324)	2.636 (1.397–4.975)	0.003
Age (yr)	0.210 (0.013)	1.021 (0.996–1.047)	0.101
TNM	0.279 (0.223)	1.322 (0.853–2.048)	0.212
Grade	0.207 (0.193)	1.229 (0.842–1.795)	0.285
Site	–0.468 (0.469)	0.627 (0.250–1.570)	0.318
p53	0.336 (0.345)	1.399 (0.712–2.751)	0.330
Gender	–0.010 (0.352)	0.990 (0.496–1.974)	0.977

DISCUSSION

p53 tumor suppressor gene located at 17q13.1, which can induce cell apoptosis. Wild-type p53 protein inhibits cell proliferation, halts cell division at the G1 checkpoint, and facilitates the injured DNA repair. p53 protein can induce cell apoptosis to prevent the mutated DNA passage to the next generation in case of the failed DNA repair. Due to the loss of cell supervision of p53 protein after mutation, cell is susceptible to entry of S phase with injured DNA and the genetic instability is the source of gene mutation and chromosomal aberration, leading to cell malignant change and tumor formation. In our experiment, p53 protein expression rate was 67.8%. Almost all the detected p53 protein is mutated because the extremely short half-life of wild-type p53 protein makes the immunohistochemical detection invalid. This expression rate is consistent with the 50-70% of p53 mutation rate in pancreatic cancer according to previous reports[2].

mdm2, a newly discovered oncogene, is located at 12q13.14. The major function of mdm2 is to inhibit the transcription activation by p53 as well as to prevent carcinogenesis. As the target gene of *p53* transcription, mdm2 can combine with p53 to form a refined feedback regulation loop. Wild-type *p53* gene induces the high expression of mdm2 protein, which, in turn, inhibits p53 transcription activity and strictly controls p53 protein level. mdm2 overexpression can block the p53-mediated transactivation, depriving *p53* gene of antineoplastic activity[5]. *mdm2* gene amplification has been found in 36% of all types of sarcomas, 10% of well-differentiated glioma as well as esophageal cancer, neuroblastoma, anaplastic astrocytoma[6]. Our study has proved that p53 protein expression rate was 88.2% (15/17) in mdm2 positive cases and 59.5% (25/42) in mdm2 negative cases, indicating the correlation between the two proteins.

Cox proportional hazards model was applied in multifactor analysis (p53, mdm2, clinicopathological parameters and survival time after surgery), indicating only mdm2 had correlation with survival time after surgery. Patients with negative mdm2 expression had longer survival time after surgery. However, various factors including sex, age, tumor site, TNM staging, differentiation rate and p53 had no correlation with survival time after surgery. Whether

p53 expression in pancreatic cancer is related to prognosis is still under debate, although our data showed that the survival time after surgery for the group with positive p53 expression was shorter than that for the group with negative p53 expression (Table 2). Some authors believe that p53 expression correlates with poor prognosis and it has been reported that p53 expression and *p53* gene mutation can serve as an indicator of prognosis[7,8]. The reason for this confusing condition is still unknown. It may be related to the antibody choice, specimen process and preservation method[9,10]. Another possible reason is that p53 protein cannot completely reflect the *p53* gene expression changes. For example, immunohistochemical staining might not detect p53 protein expression although *p53* gene abnormalities (deletion mutation, frame shift mutation, nonsense mutation) or mdm2 overexpression are present. In these cases, there is no p53 protein expression but *p53* gene expression. Thus, we believe that p53 protein expression cannot truly reflect *p53* gene change, which is related to poor prognosis.

Although multifactor analysis by Cox proportional hazards model indicated that only mdm2 correlates to the survival time after surgery, different combination of p53 protein and mdm2 protein may be related to the prognosis. As shown in Table 2, p53(+) and mdm2(+) group had shorter survival time as compared with other groups, indicating that overexpression of p53 and mdm2 protein may reflect malignant proliferation of pancreatic cancer and combined detection of the two proteins may be beneficial for the prediction of prognosis. The *mdm2* oncogene product forms a complex with the p53 protein and affects normal p53 function[9]. However, the cases in this study were too small to draw a definitive conclusion. Further studies in increased number of patients using a rigorous research design are necessary in the future.

REFERENCES

1 **Niederhuber JE**, Brennan MF, Menck HR. The National Cancer Data Base report on pancreatic cancer. *Cancer* 1995; **76**: 1671-1677

2 **Dong M**, Nio Y, Sato Y, Tamura K, Song MM, Tian YL, Dong YT. Comparative study of p53 expression in primary invasive ductal carcinoma of the pancreas between Chinese and Japanese. *Pancreas* 1998; **17**: 229-237

3 **Yuan RW**, Ding Q, Jiang HY, Qin XF, Zou SQ, Xia HS. Bcl-2, P53 protein expression and apoptosis in pancreatic cancer. *Shijie Huren Xiaohua Zazhi* 1999; **7**: 851-854

4 **Inoue S**, Tezel E, Nakao A. Molecular diagnosis of pancreatic cancer. *Hepatogastroenterology* 2001; **48**: 933-938

5 **Lev Bar-Or R**, Maya R, Segel LA, Alon U, Levine AJ, Oren M. Generation of oscillations by the p53-Mdm2 feedback loop: a theoretical and experimental study. *Proc Natl Acad Sci USA* 2000; **97**: 11250-11255

6 **Bueso-Ramos CE**, Manshouri T, Haidar MA, Huh YO, Keating MJ, Albitar M. Multiple patterns of Mdm-2 deregulation in human leukemias: implications in leukemogenesis and prognosis. *Leuk Lymphoma* 1995; **17**: 13-18

7 **Zhang SY**, Ruggeri B, Agarwal P, Sorling AF, Obara T, Ura H, Namiki M, Klein-Szanto AJ. Immunohistochemical analysis of p53 expression in human pancreatic carcinomas. *Arch Pathol Lab Med* 1994; **118**: 150-154

8 **Sinicrope FA**, Evans DB, Leach SD, Cleary KR, Fenoglio CJ, Lee JJ, Abbruzzese JL. bcl-2 and p53 expression in resectable pancreatic adenocarcinomas: association with clinical outcome. *Clin Cancer Res* 1996; **2**: 2015-2022

9 **Momand J**, Zambetti GP, Olson DC, George D, Levine AJ. The mdm2 oncogene product forms a complex with the p53 protein and inhibits p53-mediated transactivation. *Cell* 1992; **69**: 1237-1245

10 **Frebourg T**, Friend SH. The importance of p53 gene alterations in human cancer: is there more than circumstantial evidence? *J Natl Cancer Inst* 1993; **85**: 1554-1557

Science Editor Li WZ **Language Editor** Elsevier HK

PO Box 2345, Beijing 100023, China
www.wjgnet.com
wjg@wjgnet.com

ELSEVIER

World J Gastroenterol 2005;11(14):2166-2170
World Journal of Gastroenterology ISSN 1007-9327

• *BRIEF REPORTS* •

Plasma von Willebrand factor level as a prognostic indicator of patients with metastatic colorectal carcinoma

Wei-Shu Wang, Jen-Kou Lin, Tzu-Chen Lin, Tzeon-Jye Chiou, Jin-Hwang Liu, Chueh-Chuan Yen, Po-Min Chen

Wei-Shu Wang, Tzeon-Jye Chiou, Jin-Hwang Liu, Chueh-Chuan Yen, Po-Min Chen, Division of Medical Oncology, Department of Medicine, Taipei Veterans General Hospital and National Yang-Ming University School of Medicine, Taipei 112, Taiwan
Jen-Kou Lin, Tzu-Chen Lin, Division of Colorectal Surgery, Department of Surgery, Taipei Veterans General Hospital and National Yang-Ming University School of Medicine, Taipei 112, Taiwan
Supported by a Grant From the Yen Tjing-Ling Medical Foundation
Correspondence to: Dr. Po-Min Chen, Division of Medical Oncology, Department of Medicine, Taipei Veterans General Hospital, Taipei 112, Taiwan. pmchen@vghtpe.gov.tw
Telephone: +886-2-2875-7528 Fax: +886-2-2873-2184
Received: 2004-09-21 Accepted: 2004-11-23

Abstract

AIM: To evaluate the correlations of plasma von Willebrand factor (vWF) level with the distant metastasis and prognosis of patients with colorectal cancer.

METHODS: A total of 86 patients with histologically confirmed metastatic colorectal cancers receiving treatment at Taipei Veterans General Hospital were enrolled. All patients had measurable metastatic lesions and life expectancies of more than 3 mo. Plasma vWF levels were measured by immuno-turbidimetric assay and compared with results from 40 non-metastatic colorectal cancer patients and 22 healthy controls. Patients with metastatic colorectal cancer were divided into two groups according to serum vWF levels and the differences between these two groups were analyzed using χ^2 test. Data on age, gender, performance status, location of primary tumor, extent of metastasis, site of metastases, histological differentiation, serum CEA and plasma vWF levels were analyzed to determine association with survival. Survival curves were constructed by Kaplan-Meier product limit method and the data was analyzed using log-rank test on a microcomputer. Multivariate analysis using the Cox's proportional hazards regression model was then performed to determine the independent prognostic indicators among all of the possible variables.

RESULTS: Colorectal cancer patients were identified as having significantly higher plasma vWF concentrations than healthy controls ($P<0.05$). Moreover, higher vWF plasma levels were associated with advanced tumor stage ($P<0.05$) and the presence of multiple metastases ($P = 0.014$). Patients with lower vWF plasma levels ($\leqslant 160\%$) survived significantly longer than those with a higher plasma vWF level (log-rank test, $P = 0.0043$). By multivariate analysis, plasma vWF levels ($P<0.001$), the extent of metastasis ($P = 0.012$), and the performance status ($P = 0.014$) were identified as independent prognostic factors.

CONCLUSION: Our data indicates that high plasma vWF concentrations correlate with advanced diseases and significantly poor prognosis of patients with metastatic colorectal carcinoma. It may serve as a potential biological marker of disease progression in these patients.

Key words: von Willebrand factor; colorectal carcinoma; prognosis

Wang WS, Lin JK, Lin TC, Chiou TJ, Liu JH, Yen CC, Chen PM. Plasma von Willebrand factor level as a prognostic indicator of patients with metastatic colorectal carcinoma *World J Gastroenterol* 2005; 11(14): 2166-2170
http://www.wjgnet.com/1007-9327/11/2166.asp

INTRODUCTION

Recently, colorectal cancer has become one of the leading causes of cancer-related mortality in Taiwan and the incidence of colorectal cancer in Taiwan has increased over the past few decades. One possible reason is the introduction of Western foods to the local diets[1]. Blood-borne metastasis is the major cause of death from colorectal carcinoma[2]. The development of metastasis is a stepwise process that starts when cancer cells separate from a primary tumor, migrate across blood vessel walls into the bloodstream, and disperse throughout the body to generate new colonies. During the transit into the circulating system, tumor cells are exposed to fluid mechanical forces, plasma proteins, and vascular cells such as platelets. All of which may affect their survival and extravasations from the vasculature[3,4].

Von Willebrand factor (vWF) is a glycoprotein that synthesized mainly in endothelial cells and in megakaryocites[5]. It mediates the adherence of platelets to sub-endothelial matrices during vascular-endothelial damage and acts as a carrier protein for coagulation factor VIII[6]. Increased plasma vWF concentrations have been reported in various clinical conditions such as diabetes mellitus[7], myocardial infarction[8], liver diseases[9], connective tissue diseases[10], and acute infections, probably as a result of increased endothelial cell proliferation or as a part of the acute-phase reaction in response to vascular damage[11]. High plasma vWF concentrations have been reported in patients with various

types of cancer, such as prostate cancer[12], cervical and ovarian carcinoma[13], head and neck cancer[14,15], and colorectal cancer[16]. Moreover, high plasma vWF concentrations often correlate with advanced tumor staging and may have prognostic significance in these patients[12-16].

vWF plays a very important role in the pathogenesis of metastasis, by promoting the binding of tumor cells to platelets, and subsequently, to vascular subendothelium[17-20]. This interaction forms heterotypic cellular emboli, which are not easily recognized by the immune system and have more chance of attaching to the endothelial surfaces than single tumor cells[17-20]. Since blood-borne metastasis is the major cause of death from colorectal carcinoma and vWF is related to the process of metastatic dissemination of malignant cells, to evaluate its potential as a marker of tumor metastasis is warranted. In the current study we investigate the correlation of plasma vWF levels with the distant metastasis of colorectal cancer patients; furthermore, we determine the prognostic significance of plasma vWF levels in these patients.

MATERIALS AND METHODS

Patients

A total of 86 patients with histologically confirmed metastatic colorectal carcinoma receiving treatment at Taipei Veterans General Hospital were enrolled between 2002 and 2003. All patients had measurable metastatic lesions and life expectancies of more than 3 mo. They all received 5-fluorouracil (5-FU)-based systemic chemotherapy and the treatments were continued until disease progression or intolerable toxicity appeared. Salvage chemotherapy with CPT-11, oxaliplatin or capecitabine was allowed. Data on age, gender, performance status, location of primary tumor, extent of metastases, site of metastases, histological differentiation, serum CEA level, and plasma vWF levels was analyzed to determine the association with survival. The characteristics of these patients are shown in Table 1.

Methods

Plasma vWF concentrations were measured using immuno-turbidimetric assay according to manufacturer's instruction (DIAGNOSTICA STAGO, France). Briefly, this assay is based on the change in turbidity of a microparticle suspension that is measured by photometry. A suspension of latex microparticles, coated by covalent bonding with antibodies specific for vWF, is mixed with the test plasma whose vWF antigen level is to be assayed. An antigen-antibody reaction leads to an agglutination of the latex microparticles which induces an increase in turbidity of the reaction medium. The increase in turbidity is reflected by an increase in absorbance which can be measured photometrically. The cut-off level of vWF was set at 160%. The data was compared with results from 40 non-metastatic colorectal cancer patients and 22 healthy controls.

Patients with metastatic colorectal cancer were divided into two groups according to plasma vWF levels. Stratification and the differences between these two groups were analyzed using the χ^2 test[21]. Survival curves were constructed by the Kaplan-Meier product limit method and the data was analyzed by log-rank test on a microcomputer[22]. Multivariate analysis using the Cox's proportional hazards regression model was then performed to determine the independent prognostic indicators among all of the possible variables[23]. All statistical analyses were carried out with SPSS statistical software package.

RESULTS

High plasma vWF level is associated with advanced stage of colorectal carcinoma

The mean plasma level of vWF was 241.3±68.2% in patients with colorectal cancer and 110.1±27.0% in healthy controls ($P<0.001$). vWF measurements according to Dukes' stage are presented in Figure 1. In patients with tumors invading regional lymph nodes (Dukes' C, $n = 26$), the mean plasma vWF level was similar to those without regional lymph node invasion (Dukes' B, $n = 14$) (211.7±40.0% *vs* 207.9±36.0%). However, the plasma vWF level was 266.1±91.3% in patients with metastatic diseases (Dukes' D, $n = 86$), which was significantly higher than those without distant metastasis (Dukes' B or C, $P = 0.001$). As shown in Table 1, there was no significant correlation between plasma vWF concentrations and age, gender, performance status, location of tumor, histological grading, or serum carcinoembryonic antigen level. However, higher vWF plasma levels were correlated with multiple metastatic sites ($P = 0.014$) and, to some extent, trend of liver metastasis ($P = 0.110$).

Table 1 Patients' characteristics according to different plasma vWF levels

Characteristics	vWF>160%	vWF≤160%	*P*
n	53	33	
Age (yr)			0.986
<50	23	14	
50–70	18	11	
>70	12	8	
Gender			0.496
Male	36	20	
Female	17	13	
Performance status			0.656
0	32	18	
1. 2	21	15	
Primary tumor			0.825
Colon	28	16	
Rectum	25	17	
Extent of metastases			0.014
One site	20	22	
Multiple sites	33	11	
Site of metastases			0.110
Liver	37	17	
Lung	34	20	
Lymph nodes	6	3	
Peritoneum	8	5	
Others	3	1	
Histology			0.558
Well-differentiated	8	5	
Moderately-differentiated	25	19	
Poorly-differentiated	13	4	
Unknown	7	5	
Serum CEA level			0.646
≤20ng/mL	19	10	
≤20ng/mL	34	23	

CEA: Carcinoembryonic antigen; vWF: Von Willebrand factor.

High plasma vWF level is associated with poor prognosis of patients with metastatic colorectal carcinoma

As shown in Table 2, by univariate analysis the plasma vWF levels ($P<0.001$), performance status ($P = 0.022$), and extent of metastasis ($P = 0.028$) were identified as survival predicting factors, while age, gender, location of primary tumor, site of metastasis, histological differentiation, and pre-treatment serum CEA levels were not statistically significant. By multivariate analysis, plasma vWF levels ($P<0.001$), performance status ($P = 0.014$), and extent of metastasis ($P = 0.012$) were identified as independent prognostic factors. As shown in Figure 2, the survival curves plotted by Kaplan-Meier method and analyzed by log-rank test revealed that patients with plasma vWF level of less than 160% survived significantly longer than those with plasma vWF of more than 160% ($P = 0.0043$).

DISCUSSION

Metastasis is a multi-step process involved in the alterations of cell-cell adhesion, angiogenesis, degradation of extracellular matrix, escape of immune surveillance, and cell-matrix adhesion[24]. Cell-matrix adhesive interaction plays an important role in the normal organization and stabilization of the cell layer in epithelial tissue. However, in tumor cells the adhesive interaction for these cells and the subendothelial matrices is essential for their metastasis, and molecules that mediate this adhesive process may facilitate tumor cells to metastasize. vWF appears to play an important role in this process, and higher plasma vWF levels have indeed been reported in various types of cancer[12-16]. Evidence has shown that this phenomenon is related to the accelerated endothelial synthesis associated with tumor-dependent angiogenesis[3,4]. In addition, the release of thrombin by tumor cells may induce vWF production in endothelial cells and enhance the adhesion of tumor cells[25,26]. A deficiency of vWF-cleaving activity by its protease control system has recently been identified in colorectal cancer patients, and this deficiency was associated with the progression of the disease[27]. Moreover, a high vWF-positive microvessel number was also identified as an unfavorable prognostic marker for patients with stage-II and stage-III colorectal cancer[28].

The binding of vWF to several types of collagen may contribute to the attachment of platelets to the extracellular matrices of subendothelium; furthermore, a direct interaction between vWF and neoplastic cells has been demonstrated[29]. The expression of surface glycoprotein GpIb and GpIIb-IIIa complex, the adhesive ligands for vWF, has been reported in tumor cells[25,26], which may contribute to the metastatic process by promoting the binding of tumor cells to platelets via plasma vWF. Moreover, such interaction results in heterotypic cell aggregates, which are not easily recognized by the immune system and are more capable of producing adherence to endothelial surface than single tumor cells[25,26,29]. Interestingly, experiments on animals have shown that anti-platelet and anti-vWF antibodies can substantially reduce the occurrence and number of metastasis[25-27,29], indicate that plasma vWF indeed plays a crucial role in the process of metastasis of tumor cells.

A positive correlation between Dukes' stage and plasma vWF concentrations in colorectal cancer patients was recently reported[16]. Our study demonstrated a similar result that plasma vWF levels in colorectal cancer patients were significantly higher than in healthy controls, and the highest vWF plasma levels were observed in patients with metastatic diseases (Figure 1). Moreover, a higher vWF plasma level was shown to be associated with multiple metastases ($P = 0.014$) in our study (Table 1). Elevations in vWF plasma levels of patients with disseminated diseases reflect the enhancement

Table 2 Analysis of prognostic factors on survival

Variables	*n*	Univariate(*P*)	Multivariate(*P*)
Age (yr)			
<50	37	0.528	–
⩾50	49		
Gender			
Male	56	0.986	–
Female	30		
Performance status			
0	50	0.022	0.014
1. 2	36		
Site of primary tumor			
Colon	44	0.430	–
Rectum	42		
Extent of metastases			
One site	42	0.028	0.012
Multiple sites	44		
Liver metastases			
Present	54	0.658	–
Absent	32		
Lung metastases			
Present	54	0.443	–
Absent	32		
Histological differentiation			
Well/moderate	57	0.718	–
Poor/unknown	29		
Pre-treatment CEA			
⩽6 ng/mL	29	0.213	–
>6 ng/mL	57		
Pre-treatment vWF			
⩽160%	33	<0.001	<0.001
>160%	53		

CEA, carcinoembryonic antigen; vWF: von Willebrand factor; –: no significance.

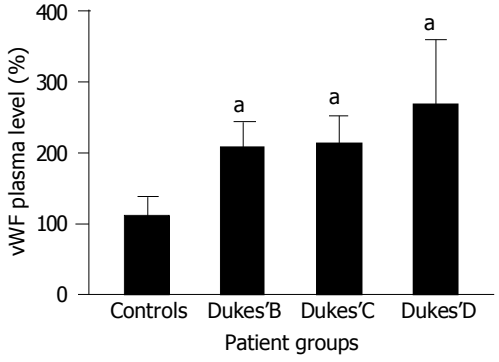

Figure 1 Plasma vWF levels according to Dukes' stages of colorectal cancer. Elevated plasma vWF levels were observed in colorectal cancer patients in a stage-dependent manner. (Data are means±SD. $^aP<0.05$ *vs* the control group).

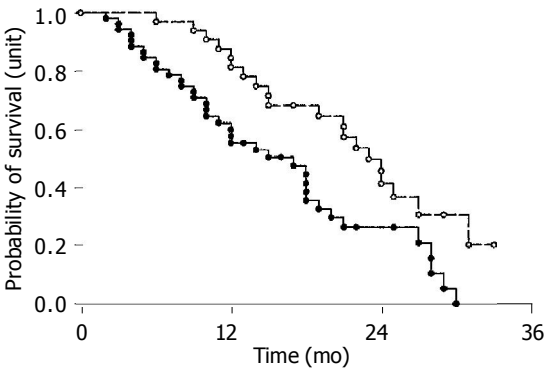

Figure 2 Survival curves according to plasma vWF levels. -○-, vWF ≤160% (n=33); -●-, vWF>160% (n = 53). Patients with plasma vWF levels of less than 160% survived significantly longer than those with vWF of more than 160% (P = 0.0043; log-rank test).

of angiogenic activity to sustain a larger tumor cell burden and the metastatic progression[16]. Furthermore, the metastatic status of these patients may represent an effect of the adhesive property of vWF, which seems to play a crucial role during the course of hematological spread[16].

Recently, a high vWF-positive microvessel number was identified as an independent prognostic marker of patients with stage-II/III colorectal carcinoma[28]. However, the relationship between plasma vWF levels and the survival of patients with metastatic colorectal cancer remains unclear. Since high plasma vWF concentrations were associated with advanced stage and multiple metastasis of colorectal cancer patients in our study, its impact on survival is of interest. In the current study, by log-rank test, patients with lower vWF plasma levels (≤160%) survived significantly longer than those with higher plasma vWF levels (Figure 2). By multivariate analysis, plasma vWF level (P<0.001) was also identified as an independent prognostic factor (Table 2).

Serum carcinoembryonic antigen (CEA) level is the most widely used marker for both prognostic predicting and post-treatment monitoring of patients with colorectal cancer[30,31]. Furthermore, serum CEA levels could also be used in the monitoring of response to systemic chemotherapy in patients with metastatic colorectal carcinoma[32]. In addition to CEA, CA19-9 is another useful serum marker for predicting the prognosis of metastatic colorectal cancer patients[33]. However, in spite of higher plasma vWF levels correlating with both advanced stage and poor prognosis of colorectal patients in our study, a higher plasma vWF level was not identified to be associated with higher serum CEA level (Table 1).

In summary, our data indicates that plasma vWF levels are elevated in colorectal cancer patients in a stage-dependent manner, and a high plasma vWF level correlates with significantly poor prognosis of patients with metastatic diseases. Plasma vWF level may serve as a potential biological marker of disease progression in colorectal cancer patients.

REFERENCES

1 **Lee JA**. Recent trends of large bowel cancer in Japan compared to United States and England and Wales. *Int J Epidemiol* 1976; **5**: 187-194
2 **Hanahan D**, Weinberg RA. The hallmarks of cancer. *Cell* 2000; **100**: 57-70
3 **Gutman M**, Fidler IJ. Biology of human colon cancer metastasis. *World J Surg* 1995; **19**: 226-234
4 **Hart IR**, Saini A. Biology of tumour metastasis. *Lancet* 1992; **339**: 1453-1457
5 **Ruggeri ZM**. Structure and function of von Willebrand factor: relationship to von Willebrand's disease. *Mayo Clin Proc* 1991; **66**: 847-861
6 **Ruggeri ZM**. von Willebrand factor. *J Clin Invest* 1997; **99**: 559-564
7 **Lufkin EG**, Fass DN, O'Fallon WV, Bowie EJ. Increased von Willebrand factor in diabetes mellitus. *Metabolism* 1979; **28**: 63-66
8 **Giustolisi R**, Musso R, Cacciola E, Cacciola RR, Russo M, Petralito A. Abnormal plasma levels of factor VIII/von Willebrand factor complex in myocardial infarction--expression of acute phase reaction or index of vascular endothelium damage? *Thromb Haemost* 1984; **51**: 408
9 **Castillo R**, Maragall S, Rodes J, Clemente C, Profitos J, Ordinas A. Increased factor VIII complex and defective ristocetin-induced platelet aggregation in liver disease. *Thromb Res* 1977; **11**: 899-906
10 **Gordon JL**, Pottinger BE, Woo P, Rosenbaum J, Black CM. Plasma von Willebrand factor in connective tissue disease. *Ann Rheum Dis* 1987; **46**: 491-492
11 **Pottinger BE**, Read RC, Paleolog EM, Higgins PG, Pearson JD. von Willebrand factor is an acute phase reactant in man. *Thromb Res* 1989; **53**: 387-394
12 **Ablin RJ**, Bartkus JM, Gonder MJ. Immunoquantitation of factor VIII-related antigen (von Willebrand factor antigen) in prostate cancer. *Cancer Lett* 1988; **40**: 283-289
13 **Facchini V**, Gadducci A, Baicchi U, Del-Bravo B, Vispi M, Teti G, Fioretti P. Factor VIIIR: Ag plasma levels in patients with cervical and ovarian carcinoma. *Eur J Gynaecol Oncol* 1988; **9**: 87-93
14 **Sweeney JD**, Killion KM, Pruet CF, Spaulding MB. von Willebrand factor in head and neck cancer. *Cancer* 1990; **66**: 2387-2389
15 **Paczuski R**, Bialkowska A, Kotschy M, Burduk D, Betlejewski S. Von Willebrand factor in plasma of patients with advanced stages of larynx cancer. *Thromb Res* 1999; **95**: 197-200
16 **Damin DC**, Rosito MA, Gus P, Roisemberg I, Bandinelli E, Schwartsmann G. Von Willebrand factor in colorectal cancer. *Int J Colorectal Dis* 2002; **17**: 42-45
17 **Gasic GJ**, Gasic TB, Galanti N, Johnson T, Murphy S. Platelet-tumor cell interactions in mice. The role of platelets in the spread of malignant disease. *Int J Cancer* 1973; **11**: 704-718
18 **Marcum JM**, McGill M, Bastida E, Ordinas A, Jamieson GA. The interaction of platelets, tumor cells and vascular subendothelium. *J Lab Clin Med* 1980; **96**: 1046-1053
19 **McCarty OJ**, Mousa SA, Bray PF, Konstantopoulos K. Immobilized platelets support human colon carcinoma cell tethering, rolling, and firm adhesion under dynamic flow conditions. *Blood* 2000; **96**: 1789-1797
20 **Morganti M**, Carpi A, Amo-Takyi B, Sagripanti A, Nicolini A, Giardino R, Mittermayer C. Von Willebrand's factor mediates the adherence of human tumoral cells to human endothelial cells and ticlopidine interferes with this effect. *Biomed Pharmacother* 2000; **54**: 431-436
21 **Fisher RA**, Yates F. Statistical Tables for Biological, Agricultural and Medical Research, 6th ed. New York: Hafner 1964
22 **Peto R**, Pike MC. Conservatism of the approximation sigma (O-E)2-E in the logrank test for survival data or tumor incidence data. *Biometrics* 1973; **29**: 579-584
23 **Thall PF**, Lachin JM. Assessment of stratum-covariate interactions in Cox's proportional hazards regression model. *Stat Med* 1986; **5**: 73-83
24 **Bogenrieder T**, Herlyn M. Axis of evil: molecular mechanisms of cancer metastasis. *Oncogene* 2003; **22**: 6524-6536
25 **Nierodzik ML**, Plotkin A, Kajumo F, Karpatkin S. Thrombin stimulates tumor-platelet adhesion *in vitro* and metastasis *in vivo*. *J Clin Invest* 1991; **87**: 229-236

26 **Nierodzik ML**, Kajumo F, Karpatkin S. Effect of thrombin treatment of tumor cells on adhesion of tumor cells to platelets *in vitro* and tumor metastasis *in vivo*. *Cancer Res* 1992; **52**: 3267-3272
27 **Koo BH**, Oh D, Chung SY, Kim NK, Park S, Jang Y, Chung KH. Deficiency of von Willebrand factor-cleaving protease activity in the plasma of malignant patients. *Thromb Res* 2002; **105**: 471-476
28 **Lackner C**, Jukic Z, Tsybrovskyy O, Jatzko G, Wette V, Hoefler G, Klimpfinger M, Denk H, Zatloukal K. Prognostic relevance of tumour-associated macrophages and von Willebrand factor-positive microvessels in colorectal cancer. *Virchows Arch* 2004; **445**: 160-167
29 **Floyd CM**, Irani K, Kind PD, Kessler CM. von Willebrand factor interacts with malignant hematopoietic cell lines: evidence for the presence of specific binding sites and modification of von Willebrand factor structure and function. *J Lab Clin Med* 1992; **119**: 467-476
30 **Wang WS**, Chen PM, Chiou TJ, Liu JH, Fan FS, Lin TC, Jiang JK, Yang SH, Yen CC, Wang HS, Lin JK. Factors predictive of survival in patients with node-positive colorectal cancer in Taiwan. *Hepatogastroenterology* 2000; **47**:1590-1594
31 **Slentz K**, Senagore A, Hibbert J, Mazier WP, Talbott TM. Can preoperative and postoperative CEA predict survival after colon cancer resection? *Am Surg* 1994; **60**: 528-531; discussion 531-532
32 **Wang WS**, Lin JK, Lin TC, Chiou TJ, Liu JH, Fan FS, Yen CC, Chen WS, Jiang JK, Yang SH, Wang HS, Chen PM. Carcinoembryonic antigen in monitoring of response to systemic chemotherapy in patients with metastatic colorectal cancer. *Int J Colorectal Dis* 2001; **16**: 96-101
33 **Wang WS**, Lin JK, Chiou TJ, Liu JH, Fan FS, Yen CC, Lin TC, Jiang JK, Yang SH, Wang HS, Chen PM. CA 19-9 as the most significant prognostic indicator of metastatic colorectal cancer. *Hepatogastroenterology* 2002; **49**: 160-164

Science Editor Guo SY **Language Editor** Elsevier HK

PO Box 2345, Beijing 100023, China
www.wjgnet.com
wjg@wjgnet.com

ELSEVIER

World J Gastroenterol 2005;11(14):2171-2173
World Journal of Gastroenterology ISSN 1007-9327

• *BRIEF REPORTS* •

Outcome of gall bladder polypoidal lesions detected by transabdominal ultrasound scanning: A nine year experience

D Chattopadhyay, R Lochan, S Balupuri, BR Gopinath, KS Wynne

D Chattopadhyay, R Lochan, S Balupuri, Hepatopancreatobiliary Surgery Unit, Freeman Hospital, Newcastle upon Tyne, NE30PL,UK
BR Gopinath, KS Wynne, Department of Surgery, South Tyneside District Hospital, South Shields, NE34 0PL, UK
Correspondence to: R Lochan, HPB Unit, Department of Surgery (level 4 Secretaries Office), Freeman Hospital, Newcastle upon Tyne, NE34 0PL, UK. rajiv.lochan@nuth.northy.nhs.uk
Telephone: +44-191-2448427 Fax: +44-191-2231483
Received: 2004-08-18 Accepted: 2004-10-05

Abstract

AIM: To determine the outcome of polypoidal lesions within the gall bladder (PLG) diagnosed by trans-abdominal scanning.

METHODS: A nine-year (1993–2002) retrospective case-note review of all patients who underwent ultrasound scanning after referral to a single Upper GI Surgeon at a District General Hospital was conducted. Patients who were diagnosed with a PLG were included in our study. A database was constructed and patient details, investigations including ultrasound scan (USS) findings, treatment and histology and final diagnosis were recorded.

RESULTS: Twenty-three (out of 651) patients were diagnosed pre-operatively by USS to have a polyp-like gall bladder lesion (PLG). Post cholecystectomy histological examination revealed 12 gallstones, 7 cholesterol polyps, 3 adenocarcinomas within polyps and 1 normal gall bladder. The specificity of USS in the diagnosis of PLG was 92.3%. All the true polyps were malignant. Overall USS had 66.66% sensitivity and 100% specificity in the pre-operative suspicion of malignancy. Using size greater than 10 mm as measured on USS as a cut-off, we find 100% sensitivity and 86.95% specificity with a positive predictive value of 50% in the diagnosis of malignancy in PLG.

CONCLUSION: A large number of PLG are in fact calculi within diseased gall bladder. In cases of gall bladder polyps more then 10 mm in size on USS further imaging (cross-sectional and/or EUS) is indicated prior to surgery. This will help in the optimal management of patients and avoid histological surprises.

Key words: Polypoidal lesion in gall bladder; Malignant polyps

Chattopadhyay D, Lochan R, Balupuri S, Gopinath BR, Wynne KS. Outcome of gall bladder polypoidal lesions detected by transabdominal ultrasound scanning: A nine year experience. *World J Gastroenterol* 2005; 11(14): 2171-2173
http://www.wjgnet.com/1007-9327/11/2171.asp

INTRODUCTION

A polypoidal lesion may be defined as an elevation on the gall bladder mucosa. Such polypoid lesions affect 5% of the adult population[1]. The majority of gall bladder polyps are benign, most commonly being cholesterol polyps, however it is their malignant transformation that is the cause for concern[1].

Initial imaging for hepatobiliary disease is usually ultrasonography, hence both surgeons and physicians are often presented with an ultrasound report suggestive of a polypoid lesion within the gall bladder (PLG)[2]. Generally polyps in the gall bladder are demonstrable on ultrasonography, only when they are over 5 mm in diameter. Sonographic differentiation between benign and malignant polyps (and calculous disease) relies greatly on the size of a single non-mobile lesion within the gall bladder. Simple cholecystectomy is curative in early gall bladder carcinoma[3]. Such curative resection is limited to cases in which the carcinoma was diagnosed in gall bladders resected for benign disease[4,5]. Their malignant potential increases with size, as demonstrated in a Japanese study where majority of malignant tumors were over 10 mm[6].

Our study was a retrospective case note review of patients referred to a consultant surgeon between 1993 and 2002. The inclusion criterion into the study was the suggestion of PLG on ultrasonography. The aim of this study was to determine the efficacy of ultrasound scan in diagnosing polyps, by correlating post cholecystectomy histopathological findings with the preoperative sonological results. The literature on existing controversy in imaging and management is thereafter reviewed and discussed briefly.

MATERIALS AND METHODS

In the nine years between April 1993 and March 2002, 751 cholecystectomies were performed at a district general hospital. Six hundred and fifty-one case notes were individually reviewed and ultrasound findings were correlated with final gall bladder histopathology report. The Ultrasound probe used was a 3.5/5.0 MHz transducer. The sonological study was performed by consultant radiologists as per hospital protocol. In cases where sonography was suggestive of PLG,

the scan was repeated by the same radiologist, to check for the mobility of the lesion in an attempt to exclude calculous etiology.

The only inclusion criterion was the presence of a solitary lesion within the gall bladder on pre-operative USS. This inclusion into the study did not differentiate between the method of definitive surgical management, i.e., laparoscopic or open procedure. The histopathological reporting was done by consultant pathologists, and only formal reports were considered.

RESULTS

Preoperative ultrasonography suspected PLG (polyp like gall bladder lesion) in 23 out of 651 patients. In the remaining 628 patients the USS diagnosis was multiple gallstones with or without acute/chronic inflammation.

Among our study group (n = 23) the female to male ratio was 16:7 with a mean age of 56.8 years. Twenty-one patients had symptomatic disease while the remaining two were symptom free.

A diagnosis of polyp like gall bladder lesion was made on the basis of: (1) An immobile gall bladder lesion with no post-acoustic shadows; (2) Normal common bile duct diameter. The range of the sizes of PLG was 2-22 mm (mean 7.91, standard deviation 4.26). Histological examination revealed multiple lesions in three patients all of which turned out to be gall bladder calculi. These results are detailed in Table 1. The sensitivity of USS in making a diagnosis of PLG was 100% (this is obvious given the inclusion criteria of our study), the proportion of patients correctly diagnosed as having a gall bladder abnormality (specificity) was 92.3%, since one patient had a histologically-normal gall bladder.

Ultrasound scan could not exclude gall bladder malignancy in two PLG cases. The suspicion about the malignant nature of these two PLG was the size of the polyp within the gall bladder (18 mm and 20 mm). In spite of the suspicion of cancer of gall bladder, no further imaging was performed in both cases because: (1) Cross sectional imaging was not widely available in the earlier years of our study; (2) Solitary lesions within the gall bladder were assumed to be due to calculous disease necessitating cholecystectomy.

In all the 23 patients laparoscopic cholecystectomy was performed. Median hospital stay was 2 d with a range of 2-5. There were no peri- or post-operative complications.

Histopathological examination of these 23 resected gall bladders revealed calculous cholecystitis in 12 (52%) cases, cholesterosis in eight patients and a focus of adenocarcinoma in three specimens. No histopathological abnormality was found in one gall bladder. No true benign polyps were seen, all the three true polyps contained a focus of adenocarcinoma.

Out of the three histologically proven gall bladder malignancies, pre-operative USS raised the suspicion of malignancy in two cases. With regard to a diagnosis of malignancy, USS had 66.66% sensitivity and 100% specificity (true positives: 2, false positives: 0, true negatives: 20, false negative: 1 [USS diagnosis was a solitary calculus]). One other gall bladder specimen was reported to have no abnormality on histopathology despite a preoperative suspicion of PLG on ultrasonography.

DISCUSSION

Majority of polypoidal lesions within the gall bladder are due to calculous biliary disease. Cholesterolosis is defined

Table 1 Summary of USS and pathological features

	Symptom	Post acoustic shadow	Lesion –number/mobility	Size mm	USS diagnosis	Histologic diagnosis
1	Bil Colic	No	1/immobile	2-3	PLG	Cholesterosis
2	Bil Colic	No	1/immobile	5	PLG	Calculi
3	Bil Colic	No	1/immobile	5	PLG	Cholesterosis
4	Bil Colic	No	1/immobile	5	PLG	Cholesterosis
5	Bil Colic	No	1/immobile	5	PLG	Calculi
6	Bil Colic	No	1/immobile	6	PLG	Cholesterosis
7	Bil Colic	No	1/immobile	6	PLG	Calculi
8	Bil Colic	No	1/immobile	7	PLG	Calculi
9	Bil Colic	No	1/immobile	8	PLG	Calculi
10	Bil Colic	No	1/immobile	8	PLG	Calculi
11	Bil Colic	No	1/immobile	9	PLG	Calculi
12	Bil Colic	No	1/immobile	9	PLG	Calculi
13	Bil Colic	No	1/immobile	10	PLG	Calculi
14	Bil Colic	No	1/immobile	12	PLG	Adenocarcinoma
15	Bil Colic	No	1/immobile	18	? malignant	Adenocarcinoma
16	Atyp pain	No	1/immobile	2-3	PLG	Cholesterosis
17	Atyp pain	No	1/immobile	5	PLG	Calculi
18	Atyp pain	No	1/immobile	5	PLG	Cholesterosis
19	Atyp pain	No	1/immobile	6	PLG	Calculi
20	Atyp pain	No	1/immobile	6	PLG	Normal
21	Atyp pain	No	1/immobile	20	? malignant	Adenocarcinoma
22	Asymp	No	1/immobile	10	PLG	Calculi
23	Asymp	No	1/immobile	12	PLG	Cholesterosis

Bil Colic – biliary colic.

as the result of accumulation of triglycerides and esterified sterols in macrophages of the lamina propria and can give ultrasonographic appearance of small polyps[7]. Such polyps are reportedly pedunculated and are attached to the gall bladder by a delicate pedicle that becomes easily detached before or during a cholecystectomy[8]. A gallstone impacted within the gall bladder wall may be easily mistaken for a polyp on ultrasound scanning[2]. Thus, several factors could contribute to the discrepancies of the USS findings and the final diagnosis after surgical excision.

In 12 of our 23 cases the PLG turned out be true gall bladder calculi. These findings are in keeping with a retrospective analysis of 41 patients with PLG who underwent cholecystectomy where the definitive diagnosis was cholesterolosis (17 of 41) or cholelithiasis (15 of 41)[2].

In our study ultrasonography was not accurate in differentiating polyps (true or pseudo that is; cholestrerol polyps) from calculi (66.7% sensitivity). This differentiation assumes significant importance given that true polyps that is, adenomas/papillomas have the potential for malignancy[9]. A level of 15 mm as a cut-off, which appears to have been used as a USS marker for malignancy has missed suspecting a 12 mm PLG as a possible malignant polyp. All the three malignant gall-bladder polyps have been above 10 mm in size. Using size greater than 10 mm as measured on USS as a marker, we find 100% sensitivity and 86.95% specificity with a positive predictive value of 50% (three lesions greater that 10 mm were non-malignant).

The efficacy of ultrasound in diagnosing gall bladder polyps is controversial as evidenced by the following two studies. In a study reported in 1993, out of 23 patients with polyps on USS only 13 (57%) true polyps were found on histology[10]. Yang *et al*[11] (1992), have reported an ultrasound scan sensitivity of 90% in detecting gall bladder polyps after reviewing post-cholecystectomy specimens with a preoperative diagnosis of polyps of the gall bladder. Sugiyama *et al* (1995), suggested routine use of endoscopic ultrasound (EUS) in the patients with a USS suggestive of a polyp. They suggested that aggregation of echogenic spots seem to be pathognomonic of cholesterol polyps. Another group[12] suggest that the nonenhanced and enhanced CT scan differentiate neoplastic from non-neoplastic PLGs. CT biliary cystoscopy has recently been suggested as a non-invasive and accurate means of assessing gall bladder polyps[13]. However, in most of the units it may not be logistically practical and financially feasible to perform EUS or CT purely to differentiate PLG.

The management of polyps found on USS is conflicting with some offering selective surgery while others offer routine laparoscopic cholecystectomy[12,14]. In our study, USS was not very specific for the diagnosis of gall bladder polyps as 52% (12 out of 23) were found to be calculi within the gall bladder. However as 22 of the 23 resected gall bladders were pathological, we suggest that gall bladder with polypoidal lesions on USS have high probability of having intrinsic gall bladder disease and hence should undergo cholecystectomy. Further a size criteria of greater than 10 mm as a marker for further investigation of the gall bladder abnormality seems reasonable. This will aid optimal management planning and avoid histological surprises.

In conclusion, ultrasound evidence of a polypoidal lesion within the gall bladder is an indication for a cholecystectomy since nearly all such gall bladders are diseased. Most of such lesions turn out to be having calculous etiology. Lesions which, measure more than 10 mm on ultrasonography need to be imaged further.

REFERENCES

1 **Myers RP,** Shaffer EA, Beck PL. Gallbladder polyps: epidemiology, natural history and management. *Can J Gastroenterol* 2002; **16**: 187-194

2 **Damore LJ,** Cook CH, Fernandez KL, Cunningham J, Ellison EC, Melvin WS. Ultrasonography incorrectly diagnoses gallbladder polyps. *Surg Laparosc Endosc Percutan Tech* 2001; **11**: 88-91

3 **Shoup M,** Fong Y. Surgical indications and extent of resection in gallbladder cancer. *Surg Oncol Clin N Am* 2002; **11**: 985-994

4 **Nevin JE,** Moran TJ, Kay S, King R. Carcinoma of the gallbladder: staging, treatment, and prognosis. *Cancer* 1976; **37**: 141-148

5 **Bergdahl L.** Gallbladder carcinoma first diagnosed at microscopic examination of gallbladders removed for presumed benign disease. *Ann Surg* 1980; **191**: 19-22

6 **Terzi C,** Sokmen S, Seckin S, Albayrak L, Ugurlu M. Polypoid lesions of the gallbladder: report of 100 cases with special reference to operative indications. *Surgery* 2000; **127**: 622-627

7 **Berk RN,** van der Vegt JH, Lichtenstein JE. The hyperplastic cholecystoses: cholesterolosis and adenomyomatosis. *Radiology* 1983; **146**: 593-601

8 **Christensen AH,** Ishak KG. Benign tumors and pseudotumors of the gallbladder. Report of 180 cases. *Arch Pathol* 1970; **90**: 423-432

9 **Majeski JA.** Polyps of the gallbladder. *J Surg Oncol* 1986; **32**: 16-18

10 **Ozdemir A,** Ozenc A S, Coskun T. Ultrasonography in the diagnosis of gallbladder polyps. *Br J Surg* 1993; **80**: 345

11 **Yang HL,** Sun YG, Wang Z. Polypoid lesions of the gallbladder: diagnosis and indications for surgery. *Br J Surg* 1992; **79**: 227-229

12 **Furukawa H,** Kosuge T, Shimada K, Yamamoto J, Kanai Y, Mukai K, Iwata R, Ushio K. Small polypoid lesions of the gallbladder: differential diagnosis and surgical indications by helical computed tomography. *Arch Surg* 1998; 133: 735-739

13 **Lou MW,** Hu WD, Fan Y, Chen JH, E ZS, Yang GF. CT biliary cystoscopy of gallbladder polyps. *World J Gastroenterol* 2004; **10**: 1204-1207

14 **Huang CS,** Lien HH, Jeng JY, Huang SH. Role of laparoscopic cholecystectomy in the management of polypoid lesions of the gallbladder. *Surg Laparosc Endosc Percutan Tech* 2001; **11**: 242-247

Science Editor Guo SY **Language Editor** Elsevier HK

PO Box 2345, Beijing 100023, China
www.wjgnet.com
wjg@wjgnet.com

ELSEVIER

World J Gastroenterol 2005;11(14):2174-2178
World Journal of Gastroenterology ISSN 1007-9327

• *BRIEF REPORTS* •

Risk factors for the recurrence of hepatocellular carcinoma after radiofrequency ablation of hepatocellular carcinoma in patients with hepatitis C

Yutaka Yamanaka, Katsuya Shiraki, Kazumi Miyashita, Tomoko Inoue, Tomoyuki Kawakita, Yumi Yamaguchi, Yukiko Saitou, Norihiko Yamamoto, Takeshi Nakano, Atsuhiro Nakatsuka, Koichiro Yamakado, Kan Takeda

Yutaka Yamanaka, Katsuya Shiraki, Kazumi Miyashita, Tomoko Inoue, Tomoyuki Kawakita, Yumi Yamaguchi, Yukiko Saitou, Norihiko Yamamoto, Takeshi Nakano, First Department of Internal Medicine, Mie University School of Medicine, 2-174 Edobashi, Tsu, Mie 514-8507, Japan
Atsuhiro Nakatsuka, Koichiro Yamakado, Kan Takeda, Department of Radiology, Mie University School of Medicine, 2-174 Edobashi, Tsu, Mie 514-8507, Japan
Correspondence to: Katsuya Shiraki, MD, PhD, 2-174 Edobashi, Tsu, Mie 514-8507, Japan. katsuyas@clin.medic.mie-u.ac.jp
Telephone: +81-592-31-5015 Fax: +81-592-31-5201
Received: 2004-09-06 Accepted: 2004-09-25

Abstract

AIM: To analyze the risk factors of hepatocellular carcinoma (HCC) recurrence after radiofrequency ablation (RFA) treatment with HCV-associated hepatitis.

METHODS: Twenty-six patients with HCV-associated HCC who were followed-up for more than 12 mo were selected for this study. Risk factors for distant intrahepatic recurrences of HCC were evaluated for patients in whom complete coagulation was achieved without recurrence in the same subsegment as the primary nodule. Twelve clinical and tumoral factors were examined: Age, gender, nodule diameter, number of primary HCC nodule, Child-Pugh classification, serum platelet, serum albumin, serum AST, post RFA AST, serum ALT, post RFA ALT, post RFA treatment.

RESULTS: Distant recurrences of HCC in remnant liver after RFA were observed in 14 cases and in the number of primary HCC nodules (P = 0.047), and the serum platelets (P = 0.030), the clear difference came out by the recurrence group and the non-recurrence group. The cumulative recurrence rates after 1 and 2 years were 30.8% and 86.8%, respectively for primary multinodular HCC, and 15.4% and 29.5% respectively, for primary uninodular HCC. In addition the 1-year recurrence rates for patients with serum albumin more than 3.4 g/dL and less than 3.4 g/dL were 23.1% for both, but the 2-years recurrence rates were 89.0% and 23.1%, respectively. The number of primary HCC nodules (relative risk, 6.970; P = 0.016) were found to be a statistically significant predictor for poor distant intrahepatic recurrence by univariate analysis.

CONCLUSION: Patients who have multiple HCC nodules, low serum platelets and low serum albumin accompanied by HCV infection, should be carefully followed because of the high incidence of new HCC lesions in the remnant liver, even if coagulation RFA is complete.

Key words: Hepatocellular carcinoma; Radiofrequency ablation

Yamanaka Y, Shiraki K, Miyashita K, Inoue T, Kawakita T, Yamaguchi Y, Saitou Y, Yamamoto N, Nakano T, Nakatsuka A, Yamakado K, Takeda K. Risk factors for the recurrence of hepatocellular carcinoma after radiofrequency ablation of hepatocellular carcinoma in patients with hepatitis C. *World J Gastroenterol* 2005; 11(14): 2174-2178
http://www.wjgnet.com/1007-9327/11/2174.asp

INTRODUCTION

Various locoregional therapies including percutaneous ethanol injection (PEI), percutaneous acetic injection and radiofrequency ablation (RFA) were performed on hepatocellular carcinoma (HCC) patients with HCV-associated hepatitis. Radiofrequency ablation (RFA) is a novel means of treating patients with both metastatic and primary liver cancer[1]. It consists of a thermal treatment technique designed to produce approximately 3-cm diameter coagulative necrosis of the tissue in a single session. Moreover, performed RFA has been used for the treatment of HCC and can be percutaneously under local anesthesia[2]. A recent prospective study found that RFA requires fewer sessions such that PEI for patients with small HCCs and the 1-year survival rate is 98%[3]. Although these therapies can achieve complete necrosis of small HCC, its recurrence is still common. The intrahepatic recurrence rate is 20% during a mean follow-up period of 18 mo[4]. However, it is unclear which factors influence intrahepatic recurrence.

The purpose of this study was to analyze the risk factors of HCC recurrence after RFA treatment with HCV-associated hepatitis.

MATERIALS AND METHODS

Clinical features of the patients

The clinical features of patients are summarized in Table 1. Among the patients diagnosed with HCC at the First

Department of Internal Medicine, Mie University Hospital, from January 2001 to October 2003, 26 patients with HCV-associated HCC who were followed-up for more than 12 mo were selected for this study. Among them 12 patients had local recurrence in the other subsegment as the primary nodule, within as early as 6 mo evident from CT scans. All patients who were anti-HCV positive were evaluated. The 19 male and seven female patients had a median age of 67.9 years, and according to the Child-Pugh classification, 15 patients (58%) had class C cirrhosis and 11 patients (42%) had class B cirrhosis. There were 13 uninodular cases and 13 multinodular cases, and biopsy was not performed if the findings of ultrasonography (US), computed tomography (CT), and angiography were all indicative of HCC, and if AFP and DCP levels were elevated. The diagnosis of HCC was established by enhanced CT and CT during hepatic anteriography (CTA) and anterioportography (CTAP) and CTA and CTAP were performed on the patients before transcatheter arterial embolization (TAE) or (RFA). The median follow-up period was 12.5 mo with recurrence and 20 mo without recurrence.

Radiofrequency ablation

We utilized RFA for local ablation therapy of HCCs. Since the gelatin sponge remains in the tumor for 2 to 3 weeks after (TACE), RFA was generally performed within 2 weeks after TACE.

RFA was performed using a 17-gauge internally cooled straight electrode (Radionics, Burlington, MA). The patients received 35 mg of pethidine hydrochloride (Opystan, Tanabe, Tokyo, Japan) intravenously before RFA for analgesia, and antibiotics were administered before and 2 to 3 d after each chemoembolization or RFA procedure.

The RF electrode was inserted into the tumor under local anesthesia. The RF generator was then activated and the power needed to maintain a temperature of 90-120 ℃ at the tip was delivered for 10-20 min. The electrode was inserted into the tumor under real-time CT fluoroscopic guidance into patients for whom multiple electrode placements were required due to a large tumor size or because the entire lesion was not visualized by US imaging. Using CT fluoroscopy, bubble formation in the tumor does not prevent additional electrode insertion into the tumor and accumulation of iodized-oil in the tumor aids precise insertion of the electrode. The electrode was placed in the tumor depending on the tumor size and shape, and the RF generator was then activated at each tumor site. The endpoint of RFA was the presence of a well-defined area of no enhancing tissue including the treated tumor with a tumor-free margin of at least 5 mm in the arterial and portal phases of enhanced CT and as seen by the MR images.

Table 1 Patient's characteristics

Gender		
Number of males		19(73%)
Number of females		7(27%)
Median age		67.9
Child-Pugh	A	15(58%)
	B	11(42%)
	C	0(0%)
Number of HCC nodules		
Uninodular		13(50%)
Multinodular		13(50%)
Mean follow-up period (months)		
With recurrence		12.5
Without recurrence		20

Therapeutic effects and diagnosis for recurrence

Helical CT scan was used to determine the therapeutic effects. Complete coagulation was defined as no enhancement in the coagulated area on the helical CT scan one week after RFA. A follow-up CT scan was performed three months after RFA. As a rule thereafter, a helical CT scan was performed every 3 mo for at least 1 year. Local recurrence of an HCC nodule was defined as the development of an enhanced area on the CT scan in the same subsegment as the primary nodule. The helical CT scan was also used to study the distant recurrence of HCC in a different subsegment of the liver. Hepatic DSA was performed to confirm not only local but also distant recurrence of HCC.

Risk factors for distant Intrahepatic recurrence of HCC

Risk factors for the distant intrahepatic recurrence of HCC were evaluated for patients for whom complete coagulation was achieved without recurrence in the same subsegment as the primary nodule. Twelve clinical and tumor factors were examined: Age, gender, nodule diameter, number of primary HCC nodule, Child-Pugh classification, serum platelet, serum albumin, serum AST, post RFA serum AST, serum ALT, post RFA serum ALT.

Statistical analysis

The unpaired *Student's t*-test was used to compare averages between groups and the χ^2-test and Fisher's exact probability test were used to compare independence. The distant intrahepatic recurrence rate was computed by Kaplan-Meier estimates and the Kaplan-Meier method and the log rank test were used to analyze the risk factors associated with the distant intrahepatic recurrences of HCC.

A stratified Cox proportional hazard regression model was used for multivariate analysis of age, gender, AST level as post RFA, platelet, Child-Pugh stage, nodule diameter, and the number of primary HCC. The results were reported as hazard ratios with 95% CI. A *P*-value of <0.05 was considered to be statistically significant for all analysis.

RESULTS

Recurrence analysis according to distant intrahepatic recurrence

Among the 26 cases, the number of HCC uninodular and multinodular nodules were 13 and 13, respectively (Table 1), and distant recurrence of HCC in the remnant liver after RFA was observed for 14 cases. Clinical and tumoral characteristics were compared between the groups with and without distant intrahepatic recurrence. No statistically significant difference was observed with regard to age, gender, nodule diameter, Child-Pugh stage, serum albumin, serum pretr-

Table 2 Comparison of patients with and without recurrence of primary HCC in the liver

Variable		With recurrence (n = 12)	Without recurrence (n = 14)	P
Age (yr)		67.8 ± 5.7	67.9 ± 7.8	NS
Gender				
Male		6	11	NS
Female		6	3	
Nodule diameter (mm)		23.5 ± 7.2	32.0 ± 24.2	NS
Number of primary HCC nodules				
Uninodular		3	10	<0.05
Multinodular		9	4	
Child-Pugh	A	6	9	NS
	B	6	5	
Platelet (/μL)		8.2 ± 3.6	13.3 ± 6.9	<0.05
Albumin (g/L)		3.2 ± 0.3	3.4 ± 0.4	NS
AST (IU/L)		197.7 ± 416.0	87.2 ± 47.2	NS
Post-RFA AST (IU/L)		72.4 ± 25.4	70.8 ± 2.96	NS
ALT (IU/L)		98.0± 121.6	76 ± 43.5	NS
Post-RFA ALT (IU/L)		49.3 ±21.4	55.4 ± 30.5	NS
Post-RFA treatment				
UDCA		10	12	NS
SNMC		5	4	
IFN		0	2	

eatment AST level, serum posttreatment AST level, serum pretreatment ALT levels, or the serum posttreatment AST level. In the number of primary HCC nodules, and the serum platelets, the difference came out intentionally by the recurrence group and the non-recurrence group.

In the number of primary HCC nodules (P = 0.047), and the serum platelets (P = 0.030), the clear difference came out by the recurrence group and the non-recurrence group. Also, no statistically significant difference was observed for UDCA therapy, and SNMC therapy after RFA treatment (Table 2). Since IFN therapy had few cases, it was not possible to compare it with other therapies about a curative effect.

Cumulative HCC recurrence rate

The longest duration of the case that we observed was 31 mo. Furthermore, the distant intrahepatic recurrence rates were analyzed based on the number of primary HCC nodules using the Kaplan-Meier method, and the recurrence rates after 1 and 2 years were 30.8%, and 86.8%, respectively for primary multinodular HCC, and 15.4% and 29.5%, respectively, for primary uninodular HCC. The primary multinodular HCC was significantly (P = 0.0136) associated with a higher distant intrahepatic recurrence rate compared with primary uninodular HCC (Figure 1). The 1-year recurrence rate for patients with serum albumin of more than 3.4 g/L and less than 3.4 g/L were 23.1% each for, but the 2-year recurrence rate they were 89.0% and 23.1%. Low (less than 3.4 g/L) serum albumin was significantly (P = 0.0236) associated with a higher recurrence rate compared with high (more than 3.4 g/L) serum albumin (Figure 2).

Multivariate analysis for risk factors of recurrence

To search for more reliable prognostic markers, a stratified Cox proportional hazard regression model was created involving eight parameters associated with decreased distant intrahepatic recurrence. The number of primary HCC nodules (relative risk, 6.970; P = 0.016) was found to be statistically significant predictors for poor distant intrahepatic recurrence by multivariate analysis (Table 3).

DISCUSSION

In this study, the rates of local and distal recurrence were 0% and 53.8% for primary HCC after RFA treatment.

Some studies reported local recurrence rates that vary from 45% to 53% for HCC patiants after RFA[22,24,25]. RFA is successful for achieving a one-session treatment for patients with small HCC using RFA with CT assistance, and RFA with CT assistance is effective for the treatment of patients with small HCC[5-21]. One of the advantages of RFA is that it can be repeatedly performed, can be combined with TACE, and can also be used according to the features of the disease and the response[7]. For patients with cirrhosis and HCC, RFA results in effective local control of disease in a significant proportion of patients and can be safely performed with minimal complications[8]. By virtue of its

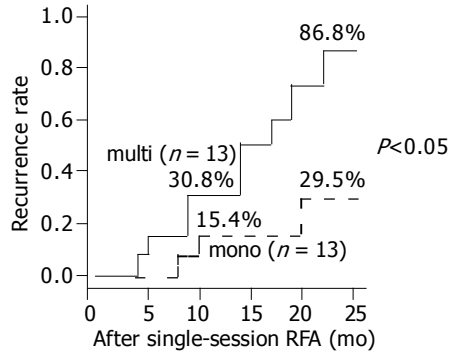

Figure 1 Distant intrahepatic recurrence curves by subsets of tumor count before RFA. The recurrence rates after 1 and 2 years were 30.8% and 86.8%, respectively, for primary multinodular HCC and 15.4% and 29.5% respectively, for primary uninodular HCC. Primary multinodular HCC was significantly (P = 0.0136) associated with a higher distant intrahepatic recurrence rate compared with primary uninodular HCC.

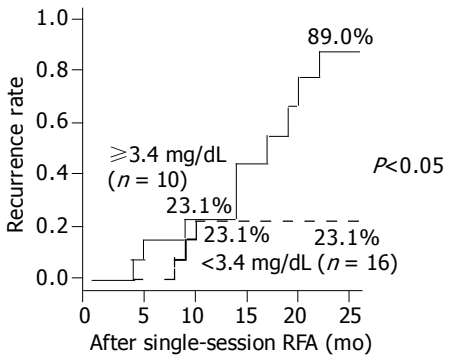

Figure 2 Distant intrahepatic recurrence curves by subsets of serum albumin before RFA. The one-year recurrence rate for patients with serum albumin of more than 3.4 g/L and less than 3.4 g/L were both 23.1%, but the two-year recurrence rates were 89.0% and 23.1%, respectively.

local curability, minimal effect on liver function, and easy repeatability for recurrence, image-guided percutaneous tumor ablations, especially RFA, will become increasingly important for the treatment of HCC[21]. RFA is a useful primary therapy for the treatment of patients with HCC, especially for cases with a poor liver reserve from cirrhosis and with multiple and deep-sited lesions. RFA also is an effective and relatively simple procedure for the treatment of liver cancers[6].

Using a variety of approaches, others have also reported high local recurrences after RFA in patients with HCC[22-24]. In contrast, our data with a local recurrence rate of 0% were lower than that of other studies[22-24]. TACE and RFA combination therapy and real-time evaluation of RFA effective area by CT in our methods provably contribute to this low local recurrence rate. Although recurrences are frequent due to various factors, for instance tumor size and the follow-up period, this study found that the distal recurrence rate is 53% for primary HCC after RFA treatment, and this result is similar to that of other studies[22-24].

In the number of primary HCC nodules ($P = 0.047$), and the serum platelets ($P = 0.030$), the difference came out intentionally by the recurrence group and the non-recurrence group. The number of primary HCC nodules (relative risk, 6.970; $P = 0.016$) was also found to be statistically significant predictors for poor distant intrahepatic recurrence by multivariate analysis. We also discovered that the primary serum albumin in patients with HCV-associated hepatitis after RFA treatment is associated with the development of distal recurrence rate.

The most important variable, which influences the local recurrence rate, is tumor size[14]. Patients who have more than two HCC nodules accompanied by HCV infection should be carefully followed because of a high incidence of new HCC lesions in the remnant liver, even if coagulation by microwave or ablation by radiofrequency is complete[11].

Our observations are consistent with these reports, and it is reasonable to argue that there may be multicentric occurrence of HCC in the remnant liver at the same frequency as that for HCV-associated cirrhosis.

In the current study, no statistically significant difference was observed in the serum pre-treatment and post-treatment AST level. The serum AFP level (relative risk, 0.621; $P = 0.596$; not shown) was not found to be a statistically significant predictor of poor distant intrahepatic recurrence by multivariate analysis.

Table 3 Multivariate analysis for prognostic factors of recurrence

Variables CI	Ungav. /fav.[1]	Relative risk	CI	*P*
Multinodular	Multinodular/ Uninodular	6.970	1.443-33.667	0.016
Post-RFA AST[2]	>40/< = 40 (IU/L)	2.438	0.213-27.956	0.474
Platelet[2]	10>/> = 10 (/μL)	2.426	0.445-13.222	0.306
Nodule diameter[2]	30>/> = 30 (mm)	1.032	0.217-4.903	0.969
Child-Pugh	B/A	0.861	0.184-4.025	0.849
Gender	Males/female	0.627	0.132-2.986	0.558
Age (yr)[2]	68>/< = 68 (yr)	0.406	0.076-2.169	0.292

[1]Unfav./fav., unfavorable *vs* favorable CI, 95%; [2]Mean.

The high serum ALT level for HCV-associated cirrohsis is associated with the rapid development of HCC[18]. Continuous elevation of ALT is important for HCC diagnosis. Patients with the high level of serum ALT for 2 years or more were at a greater risk of HCC development[17]. Patients with HCV-associated cirrhosis with a sustained high serum ALT level are at a high risk of HCC development, suggesting the possibility of the prevention of HCC development in HCV-associated cirrhosis patients by reducing inflammatory necrosis[13]. Many investigators have shown that patients with cirrhosis who have persistently high ALT levels have a high risk of developing HCC[16,19,20]. It was necessary to continue treatment with anti-inflammatory drugs following initial IFN therapy to suppress ALT below 80 IU. This prevents HCC occurrence or delays the time of HCC occurrence and prolongs patient's life span[17].

In the present study, no statistically significant difference was observed between the serum pretreatment and post-treatment AST levels and serum pretreatment and post-treatment ALT levels, indicating a high incidence of HCC recurrence in HCV-associated cirrhotic patients.

Recently, the risk of HCC occurrence was discovered to increase with the liver fibrosis stage in HCV-related liver disease[9,10]. The intrahepatic recurrence rate in C-viral and B-viral HCC is higher than that in NBNC-related HCC. Furthermore, fibrosis staging and the pathological grading of HCC are significantly linked to intrahepatic recurrence as seen by univariate analysis[13].

We did not evaluate the liver fibrosis stage for HCV-related liver disease. The serum platelet count ($P = 0.030$) for the group with recurrence was significantly higher than that for the group without recurrence. Compared with a group with the serum high platelet value, the group with a low platelet value of the recurrence rate of the HCC is clearly higher. The low level (less than 3.4 g/L) of serum albumin was significantly ($P = 0.0236$) associated with a higher recurrence rate compared with the high level (more than 3.4 g/L) of serum albumin, and this result is similar to those of previous studies[16,17,19,20]. These results suggest that the progression of fibrosis increases the recurrence of HCC with HCV-associated cirrhosis.

Serum AFP levels are significantly linked to intrahepatic recurrence as seen by univariate analysis[13]. Specifically, the level of lectin-reactive AFP is a suitable predictive marker for the early recognition of HCC during the follow-up of patients with cirrhosis[12]. In this study, no statistically significant difference was observed for the serum AFP level.

In conclusion, patients who have multiple HCC nodules, low serum platelets and serum albumin less than 3.4 g/L accompanied by HCV infection should be carefully followed, because of a high incidence of new HCC lesions in the remnant liver even if coagulation RFA is complete.

REFERENCES

1 **Fontana RJ**, Hamidullah H, Nghiem H, Greenson JK, Hussain H, Marrero J, Rudich S, McClure LA, Arenas J. Percutaneous radiofrequency thermal ablation of hepatocellular carcinoma: a safe and effective bridge to liver transplantation. *Liver Transpl* 2002; **8**: 1165-1174

2 **Francica G**, Marone G. Ultrasound-guided percutaneous

treatment of hepatocellular carcinoma by radiofrequency hyperthermia with a 'cooled-tip needle'. A preliminary clinical experience. *Eur J Ultrasound* 1999; **9**: 145-153

3 **Yamakado K**, Nakatsuka A, Ohmori S, Shiraki K, Nakano T, Ikoma J, Adachi Y, Takeda K. Radiofrequency ablation combined with chemoembolization in hepatocellular carcinoma: treatment response based on tumor size and morphology. *J Vasc Interv Radiol* 2002; **13**: 1225-1232

4 **Yamakado K**, Nakatsuka A, Akeboshi M, Shiraki K, Nakano T, Takeda K. Combination therapy with radiofrequency ablation and transcatheter chemoembolization for the treatment of hepatocellular carcinoma: Short-term recurrences and survival. *Oncol Rep* 2004; **11**: 105-109

5 **Yamasaki T**, Kurokawa F, Shirahashi H, Kusano N, Hironaka K, Okita K. Percutaneous radiofrequency ablation therapy with combined angiography and computed tomography assistance for patients with hepatocellular carcinoma. *Cancer* 2001: **91**: 1342-1348

6 **Jiang HC**, Liu LX, Piao DX, Xu J, Zheng M, Zhu AL, Qi SY, Zhang WH, Wu LF. Clinical short-term results of radiofrequency ablation in liver cancers. *World J Gastroenterol* 2002; **8**: 624-630

7 **Livraghi T**. Radiofrequency ablation, PEIT, and TACE for hepatocellular carcinoma. *J Hepatobiliary Pancreat Surg* 2003; **10**: 67-76

8 **Curley SA**, Izzo F, Ellis LM, Nicolas Vauthey J, Vallone P. Radiofrequency ablation of hepatocellular cancer in 110 patients with cirrhosis. *Ann Surg* 2000; **232**: 381-391

9 **Takano S**, Yokosuka O, Imazeki F, Tagawa M, Omata M. Incidence of hepatocellular carcinoma in chronic hepatitis B and C: a prospective study of 251 patients. *Hepatology* 1995; **21**: 650-655

10 **Yoshida H**, Shiratori Y, Moriyama M, Arakawa Y, Ide T, Sata M, Inoue O, Yano M, Tanaka M, Fujiyama S, Nishiguchi S, Kuroki T, Imazeki F, Yokosuka O, Kinoyama S, Yamada G, Omata M. Interferon therapy reduces the risk for hepatocellular carcinoma: national surveillance program of cirrhotic and noncirrhotic patients with chronic hepatitis C in Japan. IHIT Study Group. Inhibition of Hepatocarcinogenesis by Interferon Therapy. *Ann Intern Med* 1999; **131**: 174-181

11 **Izumi N**, Asahina Y, Noguchi O, Uchihara M, Kanazawa N, Itakura J, Himeno Y, Miyake S, Sakai T, Enomoto N. Risk factors for distant recurrence of hepatocellular carcinoma in the liver after complete coagulation by microwave or radiofrequency ablation. *Cancer* 2001; **91**: 949-956

12 **Shiraki K**, Takase K, Tameda Y, Hamada M, Kosaka Y, Nakano T. A clinical study of lectin-reactive alpha-fetoprotein as an early indicator of hepatocellular carcinoma in the follow-up of cirrhotic patients. *Hepatology* 1995; **22**: 802-807

13 **Koike Y**, Shiratori Y, Sato S, Obi S, Teratani T, Imamura M, Hamamura K, Imai Y, Yoshida H, Shiina S, Omata M. Risk factors for recurring hepatocellular carcinoma differ according to infected hepatitis virus-an analysis of 236 consecutive patients with a single lesion. *Hepatology* 2000; **32**: 1216-1223

14 **Hori T**, Nagata K, Hasuike S, Onaga M, Motoda M, Moriuchi A, Iwakiri H, Uto H, Kato J, Ido A, Hayashi K, Tsubouchi H. Risk factors for the local recurrence of hepatocellular carcinoma after a single session of percutaneous radiofrequency ablation. *J Gastroenterol* 2003; **38**: 977-981

15 **Pompili M**, Rapaccini GL, de Luca F, Caturelli E, Astone A, Siena DA, Villani MR, Grattagliano A, Cedrone A, Gasbarrini G. Risk factors for intrahepatic recurrence of hepatocellular carcinoma in cirrhotic patients treated by percutaneous ethanol injection. *Cancer* 1997; **79**: 1501-1508

16 **Ikeda K**, Saitoh S, Arase Y, Chayama K, Suzuki Y, Kobayashi M, Tsubota A, Nakamura I, Murashima N, Kumada H, Kawanishi M. Effect of interferon therapy on hepatocellular carcinogenesis in patients with chronic hepatitis type C: A long-term observation study of 1,643 patients using statistical bias correction with proportional hazard analysis. *Hepatology* 1999; **29**: 1124-1130

17 **Mahmood S**, Niiyama G, Kawanaka M, Nakata K, Sho M, Yasuhara Y, Ito T, Yamada G. Long term follow-up of a group of chronic hepatitis C patients treated with anti-inflammatory drugs following initial interferon therapy. *Hepatol Res* 2002; **24**: 213

18 **Tarao K**, Rino Y, Ohkawa S, Shimizu A, Tamai S, Miyakawa K, Aoki H, Imada T, Shindo K, Okamoto N, Totsuka S. Association between high serum alanine aminotransferase levels and more rapid development and higher rate of incidence of hepatocellular carcinoma in patients with hepatitis C virus-associated cirrhosis. *Cancer* 1999; **86**: 589-595

19 **Lin SM**, Lin CJ, Hsu CW, Tai DI, Sheen IS, Lin DY, Liaw YF. Prospective randomized controlled study of interferon-alpha in preventing hepatocellular carcinoma recurrence after medical ablation therapy for primary tumors. *Cancer* 2004; **100**: 376-382

20 **Shiratori Y**, Shiina S, Teratani T, Imamura M, Obi S, Sato S, Koike Y, Yoshida H, Omata M. Interferon therapy after tumor ablation improves prognosis in patients with hepatocellular carcinoma associated with hepatitis C virus. *Ann Intern Med* 2003; **138**: 299-306

21 **Shiina S**, Teratani T, Obi S, Hamamura K, Koike Y, Omata M. Nonsurgical treatment of hepatocellular carcinoma: from percutaneous ethanol injection therapy and percutaneous microwave coagulation therapy to radiofrequency ablation. *Oncology* 2002; **62 Suppl 1**: 64-68

22 **Curley SA**, Izzo F, Ellis LM, Nicolas Vauthey J, Vallone P. Radiofrequency ablation of hepatocellular cancer in 110 patients with cirrhosis. *Ann Surg* 2000; **232**: 381-391

23 **Curley SA**, Izzo F, Delrio P, Ellis LM, Granchi J, Vallone P, Fiore F, Pignata S, Daniele B, Cremona F. Radiofrequency ablation of unresectable primary and metastatic hepatic malignancies: results in 123 patients. *Ann Surg* 1999; **230**: 1-8

24 **Tranberg KG**. Percutaneous ablation of liver tumours. *Best Pract Res Clin Gastroenterol* 2004; **18**: 125-145

25 **Rossi S**, Garbagnati F, Lencioni R, Allgaier HP, Marchiano A, Fornari F, Quaretti P, Tolla GD, Ambrosi C, Mazzaferro V, Blum HE, Bartolozzi C. Percutaneous radio-frequency thermal ablation of nonresectable hepatocellular carcinoma after occlusion of tumor blood supply. *Radiology* 2000; **217**: 119-126

Science Editor Li WZ **Language Editor** Elsevier HK

PO Box 2345, Beijing 100023, China
www.wjgnet.com
wjg@wjgnet.com

ELSEVIER

World J Gastroenterol 2005;11(14):2179-2183
World Journal of Gastroenterology ISSN 1007-9327

• *BRIEF REPORTS* •

Relationships of tumor inflammatory infiltration and necrosis with microsatellite instability in colorectal cancers

Jing-Fang Gao, Gunnar Arbman, Tabasum Imran Wadhra, Hong Zhang, Xiao-Feng Sun

Jing-Fang Gao, Tabasum Imran Wadhra, Xiao-Feng Sun, Department of Oncology, Institute of Biomedicine and Surgery, University of Linköping, Linköping, Sweden
Gunnar Arbman, Department of Surgery, Vrinnevi Hospital, Norrköping, Sweden
Hong Zhang, Department of Dermatology, Institute of Biomedicine and Surgery, University of Linköping, Linköping, Sweden
Jing-Fang Gao, Department of Oncology, Institute of Biomedicine and Surgery, University of Linköping, S-581 85 Linköping, Sweden
Supported by grants from the Swedish Cancer Foundation and the Health Research Council in the South-East of Sweden
Correspondence to: Xiao-Feng Sun, Associate Professor, MD, PhD, Department of Oncology, Institute of Biomedicine and Surgery, University of Linköping, S-581 85 Linköping, Sweden. xiasu@ibk.liu.se
Telephone: +46-13-222066 Fax: +46-13-222846
Received: 2004-09-16 Accepted: 2004-10-08

Abstract

AIM: The relationships between microsatellite instability (MSI) and survival in colorectal cancer patients are not consistent. The favorable survival of patient with MSI has been suggested to be related to pronounced inflammatory infiltration; however, the reason for non-association of MSI with survival is unclear. Our aims were to investigate the associations of inflammatory infiltration and tumor necrosis (TN) with microsatellite status and clinicopathological factors in colorectal cancer patients in whom MSI was not related to survival.

METHODS: Three hundred and one colorectal adenocarcinomas were evaluated for inflammatory infiltration and 300 for TN under light microscope.

RESULTS: Low infiltration at invasive margin ($\chi^2 = 3.94$, $P = 0.047$) and in whole tumor stroma ($\chi^2 = 3.89$, $P = 0.049$) was associated with MSI, but TN was not ($\chi^2 = 0.10$, $P = 0.75$). Low infiltration was related to advanced stage ($\chi^2 = 8.67$, $P = 0.03$), poorer differentiation ($\chi^2 = 8.84$, $P = 0.03$), DNA non-diploid ($\chi^2 = 10.04$, $P = 0.002$), higher S-phase fraction ($\chi^2 = 11.30$, $P = 0.004$), positive p53 expression ($\chi^2 = 7.94$, $P = 0.01$), and worse survival ($P = 0.03$ for both univariate and multivariate analyses). Abundant TN was related to advanced stage ($\chi^2 = 17.74$, $P = 0.001$) and worse survival ($P = 0.02$ for univariate, and $P = 0.05$ for multivariate analysis).

CONCLUSION: The result that high inflammatory infiltration was not related to MSI might help explain the non-association of MSI with survival in colorectal cancer patients.

Key words: Inflammatory infiltration; Necrosis; Microsatellite instability; Prognosis; Colorectal cancer

Gao JF, Arbman G, Wadhra TI, Zhang H, Sun XF. Relationships of tumor inflammatory infiltration and necrosis with microsatellite instability in colorectal cancers. *World J Gastroenterol* 2005; 11(14): 2179-2183
http://www.wjgnet.com/1007-9327/11/2179.asp

INTRODUCTION

Colorectal cancer arises through at least two distinct genetic pathways in its carcinogenesis: microsatellite instability (MSI) and chromosomal instability[1]. MSI refers to genome-wide alteration in repetitive DNA sequence caused by deficiencies in DNA mismatch repair machinery[2], which accounts for about 10-15% of sporadic colorectal cancers and nearly all hereditary non-polyposis colorectal cancers[1]. Studies have shown that colorectal cancers with MSI are likely to be characterized by more frequent right-sided location, poor differentiation, mucinous/signet-ring cell carcinoma, and intense peri- and intra-tumoral inflammatory reaction[1,3,4]. Patients with MSI tumors appear to have a favorable prognosis compared with those with microsatellite stability (MSS) tumors[1,5-8]. The favorable prognosis associated with MSI has been suggested to be related to an enhanced inflammatory infiltration in the tumors[1,5] although the mechanism behind this phenomenon is unclear.

However, several studies including our previous two studies have reported the lack of association between MSI and survival either in entire group of colorectal cancer patients[9-14] or in subgroup with stage II colorectal cancers[15,16]. The reason for the non-association remains unclear. To our knowledge, no one has studied the association of inflammatory infiltration with microsatellite status in the patients in whom MSI is not related to survival. A recent study showed that necrosis in tumor was related to MSI-H in colorectal cancers[17]. Tumor necrosis (TN) is a common feature of solid tumors associated with a poor clinical outcome due to rapid tumor growth without sufficient blood supply[18]. However, the association of TN with microsatellite status has not been well studied. Therefore, it is interesting to evaluate the relationship of inflammatory infiltration and TN with MSI in colorectal cancers in which MSI was not related to survival. Meanwhile, we analyzed the relationship of inflammatory infiltration and TN with clinicopathological and other variables.

MATERIALS AND METHODS

Patients

Three hundred and one primary colorectal adenocarcinomas were studied for inflammatory infiltration and 300 for TN. The patients were diagnosed at the Department of Pathology, Linköping Hospital, Linköping, and Vrinnevi Hospital, Norrköping, Sweden, between 1975 and 2001. The patient's gender, age, tumor location, and Dukes' stage were confirmed from surgical and/or pathological records. Tumor growth pattern and the grade of differentiation were scored by two pathologists. The mean age of the patients was 71 years (ranging from 34 to 94 years). Tumors from the ascending and transverse colon were regarded as proximal tumors, whereas tumors from descending and sigmoid colon, and the rectum were considered distal. The tumor growth pattern was divided into expansive or infiltrative type based on pattern of growth and invasiveness. Differentiation was graded as well, moderately, poorly differentiated, and mucinous/signet-ring cell carcinoma. The data on microsatellite status[13,14], DNA ploidy, S-phase fraction (SPF)[19], and p53 expression[20] were taken from previous studies carried out at our laboratory. Microsatellite status was determined by a microsatellite analysis using the Bat26 marker; 25 cases were MSI, and 152 were MSS. DNA ploidy and SPF were measured by flow cytometry; 107 cases were DNA diploid, and 118 were non-diploid; 52 were <5% SPF, 65 were 5-10%, and 72 were >10%. p53 expression was identified with immunohistochemistry by using CM1 antibody; 117 cases were p53 negative (completely negative cases plus the cases with <5% of p53-stained tumor cells), and 114 were positive (the cases having ⩾5% of p53-stained tumor cells). No information was available about patients' age in two cases, tumor site in 7, Dukes' stage in 8, growth pattern in 21, grade of differentiation in 1, microsatellite status in 125, DNA ploidy in 75, SPF in 111, and p53 expression in 69 cases. Among 301 patients, 10 MSS and one MSI cases had received adjuvant preoperative radiotherapy, one MSS case had palliative radiotherapy, two MSS had adjuvant chemotherapy, and one MSS had palliative chemotherapy. No information was available for two cases, and the rest did not receive any radiotherapy or chemotherapy. The patients were followed up until the end of October 2001, and 125 died of colorectal cancer.

Histopathological evaluation

Three to ten sections from different parts of the tumor were examined at low magnification (×10) under light microscope by two of the authors (of whom one is a pathologist) independently in a blinded fashion without knowing the clinicopathological and other data of the patients. After the first run of the scoring, approximately 20% of the cases with disagreed score were reread independently by the two authors. Finally, about 4% of the cases with discrepant scoring were discussed under a dual-headed microscope to reach agreement on the scoring. Inflammatory infiltration and TN in the margins of the sections were not included in order to avoid artifacts. Infiltrating inflammatory cells were identified as small mononuclear cells in the stroma of tumor. The distributions of the infiltration were classified into two groups by localization: (a) those presented along the invasive margin of the tumor; (b) those distributed in entire tumor. The degree of infiltration was classified as absent, sparse, moderate, and intense according to the density of inflammatory cell[21]. Necrosis was scored as absent; <10%; 10-30%, and >30% based on the percentage of necrosis in whole tumor area[18]. Since the distributions of inflammatory infiltration and NT were often heterogeneous, the entire sections were examined to assess tumor areas including high and low inflammatory infiltration and NT. If higher infiltration or NT was more than one-third of the section, it was taken into account for scoring.

Statistical analysis

The relationships of inflammatory infiltration and TN with survival were tested using Cox's Proportional Hazard Model. Survival curves were calculated using the Kaplan-Meier method. The relationships of inflammatory infiltration and TN with other variables were tested by using the χ^2 test or Fisher exact test. Two-sided P values of less than 5% were considered statistically significant.

RESULTS

Inflammatory infiltration in relation to microsatellite status, clinicopathological and other variables

Among the 301 tumors studied, inflammatory cells at the invasive margin were absent in one case, sparse in 105, moderate in 131, and intense in 64 (Figure 1A); inflammatory cells in the tumors were absent in 17, sparse in 135, moderate in 110, and intense in 39 cases (Figure 1B). Absent, sparse, and moderate were combined as a low-level group, and

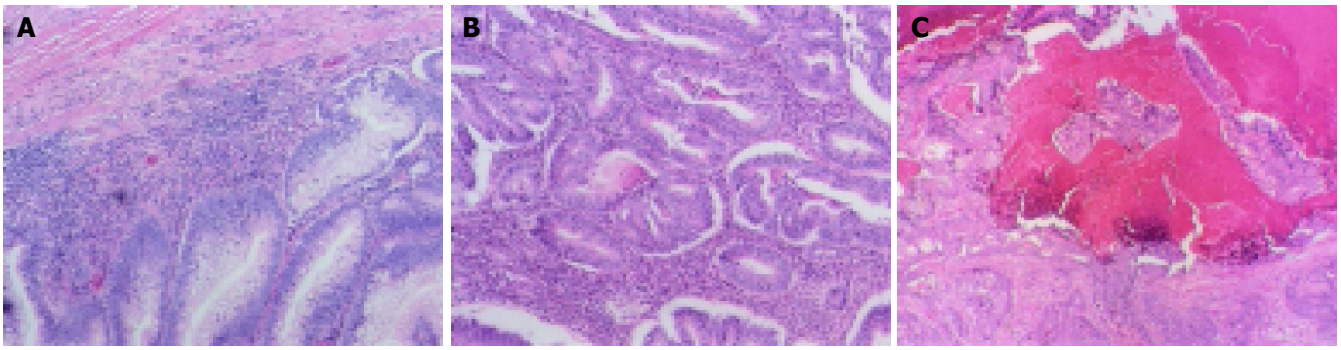

Figure 1 High inflammatory infiltration at the tumor invasive margin (A) and in the tumor (B), and TN (C). Hematoxylin and eosin-stained sections of colorectal cancer (×10).

intense as a high-level group, according to the similarities of the clinicopathological features.

The relationship of inflammatory infiltration at the invasive margin or in the tumor with microsatellite status is present in Table 1. Low inflammatory infiltration either at the invasive margin or in the tumor was lightly associated with MSI ($\chi^2 = 3.94$, $P = 0.047$ and $\chi^2 = 3.89$, $P = 0.049$).

The relationship of inflammatory infiltration at the invasive margin with clinicopathological and other variables is summarized in Table 2. The degree of inflammatory infiltration was lower in tumors with Dukes' stage D ($\chi^2 = 8.67$, $P = 0.03$), DNA non-diploid ($\chi^2 = 10.04$, $P = 0.002$), higher SPF ($\chi^2 = 11.30$, $P = 0.004$), p53 positive expression ($\chi^2 = 7.94$, $P = 0.01$), as well as poor differentiation and mucinous/signet-ring cell carcinoma ($\chi^2 = 8.84$, $P = 0.03$). Moreover, the patients with low inflammatory infiltration had worse survival than those with high infiltration ($P = 0.03$; Figure 2A), even after adjustment for patients' gender, Dukes' stage and differentiation ($P = 0.03$, data not shown). We did not find any relationship between inflammatory infiltration and patients' gender, tumor location, or growth pattern ($P>0.05$).

There was no significant relationship of inflammatory infiltration in the tumor with the above clinicopathological and other variables ($P>0.05$, data not shown).

TN in relation to MSS, and clinicopathological and other variables

Among the 300 tumors studied, necrosis was absent in 76 cases, 54 had <10%, 93 had 10-30%, and 77 had >30% of necrosis. The cases with <10% of necrosis were graded as little necrosis and the remainder as abundant necrosis (Figure 1C), based on the similarities of the clinicopathological features.

We did not find a relationship between TN and MSI ($\chi^2 = 0.10$, $P = 0.75$; Table 1). As shown in Table 2, the frequency of TN was increased from Dukes' stages A to D ($\chi^2 = 17.74$, $P = 0.001$). TN was more frequent in moderately/poorly differentiated tumors, but was the lowest in mucinous/signet-ring cell carcinomas ($\chi^2 = 22.98$, $P<0.0001$). Patients with abundant TN had worse survival than those with little TN in univariate analysis ($P = 0.02$; Figure 2B). The survival significance was borderline after adjustment for Dukes' stage and differentiation ($P = 0.05$, data not shown). There were no associations of TN with other factors including gender, age, tumor location, growth pattern, DNA ploidy, SPF, and p53 expression ($P>0.05$).

Table 1 Relationship of tumor inflammatory infiltration and necrosis with microsatellite status

Variable Category	Microsatellite stability (%)	Microsatellite instability (%)	*P*
Infiltration at the invasive margin			0.047
Low	120 (79)	24 (96)	
High	31 (21)	1 (4)	
Infiltration in the tumor			0.049
Low	71 (46)	17 (68)	
High	81 (54)	8 (32)	
Necrosis			0.75
Little	76 (51)	13 (54)	
Abundant	74 (49)	11 (46)	

Considering the relationship of inflammatory infiltration with TN, tumors with high infiltration tended to have less necrosis although the relationship did not reach statistical significance ($\chi^2 = 3.62$, $P = 0.057$).

DISCUSSION

MSI has been shown to be a favorable prognostic factor in colorectal cancer patients, even independent of tumor stage, or radiotherapy and chemotherapy[1,5-8,22,23]. The reason for this evidence has been proposed to be partly due to a stronger host response of immune system in MSI tumors than in MSS ones[1,5]. However, several other studies have reported the lack of association between MSI and survival, either in entire group of colorectal cancer patients[9,10,12] or in the subgroup with stage II colorectal cancers[15,16]. Such non-association was also shown in our previous two studies[13,14] and another Swedish study[11]. The National Cancer Institute Workshop concluded that MSI has not yet been shown conclusively to be an independent predictor of prognosis in colorectal cancer patients[2]. The reason for the non-association between MSI and survival is unclear. Subgroup variation within populations is unlikely an explanation for this evidence because the similar findings have been reported by various groups among different populations. The relationship between the degree of inflammatory infiltration and microsatellite status in the patients without association of MSI with survival has not been studied. Based on our previous findings of the non-association between MSI and

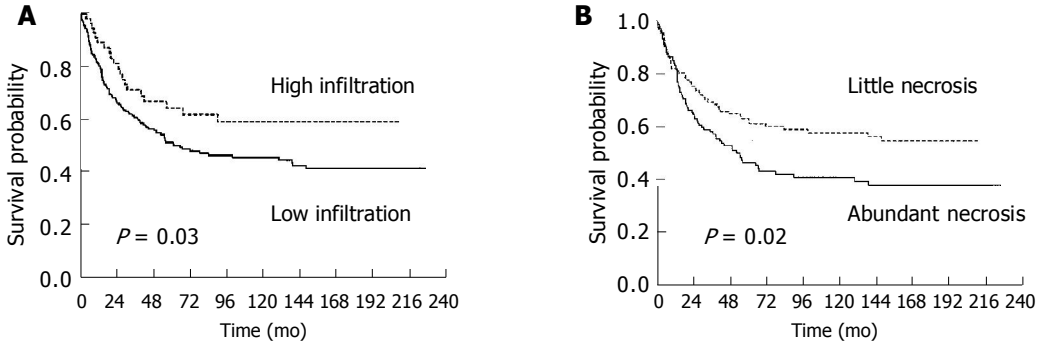

Figure 2 Tumor inflammatory infiltration at the invasive margin (A) and necrosis (B) in relation to survival in patients with colorectal cancer.

Table 2 Relationship of tumor inflammatory infiltration at the invasive margin and TN with clinicopathological and other variables

Variable	Inflammatory infiltration at the invasive margin			TN		
Category	*n*	High (%)	*P*	*n*	Abundant	*P*
Gender			0.06			0.31
Male	158	27 (17)		158	85 (54)	
Female	143	37 (26)		142	68 (48)	
Age (yr)			0.68			0.12
≤70	138	31 (22)		138	77 (56)	
>70	161	33 (21)		160	75 (47)	
Tumor location			0.55			0.75
Proximal	109	25 (23)		108	54 (50)	
Distal	185	37 (20)		185	96 (52)	
Dukes' stage			0.03			0.001
A	47	11 (23)		45	15 (33)	
B	102	26 (25)		103	45 (44)	
C	94	23 (24)		94	53 (56)	
D	50	3 (6)		50	36 (72)	
Gowth pattern			0.65			0.38
Expansive	128	25 (20)		128	64 (50)	
Infiltration	152	33 (22)		152	84 (55)	
Differentiation			0.03			<0.0001
Well	23	10 (43)		24	7 (29)	
Moderately	196	42 (21)		195	116 (60)	
Poorly	44	7 (16)		43	22 (51)	
Mucinous+signet-ring cell	37	5 (14)		37	8 (22)	
DNA ploidy			0.002			0.14
Diploid	107	32 (30)		107	53 (49)	
Non-diploid	118	15 (13)		118	70 (59)	
S-phase fraction			0.004			0.24
<5%	52	19 (37)		52	26 (50)	
5–10%	65	16 (25)		65	31 (48)	
>10%	72	8 (11)		72	44 (61)	
p53 expression			0.01			0.07
Negative	117	33 (28)		117	57 (49)	
Positive	114	15 (13)		114	69 (61)	

survival[13,14], we observed that a low level of inflammatory infiltration either at the invasive margin or in the tumor was related to MSI phenotype in the present study. Although the statistically significant differences were borderline ($P = 0.047$ and $P = 0.049$), the results provided at least an indication that pronounced inflammatory infiltration did not always accompany MSI tumors as proposed[1,3,4].

It is generally accepted that the immune system represents a specific host response to tumors. The survival advantage of pronounced infiltration of all the inflammatory cells, or various subsets of inflammatory cells such as lymphocytes and macrophages, around or within colorectal tumors has been demonstrated[21,24-26]. Anti-tumor effects of infiltrating inflammatory cells may be mediated by cytokine secretion induced by the response of inflammatory cells to tumor stimulation. The expression of two cytokines interleukin-4 (IL-4) and TN factor-α (TNF-α) in colon cancer has been found to be associated with better survival[27]. In the present study, we confirmed the previous findings in which abundant inflammatory infiltration at the invasive margin predicted a favorable prognosis in colorectal cancer patients[6,21,25]. Moreover, we found that the high level of inflammatory infiltration at the invasive margin was associated with earlier Dukes' stage, better differentiation, DNA diploid, lower SPF, and negative p53 expression. However, the degree of inflammatory infiltration in the tumor was not related to clinicopathological or other factors studied. These results indicated that the degree of inflammatory infiltration at the invasive margin, compared with that in the tumor, was more effective against the tumor.

Clinical results regarding the relationship of microsatellite status in colorectal cancer patients with adjuvant chemotherapy are fairly inconsistent. Some patients with MSI tumor had no survival benefit from chemotherapy[12,22,23] but others had[8].Reviewing all eight previous studies, that showed the non-association between MSI and survival in colorectal cancer patients, two studies were carried out on patients without chemotherapy[9,15], and one study on patients with chemotherapy, in which no survival benefit of chemotherapy was observed in MSI patients although the benefit was found in total group of the patients or microsatellite status patients[12]. Four studies did not provide information about chemotherapy[10,11,13,16]. In our previous study in 438 colorectal cancers with microsatellite status[14], 34 (8%) had received radiotherapy, 15 (3%) chemotherapy, and 7 (2%) both treatments. No information was available for 59 (13%), and the rest, 316 (73%), did not receive any adjuvant or palliative treatments. Statistical analysis showed that neither radiotherapy ($P = 0.23$) nor chemotherapy ($P = 0.84$) improved survival of the patients (unpublished data). Taken together, it seems that chemotherapy and radiotherapy were unlikely the reasons behind the non-association between MSI and survival in colorectal cancer patients. Obviously, further studies are needed to evaluate the effect of chemotherapy and radiotherapy on MSI patients.

TN is a common feature of solid tumors and caused by ischemia due to rapid tumor growth. The degree of TN reflected the level of intra-tumor hypoxia, and increased

hypoxia has been associated with high metastatic potential. TN has been previously demonstrated as an indicator of poor prognosis in several types of cancers, including colorectal cancer[18]. In the present study, abundant TN was related to poor survival, advanced Dukes' stage, and moderate/poor differentiation. Unexpectedly, the lowest frequency of TN was seen in mucinous carcinomas/signet-ring cell carcinoma that had more aggressive behaviors. This was probably due to mucinous carcinomas that had a substantial amount of mucin and were less likely to have gland formation. In addition, mucinous carcinomas usually grow slowly, which requires less blood supply, and were therefore lack of TN. Recently, Greenson *et al*[17], reported that the absence of TN was related to MSI-H in colorectal cancers. However, we could not prove this in the present study. The varying results may be due to the different characteristics of the patients and pathological features of the tumors. Besides, it may partly depend on the classification of MSI: they divided MSS into MSI-H, and microsatellite status which included MSI-low cases. Therefore, they had a lower frequency of MSI (9.8%) than ours (14%).

In conclusion, the lack of association of pronounced inflammatory infiltration with MSI might be one of the explanations for non-association between MSI and survival in colorectal cancers.

REFERENCES

1 **Gryfe R**, Gallinger S. Microsatellite instability, mismatch repair deficiency, and colorectal cancer. *Surgery* 2001; **130**: 17-20
2 **Boland CR**, Thibodeau SN, Hamilton SR, Sidransky D, Eshleman JR, Burt RW, Meltzer SJ, Rodriguez-Bigas MA, Fodde R, Ranzani GN, Srivastava S. A National Cancer Institute Workshop on Microsatellite Instability for cancer detection and familial predisposition: development of international criteria for the determination of microsatellite instability in colorectal cancer. *Cancer Res* 1998; **58**: 5248-5257
3 **Smyrk TC**, Watson P, Kaul K, Lynch HT. Tumor-infiltrating lymphocytes are a marker for microsatellite instability in colorectal carcinoma. *Cancer* 2001; **91**: 2417-2422
4 **Alexander J**, Watanabe T, Wu TT, Rashid A, Li S, Hamilton SR. Histopathological identification of colon cancer with microsatellite instability. *Am J Pathol* 2001; **158**: 527-535
5 **Gryfe R**, Kim H, Hsieh ET, Aronson MD, Holowaty EJ, Bull SB, Redston M, Gallinger S. Tumor microsatellite instability and clinical outcome in young patients with colorectal cancer. *N Engl J Med* 2000; **342**: 69-77
6 **Gafa R**, Maestri I, Matteuzzi M, Santini A, Ferretti S, Cavazzini L, Lanza G. Sporadic colorectal adenocarcinomas with high-frequency microsatellite instability. *Cancer* 2000; **89**: 2025-2037
7 **Samowitz WS**, Curtin K, Ma KN, Schaffer D, Coleman LW, Leppert M, Slattery ML. Microsatellite instability in sporadic colon cancer is associated with an improved prognosis at the population level. *Cancer Epidemiol Biomarkers Prev* 2001; **10**: 917-923
8 **Elsaleh H**, Joseph D, Grieu F, Zeps N, Spry N, Iacopetta B. Association of tumour site and sex with survival benefit from adjuvant chemotherapy in colorectal cancer. *Lancet* 2000; **355**: 1745-1750
9 **Feeley KM**, Fullard JF, Heneghan MA, Smith T, Maher M, Murphy RP, O'Gorman TA. Microsatellite instability in sporadic colorectal carcinoma is not an indicator of prognosis. *J Pathol* 1999; **188**: 14-17
10 **Ko JM**, Cheung MH, Kwan MW, Wong CM, Lau KW, Tang CM, Lung ML. Genomic instability and alterations in Apc, Mcc and Dcc in Hong Kong patients with colorectal carcinoma. *Int J Cancer* 1999; **84**: 404-409
11 **Salahshor S**, Kressner U, Fischer H, Lindmark G, Glimelius B, Pahlman L, Lindblom A. Microsatellite instability in sporadic colorectal cancer is not an independent prognostic factor. *Br J Cancer* 1999; **81**: 190-193
12 **Carethers JM**, Smith EJ, Behling CA, Nguyen L, Tajima A, Doctolero RT, Cabrera BL, Goel A, Arnold CA, Miyai K, Boland CR. Use of 5-fluorouracil and survival in patients with microsatellite-unstable colorectal cancer. *Gastroenterology* 2004; **126**: 394-401
13 **Evertson S**, Wallin A, Arbman G, Rutten S, Emterling A, Zhang H, Sun XF. Microsatellite instability and MBD4 mutation in unselected colorectal cancer. *Anticancer Res* 2003; **23**: 3569-3574
14 **Emterling A**, Wallin A, Arbman G, Sun XF. Clinicopathological significance of microsatellite instability and mutated RIZ in colorectal cancer. *Ann Oncol* 2004; **15**: 242-246
15 **Curran B**, Lenehan K, Mulcahy H, Tighe O, Bennett MA, Kay EW, O'Donoghue DP, Leader M, Croke DT. Replication error phenotype, clinicopathological variables, and patient outcome in Dukes' B stage II (T3,N0,M0) colorectal cancer. *Gut* 2000; **46**: 200-204
16 **Wang C**, van Rijnsoever M, Grieu F, Bydder S, Elsaleh H, Joseph D, Harvey J, Iacopetta B. Prognostic significance of microsatellite instability and Ki-ras mutation type in stage II colorectal cancer. *Oncology* 2003; **64**: 259-265
17 **Greenson JK**, Bonner JD, Ben-Yzhak O, Cohen HI, Miselevich I, Resnick MB, Trougouboff P, Tomsho LD, Kim E, Low M, Almog R, Rennert G, Gruber SB. Phenotype of microsatellite unstable colorectal carcinomas: Well-differentiated and focally mucinous tumors and the absence of dirty necrosis correlate with microsatellite instability. *Am J Surg Pathol* 2003; **27**: 563-570
18 **Swinson DE**, Jones JL, Richardson D, Cox G, Edwards JG, O'Byrne KJ. Tumour necrosis is an independent prognostic marker in non-small cell lung cancer: correlation with biological variables. *Lung Cancer* 2002; **37**: 235-240
19 **Sun XF**, Carstensen JM, Stal O, Zhang H, Nilsson E, Sjodahl R, Nordenskjold B. Prognostic significance of p53 expression in relation to DNA ploidy in colorectal adenocarcinoma. *Virchows Arch A Pathol Anat Histopathol* 1993; **423**: 443-448
20 **Sun XF**, Carstensen JM, Zhang H, Stal O, Wingren S, Hatschek T, Nordenskjold B. Prognostic significance of cytoplasmic p53 oncoprotein in colorectal adenocarcinoma. *Lancet* 1992; **340**: 1369-1373
21 **Nagtegaal ID**, Marijnen CA, Kranenbarg EK, Mulder-Stapel A, Hermans J, van de Velde CJ, van Krieken JH. Local and distant recurrences in rectal cancer patients are predicted by the nonspecific immune response; specific immune response has only a systemic effect-a histopathological and immunohistochemical study. *BMC Cancer* 2001; **1**: 7
22 **Colombino M**, Cossu A, Manca A, Dedola MF, Giordano M, Scintu F, Curci A, Avallone A, Comella G, Amoruso M, Margari A, Bonomo GM, Castriota M, Tanda F, Palmieri G. Prevalence and prognostic role of microsatellite instability in patients with rectal carcinoma. *Ann Oncol* 2002; **13**: 1447-1453
23 **Halling KC**, French AJ, McDonnell SK, Burgart LJ, Schaid DJ, Peterson BJ, Moon-Tasson L, Mahoney MR, Sargent DJ, O'Connell MJ, Witzig TE, Farr GH, Goldberg RM, Thibodeau SN. Microsatellite instability and 8p allelic imbalance in stage B2 and C colorectal cancers. *J Natl Cancer Inst* 1999; **91**: 1295-1303
24 **Ropponen KM**, Eskelinen MJ, Lipponen PK, Alhava E, Kosma VM. Prognostic value of tumour-infiltrating lymphocytes (TILs) in colorectal cancer. *J Pathol* 1997; **182**: 318-324
25 **Adachi Y**, Mori M, Kuroiwa S, Sugimachi K, Enjoji M. Histopathologic evaluation of survival time in patients with colorectal carcinoma. *J Surg Oncol* 1989; **42**: 219-224
26 **Funada Y**, Noguchi T, Kikuchi R, Takeno S, Uchida Y, Gabbert HE. Prognostic significance of CD8+T cell and macrophage peritumoral infiltration in colorectal cancer. *Oncol Rep* 2003; **10**: 309-313
27 **Barth RJ**, Camp BJ, Martuscello TA, Dain BJ, Memoli VA. The cytokine microenvironment of human colon carcinoma. Lymphocyte expression of tumor necrosis factor-alpha and interleukin-4 predicts improved survival. *Cancer* 1996; **78**: 1168-1178

Science Editor Li WZ **Language Editor** Elsevier HK

PO Box 2345, Beijing 100023, China
www.wjgnet.com
wjg@wjgnet.com

ELSEVIER

World J Gastroenterol 2005;11(14):2184-2187
World Journal of Gastroenterology ISSN 1007-9327

• *BRIEF REPORTS* •

Changes of ECM and CAM gene expression profile in the cirrhotic liver after HCV infection: Analysis by cDNA expression array

Xin Xu, Yi-Ming Li, Hong Ji, Chong-Zhi Hou, Ying-Bo Cheng, Fu-Ping Ma

Xin Xu, Yi-Ming Li, Hong Ji, Chong-Zhi Hou, Ying-Bo Cheng, Department of General Surgery, Second Hospital of Xi'an Jiaotong University, Xi'an 710004, Shaanxi Province, China
Fu-Ping Ma, Department of General Surgery, Second Hospital of Xianyang, Xianyang 721000, Shaanxi Province, China
Correspondence to: Xin Xu, Department of General Surgery, Second Hospital, Xi'an Jiaotong University, 157 Northern street, Xi'an 710004, Shaanxi Province, China. xuxin72722@tom.com
Fax: +86-29-87678634
Received: 2004-09-06 Accepted: 2004-11-19

Abstract

AIM: We aimed to observe the expression of extracellular matrix (ECM) and cellular adhesion molecules (CAM) in cirrhotic liver tissues after hepatitis C virus (HCV) infection.

METHODS: Twelve patients with post HCV inflammatory liver cirrhosis were selected to evaluate their liver function and other virological, pathological parameters. Then three specimens of cirrhotic patients whose health assessment results and laboratory data were similar and three normal liver specimens explanted from liver grafts prepared for liver transplantation were chosen for investigating gene expression of ECM and CAM using cDNA expression array.

RESULTS: The cDNA array assay revealed 36.7% (36/96) of genes with changes, in which 26.3% (26/96) was up-regulated and 10.1% (10/96) was down-regulated. Integrin (ITGA), collagen (COL), ADAMTS were identified as the characteristic changes of ECM and CAM gene expression levels. ITGA were demonstrated β1 and β2 sub-section changed in liver cirrhosis.

CONCLUSION: ECM and CAM play an important role in the progression of liver cirrhosis after HCV infection. The capital mechanism is related to the inflammatory cells infiltration, the activation and transformation of ECM producing cells and the imbalance between production and elimination of ECM.

Key words: Hepatitis C virus; Liver cirrhosis; Extracellular matrix; Cellular adhesion molecules; mRNA array analysis

Xu X, Li YM, Ji H, Hou CZ, Cheng YB, Ma FP. Changes of ECM and CAM gene expression profile in the cirrhotic liver after HCV infection: Analysis by cDNA expression array. *World J Gastroenterol* 2005; 11(14): 2184-2187
http://www.wjgnet.com/1007-9327/11/2184.asp

INTRODUCTION

Hepatitis C virus (HCV) infection is the major cause of liver cirrhosis according to recent studies. Olga[1] reported that about 20-25% patients with HCV infection would become liver fibrosis or/and cirrhosis. Some studies reported that HCV infection would develop to chronic liver diseases for about 18.4 years later, liver cirrhosis after 20.6 years, and liver cancer after 28.3 years, respectively. The research of the mechanisms of development of liver cirrhosis after HCV infection and prevention of cirrhosis are very important health issues[2]. In this study, we emphasized on the ECM and cellular adhesion molecules (CAM) gene expression levels that changed during liver cirrhosis after HCV infection through DNA array. We can conclude that the alterations in the expression levels of these genes might be relevant to the progression of liver cirrhosis.

It is accepted that the key reason for liver fibrosis/cirrhosis is the maladjustment of production and elimination of ECM and CAM. Unfortunately, the functions and changes of ECM and CAM genes in cirrhotic liver tissues after HCV infection are not clear.

MATERIALS AND METHODS

Materials

Normal liver specimens in control group were taken from liver grafts preparing for liver transplantation. According to the medical protocol, specimens from cirrhotic livers were collected from 12 patients with post HCV inflammatory liver cirrhosis undergoing devascularization of cardiac veins in the second hospital of Xi'an Jiaotong University from 2004 January-July. After the preoperative evaluation of liver function and judgment of apparent liver changes during operation, liver specimens were quickly obtained and conserved in liquid nitrogen. The GEArray Q Series Human Extracellular Matrix and Adhesion Molecules Gene Array and related kits were purchased from SuperArray Bioscience Corporation, which contains 96 genes encoding proteins important for the attachment of cells to their surroundings. The array includes various types of cell adhesion molecules as well as extracellular matrix (ECM) proteins, proteases and their inhibitors. These proteins play key roles in mediating cell-cell, cell-tissue and cell-extract ECM interactions and are involved in the normal processes of growth, division, differentiation and apoptosis. And these genes were important in many liver diseases, especially liver cirrhosis. Through a simple side-by-side hybridization using experimental samples and the array and reagent provided in the kit, we determine the expression profile of these matrix

Table 1 Laboratory and clinical summary data of all patients

	Sex (F/M)	Age (yr)	TBIL (μmol/L)	ALB (g/L)	Encephalopathy	Ascites	Nutritional state	Child class	Gross shape[1]
1	M	40	17.7	36.0	No	No	Fine	A	Great
2	F	45	17.4	36.9	No	No	Fine	A	Great
3	F	49	19.8	41.6	No	Small	Fine	B	Great
4	M	41	52.3	31.2	No	Mess	Weak	C	Diffuse
5	M	37	39.1	40.6	No	Small	Fine	B	Great
6	F	41	26.1	43.9	No	No	Fine	A	Less
7	M	47	10.2	40.1	No	No	Fine	A	Diffuse
8	M	55	22.5	33.8	No	Small	Fine	B	Less
9	F	38	19.6	28.4	No	Small	Fine	C	Less
10	F	40	7.6	45.3	No	Small	Fine	A	Diffuse
11	M	59	70.3	35	No	Small	Fine	C	Great
12	M	48	46.5	45.4	No	Small	Weak	B	Great

Note: [1]great – greater tubercle type of cirrhosis; less – lesser tubercle type of cirrhosis; diffuse – diffuse type of cirrhosis.

and adhesion molecules in our selected patients.

The three patients' liver tissues, which were No. 1-3 in Table 1, were chosen according to the gross shape, sex and age and Child-Pugh classification in the operation.

Clinical and pathological diagnostic standards

Based on the diagnostic resolution of Fifth National Inflammatory and Parasitic Diseases in 1995, the clinical data and pathologic sections were assured by three more surgeons and pathologists.

cDNA expression array analysis

mRNA isolation and assessing Tissue samples of liver in TRIzol were homogenized using a power homogenizer. The samples were homogenized by adding chloroform, then centrifuged at 4 ℃, and the RNA was made to remain in the aqueous phase. The RNA was precipitated from the aqueous phase by mixing with isopropyl alcohol, and the RNA pellet was washed once with 75% ethanol. The RNA was air-dried, and redissolved in RNase-free water. The absorbance was read in a spectrophotometer at 260 and 280 nm to determine the concentration and purity of RNA, and the ratio of A_{260} to A_{280} values were calculated to measure the RNA purity.

Probe synthesis and hybridization RNA was reverse-transcribed by gene-specific primers with biotin-16-dUTP. The cDNA probes were denatured and hybridized to ECM and CAM gene-specific cDNA fragments spotted on the membranes. The membranes were then washed with Wash Solution and blocked with GEA blocking solution.

Chemiluminescent detection The hybridized biotinylated probes were detected by chemiluminescent method using the alkaline phosphatase substrate, CDP-Star. The results were analyzed using GEArray Analyzer software. Each membrane comprised 96 marker genes, negative controls (pUC18 DNA and blanks) and housekeeping genes, including β-actin, GAPDH, cyclophilin A and ribosomal protein L13a. All relative expression levels of different genes were estimated by comparing their signal intensity with that of internal control.

Data analysis Using GEArray Analyzer software for background subtraction and data normalization, each GEArrayTM Q Series membranes are spotted with negative controls and housekeeping genes. All raw signal intensities were corrected for background by subtracting the minimum value to avoid the appearance of negative numbers. All signal intensities were normalized to that of a housekeeping gene.

RESULTS

Clinical data of patients

As shown in Table 2, the 3 of 12 in-hospital patients with post-HCV inflammatory liver cirrhosis were selected according to their sex, age, course and child score, and their liver were screened for further detection. During operation, the specimens were taken from at least two different regions on the liver surfaces and conserved appropriately for cDNA array assay.

Table 2 Health assessment survey and screen

Patient		Sex	Age (yr)	Progress (yr)	Child score	Liver screen and appearance
Test group	1	F	45	11	A	Greater tubercle liver cirrhosis portal vein: 1.1±0.1 cm in diameter
	2	F	49	10	B	
	3	M	40	4	A	
Control group	1	F	35	–	A	Normal
	2	F	46	–	A	
	3	M	31	–	A	

Result of 96 mRNA array screening

We carried out mRNA array assay in order to investigate the comprehensive changes in the gene expression of post HCV inflammatory liver cirrhosis. The mRNA array system, which can detect changes in the expression of 96 human genes, was used for this study. Two independent experiments: normal and cirrhotic, were conducted to clarify the role of HCV cirrhosis core protein. The results of the mRNA array are shown in Figure 1 (A) Exp.1 = normal liver/control group and (B) Exp.2 = cirrhotic liver/test group. 36.7% (36/99) genes were found to be changed in mRNA gene array assay, 26.3% was up-regulated as judged by the criterion of core signals intensity ration $\geqslant$3, and 10.1% was down-regulated as judged by the criterion of core signals intensity ration $\leqslant$0.3.

Up-regulated gene expression

As Table 3 shows the up-regulated gene expression levels in cirrhotic and normal liver tissues, COL, ITGA, ADAMTS and MMP represent higher volume production of fibrosis, intense cells adhesion, disequilibrium between ECM and ICM. Especially, COL1A1 is a rare component in normal liver tissue, which is 5.947×10^{-4}, but it increases 12.22 times to 7.266×10^{-3}. At the same time, COL3, COL4 did not increase gene expression level. Some subunits of integrin families, ITGAα10, ITGA 7, ITGA L, ITGA M, ITGA V, ITGA X, and ITGAβ2 altered their gene expression levels. The metalloproteinase, ADAMTS and MMP, gene expression levels were 3 to 90-fold in liver cirrhosis than normal.

Down-regulated genes in cirrhotic liver

Table 4 shows the down-regulated genes in cirrhotic liver. Combined with the up-regulated genes from the same family of Table 3, the different expression levels may suggest different functions of integration, promotion or inhibition.

DISCUSSION

Shimizu[3] reported that HCV infection is the "most common" cause of liver fibrosis. The production of ECM is increased in liver tissue in which HSCs are activated.

ECM gene expression in post HCV inflammatory liver cirrhosis

ECM in the liver is composed of protein and glycosaminoglycan. Biologically, ECM protein is divided into two types: constructive and adhesive ECM[4]. The stability of ECM and ICM is attributed with the production and elimination of ECM in normal liver, but this balance would be disturbed if the components produced more, or eliminated less[5,6].

The major part of constructive ECM is collagen, which is about 5-8 mg/1 g in normal liver tissue and the ratio of collagen1/collagen3 is less than 1. In cirrhotic liver, however, the content of collagen protein is 4 to 7-fold than that of normal liver. At the same time, and the ratio of collagen1/collagen3 is larger than 1. Our results showed that the

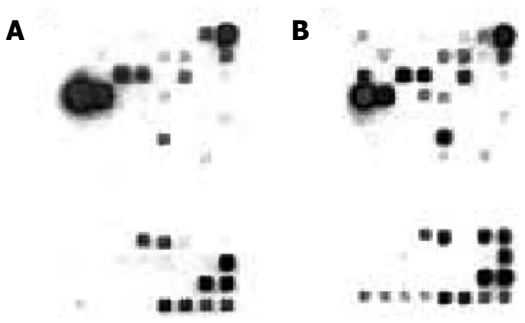

Figure 1 Results of the human ECM and adhesion molecules gene array in normal and liver cirrhosis (A) Exp.1 = normal liver/control group; (B) Exp.2 = cirrhotic liver/test group.

Table 3 Up-regulated genes in liver cirrhosis (Exp.1 = normal, Exp.2 = liver cirrhosis, N/A = 0.00 in normal)

Genename	Exp.1	Exp.2	Exp.2-Exp.1	Exp.2/Exp.1
CAM				
ITGAα10	3.531E-4	5.751E-3	5.398E-3	1.629E+1
ITGA 7	–0.000E-1	1.722E-5	1.722E-5	N/A
ITGA L	2.639E-3	7.921E-3	5.282E-3	3.002E+0
ITGA M	6.690E-4	7.043E-3	6.374E-3	1.053E+1
ITGA V	2.416E-4	2.635E-3	2.393E-3	1.091E+1
ITGA X	–0.000E-1	2.497E-3	2.497E-3	N/A
ITGAβ2	–0.000E-1	1.877E-3	1.877E-3	N/A
ICAM1	4.296E-2	3.695E-1	3.265E-1	8.600E+0
CD44	3.847E-3	9.706E-2	9.322E-2	2.523E+1
CTNN1	1.728E-1	5.052E-1	3.324E-1	2.924E+0
CST3	1.057E-1	3.735E-1	2.678E-1	3.533E+0
ECM				
CAV1	5.017E-4	5.699E-3	5.198E-3	1.136E+1
COL1A1	5.947E-4	7.266E-3	6.672E-3	1.222E+1
LAMβ1	1.301E-4	8.969E-2	8.956E-2	6.895E+2
LAMC1	–0.000E-1	3.444E-5	3.444E-5	N/A
SPP1	2.973E-4	7.781E-1	7.778E-1	2.617E+3
THBS1	1.639E-2	7.918E-1	7.754E-1	4.831E+1
Metalloproteinases				
ADAMTS1	–0.000E-1	1.860E-1	1.860E-1	N/A
ADAMTS 8	7.433E-5	7.404E-4	6.661E-4	9.961E+0
MMP15	1.858E-5	6.888E-5	5.029E-5	3.706E+0
MMP 16	–0.000E-1	3.788E-4	3.788E-4	N/A
MMP 17	–0.000E-1	6.888E-5	6.888E-5	N/A
MMP 2	3.717E-5	2.411E-4	2.039E-4	6.486E+0
MMP 8	–0.000E-1	4.305E-4	4.305E-4	N/A

Table 4 Down-regulated genes in liver cirrhosis (Exp.1 = normal, Exp.2 = liver cirrhosis)

Genename	Exp.1	Exp.2	Exp.2-Exp.1	Exp.2/Exp.1
CAM				
Integrin				
ITGA3	3.529E-1	9.885E-2	-2.541E-1	2.801E-1
ITGA5	1.388E-2	4.546E-3	-9.336E-3	3.275E-1
ITGA8	1.067E-2	2.927E-4	-1.037E-2	2.744E-2
Cadherin	2.604E-1	5.863E-2	-2.018E-1	2.252E-1
CTNND2				
ECM protein:	6.948E-2	3.960E-3	-6.552E-2	5.700E-2
SPARC				
Serine proteinases				
CTSG	1.468E-2	8.954E-4	-1.379E-2	6.099E-2
TMPRSS4	1.191E-2	-0.000E-1	-1.191E-2	-0.000E-1
HPSE	2.531E-1	3.306E-2	-2.201E-1	1.306E-1
Tissue inhibitor of metalloproteinases				
TIMP2	2.895E-2	-0.000E-1	-2.895E-2	-0.000E-1
TIMP 3	6.168E-2	3.960E-4	-6.128E-2	6.421E-3

content of collagen was 12.22-fold in cirrhotic liver than that of control group. The ratio changes of collagens in the cirrhotic liver may be the key to liver cirrhosis progression. Some researchers reported that COL2 was the most abundant collagen components in the newly formed fibrotic tissues and then COL1 increased to be the main components in mature fibrotic tissues. It is implied that the change of collagen types, concentration and the disturbance of balance between producing and elimination of collagen may produce a marked effect in the developmental period of liver cirrhosis[7]. In this study, the gene expression levels of COL1 and COL2 were up-regulated and that of TIMP2 and TIMP3 were down-regulated. It suggests the contribution of TNFβ1 to the development of cirrhosis because these changes were similar to the recent researches that TNFβ1 could promote the formation of ECM and inhibit its elimination[8].

Laminin (LAM) is the main type of adhesive ECM and performs many important biological functions. Acting as the important factor of basement membrane (BM), LAM is associated with the BM formation in liver microvascular tissue during cirrhosis. It also adjusts the pressure between Disse sinus and hepatic sinusoids. This phenomenon may be related to the by-pass blood reserve in cirrhotic liver. Our study shows that LAMB1 and LAMC1 were increased 10-fold in cirrhotic liver tissue.

CAM gene expression in post HCV inflammatory liver cirrhosis

CAM is believed to perform multiple functions in liver cirrhosis. This is clarified by the following factors: ITGA, cadherin, CD44 ICAM, and selectin, which promote the activation and homing of T, B lymph cells, infiltration of leukocytes and deposition of collagens and concentration of HA and so on. Integrin family has been classified to be over 20 kinds of dimers and 14 kinds of αsubunits and 9βsubunits. This specific membrane protein can transmit the signals of ECM and intracellular matrix (ICM), and act as an acceptor of ECM on membrane[9].

ADAMTS is one kind of medial enzyme that can help cells secrete different kinds of matrix enzymes, such as TNFα, TNFβ and so on. In our research, 7 of 19 genes were identified as core response of ADAMTS and MMPs family in HCV cirrhotic liver tissues. The up-regulated genes of MMPs were believed to be induced by down-regulated TIMP, which controlled the activity of MMPs[10].

Except for integrin family, CAM also includes the following members: cadherin, CD44 family, ICAM, immunoglobulin superfamily and selectin. We found that the expression level of cadherin was responsibly down-regulated, which indicated the cellular polarity and microstructure damages. Recently reports show that cadherin plays an important role in regulating cell adhesion and linkage formation.

Some cytokines secreted by platelets, macrophageal cells in inflammatory tissues, perform different modulatory effects on the development of liver cirrhosis[11]. It is also noteworthy that cytokines can alter the gene expression of ECM and CAM in cirrhotic liver tissue after HCV infection by producing activated oxidative components[12].

REFERENCES

1 **Olga OZ,** Nikolai DY. Invasive and non-invasive monitoring of hepatitis C virus-induced liver fibrosis: alternatives or complements? *Curr Pharm Biotechnol* 2003; **4**: 195-209
2 **Smith MW,** Yue ZN, Korth MJ, Do HA, Boix L, Fausto N, Bruix J, Carithers RL, Katze MG. Hepatitis C virus and liver disease: global transcriptional profiling and identification of potential markers. *Hepatology* 2003; **38**: 1458-1467
3 **Shimizu I.** Impact of oestrogens on the progression of liver disease. *Liver Int* 2003; **23**: 63-69
4 **Raines EW.** The extracellular matrix can regulate vascular cell migration, proliferation, and survival: relationships to vascular disease. *Int J Exp Pathol* 2000; **81**: 173-182
5 **Kozlowska J,** Loch T, Jablonska J, Cianciara J. Biochemical markers of fibrosis in chronic hepatitis and liver cirrhosis of viral origin. *Przegl Epidemiol* 2001; **55**: 451-458
6 **Sobel RA.** The extracellular matrix in multiple sclerosis: an update. *Braz J Med Biol Res* 2001; **34**: 603-609
7 **Shimizu I.** Antifibrogenic therapies in chronic HCV infection. *Curr Drug Targets Infect Disord* 2001; **1**: 227-240
8 **Calabrese F,** Valente M, Giacometti C, Pettenazzo E, Benvegnu L, Alberti A, Gatta A, Pontisso P. Parenchymal transforming growth factor beta-1: its type II receptor and Smad signaling pathway correlate with inflammation and fibrosis in chronic liver disease of viral etiology. *J Gastroenterol Hepatol* 2003; **18**: 1302-1308
9 **Quondamatteo F,** Kempkensteffen C, Miosge N, Sonnenberg A, Herken R. Ultrastructural localization of integrin subunits alpha3 and alpha6 in capillarized sinusoids of the human cirrhotic liver. *Histol Histopathol* 2004; **19**: 799-806
10 **Oda T,** Jung YO, Kim HS, Cai X, Lopez-Guisa JM, Ikeda Y, Eddy AA. PAI -1deficiency attenuates the fibrogenic response to ureteral obstruction. *Kidney Int* 2001; **60**: 587-596
11 **Bedossa P,** Paradis V. Approaches for treatment of liver fibrosis in chronic hepatitis C. *Clin Liver Dis* 2003; **7**: 195-210
12 **Powell EE,** Edwards-Smith CJ, Hay JL, Clouston AD, Crawford DH, Shorthouse C, Purdie DM, Jonsson JR. Host genetic factors influence disease progression in chronic hepatitis C. *Hepatology* 2000; **31**: 828-833

Science Editor Li WZ **Language Editor** Elsevier HK

PO Box 2345, Beijing 100023, China
www.wjgnet.com
wjg@wjgnet.com

ELSEVIER

World J Gastroenterol 2005;11(14):2188-2192
World Journal of Gastroenterology ISSN 1007-9327

• *BRIEF REPORTS* •

Clinicopathological significance of heparanase and basic fibroblast growth factor expression in human esophageal cancer

Biao Han, Jian Liu, Min-Jie Ma, Lin Zhao

Biao Han, Jian Liu, Min-Jie Ma, Lin Zhao, First Affiliated Hospital Lanzhou Medical College, Lanzhou 730000, Gansu Province, China
Supported by the Basic Research Programs of Applied Science and Technology Commission Foundation of Gansu Province, No. QS 031-c33-05
Correspondence to: Dr. Biao Han, First Affiliated Hospital, Lanzhou, Medical College, Lanzhou 730000, Gansu Province, China
Telephone: +86-931-8625200-6515
Received: 2003-11-22 Accepted: 2003-12-16

Abstract

AIM: Human heparanase is an endo-D-glucuronidase that degrades heparan sulfate/heparin and has been implicated in a variety of biological processes. The objective was to investigate the expression of heparanase (Hps) and basic fibroblast growth factor (bFGF) and their relationship to neoangiogenesis and metastasis of human esophageal carcinoma.

METHODS: Seventy-nine patients who had undergone esophageal resection for esophageal carcinoma without preoperative treatment were included in the present study. Immunohistochemistry was used to study the expression of Hps, bFGF and microvessel density (MVD) in 79 cases of esoph-ageal carcinoma. bFGF and Hps were quantitatively detected with immunohistochemistry in 79 cases of human esopha-geal carcinoma and 19 cases of adjacent normal human esophageal carcinoma. Cd34 was used to explore the MVD as a marker of endothelial cells.

RESULTS: Hps and bFGF expression in tumor tissue, being remarkably higher than that in normal esophageal tissue, were significantly correlated with clinicopathological features (depth of invasion, lymph-node metastasis and TNM stage) and MVD.

CONCLUSION: The results of this study suggest that the coexpression of Hps and bFGF plays a key role in angiogenesis, invasion and metastasis of esophageal carcinoma. Hps and bFGF may serve as a predictor of progression in esophageal carcinoma. The expression of heparanase in esophageal carcinoma enhances growth, invasion, and angiogenesis of the tumor, and bFGF seems to be a potent antigenic factor for esophageal carcinoma.

Key words: Hps; bFGF

Han B, Liu J, Ma MJ, Zhao L. Clinicopathological significance of heparanase and basic fibroblast growth factor expression in human esophageal cancer. *World J Gastroenterol* 2005; 11(14): 2188-2192
http://www.wjgnet.com/1007-9327/11/2188.asp

INTRODUCTION

For a malignant tumor cell to metastasize, it must break away from its neighbors, force its way through the surrounding stroma, and penetrate basement membranes to enter the circulation. When it arrives at its destination, these steps must be repeated in reverse order. A critical event in the process of cancer invasion and metastasis is therefore degradation of various constituents of the extra cellular matrix (ECM) including collagen, lamina, fibronectin, and heparin sulfate proteoglycans. The cell is able to accomplish this task through the concerted action of enzymes such as metalloproteinase, serine proteases, and endoglycosidases. Two essential processes required for meta-stasis are neoangiogenesis and tumor cell invasion of the basement membrane and ECM[1] H-S is an essential component of the extra cellular matrices of most tissues and is also a prominent component of blood vessels, which is essential for insolubility of the extra cellular components, cell adhesion, and locomotion[2-10]. Accordingly, cleavage of H-S by heparanase enzyme may play a decisive role in extravasations and invasion of tumor cells. So far, heparanase activity has been detected in various tumors and was found to correlate with their metastasis potentials[2,11-15]. Meanwhile, heparanase may also contribute to angiogenesis by releasing the H-S-bound growth factors such as basic fibroblast growth factor (bFGF)[6]. However, because the characterization and cloning of the enzyme has remained elusive until the recent reports of Hullet *et al*[2], and Vlodavsky *et al*[6], studies aiming at detection and evaluation of heparanase production and its *in vivo* biological role in patients with different malignancies have been hindered. Moreover, many study groups have evaluated the role of different growth factors aiming at elucidation of the biological predictor of angiogenesis in tumor.

bFGF is a potent antigenic growth factor that requires heparin or H-S for its biological activity mediated through tyrosine kinase signaling[16-20]. The activity of bFGF is stringently controlled because it can be inactive in normal tissues and becomes activated upon tissue injury, inflammation, and tumor invasion[21]. Heparanase enzyme possesses the ability to activate bFGF through structural modulation of the cell surface H-S proteoglycan[22]. Accordingly, heparanase and bFGF could play complementary biological roles

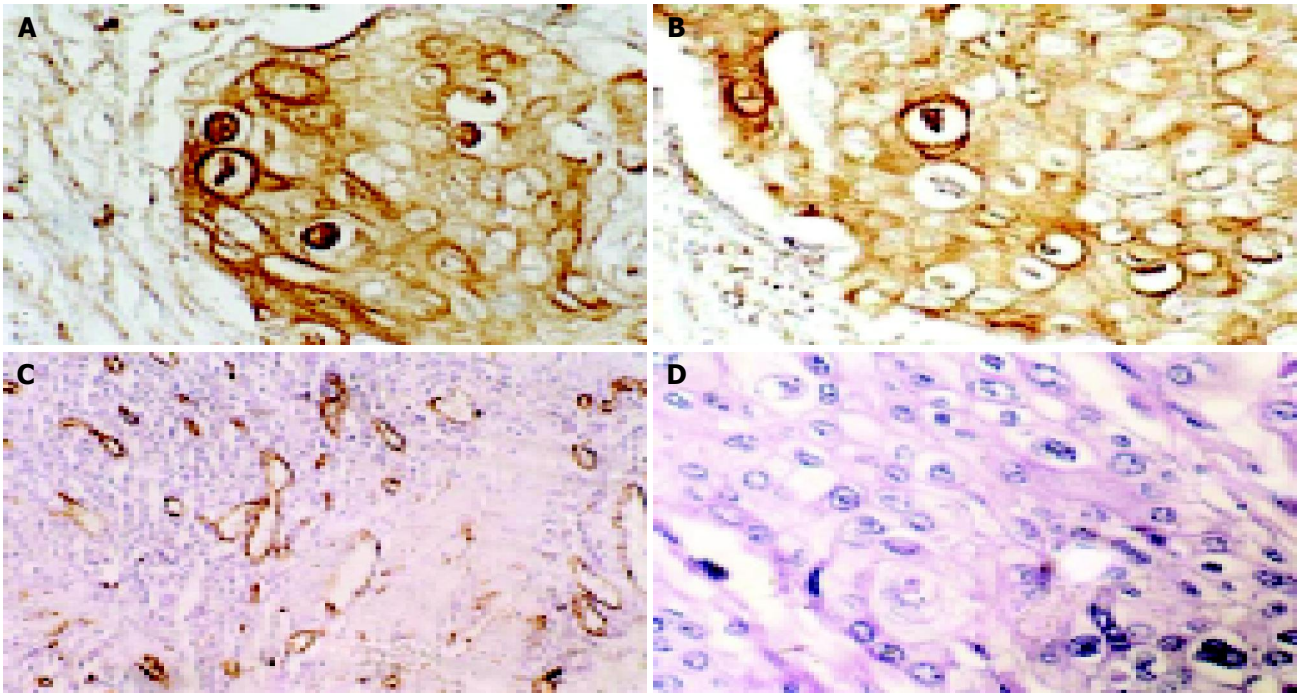

Figure 1 Immunohistochemistry SP staining and HE staining A: Heparanase-positive (nucleolus, cytoplasm, amphithecium) SP×400 B: bFGF-heparanase-positive (cytoplasm, amphithecium) SP×400 C: MVD as evaluated by immunohistochemistry with CD34 (SPx200) D: HE staining of EC SP×400.

in tumor angiogenesis and invasion. To our knowledge, expression of heparanase and its biological role in connection with bFGF expression in human esophageal carcinoma have not been evaluated so far. In the present study, we tried to find out whether bFGF and heparanase were both directly correlated to angiogenesis in human esophageal carcinoma, whether heparanase expression was associated with the degree of tumor invasiveness or not, and whether the coexpression of heparanase and bFGF enhanced tumor angiogenesis compared with expression of either factor alone.

MATERIALS AND METHODS

Patients

Seventy-nine patients undergoing esophageal carcinoma resection between 1996 and 2002 were included in the present study. None of the patients had received preoperative chemo-or embolic therapy.

The patients' ages ranged from 40 to 73 years. Tumors were staged at the time of surgery by the standard criteria for TNM staging using the Unified International esophageal carcinoma staging classification and the following morphological details were recorded: depth of invasion (pT category), lymph node involvement (pN category).

Tissue specimens

Esophageal carcinoma tissues from all of the patients were taken from the areas of tumor immediately after surgical resection. Nineteen surrounding esophageal carcinoma tissues were included. Surrounding esophageal carcinoma tissue specimens were obtained from tissues at a clear distance from the tumor edge (>5 cm), there was no evidence of nearby tumor invasion.

Antibodies and other chemicals

The following reagents were purchased from Maxim Biotech (Macim Biotech Inc., South San Francisco, CA, USA); heparan sulfate proteoglycan (RT-794), fibroblast growth factor, basic (b-FGF) (RAB-0305), CD34 (MAB-0034).

Immunohistochemistry

Immunohistochemistry was performed as described before with minor modifications[19]. Briefly, 5-μm sections were deparaffinized and rehydrated. Tissue was then denatured for 3 min in a microwave oven in citrate buffer (0.01 mol/L, pH 6.0). Blocking steps included successive incubations in 0.2% glycine, 3% H_2O_2 in methanol, and 5% goat serum. The first two steps were followed by two washes in phosphate-buffered saline (PBS). Sections were incubated with a monoc-lonal anti-human heparanase antibody diluted 1:15 in PBS, followed by incubation with horseradish peroxidase-conjugated goat-anti-mouse IgG+IgM antibodies. The preparation and specificity of this mAb have been previously described and demonstrated[19] Color was developed using either Sigma Fast 3,3-diaminobenzidine tablet sets for 10 min followed by counterstain with Mayer's hematoxylin.

Statistics

The correlation between the expression of heparanase or bFGF and micro vessel density (MVD) and clinicopathological features was analyzed. For statistical significance, the χ^2 test was used. Postoperative survival periods were computed by the method of Kaplan-Meier and compared by using the log-rank test. $P<0.05$ was taken as the level of significance for all tests. All statistical analyses were performed using the SPSS 10.0 statistical package (USA).

Table 1 Expression of Hps, bFGF, MVD in esophageal carcinoma and normal esophageal tissue

Type	*n*	Heparanase-positive (%)	bFGF-positivity (%)	MVD
Esophageal carcinoma	79	52 (65.8)	57 (72.2)	30.59±13.38
Normal esophageal tissue	19	0	3 (15.8)	13.82±4.16

Table 3 Relationship between MVD and heparanase and bFGF expression

Parameter	Hps and bFGF	bFGF and MVD	HPS and MVD
Correlation coefficient (r)	0.553	0.687	0.760
P	0.000[b]	0.000[b]	0.000[b]
Remark	Significant linear correlation	Significant linear correlation	Significant linear correlation

Note: 0.01 (two-tailed); it shows that coexpression of both heparanase and bFGF was significantly correlated with MVD ([b]*P*<0.001).

RESULTS

Expression and clinical significance of heparanase

In Table 1 Fifty-two (65.8%) esophageal carcinoma were heparanase-positive (Figure 1A and B) and 27 (34.2%) tumors had no detectable level of heparanase. Expression of heparanase was significantly higher in tumors than in normal esophageal tissue ($P = 0.01$). Heparanase expression was also associated with depth of invasion, clinical stages and lymph-node metastasis. All were significantly higher in heparanase-positive tumors compared with heparanase-negative tumors ($P<0.05$). However, there was no significant correlation between heparanase expression and tumor cell differentiation, age and gender ($P>0.05$).

Expression of bFGF and clinicopathological features of esophageal carcinoma

The bFGF-positive rate was significantly higher in esophageal carcinoma compared with that in the surrounding normal tissues ($P<0.01$), so was heparanase expression. There was a significant correlation between bFGF expression and depth of invasion, clinical stages and lymph-node metastasis ($P<0.05$ Table2).

Expression of bFGF and heparanase in tumor was significantly positively correlated with MVD expression (Figure 1C and D) ($P<0.001$; Table 3). A simple regression model was used to evaluate the correlation between MVD and bFGF and heparanase. There was a direct linear relationship between the positive expression of bFGF and heparanase and the MVD in each individual tumor ($P<0.001$).This indicates that bFGF and heparanase are directly correlated with angiogenesis in esophageal carcinoma.

Table 3 shows that coexpression of both heparanase and bFGF was significantly correlated with MVD ($P<0.001$).

Based on the level of heparanase-positivity, we divided heparanase-positivity into three groups (high; moderate; low). Postoperative survival periods were computed by the method of Kaplan-Meier and compared by using the log-rank test. (Table 4) Level of heparanase-positivity negatively correlated with the postoperative survival periods (Figure 2, Table 5, $P<0.001$).

Analysis of prognosis was computed by the method of Cox proportional hazard model. It suggested that positive expression of heparanase and bFGF, lymph node and distant metastasis and MVD were hazardous factors of postoperative survival periods.

Table 2 Expression of Hps, bFGF, MVD in esophageal carcinoma

Parameter	Hps				bFGF			MVD		
	n	+	Positive ratio(%)	*P*	+	Positive ratio(%)	*P*	Mean	SD	*P*
Gender										
Male	60	40	66.7	0.787[a]	43	71.7	0.864[a]	35.32	7.55	
Female	19	12	63.2		14	73.7		37.23	4.17	0.317[a]
Age (yr)										
<60	50	33	66	1[a]	35	70	0.614[a]	35.59	3.87	0.876[a]
⩾60	29	19	65.5		22	75.9		36.07	6.11	
Tumor cell differentiation										
High	27	17	63.0	0.921[a]	20	74.1		33.13	7.93	
Moderate	33	22	66.7		23	69.7	0.918[a]	31.92	5.29	0.878[a]
Low	19	13	68.4		14	73.7		32.52	6.17	
Depth of invasion										
T_1+T_1+T_2	28	10	35.7	0[c]	12	42.9	0[c]	23.78	4.16	0[c]
T_3+T_4	51	42	82.4		45	88.2		42.01	5.40	
Lymph-node metastasis										
N_0	32	14	43.8	0.001[c]	14	43.8		31.87	7.17	
N_1	47	38	80.9		33	70.2	0.019[b]	38.44	5.74	0.051[a]
Clinical stages										
0+I+II	38	20	60.5	0.017[b]	23	60.5		35.95	5.19	
II+IV	41	32	70.7		34	82.9	0.026	43.19	7.15	0.375[a]

Note: [a]*P*>0.05 no significant difference; [c]*P*<0.05 statistical difference; [b]*P*<0.001 significant difference.

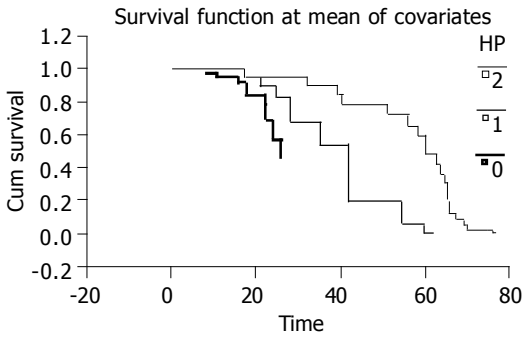

Figure 2 Heparanase-negative; 1 = heparanase- positive; 2 = strongly heparanase-positive.

DISCUSSION

H-S proteoglycan is present in the basement membrane of every vascularized organ and in the tumor stroma of several human cancers[22]. A major function of the proteoglycans is attributed to the properties of H-S[23], which is essential for insolubility of the extracellular components, cell adhesion, and locomotion[6-10]. H-S also works as a storage depot for active growth factors, of which bFGF is the most extensively studied[24]. Thus, acquisition of heparanase and splitting of H-S by a given tumor would offer such a tumor two essential features of malignancy: volatilization of the other extracellular matrix constituents, facilitating tumor invasion through blood vessels and tissues; and releasing and activation of H-S-binding growth factors and, hence, enhancing the tumor angiogenesis.

In our results, there was a direct correlation between heparanase expression and angiogenesis in esophageal carcinoma. Tumors with positive heparanase expression had a significantly higher MVD compared with heparanase-negative tumors. Accordingly, we can conclude that heparanase expression has an axial role not only in the tumor growth and invasion but also in the angiogenesis of esophageal carcinoma.

In the present study, the expression of bFGF was significantly higher in esophageal carcinoma compared with that in the surrounding and normal esophageal tissue, indicating that its up-regulation was involved in the tumor biology. Moreover, bFGF was directly correlated with MVD of esophageal carcinoma. bFGF induces neovascularization through various mechanisms including a potent mitogenic effect on the vascular and capillary endothelial cells[19,22], stimulation of endothelial migration and capillary formation, and production of plasminogen activators, proteases that are involved in the invasive property of endothelial cells during angiogenesis[25].

Table 4 Log-rank analysis of postoperative survival periods

	Statistics	df	*P*
Log rank	19.64	2	0.0001[b]
Breslow	15.66	2	0.0004[b]
Traone-ware	17.62	2	0.0001[b]

[b]*P*<0.001 significant difference.

Table 5 Variables in the equation

Variables	*P*	Odds ratio	95% CI for Exp(B)
T	0.366	1.181[a]	0.824-1.692
N	0.035	2.430[a]	1.065-5.543
BFGF	0.021	2.032[a]	1.111-3.716
MVD	0.047	1.038[a]	1.000-1.077
M	0.002	11.221[a]	-2.427-51.880
Hps	0.000	3.390[a]	2.046-5.615
Clinical stage	0.207	1.256[a]	0.819-1.924

Remark: [a]*P*>1 hazardous factor.

Moreover, heparanase expression was directly correlated with tumor size. Generally, the tumor size reflects tumor growth that is the outcome of many integrated factors, including the availability of enough nutritional support through abundant blood supply (angiogenesis) and of proliferation stimuli from active growth factors. Heparanase may influence the bioavailability of different growth factors including FGFs[26-29], vascular endothelial growth factor[30], hepatocyte growth factor[31], and PDGF[32], which are stored in H-S and possess H-S-binding sequences. It is quite reasonable to assume that the release of such growth factors may influence tumor growth and angiogenesis.

In the current study, there was an obvious synergetic effect of heparanase and bFGF expression in tumor. Coexpression of both factors was associated with higher MVD compared with expression of either factors alone. Such synergetic action may be attributed to the direct ability of heparanase to solubilize the components of ECM, which enhances endothelial cell migration during neovascularization. On the other hand, heparanase increases the biological activity of bFGF as well as of other H-S-bound growth factors like VEGF, PDGF, and HGF[33-37], which are expected to further enhance the angiogenic effect.

In conclusion, expression levels of heparanase correlate negatively with patient survival, suggesting a role of basement membrane and ECM-degrading enzymes in tumor microenvironment alterations that facilitate esophageal carcinoma cell growth, invasion, and metastasis formation. Therefore, the development of drugs acting as inhibitors or blocking agents of hps action may add a new therapeutic modality in the future treatment of pancreatic cancer.

REFERENCES

1 **Eccles SA.** Heparanase: breaking down barriers in tumors. *Nat Med* 1999; **5**: 735-736
2 **Hulett MD,** Freeman C, Hamdorf BJ, Baker RT, Harris MJ, Parish CR. Cloning of mammalian heparanase, an important enzyme in tumor invasion and metastasis. *Nat Med* 1999; **5**: 803-809
3 **Dietrich CP,** Nader HB, Straus AH. Structural differences of heparan sulfates according to the tissue and species of origin. *Biochem Biophys Res Commun* 1983; **111**: 865-871
4 **Kjellen L,** Lindahl U. Proteoglycans: structures and interactions. *Annu Rev Biochem* 1991; **60**: 443-475
5 **Yurchenco PD,** Schittny JC. Molecular architecture of basement membranes. *FASEB J* 1990; **4**: 1577-1590
6 **Vlodavsky I,** Friedmann Y, Elkin M, Aingorn H, Atzmon R, Ishai-Michaeli R, Bitan M, Pappo O, Peretz T, Michal I, Spector L, Pecker I. Mammalian heparanase: gene cloning, expression

and function in tumor progression and metastasis. *Nat Med* 1999; **5**: 793-802
7 **Jackson RL,** Busch SJ, Cardin AD. Glycosaminoglycans: molecular properties, protein interactions and role in physiological processes. *Physiol Rev* 1991; **71**: 481-539
8 **Wight TN,** Kinsella MG, Qwarnstrom EE. The role of proteoglycans in cell adhesion, migration and proliferation. *Curr Opin Cell Biol* 1992; **4**: 793-801
9 **Rapraeger AC.** The coordinated regulation of heparan sulfate, syndecans and cell behavior. *Curr Opin Cell Biol* 1993; **5**: 844-853
10 **Wight TN.** Cell biology of arterial proteoglycans. *Arteriosclerosis* 1989; **9**: 1-20
11 **Nakajima M,** Irimura T, Di Ferrante N, Nicolson GL. Metastatic melanoma cell heparanase. Characterization of heparan sulfate degradation fragments produced by B16 melanoma endoglucuronidase. *J Biol Chem* 1984; **259**: 2283-2290
12 **Freeman C,** Parish CR. A rapid quantitative assay for the detection of mammalian heparanase activity. *Biochem J* 1997; **325 (Pt 1)**: 229-237
13 **Nakajima M,** Irimura T, Di Ferrante D, Di Ferrante N, Nicolson GL. Heparan sulfate degradation: relation to tumor invasive and metastatic properties of mouse B16 melanoma sublines. *Science* 1983; **220**: 611-613
14 **Nakajima M,** Irimura T, Nicolson GL. Heparanases and tumor metastasis. *J Cell Biochem* 1988; **36**: 157-167
15 **Ricoveri W,** Cappelletti R. Heparan sulfate endoglycosidase and metastatic potential in murine fibrosarcoma and melanoma. *Cancer Res* 1986; **46**: 3855-3861
16 **Johnson DE,** Williams LT. Structural and functional diversity in the FGF receptor multigene family. Adv. *Cancer Res* 1993; **60**: 1-41
17 **Yayon A,** Klagsbrun M, Esko JD, Leder P, Ornitz DM. Cell surface, heparin-like molecules are required for binding of basic fibroblast growth factor to its high affinity receptor. *Cell* 1991; **64**: 841-848
18 **Ornitz DM,** Yayon A, Flanagan JG, Svahn CM, Levi E, Leder P. Heparin is required for cell-free binding of basic fibroblast growth factor to a soluble receptor and for mitogenesis in whole cells. *Mol Cell Biol* 1992; **12**: 240-247
19 **Rapraeger AC,** Krufka A, Olwin BB. Requirement of heparan sulfate for bFGF-mediated fibroblast growth and myoblast differentiation. *Science* 1991; **252**: 1705-1708
20 **Flaumenhaft R,** Rifkin DB. The extracellular regulation of growth factor action. *Mol Biol Cell* 1992; **3**: 1057-1065
21 **Kato M,** Wang H, Kainulainen V, Fitzgerald ML, Ledbetter S, Ornitz DM, Bernfield M. Physiological degradation converts the soluble syndecan-1 ectodomain from an inhibitor to a potent activator of FGF-2. *Nat Med* 1998; **4**: 691-697
22 **Iozzo RV,** Cohen IR, Grassel S, Murdoch AD. The biology of perlecan: the multifaceted heparan sulphate proteoglycan of basement membranes and pericellular matrices. *Biochem J* 1994; **302 (Pt 3)**: 625-639
23 **Murdoch AD,** Liu B, Schwarting R, Tuan RS, Iozzo RV. Widespread expression of perlecan proteoglycan in basement membranes and extracellular matrices of human tissues as detected by a novel monoclonal antibody against domain III and by *in situ* hybridization. *J Histochem Cytochem* 1994; **42**: 239-249
24 **Taipale J,** Keski-Oja J. Growth factors in the extracellular matrix. *FASEB J* 1997; **11**: 51-59
25 **Montesano R,** Vassalli JD, Baird A, Guillemin R, Orci L. Basic fibroblast growth factor induces angiogenesis *in vitro*. *Proc Natl Acad Sci USA* 1986; **83**: 7297-7301
26 **Mizuno K,** Inoue H, Hagiya M, Shimizu S, Nose T, Shimohigashi Y, Nakamura T. Hairpin loop and second kringle domain are essential sites for heparin binding and biological activity of hepatocyte growth factor. *J Biol Chem* 1994; **269**: 1131-1136
27 **Raines EW,** Ross R. Compartmentalization of PDGF on extracellular binding sites dependent on exon-6-encoded sequences. *J Cell Biol* 1992; **116**: 533-543
28 **Klein G,** Conzelmann S, Beck S, Timpl R, Muller CA. Perlecan in human bone marrow a growth-factor-presenting but antiadhesive extracellular matrix component for hematopoietic cells. *Matrix Biol* 1995; **14**: 457-465
29 **Folkman J,** Klagsbrun M, Sasse J, Wadzinski M, Ingber D, Vlodavsky I. A heparin-binding angiogenic protein-basic fibroblast growth factor-is stored within basement membrane. *Am J Pathol* 1988; **130**: 393-400
30 **Park JE,** Keller GA, Ferrara N. The vascular endothelial growth factor (VEGF) isoforms: differential deposition into the subepithelial extracellular matrix and bioactivity of extracellular matrix-bound VEGF. *Mol Biol Cell* 1993; **4**: 1317-1326
31 **Lyon M,** Deakin JA, Mizuno K, Nakamura T, Gallagher JT. Interaction of hepatocyte growth factor with heparan sulfate. Elucidation of the major heparan sulfate structural determinants. *J Biol Chem* 1994; **269**: 11216-11223
32 **Raines EW,** Ross R. Compartmentalization of PDGF on extracellular binding sites dependent on exon-6-encoded sequences. *J Cell Biol* 1992; **116**: 533-543
33 **Faham S,** Hileman RE, Fromm JR, Linhardt RJ. Rees DC. Heparin structure and interactions with basic fibroblast growth factor. *Science* 1996; **271**: 1116-1120
34 **Aviezer D,** Hecht D, Safran M, Eisinger M, David G, Yayon A. Perlecan, basal lamina proteoglycan, promotes basic fibroblast growth factor-receptor binding, mitogenesis, and angiogenesis. *Cell* 1994; **79**: 1005-1013
35 **Klein G,** Conzelmann S, Beck S, Timpl R, Muller CA. Perlecan in human bone marrow: a growth-factor-presenting, but antiadhesive, extracellular matrix component for hematopoietic cells. *Matrix Biol* 1995; **14**: 457-465
36 **Folkman J,** Klagsbrun M, Sasse J, Wadzinski M, Ingber D, Vlodavsky I. A heparin-binding angiogenic protein-basic fibroblast growth factor is stored within basement membrane. *Am J Pathol* 1988; **130**: 393-400
37 **Park JE,** Keller GA, Ferrara N. The vascular endothelial growth factor (VEGF) isoforms: differential deposition into the subepithelial extracellular matrix and bioactivity of extracellular matrix-bound VEGF. *Mol Biol Cell* 1993; **4**: 1317-1326

Science Editor Zhu LH **Language Editor** Elsevier HK

PO Box 2345, Beijing 100023, China
www.wjgnet.com
wjg@wjgnet.com

ELSEVIER

World J Gastroenterol 2005;11(14):2193-2196
World Journal of Gastroenterology ISSN 1007-9327

• *BRIEF REPORTS* •

Relationship between retinopathy and cirrhosis

Colakoglu Onder, Taskiran Bengur, Dayi Selcuk, Sozmen Bulent, Unsal Belkis, Maden Ahmet, Pasa Eser, Aslan S. Leyla

Colakoglu Onder, Unsal Belkis, Clinics of Gastroenterology, Izmir Ataturk Teaching and Research Hospital, Izmir, Turkey
Taskiran Bengur, Sozmen Bulent, Aslan S. Leyla, 3rd Clinics of Internal Medicine, Izmir Ataturk Teaching and Research Hospital, Izmir, Turkey
Dayi Selcuk, Maden Ahmet, Clinics of Ophthalmology, Izmir Ataturk Teaching and Research Hospital, Izmir, Turkey
Pasa Eser, Clinics of Ophthalmology, 9th September University Hospital, Izmir, Turkey
Correspondence to: Dr. Taskiran Bengur, Asit mah. 7 aralik sokak Yimenicioglu apt. No: 20/3 79106, Kilis, Turkey. barbe7426@yahoo.com
Telephone: +90-532-7015605
Received: 2004-09-20 Accepted: 2004-11-23

Abstract

AIM: To evaluate ophthalmic disorders with special attention to retinopathy in cirrhotic patients. Vitamin A deficiency-related ophthalmopathy, xerophthalmia, and color blindness may be documented in cirrhosis due to various etiologies. Retinopathy is an obscure feature of cirrhosis.

METHODS: Thirty-two cirrhotic patients, who were followed up by Clinics of Gastroenterology, Izmir Ataturk Teaching and Research Hospital, were enrolled to the study. Associated systemic diseases such as diabetes mellitus and hypertension were excluded. Thirty-two healthy volunteers took part as the control subjects. All participants had ophthalmologic examination in the same hospital.

RESULTS: Five (15.6%) of the cirrhotic subjects had soft exudate in the retina. None of the control subjects had retinopathy ($P<0.05$). Intraocular pressure (IOP) measured for both eyes were also significantly lower in the cirrhotics ($P<0.05$ *vs* $P = 0.01$). There were no statistically significant differences between the two groups in terms of other ophthalmic pathologies. The ophthalmic findings did not show up any differences according to the etiology of cirrhosis.

CONCLUSION: Soft exudates may develop in cirrhotic patients probably due to loss of synthetic function of liver and hemodynamic effects of portal hypertension. Retinopathy must be sought in cirrhosis because of its severe morbidity.

Key words: Cirrhosis; Portal hypertension; Retinopathy

Onder C, Bengur T, Selcuk D, Bulent S, Belkis U, Ahmet M, Eser P, Leyla AS. Relationship between retinopathy and cirrhosis. *World J Gastroenterol* 2005; 11(14): 2193-2196
http://www.wjgnet.com/1007-9327/11/2193.asp

INTRODUCTION

More than 60% of cirrhotic patients have clinical manifestations of portal hypertension (splenomegaly, portal-systemic collaterals, ascites)[1]. The ophthalmic pathologies of cirrhosis in the literature involve xerophthalmia, vitamin A deficiency, and color blindness. Xerophthalmia and keratoconjunctivitis observed in Sjögren's syndrome may be associated with autoimmune hepatitis and primary biliary cirrhosis. Xerophthalmia is also observed in vitamin A deficiency. It may even progress to small grayish lesions, namely Bitot's spots, and blindness. Night blindness may ensue. Vitamin A deficiency may be seen in cirrhosis since liver is the organ where vitamin A is deposited[2,3]. This is a well-documented state in primary biliary cirrhosis and alcoholic cirrhosis. Color blindness may be seen in cirrhosis especially in alcoholic type.

There are scarcely few studies about retinopathy in cirrhosis. Exudates and hemorrhage may be seen in the retina[4,5]. In these studies, associated diseases such as DM and hypertension were not excluded. Relationship between retinopathy and a variety of systemic diseases such as diabetes mellitus (DM), hypertension, blood dyscrasias (myeloproliferative disorders, plasma cell dyscrasias), Behçet's disease, sarcoidosis and systemic infections including HIV is well known. Intraretinal hemorrhage, exudate, cotton-wool spots (retinal infarcts), and papilla edema may be seen in hypertensive neuroretinopathy and diabetic retinopathy. These changes constitute an important morbidity since they may lead to blindness. Exudates are composed of extravasated plasma proteins mainly lipoproteins and are gray-yellow in color. Macrophage response is also evident. Cotton-wool spots represent microvascular infarcts due to ischemia. Axoplasmic deposits surround the infarcted area. Diabetic retinopathy comprises endothelial dysfunction, advanced glycosylated end-products, increased capillary permeability, thrombocyte dysfunction, adherence of leukocytes to endothelium, arteriovenous shunts due to obstruction of vasculature with coagulum, retinal ischemia, retinal edema, and exudates. Diabetic retinopathy is primarily related to hyperglycemia though hormonal and hemodynamic factors may modify the ongoing process[6]. Focal and diffuse arteriolar narrowing, obstructed precapillary arterioles, hemorrhage, retinal edema, and hard exudates occur in hypertensive retinopathy. There is an entity that has to be considered in the differential diagnosis, the so-called Drusen anomaly. It precedes senile macular degeneration. It does not usually result in blindness. They are characterized by asymptomatic yellow deposits

underneath the retinal pigmented layer[7].

MATERIALS AND METHODS

Thirty-two cirrhotic patients followed up by Clinics of Gastroenterology, Izmir Ataturk Teaching and Research Hospital were enrolled to the study. All patients had clinical, laboratory, and ultrasonographic features compatible with cirrhosis. Hepatitis B, alcohol, and both causes were responsible for the cirrhotic cases (16, 14, 2 patients, respectively). None of the patients had hepatitis C infection. They were neither diabetic (according to fasting and random blood glucose) nor hypertensive according to the criteria of American Diabetes Association and Joint National Committee[8,9]. They were not using any ophthalmic and antidiabetic drugs. The only two cardiovascular medicine used were propranolol (81%) and spironolactone and/or furosemide (63%) prescribed for cirrhosis. All patients had endoscopic examination within the preceding 6 mo due to several reasons and esophageal and gastric varices were detected in 84% and 44%, respectively. The control group comprised 32 healthy volunteers. None of them had a known history of DM, hypertension, known liver disease, and alcohol consumption; they were not using any drugs related to these disorders either.

Ophthalmic examination was performed following pupil dilation with 1% tropicamide drops. Color blindness was evaluated with Ishihara test. Intraocular pressure (IOP) was measured with the applanation tonometry. Schirmer 2 test and break-up time were measured to detect xerophthalmia. Standard Whatman filter paper was used for Schirmer test. Anesthetic drop was not applied. Values above 10 mm were accepted abnormal. Break-up time was measured with biomicroscope. Values ranging from 15 to 35 s were considered normal. The protocol was approved by the local ethics committee and each patient provided written informed consent.

The whole statistical analysis was performed using the SPSS 10.0 statistical software for Windows. Qualitative ophthalmic data were compared by χ^2 test and quantitative data by nonparametric tests. We compared Schirmer test results, break-up time values, and IOP measurements first by Kruskal-Wallis test and then by Mann-Whitney nonparametric test. Variables with a P value less than 0.05 was consid-ered statistically significant.

RESULTS

Mean age was 47.5±9.3 years for the cirrhotic group and 43.4±14.1 years for the control group. Male was the preponderant gender in the cirrhotic group (n = 25, 78%); only 18 (56%) were male in the other group. Eighteen (56%) of them were Child-Pugh class B, 7 (22%) were Child-Pugh class C, and 7 (22%) were Child-Pugh class A. Serum glucose, albumin, sodium levels, and platelet counts of the cirrhotic patients were as follows: 101±11 mg/dL, 3.08±0.65 g/dL, 135±5 meq/L, and 111 567±63 687/mm^3, respectively. Twenty-five patients had a mean activated partial thromboplastin time of 36.7±6.0 s. All patients had prothrombin time (PT) measured (mean 16.4±5.3 s) (Table 1).

Results of Schirmer test performed for each eye separately were similar (cirrhotics: 13.8±3.1 mm in the right *vs* 14.5±2.6 mm in the left; control subjects 15.0±1.7 mm in both eyes). In the cirrhotic group break-up time for tear film was 12.5±2.8 and 12.5±2.7 s. It was 12.2±2.1 and 11.9±2.2 s for the control subjects.

Two (6%) cirrhotic patients and one (3%) healthy volunteer were color blind. None of the cirrhotics, but two (6%) control subjects, had epithelial defect in cornea. Iris atrophy was evident in one (3%) cirrhotic patient and all control subjects had normal anterior chamber examination. Vision acuity was sound in 75% of cirrhotics and 28% of the control subjects. One patient from each group had glaucoma (3% of cirrhotics and 3% of control subjects). The two groups had no statistically significant differences in terms of ophthalmic features outlined above.

Retinal examination of cirrhotics revealed chorioretinal atrophy in two (6%) patients, Drusen anomaly in one (3%), and exudates in five (16%) (Table 2) (Figures 1A and B). In the latter group, exudates were localized bilaterally (n = 3, 60%).

Table 1 Clinical, laboratory, and endoscopic features of cirrhotic patients

	Cirrhotic group	Healthy group
Age (yr)	47.5±9.3	43.4±14.1
Gender (male/female)	25/7 (78%/22%)	18/14 (56%/44%)
Glucose (mg/dL)	101±11	
Albumin (g/dL)	3.08±0.65	
Sodium (meq/L)	135±5	
Platelet count (/mm^3)	111 567±63 687	
Gastric varices	14 (44%)	
Esophageal varices	27 (84%)	
Spider angioma	13 (41%)	
Hepatitis B	18 (56%)	–
Alcohol	16 (50%)	–
β-blocker usage	26 (81%)	–
Diuretic usage	20 (63%)	–

Table 2 Demographic clinical and laboratory features of the patients with retinopathy

	Case 1	Case 2	Case 3	Case 4	Case 5
Age (yr)	41	48	57	54	67
Gender	Male	Male	Female	Male	Male
Etiology	Alcohol	Alcohol	Hepatitis B	Alcohol	Hepatitis B
Child–Pugh class	C	C	B	B	B
Exudate	Macular and peripheral; bilateral	Macular; unilateral	Bilateral	Around macula; unilateral	Scattered; bilateral
Varices	Present[1]	Present	Present	Present	Present
Glucose	95	121	98	92	103
Plt[2] (/mm^3)	49 000	42 000	40 000	221 000	89 000
PT (s)	12.1	34.4	13.3	10.2	13.6
Drugs[3]	Present	Present	Present	Present	Present

[1]All cases had both esophageal and gastric varices except case 1. Case 1 did not have gastric varices. [2]Platelet count. [3]Beta-blocker and diuretic agents.

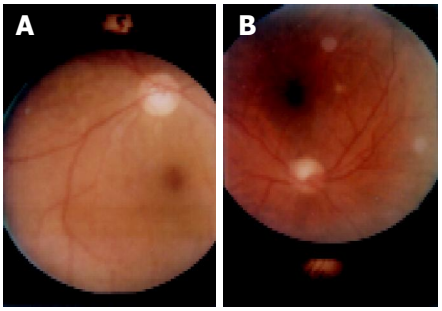

Figure 1 A: Fundus photograph of case 1. Exudate around macula and at the periphery. Retina is involved bilaterally; B: Fundus photograph of case 4. Exudate around macula. Retina is involved unilaterally.

Table 3 Schirmer test results, break-up time, and IOP values of the participants

	Cirrhotic group	Healthy group	*P*
Schirmer test[1]	13.8±3.1[2]	15.0±1.7[2]	0.046
	14.5±2.6[3]	15.0±1.7[3]	*P*>0.05
Break-up time[4]	12.5±2.8[2]	12.2±2.1[2]	*P* >0.05
	12.5±2.7[3]	11.9±2.2[3]	*P* >0.05
IOP	14.1±2.5[2]	15.4±2.1[2]	0.02
			0.01
	14.0±2.3[3]	15.3±2.0[3]	

[1]mm; [2]Right eye; [3]Left eye; [4]Seconds.

Three out of five had exudates in the macular region. One had diffuse soft exudates. None of the healthy subjects had exudates. The cirrhotic subjects had a significantly higher incidence of retinal exudates when compared to the control ones ($P<0.05$). All cirrhotics with retinopathy were also using diuretics. Among the cirrhotics without retinopathy 75% were treated with diuretics. However, retinopathy was not statistically relevant to diuretic usage. Ophthalmic features did not show up any significant differences neither among patients with or without gastric varices nor among those with or without spider angiomas. Etiology of cirrhosis was not shown to have any impact on ophthalmic findings. No significant differences were found between two groups in terms of Schirmer test results and break-up time values. The participants of both groups had IOP in the normal range. However, IOP was significantly lower in the cirrhotic group ($P<0.05$ and $P = 0.01$) (Table 3). Hence, we did not observe any significant difference between ophthalmic findings of both groups, and IOP values. Cirrhosis may occasionally cause hemorrhage in ophthalmic structures due to impaired production of coagulation factors and thrombocytopenia. In our study no hemorrhagic foci were found.

DISCUSSION

Retinopathy is not a well-studied feature of cirrhosis. Abe *et al*, compared retinal features of 85 hepatitis C patients with and without cirrhosis to those of control subjects ($n = 100$). They found that retinopathy comprises hemorrhage and exudates in 27 (31.8%) of patients. Risk factors were female gender, thrombocytopenia, systemic hypertension, a long history of liver disease, advanced age, and cirrhosis. Furthermore there was a statistically significant difference between the two groups ($P<0.01$)[4]. In our study we observed soft exudates only in the cirrhotic group. None of the healthy control subjects had exudates. This finding was statistically significant. We failed to find any statistically significant difference among Child class, platelet number, PT, and retinopathy. In addition to the results compatible with Abe's study, we took a further step by excluding the two major causes of retinopathy, i.e., hypertension and DM. In Abe's study eight patients with hepatitis C had evidence of cirrhosis. Five had hypertension and two had DM. Only two patients had neither DM nor hypertension. Therefore, our study is more focused on cirrhosis-related retinal changes by excluding hypertension and DM. In contrast to Abe's study, none of our patients had hepatitis C infection; they had alcohol and/or hepatitis B instead. Abe *et al,* showed a waxing and waning pattern during IFN therapy and suggested a possible immune pathogenesis.

Pathophysiology of retinopathy is well defined in diabetics. Since retinopathy was not searched in cirrhotics in large surveys, pathophysiology involving retinopathy in cirrhosis is unknown. Increased estrogen formation may cause hormonal modification in retinopathy. Shunts in retinal vasculature resembling intrarenal and intrapulmonary shunts observed in hepatopulmonary syndrome and hepatorenal syndrome may be operational in retinal ischemia and cotton-wool spots. In our study none of the cirrhotics had hepatorenal syndrome. Our patients were not evaluated for the presence of diagnostic criteria for hepatopulmonary syndrome, but none of them had cyanosis and clubbing. Increased hydrostatic pressure caused by high portal pressure, hypoalbuminemia in cirrhosis and resultant decreased oncotic pressure may also contribute to exudate formation via extravasation of plasma contents. A study done by Dittmer and colleagues supports this suggestion[10]. Seventeen patients with cirrhosis and portal hypertension, largely due to alcohol consumption, had ophthalmic examination before and after transjugular intrahepatic portosystemic stent shunting. Retinopathy was evident in 11 patients of which 5 were exudate in nature. Retinopathy regressed significantly or disappeared completely after this procedure which has hemodynamic contributions to the systemic circulation. These findings were attributed to the fact that cirrhosis leads to decreased retinal perfusion.

We think retinal exudates and cotton-wool spots may represent pathologic manifestations of cirrhosis in patients without DM and hypertension. Retinopathy can be present not only in hepatitis C positive cases but also in other etiologies involved in cirrhosis. Although our findings are interesting further larger studies are warranted to reach a conclusion. Also, retinal examination of Child-Pugh class A group cirrhotics and those who do not have varices may reveal more information about impact of portal hypertension on retina. In conclusion, retinopathy leading to significant morbidity in DM may be observed even in cirrhotics without DM.

REFERENCES

1 **Fauci AS**, Braunwald E, Isselbacher KJ. Harrison's principles

of internal medicine. 14th ed. The McGraw Hill companies, 1998: 1710-1717
2 **Ettl A**, Daxecker F. Xerophthalmia in liver cirrhosis. Correct diagnosis after 15 years. *Ophthalmologica* 1992; **204**: 63-66
3 **McClain CJ**, Van Thiel DH, Parker S, Badzin LK, Gilbert H. Alterations in zinc, vitamin A, and retinol-binding protein in chronic alcoholics: a possible mechanism for night blindness and hypogonadism. *Alcohol Clin Exp Res* 1979; **3**: 135-141
4 **Abe T**, Nakajima A, Satoh N, Koizumi T, Sakuragi S, Ono T, Komatsu M, Masamune O. Clinical characteristics of hepatitis C virus-associated retinopathy. *Jpn J Ophthalmol* 1995; **39**: 411-419
5 **Leonhartsberger J**. Diabetic angiopathy and liver cirrhosis. *Wien Med Wochenschr* 1978; **128**: 17-19
6 **Pickup JC**, Williams G. Textbook of Diabetes. 2nd ed. *Blackwell Science Limited* 1997: 44.1-45.1
7 **Kanski JJ**. Klinik oftalmoloji (Turkish translation). 4th ed. Butterworth-Heinemann, Nobel Tıp Kitabevleri (Turkish translation), 1999: 465-500.
8 **Report of the expert committee on the diagnosis and classification of diabetes mellitus**. *Diabetes Care* 2003; **26** Suppl 1: S5-S20
9 **Chobanian AV**, Bakris GL, Black HR, Cushman WC, Green LA, Izzo JL, Jones DW, Materson BJ, Oparil S, Wright JT, Roccella EJ. The Seventh Report of the Joint National Committee on Prevention, Detection, Evaluation, and Treatment of High Blood Pressure: the JNC 7 report. *JAMA* 2003;**289**: 2560-2572
10 **Dittmer K**, Nolte W, Tondrow M, Schworer H. Pathologic fundus changes in advanced liver cirrhosis. Reduction of symptoms after portosystemic shunt. *Ophthalmologe* 1998; **95**: 404-407

Science Editor Guo SY **Language Editor** Elsevier HK

PO Box 2345, Beijing 100023, China
www.wjgnet.com
wjg@wjgnet.com

ELSEVIER

World J Gastroenterol 2005;11(14):2197-2199
World Journal of Gastroenterology ISSN 1007-9327

• *CASE REPORT* •

Unusual clinical course of metachronous melanomas of the upper digestive system

Andrzej Dabrowski, Krzysztof Zinkiewicz, Justyna Szumilo, Witold Zgodzinski, Grzegorz Cwik, Tomasz Skoczylas, Grzegorz Wallner

Andrzej Dabrowski, Krzysztof Zinkiewicz, Witold Zgodzinski, Grzegorz Cwik, Tomasz Skoczylas, Grzegorz Wallner, 2nd Department of General Surgery, Skubiszewski Medical University of Lublin, Staszica 16, 20-081, Lublin, Poland
Justyna Szumilo, Department of Clinical Pathomorphology, Skubiszewski Medical University of Lublin, Jaczewskiego 8, 20-950, Lublin, Poland
Correspondence to: Krzysztof Zinkiewicz MD., 2nd Department of General Surgery, Skubiszewski Medical University of Lublin, Staszica 16, 20-081, Lublin, Poland. kzinek@yahoo.com
Telephone: +4881-53-241-27 Fax: +4881-53-288-10
Received: 2004-06-08 Accepted: 2004-07-27

Abstract

Melanoma of the gastrointestinal tract is a rare, highly malignant neoplasm of poor prognosis. This is description of an unusual case of surgically treated patient with two metachronous malignant melanomas of the stomach and the esophagus. The former lesion was located in the cardia and effectively treated with R0 total gastrectomy. The latter was recognized after 67 mo and appeared as irregular, flat, pigmented areas located in the mid esophagus. Subtotal esophagectomy via right-sided thoracotomy, laparotomy and left-sided cervicotomy was performed, but neoplastic cells were found in distal margin (R1). Fourteen months after esophagectomy multiple lung metastases were detected. Patient died 2 mo later.

Key words: Melanoma; Esophagus

Dabrowski A, Zinkiewicz K, Szumilo J, Zgodzinski W, Cwik G, Skoczylas T, Wallner G. Unusual clinical course of metachronous melanomas of the upper digestive system. *World J Gastroenterol* 2005; 11(14): 2197-2199
http://www.wjgnet.com/1007-9327/11/2197.asp

INTRODUCTION

Melanoma is highly malignant neoplasm with an unpredictable course. Primary melanomas of the esophagus and stomach are rare[1-9] comparing to more common metastases of melanomas from other locations especially skin[10]. The esophageal melanomas account for 0.1-0.2% of all primary tumors of this organ. This location is estimated in 2% of all cases of alimentary tract melanoma [4-6]. About 238 cases of primary esophageal melanomas were published in the literature so far, but only few cases of primary stomach location[11,12,16-19].

This description is of an unusual case of surgically treated patient with long survival with two metachronous malignant melanomas of the stomach and esophagus. In available literature no similar study is found.

CASE REPORT

A 56-year-old man was admitted to General Surgery Department of Skubiszewski Medical University of Lublin in March 1997 due to three-month history of epigastric pain, periodical vomiting with admixture of blood and the loss of body weight about 5 kg. Either family history or exposition to environmental toxic factors were not significant. Physical examination did not reveal any abnormalities. Barium swallow and endoscopic examination demonstrated ulcerated tumour located in the cardia. The biopsy specimens taken from the tumor revealed small neoplastic cells with scanty dark brown pigment that exhibited positive immunostaining for HMB-45 and negative for cytokeratin and CD45. The appropriate negative and positive controls were routinely performed and the diagnosis of malignant melanoma was established.

Extended total gastrectomy with splenectomy, omentectomy and D2 lymphadenectomy was performed on 25 March 1997 with radicality estimated as R0. The gross examination of surgical specimen showed a 1.0 cm×2.0 cm ulcerated grayish-brown tumor located just below esophagogastric junction. Microscopic examination confirmed the initial diagnosis of malignant melanoma. The tumor invaded gastric mucosa and submucosa (Figure 1). Resection margins were free of tumor. None of 20 lymph nodes contained metastases. The clinical course was complicated by 7-d high temperature and the liquid reservoir in left subphrenic region. The patient was treated conservatively.

After 67 mo period, on 21 October 2002, the patient was admitted to our Department due to mild dysphagia. Endoscopic examination demonstrated three irregular, flat, pigmented areas located at 25, 32 and 37 cm from incisors (Figure 2) as well as a single, slightly elevated nonulcerated lesion - 0.7 cm in diameter - at 25 cm from incisors. Esophagojejunal anastomosis was wide with a smooth surface. The biopsy specimens taken from the lesions contained only stratified squamous epithelium with a few scattered cells with fine brown pigment that exhibited positive immunostaining for HMB-45. The computer tomography showed a thickened esophageal wall above the esophagojejunal junction, but neither enlargement of lymph nodes nor distant metastases were demonstrated.

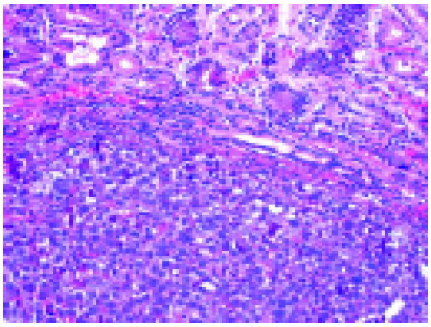

Figure 1 Gastric melanoma (HE, original magnification ×100).

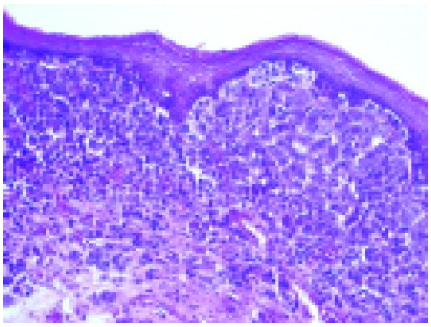

Figure 3 Esophageal melanoma (HE, original magnification ×100).

On 29 November 2002 the subtotal esophagectomy via right-sided thoracotomy, laparotomy and left-sided cervicotomy was performed. The esophageal substitute was formed with a left colon supported by middle colic artery and placed in retrosternal channel in antiperistaltic arrangement. Gross examination of 11 cm-length segment of esophagus confirmed coexistence of three flat and single elevated brownish lesions. In microscopic examination, the formers corresponded to lentiginous pattern of atypical melanocytes proliferation whereas the letter to malignant melanoma infiltrating mucosa and superficial part of submucosa (Figure 3). The diagnosis was confirmed by immunostaining (Figure 4). Scattered morphologically normal melanocytes were found in basal layer of the surface epithelium. Nineteen resected lymph nodes were free of metastases. The radicality of surgical procedure was estimated as R1 due to in situ melanoma found in distal margin.

The clinical course was complicated by intestinal fistula. The esophageal substitute was resected and the ileostomy was done. Two months later favorable results of CT and ultrasonography as well as better general conditions of the patient permitted on alimentary tract reconstruction. On 8 April 2003 izoperistaltic esophageal substitute was formed with the right colon supplied by middle colic artery by laparotomy. The cervical esophagus was anastomosed with the terminal small intestine and the large intestine was joined in the upper abdomen with previously formed reservoir from small intestine. Clinical course was uneventful and the patient was discharged 12 d after surgery.

In January 2004 the CT examination demonstrated numerous metastases in both lungs. The patient died 14 mo after subtotal esophagectomy and 2 mo after detection of lung metastases. Autopsy was not performed.

DISCUSSION

The primary melanoma of esophagus and stomach is a rare neoplasm. Some authors consider the esophageal and gastric melanomas to originate from the ectopic melanocytes, which emigrate to the digestive tract during embriogenesis[3,21]. This concept is supported by the presence of melanocytes in mucosa of the digestive tract, mainly the rectum, which was confirmed by immunohistochemical staining[20]. So-called melanosis or melanocytosis, and atypical junctional melanocyte proliferation are also reported in esophageal mucosa[15,21,22]. These lesions are observed in 25% cases of esophageal melanomas and are thought to be precursor lesions[4,5]. Due to the absence of benign melanocytes in a normal gastric mucosa, a few reports of primary gastric melanoma are questioned[17-19]. In the case presented, we revealed scattered melanocytes and proliferation of atypical melanocytes only within esophageal epithelium. However, the gastric mucosa was free of benign melanocytes both in routine staining and immunostaining (HMB-45). Locations of primary melanoma outside the gastrointestinal tract were excluded. Based on these findings as well as early stage of esophageal tumor at the time of its diagnosis (T1N0) and relatively long time between the diagnosis of gastric and esophageal tumors (67 mo) we recognized them as two metachronous primary melanomas, although the possibility that esophageal lesion was intramural metastasis of early invasive gastric melanoma could not be excluded.

The clinical symptoms of upper digestive system melanoma are not specific and similar to other tumors of this region, which result in loss of body weight, anemia or dysphagia. Malignant melanomas spread quickly by invading esophageal or gastric wall but also via lymphatic and blood vessels[11]. At

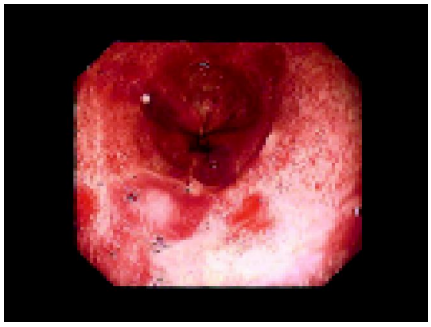

Figure 2 Endoscopic picture of esophageal melanoma.

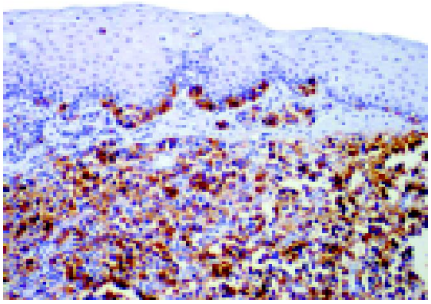

Figure 4 Strongly positive immunostaining for HMB45 in both esophageal melanoma and intraepithelial melanocytic lesion (LSAB2/HRP, original magnification ×100).

the time of diagnosis 50% of patients have distal metastases, mainly in the liver (31%), mediastinal lymph nodes (29%) and the lungs (18%)[11,12]. In our case, lung metastases were detected 12 mo after the esophagectomy. Regardless of the stage of the esophageal melanoma the prognosis always remains poor. For this melanoma the best treatment was surgery with esophagectomy as best procedure due to deep submucosal infiltration[6,8]. However, surgical treatments are regarded as a palliative therapy with a small effectiveness[12-15]. The advantages of chemo-, immuno- or radiotherapy of esophageal or gastric melanomas are also not too effective and these methods are not routinely used. The expectations for treatment of metastases and recurrent melanoma have yet to be reached.

The survival period of our patient was unusually long - he survived 7 years after the gastrectomy and 15 mo after the esophagectomy. Available case and series reports do not give any precise evidence regarding survival of the patients with primary gastric melanoma. According to literature regarding survival after diagnosis of esophageal melanoma treated by esophagectomy the results are similar to ours: 9-12 mo[11]. Rarely the survival after radical R0 esophagectomy is reported to be longer than 5 years[12]. We conclude that this topic needs more attention than has been given and hopefully in future the expectations for treatment of metastases and recurrent melanoma will be reached.

REFERENCES

1 **DeMatos P,** Wolfe WG, Shea CR, Prieto VG, Seigler HF. Primary malignant melanoma of the esophagus. *J Surg Oncol* 1997; **66**: 201-206
2 **Garfinkle JM,** Cahan WG. Primary melanocarcinoma of the esophagus; fist histologically proved case. *Cancer* 1952; **5**: 921-926
3 **De la Pava S,** Nigogosyan G, Pickren JW, Cabrera A. Melanosis of the esophagus. *Cancer* 1963; **16**: 48-50
4 **de Perrot M,** Brundler MA, Robert J, Spiliopoulos A. Primary malignant melanoma of the esophagus. *Dis Esophagus* 2000; **13**: 172-174
5 **Niezychowska K,** Zawadzki J, Wejman J. Primary malignant melanoma of the esophagus. A case report. *Pol J Pathol* 1997; **48**: 205-207
6 **Turnbull AD,** Rosen P, Goodner JT, Beattie EJ. Primary malignant tumors of the esophagus other than typical epidermoid carcinoma. *Ann Thorac Surg* 1973; **15**: 463-473
7 **Moffat RC,** Richard LB, Gnass JE. Primary malignant melanoma of the esophagus: a case report. *Can J Surg* 1972; **15**: 306-309
8 **DiCostanzo DP,** Urmacher C. Primary malignant melanoma of the esophagus. *Am J Surg Pathol* 1987; **11**: 46-52
9 **Sabanathan S,** Eng J, Pradhan GN. Primary malignant melanoma of the esophagus. *Am J Gastroenterol* 1989; **84**: 1475-1481
10 **Allen AC,** Spitz S. Malignant melanoma; a clinicopathological analysis of the criteria for diagnosis and prognosis. *Cancer* 1953; **6**: 1-45
11 **Matsutani T,** Onda M, Miyashita M, Hagiwara N, Akiya Y, Takubo K, Yamashita K, Sasajima K. Primary malignant melanoma of the esophagus treated by esophagectomy and systemic chemotherapy. *Dis Esophagus* 2001; **14**: 241-244
12 **Chalkiadakis G,** Wihlm JM, Morand G, Weill-Bousson M, Witz JP. Primary malignant melanoma of the esophagus. *Ann Thorac Surg* 1985; **39**: 472-475
13 **Adili F,** Monig SP. Surgical therapy of primary malignant melanoma of the esophagus. *Ann Thorac Surg* 1997; **63**: 1461-1463
14 **Herman J,** Duda M, Lovecek M, Svach I. Primary malignant melanoma of the esophagus treated by endoscopic ablation and interferon therapy. *Dis Esophagus* 2001; **14**: 239-240
15 **Volpin E,** Sauvanet A, Couvelard A, Belghiti J. Primary malignant melanoma of the esophagus: a case report and review of the literature. *Dis Esophagus* 2002; **15**: 244–249
16 **Aagaard MT,** Kristensen IB, Lund O, Hasenkam JM, Kimose HH. Primary malignant non-epithelial tumours of the thoracic oesophagus and cardia in a 25-year surgical material. *Scand J Gastroenterol* 1990; **25**: 876-882
17 **Macak J.** Melanoma of the stomach: reality or fiction? *Pathologica* 1998; **90**: 388-390
18 **Liang JT,** Yu SC, Lee PH, Chang KJ, Fang CL, Lin WJ, Chuang SM. Endoscopic diagnosis of malignant melanoma in the gastric cardia--report of a case without a detectable primary lesion. *Endoscopy* 1995; **27**: 409
19 **Alazmi WM,** Nehme OS, Regalado JJ, Rogers AI. Primary gastric melanoma presenting as a nonhealing ulcer. *Gastrointest Endosc* 2003; **57**: 431-433
20 **Clemmensen OJ,** Fenger C. Melanocytes in the anal canal epithelium. *Histopathology* 1991; **18**: 237-241
21 **Alberti JE,** Bodor J, Torres AD, Pini N. Primary malignant melanoma of the esophagus associated with melanosis of the esophagus and stomach. *Acta Gastroenterol Latinoam* 1984; **14**: 139-148
22 **Le Douarin NM.** Cell migrations in embryos. *Cell* 1984; **38**: 353-360

Science Editor Li WZ **Language Editor** Elsevier HK

PO Box 2345, Beijing 100023, China
www.wjgnet.com
wjg@wjgnet.com

ELSEVIER

World J Gastroenterol 2005;11(14):2200-2202
World Journal of Gastroenterology ISSN 1007-9327

• *CASE REPORT* •

Etiological role of brucellosis in autoimmune hepatitis

Colakoglu Onder, Taskiran Bengur, Adnan Kirci, Tunakan Mine, Buyrac Zafer, Unsal Belkis, Aksoz Kadir, Yorukoglu Gazi

Colakoglu Onder, Adnan Kirci, Buyrac Zafer, Unsal Belkis, Aksoz Kadir, Yorukoglu Gazi, Clinics of Gastroenterology, Izmir Ataturk Training and Research Hospital, Izmir, Turkey
Taskiran Bengur, 3rd Clinics of Internal Medicine, Izmir Ataturk Training and Research Hospital, Izmir, Turkey
Tunakan Mine, Department of Pathology, Izmir Ataturk Training and Research Hospital, Izmir, Turkey
Supported by the Authors Have no Financial or Other Relationship that Might Lead to a Conflict of Interest
Correspondence to: Dr. Taskiran Bengur, Asit mah. 7 aralik sokak Yimenicioglu apt. No. 20/3 79106, Kilis, Turkey. barbe7426@yahoo.com
Telephone: +90-532-7015605
Received: 2004-09-20 Accepted: 2004-11-23

Abstract

To show that brucellosis may trigger autoimmune hepatitis (AIH), in addition to nonspecific liver involvement and toxic hepatitis, due to a class effect of tetracycline family used for treatment. We present a female patient admitted to our hospital due to partially improved fatigue and elevated liver enzymes following doxycycline and streptomycin usage for brucellosis. Brucellosis is endemic in our country, Turkey. It may involve any organ in the body. Liver is frequently involved. Doxycycline used for treatment occasionally may lead to hepatotoxicity. AIH is a necroinflammatory disease of the liver. Certain drugs (e.g., minocycline), toxins, and viruses (hepatitis B, hepatitis C, EBV, *etc.*) can trigger AIH. Only one case of AIH probably caused by doxycycline and brucellosis was reported. We discuss the relationship between brucellosis, AIH, and hepatotoxicity of doxycycline. Brucellosis may trigger AIH.

Key words: Brucellosis; Autoimmune hepatitis; Doxycycline

Onder C, Bengur T, Kirci A, Mine T, Zafer B, Belkis U, Kadir A, Gazi Y. Etiological role of brucellosis in autoimmune hepatitis. *World J Gastroenterol* 2005; 11(14): 2200-2202
http://www.wjgnet.com/1007-9327/11/2200.asp

INTRODUCTION

Brucellosis can present with various manifestations and may involve any organ in the body. Hepatic pathology comprises noncalcified granulomas, suppurative abscesses, and mononuclear cell infiltration. Liver and spleen enlarge in 15-20% of cases. Elevated liver enzymes and bilirubin levels accompany these pathologies[1].

Doxycycline, used for brucellosis, can cause toxic hepatitis. Doxycycline may lead to microvesicular fatty infiltration as the other members of the tetracycline family. There is only one report about toxic hepatitis caused by doxycycline in human despite various studies done on rats by Böcker *et al*, showing microvesicular fatty infiltration with 50-100 mg/kg doxycycline[2-5]. Hepatocytes are filled with fat droplets that do not displace the nucleus. They occur as a result of beta oxidation of fatty acids. Fatty infiltration is either diffuse or zonal. It is partially correlated with dosage[6]. Streptomycin, another drug used for brucellosis, has no known hepatotoxicity.

Autoimmune hepatitis (AIH) is a necroinflammatory disease that may lead to chronic hepatitis and cirrhosis. Its etiopathogenesis is not clear. Various clues indicate that some viruses (HBV, HCV, coxsackie, EBV, *etc.*), some drugs (minocycline in type 1 AIH, *etc.*), and toxins can trigger AIH[7-9]. Histological findings of AIH are portal hepatitis, interface hepatitis, panacinar hepatitis, and cirrhosis; even there may be no pathologic features. Interface hepatitis is characterized by gamma globulin deposition in hepatic mesenchymal cells in periportal area with lymphocyte, plasmocyte, and histiocyte infiltration. Although these features are not entirely specific for AIH, they are frequently and most severely observed in AIH. Destructive bile duct injury does not support AIH while periductal lymphoid aggregates or mixed inflammatory infiltrates are acceptable in cases with interface hepatitis and appropriate clinical findings. Presence of destructive cholangitis and ductopenia suggests primary sclerosing cholangitis (PSC), while nondestructive cholangitis suggests primary biliary cirrhosis (PBC). Diagnosis of AIH is difficult not solely due to histopathologic findings but also due to alcohol usage, viral markers, biochemical and immunologic markers. Nevertheless a scoring system was developed to increase the specificity of diagnosis of AIH (Table 1). Some features (destructive cholangitis or ductopenia) of PBC or PSC may accompany those of AIH, namely overlap syndromes. Some infectious agents or some drugs may trigger overlap syndromes as well as AIH[10].

The case described below is a good example about difficulties in defining the etiology in a patient with impaired liver enzymes.

CASE REPORT

A woman, who was diagnosed with brucellosis by serological and clinical means three months ago, received a treatment regimen of doxycycline and streptomycin. She was admitted to hospital because of partially improved fatigue and elevated liver enzymes.

Biochemical tests yielded AST 140 IU/L, ALT 122 IU/L,

Table 1 AIH scoring system

Category	Feature	Score	Patient
Gender	Female	+2	+2
ALP:AST (or ALT) ratio	<1.5	+2	–2
	1.5–3.0	0	
	>3.0	–2	
Gamma globulin or Ig G levels over normal values	>2.0	+3	+3
	1.5–2.0	+2	
	1.0–1.5	+1	
	<1.0	0	
ANA, SMA, or anti-LKM1 titer	>1:80	+3	+3
	1:80	+2	
	1:40	+1	
	<1:40	0	
AMA	Positive	–4	–4
Viral markers	Positive	–3	+3
	Negative	+3	
Drugs	Yes	–4	–4
	No	+1	
Alcohol	<25 g/d	+2	+2
	>60 g/d	–2	
HLA	DR3 or DR4	+1	
Immune disease	Thyroiditis, colitis, synovitis, others	+2	0
Other liver-related antibodies	Anti-SLA/LP, anti-aktin, anti-LC1, p-ANCA	+2	0
Histologic features	Interface hepatitis	+3	+3
	Plasmocytes	+1	+1
	Rosette formation	+1	0
	None of the above	–5	0
	Biliary changes	–3	–3
	Other features	–3	0
Response to therapy	Complete	+2	+2
	Relapse	+3	
Score before therapy			
Absolute diagnosis		>15	6
Probable diagnosis		10–15	

Abbreviations: ALP, serum alkaline phosphatase level; AST, serum aspartate aminotransferase level; ALT, serum alanine aminotransferase level; ANA, antinuclear antibody; SMA, smooth muscle antikoru; anti-LKM1, antibody against liver/kidney type 1; AMA, anti-mitochondrial antibody; anti-SLA/LP, antibody against soluble liver antigen/liver pancreas; anti-LC1, antibody against liver cytosole type 1; p-ANCA, perinuclear anti-neutrophilic cytoplasmic antibody.

ALP 1 558 IU/L, GGT 1 190 IU/L and total bilirubin 2.48 mg/dL. Albumin/globulin ratio was reversed despite a normal level of albumin. Polyclonal gammopathy was detected on protein electrophoresis. Serum glucose, lipid, urea, creatinine levels and prothrombin time were normal. Anti-HBsAg, HBsAg, anti-HBc Ig G/M, anti-HBe Ag, HBeAg, anti-HCV, anti-HDV, anti-HEV, anti-HAV Ig G/M, and anti-HIV were negative. HBV-DNA and HCV-RNA were also evaluated; they were negative too. Immunologic markers of AIH (ANA, AMA, ASMA, p-ANCA, and anti-LKM1) were negative save ANA and AMA (1/640 and 1/320, respectively). Serologic tests for brucellosis were repeated; Rose-Bengal test was three positive and *Brucella abortus* titer was positive (1/320) for Coombs' test. Liver biopsy was performed and it yielded plasmocyte infiltration, interface hepatitis, and nondestructive bile duct injury suggesting PBC (Figure 1). AIH score was six. The case was diagnosed to be overlap syndrome that comprised AIH and PBC. Methyl prednisolone 40 mg/d and ursodeoxycholicacid (UDCA) 15 mg/(kg • d) were administered. All liver function tests returned to normal after a month. She is still taking maintenance treatment of steroid and UDCA.

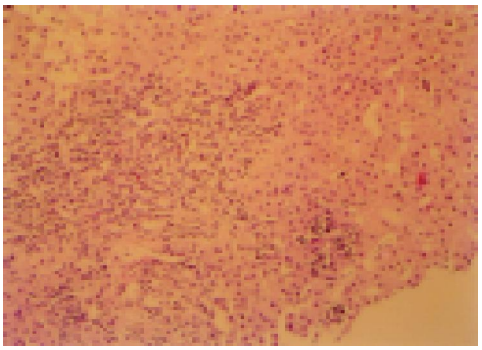

Figure 1 Areas of focal necrosis and periportal biliary piecemeal necrosis (HE ×440).

DISCUSSION

Liver involvement due to brucellosis recurrence and toxic hepatitis was suspected at admission. Microvesicular fatty infiltration, suggesting toxic hepatitis due to tetracycline and doxycycline, was not evident. Hence, histopathology did not support toxic hepatitis. Liver biopsy yielded bile duct injury, interface hepatitis, and plasmocyte infiltration. As a result we focused on AIH and evaluated immunologic markers of AIH. ANA positivity supported AIH. Increased gamma globulin levels, female gender, negative viral markers, and absence of alcohol usage also supported the diagnosis. Unfortunately anti-SLA/LP, anti-aktin, anti-LC1, and HLA tests were unavailable.

AST and ALT levels (3.5 and 3.0 times UNL) in our case were not in the range of a typical AIH case (more than 5.0 times UNL). In most cases of AIH, AST and ALT are below 500 IU/L. Bile duct injury and increased ALP/AST and ALP/ALT ratio indicated cholestatic component. Absence of ductopenia, nondestructive nature of cholangitis, and periductal infiltration supported PBC in spite of PSC component. AMA positivity was also valid for PBC. As in PBC, ALP was predominantly elevated than AST and ALT.

The case was diagnosed with an overlap syndrome according to the AIH scoring system probably triggered by doxycycline. Clinical and biochemical response to steroid and UDCA therapy is achieved.

Liver involvement in brucellosis is not restricted to granulomatous hepatitis; nonspecific cell infiltration (mononuclear cell and plasmocyte) is evident in most cases. This finding suggests that hepatic involvement of brucellosis may contribute to hepatic injury in our case. Furthermore, an overlap syndrome triggered by brucellosis is also open to discussion. Whether brucellosis or doxycycline is a trigger of overlap syndrome is an important question waiting for an answer. We think that our case demands attention since there is only one case in the literature about hepatitis developed after brucellosis infection and doxycycline usage[11].

REFERENCES

1 **Fauci AS,** Braunwald E, Isselbacher KJ. Harrison's principles of internal medicine. 14th ed. The McGraw Hill companies, 1998: 969-971

2 **Hopf G,** Bocker R, Estler CJ. The influence of tetracyclines on the aggregation of free and membrane-bound polysomes and on the RNA content of the liver of mice. *Naunyn Schmiedebergs Arch Pharmacol* 1988; **338**: 455-458

3 **Hopf G,** Bocker R, Estler CJ. Comparative effects of tetracycline and doxycycline on liver function of young adult and old mice. *Arch Int Pharmacodyn Ther* 1985; **278**: 157-168

4 **Bocker R,** Estler CJ, Muller S, Pfandzelter C, Spachmuller B. Comparative evaluation of the effects of tetracycline, rolitetracycline and doxycycline on some blood parameters related to liver function. *Arzneimittelforschung* 1982; **32**: 237-241

5 **Bocker R,** Estler CJ, Maywald M, Weber D. Comparative evaluation of the effects of tetracycline and doxycycline on blood and liver lipids on male and female mice. *Arzneimittelforschung* 1981; **31**: 2118-2120

6 **Topcu AW,** Soyletir G. Ilaclara ve toksik maddelere bagli karaciger hasari. 1st ed. Nobel kitap evi, 1996: 152-172

7 **Angulo JM,** Sigal LH, Espinoza LR. Coexisptent minocycline-induced systemic lupus erythematosus and autoimmune hepatitis. *Semin Arthritis Rheum* 1998; **28**: 187-192

8 **Elkayam O,** Yaron M, Caspi D. Minocycline-induced autoimmune syndromes: an overview. *Semin Arthritis Rheum* 1999; **28**: 392-397

9 **Eichenfield AH.** Minocycline and autoimmunity. *Curr Opin Pediatr* 1999; **11**: 447-456

10 **Zakim D,** Boyer T. Hepatology: a textbook of liver diseases. 4th ed. *Saunders Company* 2003: 1163-1202

11 **Selimoglu MA,** Ertekin V. Autoimmune hepatitis triggered by Brucella infection or doxycycline or both. *Int J Clin Pract* 2003; **57**: 639-641

Science Editor Guo SY **Language Editor** Elsevier HK

PO Box 2345, Beijing 100023, China
www.wjgnet.com
wjg@wjgnet.com

ELSEVIER

World J Gastroenterol 2005;11(14):2203-2205
World Journal of Gastroenterology ISSN 1007-9327

• *CASE REPORT* •

Extraskeletal myxoid chondrosarcoma metastatic to the pancreas: A case report

C Fotiadis, A Charalambopoulos, S Chatzikokolis, GC Zografos, M Genetzakis, R Tringidou

C Fotiadis, A Charalambopoulos, S Chatzikokolis, Third University Department of General Surgery, Athens School of Medicine, Athens, Greece
GC Zografos, M Genetzakis, First University Department of General Surgery, Athens School of Medicine, Ippokration Hospital, Athens, Greece
R Tringidou, Department of Pathology, Sotiria Hospital, Athens, Greece
Correspondence to: C Fotiadis, MD, Third University Department of General Surgery, Athens School of Medicine, Athens, Greece. costfot@b_online.gr
Telephone: +11-30210-5326411 Fax: +11-30210-8133184
Received: 2004-10-23 Accepted 2004-11-29

Abstract

Extraskeletal myxoid chondrosarcoma (EMC) is a low-grade sarcoma characterized by developing metastases and local recurrence in high rate. It is mainly deep seated in the proximal extremities. The most common metastatic sites are the lungs, soft tissues, lymph nodes, bones and the brain. To our knowledge, no case of clearly defined EMC has been reported to date developing a metastasis in the pancreas. We describe a case of a man suffering from EMC who developed a single pancreatic metastasis 20 years after the initial diagnosis. A 49-year-old man was submitted to surgical excision of an EMC, in left thigh, 20 years ago. Fourteen years after the initial diagnosis a local recurrence in left thigh occurred. Multiple lesions of metastatic origin, in both lungs, were excised via thoracotomies until the time being. In 2003, as a part of a periodically performed imaging control, an abdominal CT scan was performed revealing a solid lesion in the pancreas. Distal pancreatectomy was performed. The histopathology of the excised specimen proved to be the one of metastatic lesion of EMC. The above-mentioned case of EMC is, as far as we know, the first one described developing a certain pancreatic metastasis.

Key words: Extraskeletal myxoid chondrosarcoma; Metastasis; Pancreas

Fotiadis C, Charalambopoulos A, Chatzikokolis S, Zografos GC, Genetzakis M, Tringidou R. Extraskeletal myxoid chondrosarcoma metastatic to the pancreas: A case report. *World J Gastroenterol* 2005; 11(14): 2203-2205
http://www.wjgnet.com/1007-9327/11/2203.asp

INTRODUCTION

Extraskeletal myxoid chondrosarcoma (EMC) was described firstly by Stout and Verner[1] in 1953 and as a distinct clinicopathologic entity by Enziger and Shiraki[2] in 1972. It is generally viewed as a low-grade sarcoma composed of primitive chondroid cells in an abundant myxoid matrix resembling embryonic cartilage and presenting a high rate of survival. However, despite the protracted clinical course, it is characterized by developing metastases and local recurrence in high rate and finally high mortality[3].

EMC represents 2.5% of soft tissue sarcomas and the male to female ratio is 2:1. At the time of diagnosis, the median tumor size ranges from 1 to 25 cm in diameter, while the patient's median age is 50 years (ranging from 6 to 90 years)[1,4-6]. EMC is mainly deep seated in the proximal extremities, most frequently presenting as a painful soft tissue mass. Almost half of the cases will recur during the clinical course[4,6].

About half of the cases of EMC will develop metastases, which is proved to be an adverse prognostic factor with regard to survival[4]. The location of metastases depends on the primary site of the lesion. The most common metastatic sites[4] are the lungs, soft tissues, lymph nodes, bone[7] and the brain. Rare cases of metastatic EMC are noted in the liver[8], the mandibular[9], the retroperitoneum[10] and the right ventricle[11].

The detection of metastases varies from 6 to 15 years after the initial diagnosis of the tumor, while survival after detection ranges from a few months to 18 years[4]. Metastases are detected before identification of the primary lesion or at the time of diagnosis in almost one-third of cases developing metastases. Significant adverse prognostic factors, with regard to metastases, are larger tumor size, microscopic tumor necrosis and higher Ki67 values[4].

We describe a case of a man suffering from EMC who developed a single pancreatic metastasis 20 years after the initial diagnosis. To our knowledge, no case of clearly defined EMC has been reported to date developing a metastasis in the pancreas.

CASE REPORT

A 49-year-old man was submitted to surgical excision of a soft tissue mass of unknown origin, in left thigh, 20 years ago. The histopathologic diagnosis of the surgical specimen, 2.5 cm in diameter, was referring to myxoid liposarcoma of the thigh. Fourteen years after the initial diagnosis, in 1997, a local recurrence in left thigh occurred, viewed in MRI. The lesion, 3 cm×2 cm×2 cm in dimensions, was being excised and the histopathologic findings showed EMC. Moreover, a piece of left femur 1.5 cm×1.5 cm×1 cm also excised, proved bone superficially permeated by the lesion. A review of the histological slides of the primary

tumor also revealed EMC.

In 2000, an imaging control was performed because of developing the local recurrence three years ago. Multiple lesions of metastatic origin in both lungs were found. The patient was submitted to thoracotomy and four lesions, ranging in diameter from 0.6 to 3 cm, were excised from both lungs. The lesions proved to be metastatic of EMC. During recent three years, three surgical excisions of metastatic lesions in both lungs took place: thoracotomy in 2002 for two lesions and two thoracotomies in 2003.

In May of 2003, as a part of a periodically performed imaging control, an abdominal CT scan initially as well as an MRI were performed. These studies revealed a solid, in morphology, lesion with distinct margins, about 9 cm × 6 cm in dimensions (Figure 1A). This lesion was viewed just anterior to the body and the tail of the pancreas, giving the impression to be of pancreatic origin. The clinical and imaging features of the lesion were claiming to be of metastatic nature from EMC. As a part of the diagnosis process, a biopsy of the tumor after CT-guided FNA was performed, but the material of aspiration was not of any diagnostic significance.

Laparotomy was decided, firstly to determine the nature of the tumor and secondly for therapeutical reasons, if feasible. The lesion, previously described, was discovered originating from the body and the tail of the pancreas. Distal pancreatectomy was performed (Figure 1B-D).

The histological examination of the excised specimen proved to be the one of the metastatic lesion of EMC (Figure 1E) including tumor cells oval to round in shape, as well as some spindled ones, with light colored/eosinophilic cytoplasm. They were arranged, as single ones or in small groups, in an abundant myxoid matrix. The immunohistochemical staining results were positive in vimentin, *a1-antithrypsin, a1-antichymothrypsin, lysozyme* and *protein S-100,* while negative in all the epithelial factors.

During the most recently performed follow-up of the patient, five months after the pancreatectomy, a CT of the chest revealed a, possibly metastatic, lesion in the right medial lobe 1.2 cm in diameter. Furthermore, an abdominal CT imaged a slightly viewed lesion in the quadrate lobe of the liver, which could not be characterized, because of its dimensions, without excluding the metastatic nature.

DISCUSSION

EMC is a rare neoplasm of soft tissue located in the proximal extremities and limb girdles in 60% of cases, the trunk (20%) and the distal extremities (20%). Distal is defined as those lesions distal to the knee or elbow[1,4]. Most tumors arise within skeletal muscle or tendious structures although some involve deep subcutis[4]. Involving skin or invading bone is extremely rare.

The local recurrence rate is about 45-50% and is not a prognostic factor of survival[4]. Time passing between the initial diagnosis and the first local recurrence ranges from a few months to 18 years. With regard to local recurrence, adverse prognostic factors are female sex and higher mitotic rate[4].

The differential diagnosis of EMC is broad and depends on whether the individual case is hypercellular, hypocellular or a typical EMC. Benign and malignant tumors are included, as mixed myoepithelial tumors[12], chondroid lipoma[13], myxoid liposarcoma, myxofibrosarcoma[4], low-grade fibromyxoid sarcoma, myxoid variants of ossifying fibromyxoid tumor of soft tissues[14] and myxoid sclerosing

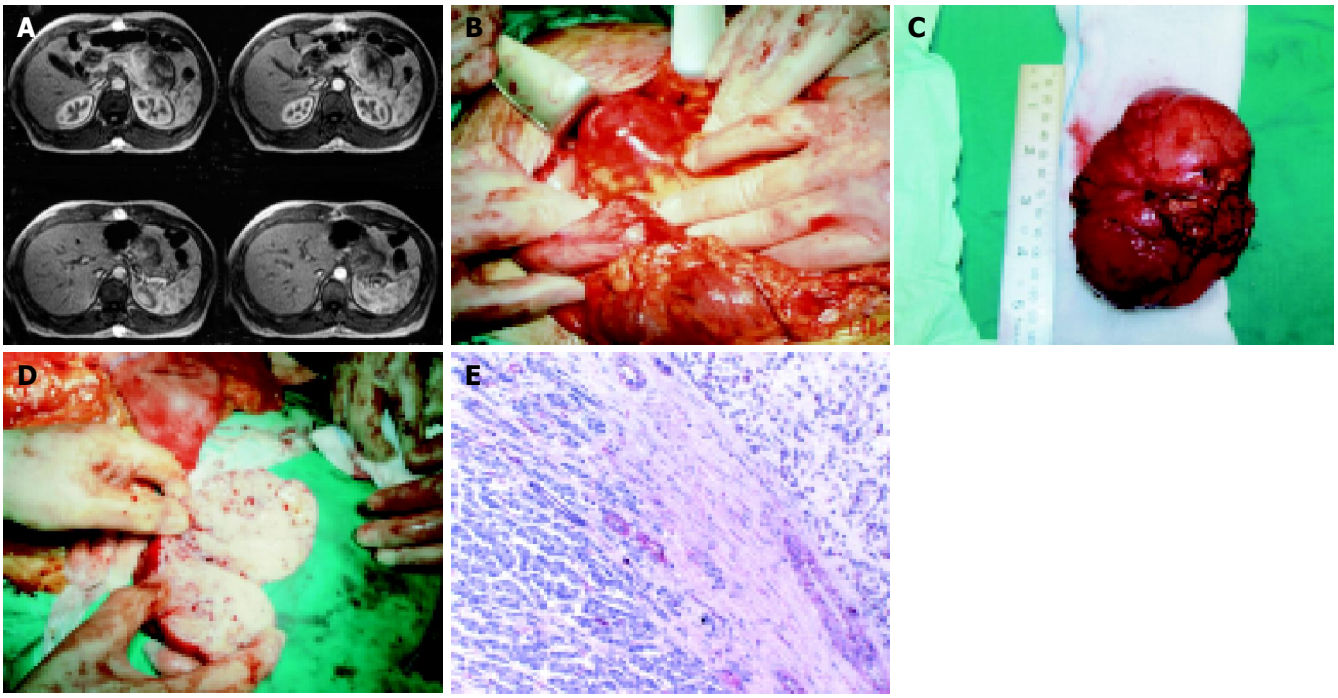

Figure 1 A: The abdominal CT scan revealing the pancreatic metastatic lesion; B: The pancreatic metastatic lesion while excised; C: The excised surgical specimen; D: A section of the surgical specimen; E: Normal pancreatic tissue (1) and tumor cells of the metastatic EMC (2) separated by connective tissue (× 400).

epithelioid fibrosarcoma.

EMC has usually a multilobular configuration with an incomplete fibrous capsule, but some cases are infiltrative. Most have fibrous septa traversing the lesion and an abundant myxoid matrix. The tumor cells, primitive chondroid, are arranged in delicate intersecting strands and rings, but in some tumors forming small balls and clusters due to loss of cell's cohesion[4]. Some cases are viewed with epithelioid and/or rhabdoid cells. Cellular areas with minimal or even absent myxoid matrix are observed in several cases, while other cases are hypocellular and composed of elongated, spindled cells reminiscent to fibroblasts and myofibroblasts, this way confusing differential diagnosis. Histologic features, including necrosis, increased cellularity, high mitotic rate, pleomorphism, epithelioid features, rhabdoid cells and spindled foci are not proven to affect prognosis[4].

A recurrent *t (9:22) (q22:q12)* translocation has been reported in EMC involving the *EWS gene* at *22q12* and a novel gene at *9q22* designated *TEC* or *CHN*, which encodes for a novel orphan nuclear receptor. Two major types of EWS-TEC fusion transcripts have been identified, accounting for 75% of EMC[15,18]. Recent findings suggest that a specific gene, *TAF2N* (member of *TLS/FUS* family, where *EWS gene* also belongs to), can replace *EWS gene* in the fusion transcript. The novel *TAF2N-TEC gene* fusion could account for those 25% of cases that lack[19].

The study of certain immunohistochemical features reveals some of them, as *p53* and *Ki67,* with negative or extremely weak immunostaining, while others, as *protein S-100, vimentin, PCNA, bcl-2, enolase, EMA* and *laminin,* with variant degrees of staining, without however any prognostic role[4,5,20].

CT and MRI possess a major role during the diagnostic procedure, with the latter frequently imaging tumors of lobulated appearance with enhancement following contrast injection[4]. The role of cytogenetics in the diagnosis becomes extremely important, particularly in view of hypercellular, nonmyxoid and potentially solid variants of EMC[15-18]. The biopsy of the tumor after fine needle aspiration (FNA) has not yet been proved of significance in diagnosis[21].

The treatment of EMC is problematic because it has the propensity to recur locally and most cases do not respond well to chemotherapy[22] and radiation. Complete surgical excision, when feasible, remains the primary treatment modality for EMC, with radiation therapy and chemotherapy reserved for unique cases[4]. Specific surgical modifications could decrease the postoperative complications.

It seems that certain clinical features such as tumor's size, its location (proximal of the extremities), patient's age and the presence of metastases are significant adverse prognostic factors of survival, although not clearly defined[4]. The estimation of 5-, 10- and 15-year survival rates of EMC is accounted up to 90%, 70% and 60%, respectively[4].

There are two references in the literature describing pancreatic metastases, but the histopathologic character of the chondrosarcoma is not clearly defined.

Concluding, the case of EMC, mentioned above, is, as far as we know, the first one described developing a certain pancreatic metastasis.

REFERENCES

1 **Stout AP**, Verner EW. Chondrosarcoma of the extraskeletal soft tissues. *Cancer* 1953; **6**: 581-590
2 **Enzinger FM**, Shiraki M. Extraskeletal myxoid chondrosarcoma. An analysis of 34 cases. *Hum Pathol* 1972; **3**: 421-435
3 **Saleh G**, Evans HL, Ro JY, Ayala AG, Extraskeletal myxoid chondrosarcoma. A clinicopathologic study of ten patients with long term follow-up. *Cancer* 1992; **70**: 2827-2830
4 **Meis-Kindblom JM**, Bergh P, Gunterberg B, Kindblom LG. Extraskeletal myxoid chondrosarcoma: a reappraisal of its morphologic spectrum and prognostic factors based on 117 cases. *Am J Surg Pathol* 1999; **23**: 636-650
5 **Okamoto S**, Hisaoka M, Ishida T, Imamura T, Kanda H, Shimajiri S, Hashimoto H. Extraskeletal myxoid chondrosarcoma: a clinicopathologic, immunohistochemical, and molecular analysis of 18 cases. *Hum Pathol* 2001; **32**: 1116-1124
6 **Saleh G**, Evans HL, Ro JY, Ayala AG. Extraskeletal myxoid chondrosarcoma. A clinicopathologic study of ten patients with long-term follow-up. *Cancer* 1992; **70**: 2827-2830
7 **Takeda A**, Tsuchiya H, Mori Y, Nonomura A, Tomita K. Extraskeletal myxoid chondrosarcoma with multiple skeletal metastases. *J Orthop Sci* 2000; **5**: 171-174
8 **Ryan JM**, Dupuy DE, Pitman M, Boland GW, Hahn PF, Mueller PR. Metastases to the liver from extraskeletal myxoid chondrosarcoma and successful treatment with percutaneous ethanol injection. *Clin Radiol* 2000; **55**: 314-317
9 **Englert TP**, Kahn MR, Bushkoff SH, Mendelow H. Mandibular metastasis of an extraskeletal myxoid chondrosarcoma arising on the plantar surface of the foot: report of case. *J Oral Surg* 1978; **36**: 401-405
10 **Gebhardt MC**, Parekh SG, Rosenberg AE, Rosenthal DI. EMC of the knee. *Skeletal Radiol* 2000; **28**: 354-358
11 **Banfic L**, Jelic I, Jelasic D, Cuzic S. Heart metastasis of extraskeletal myxoid chondrosarcoma. *Croat Med J* 2001; **42**: 199-202
12 **Kilpatrick SE**, Hitchcock MG, Kraus MD, Calonje E, Fletcher CD. Mixed tumors and myoepitheliomas of soft tissue: a clinicopathologic study of 19 cases with a unifying concept. *Am J Surg Pathol* 1997; **21**: 13-22
13 **Meis JM**, Enzinger FM. Chondroid lipoma: A unique tumor simulating liposarcoma and myxoid chondrosarcoma. *Am J Surg Pathol* 1993; **17**: 1103-1112
14 **Enzinger FM**, Weiss SW, Liang CY. Ossifying fibromyxoid tumor of soft parts. A clinicopathological analysis of 59 cases. *Am J Surg Pathol* 1989; **13**: 817-827
15 **Hirabayashi Y**, Ishida T, Yoshida MA, Kojima T, Ebihara Y, Machinami R, Ikeuchi T. Translocation (9;22)(q22;q12). A recurrent chromosome abnormality in extraskeletal myxoid chondrosarcoma. *Cancer Genet Cytogenet* 1995; **81**: 33-37
16 **Stenman G**, Andersson H, Mandahl N, Meis-Kindblom JM, Kindblom LG. Translocation t(9;22)(q22;q12) is a primary cytogenetic abnormality in extraskeletal myxoid chondrosarcoma. *Int J Cancer* 1995; **62**: 398-402
17 **Sjogren H**, Wedell B, Meis-Kindblom JM, Kindblom LG, Stenman G. Fusion of the NH2-terminal domain of the basic helix-loop-helix protein *TCF12* to *TEC* in extraskeletal myxoid chondrosarcoma with translocation *t (9; 15) (q22; q21). Cancer Res* 2000; **60**: 6832-6835
18 **Brody RI**, Ueda T, Hamelin A, Jhanwar SC, Bridge JA, Healey JH, Huvos AG, Gerald WL, Ladanyi M. Molecular analysis of the fusion of *EWS* to an orphan nuclear receptor gene in extraskeletal myxoid chondrosarcoma. *Am J Pathol* 1997; **150**: 1058
19 **Sjogren H**, Meis-Kindblom J, Kindblom LG, Aman P, Stenman G. Fusion of the *EWS-related gene TAF2N* to *TEC* in extraskeletal myxoid chondrosarcoma. *Cancer Res 1999;* **59**: 5064-5067
20 **Oliveira AM**, Sebo TJ, McGrory JE, Gaffey TA, Rock MG, Nascimento AG. Extraskeletal myxoid chondrosarcoma: a clinicopathologic, immunohistochemical, and ploidy analysis of 23 cases. *Mod Pathol* 2000; **13**: 900-908
21 **Jones H**, Ozua PO, Lee DM. Diagnosis of EMC by FNA. *Cytopathol* 1995; **6**: 273-276
22 **Patel SR**, Burgess MA, Papadopoulos NE, Linke KA, Benjamin RS. Extraskeletal myxoid chondrosarcoma. Long-term experience with chemotherapy. *Am J Clin Oncol* 1995; **18**: 161-163

Science Editor Guo SY **Language Editor** Elsevier HK

PO Box 2345, Beijing 100023, China
www.wjgnet.com
wjg@wjgnet.com

ELSEVIER

World J Gastroenterol 2005;11(14):2206-2209
World Journal of Gastroenterology ISSN 1007-9327

• *CASE REPORT* •

Extrahepatic portal vein aneurysm: Two case reports of surgical intervention

Bi Jin, Yuan Sun, Yi-Qing Li, Yu-Guo Zhao, Chuan-Shan Lai, Xian-Song Feng, Chi-Dan Wan

Bi Jin, Yuan Sun, Yi-Qing Li, Yu-Guo Zhao, Chuan-Shan Lai, Department of Vascular Surgery, Union Hospital, Huazhong Science and Technology University, Wuhan 430022, Hubei Province, China
Xian-Song Feng, Chi-Dan Wan, Department of Portal Hypertension Surgery, Union Hospital, Huazhong Science and Technology University, Wuhan 430022, Hubei Province, China
Correspondence to: Dr. Bi Jin, Department of Vascular Surgery, Union Hospital, Huazhong University of Science and Technology, Wuhan 430022, Hubei Province, China. jinbi2000@hotmail.com
Telephone: +86-27-85726396
Received: 2004-07-07 Accepted: 2004-07-22

Abstract

We report two cases of extrahepatic portal vein aneurysm, and both of them underwent surgical intervention. The first case had a mild pain in right upper quadrant of the abdomen; the second had no obvious symptoms. Physical examination revealed nothing abnormal. Both of them were diagnosed by magnetic resonance imaging angiography (MRA). One of the aneurysms was located at the main portal vein, the other, at the confluence of the superior mesenteric vein and the splenic vein, and these two places are exactly the most common locations of the extrahepatic portal vein aneurysm reported in the literature (30.7% each site). The first case underwent aneurysmorrhaphy and the second case, aneurysm resection with splenectomy. Both of them recovered soon after the operation, and the symptom of the first case was greatly alleviated. During the follow-up of half a year, no complication and adverse effect of surgical intervention was found and the color Doppler ultrasonography revealed no recurrence of the aneurysmal dilation. We suggest that surgical intervention can alleviate the symptom of the extrahepatic portal vein aneurysm and prevent its complications effectively and safely for low risk patients.

Key words: Extrahepatic portal vein aneurysm; Surgical intervention; Splenectomy

Jin B, Sun Y, Li YQ, Zhao YG, Lai CS, Feng XS, Wan CD. Extrahepatic portal vein aneurysm: Two case reports of surgical intervention. *World J Gastroenterol* 2005; 11(14): 2206-2209
http://www.wjgnet.com/1007-9327/11/2206.asp

INTRODUCTION

Extrahepatic portal vein aneurysm is a rare clinical entity that can be caused by hepatic disease with portal hypertension or by the malformation of vein[1], and there are no more than 50 cases reported in the literature. The first entity was reported by Barzilai and Klekner in 1956[2]. It can happen at any age and with no sexual preference. In most cases it was asymptomatic, so it is not easy to be discovered. It is defined as a focal dilatation of the portal venous system that presents a fusiform or saccular configuration[3-6]. Ultrasonographic studies have been conducted to evaluate the normal dimensions of the portal vein but considerable variations of the mean portal vein diameter have been reported[7-9]. Douts and Pearce[10] reported the maximal diameter of the portal vein as approaching 19 mm. So a diameter greater than 20 mm is therefore regarded as diagnostic standard of extrahepatic aneurysm[3]. The two most common locations are the main portal vein and the confluence of the superior mesenteric vein and the splenic vein[11]. In this paper, two cases of extrahepatic portal vein aneurysm and their surgical treatment are presented. One is an aneurysm locating at the truncus of the portal vein; the other is a splenic vein aneurysm at the confluence of the superior mesenteric vein and the splenic vein.

CASE REPORT

Case 1

A 45-year-old woman presented with intermittent right upper quadrant pain that had lasted for 6 mo. Physical examination revealed nothing abnormal. She had a history of hypertension for 10 years. Laboratory analysis was within normal limits except fasting blood glucose, which was 11.8 mmol/L. The magnetic resonance imaging angiography (MRA) revealed an aneurysmal dilation at the truncus of the portal vein, measuring 3.0 cm×3.8 cm in diameter, and the distance between the body of the aneurysm and the bifurcation of the portal vein was 0.8 cm (Figure 1A). To prevent the complications of the aneurysm and relieve the abdominal pain, an operation was performed. During the operation, we carefully separated the aneurysm which was located at the truncus of the portal vein from the hepatoduodenal ligament. The diameter of the aneurysm was about 3 cm×4 cm (Figure 1B). The common hepatic artery and the common bile duct were compressed, but the dimension of the duct above the aneurysm had not increased. No abnormality of the liver and spleen was found. After both sides of the aneurysm were blocked with elastic band, we used a Satinsky claw to divide the body of the aneurysm into two parts and resected the redundant part. The remaining wall of portal vein was sutured, so its diameter had a marked reduction (Figure 1C). In the end, we relaxed the elastic band, and made sure of no hemorrhage of the portal vein.

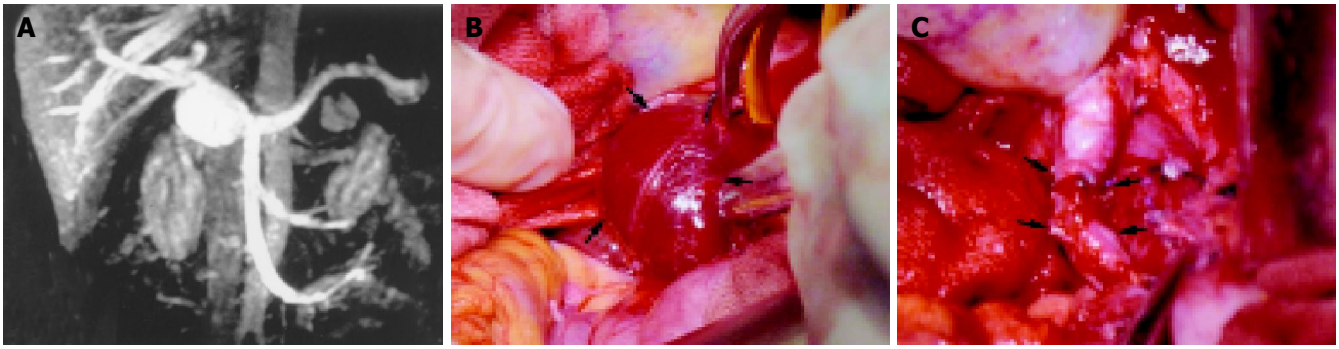

Figure 1 A: MRA revealed a fusiform dilation of the portal vein, measuring 3.0 cm×3.8 cm in diameter. B: During the operation, the aneurysm was exposed. C: After the aneurysm was resected, the dimension of the portal vein was greatly reduced.

Pathological examination diagnosed the specimen of the aneurysm as congenital amyoplasia. After the operation, anticoagulant was administered for a week. The patient recovered soon and the symptom was greatly alleviated. During half a year's follow-up with Doppler ultrasonography, no stricture and dilation of portal vein was detected, and there was no sign of thrombosis. The symptom has not recurred.

Case 2

A 34-year-old woman without clinical manifestation was detected of an aneurysmal dilatation of portal vein in a routine physical examination by the abdominal Doppler ultrasonography. Physical examination and the laboratory analysis including liver-associated enzymes were unremarkable. She suffered from schistosomiasis 20 years ago. MRA revealed an aneurysmal dilation at the confluence of the superior mesenteric vein and the splenic vein. The maximal diameter of the aneurysmal dilation was 4 cm approximately. No other abnormality was revealed (Figure 2 A). A surgical intervention was performed to prevent the complications of the aneurysm. On celiotomy, the aneurysm which measured about 3 cm×4 cm was found situated at the confluence of the splenic vein and the superior mesenteric vein. It had a pedicle connected to the distal extremity of the splenic vein (Figure 2B). There was no obvious abnormality of the liver and spleen. We resected the spleen at first, then separated the pedicle of the aneurysm and ligated it with silk thread. So the aneurysm could be resected without great difficulty (Figure 2C). Pathologic diagnosis confirmed the specimen to be a true aneurysm of the splenic vein. She had no discomfort during a half year's follow-up, and no abnormality of the portal vein was observed by the Doppler ultrasonography.

DISCUSSION

The portal vein is a unique vessel because of the presence of capillaries on both ends of the system and the absence of valves. The etiology is considered to be congenital; secondary to portal hypertension, chronic hepatic disease or associated with abnormal weakness of the vein wall[5]. And there were some other rare causes reported: Yang *et al*[12], reported a portal vein aneurysm caused by gastric adenocarcinoma invading the portal venous system. Tolgonay *et al*[13], reported a case of a splenic vein aneurysm that appeared and regressed in parallel with splenic size during the course of a systemic infection in a patient with leukemia. In this case, the portal blood flow which is associated with most forms of inflammatory diseases was considered to be related to the cause of portal vein aneurysm. Though various causes were discussed in the literature, the etiology still remains controversial, and the cause in majority of cases is difficult to determine. Expanded use of noninvasive medical imaging techniques has increased the number of patients with portal vein aneurysm but without portal hypertension

Figure 2 A: MRA revealed an aneurysmal dilation at the confluence of the splenic vein and the superior mesenteric vein. The maximal diameter of the aneurysm was 4 cm approximately. B: The aneurysm which measured about 3.0 cm×4.0 cm was exposed. C: The splenic aneurysm was resected.

or chronic liver disease. Portal hypertension was reported in 10 of 12 cases (83%) before 1985 in the literature but in only 2 of 11 cases (18%) after 1985. Chronic liver disease was reported in 9 of 12 cases (75%) before 1985 but in only 2 of 11 cases (18%) after 1985. These data suggest that neither the relationship between portal aneurysm and portal hypertension nor the relationship between portal aneurysm and chronic hepatic disease[2] is as strong as previously understood. The affirmative etiology still needs to be investigated for a long time with analyses of more entities. Neither of our patients had history or clinical evidence of underlying liver disease, portal hypertension, or other disease states that would predispose them to the development of aneurysms. Though one of the cases had a history of schistosomiasis, but during the operation no abnormality of the liver and no signs of portal hypertension were found.

Though most of the patients with portal vein aneurysm were asymptomatic or presented with mild abdominal pain[2,11,14,15], some patients presented with jaundice and gastrointestinal bleeding[6,16-19]. Complications of portal vein aneurysm include thrombosis, aneurysmal rupture, complete occlusion of the portal vein, portal-systemic shunt and pressure effects on adjacent viscera. Large extrahepatic portal vein aneurysms can cause obstruction of the common bile duct and duodenum. Patients may present with recurrent abdominal pain and obstructive jaundice. Acute thrombosis of the portal vein aneurysm can result in severe life-threatening portal hypertension[5,11,20-22]. One of our two patients had compression symptoms, the other was free from any discomfort, and neither of them had jaundice and gastrointestinal symptoms.

The two cases were both discovered by color Doppler ultrasonography, and then confirmed by MRA (Figures 1A and 2A). Portal vein aneurysm can easily and confidently be established by color Doppler ultrasonography, and it is not very expensive. So color Doppler ultrasonography can be used in follow-up of most of the patients. Computerized tomography angiography, MRA can also determine the location and its relation of the adjacent organs. It is most important that they play a potential role in determining the surgical or therapeutic approach because they can supply adequate information for the surgeons. All of them are non-invasive methods. Angiography is mandatory only in determining surgical approach or when a portacaval fistula is present[3].

In the past two decades no mortalities of portal vein aneurysm have been reported. Most of the patients keep well with the aneurysm remaining stable in size during follow-up[4,15,23-25]. It is received mostly that for asymptomatic patients without evidence of portal hypertension or cirrhosis, conservative management with regular follow-up is advisable[6,11]. But not everyone agreed with this opinion, the more current surgery literature notes that prophylactic surgery for these aneurysms is cautiously recommended for low-risk patients[26]. We think surgical intervention should be considered once symptoms arise or the aneurysm expands, indicating an increased risk of thrombosis or rupture. In the literature, seven patients underwent surgical interventions for their extrahepatic portal vein aneurysms[4,5,17,27].

Both the patients underwent surgical intervention. For the main portal vein aneurysm, an aneurysmorrhaphy operation was performed. The splenic vein aneurysm was resected after splenectomy. The aim of surgical intervention is to relieve the compression symptoms of the aneurysm and prevent the occurrence of the complications. As for the aneurysms located at the main portal vein, the methods of surgical intervention included aneurysmorrhaphy, mesocaval shunt and portacaval shunt. All were documented as having good clinical outcomes during the early postoperative period[28]. For patients with portal hypertension, a portal-systemic shunt operation is recommended. It avoids dissection or mobilization of the aneurysm, which may be injurious and will bring great difficulty to the operation[17]. A shunting procedure helps to reduce the portal venous pressure, which may prevent the progressive dilatation of the portal vein aneurysm[27]. For patients without portal hypertension, aneurysmorrhaphy is advocated as it can preserve the portal blood flow without the complications of portal-systemic shunting, such as encephalopathy. And laminar flow in the portal vein is restored, so stasis of portal blood flow which tends to result in thrombosis can be avoided. Risk of rupture is also reduced as the lateral wall tension is diminished by reduction of the radius after aneurysmorrhaphy[28]. The surgical treatment of splenic vein aneurysm includes aneurysm resection with splenectomy, splenorenal shunt, and distal pancreatectomy[29,30], all of which can procure good results.

For patients with greatly impaired hepatic function or those intolerant to shunting or devascularization surgery, non-surgical and less invasive treatments could be considered. Some held the opinion that the increased blood flow in portal hypertension come mainly from the splenic vein. So partial splenic embolization can decrease the blood flow and pressure of the main portal vein, equivalent to the conjoint effects of splenectomy and devascularization[31].

Before operation, somatostatin can be used in the patients with high portal hypertension for it can effectively lower the portal venous pressure with little side effect. Antico-agulant should be used during the postoperative period to avoid thrombosis.

After careful evaluation of our two patients, surgical interventions were performed successfully and they both experienced an uncomplicated postoperative course. No recurrence of aneurysm was discovered by color Doppler ultrasonography in half a year's follow-up. We suggest that the surgical intervention can relieve the symptoms and prevent the occurrence of the complications effectively and safely for low risk patients. And it should be greatly emphasized that the management should be on a case-by-case basis, depending on the size and anatomy of the aneurysm, as well as the symptoms and clinical condition of the patient[28]. In summary, extrahepatic portal vein aneurysm is a rare condition, which will be increasingly recognized in the practise of vascular surgery.

REFERENCES

1 **Glazer S,** Gaspar MR, Esposito V, Harrison L. Extrahepatic portal vein aneurysm: report of a case treated by thrombectomy and aneurysmorrhaphy. *Ann Vasc Surg* 1992; **6**: 338-343

2 **Barzilai R,** Kleckner MS. Hemocholecyst following ruptured

aneurysm of portal vein; report of a case. *AMA Arch Surg* 1956; **72**: 725-727
3 **Gallagher DM,** Leiman S, Hux CH. In utero diagnosis of a portal vein aneurysm. *J Clin Ultrasound* 1993; **21**: 147-151
4 **Ohnami Y,** Ishida H, Konno K, Naganuma H, Hamashima Y, Zeniya A, Masamune O. Portal vein aneurysm: report of six cases and review of the literature. *Abdom Imaging* 1997; **22**: 281-286
5 **Dognini L,** Carreri AL, Moscatelli G. Aneurysm of the portal vein: ultrasound and computed tomography identification. *J Clin Ultrasound* 1991; **19**: 178-182
6 **Brock PA,** Jordan PH, Barth MH, Rose AG. Portal vein aneurysm: a rare but important vascular condition. *Surgery* 1997; **121**: 105-108
7 **Weinreb J,** Kumari S, Phillips G, Pochaczevsky R. Portal vein measurements by real-time sonography. *AJR Am J Roentgenol* 1982; **139**: 497-499
8 **Webb LJ,** Berger LA, Sherlock S. Grey-scale ultrasonography of portal vein. *Lancet* 1977; **2**: 675-677
9 **Bolondi L,** Gandolfi L, Arienti V, Caletti GC, Corcioni E, Gasbarrini G, Labo G. Ultrasonography in the diagnosis of portal hypertension: diminished response of portal vessels to respiration. *Radiology* 1982; **142**: 167-172
10 **Doust BD,** Pearce JD. Gray-scale ultrasonic properties of the normal and inflamed pancreas. *Radiology* 1976; **120**: 653-657
11 **Lopez-Machado E,** Mallorquin-Jimenez F, Medina-Benitez A, Ruiz-Carazo E, Cubero-Garcia M. Aneurysms of the portal venous system: ultrasonography and CT findings. *Eur J Radiol* 1998; **26**: 210-214
12 **Yang DM,** Yoon MH, Kim HS, Jin W, Hwang HY, Kim HS. CT findings of portal vein aneurysm caused by gastric adenocarcinoma invading the portal vein. *Br J Radiol* 2001; **74**: 654-656
13 **Tolgonay G,** Ozbek SS, Oniz H, Suzer E, Yurdakul LO. Regression of splenic vein aneurysm following resolution of splenomegaly. *J Clin Ultrasound* 1998; **26**: 98-102
14 **Atasoy KC,** Fitoz S, Akyar G, Aytac S, Erden I. Aneurysms of the portal venous system. Gray-scale and color Doppler ultrasonographic findings with CT and MRI correlation. *Clin Imaging* 1998; **22**: 414-417
15 **Ozbek SS,** Killi MR, Pourbagher MA, Parildar M, Katranci N, Solak A. Portal venous system aneurysms: report of five cases. *J Ultrasound Med* 1999; **18**: 417-422; quiz 423
16 **Leonsins AJ,** Siew S. Fusiform aneurysmal dilatation of the portal vein. *Postgrad Med J* 1960; **36**: 570-574
17 **Thomas TV.** Aneurysm of the portal vein: report of two cases, one resulting in thrombosis and spontaneous rupture. *Surgery* 1967; **61**: 550-555
18 **Hermann RE,** Shafer WH. Aneurysm of the portal vein and portal hypertension, first reported case. *Ann Surg* 1965; **162**: 1101-1104
19 **Sedgwick CE.** Cisternal dilatation of portal vein associated with portal hypertension and partial biliary obstruction. *Lahey Clin Bull* 1960; **11**: 234-237
20 **Fukui H,** Kashiwagi T, Kimura K, Goto M, Takei Y, Kasahara A, Kawano S, Fusamoto H, Kozuka T, Kamada T. Portal vein aneurysm demonstrated by blood pool SPECT. *Clin Nucl Med* 1992; **17**: 871-873
21 **Tsukuda S,** Sugimoto E, Watabe T, Amanuma M, Heshiki A. A case of extrahepatic portal vein aneurysm with massive thrombosis: diagnosis with reconstruction images from helical CT scans. *Radiat Med* 1998; **16**: 301-303
22 **Baker BK,** Nepute JA. Computed tomography demonstration of acute thrombosis of a portal vein aneurysm. *Mo Med* 1990; **87**: 228-230
23 **Thompson PB,** Oldham KT, Bedi DG, Guice KS, Davis M. Aneurysmal malformation of the extrahepatic portal vein. *Am J Gastroenterol* 1986; **81**: 695-697
24 **Itoh Y,** Kawasaki T, Nishikawa H, Ochi J, Miura K, Moriyasu F. A case of extrahepatic portal vein aneurysm accompanying lupoid hepatitis. *J Clin Ultrasound* 1995; **23**: 374-378
25 **Boyez M,** Fourcade Y, Sebag A, Valette M. Aneurysmal dilatation of the portal vein: a case diagnosed by real-time ultrasonography. *Gastrointest Radiol* 1986; **11**: 319-321
26 **Calligaro KD,** Ahmad S, Dandora R, Dougherty MJ, Savarese RP, Doerr KJ, McAffee S, DeLaurentis DA. Venous aneurysms: surgical indications and review of the literature. *Surgery* 1995; **117**: 1-6
27 **Andoh K,** Tanohata K, Asakura K, Katsumata Y, Nagashima T, Kitoh F. CT demonstration of portal vein aneurysm. *J Comput Assist Tomogr* 1988; **12**: 325-327
28 **Lau H,** Chew DK, Belkin M. Extrahepatic portal vein aneurysm: a case report and review of the literature. *Cardiovasc Surg* 2002; **10**: 58-61
29 **Loewenthal M,** Jacob H. Aneurysm of the splenic vein; report of a case. *Acta Med Orient* 1953; **12**: 170-173
30 **Torres G,** Hines GL, Monteleone F, Hon M, Diel J. Splenic vein aneurysm: is it a surgical indication? *J Vasc Surg* 1999; **29**: 719-721
31 **Numata S,** Akagi K, Sakino I, Ogata H, Kawadoko T, Suzuki N, Nomiyama K, Tsuji H, Fujishima M. Partial splenic embolization for the treatment of liver cirrhosis with hypersplenism: assessment of clinical response and liver function. *Nihon Shokakibyo Gakkai Zasshi* 1997; **94**: 526-531

Science Editor Gou SY **Language Editor** Elsevier HK

PO Box 2345, Beijing 100023, China
www.wjgnet.com
wjg@wjgnet.com

ELSEVIER

World J Gastroenterol 2005;11(14):2210
World Journal of Gastroenterology ISSN 1007-9327

Acknowledgements to Reviewers of *World Journal of Gastroenterology*

Many reviewers have contributed their expertise and time to the peer review, a critical process to ensure the quality of *World Journal of Gastroenterology*. The editors and authors of the articles submitted to the journal are grateful to the following reviewers for evaluating the articles (including those were published and those were rejected in this issue) during the last editing period of time.

Andrew Seng Boon Chua, M.D.
Department of Gastroenterology, Gastro Centre Ipoh, 31, Lebuhraya Taman Ipoh, Ipoh Garden South, 32400, Ipoh, Perak, Malaysia

Zong-Jie Cui, Professor
Institute of Cell Biology, Beijing Normal University, Beijing 100875, China

Curt Einarsson, Professor
Department of Medicine, Karolinska institute, Karolinska University Hospital Huddinge, Dept of Gastroenterology and Hepatology, K 63, Huddinge SE-141 86, Sweden

Michael W Fried, Professor
Department of Gastroenterology and Hepatology, Division of Digestive Diseases, University NC, Division of Gastroenterology, University Hospital Zurich, Raemistrasse 100, Zurich CH- 8091, Switzerland

Jaime Guardia, Professor
Internal Medicine and Liver Unit, Hospital Universitari 'Vall d'Hebron'. Universitat Autonoma de Barcelona, Hospital Universitari Vall d'Hebron, Pg Vall d'Hebron, 119, Barcelona 08035, Spain

De-Wu Han, Professor
Shanxi Medical University, 86 Xinjian South Road, Taiyuan 030001, Shanxi Province, China

Shao-Heng He, Professor
Medical College of Shantou University, 22 Xinling Rd, Shantou, Guangdong, Shantou 515031, Guangdong Province, China

Fu-Lian Hu, Professor
Department of Gastroenterology, Peking University First Hospital, 8 Xishiku St, Xicheng District, Beijing 100034, China

Wayne HC Hu, M.D.
Department of Medicine, University of Hong Kong, 302, New Clinical Building, Queen Mary Hospital, Pokfulam Road, Hong Kong SAR, China

Richard A Kozarek, M.D.
Department of Gastroenterology, Virginia Mason Medical Center, 1100 Ninth Avenue, P.O. Box 900, Seattle 98111-0900, United States

Shiu-Ming Kuo, M.D.
University at Buffalo, 15 Farber Hall, 3435 Main Street, Buffalo 14214, United States

Ai-Ping Lu, Professor
China Academy of Traditional Chinese Medicine, Dongzhimen Nei, 18 Beixincang, Beijing 100700, China

Reza Malekzadeh, Professor
Director , Digestive Disease Research Center, Tehran University of Medical Sciences, Shariati Hospital, Kargar Shomali Avenue, 19119 Tehran, Iran

Hisato Nakajima, M.D.
Department of Gastroenterology and Hepatology, The Jikei University School of Medicine, 3-25-8, Nishi-Shinbashi, Minato-ku, Tokyo 105-8461, Japan

Christian Rabe, M.D.
Resident, Department of Medicine 1, University of Bonn Sigumund-Freud-Strasse 25 D 53105 Bonn, Germany

Kiichi Tamada, M.D.
Department of Gastroenterology, Jichi Medical Shool, 3311-1 Yakushiji, Minamikawachi,Kawachigun, Tochigi 329-0498, Japan

Akihito Tsubota, Assistant Professor
Institute of Clinical Medicine and Research (ICMR), Jikei University School of Medicine, 163-1 Kashiwa-shita, Kashiwa, Chiba 277-8567, Japan

Jian-Zhong Zhang, Professor
Department of Pathology and Laboratory Medicine, Beijing 306 Hospital, 9 North Anxiang Road, PO Box 9720, Beijing 100101, China

Xiao-Hang Zhao, Professor
State Key Laboratory of Molecular Oncology, Cancer Institute of Chinese Academy of Medical Sciences, 17 Panjiayuan, Chaoyangqu, Beijing 100021, China

Shu Zheng, Professor
Scientific Director of Cancer Institute, Zhejiang University, Secondary Affiliated Hospital, Zhejiang University, 88# Jiefang Road, Hangzhou 310009, Zhejiang Province, China

PO Box 2345, Beijing 100023, China
www.wjgnet.com
wjg@wjgnet.com

ELSEVIER

World J Gastroenterol 2005;11(14):Appendix 1
World Journal of Gastroenterology ISSN 1007-9327

Meetings

Major meetings coming up

Digestive Disease Week
106th Annual Meeting of AGA, The American Gastroenterology Association
May 14-19, 2005
www.ddw.org/
Chicago, Illinois

13th World Congress of Gastroenterology
September 10-14, 2005
www.wcog2005.org/
Montreal, Canada

13th United European Gastroenterology Week, UEGW
October 15-20, 2005
www.uegf.org/
Copenhagen, Denmark

American College of Gastroenterology Annual Scientific Meeting
October 28-November 2, 2005
www.acg.gi.org/
Honolulu Convention Center, Honolulu, Hawaii

Events and meetings in the upcoming 6 months

EASL 2005 the 40th annual meeting
April 13–17, 2005
www.easl.ch/easl2005/
Paris, France

World Congress on Gastrointestinal Cancer
June 15–18, 2005
Barcelona

Digestive Disease Week *DDW 106th Annual Meeting*
May 15–18, 2005
www.ddw.org
Chicago, Illinois

Events and meetings in 2005

Canadian Digestive Disease Week Conference
February 26-March 6, 2005
www.cag-acg.org
Banff, AB

2005 World Congress of Gastroenterology
September 12–14, 2005
Montreal, Canada

International Colorectal Disease Symposium 2005
February 3–5, 2005
Hong Kong

13th UEGW meeting *United European Gastroenterology Week*
October 15–20, 2005
www.webasistent.cz/guarant/uegw2005/
Copenhagen-Malmoe

7th International Workshop on Therapeutic Endoscopy
September 10–12, 2005
www.alfamedical.com
Theodor Bilharz Research Institute

EASL 2005 the 40th annual meeting
April 13–17, 2005
www.easl.ch/easl2005/
Paris, France

Pediatric Gastroenterology, Hepatology and Nutrition
March 13, 2005
Jakarta, Indonesia

21st annual international congress *of Pakistan society of Gastroenterology & GI Endoscopy*
March 25–27, 2005
www.psgc2005.com
Peshawar

8th Congress of the Asian Society of HepatoBiliary Pancreatic Surgery
February 10–13, 2005
Mandaluyong, Philippines

APDW 2005 - Asia Pacific Digestive Week 2005
September 25–28, 2005
www.apdw2005.org
Seoul, Korea

World Congress on Gastrointestinal Cancer
June 15–18, 2005
Barcelona

British Society of Gastroenterology Conference (BSG)
March 14–17, 2005
www.bsg.org.uk
Birmingham

Digestive Disease Week *DDW 106th Annual Meeting*
May 15–18, 2005
www.ddw.org
Chicago, Illinois

70th ACG Annual Scientific Meeting and Postgraduate Course
October 28-November 2, 2005
Honolulu Convention Center, Honolulu, Hawaii

Events and meetings in 2006

EASL 2006 - THE 41ST ANNUAL MEETING
April 26–30, 2006
Vienna, Austria

Canadian Digestive Disease Week Conference
March 4–12, 2006
www.cag-acg.org
Quebec City

XXX pan-american congress of digestive diseases *XXX congreso panamericano de anfermedades digestivas*
November 25-December 1, 2006
www.gastro.org.mx
Cancun

World Congress on Gastrointestinal Cancer
June 14–17, 2006
Barcelona, Spain

7th World Congress of the International Hepato-Pancreato-Biliary Association
September 3–7, 2006
www.edinburgh.org/conference
Edinburgh

71st ACG Annual Scientific Meeting and Postgraduate Course
October 20–25, 2006
Venetian Hotel, Las Vegas, Neveda

PO Box 2345, Beijing 100023, China
www.wjgnet.com
wjg@wjgnet.com

ELSEVIER

World J Gastroenterol 2005;11(14):Appendix 2-3
World Journal of Gastroenterology ISSN 1007-9327

Instructions to authors

GENERAL INFORMATION

World Journal of Gastroenterology (*WJG,* ISSN 1007-9327 CN 14-1219/R) is a weekly journal of more than 48 000 circulation, published on the 7th, 14th, 21st and 28th of every month.

Original Research, Clinical Trials, Reviews, Comments, and Case Reports in esophageal cancer, gastric cancer, colon cancer, liver cancer, viral liver diseases, *etc*., from all over the world are welcome on the condition that they have not been published previously and have not been submitted simultaneously elsewhere.

Published jointly by
The WJG Press and Elsevier Inc.

SUBMISSION OF MANUSCRIPTS

Manuscripts should be typed double-spaced on A4 (297×210 mm) white paper with outer margins of 2.5 cm. Number all pages consecutively, and start each of the following sections on a new page: Title Page , Abstract, Introduction, Materials and Methods, Results, Discussion, Acknowledgements, References, Tables, Figures and Figure Legends. Neither the Editors nor the Publisher is responsible for the opinions expressed by contributors. Manuscripts formally accepted for publication become the permanent property of The WJG Press and Elsevier Inc., and may not be reproduced by any means, in whole or in part without the written permission of both the Authors and the Publisher. We reserve the right to put onto our website and copy-edit accepted manuscripts. Authors should also follow the guidelines for the care and use of laboratory animals of their institution or national animal welfare committee.

Authors should retain one copy of the text, tables, photographs and illustrations, as rejected manuscripts will not be returned to the author(s) and the editors will not be responsible for the loss or damage to photographs and illustrations.

Online submission
Online submission is strongly advised. Manuscripts should be submitted through the Online Submission System at: http://www.wjgnet.com/index.jsp. Authors are highly recommended to consult the ONLINE INSTRUCTIONS TO AUTHORS (http://www.wjgnet.com/wjg/help/instructions.jsp) before attempting to submit online. Authors encountering problems with the Online Submission System may send an email describing the problem to wjg@wjgnet.com for assistance. If you submit manuscript online, do not make a postal contribution. A repeated online submission for the same manuscript is strictly prohibited.

Postal submission
Send 3 duplicate hard copies of the full-text manuscript typed double-spaced on A4(297×210 mm) white paper together with any original photographs or illustrations and a 3.5 inch computer diskette or CD-ROM containing an electronic copy of the manuscript including all the figures, graphs and tables in native Microsoft Word format or *.rtf format to:

World Journal of Gastroenterology
Apartment 1066 Yishou Garden,
58 North Langxinzhuang Road,
PO Box 2345, Beijing 100023, China
E-mail: wjg@wjgnet.com
http: //www.wjgnet.com

MANUSCRIPT PREPARATION

All contributions should be written in English. All articles must be submitted using a word-processing software. All submissions must be typed in 1.5 line spacing and in word size 12 with ample margins. The letter font is Tahoma. For authors originating from China, one copy of the Chinese translation of the manuscript is also required (excluding references). Style should conform to our house format. Required information for each of the manuscript sections is as follows:

Title page
Full manuscript title, running title, all author(s) name(s), affiliations, institution(s) and/or department(s) where the work was accomplished, disclosure of any financial support for the research, and the name, full address, telephone and fax numbers and email address of the corresponding author should be involved. Titles should be concise and informative (removing all unnecessary words), emphasize what is NEW, and avoid abbreviations. A short running title of less than 40 letters should be provided. List the author(s)' name(s) as follows: initials and/or first name, middle name or initial(s) and full family name.

Abstract
An informative, structured abstract of no more than 250 words should accompany each manuscript. Abstracts for original contributions should be structured into the following sections: AIM: Only the purpose should be included. METHODS: The materials, techniques, instruments and equipments, and the experimental procedures should be included. RESULTS: The observatory and experimental results, including data, effects, outcome, *etc*. should be included. Authors should present *P* value where necessary, and the significant data should accompany. CONCLUSION: Accurate view and the value of the results should be included.

The format of structured abstracts is at: http://www.wjgnet.com/wjg/help/11.doc

Key words
Please list 3-10 key words that could reflect content of the study.

Text
For most article types, the main text should be structured into the following sections: INTRODUCTION, MATERIALS AND METHODS, RESULTS and DISCUSSION, and should include appropriate Figures and Tables. Data should be presented in the body text or Figures and Tables, not both.

Illustrations
Figures should be numbered as 1, 2, 3 and so on, and mentioned clearly in the main text. Provide a brief title for each figure on a separate page. No detailed legend should be involved under the figures. This part should add into the text where the figures are applicable. Digital images: black and white photographs should be scanned and saved in TIFF format at a resolution of 300 dpi; color images should be saved as CMYK (print files) and not RGB (screen-viewing files). Place each photograph in a separate file. Print images: supply images of size no smaller than 126×76 mm printed on smooth surface paper; label the image by writing the Figure number and orientation using an arrow. Photomicrographs: indicate the original magnification and stain in the legend. Digital Drawings: supply files in EPS if created by Freehand and Illustrator, or TIFF from Photoshop. EPS files must be accompanied by a version in native file format for editing purposes. Scans of existing line drawings should be scanned at a resolution of 1200 dpi and as close as possible to the size at which they will appear when printed, not smaller. Please use uniform legends for the same subjects. For example: Figure 1 Pathological changes of atrophic gastritis after treatment. A: ...; B: ...;C: ...; D: ...; E: ...; F: ...; G: ...

Tables
Three-line tables should be numbered as 1, 2, 3 and so on, and mentioned clearly in the main text. Provide a brief title for each table. No detailed legend should be involved under the tables. This part should add into the text where the tables are applicable. The information should complement but not duplicate that contained in the text. Use one horizontal line under the title, a second under the column heads, and a third below the Table, above any footnotes. Vertical and italic lines should be omitted.

Notes in tables and illustrations
Data which is not statistically significant should not be noted. $^{a}P<0.05$, $^{b}P<0.01$ ($P>0.05$ should not be noted). If there are other series of *P* values, $^{c}P<0.05$ and $^{d}P<0.01$ are used; Third series of *P* values can be expressed as $^{e}P<0.05$ and $^{f}P<0.01$. Other notes in tables or under

illustrations should be expressed as ^1F, ^2F, ^3F; or some other symbols with a superscript (Arabic numerals) in the upper left corner. In a multi-curve illustration, each curve should be labeled with ●, ○, ■, □, ▲, △, *etc*. in a certain sequence.

Acknowledgments

Brief acknowledgments of persons who have made genuine contributions to the manuscripts and who endorse the data and conclusions are included. Authors are responsible for obtaining written permission to use any copyrighted text and/or illustrations.

References

Cited references should mainly be drawn from journals covered in the Science Citation Index (http://www.isinet.com) and/or Index Medicus (http://www.ncbi.nlm.nih.gov/PubMed) databases. Mention all references in the text, tables and figure legends, and set off by consecutive, superscripted Arabic numerals. References should be numbered consecutively in the order in which they appear in the text. Abbreviate journal title names according to the Index Medicus style (http://www.ncbi.nlm.nih.gov/entrez/query.fcgi?db=journals). Unpublished observations and personal communications are not listed as references. The style and punctuation of the references conform to ISO standard and the Vancouver style (5th edition); see examples below. Reference lists not conforming to this style could lead to delayed or even rejected publication status. Examples:

Standard jounal article (list all authors and include the PubMed ID [PMID] where applicable)

1 **Das KM,** Farag SA. Current medical therapy of inflammatory bowel disease. *World J Gastroenterol* 2000; 6: 483-489 [PMID: 11819634]

2 **Pan BR**, Hodgson HJF, Kalsi J. Hyperglobulinemia in chronic liver disease: Relationships between *in vitro* immunoglobulin synthesis, short lived suppressor cell activity and serum immunoglobulin levels. *Clin Exp Immunol* 1984; 55: 546-551 [PMID: 6231144]

3 **Lin GZ,** Wang XZ, Wang P, Lin J, Yang FD. Immunologic effect of Jianpi Yishen decoction in treatment of Pixu-diarrhoea. *Shijie Huaren Xiaohua Zazhi* 1999; 7: 285-287 [CMFAID:1082371101835979]

Books and other monographs (list all authors)

4 **Sherlock S,** Dooley J. Diseases of the liver and billiary system. 9th ed. Oxford: Blackwell Sci Pub, 1993: 258-296

Chapter in a book (list all authors)

5 **Lam SK.** Academic investigator's perspectives of medical treatment for peptic ulcer. In: Swabb EA, Azabo S. Ulcer disease: investigation and basis for therapy. New York: Marcel Dekker, 1991: 431-450

Electronic journal (list all authors)

6 **Morse SS.** Factors in the emergence of infectious diseases. Emerg Infect Dis serial online, 1995-01-03, cited 1996-06-05; 1(1):24 screens. Available from: URL: http//www.cdc.gov/ncidod/EID/eid.htm

PMID requirement

From the full reference list, please submit a separate list of those references embodied in PubMed, keeping the same order as in the full reference list, with the following information only: (1) abbreviated journal name and citation (e.g. *World J Gastroenterol* 2003;9(11): 2400-2403; (2) article title (e.g. Epidemiology of gastroenterologic cancer in Henan Province, China; (3) full author list (e.g. Lu JB, Sun XB, Dai DX, Zhu SK, Chang QL, Liu SZ, Duan WJ; (4) PMID (e.g. 14606064). Provide the full abstracts of these references, as quoted from PubMed on a 3.5 inch disk or CD-ROM in Microsoft Word format and send by post to The *WJG* Press. For those references taken from journals not indexed by *Index Medicus*, a printed copy of the first page of the full reference should be submitted. Attach these references to the end of the manuscript in their order of appearance in the text.

Inappropriate references

Authors should always cite references that are relevant to their article, and avoid any inappropriate references. Inappropriate references include those that are linked with a hyphen and the difference between the two numbers at two sides of the hyphen is more than 5. For example, [1-6], [2-14] and [1,3,4-10,22] are all considered as inappropriate references. Authors should not cite their own unrelated published articles.

Statistical data

Present as mean±SD and mean±SE.

Statistical expression

Express *t* test as *t*(in italics), *F* test as *F*(in italics), chi square test as χ^2 (in Greek), related coefficient as *r*(in italics), degree of freedom as γ(in Greek), sample number as *n*(in italics), and probability as *P*(in italics).

Units

Use SI units. For example: body mass, m(B) = 78 kg; blood pressure, p (B)=16.2/12.3 kPa; incubation time, t(incubation)=96 h, blood glucose concentration, c(glucose) 6.4±2.1 mmol/L; blood CEA mass concentration, p(CEA) = 8.6 24.5 μg/L; CO_2 volume fraction, 50 mL/L CO_2 not 5% CO_2; likewise for 40 g/L formaldehyde, not 10% formalin; and mass fraction, 8 ng/g, *etc*. Arabic numerals such as 23,243,641 should be read 23 243 641.

The format about how to accurately write common units and quantum is at: http://www.wjgnet.com/wjg/help/15.doc

Abbreviations

Standard abbreviations should be defined in the abstract and on first mention in the text. In general, terms should not be abbreviated unless they are used repeatedly and the abbreviation is helpful to the reader. Permissible abbreviations are listed in Units, Symbols and Abbreviations: A Guide for Biological and Medical Editors and Authors (Ed. Baron DN, 1988) published by The Royal Society of Medicine, London. Certain commonly used abbreviations, such as DNA, RNA, HIV, LD50, PCR, HBV, ECG, WBC, RBC, CT, ESR, CSF, IgG, ELISA, PBS, ATP, EDTA, mAb, can be used directly without further mention.

Italicization

Quantities: *t* time or temperature, *c* concentration, *A* area, *l* length, *m* mass, *V* volume.
Genotypes: *gyr*A, *arg* 1, *c myc*, *c fos*, *etc*.
Restriction enzymes: *Eco*RI, *Hin*dI, *Bam*HI, *Kbo* I, *Kpn* I, *etc*.
Biology: *Helicobacter pylori, H pylori, E coli, etc*.

SUBMISSION OF THE REVISED MANUSCRIPTS AFTER ACCEPTED

Please revise your article according to the revision policies of *WJG*. The revised version including manuscript and high-resolution image figures (if any) should be copied on a floppy or compact disk. Author should send the revised manuscript, along with printed high-resolution color or black and white photos, copyright transfer letter, the final check list for authors, and responses to reviewers by a courier (such as EMS) (submission of revised manuscript by e-mail or on the WJG Editorial Office Online System is NOT available at present).

Language evaluation

The language of a manuscript will be graded before sending for revision. (1) Grade A: priority publishing; (2) Grade B: minor language polishing; (3) Grade C: a great deal of language polishing; (4) Grade D: rejected. The revised articles should be in grade B or grade A.

Copyright assignment form

It is the policy of WJG to acquire copyright in all contributions. Papers accepted for publication become the copyright of WJG and authors will be asked to sign a transfer of copyright form. All authors must read and agree to the conditions outlined in the Copyright Assignment Form (which can be downloaded from http://www.wjgnet.com/wjg/help/9.doc).

Final check list for authors

The format is at: http://www.wjgnet.com/wjg/help/13.doc

Responses to reviewers

Please revise your article according to the comments/suggestions of reviewers. The format for responses to the reviewers' comments is at: http://www.wjgnet.com/wjg/help/10.doc

Proof of financial support

For paper supported by a foundation, authors should provide a copy of the document and serial number of the foundation.

Publication fee

Authors of accepted articles must pay publication fee.

PO Box 2345, Beijing 100023, China
www.wjgnet.com
wjg@wjgnet.com

ELSEVIER

World J Gastroenterol 2005;11(14):Appendix 4
World Journal of Gastroenterology ISSN 1007-9327

World Journal of Gastroenterology standard of quantities and units

Number	Nonstandard	Standard	Notice
1	4 days	4 d	In figures, tables and numerical narration
2	4 days	four days	In text narration
3	day	d	After Arabic numerals
4	Four d	Four days	At the beginning of a sentence
5	2 hours	2 h	After Arabic numerals
6	2 hs	2 h	After Arabic numerals
7	hr, hrs,	h	After Arabic numerals
8	10 seconds	10 s	After Arabic numerals
9	10 year	10 years	In text narration
10	Ten yr	Ten years	At the beginning of a sentence
11	0,1,2 years	0,1,2 yr	In figures and tables
12	0,1,2 year	0,1,2 yr	In figures and tables
13	4 weeks	4 wk	
14	Four wk	Four weeks	At the beginning of a sentence
15	2 months	2 mo	In figures and tables
16	Two mo	Two months	At the beginning of a sentence
17	10 minutes	10 min	
18	Ten min	Ten minutes	At the beginning of a sentence
19	50% (*V/V*)	500 mL/L	
20	50% (m/*V*)	500 g/L	
21	1 M	1 mol/L	
22	10 μM	10 μmol/L	
23	1N HCl	1 mol/L HCl	
24	1N H_2SO_4	0.5 mol/L H_2SO_4	
25	4rd edition	4^{th} edition	
26	15 year experience	15- year experience	
27	18.5 kDa	18.5 ku,18 500u or M_r18 500	
28	25 $g.kg^{-1}/d^{-1}$	25 g/(kg·d) or 25 g/kg per day	
29	6900	6 900	
30	1000 rpm	1 000 r/min	
31	sec	s	After Arabic numerals
32	1 pg $\cdot L^{-1}$	1 pg/L	
33	10 kilograms	10 kg	
34	13 000 rpm	13 000 *g*	High speed; *g* should be in italic and suitable conversion.
35	1000 *g*	1 000 r/min	Low speed. *g* cannot be used.
36	Gene bank	GenBank	International classified genetic materials collection bank
37	Ten L	Ten liters	At the beginning of a sentence
38	Ten mL	Ten milliliters	At the beginning of a sentence
39	umol	μmol	
40	30 sec	30 s	
41	1 g/dl	10 g/L	10-fold conversion
42	OD_{260}	A_{260}	"OD" has been abandoned.
43	One g/L	One microgram per liter	At the beginning of a sentence
44	*A*260 nm	A_{260}nm	*A* should be in italic.
	^bP<0.05	^aP<0.05	In Table, no note is needed if there is no significance in statistics: ^aP<0.05, ^bP<0.01 (no note if P>0.05). If there is a second set of P value in the same table, ^cP<0.05 and ^dP<0.01 are used for a third set: ^eP<0.05, ^fP<0.01.
45	**F*=9.87, §*F*=25.9, #*F*=67.4	^1F=9.87,^2F=25.9, ^3F=67.4	Notices in or under a table
46	KM	km	kilometer
47	CM	cm	centimeter
48	MM	mm	millimeter
49	Kg, KG	kg	kilogram
50	Gm, gr	g	gram
51	nt	N	newton
52	l	L	liter
53	db	dB	decibel
54	rpm	r/min	rotation per minute
55	bq	Bq	becquerel, a unit symbol
56	amp	A	ampere
57	coul	C	coulomb
58	HZ	Hz	
59	w	W	watt
60	KPa	kPa	kilo-pascal
61	p	Pa	pascal
62	ev	EV	volt (electronic unit)
63	Jonle	J	joule
64	J/mmol	kJ/mol	kilojoule per mole
65	10×10×10cm^3	10 cm×10 cm×10 cm	
66	N·km	KN·m	moment
67	$\bar{x}$±s	mean±SD	In figures, tables or text narration
68	Mean±SEM	mean±SE	In figures, tables or text narration
69	*im*	im	intramuscular injection
70	*iv*	iv	intravenous injection
71	Wang et al	Wang *et al.*	
72	EcoRI	*Eco*RI	*Eco* in italic and RI in positive. Restriction endonuclease has its prescript form of writing.
73	Ecoli	*E.coli*	Bacteria and other biologic terms have their specific expression.
74	Hp	*H pylori*	
75	Iga	*Iga*	writing form of genes
76	*igA*	IgA	writing form of proteins
77	-70 kDa	~70 ku	